VULNERABILITY ASSESSMENT OF CURRENT MASONRY BUILDING STOCK IN ALBANIA

A THESIS SUBMITTED TO
THE FACULTY OF ACHITECTURE AND ENGINEERING
OF
EPOKA UNIVERSITY

BY

MARJO HYSENLLIU

IN PARTIAL FULFILLMENT OF THE REQUIREMENTS
FOR
THE DEGREE OF DOCTOR OF PHILOSOPHY
IN
CIVIL ENGINEERING

JUNE, 2020

Approval of the thesis:

VULNERABILITY ASSESSMENT OF CURRENT MASONRY BUILDING STOCK IN ALBANIA

submitted by……………………… in partial fulfillment of the requirements for the degree of **Doctor of Philosophy in Department of Architecture and Engineering, Epoka University** by,

Prof. Dr. ……………... ______________________
Dean, Faculty of Architecture and Engineering

Prof. Dr. ………….. ______________________
Head of Department, **Computer Engineering, EPOKA University**

Prof. Dr. …………… ______________________
Supervisor, **………………. Dept., EPOKA University**

Prof. Dr. …………… ______________________
Co-Supervisor (if available), **………….. Dept., …………..University**

Examining Committee Members:

Prof. Dr. …………….. ______________________
………………. Dept., ………….. University

Prof. Dr. ……………. ______________________
………………. Dept., ………….. University

Assoc. Prof. Dr. ,,,,,,,,,,,,,,,,,,,, ______________________
………………. Dept., ………….. University

Assoc. Prof. Dr. …………………. ______________________
………………. Dept., ………….. University

Assist. Prof. Dr. ……….. ______________________
………………. Dept., ………….. University

Date: 15.06.2020

I hereby declare that all information in this document has been obtained and presented in accordance with academic rules and ethical conduct. I also declare that, as required by these rules and conduct, I have fully cited and referenced all material and results that are not original to this work.

Name, Last name: Marjo Hysenlliu

Signature:

ABSTRACT

VULNERABILITY ASSESSMENT OF CURRENT MASONRY BUILDING STOCK IN ALBANIA

Hysenlliu, Marjo

Ph.D., Department of Architecture and Engineering

Supervisor: Assoc. Prof. Dr. Huseyin Bilgin

Recent devastating earthquakes in Albania have shown the inadequate seismic performance of existing building stock. In Albania, template designs developed by the General Directorate of Construction Affairs are used for many of the buildings intended for residential as well as governmental services (administrative centers, health clinics, hospitals, schools etc.) as common practice to save on architectural fees and ensure quality control. For that reason, these buildings must be dealt with firstly.

This study evaluates seismic performance of residential buildings with the selected template designs in Albania considering inelastic behavior of masonry components. Nineteen masonry buildings from ten different template designs were selected to represent major percentage of residential buildings in medium-size cities located in high seismic regions of Albania. Selection of template designed buildings and material properties were based on field investigation and a detailed archive study on public and private buildings in several cities of Albania. Capacity curves of investigated buildings were determined by pushover analyses conducted in two principal directions by using TREMURI software package. The inelastic dynamic characteristics were represented by equivalent single-degree-of-freedom (SDOF) systems and their seismic displacement demands were calculated under selected ground motions from near and far-field recordings. Seismic performance evaluation was carried out in accordance with Eurocode 8 that has similarities with FEMA-356 guidelines. Reasons of building damages in recent earthquakes are examined using the results of performance assessment of investigated buildings. The effects of material quality, building height, the date of construction on the seismic performance of residential buildings were investigated. The detailed examination of capacity curves and performance evaluation identified deficiencies and possible solutions for template designs. Seismic capacity evaluation was carried out in accordance with Eurocode 8.

Evaluation of the capacity curves for the investigated buildings points out that material quality, detailing, aging and height have significant role in both displacement and lateral strength capacity of buildings. Also, performance of public buildings improves as the amount of load bearing wall increases, emphasizing its importance, especially in countries where construction with poor detailing is a common problem.

Insufficient performance of residential buildings makes the development of the effective and affordable retrofitting techniques essential. The most convenient technique in Albania where poor material and construction quality is a common problem, seems the adding steel grids to increase lateral load capacity and decrease displacement demands. Besides this technique, adding encirclements and polymer grids could be alternative methods to increase the stiffness and the deformation capacity of the existing masonry buildings. As a result, existing deficiencies in load bearing walls are less pronounced and poor construction quality in buildings is somewhat compensated. Analytical findings of this study are also compared with the induced damages on masonry buildings after 2019 Albanian Earthquakes. Finally, conclusions are provided, and future research needs on the topic are outlined.

Keywords: Macro modeling, masonry structures, pushover analysis, performance based seismic evaluation, seismic capacity, template designs.

ABSTRAKT

VLERESIMI I DEMTUESHMERISE I FONDIT TE NDERTESAVE ME KONSTRUKSION MURATURE NE SHQIPERI

Hysenlliu, Marjo

Doktoraturë, Departamenti i Arkitekturës dh Inxhinierisë së ndërimit

Udhëheqësi: Assoc. Prof. Dr. Huseyin Bilgin

Tërmetet e fundit shkatërruese në Shqipëri kanë treguar performancën e pamjaftueshme sizmike të stokut të ndërtesave ekzistuese. Në Shqipëri, modelet e miratuara nga Institutet e Standartëve të Projektimit të Ndërtimit janë përdorur për shumë prej ndërtesave të destinuara për banesa, si dhe shërbime qeveritare (qëndra administrative, klinika shëndetësore, spitale, shkolla, etj.) Si praktikë e zakonshme për të kursyer në tarifat arkitektonike dhe për të siguruar kontrollin e cilësisë. Për këtë arsye, këto ndërtesa duhet të anzalizohen.

Ky studim vlerëson performancën sizmike të ndërtesave residenciale me modelet e zgjedhura nga stoku i banesave në Shqipëri duke marrë parasysh sjelljen joelastike të përbërësve të muraturës. Nëntëmbëdhjetë ndërtesa murature nga dhjetë modele të ndryshme u zgjodhën për të përfaqësuar përqindjen më të madhe të ndërtesave të banimit në qytete të vendosura në rajone me risk të madh sizmik në Shqipëri. Përzgjedhja e ndërtesave të projektuara me modele shabllon dhe provave materiale u bazuan në investigimin në terren dhe një studim të detajuar arkivor mbi ndërtesat publike dhe private në disa qytete të Shqipërisë. Kurba e kapaciteteve të secilës godinës së hetuar u përcaktuan nga analizat pushover të bëra në dy drejtimet kryesore duke përdorur paketën kompjuterike TREMURI. Karakteristikat dinamike inelastike u përfaqësuan nga sisteme ekuivalente me një shkallë lirie dinamike (SDOF) dhe kapiciteti i tyre për zhvendosje sizmike u llogarit nga lëvizjet nëntokësore të zgjedhura, me epiqendër të thellë dhe të cekët të tyre. Vlerësimi i performancës sizmike u krye në përputhje me Eurocode 8 që ka ngjashmëri me udhëzimet FEMA-356. Arsyet e dëmtimit të ndërtesave në tërmetet e fundit u shqyrtuan duke përdorur rezultatet e vlerësimit të performancës së ndërtesave të hetuara. U investiguan efektet e cilësisë së materialit, lartësia e ndërtesës dhe data e ndërtimit në performancën sizmike të ndërtesave të banimit. Ekzaminimi i detajuar i kurbave të kapaciteteve dhe vlerësimi i performancës identifikuan mangësitë dhe zgjidhjet e mundshme për modelet e godinave. Vlerësimi i kapacitetit sizmik u krye në përputhje me Eurocode 8. Vlerësimi i kurbave të kapacitetit për ndërtesat e hetuara tregon se cilësia e materialit, detajimi, vjetërsia dhe lartësia kanë një rol të rëndësishëm si në zhvendosjen anësore ashtu edhe në kapacitetin e ndërtesave. Gjithashtu, performanca e ndërtesave residenciale përmirësohet me rritjen e sasisë së mureve mbajtëse, duke theksuar rëndësinë e tyre, veçanërisht në vendet ku ndërtimi me konstuksion të dobët është një problem i zakonshëm.

Performanca e pamjaftueshme e ndërtesave të banimit e bën të domosdoshme zhvillimin e teknikave efektive dhe të përballueshme të rikonstruksionit.

Teknika më e përshtatshme në Shqipëri, ku cilësia e dobët e materialit dhe e ndërtimit është një problem i zakonshëm, është shtimi i rrjeteve të çelikut për të rritur kapacitetin e ngarkesës anësore dhe për të zvogëluar zhvendosjet në rast tërmeti. Përveç kësaj teknike, shtimi i rrethimeve dhe rrjetave me polimer mund të jetë metoda alternative për të rritur ngurtësinë dhe aftësinë e deformimit të ndërtesave ekzistuese të muraturës. Si rezultat, mangësitë ekzistuese në muret mbajtëse janë më pak të theksuara dhe cilësia e dobët e ndërtimit në ndërtesa është disi e kompensuar. Gjetjet analitike të këtij studimi krahasohen edhe me dëmet e shkaktuara në ndërtesat e muraturave pas Tërmetit të Durrësit të vitit 2019. Në fund, jepen përfundime, dhe nevojat e kërkimit të ardhshëm mbi temën janë përshkruar.

Fjalët kyçe: konstruksione murature, makro-modelim, analiza e bazuar në spektrin e projektimit, analiza kohë-histori, analiza e dëmtueshmërisë së strukturave

Dedicated to my family

ACKNOWLEDGEMENTS (optional)

I would like to express my special thanks to my supervisor Prof. Dr. Huseyin Bilgin for his continuous guidance, encouragement, motivation and support during all the stages of my thesis. I sincerely appreciate the time and effort he has spent to improve my experience during my graduate years.

I am also deeply thankful to………………..

My sincere acknowledgements go to my thesis progress committee members, ………………………………………….., for their comments and suggestions throughout the entire thesis.

I deeply thank to ……………………….

I am especially grateful to …………

I would like to thank to …………….

TABLE OF CONTENTS

LIST OF TABLES

TABLES

LIST OF FIGURES

Figure 29. Limit state rotations according to EC-8 and bilinear force-deformation relationship for a masonry pier………… [EN 1998-1, 2004]……………………….. 58

LIST OF ABBREVIATIONS

KTP	Kushti Teknik i Projektimit (Technical Code of Design)
EU	European Union
EC	EuroCode
ASTM	American Society for Testing and Materials
ATC	Applied Technology Council
FEMA	Federal Emergency Management Agency
INSTAT	Institute of statistics of Albania
IN	Institute of Construction of Albania
$[E]$	Masonry modulus of elasticity KTP
$[R_n]$	Design compressive strength of masonry KTP
$[Q_k]$	Weight of building KTP
$[\beta]$	Dynamic coefficient KTP
$[k_c]$	Seismic coefficient KTP
$[m_k]$	Behaviour factor KTP
$[T]$	Period of structure
$[X_{(xk)}]$	Displacement corresponding to the response of mass in the system
$[\eta_{ki}]$	Coefficient floor distribution KTP
$[K_r]$	Importance factor KTP
$[\psi]$	Coefficient for elasto-plastic work KTP
$[f_b]$	Brick compressive strength EC6
$[f_m]$	Mortar compressive strength EC6
$[f_k]$	Compressive strength of masonry EC6

$[f_t]$	Tensile strength of masonry EC6
$[f_{vk}]$	Shear strength of masonry EC6
$[f_{vk0}]$	Initial shear strength of masonry EC6
$[\sigma_d]$	Vertical compressive stress of masonry
$[G]$	Shear modulus of masonry
$[M_W]$	Seismic magnitude in Rihter Scale
$[q]$	Behaviour factor EC8
$[S]$	Soil factor EC8
$[T_B, T_C, T_D]$	Characteristic periods of response spectrum EC8
$[ag]$	Ground acceleration
$[P.G.A.]$	Peak ground acceleration
$[\varepsilon ult]$	Ultimate strain
$[Eb]$	Brick modulus of elasticity
$[W_A]$	Water Absorption
$[f_m{}']$	Peak compressive stress
$[\varepsilon_m{}']$	Strain at peak compressive stress
$[v]$	Poisson coefficient
URM	Unreinforced masonry building
G	Gravity loads of structure
P	Live load of structure
UNDP	United Nations Development Programme
IGJEUM	Institute of Geosciences, Energy, Water and Environment
$[\sigma - \varepsilon]$	Stress-strain relationship

$[f_x]$	Flexural strength of masonry
EN	European Normative
K	Empirical coefficient depending on masonry classification EC6
$[f_{xk1}]$	Flexural strength with a plane of failure parallel to the bed joints
$[f_{xk2}]$	Flexural strength with a plane of failure perpendicular to the bed joints
$[\sigma - \varepsilon]$	Stress-strain relationship
$[\sigma_{max}]$	Maximum axial stress of masonry pier element
$[\tau_{max}]$	Maximum tranversial stress of masonry pier element
$[G_f]$	Tensile fracture energy
$[G_{fc}]$	Compressive fracture energy
$[C_f]$	Correction factor of prism strength varying from h/t ratio
$[f_{prism}]$	Prism compressive strength
$[F_{max}]$	Maximal applied force
$[M - 25]$	Compressive strength given in Marka, 10Marka=1MPa
$[w]$	The axial displacement of macro element
$[u]$	The transversal displacement of macro element
$[j]$	Rotation of macro element
$[d]$	the axial displacement of macro element
$[f]$	the axial rotation of macro element
$[a]$	degree of damage
$[g_p]$	plastic flow
$[\sigma_{el}]$	Elastic limit of vertical compressive stress of masonry

$[\gamma_{el}]$	Elastic limit of shear deformation of masonry
$[\tau_{el}]$	Elastic limit of shear stress of masonry
$[\varepsilon_{el}]$	Elastic strain of shear stress of masonry
$[\gamma_{el}]$	Elastic limit of shear deformation of masonry
$[d_y]$	Yield displacement of structure N2 method
$[d_m]$	Ultimate displacement of structure N2 metod
$[LS2]$	Minor damage limit state of structure
$[LS3]$	Extensive damage limit state of structure
$[LS4]$	Complete damage limit state of structure
$[w]$	Axial displacement of wall pier element 3muri approach
$[u]$	Tranversal displacement of wall pier element 3muri approach
$[j]$	Rotation of wall pier element 3muri approach
$[d]$	Axial displacement of macro-element wall pier 3muri approach
$[f]$	Tranversial displacement of macro-element wall pier 3muri approach
$[j]$	Rotation of wall pier element 3muri approach
$[T]$	Tension of wall pier element 3muri approach
$[U]$	Displacement vector N2-method
$[R]$	Inertial force vector N2-method
$[1]$	Unit vector N2-method
$[a]$	The ground acceleration as a function of time N2-method
$[P]$	Statically applied exernal loads N2-method
$[m^*]$	Equivalent mass of SDOF system N2-method
$[d^*]$	Displacement of equivalent SDOF system N2-method

$[F^*]$	Force of equivalent SDOF system N2-method
$[V]$	Base shear force of MDOF system N2-method
$[\Gamma]$	Modal participation factor of MDOF system to the MDOF model N2-method
$[T^*]$	Initial period of equivalent SDOF system N2-method
$[K^*]$	Elastic stiffness of equivalent SDOF system N2-method
$[\mathrm{d}_\mathrm{y}^*]$	Yield displacement of bilinear capacity curve N2-method
$[K^*]$	Elastic stiffness of equivalent SDOF system N2-method
$[\mathrm{E}_\mathrm{m}^*]$	Energy of dissipation of equivalent SDOF system N2-method
$[\mu]$	Ductility factor N2-method
$[PF_1]$	Modal participation factor for the first mode in FEMA440
$[\propto_1]$	Modal mass coefficient for the first mode in FEMA440
$[w_i]$	Weight assigned to level i of the structure
$[\varphi_{i1}]$	Amplitude of mode 1 at level i
$[n]$	roof level
$[W]$	building dead weight plus likely live loads
$[\propto]$	Slope of idealized pushover curve in FEMA440
$[a_{pi}]$	Spectral acceleration of point in FEMA440
$[d_{pi}]$	Spectral displacement of point i in FEMA440
$[a_y]$	Spectral acceleration of yield point in FEMA440
$[d_y]$	Spectral displacement of yield point in FEMA440
$[\mu]$	Ductility value in FEMA440
$[\beta_{eff}]$	Effective damping in FEMA440

$[\beta_0]$	Initial damping (5%) in FEMA440
$[T_{eff}]$	Effective period in FEMA440
$[T_0]$	Initial period in FEMA440
$[B(\beta_{eff})]$	Spectral reduction factor in FEMA440
DL	Damage Limitation state EC-8
SD	Significant damage state EC-8
NC	Near Collapse state EC-8

CHAPTER 1

INTRODUCTION

1.1 General

Since Albania is a country located in Balkan penisula which is surrounded by active seismic zones, vulnerability assessment of the existing building is an urgent need to prevent the possible casaulities and induced economic losses as experienced by other neighboring countries in the region (Turkey, Italy, Montenegro, Greece and North Macedonia). [Bilgin H., Hysenlliu M., 2019] The boom of the masonry structures was during the communist era, when the state itself, had a good structure and budget for building these typologies of structures in mass, for residents all over the country. But these building inherit all the disadvantages and backwardness of the conditions of the 45-90 era, when the country was under an extreme poverty and total lack of construction materials. At this time buildings were designed with standardized templates, all over the country. Masonry is one of the most common structural types for low to mid-rise buildings in the Albania like in many other earthquake prone countries worldwide (USA, New Zeland, Italy, Japan and Turkey). It is used both for public and residental buildings. They were designed and built by using template designs in different time and periods, but mainly between1940-1990s. This typology was observed as one of the highly susceptible types

to earthquake damages according to the recent reconnaissance team reports [Kaplan et. al., 2014; Goda et al, 2015; Sorrentino et. al., 2019; Bilgin and Hysenlliu, 2020]. Therefore, masonry structures have high seismic vulnerability over the region. In other words, a moderate or big seismic activity may result in a tragic consequence associated with the masonry building stock in the region. Building codes also, have played a significant role. Albania building codes [KTP-1963, KTP-1978 and KTP-1989], have significant changes within one another, but also very verified deficiency. This comes from lack of knowledge of the time especially on seismic calculations, compared to nowadays acepted worldwide [EC and ASTM]. Lacking of seismic analysis in KTP-63 and low considered demand of KTP-78, implies that the entire stock of pre 89s era to be reconsidered and re-analyzed with today updated codes. Also on this buildings many interventions are done, especially after the 90s. Added stories and interventions on first floor are very popular among these building types.

1.2 Objective of the study

As overall objective of the study is making a full assessment of the entire stock of the masonry building, highlighting the building types that have higher risk under seismic action. To achieve this objective, first a full study is made on the database of the current building stock, to choose represantitive templates for all the population. 19 buildings of 10 different templates are choosen to represent the building stock. To proper model the masonry structures, several tests are conducted to define the mechanical characteristics of the buildings. Six different tests are performed on specimens from these buildings and the results are also revised with EC guidance. Three dimensional models of the structures are prepared for modal, pushover and time history analysis by a user-friendly software as 3muri, specialized for masonry buildings. [3muri software package] To make a full assessment of the seismic hazard, three different analysis are conducted to all the buildings: the non-linear pushover analysis, the N-2 spectrum based analysis [Fajfar p. et al, 2005; EN1998, 2005] and the displacement based time history analysis, All the three are done seperatively and their results are compared to show the compability of each the similarity and differences of the results. Also for time history analysis the earthquake records are diveded in two groups: near field and far field records, to show the different effect of both cases. During the timeline of this study, a strong earthquake of Magnitude M_w=6.4 hitted Durres region, causing many casualites on Durres, Tirana and Lezhe region. [IGJEUM, 2020] The building stock of these region has a significant part of masonry buildings, wich were priorly analysed on this study. The real damage on these buildings is inspected in-site and evaluated using EC-8 guidancee [EN1998-1, 2004], and are compared with the results of performance based and time-history analysis.

1.3 Scope and methodology

In order to recognize the most critical regions and make a rational estimation to mitigate the future earthquake consequences associated with the masonry buildings, a proper assessment of seismic risk in existing buildings should be quantitively estimated through analytical methods. To achive a proper assessment of the buildings, the first step is choosing the proper modelling methodology. Modelling of masonry buildings has always been a challenging task because of the presence of joints as the major source of weakness and also nonlinearity and discontinuity. In this study is used a macro-modelling technique, based on pier and sprandels idealization of the masonry wall. This approach is integrated in 3muri software package, and gives reliabile and verified results. [Cattari S., et.al, 2015; Penna A., et. al.,2014; R. Marques, PB Lourenco, 2014; Lagomarsino S, et.al., 2013; Galasco A. et.al 2006; Galasco A. et.al 2004; Penna A. et.al., 2004; Galasco A. et.al., 2002] The masonry walls are modelled as non-linear elements, taking in consideration both elastic and plastic phases. The basic mechanical charachteristics of the walls, since these buildings are old, and some of them are done with poor materials and workmanship, are determinded by doing experimental tests on speciemens extracted from real buildings. Compressive strength test and tensile flexural test is done for both brick and mortar specimens to determine compressive and tensile strength of both. For masonry, prism test and triplet shear test are conducted to determine, compressive strength, initial shear strength and shear strength of masonry. To determine capacity of the idealized SDOF for each building, pushover analysis is performed, with 3muri software [3muri software package]. As given in the EC-8 the capacity is evaluated in three limit states DL (damage limitation), SD (significant damage) and NC (near collapse) referring to the damage state of building. The first seismic analyze is the spectrum based approach. Following the guidance of EC-8, 3muri analyses and gives the peak ground acceleration of the earthquke spectrum for each limit state.[EN1998-1, 2004] For nonlinear response history analyses, the selection of acceleration records is an important step because the use of acceleration records with same features can exaggerate or underestimate the building response. To comparatively investigate influence of the far- field and near-field earthquakes on the seismic response of the URM template designs, a total of 78 near-fault and 68 far-fault ground motions recorded on dense-to-firm soil sites are used for seismic performance evaluation of the considered buildings. The output of the two analysis, to make it more easy comparable and simple, is prepared in charts. The ratio of exceendance of each limit state is given in percentage of the buldings population. According to the analysis this data is given under the selected earthquakes or the spectra peak ground acceleration. In the last part of the study, some investigation methods are proposed as given in EC, to proper assess the damage, that occured in masonry buildings in Tirane, Durres, Thumane and Vore on the 26.11.2019 earthquake. Comparison between the real damage and the predictions of the two analysis are mostly in accordance.

1.4 Brief description of the content

The study is divided in eight chapters.

Chapter one gives an introduction to the study.

Chapter two gives a full literature review on this topic. Here are discussed prior studies on testing of materials, pushover analysis of masonry buildings, spectrum based assessment and time-history analysis. It starts with a review of regulations on masonry buildings of KTP and EC. The failure mechanism of the masonry walls and how they affect the material properties are given on this chapter. The damage limit states are presented here and the description of capacity of the buildings and demand from the seismic data. Also, here is presented a review of the seismic hazard of Albania and the earthquake ground motions choosen for time-history analysis. This earthquake records are divided by the epicentral depth to near-fault and far-fault earthquakes. In total are chosen 78 near-fault records and 68 far-faults records.

Chapter three gives a full view of the building stock and of the template buildings considered in this study. Based on time of construction, height of the building, material of construction and seismicity of the zone are choosen 19 buildings of 10 different templates. The mechanical characteristics are given for each building, as in the project blueprints.

Chapter four presents the mechanical properties of each building. The test of bricks, mortar and masonry are performed and the material characteristics for each building are determined. This part is crucial because many of these buildings are very old and materials have degraded with time. The mechanical properties, in most of the cases, are lower than the project blueprints. With these values three dimensional non-linear macro-models are generated with 3muri software package.

Chapter five gives the full results of all pushover cases. In total are performed 24 cases of non-linear pushover analysis for each building.The capacity curves are evaluated in both directions and the performace levels, according to EC-8 guidance. The failure mechanisms of buildings with and without interventions are compared to show how the interventions affect performance.

Chapter six gives the full analysis and results of both force-based N-2 spectrum analysis and displacement based time-history analysis. The output of the two analyses is prepared in charts to easy compare the results. Comparisons are done between the two analyses, different building types and near-fault and far-fault earthquakes.

Chapter seven presents the results from the investigations done on several masonry buildings in Tirane, Durres, Thumane and Vore after the earthquake sequence of 26 November 2019. The buildings performance is evaluated after in-site inspection and are compared with results of spectrum based and time-history analysis.

Chapter eight summarizes the results of this study.

CHAPTER 2

LITERATURE REVIEW

This chapter presents a summary review of the past thoretical and experimental studies on the seismic response of masonry structures with special attention given to their displacement capacity under seismic shakings.

To proper assess the buildings vulnerability, different authors have developed different theories and assessment methods. In this chapter, are reviewed some papers and literature on the following topics:

- building codes and masonry building stock
- seismicity and other characteristics of Albanian territory
- material characteristics of the masonry buildings and how to determine them
- modelling techniques of masonry buildings
- pushover analysis of masory buildings
- spectrum based and time history analysis
- vulnerability assessment of masonry builidings

2.1 Earthquake resistant design codes and regulations

To proper assess the performance of the existing masonry building stock, first the Albanian building codes, that guided the design and projection of those, should be understood. Since Albania is a state in Europe and heading towards EU, EC are also to be adopted as a legislation regarding construction, so a comparison of them with KTP is necessary for understanding the code deficiencies. The related standards are EC-6 [EN 1996-1, 2005] which gives rules and specifications for masonry structures and EC-8 [EN 1998-1, 2004] that gives basics of seismic design requirements for structures. The first Albanian code was KTP-1952, a good paper regulating construction for the time it was published, but with great deficiencies. [KTP-52, 1952] Seismic analysis was not known then, and building were projected with a simplified calculation and mostly based on recommendations from prior experience. In 1963, the KTP-1963 was published and was used as the basic paper for regulating the construction. [KTP-63, 1963] The section for masonry was the widest since it was the basic technique of the time.

Seismic demand was taken in consideration in this code, but the seismic intensity of the zones was taken very low compared to the real seismic hazard of today's practice. The Albanian KTP-78 is the main reference for masonry structures, and also has seismic calculation integrated. The first seismic map of Albania, was developed in 1952 by the Institute of Science of that time. Till then, a lot of work is done in this topic by different authors at different times. The 1979 earthquake near Shkodra was very devastating, and many 5 story high masonry structures, constructed with the old KTP-63 had major damages, even diagonal cracks on the load bearing walls. So the seismic demand was again updated, and later even in the KTP-89 that is currently in law in Albania. But even though a seismic analysis based on a projection spectrum was incorporated till early, the spectrum properties of KTP-78 and KTP-89 if compared to the EN 1998-1, have very lowered seismic demand. [KTP-9-78, 1978; KTP-N2-89, 1989; EN 1998-1, 2004]

2.1.1 KTP 9 - 78 Masonry design code

This code was published in 1978. All the cases for walls of different materials are specified in this code. For the compression strength of the elements the below tables are suggested in this code:

Table 1: Design compressive strength for wall with 12 cm thickness of brick rows [KTP-9-78, 1978]

Clay brick class (kg/cm^2)	**Mortar class kg/cm^2**						
	100	75	50	25	15	4	0
150	22	20	18	15	13.5	12	8
100	18	17	15	13	11	9	6
75	15	14	13	11	9	7	5
50	-	11	10	9	7.5	6	3.5

Table 2: Design compressive strength for wall with 18 cm thickness of brick row [KTP-9-78, 1978]

Clay brick class (kg/cm^2)	**Mortar class kg/cm^2**						
	100	75	50	25	15	4	0
100	20	18	17	16	14.5	13	9
75	16	15	14	13	11.5	10	7
50	12	11.5	11	10	9	8	5

Table 3: Design compressive strength for massive concrete wall [KTP-9-78, 1978]

Stone class kg/cm2	**Concrete class kg/cm2**		
	100	75	50
Above 200	27	22	18
Below 200	-	18	15

Table 4: Masonry wall design tensile and shear strength [KTP-9-78, 1978]

Type of strength	**Mortar class kg/cm2**			
	100-50	25	15	4
Tensile strength				
Along bed joints	1.6	1.1	0.5	0.2
Across bed joints	0.8	0.5	0.3	0.1
Shear strength				
Along bed joints	1.6	1.1	0.5	0.2
Across bed joints	2.4	1.6	0.8	0.4
Principal tensile strength	1.2	0.8	0.4	0.2

The modulus of elasticity is calculated as follows:

$E = 0.5 * \alpha * R_n$ (1) ,for limit state design

$E = 0.8 * \alpha * R_n$ (2) ,for calculating deformation

Where R_n is the design compressive strength of the wall.

Coefficient "α" is found at the table below

Table 5: Coefficient "α" for masonry wall [KTP-9-78, 1978]

Type of wall	**Mortar class kg/cm2**			
	100-50	25	4	0
Clay bricks and concrete blocks	1000	750	500	350
Clay bricks with vertical holes	2000	1500	1000	-
Clay brick with horizontal holes	1500	1000	750	-

Seismic evaluation is done by considering the equivalent earthquake force in KTP is evaluated by the formula: $E = Q_k * k_c * \beta * m_k$ (3)

Q_k- weight of building β - dynamic coefficient k_c-seismic coefficient

m_k- behaviour factor $Q_k = G + 0.8P$ (4)

$\beta = \frac{0.9}{T}$ $0.65<\beta_i<2$ where $T = 0.045 n_{stories}$ (5)

$k_c = 0.025$ when intensity scale VII

$k_c = 0.05$ when intensity scale VIII (6)

$k_c = 0.1$ when intensity scale IX

Behaviour factor m_k is a coefficient that depends on the form of deformation while $X_{(xk)}$ and $X_{(xj)}$ are the displacements in the k point and all j points correspondent to the response of all masses in the system. $m_k = \frac{X_{(xk)} * \sum_j^n QX_{(xj)}}{\sum_j^n Q_j * X_{xj}{}^2}$ (7)

2.1.2 KTP 9 - 89 Masonry design code

Seismic force was evaluated: $E_{ki} = K_E * K_r * \psi * \beta_i * \eta_{ki} * Q_k$ (8)

Q_k- vertical force of construction which is sum of 0.9 weight of construction, 0.4 loads with short duration, 0.8 load with long duration. Interim load is multiplied by

$\eta = 0.3 + \frac{0.6}{\sqrt{n}}$ (9)

$\eta_{ki} = \frac{3k}{2n+1}$ (10) coefficient floor distribution

n- floors number k - floor number from bottom n - number of floors

K_E- seismic coefficient K_r- importance factor

ψ- coefficient for elasto-plastic work β_i- dynamic coefficient

$T_i = 0.045 n_{floors}$ (period of free vibrance) (11)

$\beta_i = 0.8/T \quad 0.65<\beta_i<2 \qquad (12)$

Spectral acceleration as follows: $S_a = K_E * K_r * \psi * \beta_i * g \qquad (13)$

Table 6: Values of structural coefficient [KTP-N2-89, 1989]

Description of building	Structural coefficient ψ
Construction with reinforced concrete (frames combined with vertical walls)	0.28
Construction with reinforced concrete walls	0.3
Building with unreinforced masonry walls	0.45
Building with reinforced masonry walls	0.38

$\beta_i = 0.7/T \quad 0.65<\beta_i<2.3$ for first soil category

$\beta_i = 0.8/T \quad 0.65<\beta_i<2$ for second soil category (14)

$\beta_i = 1.1/T \quad 0.65<\beta_i<1.7$ for third soil category

Table 7: Value of importance factor K_r [KTP-N2-89, 1989]

Category	Description of building	Importance factor
I	Extraordinary importance	1.5 - 4
II	Special importance	1.2 - 1.5
III	Normal importance	1
IV	Secondary importance	0.5
V	Temporary	0

Table 8:Value of seismic coefficient K_E [KTP-N2-89, 1989]

Category of soil	Seismic intensity		
	VII	VIII	IX
I	0.08	0.16	0.27
II	0.11	0.22	0.36
III	0.14	0.26	0.42

2.1.3 Eurocode 6 and 8

EN-1996 is the basic code of construction for masonry structures used in EU.[EN 1996-1] The Albanian Code has significant changes and deficiencies compared to EN-1996.

The characteristic compressive strength of unreinforced masonry made with general purpose mortar, with all joints to be considered as filled can be calculated:

$f_k = k * f_b^{0,65} * f_m^{0.25}$ (15) f_b - brick strength f_m - mortar strength

Table 9: Value of k factor [EN 1996-1, 2005]

k=0.6	Solid bricks	**k=0.5**	More than 1 brick width
k=0.55	Rectangular vertical holes on brick	k=0.45	More than 1 brick width
k=0.5	Circular vertical holes on bricks	k=0.4	More than 1 brick width

Characteristic shear strength of masonry may be given by tests calculated (lower value)

$f_{vk} = f_{vk0} + 0.4 * \sigma_d$ (16) or $f_{vk} = 0.065 * f_b$ (17) where:

f_{vk0} - mortar brick cohesion σ_d - vertical stress or as below:

Table 10: Shear strength of masonry (part of table) [EN 1996-1, 2005]

Masonry Unit	Mortar	f_{vk0}	f_{vk} (lower limit)
Solid clay bricks (group 1)	M10 - M20	0.3	1.7
	M2.5-M9	0.2	1.5
	M1-M2	0.1	1.2

The short term secant modulus of elasticity is taken: $E = 1000 * f_k$ (18)

When calculating structure in serviceability limit state $E = 600 * f_k$ (19)

The shear modulus G is taken 40% of the elastic modulus E.

Possible construction inclination is limited to: $\nu = \frac{1}{100 * \sqrt{h_{tot}}}$ (20)

EN-1998 specifies general rules for seismic design of structures.[2] Although it does not mention in detail masonry seismic design there are some recommendations to be considered like the compressive strength limits. The minimum masonry compressive strength is: - normal to bed face (vertical) - $f_{b,min} = 5MPa$

-parallel to bed face (horizontal) - $f_{b,min} = 2MPa$

The seismic load depends on the ground acceleration and on the type of the soil. The classification of the soil depends on the ground type acceleration and on the type of the soil. The classification of the soil is given in the table below:

Table 11: Ground categories [EN 1998-1, 2004]

Ground type	Description	Parameters		
		$v_{s,30}$ (m/s)	NSPT (blow/30cm)	C_u (kPa)
A	Rock or other rock like geological formation, including at most 5m of weaker material of the surface	>800	-	-
B	Deposits of very dense sand, gravel, or very stiff clay, at least several tens of meters in thickness, characterised by a gradual increase of mechanical properties with depth.	360-800	>50	>250
C	Deep deposits of dense or medium dense sand, gravel or stiff clay with thickness from several tens of hundreds of meters.	180-360	15-50	70-250
D	Deposits of loose to medium cohesion-less soil (with or without some soft), or of predominantly soft to firm cohesive soil	<180	<15	<70
E	A soil profile consisting of a surface alluvium layer with vs values of type C or D and thickness varying between about 5m and 20m, underlain by stiffer material with vs > 800m/s			
S1	Deposits consisting, or containing a layer at least 10 m thick, of soft clays/silts with a high plasticity index (PI>40) and high water content	<100	-	10-20
S2	Deposits of liquefiable soils, of sensitive clays, or any other soil profile not included in types A-E or S1			

The seismic action is represented by the response spectrum defined in EN 1998-1.

There are two types of response spectrums according to EN 1998-1 in basis of magnitude:

Type 1 - is used when expected magnitudes M > 5.5

Type 2 - is used when expected magnitudes M < 5.5

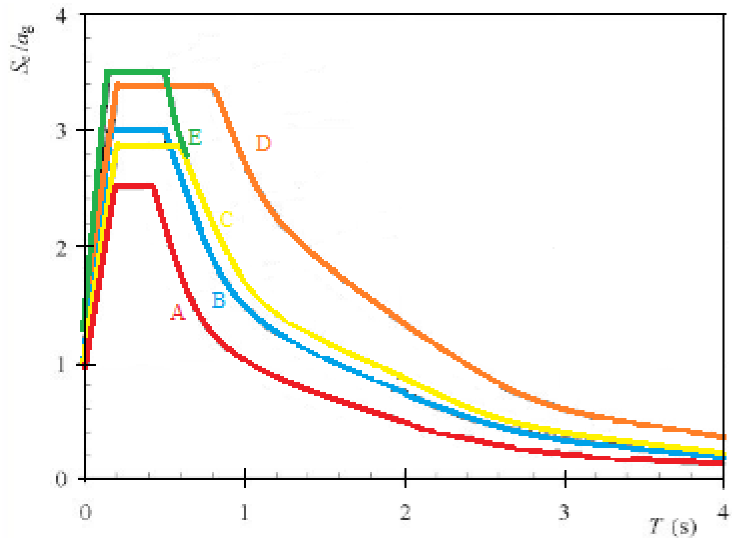

Figure 1: Type 1 elastic response spectra for ground types A-E

Table 12:Values of parameters describing the response spectra [EN 1998-1, 2004]

Ground type	**S**	**$T_B(s)$**	**$T_C(s)$**	**$T_D(s)$**
A	1.0	0.15	0.4	2.0
B	1.2	0.15	0.5	2.0
C	1.15	0.2	0.6	2.0
D	1.35	0.2	0.8	2.0
E	1.4	0.15	0.5	2.0

The behaviour factor "q" is given in the table below.

Table 13: Behaviour factor for masonry [EN 1998-1, 2004]

Type of construction	**q**
Unreinforced masonry in accordance with EN 1996 alone (recommended only for low seismicity cases)	1.5
Unreinforced masonry in accordance with EN 1998-1	1.5 - 2.5
Confined masonry	2.0 - 3.0
Reinforced masonry	2.5 - 3.0

With the above values and the peak ground acceleration "ag" is calculated the design response spectrum using the following relationships:

$$0 \le T \le T_B \qquad S_D(T) = a_g * S * \left[\frac{2}{3} + \frac{T}{T_B}\left(\frac{2.5}{q} - \frac{2}{3}\right)\right]$$

$$T_B \le T \le T_C \qquad S_D(T) = a_g * S * \frac{2.5}{q}$$

$$T_C \le T \le T_D \qquad S_D(T) = \begin{cases} = a_g * S * \frac{2.5}{q} * \frac{T_C}{T} \\ \ge \beta * a_g \end{cases} \tag{21}$$

$$T \ge T_D \qquad S_D(T) = \begin{cases} = a_g * S * \frac{2.5}{q} * \frac{T_C * T_D}{T^2} \\ \ge \beta * a_g \end{cases}$$

2.1.4 Seismic demand in acceleration-displacement format

The inelastic acceleration spectrum should be converted in acceleration-displacement format to proper compare it with the building capacity in the same format. For an elastic SDOF sytem the relationship is as follows:

$$S_{de} = \frac{T^2}{4\pi^2} S_{ae} \tag{22}$$

where: S_{ae} – elastic acceleration

S_{de} – displacement spectrum

A typical smooth elastic acceleration spectrum for 5% damping, normalized to a peak ground acceleration of 1.0g, and the corresponding elastic displacement spectrum, are shown in the figure below:

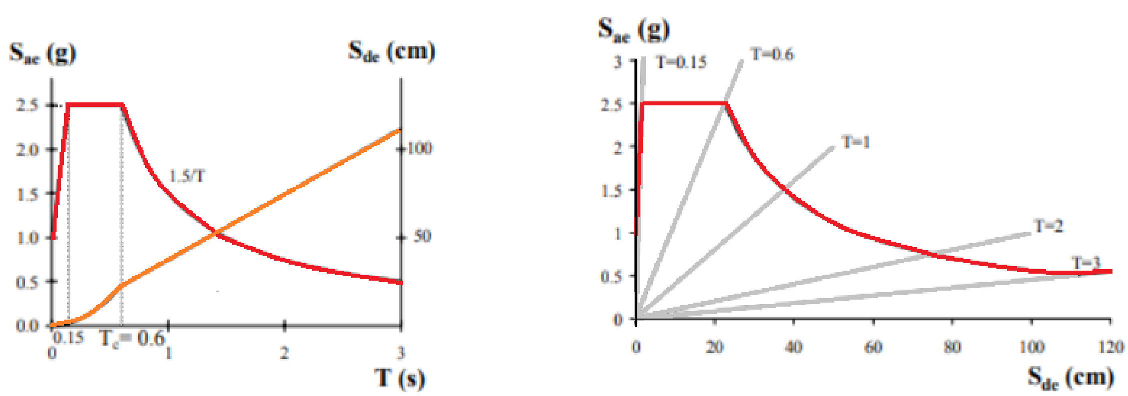

Figure 2: Typical elastic acceleration (S_{ae}) and displacement spectrum (S_{de}) for 5% damping normalized to 1.0g peak ground acceleration: traditional and acc-disp format [Fajfar P.et. al., 2000]

Vidic et.al. ,1994 gives the following relationship between spectrum acceleration (S_a) and the displacement spectrum (S_d): $S_a = \frac{S_{ae}}{R_\mu}$ (23)

$$S_d = \frac{\mu}{R_\mu} S_{de} = \frac{\mu}{R_\mu} \frac{T^2}{4\pi^2} S_{ae} = \mu \frac{T^2}{4\pi^2} S_a \qquad (24)$$

μ is the ductility factor defined as the ratio between te maximum displacement and the yield displacement, and R_μ is the the reduction factor due to ductility, from the hysteric energy dissipation of ductile structures. In the N2 method, the use of the bilinear spectrum takes in consideration the reduction factor:

$$R_\mu = (\mu - 1)\frac{T}{T_C} + 1 \qquad T < T_C \qquad (25)$$

$$R_\mu = \mu \qquad T \geq T_C \qquad (26)$$

T_C is the characteristic period of the ground motion.

This equations (25) ad (26) are a simple version of the formualae proposed by Vidic et.al. (1994). [Vidic et.al. ,1994] Starting from the elastic design spectrum shown in figure 1, using equations 2 and 5 the demand spectra in acc-disp format is obtained and shown in figure 2.

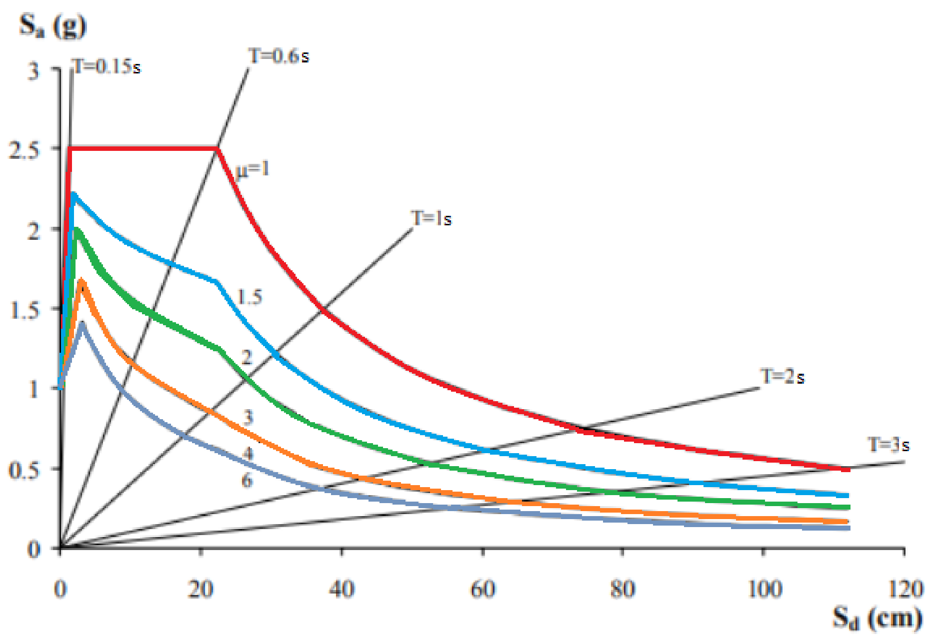

Figure 3: Demand spectra for constant ductilities on Sa-Sd format normalized to 1.0g p.g.a. [Fajfar P.et. al., 2000]

2.1.5 Code comparison

As was highlighted before, KTP-78 and KTP-89, have serious deficiency and take lower seismic consideration to EC. To show this deficiency, below are shown the results for the seismic consideration in a five story building. The base shear force for weight is calculated by taking in consideration all the three codes. In the figure below are shown the plan and facade of the template building. The first and second story have a width of 38cm, while others of 25cm. The building is supposed to be in a soil of mid conditions, category B according KTP or category C for EC-8. The seismic intensity of the zone is supposed VII MM for KTP and ag/g=15% for EC-8. The calculations are shown in appendix section.

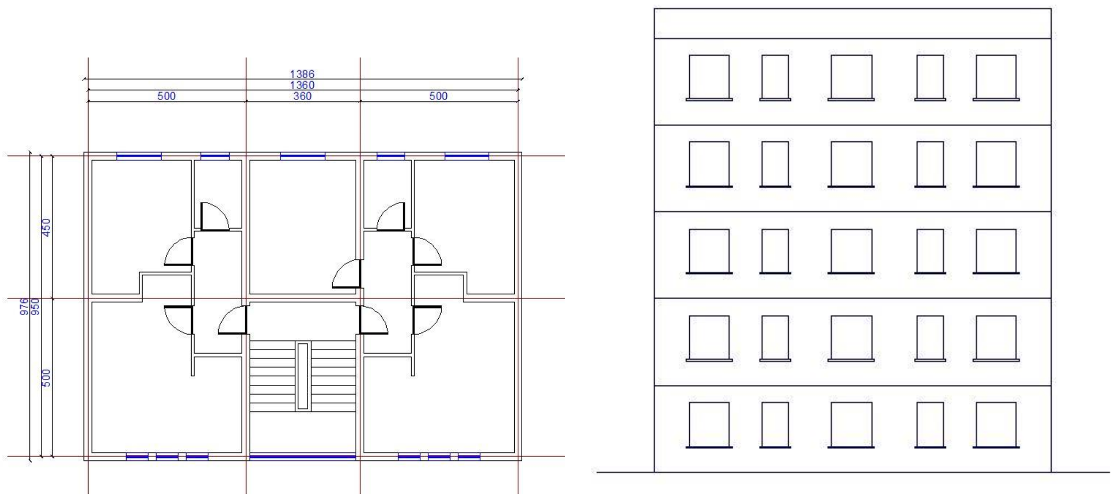

Figure 4: Template building taken in consideration

As can be seen, the difference in value between KTP-89 and EC-8 is almost half the seismic force. In the table below are compared the buildings of different era and code seismic characteristics. [KTP-N2-89, 1989; EN 1998-1, 2004]

Table 14: Characteristics of calculations and projection of buildings of different era

Period of construction	**Before 1963**	**1963-1978**	**1978-1990**	**After 1990**	
Building code	KTP-1952	KTP-1963	KTP-1978	KTP-1989	EN-1998
Code Characteristics	great deficiency	very low seismic demand	Low seismic demand	Acceptable seismic demand	High seismic demand
Seismic force consideration	Not known at time	Seismic demand was taken in consideration	$E = Q_k * k_c * \beta * m_k$	$E_{ki} = K_E * K_r * \psi * \beta_i * \eta_{ki} * Q_k$	$E_{ki} = a_g * S * \left[\frac{2.5}{q}\right] * Q_k$
Natural Period		by giving recommenda-tions for different structures	$T = 0.045n_{st} = 0.225s$	$T = 0.045n_{st} = 0.225s$	$T = 0.045n_{st} = 0.225s$
Seismic coefficient			$k_C = 0.1$	$k_E = 0.36$	$a_g = 0.15$
Dynamic coefficient			$\beta = \frac{0.9}{T}$ $\beta = 2$	$\beta = \frac{0.8}{T}$ $\beta = 2$	$T_B < T < T_c$ $T_B = 0.2$ $T_C = 0.6$
Behaviour factor			$m_k = 0.45$	$\psi = 0.45$	$q = 2.5$
Weight of structure			$G + 0.8P$	$0.9G + 0.8P$	$G + 0.3P$
Seismic force calculated			$246.3kN$	$730.8kN$	$1483.4kN$

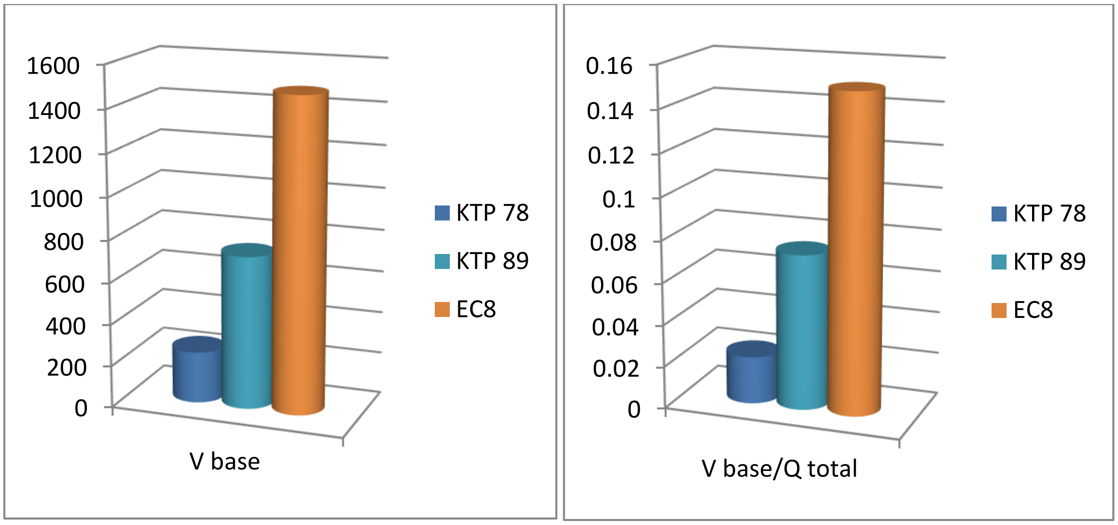

Figure 5: Changes of seismic demand among different design codes

2.2 Earthquake ground motion, seismiz hazard and seismic zonation

2.2.1 Earthquake ground motion

An earthquake is manifested as ground shaking caused by the sudden release of energy in the Earth's crust. Earthquake occurence is explanied by the theory of large-scale tectonic plate movement. When two ground masses move to one another, elastic strain energy due to tectonic process is stored and then released through the rupture of the interface zone. This energy travels in form of seismic waves from the epicentre zone to the building in surface, where it is felt as a shaking. [Elnashi A.S. et.al., 2003] The shaking felt is generally a combination of these waves. There are many types of seismic waves that are generated during this process, but the most important are the longitudinal or primary waves and tranverse or secondary waves. Primary waves causes alternate push or compression and tensile stresses between the soil during their travel, meanwihle secondary waves causes vertical and horizontal side to side motion during their travel causing shear stresses. The longditunal waves travel faster around 50-60% of the speed of tranverse waves. This two types longditunal and tranverse waves are also called body waves. The other types are surface waves such as Love waves and Rayleigh waves and they are generated by the constructive interference of body waves travelling paralel to the ground surface and underlying boundaries. The combination of this waves hits the structure and the lateral and vertical components are measured and affect the performance of the building. This waves are measured using seismographs and for each component are given the displacent, velocity and acceleration to time. In the figure below are shown the seismograms from 26 Novemember 2019 earthquake, on Tirana station. [IGJEUM, 2020]

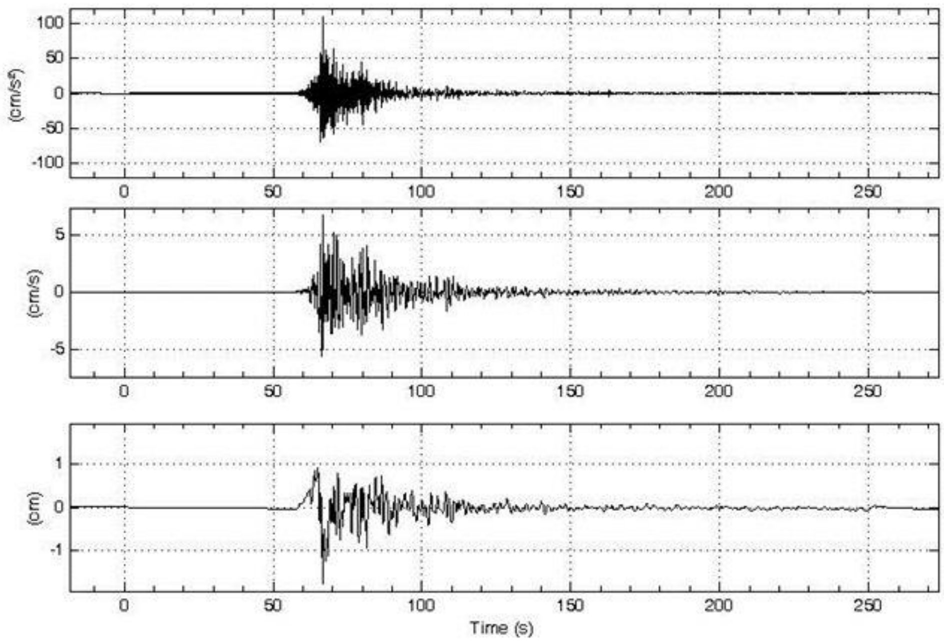

Fig 6. November 26, 2019 Earthquake N-S component [IGJEUM, 2020]

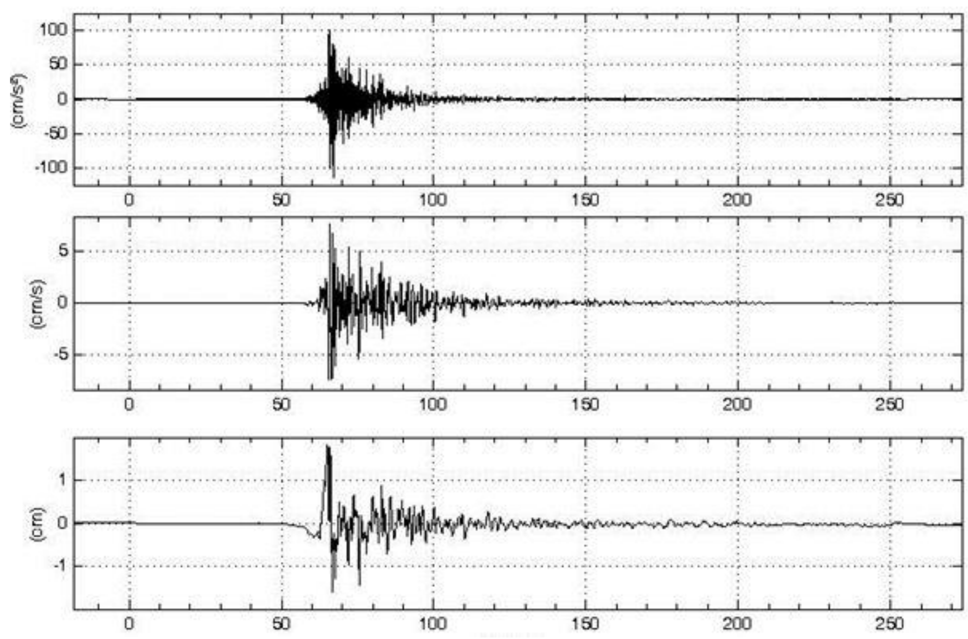

Fig 7. November 26, 2019 Earthquake E-W component [IGJEUM, 2020]

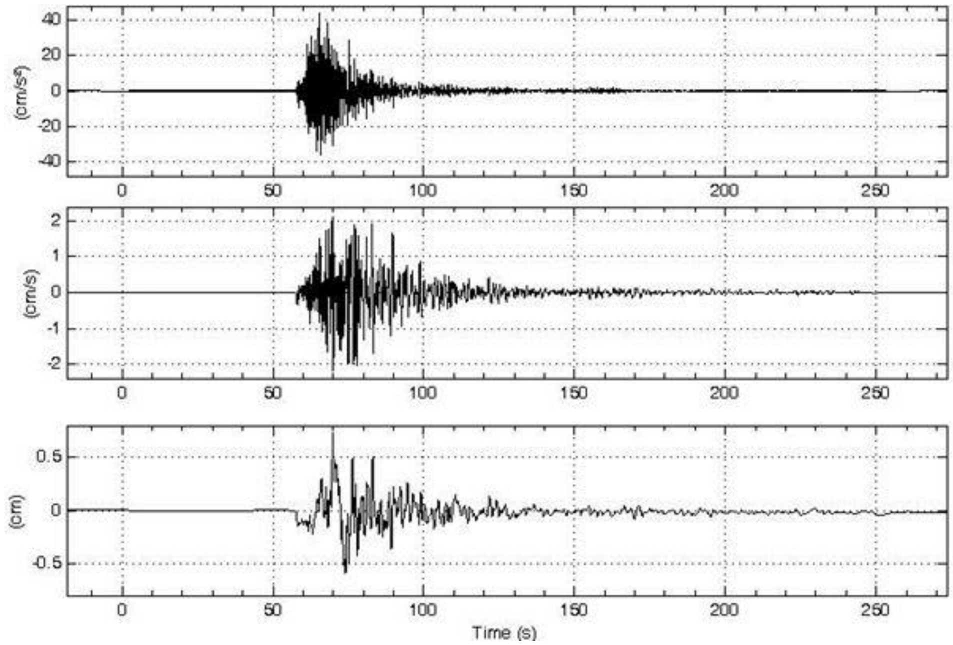

Fig 8. November 26, 2019 Earthquake Z- component [IGJEUM, 2020]

2.2.2 Earthquake measuring parameters

The earthquakes have various defining parameters, among those the most important are:

-Intensity, is a qualitative measure wich is a non-instrumental perceptibility measure of damage to structures, ground surface effects and human reaction to earthquake shaking. The scale used in Europe is the Modified Mercalli scale with 12 levels of intensity. In Albanian teritorry the expected maximum intensity is around IX for strong ground motion

-Magnitude, is a quantitative measure of earthquake size and fault dimensions. The Rihter scale is mostly used in Europe and Albania, wich compares the ampiltude of the earthquake with the standard earthquake considered as of magnitude Mw=1. The strongest recorded earthquake in Albanian terittory was of M=6.9 near Shkodra

-Epicentral depth, wich measures the depth of the epicentre of earthquake. This parameter is very important because near fault earthquakes affect more the buildings comparing to far fault earthquakes.

-Peak ground acceleration, which reffers to the ampiltude of acceleration during the strong motion sequence. These values are very important because the determination of the limit states is based on this parameter.

-Return period, wich refers to the amount of time that the earthquake with the given magnitude has a probability to hit the seismic zone. In EC-8 [EN 1998-1, 2004] very important are the expected earthquakes with a return period of 95 years and 475 years, wich are used for the limit state design

2.2.3 Seismicity of Albania

Albania is a country of moderate seismic hazard. Taking place on the Alpine-Mediterranean seismic plate, in the region historically have occurred high intensity earthquakes. The seismicity of Albania is characterised from an intensive seismic micro-activity (1.0<M<3.0), from many small earthquakes (3.0<M<5.0), rare medium-sized earthquakes (5.0<M<7.0), and very rarely from strong earthquakes (M>7.0).

Table 15: Major earthquakes in Albania

Date	**Area affected**	**Mw**	**Depth (km)**	**Casualities**	
				Dead	Injured
26.11.2019	Durres	6.4	20	52	3000+
21.09.2019	Durres	5.6	10	-	108
09.01.1988	Tirana	5.4	24	-	-
16.11.1982	Fier	5.6	22	1	12
15.04.1979	Shkoder	6.9	10	136	1000+
30.11.1967	Diber	6.6	20	12	174
18.03.1962	Fier	6.0	-	5	77
26.05.1960	Korce	6.4	-	7	127
01.09.1959	Fier	6.2	20	2	-
27.08.1942	Diber	6.0	33	43	110
21.11.1930	Vlore	6.0	35	30	100
26.11.1920	Tepelene	6.4	-	36	102
06.01.1905	Shkoder	6.6	-	200	500

First map of seismic zone intensity in Albania dates back to 1952 from the Science Institution and the ministry of the time. Since then it has been updated many times till the 1979 map, that is still the in law map for seismic evaluation. KTP-63 and KTP-78 are based on the map prior of 79s that has lower seismic consideration comparing to the updated values because of the lack of knowledge of the time. Several authors have studied this topic, like A.Fundo et.al., "Probabilistic seismic hazard assessment of Albania" Tirane (2012). [A.Fundo et.al., 2012] The strongest earthquake in Albania have occurred in North-West part in Shkodra. The earthquake of 01.06.1905 with magnitude Ms=6.6. The duration of the earthquake was 10-12 sec and caused big damage. There were completely destroyed about 1500 dwelling houses only in Shkodra, and all other buildings were heavily damaged. Also the walls of Shkodra caste were damaged and partly fallen. The earthquake of 15.04.1979 was one of the strongest earthquakes occurred in Balkan Penisula during 20th century. Its magnitude is evaluate 6.6 to 7.2. The epicentre of this earthquake is in the coastal area, near Petrovac, Montenegro. Many foreshocks occurred about two weeks before the main shock of 15 April, and the aftershocks continued for more than 9 months. A strong aftershock occurred on 24 May with magnitude Ms=6.3. [Sulstarova et.al., 2005] This earthquake was a major reason that lead to updates to the seismic code and seismic zonation map update. The today map is still based on the maximum intensity zonation, and not in peak ground acceleration, but different authors have worked on this topic. Another stong earthquake occured on Durres on 26.11.2019 with Ms=6.4. The epicentre was very near to the most populous and urban zone of Albania and casualities were very high. Especially old masonry buildings, in Thumane, Vore and Kombinat in Tirana, were highly damaged and some even collapsed. This earthquake and his casualitites will be studied in depth in this study and the results of all analysis will be compared with the real damage occured on buildings during this earthquake.

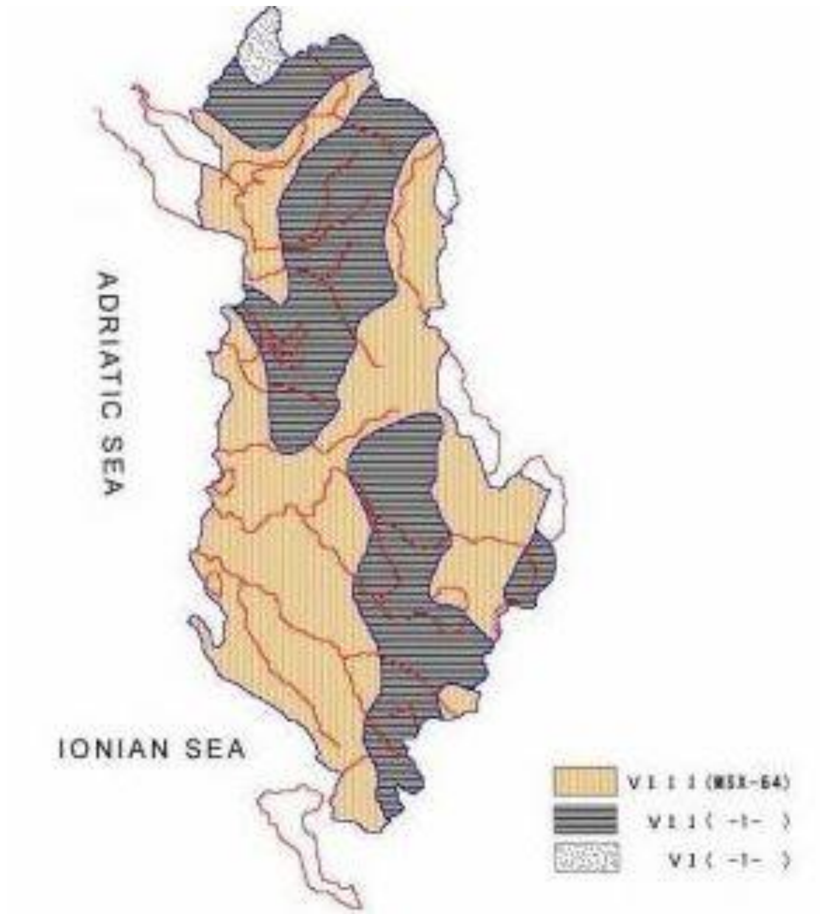

Figure 9: Map of seismic intensity zoning for Albania [KTP-9-78, 1978]

2.2.4 Probabilistic seismic hazard maps

The seismic source zones of Albania, characterised from evidences from earthquake catologues, active fault and present days tectonic regime, are the necessary main inputs for calculation of seismic hazard. [Sulstarova et.al., 2005] In Albania and in its surroundings, the following 9 seismic zones are defined:

1.Lezha-Ulqini (LU) zone 2.Peri-Adriatic Lowland (PL) zone

3.Ionian Coast (IC) zone 4.Korca-Ohrid (KO) zone

5.Elbasan-Diber-Tetova (EDT) zone 6.Kukes-Peshkopi (KP) zone

7.Shkodra-Tropoja (ST) zone 8.Peja-Prizreni (PP) zone

9.Skopje (Sk) zone

The catalogue of Albanian earthquakes used includes earthquakes with magnitude Ms>4.5 that occurred in the region between 39.0° N and 43.0° N and 18.5°E and 21.5°E between years 58 and 2005. [Sulstarova et.al., 2005] The best estimates of maximum magnitude are made by considering the largest earthquakes known from similar tectonic environments. All this data input are analysed using probabilistic approach and proper attenuation method in order to obtain the Probabilistic Hazard Map of Albania.

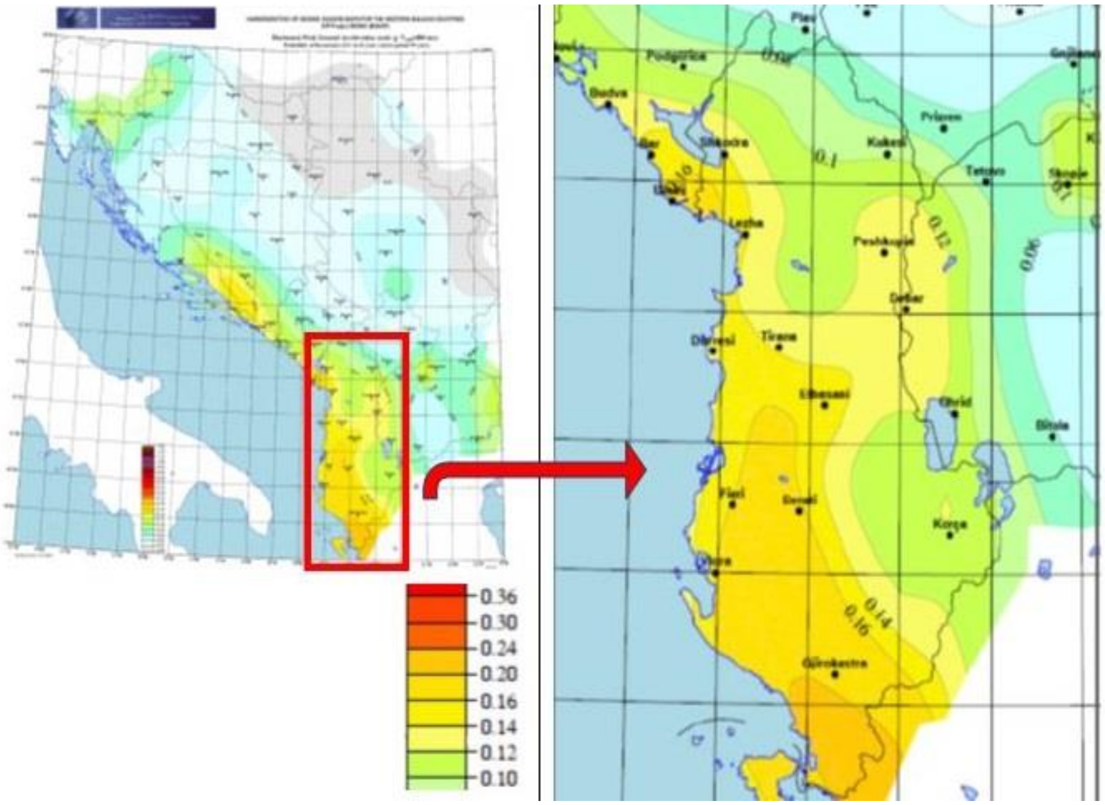

Figure 10: Probabilistic seismic hazard map for horizontal PGA, with the return period of 95 years, for hard rock conditions ($V_{s30} \geq 800$ m/sec). [NATO SfP Project No. 983054, 2008]

The seismic zonation map of Albania is based on the intensity values, also because Albania KTP-89 calculations are based on this parameter. But later codes like EC-6 and EC-8 and other worldwide accepted codes are based on the peak ground acceleration values. Probabilistic seismic hazard map for horizontal PGA are calculated with probabilistic methods and are given for different return periods. For an earthquake with peak ground acceleration within the extents of the map with the return period of 95 years, the building should perform in DL state. Meanwhile for an earthquake with peak ground acceleration within the extents of the return period of 475 years, buildings should perform in SD state. the seismic hazard maps for horizontal PGA, with the return period of 95 and 475 years, respectively, are shown for hard rock conditions (Fig 8-9).

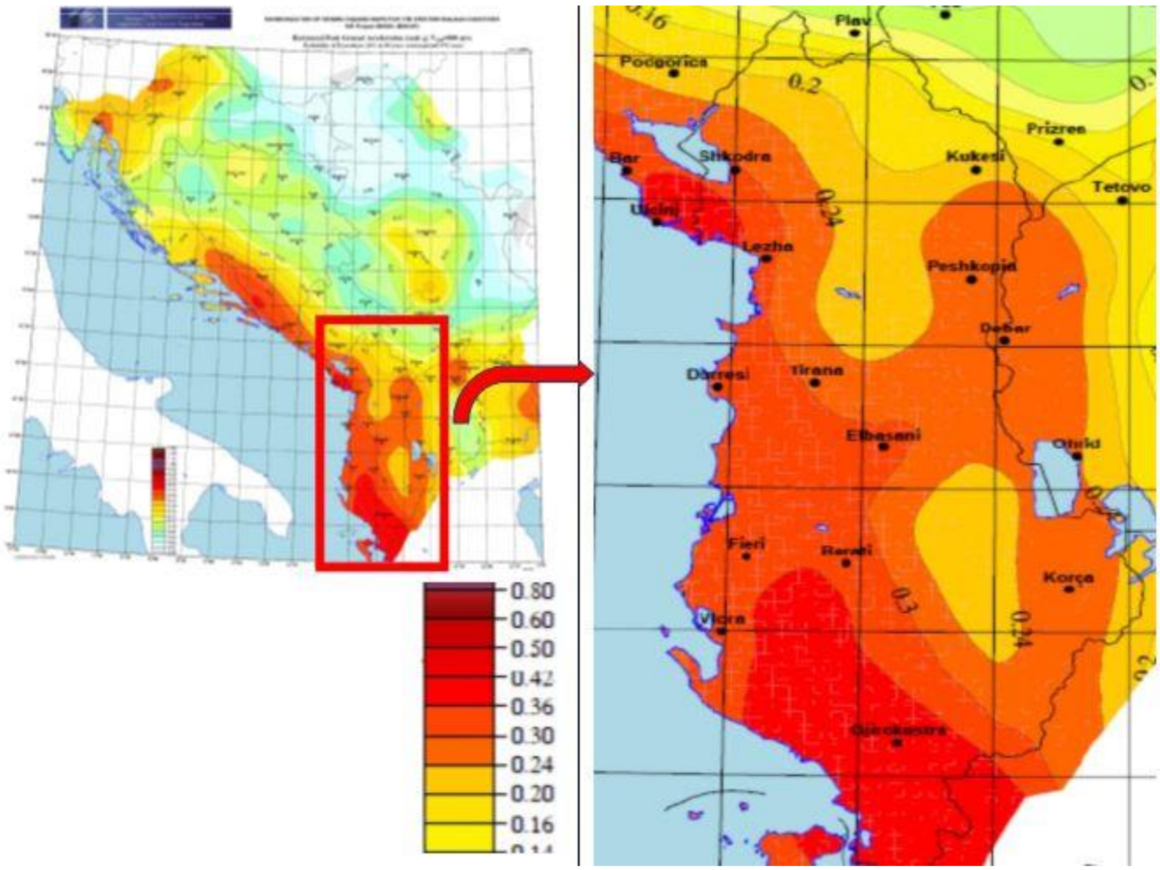

Figure 11: Probabilistic seismic hazard map for horizontal PGA, with the return period of 475 years, for hard rock conditions ($V_{s30} \geq 800$ m/sec). [NATO SfP Project No. 983054, 2008]

As can be seen from the maps below in many cities with a high population of masonry buildings such as Durres, Shkodra, Elbasan, Tirane,Vlora the expected peak ground acceleration for an earthquake with return period of 95 years is around 20%g, meanwhile for an earthquake with return period of 475 years is around (30-40)%g. If this values are compared with the values of 26 November 2019 earthquake, in most of the zones this values are near the values of 95 years of return period.

2.2.5 Earthquake ground motion records used in the dynamic analysis

In nonlinear response history analyses, the selection of acceleration records is an important step because the use of acceleration records with same features can exaggerate or underestimate the building response. Past earthquake reconnaissance team reports and the evidence of the observed structural damage and collapses have shown that damage to structures is increased under near field ground motions. In terms of the difference between the absolute and relative energy input to structural systems, near field records have more significant effect than far-field records. [Kalkan E. et.al, 2007] Many authors have studied this topic, especially for reinforced concrete buildings. To comparatively investigate influence of the far- field and near-field earthquakes on the seismic response of the URM template designs, a total of 78 near-fault and 68 far-fault ground motions recorded on dense-to-firm soil sites are used for seismic performance evaluation of the considered buildings. The tables below list major attributes of records considered in this study.

Table 16: List of near fault earthquakes taken in consideration for time history analysis

No	Year	Earthquake	M_w	Record and component	D (km)	Site	PGA (g)	PGV (cm/s)	PGD (cm)
1	1979	IMPERIAL VALLEY	6.5	CHIHUAHUA, 012 (UNAM/UCSD STATION 6621)	-		0.27	24.85	9.13
2	1979	IMPERIAL VALLEY	6.5	CHIHUAHUA, 282 (UNAM/UCSD STATION 6621)	-		0.254	30.12	12.91
3	1979	IMPERIAL VALLEY	6.5	CHIHUAHUA, DWN (UNAM/UCSD STATION 6621)	-		0.218	5.13	1.28
4	1979	IMPERIAL VALLEY	6.5	EL CENTRO ARRAY #6, 140 (CDMG STATION 942)	1.00	D	0.41	64.83	27.57
5	1979	IMPERIAL VALLEY	6.5	EL CENTRO ARRAY #6, 230 (CDMG STATION 942)	1.00	D	0.439	109.80	65.82
6	1979	IMPERIAL VALLEY	6.5	EL CENTRO ARRAY #6, UP (CDMG STATION 942)	1.00	D	1.655	57.69	25.82
7	1979	IMPERIAL VALLEY	6.5	EL CENTRO ARRAY #7, 140 (USGS STATION 5028)	0.60	D	0.338	47.60	24.65

8	1979	IMPERIAL VALLEY	6.5	EL CENTRO ARRAY #7, 230 (USGS STATION 5028)	0.60	D	0.463	109.24	44.71
9	1979	IMPERIAL VALLEY	6.5	EL CENTRO ARRAY #7, UP (USGS STATION 5028)	0.60	D	0.544	26.37	9.32
10	1979	IMPERIAL VALLEY	6.5	BONDS CORNER, 140 (USGS STATION 5054)	2.50	D	0.084	3.61	0.34
11	1979	IMPERIAL VALLEY	6.5	BONDS CORNER, 230 (USGS STATION 5054)	2.50	D	0.1	8.18	1.42
12	1979	IMPERIAL VALLEY	6.5	BONDS CORNER, UP (USGS STATION 5054)	2.50	D	0.052	0.90	0.02
13	1980	IRPINIA EQ / ITALY	6.9	STURNO, 000	10.8	C	0.251	36.39	11.58
14	1980	IRPINIA EQ / ITALY	6.9	STURNO, 270	10.8	C	0.358	51.82	32.02
15	1980	IRPINIA EQ / ITALY	6.9	STURNO, UP	10.8	C	0.26	25.59	10.27
16	1985	NAHANNI, CANADA	6.8	SITE 1, 010	6.00	B	0.978	46.05	9.64
17	1985	NAHANNI, CANADA	6.8	SITE 1, 280	6.00	B	1.096	46.13	14.52
18	1985	NAHANNI, CANADA	6.8	SITE 1, UP	6.00	B	2.086	40.60	12.29
19	1985	NAHANNI, CANADA	6.8	SITE 2, 240	6.00	B	0.489	29.26	7.54
20	1985	NAHANNI, CANADA	6.8	SITE 2, 330	6.00	B	0.323	33.13	6.57
21	1987	SUPERSTITION HILLS	6.6	PTS, 225 (USGS STATION 5051)	0.70	D	0.455	112.00	52.83
22	1987	SUPERSTITION HILLS	6.6	PTS, 315 (USGS STATION 5051)	0.70	D	0.377	43.90	15.25
23	1989	LOMA PRIETA	6.9	BRAN, 000			0.481	55.74	11.69
24	1989	LOMA PRIETA	6.9	BRAN, 090			0.526	41.91	11.86

25	1989	LOMA PRIETA	6.9	BRAN, UP			0.505	16.28	9.14
26	1989	LOMA PRIETA	5.1	CORRALITOS, 000 (CDMG STATION 57007)	5.1	D	0.644	55.16	10.82
27	1989	LOMA PRIETA	5.1	CORRALITOS, 090 (CDMG STATION 57007)	5.1	D	0.479	45.50	11.29
28	1989	LOMA PRIETA	5.1	CORRALITOS, UP (CDMG STATION 57007)	5.1	D	0.455	17.70	7.11
29	1989	LOMA PRIETA	6.9	SARATOGA ALOHA AVE, 000 (CDMG STATION 58065)	4.1	C	0.512	51.15	16.24
30	1989	LOMA PRIETA	6.9	SARATOGA ALOHA AVE, 090 (CDMG STATION 58065)	4.1	C	0.324	42.61	27.61
31	1989	LOMA PRIETA	6.9	SARATOGA ALOHA AVE, UP (CDMG STATION 58065)	4.1	C	0.389	26.86	15.21
32	1992	ERZICAN / TURKEY	6.7	ERZICAN EAST-WEST COMP	4.4	D	0.496	64.30	21.92
33	1992	ERZICAN / TURKEY	6.7	ERZICAN - NORTH-SOUTH COMP	4.4	D	0.515	83.95	27.66
34	1992	ERZICAN / TURKEY	6.7	ERZICAN -UP COMP	4.4	D	0.248	18.38	7.55
35	1992	CAPE MENDOCINO	7.1	CAPE MENDOCINO, 000 (CDMG STATION 89005)	9.5	B	1.497	125.57	39.74
36	1992	CAPE MENDOCINO	7.1	CAPE MENDOCINO, 090 (CDMG STATION 89005)	9.5	B	1.039	41.33	12.18
37	1992	CAPE MENDOCINO	7.1	CAPE MENDOCINO, UP (CDMG STATION 89005)	9.5	B	0.754	63.08	110.3
38	1992	CAPE MENDOCINO	7.1	PETROLIA, 000 (CDMG STATION 89156)	9.5	B	0.59	48.32	21.97
39	1992	CAPE MENDOCINO	7.1	PETROLIA, 090 (CDMG STATION 89156)	9.5	B	0.662	90.08	29.01
40	1992	CAPE MENDOCINO	7.1	PETROLIA, UP (CDMG STATION 89156)	9.5	B	0.163	24.55	28.44

41	1992	LANDERS 6/28/92	7.3	LUCERNE, 260 (SCE STATION 24)	2.0	B	0.727	146.03	217.1
42	1992	LANDERS 6/28/92	7.3	LUCERNE, 345 (SCE STATION 24)	2.0	B	0.789	32.94	52.78
43	1992	LANDERS 6/28/92	7.3	LUCERNE, UP (SCE STATION 24)	2.0	B	0.818	46.08	22.23
44	1994	NORTHRIDGE	6.7	CA:LA;SEPULVEDA VA, BLD 40 GND; 270	9.5	D	0.749	78.10	13.39
45	1994	NORTHRIDGE	6.7	CA:LA;SEPULVEDA VA, BLD 40 GND; 360	9.5	D	0.934	76.15	17.39
46	1994	NORTHRIDGE	6.7	CA:LA;SEPULVEDA VA, BLD 40 GND; UP	9.5	D	0.454	25.16	10.88
47	1994	NORTHRIDGE	6.7	NORTHRIDGE - SATICOY, 090 (USC STATION 90003)	13.3	D	0.368	28.96	8.44
48	1994	NORTHRIDGE	6.7	NORTHRIDGE - SATICOY, 180 (USC STATION 90003)	13.3	D	0.477	61.46	22.07
49	1994	NORTHRIDGE	6.7	RINALDI RECEIVING STA, 228	8.6	D	0.825	160.33	29.62
50	1994	NORTHRIDGE	6.7	RINALDI RECEIVING STA, 318	8.6	D	0.487	74.54	26.96
51	1994	NORTHRIDGE	6.7	RINALDI RECEIVING STA, UP	8.6	D	0.834	44.04	10.06
52	1994	NORTHRIDGE	6.7	SYLMAR - HOSPITAL, 090 (CDMG STATION 24514)	6.4	D	0.604	78.37	16.82
53	1994	NORTHRIDGE	6.7	SYLMAR - HOSPITAL, 360 (CDMG STATION 24514)	6.4	D	0.843	130.40	31.96
54	1994	NORTHRIDGE	6.7	SYLMAR - HOSPITAL, UP (CDMG STATION 24514)	6.4	D	0.535	19.42	9.35
55	1999	KOCAELI / TURKEY	7.4	IZMIT, 090 (ERD)	4.3	B	0.22	29.78	17.13
56	1999	KOCAELI / TURKEY	7.4	IZMIT, 180 (ERD)	4.3	B	0.152	22.61	9.81
57	1999	KOCAELI / TURKEY	7.4	IZMIT, UP (ERD)	4.3	B	0.146	13.12	6.67

58	1999	KOCAELI / TURKEY	7.4	YARIMCA, 330 (KOERI)	3.3	D	0.349	62.16	50.98
59	1999	KOCAELI / TURKEY	7.4	YARIMCA, 060 (KOERI)	3.3	D	0.268	65.72	57.03
60	1999	KOCAELI / TURKEY	7.4	YARMICA, UP (KOERI)	3.3	D	0.242	30.81	29.56
61	1999	CHI-CHI 09/20/99	7.6	TCU065, E	2.5	D	0.814	126.18	92.59
62	1999	CHI-CHI 09/20/99	7.6	TCU065, N	2.5	D	0.603	78.79	60.75
63	1999	CHI-CHI 09/20/99	7.6	TCU065, V	2.5	D	0.272	77.05	53.71
64	1999	CHI-CHI 09/20/99	7.6	TCU067, E	1.1	D	0.503	79.58	93.12
65	1999	CHI-CHI 09/20/99	7.6	TCU067, N	1.1	D	0.325	66.70	45.96
66	1999	CHI-CHI 09/20/99	7.6	TCU067, V	1.1	D	0.225	42.70	28.49
67	1999	CHI-CHI 09/20/99	7.6	TCU084, E	11.4	C	1.157	114.74	31.44
68	1999	CHI-CHI 09/20/99	7.6	TCU084, N	11.4	C	0.417	45.58	21.27
69	1999	CHI-CHI 09/20/99	7.6	TCU084, V	11.4	C	0.34	25.30	11.94
70	1999	CHI-CHI 09/20/99	7.6	TCU102, E	1.2	D	0.298	112.45	89.2
71	1999	CHI-CHI 09/20/99	7.6	TCU102, N	1.2	D	0.169	77.16	44.88
72	1999	CHI-CHI 09/20/99	7.6	TCU102, V	1.2	D	0.189	56.21	48.75
73	1999	DUZCE 11/12/99	7.4	DUZCE, 180 (ERD)	11.0	D	0.348	59.97	42.11
74	1999	DUZCE 11/12/99	7.4	DUZCE, 270 (ERD)	11.0	D	0.535	83.49	51.62

75	1999	DUZCE 11/12/99	7.4	DUZCE, UP (ERD)	11.0	D	0.357	22.63	19.41
76	2002	ALASKA 11/03/02	7.9	PS10, 047	5.0	D	0.319	134.73	102.7
77	2002	ALASKA 11/03/02	7.9	PS10, 317	5.0	D	0.318	75.97	77.99
78	2002	ALASKA 11/03/02	7.9	PS10, UP	5.0	D	0.241	51.07	27.5

Table 17: List of far fault earthquakes taken in consideration for time history analysis

No	Year	Earthquake	M_w	Record and component	D (km)	Site	PGA (g)	PGV (cm/s)	PGD (cm)
1	1971	San Fernando 2/9/1971	6.6	LA HOLLYWOOD STOR LOT, 090 (USGS STATION 135)	62.2	C	0.21	18.93	12.42
2	1971	San Fernando 2/9/1971	6.6	LA HOLLYWOOD STOR LOT, 180 (USGS STATION 135)	62.2	C	0.174	14.87	6.32
3	1971	San Fernando 2/9/1971	6.6	LA HOLLYWOOD STOR LOT, UP (USGS STATION 135)	62.2	C	0.136	4.30	1.46
4	1976	Friuli, Italy 5/6/1976	6.5	Tolmezzo, 000	37.7	C	0.351	22.03	4.11
5	1976	Friuli, Italy 5/6/1976	6.5	Tolmezzo, 270	37.7	C	0.315	30.80	5.09
6	1976	Friuli, Italy 5/6/1976	6.5	Tolmezzo, UP	37.7	C	0.268	10.70	2.51
7	1979	Imperial valley 10/15/1979	6.9	DELTA, 262 (UNAM/UCSD STATION 6605)	43.6	D	0.238	26.00	11.99
8	1979	Imperial valley 10/15/1979	6.9	DELTA, 352 (UNAM/UCSD STATION 6605)	43.6	D	0.351	33.02	19.03
9	1979	Imperial valley 10/15/1979	6.9	DELTA, DWN (UNAM/UCSD STATION 6605)	43.6	D	0.145	14.79	8.57
10	1979	Imperial valley 10/15/1979	5.2	EL CENTRO ARRAY #11, 140 (USGS STATION 5058)	30.3	D	0.364	34.44	16.08

11	1979	Imperial valley 10/15/1979	5.2	EL CENTRO ARRAY #11, 230 (USGS STATION 5058)	30.3	D	0.38	42.14	18.63
12	1979	Imperial valley 10/15/1979	5.2	EL CENTRO ARRAY #11, UP (USGS STATION 5058)	30.3	D	0.14	11.09	6.8
13	1987	SuperstitionHills02 11/24/87	6.5	EL CENTRO IMP CO CENTER, 000 (CDMG STATION 01	18.5	B	0.358	46.36	17.53
14	1987	SuperstitionHills02 11/24/87	6.5	EL CENTRO IMP CO CENTER, 090 (CDMG STATION 01	18.5	B	0.258	40.87	20.1
15	1987	SuperstitionHills02 11/24/87	6.5	EL CENTRO IMP CO CENTER, UP (CDMG STATION 01	18.5	B	0.128	8.36	4.89
16	1987	SuperstitionHills02 11/24/87	6.5	POE, 270 (USGS STATION TEMP)	14.7	B	0.446	35.80	8.82
17	1987	SuperstitionHills02 11/24/87	6.5	POE, 360 (USGS STATION TEMP)	14.7	B	0.3	32.80	11.28
18	1989	LOMA PRIETA 10/18/89	7.1	CAPITOLA, 000 (CDMG STATION 47125)			0.529	35.01	9.13
19	1989	LOMA PRIETA 10/18/89	7.1	CAPITOLA, 090 (CDMG STATION 47125)			0.443	29.21	5.49
20	1989	LOMA PRIETA 10/18/89	7.1	CAPITOLA, UP (CDMG STATION 47125)			0.541	17.86	2.63
21	1989	LOMA PRIETA 10/18/89	7.1	GILROY ARRAY #3, 000 (CDMG STATION 47381)	14.4	D	0.555	35.69	8.26
22	1989	LOMA PRIETA 10/18/89	7.1	GILROY ARRAY #3, 090 (CDMG STATION 47381)	14.4	D	0.367	44.67	19.33
23	1989	LOMA PRIETA 10/18/89	7.1	GILROY ARRAY #3, UP (CDMG STATION 47381)	14.4	D	0.338	15.46	6.97
24	1992	CAPE MENDOCINO 04/25/92	7.0	RIO DELL OVERPASS FF, 360 (CDMG STATION 89324)	18.5	D	0.549	42.00	19.55
25	1992	CAPE MENDOCINO 04/25/92	7.0	RIO DELL OVERPASS FF, UP (CDMG STATION 89324)	18.5	D	0.195	10.54	7.02

26	1992	CAPE MENDOCINO 04/25/92	7.0	RIO DELL OVERPASS FF, 270	18.5	D	0.195	10.54	7.02
27	1992	LANDERS 7/23/92	7.3	COOLWATER, LN (SCE STATION 23)	69.2	C	0.283	25.64	13.71
28	1992	LANDERS 7/23/92	7.3	COOLWATER, TR (SCE STATION 23)	69.2	C	0.417	42.34	13.81
29	1992	LANDERS 7/23/92	7.3	COOLWATER, UP (SCE STATION 23)	69.2	C	0.174	9.95	4.01
30	1992	LANDERS 06/28/92	7.3	YERMO FIRE STATION, 270 (CDMG STATION 22074)	23.6	D	0.245	51.44	43.85
31	1992	LANDERS 06/28/92	7.3	YERMO FIRE STATION, 360 (CDMG STATION 22074)	23.6	D	0.152	29.71	24.63
32	1992	LANDERS 06/28/92	7.3	YERMO FIRE STATION, UP (CDMG STATION 22074)	23.6	D	0.136	12.96	4.98
33	1994	NORTHRIDGE EQ 1/17/94	6.7	BEVERLY HILLS - 12520 MULH, 035 (USC STATION 90014			0.617	40.86	8.57
34	1994	NORTHRIDGE EQ 1/17/94	6.7	BEVERLY HILLS - 12520 MULH, 125 (USC STATION 90014			0.444	30.19	4.83
35	1994	NORTHRIDGE EQ 1/17/94	6.7	BEVERLY HILLS - 12520 MULH, UP (USC STATION 90014)			0.314	14.01	1.31
36	1994	NORTHRIDGE EQ 1/17/94	6.7	BEVERLY HILLS - 14145 MULH, 009 (USC STATION 90013	19.6	C	0.416	58.94	13.15
37	1994	NORTHRIDGE EQ 1/17/94	6.7	BEVERLY HILLS - 14145 MULH, 279 (USC STATION 90013	19.6	C	0.516	62.78	11.07
38	1994	NORTHRIDGE EQ 1/17/94	6.7	BEVERLY HILLS - 14145 MULH, UP (USC STATION 90013)	19.6	C	0.327	16.83	2.56
39	1994	NORTHRIDGE EQ 1/17/94	6.7	CANYON COUNTRY - W LOST CANYON, 000 (USC STATION 9	13.0	D	0.41	43.03	11.71
40	1994	NORTHRIDGE EQ 1/17/94	6.7	CANYON COUNTRY - W LOST CANYON, 270 (USC STATION 9	13.0	D	0.482	45.38	12.54

41	1994	NORTHRIDGE EQ 1/17/94	6.7	CANYON COUNTRY - W LOST CANYON, UP (USC STATION 90	13.0	D	0.318	20.32	5.18
42	1995	KOBE 01/16/95	6.9	NISHI-AKASHI, 000	22.5	D	0.509	37.29	9.53
43	1995	KOBE 01/16/95	6.9	NISHI-AKASHI, 090	22.5	D	0.503	36.67	11.26
44	1995	KOBE 01/16/95	6.9	NISHI-AKASHI, V	22.5	D	0.371	17.42	5.64
45	1995	KOBE 01/16/95	6.9	SHIN-OSAKA, 000	19.2	D	0.243	37.86	8.55
46	1995	KOBE 01/16/95	6.9	SHIN-OSAKA, 090	19.2	D	0.212	27.94	7.64
47	1995	KOBE 01/16/95	6.9	SHIN-OSAKA, V	19.2	D	0.06	6.39	2.16
48	1999	KOCAELI 08/17/99	7.4	ARCELIK, 000 (KOERI)	17.0	C	0.219	17.69	13.65
49	1999	KOCAELI 08/17/99	7.4	ARCELIK, 090 (KOERI)	17.0	C	0.15	39.55	35.58
50	1999	KOCAELI 08/17/99	7.4	ARCELIK, DWN (KOERI)	17.0	C	0.086	8.57	5.52
51	1999	KOCAELI 08/17/99	7.4	DUZCE, 180 (ERD)	17.1	D	0.312	58.88	44.13
52	1999	KOCAELI 08/17/99	7.4	DUZCE, 270 (ERD)	17.1	D	0.358	46.39	17.62
53	1999	KOCAELI 08/17/99	7.4	DUZCE, UP (ERD)	17.1	D	0.229	20.41	17.02
54	1999	CHI-CHI 09/20/99	7.6	CHY101, E	11.1	D	0.353	70.64	45.3
55	1999	CHI-CHI 09/20/99	7.6	CHY101, N	11.1	D	0.44	115.0 0	68.76
56	1999	CHI-CHI 09/20/99	7.6	CHY101, Vertical	11.1	D	0.165	27.99	19.73

57	1999	CHI-CHI 09/20/99	7.6	TCU045, E	26.0	C	0.474	36.70	50.68
58	1999	CHI-CHI 09/20/99	7.6	TCU045, N	26.0	C	0.512	39.09	14.35
59	1999	CHI-CHI 09/20/99	7.6	TCU045, Vertical	26.0	C	0.361	21.46	22.96
60	1999	DUZCE 11/12/99	7.1	BOLU, 000 (ERD)	12.0	D	0.728	56.49	23.07
61	1999	DUZCE 11/12/99	7.1	BOLU, 090 (ERD)	12.0	D	0.822	62.12	13.56
62	1999	DUZCE 11/12/99	7.1	BOLU, UP (ERD)	12.0	D	0.203	17.33	14.29
63	1990	IRAN_MANJIL 06/20/90	7.4	LONGITUDINAL COMP	74.0	-	0.515	43.26	14.92
64	1990	IRAN_MANJIL 06/20/90	7.4	TRANSVERSE COMP	74.0	-	0.496	55.55	20.83
65	1990	IRAN_MANJIL 06/20/90	7.4	VERTICAL COMP	74.0	-	0.538	44.79	26.17
66	1999	HECTOR MINE OCT 16, 1999	7.1	HEC, 000	22.0	-	0.266	28.58	22.54
67	1999	HECTOR MINE OCT 16, 1999	7.1	HEC, 090	22.0	-	0.337	41.75	13.96
68	1999	HECTOR MINE OCT 16, 1999	7.1	HEC, VER	22.0	-	0.15	12.08	6.92

2.2.6 Geotechnical characteristics of Albanian territory

A good paper on this topic was published by Aliaj Sh, (2000). [Aliaj Sh. et.al., 2000] The geotechnical map, compiled on a scale of 1:200000, divides its territory into three zones of natural slopes stability: stable terrains, relatively stable terrains and unsable terrain. Stable terrain cover about 56.5% of the country, relatively stable terrain covers about 33.6% and naturally unstable terrain covers about 9.8% of territory. Stable zones are composed of strong rocks represented by intrusive and effusive magmatic rocks, limestone's of different ages, dolomites,breccias and conglomeration of carbonate and siliceous cementation, metamorphic rocks and schists. The relatively stable terrains are made of conglomeratic rocks of the loma suite, effusive-sedimentary rocks, schistose rocks, sand schists, epavoric rocks and partly molasses of sands-conglomerates.The unstable terrains are made of various kind of schists, molassess and to a lesser extent, of sand-conglomerates.

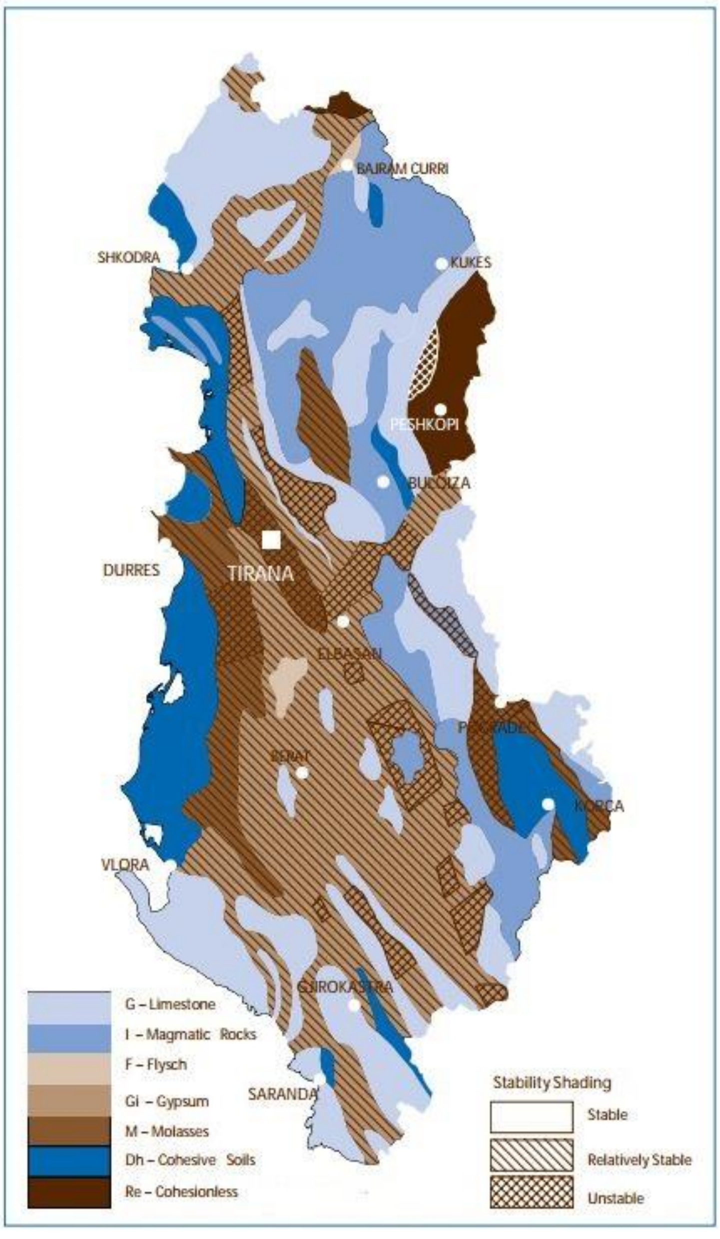

Figure 12: Geotechnical map of Albania [Aliaj Sh. et.al., 2000]

2.3 Basic failure mechanisms of masonry walls

2.3.1 In plane and out of plane response of masonry walls

For masonry structures and their response under gravity and seismic loads, many experiments have been done and many authors have reached to similar results. The basics of building codes, in the design of new structures are based on the concept of preventing the local brittle failue modes, wich are associated with out-of-plane response of the walls. If these brittle failure modes are prevented, a ductile global behaviour governed by the in-plane response of the wall develops, wich is far more acceptable to give solution to engineering problems. Details as given in section 2.1 give recommendation about requirements of values for the strength of units and mortar, effective connections between intersecting walls and between walls and diaphragms, requiring sufficient in-plane stiffness of diaphragms and limiting the minimum thickness and maximum slenderness of walls, in order to prevent the local brittle failure modes. [Sapmanpour A.H., 2017]

2.3.2 Basic failure mechanism of masonry walls

Different failure mechanisms are noted in masonry under different loading conditions. Also the fact that masonry is a isotropic material contributes in this variety. Compression failure is a very critic failure, because it develops very quickly and leads the entire wall or building to collapse.

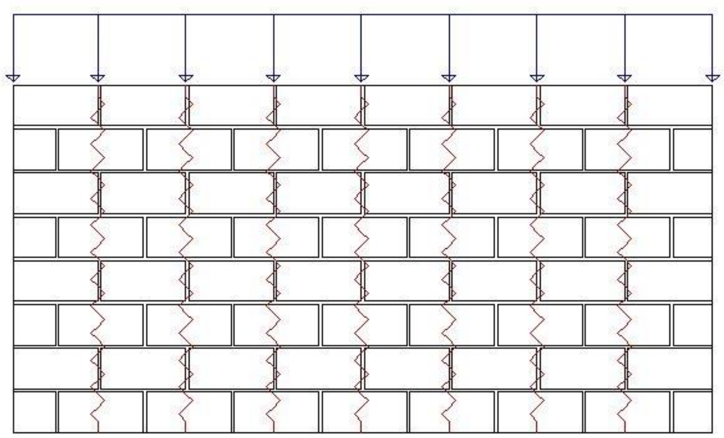

Figure 13: Compression failure of masonry

This type of failure is caused by overloading of masonry wall. The bricks start to break in the middle forming several columns inside the wall, till the wall entire collapses.

If the wall is properly designed according to code, this failure type should not happen.

The most common failure type in masonry structures is diagonal shear failure. The main cause of this failure type is the earthquake ground motion that produces horizontal inertia forces. These forces are transmitted through the slabs or any perpendicular walls. This failure is caused by principal tensile strength analogue to concrete walls, with the slight difference that the cracks follow the bricks faces.

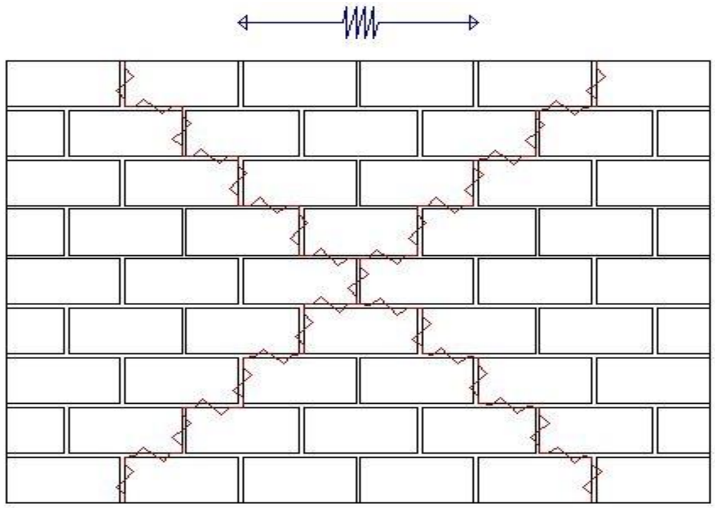

Figure 14: Shear failure of masonry

In this case of shear failure mode, the response of the wall is characterized by rapid streength and stiffness degradation, moderate energy dissipation and limited displacement capicity. [Sapmanpour A.H., 2017] In general this failure governs the in-plane response of URM walls subjected to seismic loads. Shear strength, is defined as the strength of masonry subjected to shear forces and is a combination of initial shear strength at zero compressive strength f_{vko} plus the design compressive stress perpendicular to shear. Several authors have conduted tests and made comparisons between different testing methods. The recommended values about shear strength are given in EC-8 [EN 1998-1, 2004] and Tomazevic equations [Tomazevic M., 1999].

2.3.3 Other types of failures

Another kind of failure is sliding failure of masonry. This kind of failure is not common, but can happen in some cases like in the figure. If the action that causes the failure is not lasting for a relatively long time, the structure does not reach collapse phase.

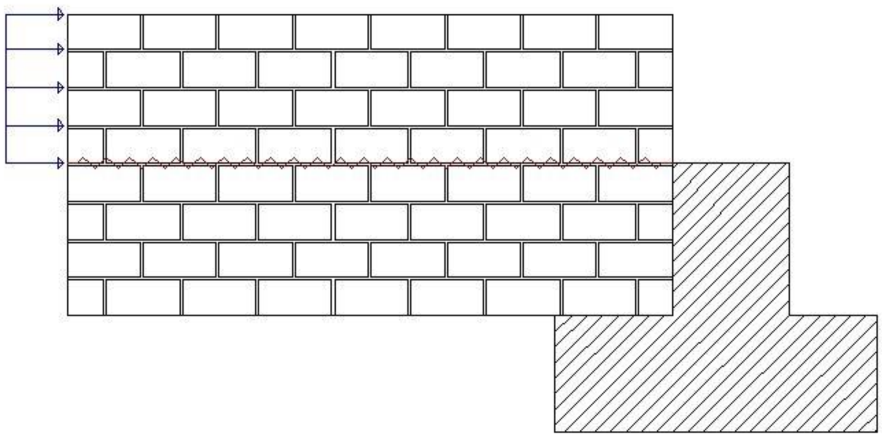

Figure 15:Sliding failure of masonry

The masonry has relatively small out of plane resistance. In the figure are shown bending situations that can be caused by eccentricity of the axial load applied. In reality small eccentricities cannot be avoided completely, but the wall has to be checked for stress limits at the most unfavourable places. Usually in seismic design this out of plane resistance is neglected. When applying the seismic force, walls are considered as membranes favouring the safety.

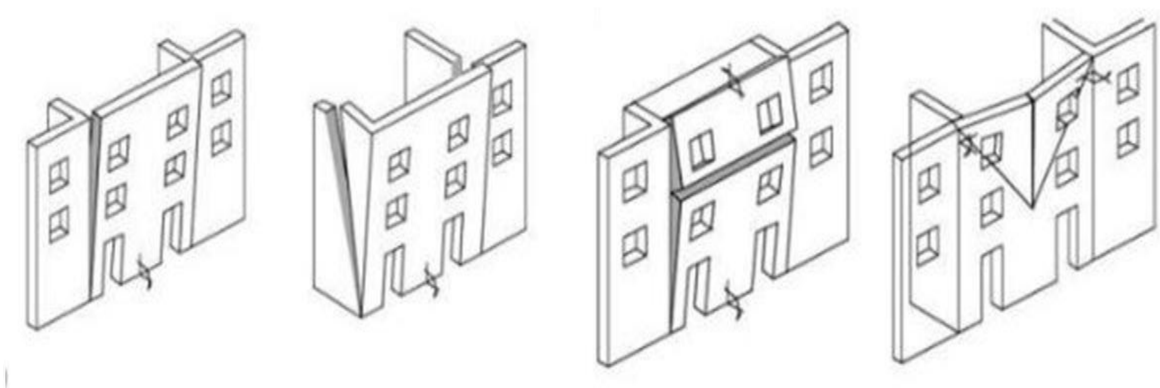

Figure 16: Out of plane failure of masonry [Salat Z., 2015]

Tensile flexural failure of masonry technically may happen at walls with small width/height ratio, which carry small static load. In this case horizontal force causes significant tensile forces at one side and compressive at the other. Considering that tensile forces at one side and compressive at the other. Considering that the tensile resistance is negligible the corresponding cracks happens first. Than after detaching a part from the left side the rest remaining contact has to carry the static load plus bending compressive stress. If the stress exceeds masonry compression limit value, than toe crushing is likely to happen.

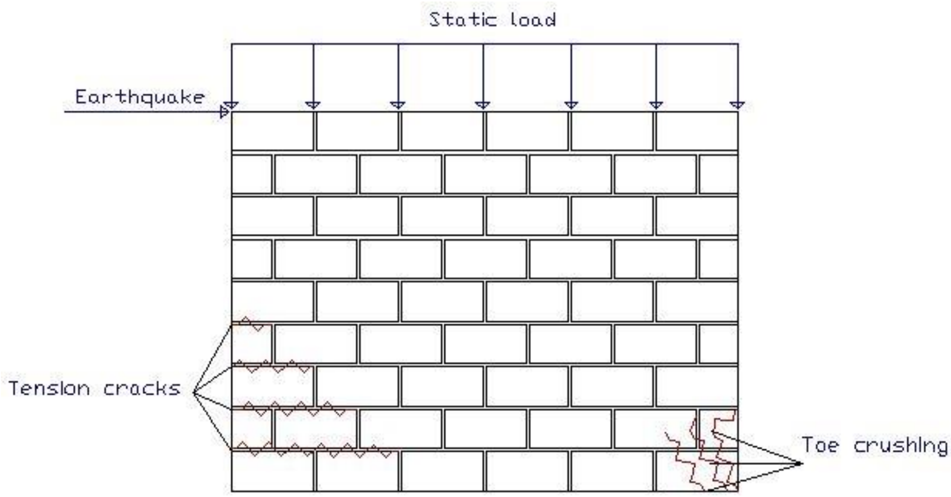

Figure 17: Flexural bending failure of masonry with (or without) toe crushing

2.4 Mechanical properties of masonry walls

Masonry is a typical composite construction material and its properties are defined by the properties of the raw materials, and the interaction between them. These material consists in masonry units, bonding material, concrete infill and reinforcing steel. Depending on how these materials are composed together in a structure, masonry is divided in subgroups: unreinforced masonry, confined masonry and reinforced masonry.Unreinforced masonry consist of masonry units (brick or stone) bonded with mortar. Most of the Albanian building stock are of unreinforced masonry. Confined masonry consist on masonry units, mortar and reinforcing steel. Some of the late buildings in the stock have this type used especially in seismic zones. Reinforced masonry, consists of masonry units, mortar, reinforcing steel and concrete infill. Because of its complexity, masonry and its constituent masonry should comply with specific requirements of standards and codes, especially when they are used for the construction of engineered structures, where the resistance of elements and the entire structure to gravity and seismic loads is verified by calculation. [Tomazevic M., 1999] The basic requirements of masonry materials are specified in EN1996 "Design of masonry structures" [EN 1996-1, 2005]. Additional requirements for masonry materials and construction system to be considered in seismic zones are given in EN1998 "Design provisions for earthquake resistance of structures" [EN 1998-1, 2004]

2.4.1 Brick and mortar characteristics

The basic characteristic of masonry units is the load bearing capacity. Apart from this there are some requirements when selecting the most suitable units like:

-adequate thermal and sound insulation capacity of masonry

-reduction of the weight of the building to reduce the seismic loads

-durability of units to breakage

-economy of construction

In some early buildings of the Albanian stock like the template of 40s, is used adobe and stone masonry. In the other buildings are used clay and silicate brick masonry. The clay bricks mostly used are of M-5 and M-7.5 and silicate bricks are of M-7.5 and M-10. Other bricks types are used like hollow bricks, but for non load bearing walls. Some late templates like the 1983s, have unreinforced masonry where the walls are with reinforced concrete columns at the corners of the building. As recommended byEN771 1-6 [EN771 1-6, 2004] the lowest mean values of compressive strength of masonry units to be used are:

-clay units minimum $f_b = 2.5\text{MPa}$

-calcium silicate units min $f_b = 5\text{MPa}$

-concrete aggregate units: min $f_b = 1.8\text{MPa}$

-autoclaved aerated units min $f_b = 1.8\text{MPa}$

-manufactured stone units $f_b = 15\text{MPa}$

Mortar is a mixture of inorganic binders (lime and/or cement), aggregates and water which binds together masonry units. For improving workability or other qualities are used additives. Different types of mortar are described as: [EN 1996-1, 2005]

-general purpose mortar, which is the traditional type of mortar used in joints with thickness greater than 3mm and in which only dense aggregate is used.
-thin layer mortar, which intended for use in masonry with thickness of joints 1-3mm.
-lightweight mortar made using expanded clay, expanded shale or other materials
The mortar compressive strength can be prescribed by the mixing ratios, or can be evaluated from compression tests.

Table 18: Typical strength of general purpose mortars [EN 1996-1, 2005]

Mortar type	Mean compressive strength	Approximate composition in parts of volume		
		Cement	Hydrated lime	Sand
M-2.5	2.5MPa	1	1.25-2.5	2.25 - 3 times cement and lime
M-5	5MPa	1	0.5-1.25	
M-10	10MPa	1	0.25-0.5	
M-20	20MPa	1	0-0.25	

According to EN1998 [EN 1998-1, 2004], for the unreinforced masonry and confined masonry, the minimum compressive strength $f_m = 5$MPa. In the building of Albanian stock this minimum is not respected because most of the buildings are realized with M2.5.

2.4.2 Masonry properties

When verifying the load-bearing capacity of masonry walls and structures to vertical and lateral loads, the values of mechanical properties of masonry are more important as an assemblage of units, than of the characteristics of the units themselves. But as we said these masonry properties are imposed by the material properties. In EC-6 [3] are defined the following characteristics, as the basics and recommends obtaining them by standard test methods of EN1052 [EN1052-1, EN1052-2, EN1052-3, EN1052-4 and EN1052-5]:

f_k - compressive strength of masonry
f_v - shear strength of masonry
f_x - flexural strength of masonry
$\sigma - \varepsilon$ - stress-strain relationship

In addition to mechanical characteristics specified by EN1996 [EN 1996-1, 2005], the following mechanical properties of masonry and masonry elements are also needed in numerical verification:

f_t - tensile strength of masonry, as an equivalent to f_v shear strength

E- modulus of elasticity G- shear modulus μ - ductility factor

2.4.3 Compressive strength fk

Different codes recommends testing procedures for determining the following properties. EN1052 [EN1052-1, 1998] for defining compressive strength determines testing procedure of masonry wallets or masonry walls. Wallets are at least 1.5 units length and 3 units height, or walls of 1.0-1.8m long and 2.4-2.7m high. The specimens are tested in compressing machine and are tested at least 3 specimens.

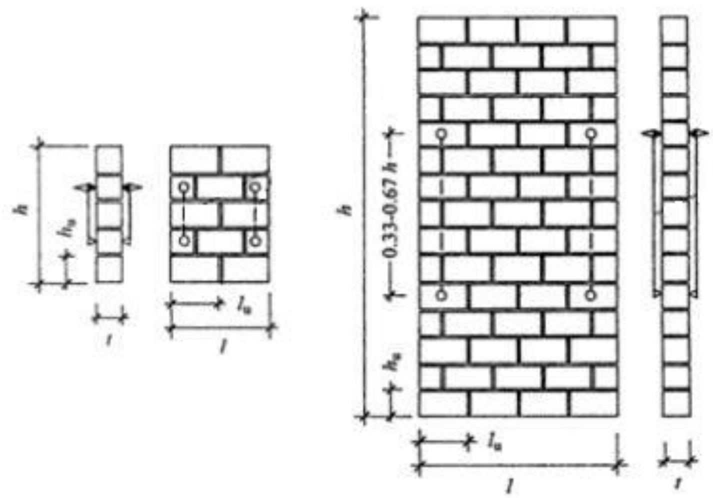

Figure 18: Testing specimens of compressive test [EN1052-1, 1998]

Also values and recommendations are given for correlation between them and the material properties. In case that no test data are available the characteristic compressive strength of URM. EN1052 [EN1052-3, 1998] gives the following correlation:

$$f_k = K * f_b^{0.7} * f_m^{0.3} \text{ (MPa)} \qquad (27)$$

f_b - normalized mean compressive strength of brick units

f_m - normalized mean compressive strength of mortar

K - empirical coefficient depends on masonry classification

To obtain the normalized compressive strength of masonry units, the mean compressive strength of the tested units is multiplied by the δ factor. The values of this factor are given in EC-6 [EN1996-1, 2005] and presented in table below.

Table 19: Values of δ factor [EN1996-1, 2005]

Height of unit (mm)	Least horizontal dimension of unit (mm)				
	50	**100**	**150**	**200**	**250 or more**
50	0.85	0.75	0.7	n/a	n/a
65	0.95	0.85	0.75	0.7	0.65
100	1.15	1	0.9	0.8	0.75
150	1.3	1.2	1.1	1	0.95
250	1.45	1.35	1.25	1.15	1.1
>250	1.55	1.45	1.35	1.25	1.15

2.4.4 Shear strength f_{vk} and flexural strength f_{xk}

Shear strength, is defined as the strength of masonry subjected to shear forces and is a combination of initial shear strength at zero compressive strength f_{vko} plus the design compressive stress perpendicular to shear. $f_{vk} = f_{vko} + 0.4\sigma_d$ (28)

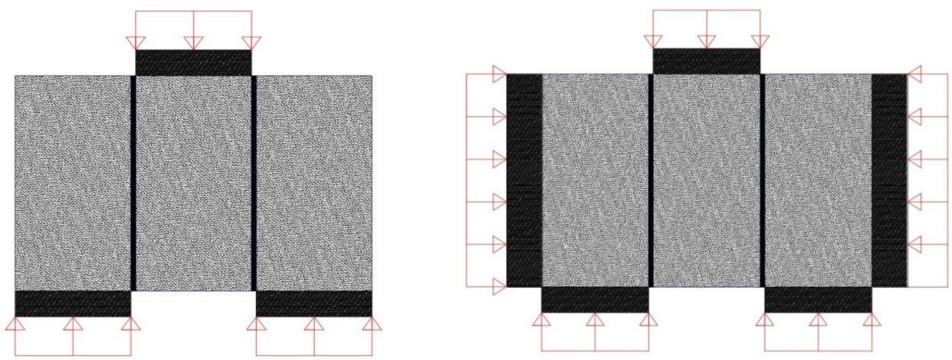

Figure 19: Determination of the initial shear strength and triplet shear strength [EN1052, 1998]

For determining f_{vko} EN1052-3 recommends the triplet test, the specimens are shown below and are tested at least five triplets. The minimum value is 0.03MPa. The minimum value of f_{vk} is $0.065f_b$. Another approach is by correlating the shear strength with tensile strength. If the strength of masonry walls is verified for out of plane loads, f_{xk} flexural strength is the governing parameter. In the EC is defined f_{xk1} flexural strength having a plane of failure parallel to the bed joints and f_{xk2} flexural strength having a plane of failure perpendicular to the bed joints.

The recommendations give the equations:

$f_{xk1} = 0.035 f_b$ with filled and unfilled perpendicular joints

$f_{xk2} = 0.035 f_b$ with filled perpendicular joints (29)

$f_{xk2} = 0.025 f_b$ with unfilled perpendicular joints

or from tables with recommendations for different types of masonry and mortar strength.

2.4.5 Tensile strength f_t

Tensile strength in masonry has values relatively low, so it is neglected many times in calculations. But in non-linear analysis it is important because it gives effect on the lateral load-bearing capacity of the structure. Backes [Backes H.P. et.al., 1985] has tested many masonry walls and found that the value of tensile strength of masonry is between: $0.09\text{MPa} \leq$ ft $\leq 0.82\text{MPa}$ (30). Soric recommends tensile strength to be taken as 10% of compressive strength. [Soric Z., 1987]

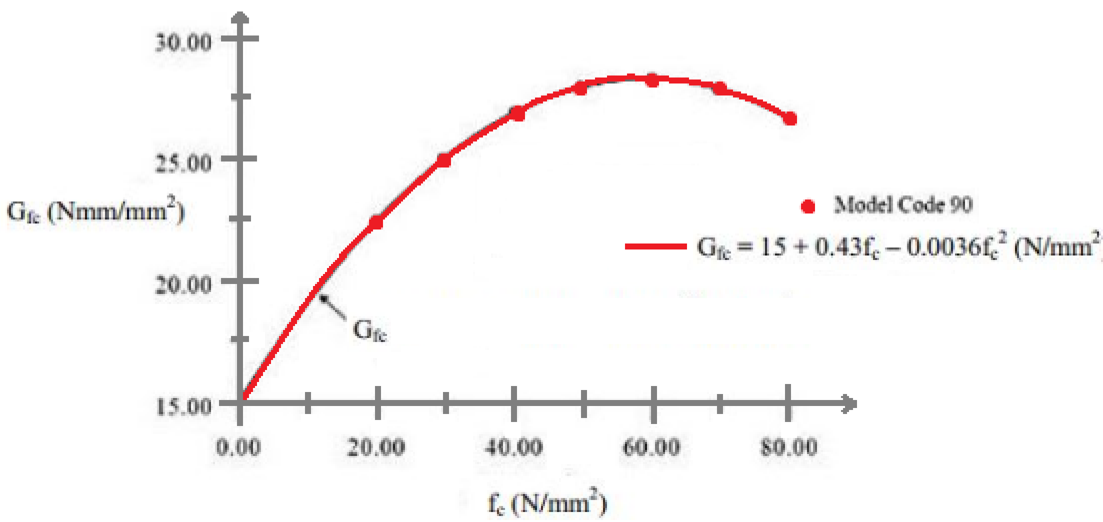

Figure 20: Compressive fracture energy [CEB-FIP Model Code 90, 1993]

Lourenco based on Model Code90 for concrete [Lourenco et.al., 2004; CEB-FIP Model Code 90, 1993], where the fracture energy is calculated by the expression:

$G_f = 0.025 * (2 * f_t)^{0.7}$ (N/mm2) (31)

The ratio between tensile and compressive strength is assumed 5%. The ductility index is defined as $\mu = \frac{G_f}{F_t}$ (32) and for the brick has a recommended value of 0.029. [Lourenco P.B. et.al, 2004]

The determination of the compressive fracture energy is as well based on the Model Code90 [CEB-FIP Model Code 90, 1993], for a peak strain of 0.2% as shown in figure.

The equation of this function is given as below:

$G_{fc} = 15 + 0.43 * f_k - 0.0036 * f_k^2$ (32)

For: $f_c < 12N/mm^2$ d=1.6mm

$f_c > 80N/mm^2$ d=0.33mm

as recommended by Lourenco.

2.4.6 Stress-strain (σ-ε) relationship

The σ-ε diagram can be obtained by monitoring compression test of wall with the right sensors. The modulus of elasticity E can be evaluated as secant modulus at service load condition one third of compressive strength. If there are no experimental data, EC-6 recommends to take the modulus equal to $E = 1000 * f_k$ (MPa) (33)

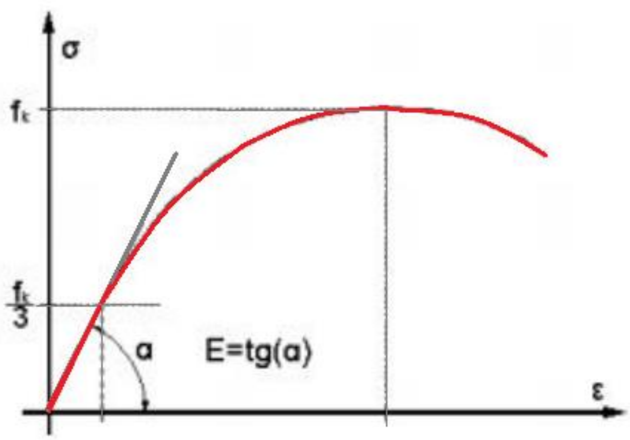

Figure 21: Evaluating modulus of elasticity from σ-ε diagram

Tomazevic proposes $200f_k \leq E \leq 2000f_k$ (34) [Tomazevic M., 1999], Binda recommends $E = 900N/mm^2$ (35) [Binda L. et.al., 2007] for rural poor buildings and palaces $E = 900 - 1500\ N/mm^2$ (36). KTP-78 [KTP-9-78, 1978] recommends similar values and are given in function of α coefficient depending on the wall type and mortar strength. $E = \alpha * f_k$ (37). The shear modulus G can be obtained as 40% of the modulus of elasticity as recommended by EN1996 [EN 1996-1, 2005]. In many studies is showed that this value is very high comparing to reality and that real values vary from 6% to 25%. If shear modulus is expressed in the terms of tensile strength, is recommended the value $G = 2000f_t$ (38). Since the range of variation of the possible values of strength and deformability characteristics of masonry is very wide, it is recommended that the data obtained by testing is more reliable than analytical formulations.

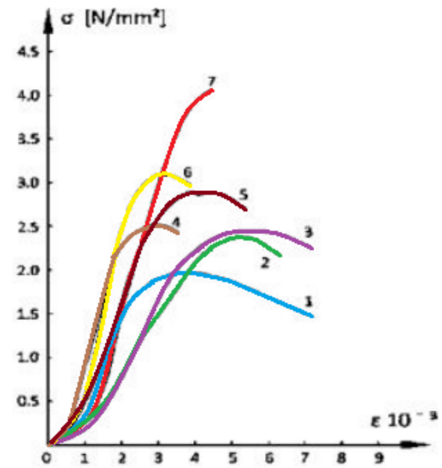

Figure 22: Experimental diagrams of masonry under pressure [Lourenco P.B, et.al., 2004]

In compressive tests masonry shows an elasto-plastic deformation diagram. In the begging with the increasing of the load, micro cracks inside the wall are formed and the deformation is slow and in linear and elastic relationship with pressure. After passing ultimate elastic state, macro-cracks starts to form. These are plastic deformation and are viewed by human eye. Increasing of load, implies increasing deformation to the cracking point. Different studies like Binda et.al., 2007, have shown that high strength masonry perform more in an elastic phase having lesser plastic deformation before failure (ductility) and lower strength masonry have more plastic deformation (ductility). [Binda L. et.al., 2007] $\sigma - \varepsilon$ diagram is given by different authors and the non-linear part has significant importance. Turnsek-Cacovic have reported the relationship between $\sigma - \varepsilon$ as in the figure with 2 phases. [Turnsek-Cacovic, 1971]

The elastic part with $\sigma = E * \varepsilon$ and the plastic part with a parabolic relationship:

$$\frac{\sigma}{f_k} = 6.4 * \frac{\varepsilon}{\varepsilon_k} - 5.4 \left(\frac{\varepsilon}{\varepsilon_k}\right)^{1.17} \quad (39)$$

where ε_{mu} ultimate strain, and ε_k and f_k the strain and stress corresponding.

EN1996 gives a similar relationship, but that continues linear in the plastic phase.

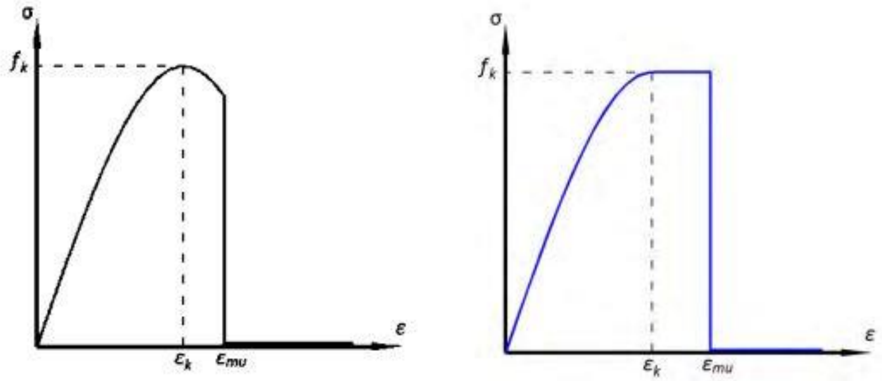

Figure 23: σ-ε diagram as in [Turnsek-Cacovic, 1971] and [EN 1996-1]

2.5 Modelling techniques of masonry buildings

2.5.1 Model typologies

Analysis and numerical modelling of masonry structures is one of the greatest challenges faced by structural engineers. The presence of joints is the major source of weakness, as well as discontinuty, nonlinearity and the existence of uncertainities in the material and geometrical properties.

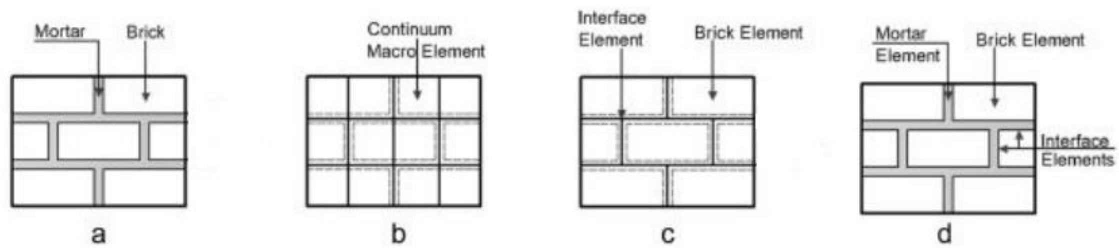

Figure 24: Masonry sample (a), One-phase macro-element (b), two-phase micro-modelling (c), three-phase micro-modelling (d) [Asteresis P.G. et.al., 2015]

Below is given a summary of different analytical proceduress in three levels of refinement for masonry models:

Macro-modeling (or as one phase-material) where the units, mortar and the unit-mortar interface are smeared out in a homogenous continuum. So masonry is taken as an homogenous, isotropic or anisotropic continuum medium.

Simplified micro-modelling or meso-modelling (as a two phase material), where the bricks are represented as fictitious expanded bricks by continuum elements with the same size as the original bricks plus the joint thickness. The mortar joint is also modeled as an interace with zero thickness. This approach leads to the reduction of the computational effort and yields a model that is applicable to a wider range of structures.

Micro-modelling (or three-phase materials), where the units and mortar in the joints are represented by continuum elements, whereas the unit-mortar interface is represented by discontinuum elements. This models leads to more accurate results but the level of refinement means that the corresponding analysis is computationally intensive, limiting is application to small scale laboratory.

These three basic models are also divided in sub-categories and the capabilities and limitation of each case. Asteris P. have studied this topic related to computional softwares that use different approaches, compared to full scale experimental tests. In most of the cases macro-modelling, gives acceptable results. [Asteresis P.G. et.al., 2015]

2.5.1 Non-linear modelling with software

3muri is based on a finite element methodology for modelling masonry structures. [3muri software package] The software proposes the line finite element, which is represented by its axis. Below is showed a review from the theoretical modelling part of 3muri manual. The non-linear macro-element model, representative of a whole masonry panel, proposed by Gambarotta and Lagomarsino, (1996) , permits with a limited number of degrees of freedom (eight), to represent the two main in-plane masonry failure modes, bending-rocking and shear-sliding (with friction) mechanism, on the basis of mechanical assumptions. [Gambarotta L. et.al., 1996]

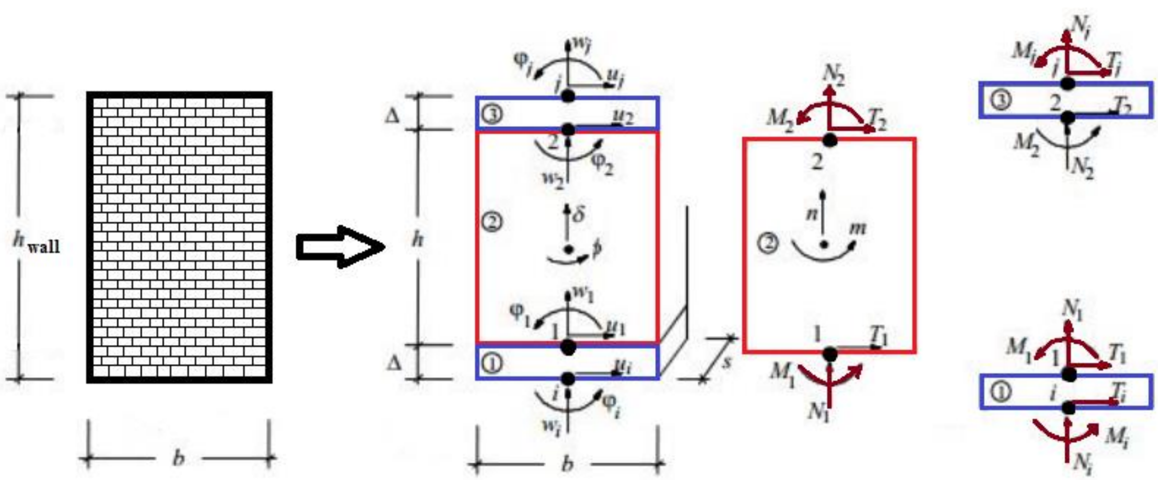

Figure 25: 3Muri finite element view [Gambarotta L. et.al., 1996]

A wall of width b and thickness s, consist of three parts: axial deformability which is concentrated in the two extremity elements 1 and 3, of infinitesimal thickness D, infinitely rigid to shear actions. The tangential deformability is situated in the central body, of height h, which is non-deformable axially and in flexure. The complete cinematic model for the macro-element must examine three degrees of freedom for the nodes i and j, and those of the interface 1 and 2. If we specify the axial displacement with w, transversal displacement with u, and rotations with j, it can be affirmed that $u_1 = u_i$, and $u_2 = u_j$. The elements 1 and 3 have infinite shearing resistance and a thickness of D tending towards zero. Also can be affirmed that $w_1 = w_2 = d$, $j_1 = j_2 = f$. The central body is axially and flexurally rigid and d, f represent the axial displacement and the rotation, respectively. So the total number of degree of freedom is eight, where six are displacement components for the extremity nodes ($u_i, w_i, j_i, u_j, w_j, j_j$) and two macro-element components (d and f). Hypothesizing a mono-lateral elastic contact in interfaces 1 and 2, represents the absence of significant traction resistance in the material from the overturning mechanism. The shear resistance mechanism is schematized by considering a state of uniform tension in the central module, (assuming $T_i = T_j$), through a joint between the cinematic components (u_i, u_j, f) the tension state and the descriptive variables of the plastic behaviour (degree of damage a and plastic flow g_p). Cracking damage in the diagonal spandrel beams, where shear-sliding mechanism are found, can be represented through the inelastic displacement component g_p which is activated when the Coulomb attrition limit condition is exceeded. The joint allows the cyclical evolution of the rigidity degradation and associated deterioration of resistance to the progressive shearing damage to be described using the variables a and g_p [Gambarotta L. et.al., 1996]. The bending behaviour of the element is concentrated in two extremities. The relationship which links the axial compression N and the moment M is derived directly from the joint elastic equations. If the pressure centre is inside the central inertial core the extremity of the wall will not be choked. 3muri is based on the EC which for calculation of existing masonry specifies:

-for bending compression maximum drift (strain) is 0.8%, $\sigma_{max} = 1.8MPa$ (40)

-for shear failure maximum drift (strain) is 0.4%, $\tau_{max} = 0.06MPa$ (41)

The behaviour is modelled as elastic- perfectly plastic idealized curve. The maximum elastic strain is not specified directly but using the 3Muri software values for elastic modulus "E" and shear modulus "G" can be calculated as below:

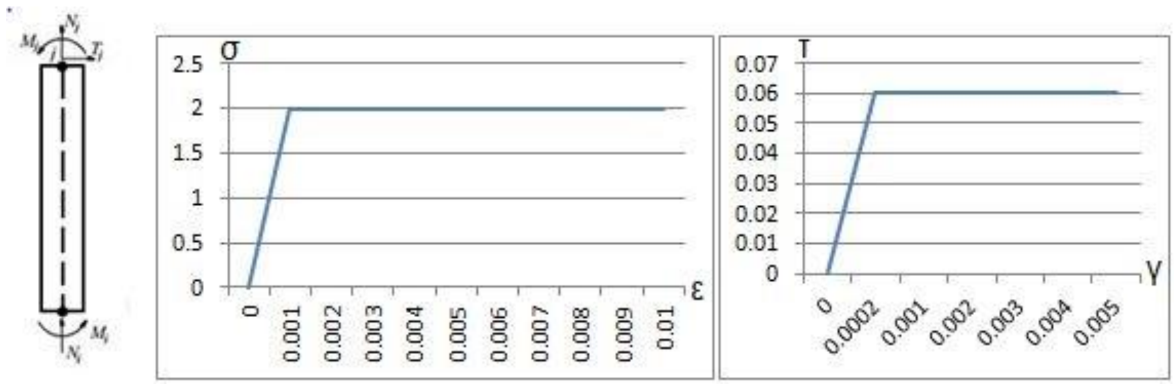

Figure 26: 3muri finite element, compression strain curve, shear strain curve

The maximum elastic strain is calculated using maximum stress and elastic modulus:

$$\varepsilon_{el} = \frac{\sigma_{el}}{E} = \frac{1.8MPa}{1800MPa} = 0.001 \qquad (42)$$

The maximum elastic shear drift is calculated using maximum stress and shear modulus:

$$\gamma_{el} = \frac{\tau_{el}}{G} = \frac{0.06MPa}{300MPa} = 0.0002 \qquad (43)$$

2.6 Basics of assessment and analysis of masonry structures

2.6.1 Performance based assessment

Design of building structures is based on assessing the performance of the structure under gravity, live and lateral loads. This assessments predicts and limits the damage on the structure under the circumstances, it is calculated. The relevant design situations shall be selected taking into account the circumstances under wich the structure is required to fulfil its function. The basic hazard, and the worst scenario for masonry buildings in Albania, in most of the cases, comes from the combination of gravity, live and seismic loads.

2.6.2 Description of damage limit states

A damage limit state, classifies the damage that occurs in a building under different loads and scenarios. By limiting the maximum amount of damage expected, the performance of the sctructure under this scenario can be controlled by the designer. To evaluate how the buildings reacts to a load scenario and studying the structure with different methods, from unloaded conditions to the maximum load that the structure can bear, is reffered as capacity evaluation of the structure. So, basically the capacity of the structure, measures the structure ability to bear loads. Capacity evaluation can be made by different methods, but the most popular, and that gives easier and reliable solution is the pushover analysis. Non-linear pushover analysis calculates the capacity curve of the equivalent single degree of freedom model of the structure. Capacity curve gives the relation between the base shear force of the structure to the displacement of the top roof level.

2.6.3 Basics of pushover analysis

To properly determine the capacity of the building in the literature are given various ways and analysis. The capacity of a structure is defined as the maximum lateral load it can bear, under gravity and live loads, without failing. As for single elements of the structure the failure point is clear, for the whole structure, the failure point is reached when the first element fails. So for example eventhough only one slab can fail and the other elements of the structure can still have capacity to bear loads, the structure is considered to have reach the failure point. The entire EC-6 and EC-8 design is based on the concept that all the structural elements should have the capacity to bear loads and guarantee the safety of each element. Pushover analysis is performed by subjecting the structure to a monotonically increasing pattern of lateral forces, representing the inertial forces. Those representing load conditions that would be experienced by the structure during ground shakings. With this method, a characteristic nonlinear force-displacment relationship of the MDOF system can be determined. The base shear force and the top roof displacement have been used mostly in literature [KTP-N2-89, 1989; EN 1996-1, 2005; EN 1998-1, 2004] and also in this parer as representative of force and displacement. Different assumpions are made about the shapes of load patterns and give similar results. In 3muri approach [Galasco A.et.al, 2006] are two load pattern applied: first mode shape distribution (static), based on the fundamental mode shape of the structure, and a uniform load distribution to all stories. The vector of lateral loads P used in the pushover analysis, in the N2 method, is determined as: $P = p\Psi = pM\varphi$ (44)

Where: M-the diagonal mass matrix p- magnitude of the force

Ψ-factor for distribution of lateral loads φ-displacement shape

The lateral force in the i-th level is proportional to the component φ_i of the assumed displacement shape φ, weighted by the story mass m_i is as follows: $P = pm_i\varphi_i$ (45)

2.6.4 Equivalent SDOF model and capacity diagram

The seismic demand of the structure, in the N2 method, is taken in consideration by using response spectrum. The outcome of the pushover analysis is the diagram of the global force versus top displacement curve or capacity curve. This curve is used do determine the basic characteristics of the structure as stiffnes, strength and ductility.

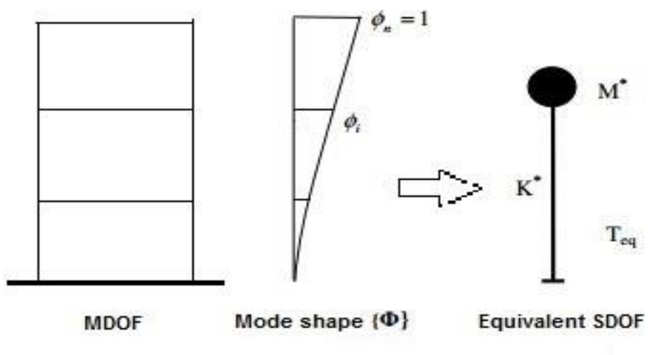

Figure 27: Transformation of MDOF to SDOF

The structure is modeled as a SDOF system and the procedure followed in N2 method is given below [EN1998, 2004]. The equation of motion of a planar MDOF model, that includes only lateral translational degrees of freedom: $M\ddot{U} + R = M1a$ (46)

Where: U-vector representing displacement R-vector of inertial forces

1-unit vector a-the ground acceleration as a function of time

Eventhough damping is not included in the equation, its influence is taken in consideration in the design spectrum. The basic and most critical assumption in the procedure is that the displacement shape φ is constant and the displacement vector is defined as follows:

$U = \varphi D_t$ (47)

Where D_t is the time-dependent top displacement. The vector φ is normalized in such a way that the component at the top is equal to 1. The internal forces R are equal to the statically applied external loads from static equations.

$P = R$ (48)

By substituting equations 6,9 and 10 into equation 8, and my multiplying with φ^T:

$\varphi^T M\varphi\ddot{D}_t + \varphi^T M\varphi p = -\varphi^T M1a$ (49)

After multiplying and dividing with $\varphi^T M 1 a$, the equation can be written as follows:

$$m^* \ddot{D}^* + F^* = -m^* a \qquad (50)$$

Where m^* is the equivalent mass of the SDOF system:

$$m^* = \varphi^T M 1 = \sum m_i \, \varphi_i \qquad (51)$$

And D^* and F^* are the displacement and force of the equivalent SDOF system:

$$D^* = \frac{D_t}{\Gamma} \qquad (52) \qquad\qquad F^* = \frac{V}{\Gamma} \qquad (53)$$

V is the base shear of the MDOF model:

$$V = \sum P_i = \varphi^T M 1 p = p \sum m_i \, \varphi_i = p m^* \qquad (54)$$

The modal participation factor Γ controls the transformation of the MDOF system to the SDOF model is defined as: $\Gamma = \frac{\varphi^T M \, 1}{\varphi^T M \, \varphi} = \frac{\sum m_i \varphi_i}{\sum m_i {\varphi_i}^2} = \frac{m^*}{\sum m_i {\varphi_i}^2}$ (55)

Γ is equivalent to PF_1 in capacity spectrum method, and to C_0 in the displacement coefficient method. [ATC 40, FEMA 273]

2.6.5 Bilinear capacity curve

The graphical procedure in the N2 method, requires that the post-yield stiffess is equal to zero. The influence of moderate strain hardening is incorporated in the demand spectra. This approach has its limitations, but gives acceptable results for most of the cases [Fajfar P. et.al, 2000] . For the above reasons, but also for simplicity, in calculation the capacity curve can be idealised as bilinear by equating the surface under the curves, of both real and bilinear, and maintaining the initial elastic stiffness. From the bilinear curve the yield strength F_y m and the elastic stiffness K_e. The initial period T^* of the equivalent SDOF system will be:

$$T_{eq} = 2\pi \sqrt{\frac{m^*}{K^*}} \qquad (56)$$

where K^* defines the elastic stiffness of the equivalent SDOF system.

$$K^* = \frac{F_y^*}{d_y^*} \qquad (57)$$

Equalizing the surfaces between the two curves d_y^* can be defined by the following equation:

$$d_y^* = 2\left(d_m^* - \frac{E_m^*}{F_y^*}\right) \qquad (58)$$

where:

d_y^* - yield displacement of bilinear curve $\qquad$ E_m^* - energy (surface) under both graphs

The program generates automatically this bilinear curve based on N2 [EN1998; 2004].

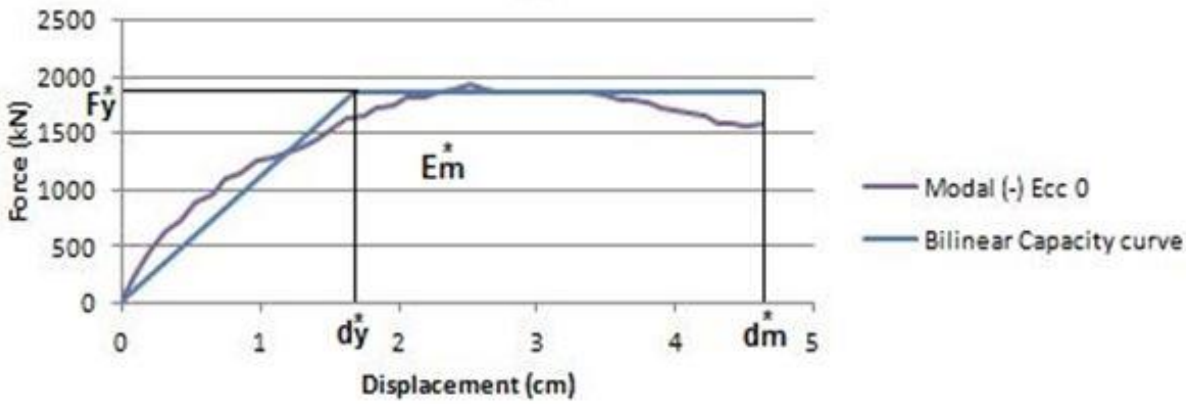

Figure 28: Bi-linearization of pushover curve

In the figure above can easily be determined the strength of the building Vy, the initial elastic stiffness E=tgα and the ductility μ=du/dy. Strength is defined as the maximum load bearing capacity of the structure. But this is not always the determining factor because of the plastic phase, when eventhough the lateral force remains constant, the structure has still reserve in displacement. This reserve is called plastic phase or ductility of the building, and is measured by the ductility factor. In masonry buildings ductility can take values in a range from μ=1.5-2.5.

2.6.6 Performance evaluation of MDOF system N2-method

The displacement demand of the SDOF model S_d is transformed into the maximum top displacement D_t of the MDOF system (target displacement) by using eq.14.

The local seismic demand can be determined by a pushover analysis. Under monotically increasing lateral loads with a fixed patterns as discussed before, the structure is pushed to its target top displacement D_t. It is assumed that the distribution of deformations throughout the structure in the static pushover analysis approximately corresponds to that which would be obtained in the dynamic analyses. Studies [Fajfar P. et.al., 2005; Vidic T. et.al., 1994; Miranda E., 2000] show that D_t represents a mean value for the applied earthquake loading, and there is a considerable scatter out the mean. In FEMA 273 [FEMA, 1997] it is recommended to carry out the analysis to at least 150% of the calculated top displacement. The expected performance can be assessed by comparing the seismic demands, with the capacities for the relevant performance level. Global performance can be verified by comparing displacement capacity and demand.

2.6.7 Capacity versus demand of the buildings and performance targets

Capacity evaluation of the investigated URM residential buildings is performed using Eurocode 8 [EN 1998-1, 2004]. Three damage limit states levels, i.e., "Damage Limitation" (DL), the limit state "Significant Damage" (SD) and the limit state "Near Collapse" (NC) are considered as specified in this code and several other international guidelines such as FEMA-356, ATC-40, and FEMA-440.[FEMA-356, 2000,1997; ATC-40, 1996; FEMA-440, 2005] Part 3 of EC-8 addresses the seismic evaluation of existing buildings and provides – unlike its counterpart for newly designed structures Eurocode 8, Part 1 – estimates of drift capacities of unreinforced masonry piers. For URM spandrels, such drift capacities are not identified. This section reviews the drift values and the corresponding limit states definitions in EC-8 [EN1998-3, 2004] for URM piers. For the "DL" limit state, the strength and stiffness of the URM structure should not be significantly weakened and permanent drifts should be negligible. For a single structural component, this limit state is associated with the yield point of the force-deformation curve, i.e., with the end of the branch corresponding to the elastic behavior. The "yield" drift θ_y, which corresponds to the limit state rotation "Damage Limitation" (θ_{DL}), is the intersection of the elastic branch and the pier strength. The second limit state "SD" is the limit state on which the seismic assessment of structures is typically based as it describes the limit state which is acceptable for a return period of 475 years of the seismic action. For masonry piers, Eurocode 8 defines drift capacities which are based on the failure mode (shear vs. flexure) and the shear aspect ratio H_0/L where H_0 is the height of zero moment and L the wall length of the pier:

Pier Shear failure: $\delta_{SD} = 0.4\%$ Pier Flexural failure: $\delta_{SD} = 0.80\% (H_0/ L)$ (59)

Equations give the drift capacities for the limit state "Significant Damage" (SD). To obtain the drift capacity at "Near Collapse" limit state (NC), the drift capacities of The above equations are multiplied by a factor 4/3 [EN 1998-1, 2004]. Other design codes use similar approaches. [Petry and Beyer, 2014; Kržan et al., 2015].

For an entire structure, EC-8 associates the limit state “NC” with “the roof displacement at which the total base shear has dropped below 80% of the peak resistance of the structure, due to progressive damage and failure of lateral load resisting components. For single structural elements such as a pier or a spandrel, Eurocode 8 does not specify by how much the strength of the element has dropped when the element reaches the limit state “NC” but defines only qualitatively that the piers might have lost most of their lateral strength and stiffness but should still be able to transfer vertical loads to the underlying soil through their foundation. EC-8 approximates the base shear force-drift relationship of masonry piers by a bilinear curve.

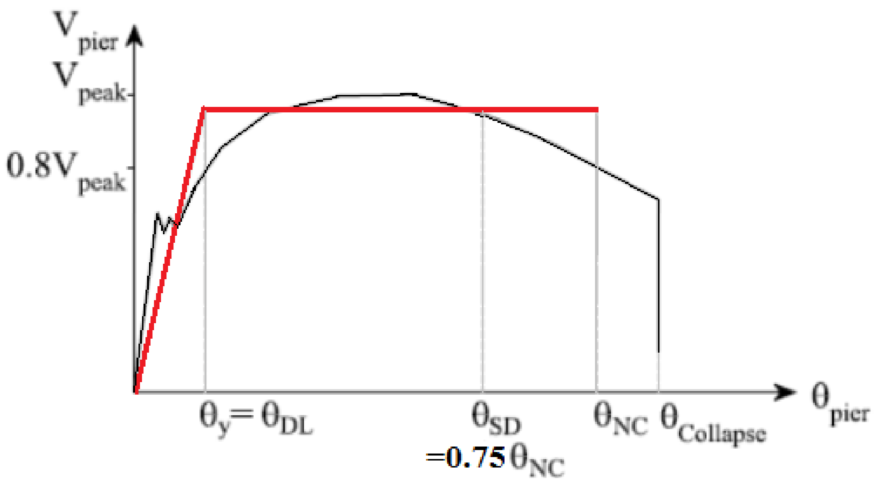

Figure 29: Limit state rotations according to EC-8 and bilinear force-deformation relationship for a masonry pier [EN 1998-1, 2004]

In addition to the drift limits noted above, it furnishes estimates of the pier strength. The elastic stiffness of the pier can be calculated from gross sectional properties and a stiffness reduction factor of 0.5 to account for cracking. Eurocode 8 provides therefore all input parameters required for establishing the base shear force-drift relationship of masonry piers. As outlined in the above, Eurocode 8 does not provide any guidance for establishing the force-deformation relationship of masonry spandrel or their limit state rotations. The definition of the limit state “NC” for a global structure refers to a very heavily damaged structure with low residual lateral strength and stiffness although the vertical elements are still capable of sustaining vertical loads. As the spandrels are not necessary to transmit the vertical loads to the foundation, the spandrels could have zero lateral strength and stiffness when the structure reaches the limit state “NC”. The rotation θ_{NC} could therefore be defined as the rotation associated with partial collapse of the spandrel ($\theta_{Collapse}$), i.e. with the maximum rotation applied during quasi-static cyclic testing. The quasi-static cyclic tests on masonry spandrels showed that the collapse of spandrels supported on timber lintels is caused by the collapse of the lintel supports and that the collapse of spandrels supported on masonry arches starts with the collapse of the arch [Beyer K. et.al, 2012]. However, to be consistent with the definition of the limit rotation θ_{NC} for piers, the limit rotation θ_{NC} of spandrels is defined as the rotation where the residual strength drops by 20%. For the limit state “SD”, EC-8 refers to a structure which is significantly damaged but has still some residual lateral strength and stiffness. The structure can “sustain after-shocks of moderate intensity” but is “likely to be uneconomic to repair”. For masonry spandrels, this definition seems to apply best to the state before the onset of strong material degradation. The onset of degradation can be monitored either visually or be determined from the force-rotation relationship of the spandrel as the rotation θ_{SD} before the residual strength deviates from the linear trendline describing the force-rotation relationship of the residual strength regime [Beyer K., 2013].

2.7 Results on similar studies

2.7.1 Assessment on Albanian building stock

Albanian building stock consists of different buildings, different types and of different era. Masonry buildings occupy a considerable place in civil engineering of our country. They are built in different era and periods, from the 40s to the 90s of the XX century. According to the census of 2001 [INSTAT, 2002], the total population of Albania consists of 3069275 inhabitants, 726894 households, 512387 buildings and 785515 dwellings. The housing stock is characterised by a low number of dwellings per buildings on average 1.53, especially in rural areas 1.14 and town of less than 10000 inhabitants. In towns with more than 10000 inhabitants, the number of dwellings per buildings is on average 2.58. It is largest in Tirana at 2.80. Below are classified the buildings by the principal construction material. Brick or stone masonry buildings compose 88.3% of the masonry building stock.

Table 20: Buildings by time of construction [UNDP, 2003]

Principal construction material	Total	Before 1945	1945-1963	1963-1978	1978-1990	After 1990
Prefabricated	4.5%	-	-	-	6.1%	9.5%
Brick or stone masonry	88.3%	92.5%	93.1%	92.2%	88.8%	80.9%
Wood and other materials	7.2%	7.5%	6.9%	7.8%	6.9%	9.6%

Even today the number of building with principal material of brick or stone masory is estimateed more than 60% of the building entire stock. Many authors, have made estimations about the seismic risk of the building stock. In the paper presented by UNDP, (2003), the seismic risk estimations are based on various scenarios of earthquakes,that can happen in different fault zones. [UNDP, 2003] Fifteen scenario earthqaukes have been selected and represent realistically, the most probable seismic disaster scenarios that could generate a severe adverse impact of the population, material property and economy. To estimate reliably the scale of possible seismic impacts, the risk assessment is conducted for pre-selected characteristic return periods. A return period of 475 years is adopted because it is the refrent one in EC-8 for SD limit state. In the above table are shown the % of territory exposed to an excitation level for adopted return periods of scenario earthquakes. For adopted return periods of 50, 100, 200 and 475 years, the scenario event demands are presented in terms of the expected number of structurally damaged buildings (corresponding SD limit state) and/or to be evacuated and totally damaged and/or collapsed buildings and related percentage in respect to the total residental building stock of the country. The greatest demand on the national civil emergency system would result from earthquakes occuring in Durres, Elbasan, Berat, or Vlora. The seismic sources capable of generating structural damage and collapse ranges from 1.9% (±10% in Elbasan) to 1.2% (±10% in Durres) of the national building stock for a return period 50 years. For a return period of 200 years the values range from 7.1% (±10% in Durres) to 5.2% (±10% in Berat). For a return period of 475 years, the energetic potential in combination with the patterns (typology and concentration) of construction, are capable of creating a catastrophe at the national level.

Table 21: Territory of the country by excitation levels for adopted return periods of scenario earhquakes [UNDP, 2003]

Return period of earthquake	**Excitation level**			
	<15%g	**(15-30)%g**	**(30-45)%g**	**(45-60)%g**
50 years	99.4%	0.6%		
100 years	73.2%	26.8%		
200 years	34.3%	65.2%	0.5%	
475 years	18.7%	42.4%	39.0%	
1000 years	12.7%	23.2%	39.6%	24.5%

Another author that has studied Albania building stock and especially masonry buildings is Baballeku M. in his PhD thesis "Assessment of structural damage to templatew buildings of educational system" (2014) [Baballeku M., 2014]. This study presents a methodology for assessing damage to the template buildings used for educational system in Albania based on fragility assessment. These building are in general of masonry structures, almost all of unreinforced masonry, with height no more than 4 floors. The schools projects and templates are from 1960-1979 and some even build after 79s, with the old codes KTP-63 and KTP-78 that have serious verified deficiency in seismic evaluation. For realising the seismic modelling of the building is used sap2000 software, wich uses a macro-modelling technique with 3 layered nonlinear shells. The first shell takes in consideration compressive-tensile stresses even in non-linear phase, the second shell takes in consideration diagonal shear failure and the third compressive-tensile stress and strain in linear phase. As conclusion in this study is shown that for the buildings studied if we refer to KTP seismic demand, the educational buildings of Albania have a high probability to have lesser or moderate damages, but referring to EC seismic demand the probability of high damages on this building types increases significantly. Bilgin H. and Huta M. (2018) have also made an vulnerability assessment of two URM buildings having typical architectural configurations common for residential use. [Bilgin H. et.al., 2018] Both buildings are of URM and are of clay brick masonry structures constructed in 60s and 80s, respectively. The first building is a three-story URM and the second one confined masonry and five story high. Mechanical characteristics of the building of masonry walls are determined by experimental test of the buildings material and correlations given by the ASTM standard codes.[ASTM, 2008] For both models a global numerical model building was built, and masonry elements are simulates as non-linear. This building are modelled with proper elements characteristics using the software DIANA v9.6 with a micro-modelling technique. Then displacement demands are calculated for both EC-8 and FEMA440. [EN1998, 2005; FEMA440, 2005] The results of the study showed that URM building displays higher displacement and shear force demands that can be directly related to damage or collapse. On the other hand, the confined one exhibits relatively higher seismic resistance by indicating moderate damage. Also effects of demand estimation approaches on performance assessment of URM building were compared. Deficiencies and possible solutions to improve the capacity of such buildings are given.

2.7.2 Non-linear pushover analysis by different authors

The literature for this part is very wide, because this kind of approach is very popular and gives verified results. Two authors are presented here that have studied Italian building stock. Capsulla C. et.al., (2016). in their study "Seismic safety assessment of a masonry building according to Italian guidelines on Cultural Heritage: simplified mechanical-based approach and pushover analysis" [Capsulla C. et.al., 2016] have presented a seismic safety assessment of a case study of a masonry building located in Naples, together with a critical appraisal of the methods used. This masonry building was built before the introduction of proper seismic code provisions, so it can be representative of many other similar cases of vulnerable historical buildings in earthquake-prone urban areas. This building was analyzed with the simplified code method (LV1) of Italian Guideline on Cultural Heritage [NTC, 2008]. . In this guidelines are three levels of investigation and assessment:

LV1- territorial-scale seismic evaluation through a simplfied mechanical-based approach

LV2- seismic evaluationto be used in case of local interventions on a building

LV3- accurate evaluation of the seismic safety of a building

From the LV1 assessment, the reference seismic action of the site for the SLV limit-state as characterised by return period of 475 years, the maximum ground acceleration is 0.166g, with a safety factor fa=0.484.

The LV3 assessment is performed through nonlinear static analysis by using 3Muri software program, the same as in this study. The weaker direction was identified along the axis of the shorter dimension in plan of the building and a prevailing failure mechanism of the masonry piers was observed in this direction due to bending. The safety indexes obtained by both approaches appear to the same order of magnitude, especially considering the deformability of the timber and steel floors in their plane. Also a comparison between models with rigid and flexible diaphragms was carried out within the LV3 pushover analysis, and a decrease of safety index and shear capacity, of the building about 41% and 35% respectively, were obtained when flexible floors were assumed, while the displacement capacity decreased about 72%. Although there are still many uncertainites in the modelling criteria for flexible floors, the result does confirm that the stiffness of horizontal structures plays an important role on the global displacement of a masonry building. In conclusion, the LV1 method is capable of providing only some information in agreement with the structural behaviour of the buildings, since many aspects, such as the reference global models abd the failure modes of piers and sprandels are still quite difficult to be represented by non-dimensional parameters. In our study, the non-linear pushover analysis is similar to the LV3 analysis of Italian Code and also buildings with similar plan and height exist in Albania.

Formisano A. and Chieffo N. on their study have presented a seismic assessment of the responce of a typical residental masonry building located in Mirabello, a district of Ferrarra, damaged by the earthqauke that in 2012 hit the Emilia Romagna region of Italy. [Formisano A. et.al., 2018] After the geometrical and mechanical characterization of the building, non-linear static analyses are carried out by using different softwares to assess the most probable seismic response of the investigated housing construction. The series of main earthquakes that hit the Emilia-Romagna region of Italy on 20 May 2012 was of a magnitude scale M=5.9 and on 29 May 2012 of a magnitude scale of M=5.8. Eventhough the magnitude was relatively low comparing to other seismic events with high casualities but thiz zone was considered as a low seismic hazard region according to Italian codes. The expected peak ground acceleration was around (10-15)%g, meanwhile the earthquakes near the epicentre imposed a peak ground acceleration around 30% g. In the zone the most considerable part of the buildings were of masonry as principal construction material. The damages detected on the building were failure of masonry chimneys with the consequent collapse of some portions of the roof, settlements of the foundation structure along the short sides of the building resulting in the consequent detachement of all perimeter sidewalks, numerous medium size craks in the bearing masonry walls and in the masonry corners, slight detachment between floors and masonry walls, detachment between the roof and the masonry walls below, detachment of roof covering elements and subsequent infiltration of rainwater causing damages to both real estate units and staircases. Non-linear analyses are performed for this building by using 3 different software packages Pro-Sap, 3Muri and 3D Macro. If compared to Albania stock buildings, the slabs here are with dead loads that vary from 2-3kN/m^2 a highly reduced value comparing to Albanian masonry buildings with more heavy and rigid slabs, with load variation 4-4.5kN/m^2. In this study the results of each software are compared in both direction and in terms of stiffness they are almost the same for all the software, meanwhile in terms of displacement the results varies more, but the range is acceptable.Considering the maximum peak ground acceleration occured in Mirabello ar the life safety limit state (0.16g), from the comparison of achived results it has been detected as, for the collapse condition. The discretised method provides the highest damage forecasts, with the damage exceedance probabilities greater than those achived with the lognormal distribution based procedure.

2.8 Earthquake of 26 November 2019 Durres caualities

On November 26, 2019, an earthquake hit the central western part of Albania. It was assessed as M_w 6.4. Its epicenter was located offshore north western Durrës, about 7 km north of the city and 30 km west from the capital city of Tirana. Its focal depth was about 10 km. The most affected areas are the Durres city and the Thumane town, while damage was also observed in Laç town, Fushe-Kruje town, Kamez, Vore and Tirana city. The earthquake charachteristics will be given in more detail in chapter VII.

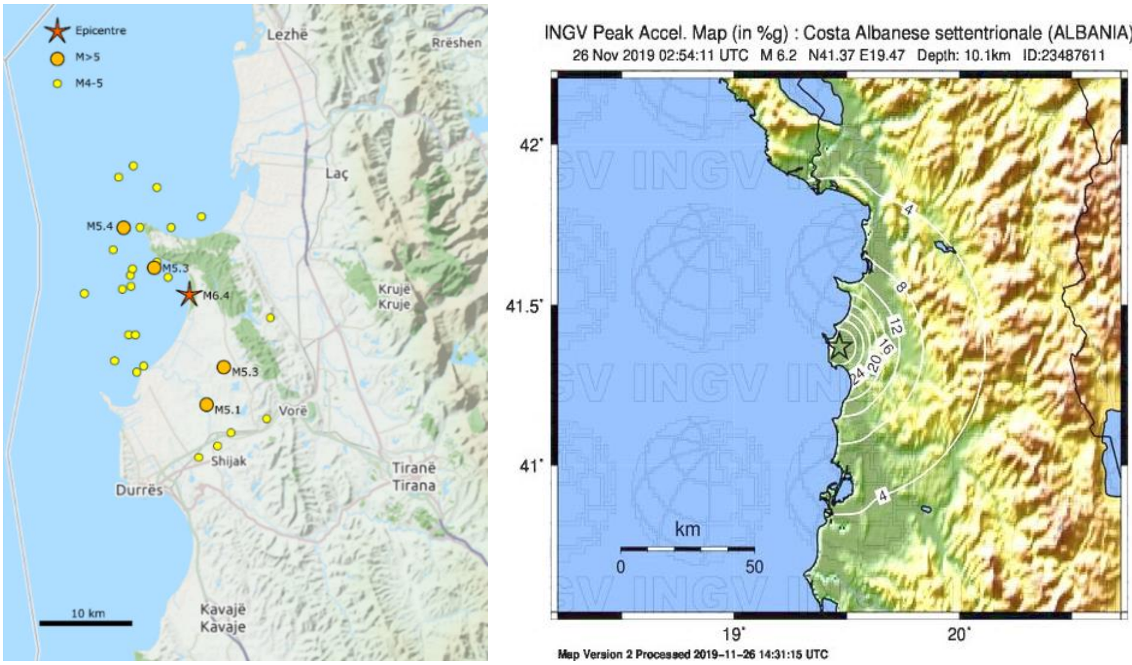

Figure 30: Location of epicenter and aftershocks of the 26 Novemember earthquake (left), Peak ground acceleration map (right) [http://shakemap.rm.ingv.it/shake/23487611/pga.html]

2.8.1 Criteria for post-earthquake building damage inventory and usability classification

In EC-8 the criteria for classifing post-earthquake building damage inventory and usability classifies the buildings in five damage degrees. The first two levels DS1 and DS2 classify the buildings wich are immeditalely usable after the earthquake and don't need repair. These building have slight non-structural damage and very isolated and neglible structural damage. The next levels DS3 and DS4 classify the buildings as temporarely unusable. These buildings have extensive non-structural damage and considerable structural damage, but yet repairable structural system. The last level DS5 classifies the building as unusable. This buildings is destroyed or has partially or totally collapsed structural system. The regulations and reccomendations about the investigation process give also the damage desciption for damage degree, to use for proper investigation of the building.

Table 22: Criteria for post-earthquake building damage inventory and usability classification [EMS-98; 1998]

Damage Degree (DS)	Usability category	Damage state	Damage description	Notes
DS-1	Immediately Usable	None: Slight non-structural damage and very isolated neglible structural damage	Without visible damage to structural elements. Possible fine cracks in the wall and ceiling mortar. Hardly visible non-structural and structural damage.	Buildings of damage degree D1 and/or D2 are without decreased seismic capacity and do not pose danger to human life. Immediately usable, or usable after removal of local hazards (instable or cracked chimneys, attics or gable walls)
DS-2			Cracks to the wall and ceiling mortar. Falling of large patches of mortar from wall and ceiling surface. Considerable cracks, or patial failure of chimneys, attics and gable walls. Disturbance partial sliding, sliding and failing down of roof covering. Cracks in structural members. Building classified here are without decreased seismic capacity and do not pose danger to human life. Immediately usable, or usable after removal of local hazards.	
DS-3	Temporary unusable	Severe: Extensive non-structural damage and considerable structural damage but reparaible structural system	Diagonal cracks or other cracks to structural walls, walls between windows and similar structural elements. Large cracks in reinforced structural members: columns, beams, RC walls. Partially failer or failed chimneys, attics or gable walls, disturbance, sliding and failing down of roof covering.	Buildings of damage degree DS3 and/or DS4 are of significantly decreased seismic capacity. Limited entry is permitted unusable before repair and strengthening. Needs for supporting and protection of the and
DS-4			Large cracks with or without detachment of walls with crushing of materials. Large cracks with crushed materials of walls between window and similar elements of	

			structural walls. Large cracks with small dislocation of RC's structural elements: column, beam, RC walls. Slight dislocation of structural elements and the whole building.	its surroundings should be considered.
DS-5	Unusable	Total: Destroyed, paritally or totally collapsed structural system	Structural elements and their connections are extremely damaged and dislocated. A large number of crushed structural elements. Considerable dislocation of the entire building and deleveling of roof structure. Partially or completely failed buildings.	Buildings of damage degree DS5 are unsafe with possible sudden collapse. Entry is prohibited. Protections of streets and neighboring vuildings is required. Decision on demolotion should be based on economic study considering repair and strengthening. as alternatives.

2.8.2 Earthquake casualities

Two hotels and two apartment blocks collapsed in Durres. Four buildings, including a five-story apartment block, collapsed in Koder-Thumane and the town was the hardest hit from the earthquake. In the table below, are shown the results of damage inspections done on the damaged building in Durres, Lezhe and Tirane by the Construction Institute of Albania. A total of 44582 building were inspected and as can be see below more then 1055 buildings in total were classified as DS4 and DS5, buildings that have serious damage on structural system.

Table 23: Number of buildings investigated by Construction Institute and damage state [Construction Institute of Albania, 2020]

City	DS0	DS1	DS2	DS3	DS4	DS5	Total
DURRES	**22605**	**2761**	**2384**	**1735**	**1855**	**626**	**31966**
Durres	13737	1801	1210	804	582	205	18339
Kruje	1672	529	582	454	690	137	4064
Shijak	7196	431	592	477	583	284	9563
LEZHE	**494**	**364**	**421**	**326**	**402**	**43**	**2050**
Kurbin	343	244	294	196	215	28	1320
Lezhe	150	110	112	126	166	9	673
Mirdite	1	10	15	4	21	6	57
TIRANE	**5651**	**1560**	**1258**	**737**	**974**	**386**	**10566**
Kamez	138	233	163	46	65	18	663
Kavaje	18	89	137	126	108	12	490
Tirane	207	528	481	348	458	60	2082
Vore	5288	710	477	217	343	296	7331
TOTAL	**28750**	**4685**	**4063**	**2798**	**3231**	**1055**	**44582**
	64%	11%	9%	6%	7%	2%	

As can be seen a very high % of the building stock was affected by the eqarthquake and also many buildings that are in-depth analysed on this study have suffered damage and even collapsed from this earthquake. A full damage investigation and evaluation will be given in detail in chapter VII.

CHAPTER 3

DESCRIPTION OF THE TEMPLATE DESIGN,

3.1 Masonry builfding stock and choosen templates

Masonry buildings occupy a considerable place in civil engineering of our country. They are built in different era and periods, from the 40s to the 90s of the XX century. Typical rural buildings in Albania are traditionally built with load bearing walls. The old Tirana building style for example it is characterized by the fire room in the middle as a nucleus, surrounded by other rooms. [AQTN, 1999] Masonry is one of the most used materials all around the world for low to medium rise buildings. In Albania it was used both for public and government buildings as a low cost method. Today these buildings are in use and mainly serve for residential purposes.

3.1.1 Historical features

Characteristic Albanian dwellings have been the result of architecture, economic, political and other historical factors. They had simple plans and the mainly necessary functional rooms. The buildings in cities like Berat, Scodra, Argirocasto had their own regional characteristics, with the so called cardak, which linked all the rooms in the building. After ottoman period, Albanian engineering and architecture due to political and economic factors was influenced mostly form Italian politics and architecture. In these years, Tirana, as the new capital of Albania was growing faster and some hoods were created from zero. Most of them were built with templates and types in series in different places. Palaces as the "Moskat" template were built in 1940 in the quarters between "Muhamet Gjollesha" street and "Sami Frasheri" street. [AQTN, 1999] During the communsit era, although the regime had many negative aspects in the development of the economy, the population in these years, doubled in size . These raised a great demand for new buildings and houses for the new residents of the state. The first buildings where constructed 1-2 story high with random materials. The first template design began in 1949 with two story high adobe buildings. Masonry buildings began in the early 50s and their height was not more than 5 stories in all the stock buildings. These because the technology of the time needed using elevators and producing them in Albania was not possible economically.During all this time till the late 80s, unreinforced masonry buildings of both silicate and clay bricks are the principal building type for residental buildings. After developments in civil engineering, but a crisis in economy of socialist republics, the building templates were also constructed of reinforced concrete skeleton. Masonry was used as a non load bearing material only for screening walls in the building. Later also major developments were implemented as use of slabs of pre-stressed reinforced concrete, or nuclei buildings with combined forms and variation.After the fall in communism in 1990 in Albania, civil engineering boomed over other aspects of the economy. A massive immigration of the population from rural areas, to the urban area happened right after the regime fall. Massive population raise in city such as Tirana or Durres and also opening of economy implied a great demand for shops and stores. Although new buildings were constucted with reinforced concrete beam- columns load bearing system, at this era, very much interventions are done to the existing buildings, especially the ones near main roads. Interventions like openings on the first floor are done in many cases without a civil engineer and a proper project. Also added floor and side addings are very popular among masonry stock buildings. These interventions have serious impact on lowering the buliding capacity, not to mention the degradation and other factors.

3.1.2 Template design

The beliefs of the regime were also projected in the buildings body. The institutes and government made laws for equality and standardization. [Bego M., 2009]

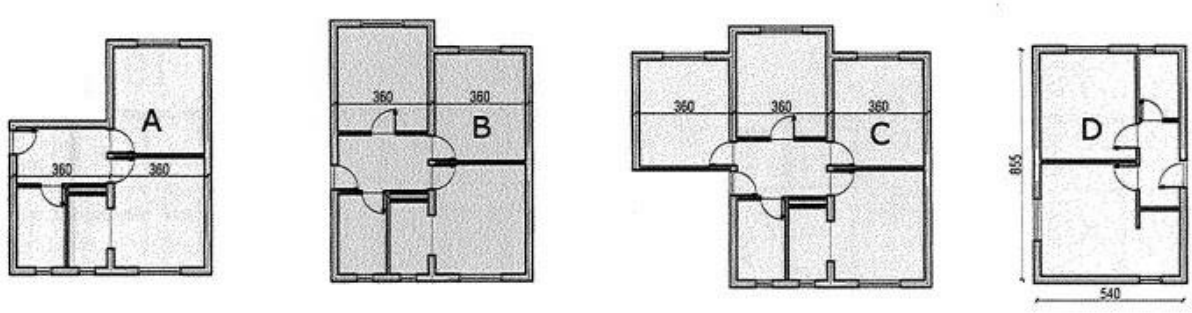

Figure 31: Apartment section types approved by the state [Bego M., 2009]

So buildings were made by combination of standard apartments approved. The sections projected economy and development over time. The first sections of pre 60s era, where with smaller apartments accepting the standard 2 room and kitchen one for housing two families.Then since the kitchen was the most frequented part of the house was accepted the rise of $10m^2$ area, and then an annex within the kitchen. After the year 1965 new technologies and developments were available and the light space was available to 5.4m - 6m. Till the beginning of the 70s, several templates where proposed, with more comfortable plans for living having 3 to 4 apartments and with light space 5.4m with longitudinal sustaining walls for a lighter structure. In the years that passed, the sector of characterisation in the institute, prepared brochures every year with template section to be used in construction. The first batches date back to 1959, with building up to 4 stories and templates similar to one another. Second batches than on 1972 with building up to 5 stories. Than more on 1978, 1983 and continued till 1989 when this sector approved new types with the new updated codes of the year. The template design of the era, makes easier the problem of studying the building stock, because some template are more populous and most used among others. Many buildings in Kombinat, Tirana, for example, were designed using the standard template 77/5.

3.1.3 Classification of masonry building stock

The basis of classification for masonry structures are determined by four pillars: time of construction, height of building, material used and building location.

3.1.3.1 Classification by time of construction

From time of construction buildings are classified mainly by the code that are projected. They can be classified as below:

-Buildings constructed before 1963: Based on prior experience, no seismic evaluation

-Buildings constructed from 1964 to 1978: Based on KTP-63, very low seismic consideration

-Buildings constructed from 1979 to 1990: Based on KTP-78, low seismic consideration

-Buildings constructed after 1991: Based on KTP-89, small population of buildings with load bearing masonry walls.

The choosen templates in the thesis are named A before 1963, B from 64 to 78 and C from 79 to 90.

3.1.3.2 Classification by height

The classification of height is based on the number of stories each building has. The Albanian building stock has maximum 6 story buildings with load bearing masonry walls. Most of the buildings prior of KTP-63, were no more than 4 stories, and later up to 5. In many buildings problem are the added stories, that imply an increased seismic demand, with all the deficiency that KTP-78 itself has. The tallest buildings are the ones, in wich is excpexted more damage and risk in seismic scenario.

3.1.3.3 Classification by material of construction

By the materials used these buildings can be classified in two major groups, unreinforced masonry and confined masonry. Unreinforced masonry are most common and before KTP-78, very few buildings had confinement columns, on the load bearing walls. These buildings are of both clay bricks masonry and silicate brick masonry. Buildings with clay brick masonry perform more resistent to atmospheric agents comparing to silicate ones. For the compressive strength of the bricks used on most of the stock the clay bricks are with $f_k = 7.5\text{MPa}$, meanwhile the silicate bricks used have more compressive strength $f_k = 10\text{MPa}$ on most of the buildings. Mortar strength also varies and mostly are used cement or lime mortar with $f_k = 2.5\text{MPa}$ and $f_k = 5\text{MPa}$. The bonding between clay and mortar is better than silicate-mortar, giving so a greater value of f_{vk} shear strength of masonry. The confined masonry buildings are of the 1978 to 1990 era, and have perimeter columns of C12/15 for increasing lateral resistance of the shear walls. Also the slab types varies on buildings and era of construction but most of them are rigid slabs of reinforced concrete. Foundation are constructed with stoned of M>200 and are calculated for [σ]=2kg/cm2.

3.1.3.4 Classification by location

Location of the buildings affects many factors of the performance of the buildings. Site conditions, climatic effects and seismicity of the zone as the most governing factor. Albania can be divided in three zones, from the seismic risk, where the intensity scale of projection varies VI, VII and VIII. Also some zones where considered with lower seismic intensity in KTP-63 and KTP-78, implying a lowered seismic consideration on projection. This topic will be discussed later on this chapter.

3.1.4 Choosen template buildings

The templates are choosen based on the above classification. The population of each template is the basic criteria, but also template are choosen to represent all the material types that are used in the stock, all the building heights on each era they are built, and also the ones that are distributed mostly in all cities of the country. Also some templates that have irregular shapes and verified seismic deficiency have been taken in consideration. For each choosen template are given at least 4 buildings in different locations, and also are highlited some of them, that have interventions like added stories or openings on first floors. In total are choosen 10 templates, and 19 buildings from these templates are analyzed later.

3.1.4.1 A1 Template

This template is the oldest in the list of the year 1940, but the buildings are near the "ish blloku" zone in Tirana, and they are well maintenied and interventions are done with project so no severe damage is observed. The buildings have plan dimensions of (56.65*11.65)m. Building has two entrances, four apartments and is symmetric. In the template project, it was projected for two stories of 2.8m height. In some of the buildings of this template are built extra stories later, after the 90s period (the MOSKAT buildings in Tirana). Inside and outside walls of the building are 25cm and non load bearing walls are 12cm. For masonry are used clay bricks of strength 5MPa as given in the project. The mortar used is lime mortar as defined in the project with ratio 1:3 (lime : sand). Specifications of the mortars and the procedure of preparing are given in K.Cika "Cement and concrete" [K.Cika, 1969]. For 1m3 sand is used 0.333m3 lime and 200liters water

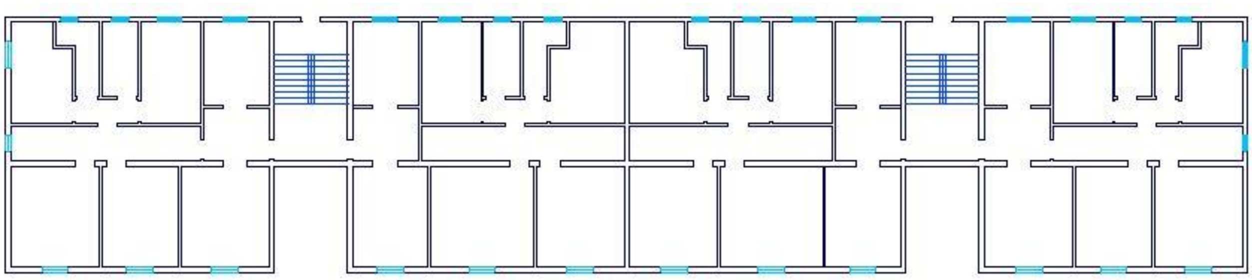

Figure 32: Template A1 plan view [AQTN, 2018]

Three buildings are choosen of this template with 2 floors, 3 floors and 4 floors. In the latest two, additional floor were added later.

3.1.4.2 A2 Template

This template is of year 1958, reffered as 58/2 in the manual of Construction Institute. The building representing this template is located at "Sulejman Delvina" street in Tirana. The buildings has plan dimensions of (26.94*12.14)m. Inside and outside walls of the building are 25cm, with red clay bricks M-75 and lime mortar M-25. Non sustaining walls are 12cm. Slabs and beams are of mounting panels. Foundations are made with concrete, under the sustaining walls, and of bricks under the non sustaining walls. Reinforced concrete belts are added to the sustaining walls in the pavement and ceiling level. The mortar used in masonry is mixed mortar as defined in the project with ratios 1:0.7: 5.80 (cement: lime: sand). For 1m3 sand is used 0.122m3 lime, 145kg cement of 20MPa and 200liters water. Two buildings of these template are taken in consideration, one with seismic divide and one without.

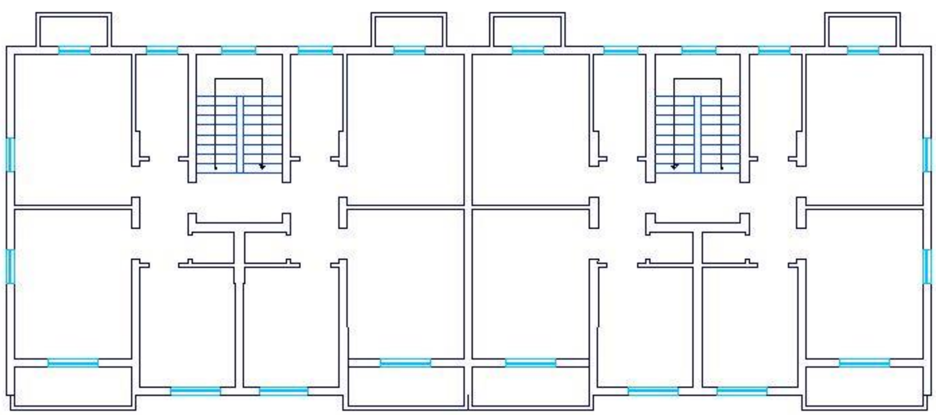

Figure 33: Template A2 plan view [AQTN, 2018]

3.1.4.3 B1 Template

This template is of year 1963, reffered as 63/1 in the manual of Construction Institute. The building representing this template stock is located near Lapraka in Tirana. In this hood are 3 buildings of this type. The specimens are taken from one building that is very much damaged and degraded. The template 63/1 is for three story buildings and has a (21.85*10.07) m plan dimension, symmetric in one direction and a story height 285cm. Total height of the building is 840cm. The load bearing walls have a thickness of 25cm in all three stories. The walls are masonry with solid red clay bricks of M75 with strength 7.5MPa.The mortar used in this building is lime mortar with ratio 1:2 (lime : sand). For 1m3 sand is used 0.5m3 lime and 200liters water. There are 2 buildings of these type, the first with 3 floors and second with one additional floor added later.

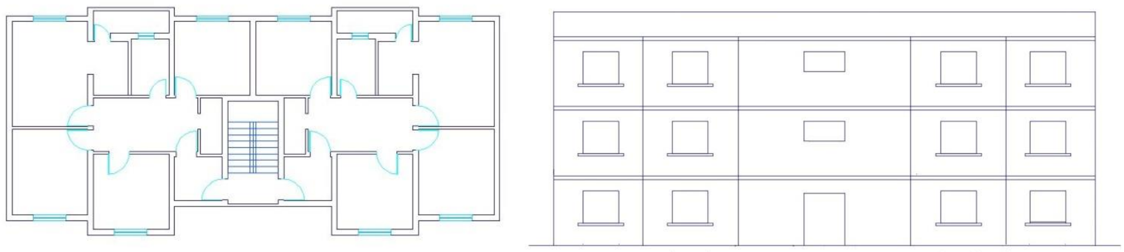

Figure 34: Template B1 plan and façade view [AQTN, 2018]

3.1.4.4 B2 Template

This template is of year 1963, reffered as 69/3 in the manual of Construction Institute. The building chosen from this template is located in Corovode, near Berat .The template 69/3 has plan dimensions of (15.44*13.49) m and a nearly square form.

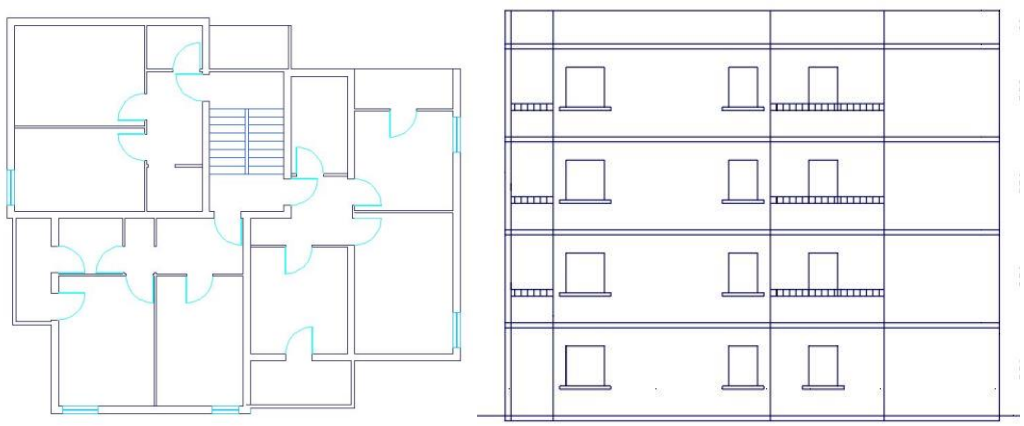

Figure 35: Template B2 plan and façade view [AQTN, 2018]

The buildings has 4 floors with story height of 285 cm. Load bearing walls are of silicate bricks M-75 and mortar M-25. The first and second floor walls are 38cm and third and fourth floor of 25cm. Non load bearing walls are 8cm thick with hollow bricks. The mortar used in this building is mixed mortar with ratio 1:0.7:8.8 (cement: lime: sand). For 1m3 sand is used 145kg cement M200, 0.124m3 lime and 200liters water. There are two buildings of these type, one with regular wall width, and one with 38cm wall in all stories. These building is located in Kukes, and this solution is done for climatic issues.

3.1.4.5 B3 Template

This template is of year 1972, reffered as 72/1 in the manual of Construction Institute. The building chosen for the tests is Elbasan near "28 Nentori" street. This building has plan dimensions of (18.32*12.43) m. Its 5 story high with 285cm height for each story. The sustaining walls are built with clay bricks M75 (strength 7.5 MPa). The mortar is M25 of strength 2.5MPa. The wall thickness is 38cm in the first and second floor, than 25cm on the remaining. The partition walls are with hollow clay bricks. The concrete corner columns and slabs are constructed with M150 concrete. The foundations, also performed with mass concrete 10MPa. Mortar used in this building is cement mortar with ratio 1:5.20 (cement: water). For 1m3 sand is used 190 kg cement M200, and 170 liters water. There are two buildings of the template both 5 floors but in one interventions are done in first floor.

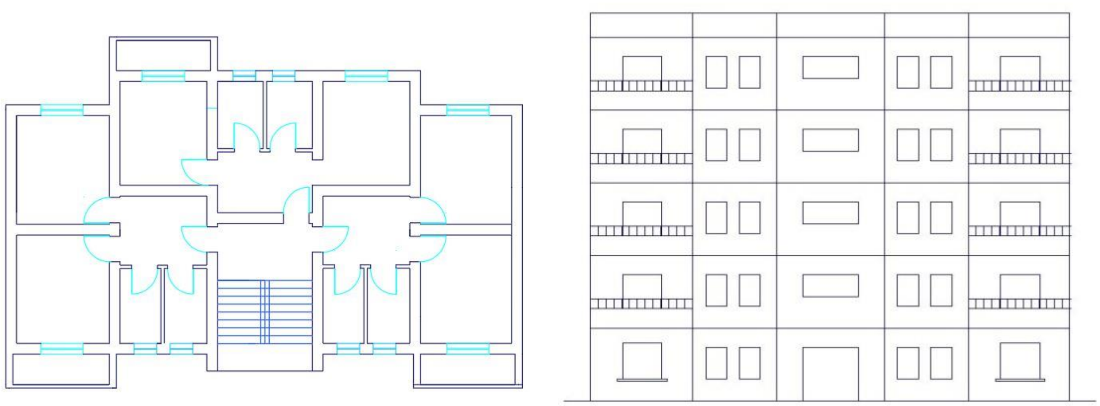

Figure 36: Template B3 plan and façade view [AQTN, 2018]

3.1.4.6 B4 Template

This template is of year 1972, reffered as 72/3 in the manual of Construction Institute. The building chosen from this template is located in Porcelan, Tirane Plan dimensions of the building are (21.12*17.12) m. Its 5 story high with 285cm height for each story. The sustaining walls are built with silicate bricks M75 (strength 7.5 MPa) and mortar M50 of strength 5MPa. The wall thickness is 38cm in the first and second floor, than 25cm on the remaining. The partition walls are with hollow clay bricks. The concrete corner columns and slabs are constructed with M150 concrete. The foundations, also performed with mass concrete 10MPa. Mortar used in this building is cement mortar with ratio 1:4.80 (cement: water). For 1m3 sand is used 260 kg cement M300, and 170 liters water.

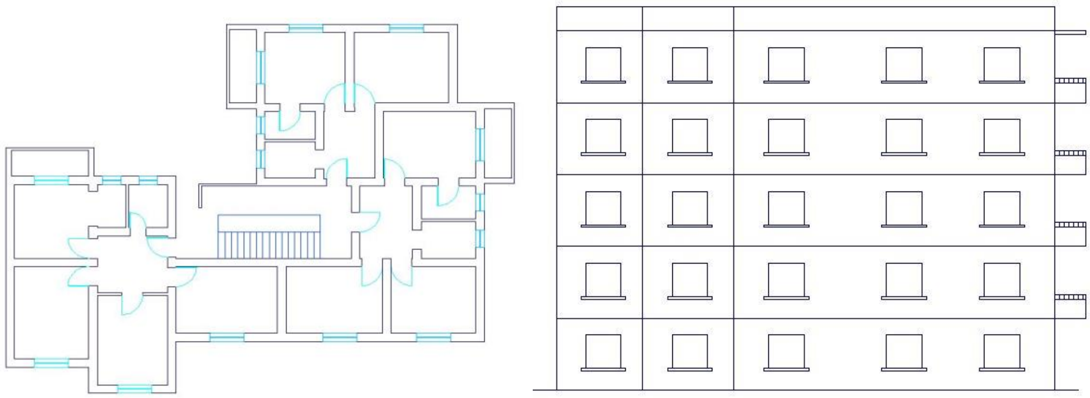

Figure 37: Template B4 plan and façade view [AQTN, 2018]

3.1.4.7 C1A and C1B Template

This is the most used template in our country and two buildings are chosen for the two types of materials. One building is located in Tirana near "Rruga e Kavajes" (clay bricks). The template 77/5 was projected for seismicity of 7 and 8 scale. The masonry is constructed with two types of bricks: red bricks of M-75 and mortar M-50, silicate bricks M-100 and mortar M-50. Mortar used in our building is cement mortar with ratio 1:4.80 (cement: water). For 1m3 sand is used 260kg cement M300, and 170liters water. Non sustaining walls have bricks with openings and mortar M-15. Lintels are realized with reinforced concrete, and slabs with reinforced ceramics, and concrete M-200. Foundation are realized with stones of M>200 and are calculated for [σ] = 2kg/cm2. There are four buildings of these template C1A 5 floor with clay building, C1A with intervention in first floor, C1B with 5 floors with silicate buildings and C1B 6 floors, with one added floor later.

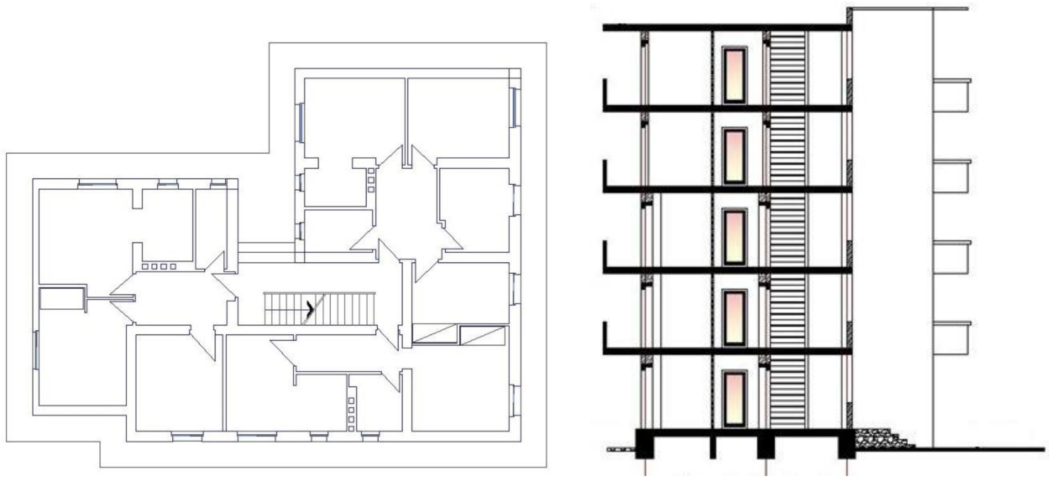

Figure 38: Building C1 plan view and facade view [AQTN, 2018]

3.1.4.8 C2 Template

This template is of year 1983, reffered as 83/3 in the manual of Construction Institute. The building chosen from this template is located in Tirana at "Ali Demi". The template 83/3 has plan dimensions of (24.44*9.04) m. Its 5 story high with 285cm height for each story. The sustaining walls are built with clay bricks M-75 (strength 7.5 MPa) and mortar M-25 of strength 2.5MPa. The mortar used in this building is mixed mortar with ratio 1:0.7:8.8 (cement: lime: sand). For 1m^3 sand is used 145kg cement M200, 0.124m3 lime and 200 liters water. The wall thickness is 38 cm in the first and second floor, than 25 cm on the remaining. The partition walls are with hollow clay bricks. There are two buildings of these type, one with 5 floor and the other with additional floor added later.

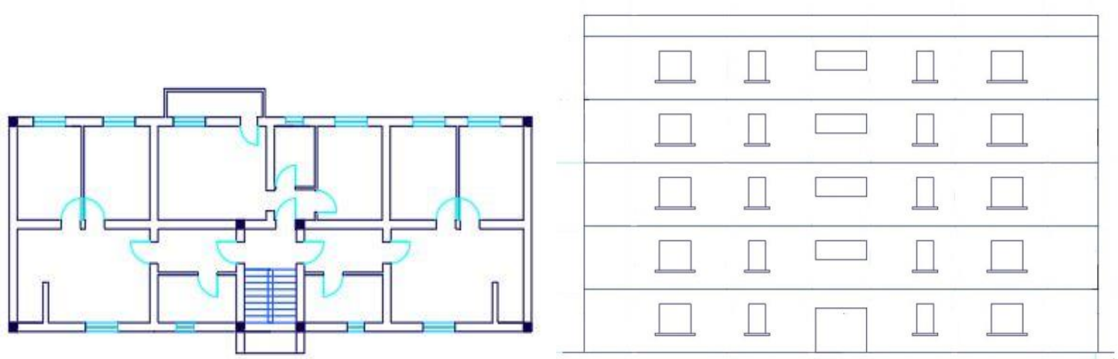

Figure 39: Building C2 plan view and facade view [AQTN, 2018]

3.1.4.9 C3 Template

This template is of year 1983, reffered as 83/10 in the manual of Construction Institute.

The building chosen from this template is located in "Andon Profka" street in Fier. The template 83/10 was calculated for terrain with strength $[\sigma] = 2\mathrm{kg/cm^2}$ and seismicity VII-VIII scale. The building has 5 floors with dimensions in plan (20.64*17.6) m. The slabs are of pre-stressed concrete span less than 420cm and reinforced concrete for span more than 4.4m.The masonry is realized with red clay bricks M-75 and mortar M-50. Mortar used is cement mortar with ratio 1:3.40 (cement: water). For 1m3 sand is used 370 kg cement M300, and 170 liters water. The non sustaining walls are with bricks with openings (8-12) cm and mortar M-15, as given by the project.

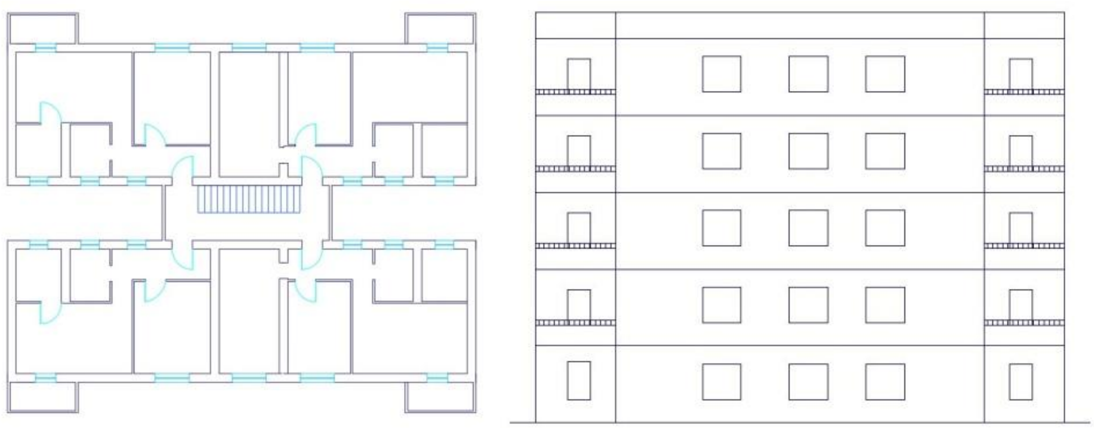

Figure 40: Building C3 plan view and facade view [AQTN, 2018]

3.1.4.10 Choosen buildings

In total are choosen 19 building from the templates above. From the first period before 1963 era are in total five buildings, three of them of template A1, one original and the others with one and two added floors. The buildings of template A2 comprise two story buildings, one with seismic divide and the other without. From the second period 1963-1978 era, are choosen seven buildings from the four templates with different heights, different materials and different issues such as intervention or added stories. From the third era, after 1978 are choosen seven buildings of three different templates, where the most are of C1 template. This buildings are the highest in height, with five and six story high. In the table below are summarized the basic charcteristics of each building.

Table 24: Summary of the studied buildings and their properties

Building	Height	Brick	Mortar	Time of construction	Issues
A1	2 stories	clay M-5	lime M-2.5	1940	-
A1 3fl	3 stories	clay M-5	lime M-2.5	1940	1 added story
A1 4fl	4 stories	clay M-5	lime M-2.5	1940	2 added story
A2	2 stories	clay M-7.5	mixed M-2.5	1958	no seismic divide
A2 half	2 stories	clay M-7.5	mixed M-2.5	1958	with seismic divide
B1	3 stories	clay M-7.5	lime M-5	1963	-
B1 4fl	4 stories	clay M-7.5	lime M-5	1963	1 added story
B2	4 stories	silicate M-7.5	cement M-2.5	1969	-
B2 38cm	4 stories	silicate M-7.5	cement M-2.5	1969	projection deficiency
B3	5 stories	clay M-7.5	cement M-2.5	1973	-
B3 int	5 stories	clay M-7.5	cement M-2.5	1973	intervention first floor
B4	5 stories	silicate M-7.5	cement M-5	1973	-
C1A	5 stories	clay M-7.5	cement M-5	1978	-
C1A int	5 stories	clay M-7.5	cement M-5	1978	intervention first floor
C1B	5 stories	silicate M-10	cement M-5	1978	-
C1B 6fl	6 stories	silicate M-10	cement M-5	1978	1 added story
C2	5 stories	clay M-7.5	mixed M-5	1983	-
C2 6fl	6 stories	clay M-7.5	mixed M-5	1983	1 added story
C3	5 stories	clay M-7.5	cement M-5	1983	-

CHAPTER 4

ANALYTICAL MODELLING AND ASSESSMENT

4.1 Non-linear modelling of masonry buildings

Modelling of masonry structures has always been a difficult problem because of the presence of joints as the major source of weakness and also nonlinearity and discontinuity of the material. A proper model must take in consideration both the behaviour of brick and mortar units and the interaction between them.

4.1.1 Macro modelling techniques

In this technique the materials are not modelled as divided elements, but with equivalent elements (like plates for example) that have equivalent properties. No distinction are made between the individual units and joints, and masonry is taken in account as a homogenous, isotropic or anisotropic continuum medium. The influence of existing mortar joints is the major source of weakness of this approach and nonlinearity cannot be taken in consideration.

4.1.2 Micro modelling techniques

Micro-modelling is a more detailed type of modelling. Properties of both units and mortar are used and crack patterns are defined prior to the analysis. This technique uses a finite element methodology. Units and mortar in joints are represented by continuum elements, and the unit-mortar interface is presented by discontinuum element. This model leads to more accurate results, but is more computationally intensive.

4.1.3 Meso modelling techniques

- Meso-modelling is a balanced approach between the two first. This technique can also be understood as a simplified micro-modelling. The bricks are represented by continuum elements with the same size as the original bricks dimension plus joint thickness. The mortar joint is modelled with zero thickness and the interface stiffness is deduced from the stiffness or real joints. This approach leads to the reduction of the computational effort. More information is given in chapter II about this topic.

4.1.4 Tremuri modelling methodology

3muri is based on a finite element methodology for modelling masonry structures. The software proposes the line finite element, which is represented by its axis. The non-linear macro-element model, representative of a whole masonry panel, proposed by Gambarotta and Lagomarsino, permits with a limited number of degrees of freedom,to represent the two main in-plane masonry failure modes, bending-rocking and shear-sliding (with friction) mechanism, on the basis of mechanical assumptions.[Gambarotta L. et.al., 1996] A wall consist of three parts: axial deformability which is concentrated in the two extremity elements, of infinitesimal thickness D, infinitely rigid to shear actions. The tangential deformability is situated in the central body, of height h, which is non-deformable axially and in flexure.

4.1.5 A detailed tremuri modelling example

The first step of software modelling is drawing the perimeter and inside walls of the building. This can be done manually in the program, but the easiest way is two import the plan view from the .dxf file version generated with Autocad. In the plan view, the walls are represented only by its axis line. The thickness of walls and opening are generated later by specific commands on the software. The non-sustaining walls are deleted from the first drawing, because they do not contribute in the stiffness of the structure, but they are taken in consideration as additive gravitational loads, when modelling the slabs.

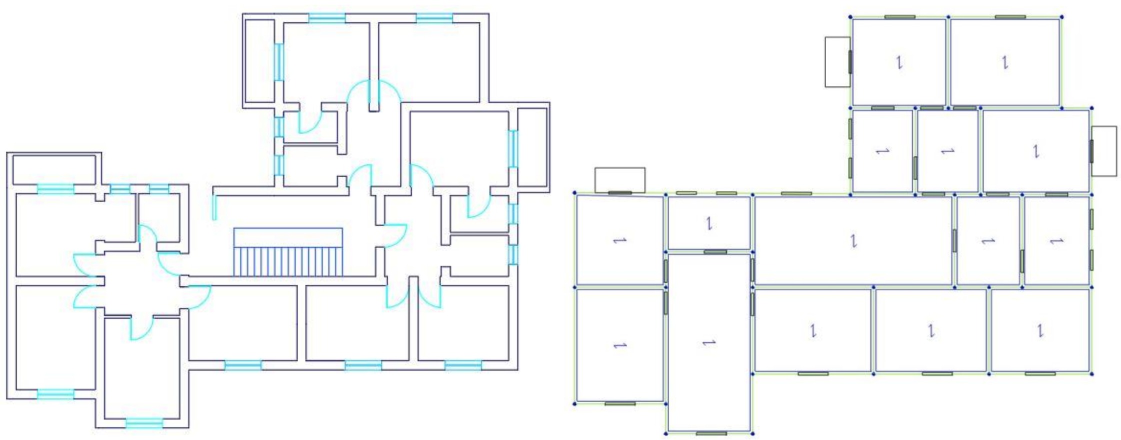

Figure 41: B4 Building plan view in Autocad and model plan view in 3muri

After the import of .dxf drawing, with the insert wall command, each structural wall is inserted using the plan and intersections between axis lines. Walls should be inserted with the perimeter nodes, and the software automatically generates joints in points of wall intersections with each other. Next in the section structure of the software, firstly for the walls with draw opening command, are created the openings (spaces) of the walls in part when they are windows or doors. After this in the materials sections, are defined the masonry material characteristics, according to Turnsek-Cacovic or EC, as discussed in chapter II. Slabs are defined with the draw floor command and selecting rigid floor, if the slab can be considered as a rigid diaphragm, or the slab type like r.c. concrete with masonry infills, depending to the slabs of the real building. For model B4 slabs are modelled as r.c. concrete with masonry in-fills with slab parameters $b = 10cm, h = 15cm, i = 50cm, s = 5cm$, $E_{conc} = 15000N/mm^2$, addition load from partition walls $1.3kN/m^2$an probable live load $2kN/m^2$ as defined in EC.

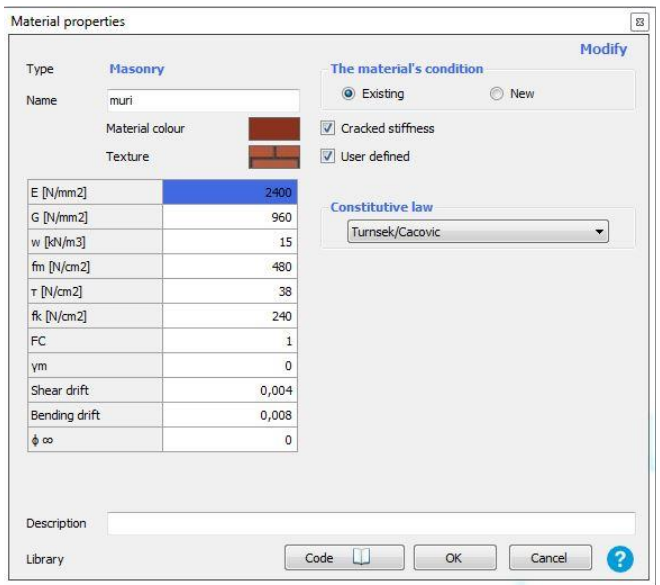

Figure 42: Masonry properties for building B4

Balconies are added with the insert balcony command with their geometry and characteristics. The additive loads of non-load bearing walls can also be add using the command insert loads and adding them in the plan in their original, rather than adding them as additive loads to the slabs.With the insert wall segment attributes, all the walls are selected and are inserted the material properties as defined before, and the wall section thickness and height.

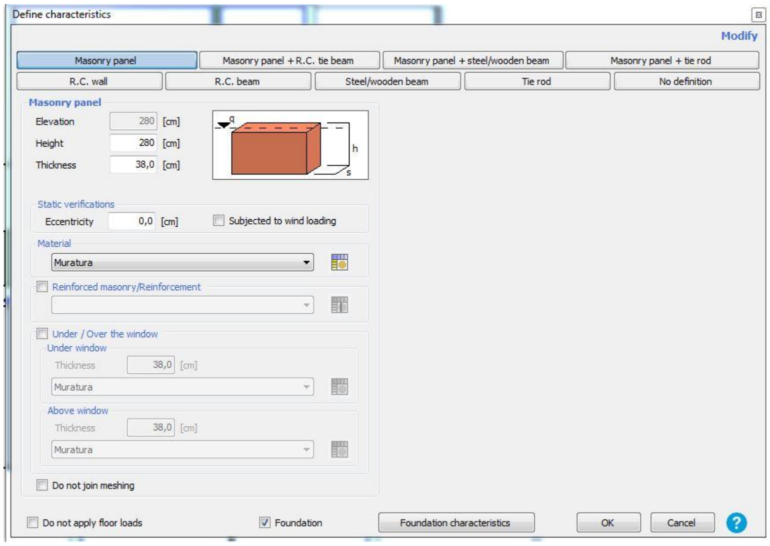

Figure 43. Masonry walls segment attributes

Walls are considered as layered non-linear materials according to Turnsek-Cacovic approach as defined in EC-6 Also the foundation types can be selected within this command, and are considered pinned for the B4 building. Next the level management command is used to duplicate the floors, with the same characteristics, as the first floor, and also defining their height. For the third, fourth and fifth floor the insert wall segment attributes is repeated, because of the thickness reduction in upper floors.

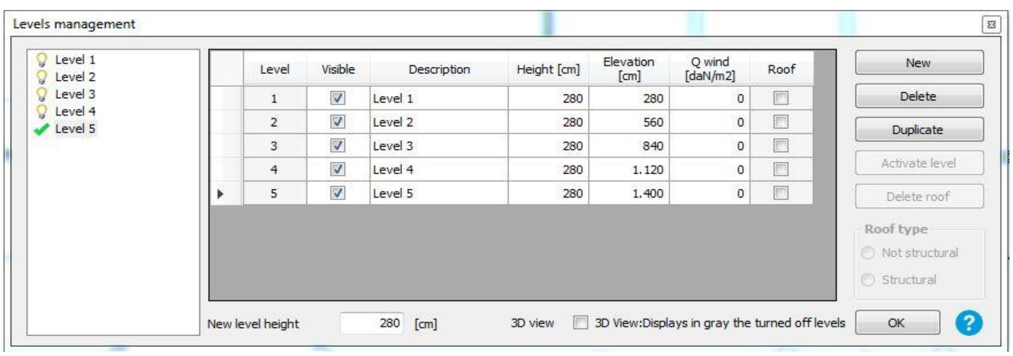

Figure 44: Level management of building

In the end the compute model mesh, creates the mesh of the program and makes it ready for analysis and also checks the model for discontinuities. Also the global static verification can be made in this moment to verify the building from gravity loads.

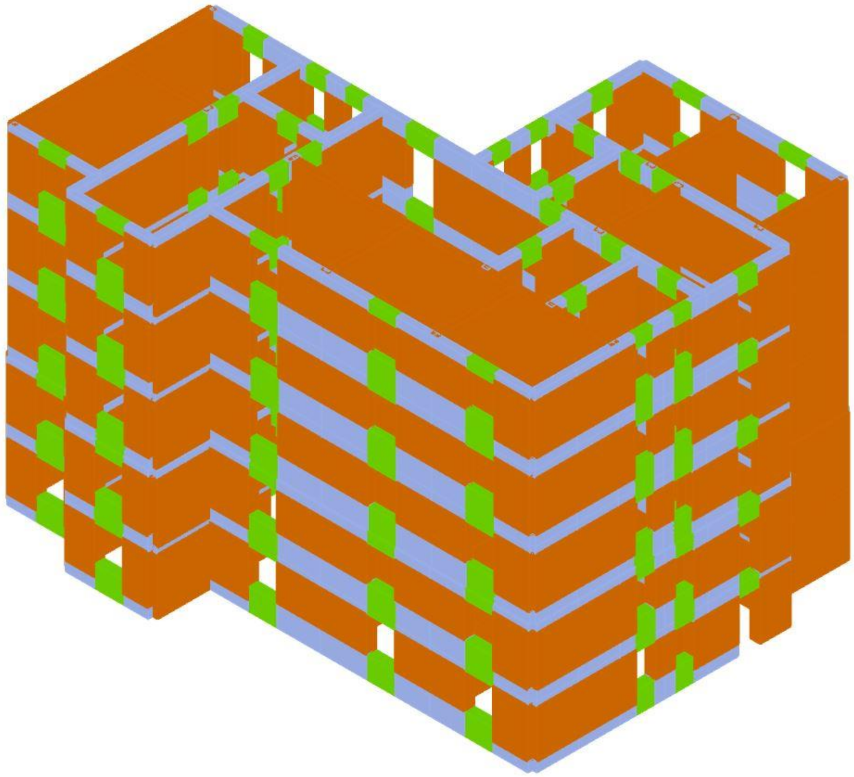

Figure 45: Model and meshing of building B4

After the modelling generation a global static verification can be generated, for verifying the system from static loads and combinations of EC. (1.35G). If any value is not proper, is shown in the element and the properties that should be changed, in local or global level.

Modal analysis also can easily be generated using 3muri. The differential equation [9], induced by an earthquake motion to a MDOF is as below:

$[M]\{\ddot{U}\} + [C]\{\dot{U}\} + [K]\{U\} = -[M]\{l\}\ddot{u}_g$ (60) where:

$[M]$ - mass matrix $[C]$ - damping matrix $[F]$ - storey force vector

$\{l\}$ - influence vector charactering displacement of masses when a unit ground is statically applied $\ddot{u}_g$ - the ground acceleration history

By assuming a single shape vector, $\{\phi\}$, which is independent of time, and defining a relative displacement vector, U, of the MDOF system as

$U = \{\phi\}u_t$ where u_t denotes the top roof displacement, the governing differential equation of the system is transformed to:

$[M]\{\phi\}\ddot{u}_t + [C]\{\phi\}\dot{u}_t + [K]\{\phi\}u_t = -[M]\{l\}\ddot{u}_g$ (61)

To define the modal matrix $\{\phi\}$ firstly is done a free vibration modal analysis. This analysis is done to define the natural frequency of vibration ω_i for every mode, and the modal shapes $\{\phi\}_i$. The equation that is used for defining the $\{\varphi\}_i$ vector is

$([k] - \omega_i^2[m]) * \{\varphi\}_i = 0$ (62) but firstly are calculated the frequencies for each mode from: $\det\left|[k] - \omega_i^2[m]\right| = 0$ (63)

Table 25: Period and mass participation of first 12 modes for building B4

Mode	T [s]	mx [kg]	Mx [%]	my [kg]	My [%]	mz [kg]	Mz [%]
1	0.25938	64268	4,60	970987	69,49	13	0,00
2	0.23303	894028	63,98	58016	4,15	64	0,00
3	0.20304	101428	7,26	9068	0,65	66	0,00
4	0.09349	14444	1,03	242253	17,34	163	0,01
5	0.08745	205358	14,70	14202	1,02	1557	0,11
6	0.07753	11555	0,83	302	0,02	5845	0,42
7	0.06762	185	0,01	110	0,01	1063210	76,09
8	0.06506	1984	0,14	2407	0,17	24767	1,77
9	0.06099	116	0,01	264	0,02	356	0,03
10	0.05625	5501	0,39	6	0,00	2184	0,16
11	0.05542	372	0,03	2716	0,19	13521	0,97
12	0.05198	1186	0,08	32432	2,32	683	0,05

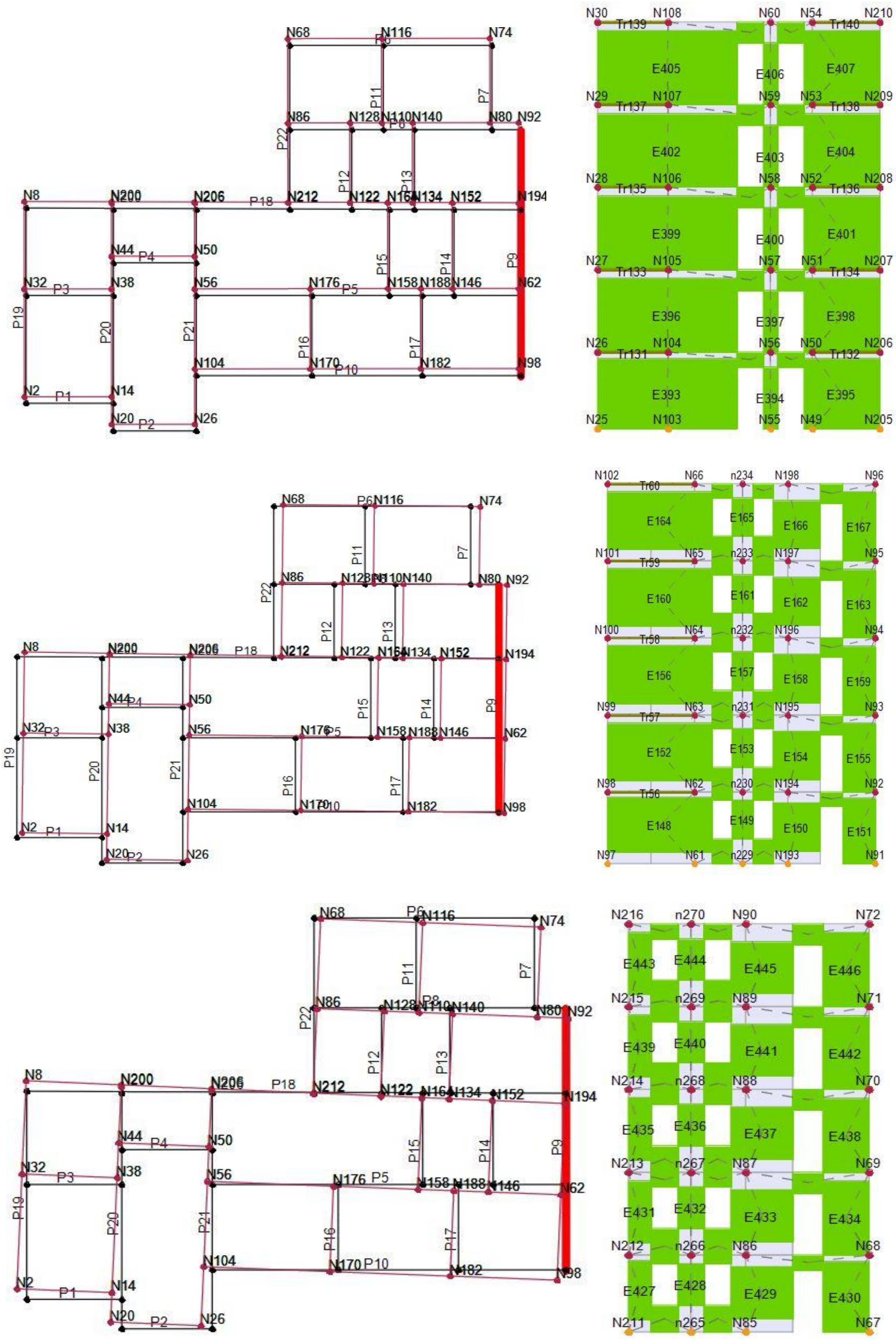

Figure 46: Plan and walls deformed shape for first three modes of vibration

4.2 Determination of the mechanical characteristics of the materials of masonry structures

To proper determine the mechanical properties of the masonry buildings two different approaches are followes. Firstly as given in chapter 2.5, the mechanical properties are calculated from the project blueprint values, and the correlation given in EC-6 [EN 1996-1, 2005]. Secondly, because this buildings are of 50 years old and more and the degradation of materials, especially mortar, six tests are performed on each building and the values are revised. The mimum of the compressive and shear strength from the first and second approach is taken in consideration in the building model later. The results for each building are presented below.

4.2.1 Mechanical properties of the studied buildings from the project blueprints

For the load-bearing masonry walls of the studied templates above, are given the parameters of the used materials. The parameters needed for numerical modeling, are calculated from the correlation of EC.The values of compressive and tensile strength are shown in the table below. This values are for the load bearing walls.

Table 26: Brick and masonry parameters from project blueprints

Building Template	**Brick properties**			**Mortar properties**		
	Type	f_b $[MPa]$	f_{bt} $[MPa]$	Type	f_m $[MPa]$	f_{mt} $[MPa]$
A1	Clay	5	0.5	Lime	2.5	0.25
A2	Clay	7.5	0.75	Mixed	2.5	0.25
B1	Clay	7.5	0.75	Lime	2.5	0.25
B2	Silicate	7.5	0.75	Cement	2.5	0.25
B3	Clay	7.5	0.75	Cement	2.5	0.25
B4	Silicate	7.5	0.75	Cement	5	0.5
C1	Clay	7.5	0.75	Cement	5	0.5
C1'	Silicate	10	1	Cement	5	0.5
C2	Clay	7.5	0.75	Mixed	2.5	0.25
C3	Clay	7.5	0.75	Cement	5	0.5

From this values, are calculated the masonry properties that are needed for numerical modeling of these buildings. These value will be revised later after the testing procedure of the chosen buildings from each template.Compressive strength of masonry is calculated by the EC-6 [EN 1996-1, 2005] recommendation:

$f_k = K * f_b^{0.7} * f_c^{0.3}$ (64) (values of f_b and f_m are normalized with δ factor)

Young modulus $E = 1000 * f_k$ (65)

Compressive fracture energy $G_{fc} = 15 + 0.43 * f_k - 0.0036 * f_k^2$ (66)

Tensile strength $f_t = 0.05 * f_k$ (67)

Tensile fracture energy $G_f = 0.1MPa$ (68)

Shear strength $f_{vk} = f_{vko} + 0.4\sigma_d$ (69)

$f_{vko} = 0.2$ (70) when clay bricks are used or silicate bricks M-10

$f_{vko} = 0.15$ when silicate bricks M-7.5 used as recommended in EC,

the maximum value of $f_{vk} = 0.065 f_b$ $\sigma_d = 1MPa$

$f_{xk1} = 0.035 f_b$ with filled and unfilled perpendicular joints

$f_{xk2} = 0.035 f_b$ (71) with filled perpendicular joints $f_{xk2} = 0.025 f_b$ with unfilled perpendicular joints

Shear modulus $G = 0.25E$ (72) Poisson ratio $\nu = 0.2$

Table 27: Calculated parameters from the projected building characteristics

Building Template	f_k [MPa]	f_{vk} [MPa]	f_{vk0} [MPa]	f_t [MPa]	f_{xk1} [MPa]	f_{xk2} [MPa]	E [MPa]	G [MPa]	G_{fc} [MPa]	ν
A1	1.49	0.325	0.15	0.07	0.175	0.13	1490	373	2.38	0.2
A2	1.97	0.4875	0.2	0.1	0.26	0.19	1977	494	3.16	0.2
B1	1.97	0.4875	0.2	0.1	0.26	0.19	1977	494	3.16	0.2
B2	1.97	0.4875	0.15	0.1	0.26	0.19	1977	494	3.16	0.2
B3	1.97	0.4875	0.2	0.1	0.26	0.19	1977	494	3.16	0.2
B4	2.43	0.4875	0.15	0.12	0.26	0.19	2430	608	3.89	0.2
C1	2.43	0.4875	0.2	0.12	0.26	0.19	2430	608	3.89	0.2
C1'	2.97	0.65	0.2	0.15	0.35	0.25	2970	744	4.76	0.2
C2	1.97	0.4875	0.2	0.1	0.26	0.19	1977	494	3.16	0.2
C3	2.43	0.4875	0.2	0.12	0.26	0.19	2430	608	3.89	0.2

For building A2 masonry properties:

$f_b = \mathbf{7.5}\boldsymbol{MPa}$ clay bricks, $f_m = \mathbf{2.5}\boldsymbol{MPa}$ mixed mortar

$f_k = K * f_b^{0.7} * f_c^{0.3} = 0.6 * (0.8 * 7.5)^{0.7} * (0.85 * 2.5)^{0.3} = \mathbf{1.977}\boldsymbol{MPa}$

$f_{vko} = \mathbf{0.2}\boldsymbol{MPa}$ clay bricks are used,

$f_{vk} = f_{vko} + 0.4\sigma_d = 0.2 + 0.4 * 1 = 0.6MPa,$

$f_{vk} = 0.065 f_b = 0.065 * 7.5 = \mathbf{0.4875}\boldsymbol{MPa}$

$f_{xk1} = 0.035 f_b = 0.035 * 7.5 = \mathbf{0.26}\boldsymbol{MPa},$ $f_{xk2} = 0.025 f_b = 0.025 * 7.5 = \mathbf{0.19}\boldsymbol{MPa}$

$E = 1000 * f_k = 1000 * 1.97 = \mathbf{1977MPa,}$

$G = 0.25E = 0.25 * 1970 = \mathbf{494}\boldsymbol{MPa}$

$G_{fc} = 15 + 0.43 * f_k - 0.0036 * f_k^2 = 15 + 0.43 * 1.97 - 0.0036 * 1.97^2 = \mathbf{3.16}\boldsymbol{MPa}$

$G_f = 0.1MPa, \ \ \nu = 0.2$

4.3 Theoretical basics of performed laboratory tests

Assessment of an existing building, requires a proper investigation of the template. Geometry of the building and material properties are the basics for every modelling technique, implementing element, piers and global properties of the structure. Recommendations from the codes, and also testing methods are available for representing the real performance of masonry.

4.3.1 Methodology of investigation and characterisation

For investigation and characterisation of the structures is followed the methodology presented in ICOMOS-Recommendations for Heritage [IOCOMOS, 2003].

This methodology is divided in two phases:

Knowledge phase:

-historical investigation (obtaining the project of the structure and checking for interventions during time)

-description of the building (analysis of elements for geometrical and material properties)

-survey and description of the damage (possible causes of observed damage if any)

- in-situ and laboratory tests (characterisations of material and structural behaviour through experimental tests)

Numerical phase:

Modelling of the structure in the most effective approach.

4.3.2 Laboratory tests

The laboratory tests are done to the guidance of EC and ASTM codes [EN1052, 1998; ASTM C109, 2008]. They are divided in three basic sections:

- the brick tests - the mortar tests - the masonry prism tests

The tests are done to compare the values of the project with the real values from the tests. This because many buildings are built before 50 or more years and materials are degraded with time. EC and ASTM give reccomendations and correlations for defining masonry characteristics from the brick and mortar properties, but prism test are also done to verify this values.

4.3.2.1 Brick tests

ASTM C67-09 [ASTM C67-09, 2008] gives the procedure as follows, fkor the determination of the solid brick compressive strength:

Five specimens of dimension (250*125*60) mm should be tested. The test specimens should consist of dry half bricks, full height and width of the unit, with length equal to one half the full length of the unit. The units are tested flat-wise, the load should be applied perpendicular to the bed surface of the brick in the stretcher position. They should be centred under the spherical upper bearing. The load is applied up to one half of the expected maximum load, at any convenient rate, after which, the controls of the machine should be adjusted so that the remaining load is applied at a uniform rate.

Figure 47: Brick compression test

The compressive strength of each specimen is calculated: $C = W/A$ (73)

C - compressive strength of the specimen (kg/cm2)

W - maximum load

A - average area of the gross areas of the upper and lower bearing surfaces

For both silicate and clay bricks the procedure is the same in ASTM.

For determinations of the solid brick weights the procedure is as below:

Five full specimens of dimensions (250*120*65)mm should be tested.

The specimens are dried in a ventilated oven at 110°C for not less than 24h and until two successive weightings at intervals of 2h show an increment loss not greater than 0.2% of the last previously determined weight of the specimen.

After this process, the specimens are cooled in a drying room maintained at a temperature 24 ± 8°C with a relative humidity between (30-70)%. The units are stored free from drafts, not stacked, with separate placement, for a period of at least 4h and until the surface temperature is ± 2.8° of the drying room temperature. Then the specimen can be weighted. Tensile strength for bricks is obtained by the brick tensile flexural strength ASTM C67-10 [ASTM C67-10, 2008]. Tensile strength is tested on a series of single bricks supported by steel roller bearings, simple beam system. Load is applied gradually through a steel rod on top of the bricks acting like a concentrated load. The samples are of dimensions (40*40*160) mm

Figure 48: Tensile flexural tests and failure mechanism of solid clay bricks

4.3.2.2 Mortar tests

For the mortar tests of unreinforced masonry, samples of mortar are collected in the areas where the connection between solid bricks units and mortar has failed. Due to the irregular shape of the samples, capping is required to be done according to ASTM C109/C 109M-02 regulations [ASTM C109/C, 2008]. The depressions at the samples are filled with mortar composed of 1 part by weight of cement and 2.75 parts of sand. The specimens are aged at least 48h before capping them. In this perspective, samples of mortars with (500*500) mm dimensions are prepared in the moist closet or moist room.

Figure 49: Compressive (left) and flexural (right) strength tests of mortar samples

They are kept in moist room from 20h to 72h with their upper surfaces exposed to the moist air but protected from dripping water. After their removal from the moist closet in the case of 24h specimens, they are tested within 30 minutes. The average compressive strength of the 5 samples is taken as the compressive strength. When it is impossible to take samples of the mortar the strength is taken according to the project and KTP-89. [KTP-N2-89, 1989]

The same procedure is for the flexural strength of mortar samples. The samples are constructed of dimensions 40*40*160mm. Tensile strength is tested on a series of mortar samples supported by steel roller bearings, simple beam system. Load is applied gradually through steel rod on top of the bricks acting like a concentrated load.

4.3.2.3 Masonry tests

Prism testing is a laboratory test for calculating the compressive strength of a masonry prism. The procedure is described in EN1052-1 [EN1052-1, 1998]. A minimum of three prisms should be constructed, using the same materials and workmanship as used in the project. The mortar bedding, joint thickness, joint tooling, bonding arrangement and grouting pattern should be the same as in the project. No structural reinforcement should be included, however, metals wall ties may be included if used in the project. The prism thickness should be the same as that of the actual construction. The prism length should be equal to or greater than the prism thickness. The height of the prism should be at least twice the prisms thickness or a minimum 375mm. Prisms should be subjected to atmospheric conditions similar to those of the masonry they represent for a period of 48 hour to being prepared for transportation to the testing laboratory. Prisms should be secured and transported in such a manner so as not to damage them.

Figure 50: Specimens of prism clay masonry (left), silicate masonry (right)

After prisms are delivered to the laboratory, they should be cured in laboratory air, free of drafts at 24°C with ±8°C, with a relative humidity between 30-70% for a period of 26 additional days. Proper capping of prisms cannot be over-emphasized. Brick units are not perfectly formed and their bearing surfaces may not be parallel and free from surface irregularities. The purpose of capping the bearing surfaces is to assure reasonably parallel and smooth bearing planes. The capping material itself should have a compressive strength in excess of that expected of the prisms to insure that the capping material does not fail before the prism. Prisms should be centred under the spherical upper bearing block of testing machine so that the resulting load will be applied through the centre of gravity of each specimen. The ultimate compressive strength of a prism is calculated by dividing the maximum compressive load by the cross-sectional area of the prism.

Figure 51: Masonry prism failure

Triplet testing of masonry is a test for determining the shear strength of masonry walls.The shear strength of masonry triplets was obtained as described in EN 1052-3 [EN 1052-3, 1998]. The specimens consist of three bricks bonded with mortar of same recipe and workmanships as in the original projects. Three sets of triplets are tested under no compressive force for determining f_{vko} value. Then three others sets of triplets are tested with the presence of compressive test as given in the Code. Two load cells were used to carry out the shear tests. One load cell was used for applying the shear force and the other applying the compressive force acting perpendicular to the shear force, as shown in the figure below

Figure 52: Masonry triplet specimen and test procedure

The shear strength, f_v is calculated according to EN 1052-3 [EN 1052-3, 1998] as:

$f_v = \frac{F_{max}}{2A}$ (74) where F_{max} is the maximal shear force and A is the cross sectional area of the joint. Additionally, the characteristic value of the shear strength f_{vk} is calculated:

$$f_{vk} = 0.8 f_v \quad (75)$$

4.4 Buildings investigation and results

4.4.1 Building A1

This template and building is the oldest in the list, but the buildings are near the "ish blloku" zone in Tirana, and they are buildings where maintenance and good interventions are done so no severe damage is observed. The buildings has plan dimensions of (56.65*11.65) m. Building has two entrances and four apartments and is symmetric. Building has two stories of 2.8 m height. In some of the buildings of these template are built extra stories later in the after 90s period (in two of these building also known as MOSKAT). Inside and outside walls of the building are 25 cm and non load bearing walls are 12 cm. For masonry are used clay bricks of strength 5 MPa as given in the project. The mortar used is lime mortar as defined in the project with ratio 1:3 (lime: sand). Specifications of the mortars and the procedure of preparing are given in Cika K.,(1969) [Cika K., 1969] For 1m^3 sand is used 0.333m3 lime and 200liters water. In the tests the mortar samples are taken from the building and are filled in the samples with mortar of this ratios. Also same ratio for the mortar mixes is used when preparing samples for prism testing and triplet testing. In the below figure are shown the positions where the bricks and mortar samples are extracted from the building as the given procedure above and below the test results.

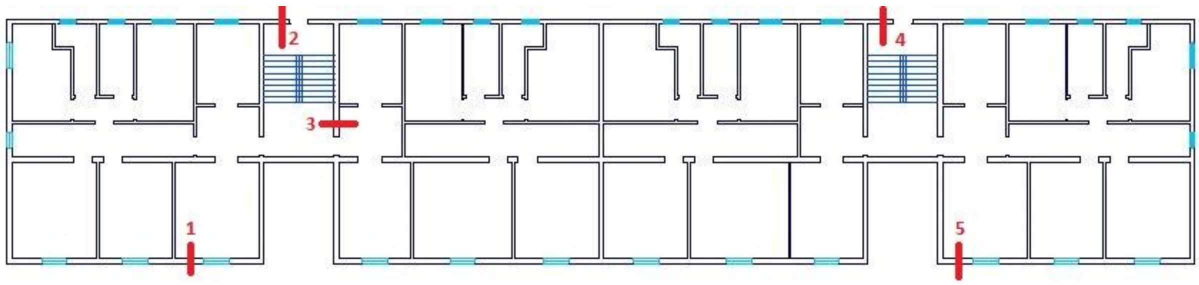

Figure 53: Template A1 (40/1) and locations where materials are extracted

From the test results are obtained the following values:

Brick tests: $f_b = 5\mathrm{MPa}$ $f_{bt} = 1\mathrm{MPa}$ $\rho_b = 1548\,\mathrm{kg/m^3}$

Mortar tests: $f_m = 2.3\mathrm{MPa}$ $f_{mt} = 0.45\mathrm{MPa}$

Masonry tests: $f_k = 1.43\mathrm{MPa}$ $f_{vk} = 0.3$ $f_{vk0} = 0.15$

4.4.2 Building A2

The building representing this template stock is located at "Sulejman Delvina" street in Tirana. The buildings has plan dimensions of (26.94*12.14) m. Inside and outside walls of the building are 25cm, with red clay bricks M-75 and lime mortar M-25. Non sustaining walls are 12cm. Slabs and beams are of mounting panels. Foundations are made with concrete, under the sustaining walls, and of bricks under the non sustaining walls. Reinforced concrete belts are added to the sustaining walls in the pavement and ceiling level. The mortar used in masonry is mixed mortar as defined in the project with ratios 1:0.7: 5.80 (cement: lime: sand). For 1m3 sand is used 0.122m3 lime, 145kg cement of 20MPa and 200liters water. In the tests the mortar samples are taken from the building and are filled in the samples with mortar of this ratios. Also same ratio for the mortar mixes is used when preparing samples for prism testing and triplet testing. In the below figure are shown the positions where the bricks and mortar samples are extracted from the building as the given procedure above and below the test results.

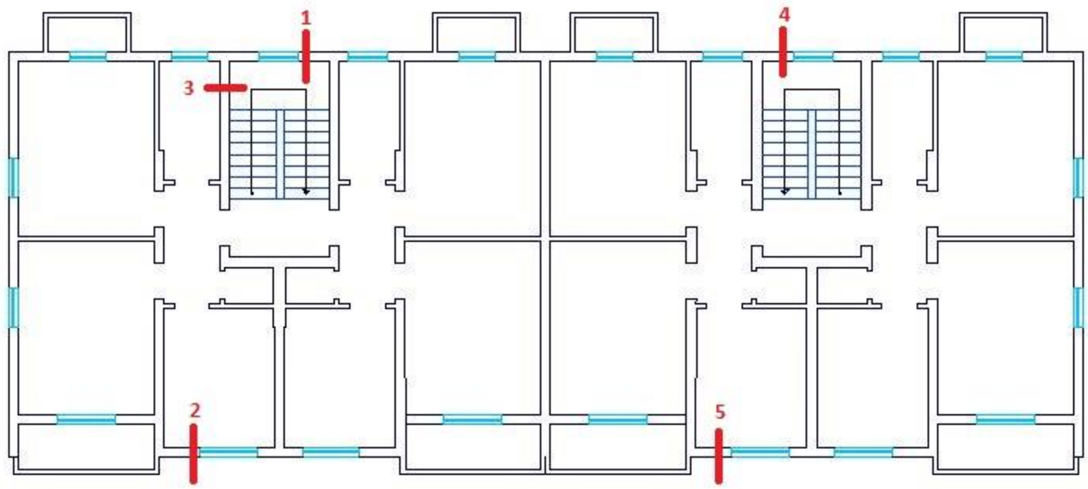

Figure 54: Template A2 (58/2) and locations where materials are extracted

Brick tests: $f_b = 7MPa$ $f_{bt} = 1.5MPa$ $\rho_b = 1730\,kg/m^3$

Mortar tests: $f_m = 2.13MPa$ $f_{mt} = 0.5MPa$

Masonry tests: $f_k = 1.83MPa$ $f_{vk} = 0.33$ $f_{vk0} = 0.17$

4.4.3 Building B1

The building representing this template stock is located near Lapraka in Tirana. In this hood are 3 buildings of this type. The specimens are taken from one building that is very much damaged and degraded. The template 63/1 is for three story buildings and has a (21.85*10.07) m plan dimension, symmetric in one direction and a story height 285cm. Total height of the building is 840cm. The load bearing walls have a thickness of 25cm in all three stories. The walls are masonry with solid red clay bricks of M75 with strength 7.5MPa.The mortar used in this building is lime mortar with ratio 1:2 (lime : sand). For 1m3 sand is used 0.5m3 lime and 200liters water. In the tests the mortar samples are taken from the building and are filled in the samples with mortar of this ratios. Also same ratio for the mortar mixes is used when preparing samples for prism testing and triplet testing. In the below figure are shown the positions where the bricks and mortar samples are extracted from the building as the given in the procedure above and the test results.

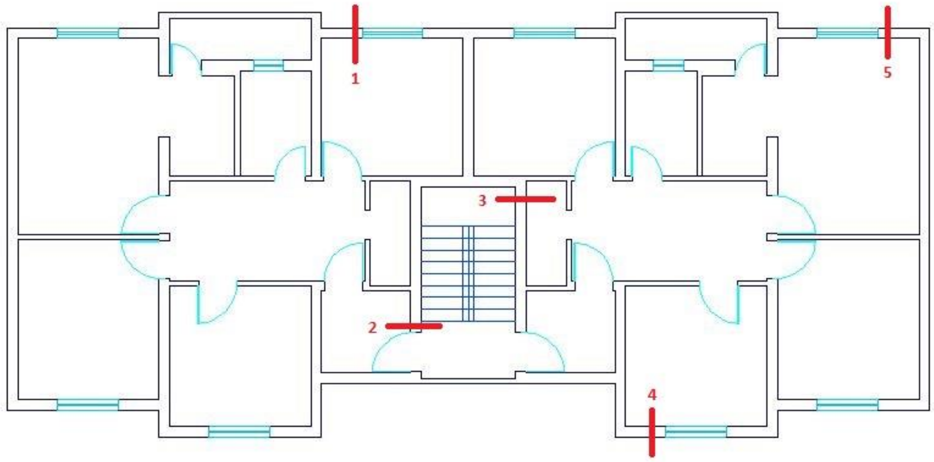

Figure 55: Template B1 (63/1) and locations where materials are extracted

Brick tests: $f_b = 7.2\text{MPa}$ $f_{bt} = 1.7\text{MPa}$ $\rho_b = 1809\ \text{kg/m}^3$

Mortar tests: $f_m = 2.23\text{MPa}$ $f_{mt} = 0.5\text{MPa}$

Masonry tests: $f_k = 1.87\text{MPa}$ $f_{vk} = 0.34$ $f_{vk0} = 0.17$

4.4.4 Building B2

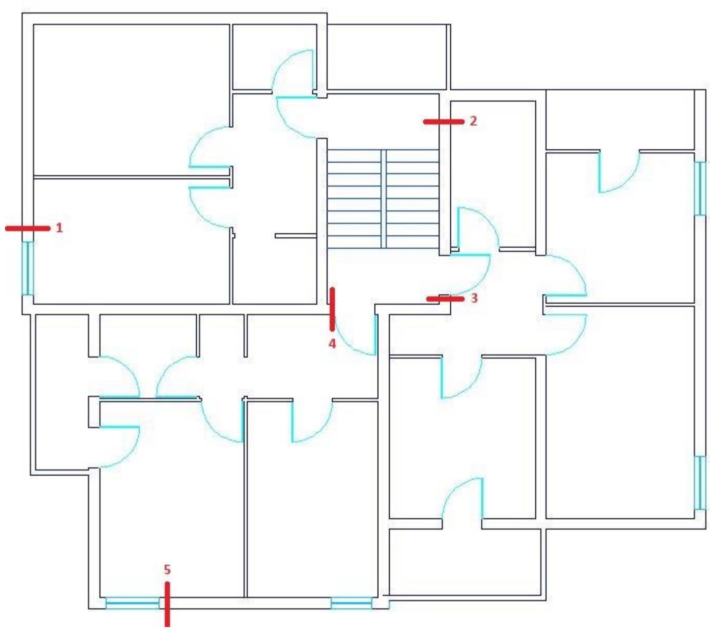

Figure 56: Template B2 (69/3) and locations where materials are extracted

The building chosen from this template is located in Corovode, near Berat .The template 69/3 has plan dimensions of (15.44*13.49) m and a nearly square form. The buildings has 4 floors with story height of 285 cm. Load bearing walls are of silicate bricks M-75 and mortar M-25. The first and second floor walls are 38cm and third and fourth floor of 25cm. Non load bearing walls are 8cm thick with hollow bricks. The mortar used in this building is mixed mortar with ratio 1:0.7:8.8 (cement: lime: sand). For 1m3 sand is used 145kg cement M200, 0.124m3 lime and 200liters water. In the tests the mortar samples are taken from the building and are filled in the samples with mortar of this ratios. Also same ratio for the mortar mixes is used when preparing samples for prism testing and triplet testing. In the above figure are shown the positions where the bricks and mortar samples are extracted from the building as the given procedure above and below the test results.

Brick tests: $f_b = 7.2\text{MPa}$ $f_{bt} = 1.7\text{MPa}$ $\rho_b = 2100\,\text{kg/m}^3$

Mortar tests: $f_m = 2.23\text{MPa}$ $f_{mt} = 0.63\text{MPa}$

Masonry tests: $f_k = 1.88\text{MPa}$ $f_{vk} = 0.35$ $f_{vk0} = 0.19$

4.4.5 Building B3

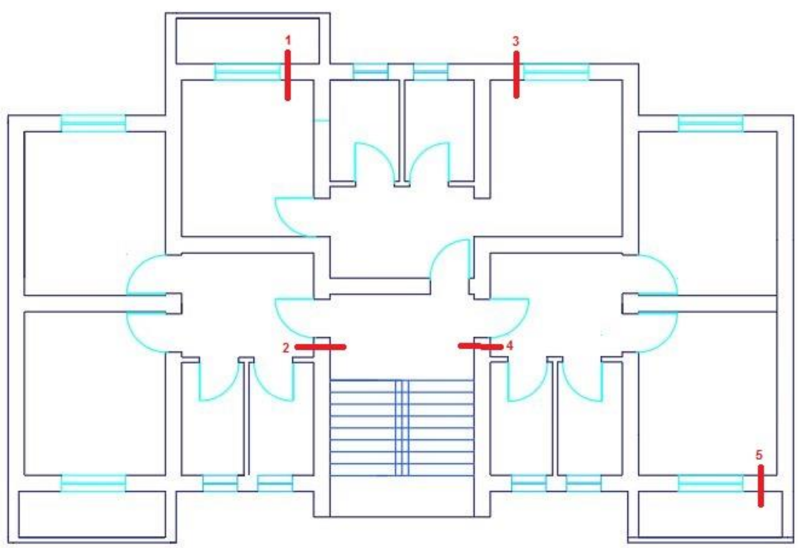

Figure 57: Template B3 (72/1) and locations where materials are extracted.

The building chosen for the tests is Elbasan near "28 Nentori" street. This building has plan dimensions of (18.32*12.43) m. Its 5 story high with 285cm height for each story. The sustaining walls are built with clay bricks M75 (strength 7.5 MPa). The mortar is M25 of strength 2.5MPa. The wall thickness is 38cm in the first and second floor, than 25cm on the remaining. The partition walls are with hollow clay bricks. The concrete corner columns and slabs are constructed with M150 concrete. The foundations, also performed with mass concrete 10MPa. Mortar used in this building is cement mortar with ratio 1:5.20 (cement water). For 1m3 sand is used 190kg cement M200, and 170liters water. In the tests the mortar samples are taken from the building and are filled in the samples with mortar of this ratios. Also same ratio for the mortar mixes is used when preparing samples for prism testing and triplet testing. In the above figure are shown the positions where the bricks and mortar samples are extracted from the building as the given procedure above and below the test results.

Brick tests: $f_b = 7.3\text{MPa}\ \ f_{bt} = 1.9\text{MPa}\ \rho_b = 1705\,\text{kg/m}^3$

Mortar tests: $f_m = 2.4\text{MPa}\ \ f_{mt} = 0.62\text{MPa}$

Masonry tests: $f_k = 1.9\text{MPa}\ \ f_{vk} = 0.35\ \ f_{vk0} = 0.18$

4.4.6 Building B4

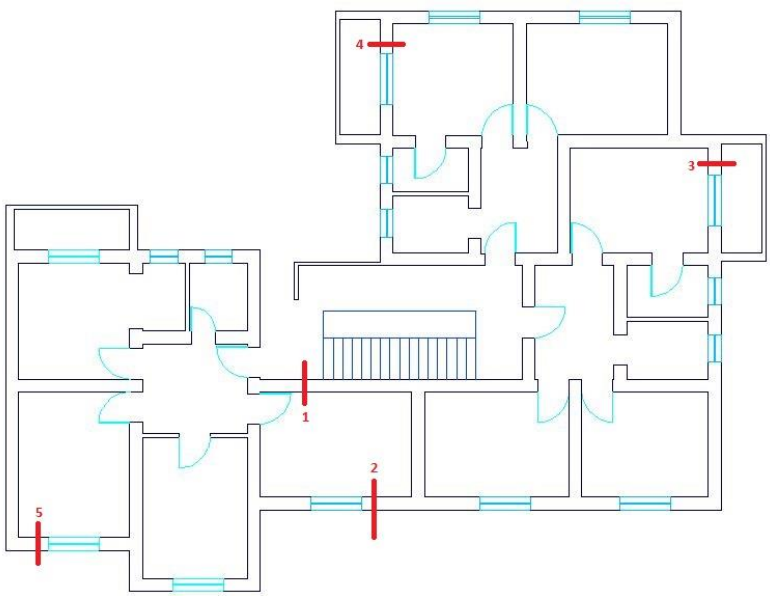

Figure 58: Template B4 (72/3) and locations where materials are extracted.

The building chosen from this template is located in Porcelan, Tirane Plan dimensions of the building are (21.12*17.12) m. Its 5 story high with 285cm height for each story. The sustaining walls are built with silicate bricks M75 (strength 7.5 MPa) and mortar M50 of strength 5MPa. The wall thickness is 38cm in the first and second floor, than 25cm on the remaining. The partition walls are with hollow clay bricks. The concrete corner columns and slabs are constructed with M150 concrete. The foundations, also performed with mass concrete 10MPa. Mortar used in this building is cement mortar with ratio 1:4.80 (cement: water). For 1m3 sand is used 260kg cement M300, and 170liters water. In the tests the mortar samples are taken from the building and are filled in the samples with mortar of this ratios. Also same ratio for the mortar mixes is used when preparing samples for prism testing and triplet testing. In the above figure are shown the positions where the bricks and mortar samples are extracted from the building as the given procedure above and below the test results.

Brick tests: $f_b = 7.38\text{MPa}$ $f_{bt} = 1.71\text{MPa}$ $\rho_b = 1750\,\text{kg/m}^3$

Mortar tests: $f_m = 4.8\text{MPa}$ $f_{mt} = 0.95\text{MPa}$

Masonry tests: $f_k = 2.4\text{MPa}$ $f_{vk} = 0.37$ $f_{vk0} = 0.2$

4.4.7 Building C1

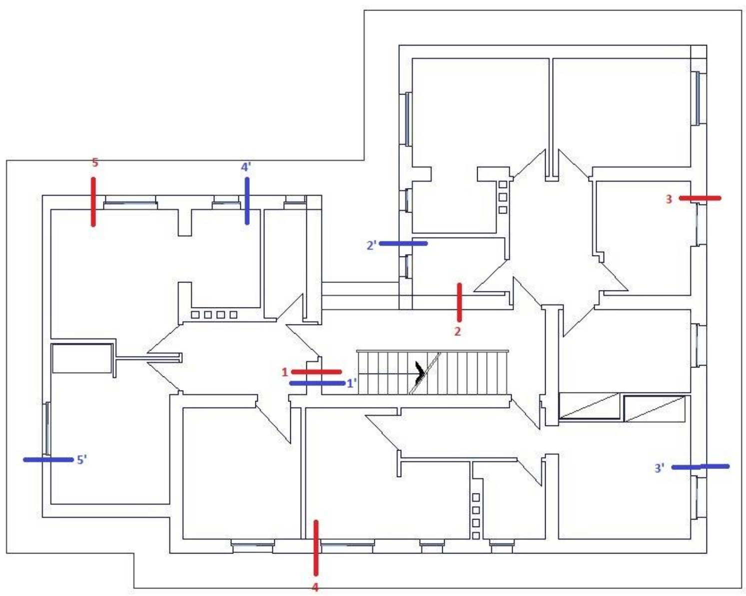

Figure 59: Template C1 (77/5) and locations where materials are extracted.

This is the most used template in our country and two buildings are chosen for the two types of materials. One building is located in Tirana near "Rruga e Kavajes" (clay bricks) and one in Vlore near boulevard "Ismail Qemali" (silicate bricks). The template 77/5 was projected for seismicity of 7 and 8 scale. The masonry is constructed with two types of bricks: red bricks of M-75 and mortar M-50, silicate bricks M-100 and mortar M-50. Mortar used in the first building is cement mortar with ratio 1:4.80 (cement: water). For 1m3 sand is used 260kg cement M300, and 170liters water. Mortar used in the second building is cement mortar with ratio 1:3.40 (cement: water). For 1m3 sand is used 370kg cement M300, and 170liters water. Non sustaining walls have bricks with openings and mortar M-15. Lintels are realized with reinforced concrete, and slabs with reinforced ceramics, and concrete M-200. Foundation are realized with stones of M>200 and are calculated for [σ] = 2kg/cm2. In the above figure are shown the positions where the bricks and mortar samples are extracted from the building as the given procedure above and below the test results.

-Clay building

Brick tests: $f_b = 7.48\text{MPa}$ $f_{bt} = 1.71\text{MPa}$ $\rho_b = 1766\,\text{kg/m}^3$

Mortar tests: $f_m = 4.8\text{MPa}$ $f_{mt} = 1.1\text{MPa}$

Masonry tests: $f_k = 2.42\text{MPa}$ $f_{vk} = 0.36$ $f_{vk0} = 0.2$

-Silicate building

Brick tests: $f_b = 10\text{MPa}$ $f_{bt} = 2.59\text{MPa}$ $\rho_b = 2106\,\text{kg/m}^3$

Mortar tests: $f_m = 5.06\text{MPa}$ $f_{mt} = 1\text{MPa}$

Masonry tests: $f_k = 3\text{MPa}$ $f_{vk} = 0.4$ $f_{vk0} = 0.2$

4.4.8 Building C2

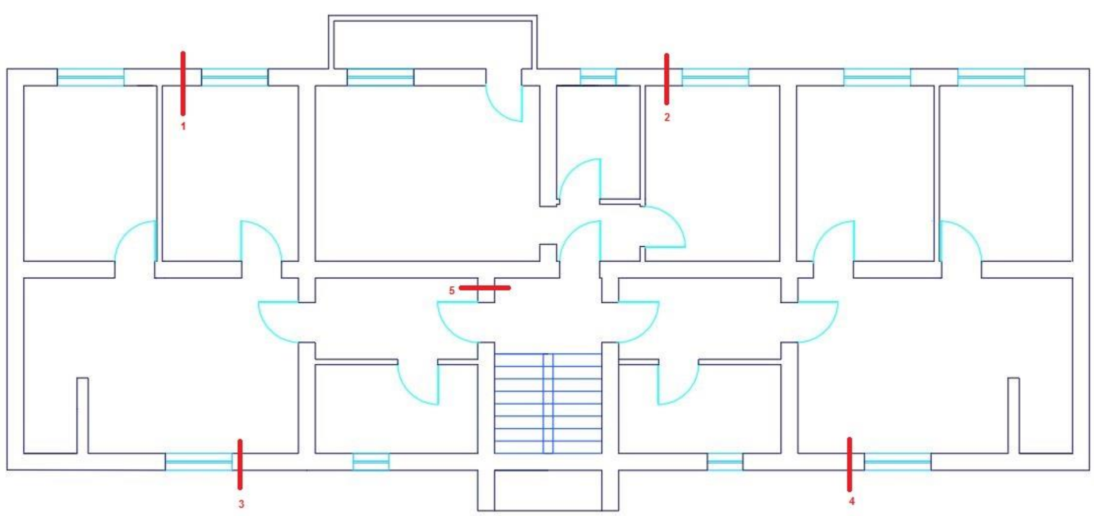

Figure 60: Template C2 (83/3) and locations where materials are extracted.

The building chosen from this template is located in Tirana at "Ali Demi". The template 83/3 has plan dimensions of (24.44*9.04) m. Its 5 story high with 285cm height for each story. The sustaining walls are built with clay bricks M-75 (strength 7.5 MPa) and mortar M-25 of strength 2.5MPa. The mortar used in this building is mixed mortar with ratio 1:0.7:8.8 (cement: lime: sand). For 1m3 sand is used 145kg cement M200, 0.124m3 lime and 200liters water. The wall thickness is 38cm in the first and second floor, than 25cm on the remaining. The partition walls are with hollow clay bricks. In the above figure are shown the positions where the bricks and mortar samples are extracted from the building as the given procedure above and below the test results. In the tests the mortar samples are taken from the building and are filled in the samples with mortar of this ratios. Also same ratio for the mortar mixes is used when preparing samples for prism testing and triplet testing.

Brick tests: $f_b = 7.55\text{MPa}$ $f_{bt} = 1.82\text{MPa}$ $\rho_b = 1934\,\text{kg/m}^3$

Mortar tests: $f_m = 2.57\text{MPa}$ $f_{mt} = 0.65\text{MPa}$

Masonry tests: $f_k = 1.91\text{MPa}$ $f_{vk} = 0.35$ $f_{vk0} = 0.19$

4.4.9 Building C3

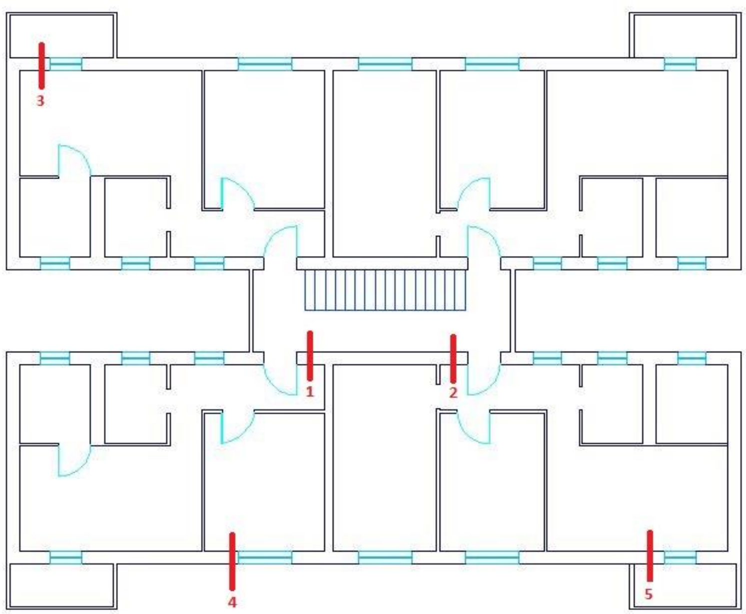

Figure 61: Template C3 (83/10) and locations where materials are extracted.

The building chosen from this template is located in "Andon Profka" street in Fier. The template 83/10 was calculated for terrain with strength $[\sigma] = 2\mathrm{kg/cm^2}$ and seismicity VII-VIII scale. The building has 5 floors with dimensions in plan (20.64*17.6)m. The slabs are of pre-stressed concrete span less than 420cm and reinforced concrete for span more than 4.4m.The masonry is realized with red clay bricks M-75 and mortar M-50. Mortar used is cement mortar with ratio 1:3.40 (cement: water). For 1m^3 sand is used 370 kg cement M300, and 170liters water. The non sustaining walls are with bricks with openings (8-12) cm and mortar M-15, as given by the project. In the tests the mortar samples are taken from the building and are filled in the samples with mortar of this ratios. Also same ratio for the mortar mixes is used when preparing samples for prism testing and triplet testing. In the above figure are shown the positions where the bricks and mortar samples are extracted from the building as the given procedure above and below the test results.

Brick tests: $f_b = 7.55\mathrm{MPa}$ $f_{bt} = 1.85\mathrm{MPa}$ $\rho_b = 1877\ \mathrm{kg/m^3}$

Mortar tests: $f_m = 5.12\mathrm{MPa}$ $f_{mt} = 1.12\mathrm{MPa}$

Masonry tests: $f_k = 2.48\mathrm{MPa}$ $f_{vk} = 0.39$ $f_{vk0} = 0.2$

4.5 Final revised values of material characteristics and properties

The strength of bricks and mortar for every masonry wall are very important because all other parameters depend on them. Also the f_k value calculated from prism testing is much more reliable than the value correlated by the f_b and f_m from the standard EC-6 [EN1996-1, 2005] correlation. In all cases f_b and f_m values taken for modelling are the lowest of the test or the project. In all the tested building can be spotted that the values have a maximum loss in strength of 0.5MPa (58/2 building). For the earliest template A1 the compressive strength of brick and mortar are almost the same as the projected values. Still this values are the lowest in the list. The A2 building has the biggest loss in strength parameters with 7MPa (experimental) versus 7.5MPa (projected) and 2.13MPa (experimental) versus 2.5MPa (projected). The compressive strength of masonry f_k is calculated from equation (63) and compared to the f_k from prism test. The lowest value is taken as the compressive strength of masonry. Templates B1, B2 and B3 also have significant drop in values of compressive strength of materials. The same procedure is repeated for them and the lowest values are accepted, for defining masonry walls. In the other four templates the values of the tests and the projected values have no significant change. For the shear strength with and without compression f_{vk} , f_{vk0} in all times are accepted the values from the test as more relevant and recommended by the code. The other parameters are correlated in the same way from f_k. The following values of mechanical properties are accepted as the basics parameters for designing masonry walls in each building.

Table 28: Comparison of compressive strength of brick, mortar and masonry of projected values and experimental ones.

Building Template	$f_b\ proj$ $[MPa]$	$f_b\ exp$ $[MPa]$	$f_m\ proj$ $[MPa]$	$f_m exp$ $[MPa]$	$f_k proj$ $[MPa]$	$f_k exp$ $[MPa]$
A1	5	5	2.5	2.3	1.49	1.43
A2	7.5	7	2.5	2.13	1.97	1.94
B1	7.5	7.2	2.5	2.23	1.97	1.87
B2	7.5	7.3	2.5	2.35	1.97	1.88
B3	7.5	7.25	2.5	2.4	1.97	1.9
B4	7.5	7.38	5	4.8	2.43	2.4
C1	7.5	7.48	5	4.8	2.43	2.42
C1'	10	10.06	5	5.06	2.97	3
C2	7.5	7.6	2.5	2.57	1.97	1.94
C3	7.5	7.55	5	5.12	2.43	2.479

Table 29: Brick and mortar properties for analysed buildings

Building Template	**Brick properties**			**Mortar properties**		
	Type	f_b $[MPa]$	f_{bt} $[MPa]$	Type	f_m $[MPa]$	f_{mt} $[MPa]$
A1	Clay	5	1.1	Lime	2.3	0.45
A2	Clay	7	1.5	Mixed	2.1	0.5
B1	Clay	7.2	1.7	Lime	2.2	0.5
B2	Silicate	7.3	1.9	Cement	2.35	0.65
B3	Clay	7.25	1.7	Cement	2.4	0.6
B4	Silicate	7.4	1.65	Cement	4.8	0.95
C1	Clay	7.5	1.7	Cement	4.8	1.1
C1'	Silicate	10	2.6	Cement	5	1
C2	Clay	7.5	1.8	Mixed	2.5	0.65
C3	Clay	7.5	1.85	Cement	5	1.1

Table 30: Revised masonry wall properties for analysed building

Building Template	f_k $[MPa]$	f_{vk} $[MPa]$	f_{vk0} $[MPa]$	f_t $[MPa]$	f_{xk1} $[MPa]$	f_{xk2} $[MPa]$	E $[MPa]$	G $[MPa]$	G_{fc} $[MPa]$	ν
A1	1.43	0.3	0.15	0.072	0.180	0.129	1430	358	2.38	0.2
A2	1.94	0.33	0.17	0.097	0.245	0.175	1940	485	3.1	0.2
B1	1.87	0.34	0.175	0.094	0.252	0.18	1870	467	2.99	0.2
B2	1.88	0.345	0.19	0.094	0.256	0.183	1880	470	3	0.2
B3	1.9	0.35	0.18	0.095	0.254	0.181	1900	475	3.04	0.2
B4	2.4	0.37	0.2	0.12	0.258	0.185	2400	600	3.84	0.2
C1	2.42	0.36	0.2	0.121	0.262	0.187	2420	605	3.87	0.2
C1'	2.97	0.4	0.22	0.149	0.352	0.252	2970	742	4.75	0.2
C2	1.94	0.35	0.185	0.097	0.266	0.19	1940	485	3.1	0.2
C3	2.43	0.39	0.2	0.122	0.264	0.189	2430	607	3.89	0.2

CHAPTER 5

PUSHOVER ANALYSIS

5.1 Procedure of non-linear pushover analysis

The structures are firstly modelled with the technique discussed in chapter IV using 3muri software package and by assigning proper element and materials nonlinearity. [3muri software package] The procedure presented in chapter 2.6 is followed for the 19 studied buildings. For each building are computed 24 analysis, combining different load cases, direction and eccentricity.

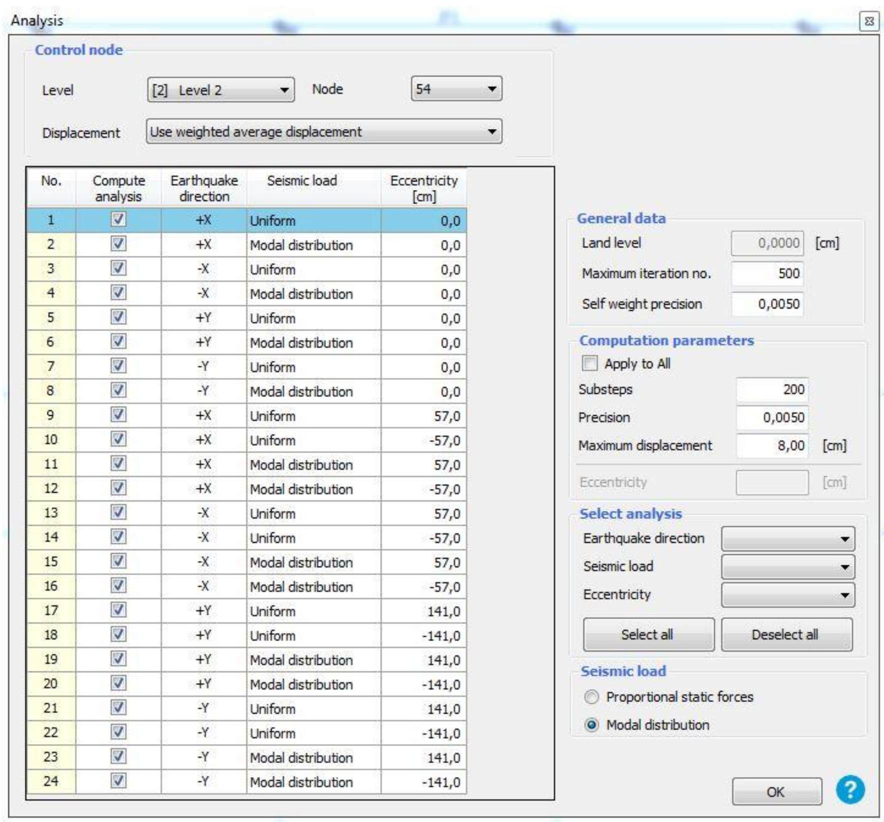

Figure 62: Computed pushover analysis cases

Two load patterns are taken in consideration, first mode shape distribution based on the fundamental mode shape of the structure, and an uniform load distribution to all stories as reccomended by different authors for N-2 and 3muri approach. [Fajfar p. et al, 2005; EN1998, 2005; Galasco A. et.al., 2006; 3muri software package] The load shapes are proportional to mass, shape and force as given in equations (44) and (45) in section 2.6.3. In the figure above are shown the 24 pushover cases for A2 building analysis.

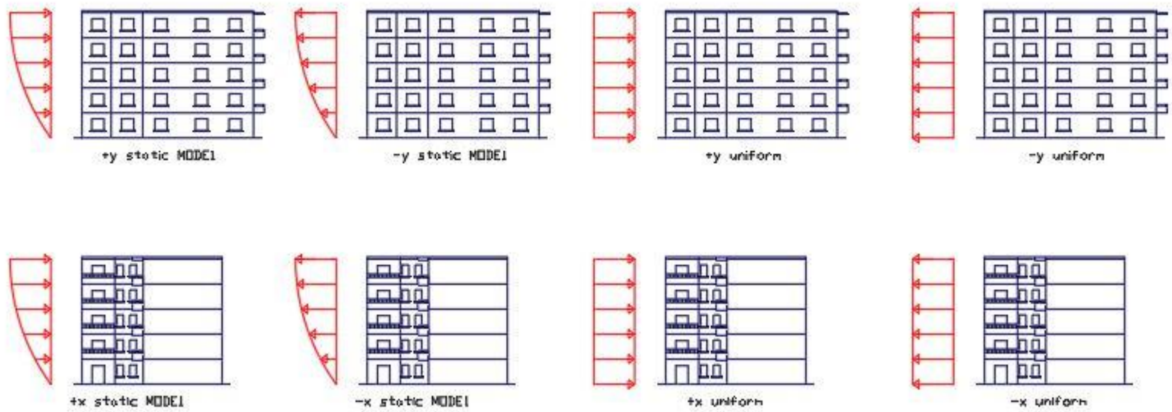

Figure 63: Load patterns and different cases of pushover analysis

The analysis procedure is generated automatically by the program and is theorical base is given in section 2.6.4. The output of pushover analysis in 3muri is the force-displacement curve. For each direction x and y from the 12 curves, the worst scenario (the case with least energy dissipation) is choosen as the representative capacity curve in that direction. The curve is then bilinearized following N-2 procedure given in section 2.6.5

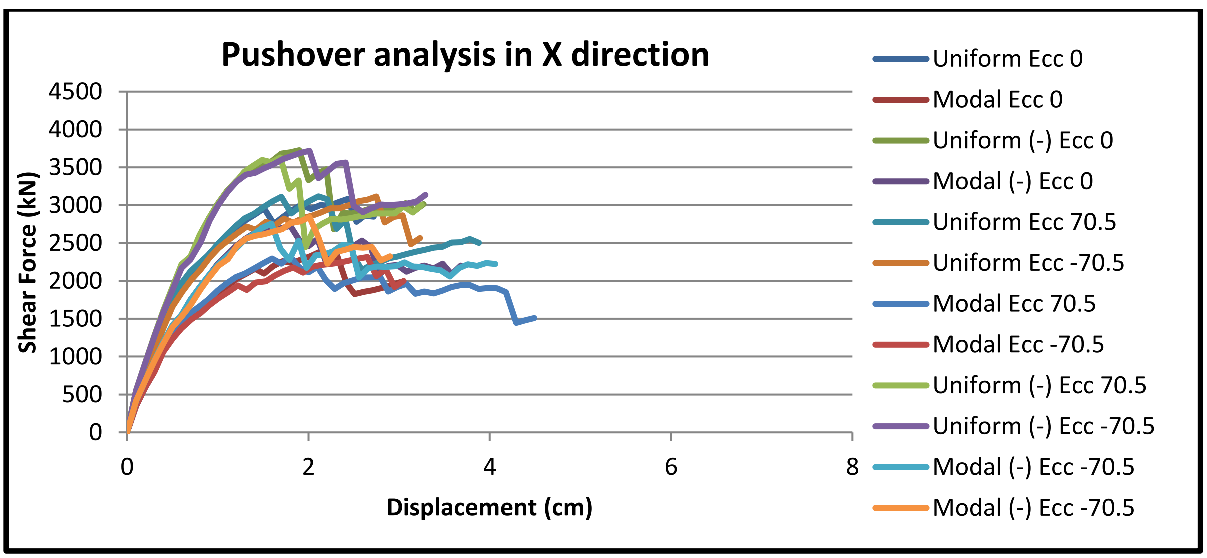

Figure 64: Pushover analysis for x-dir, 12 load patterns of building C1A

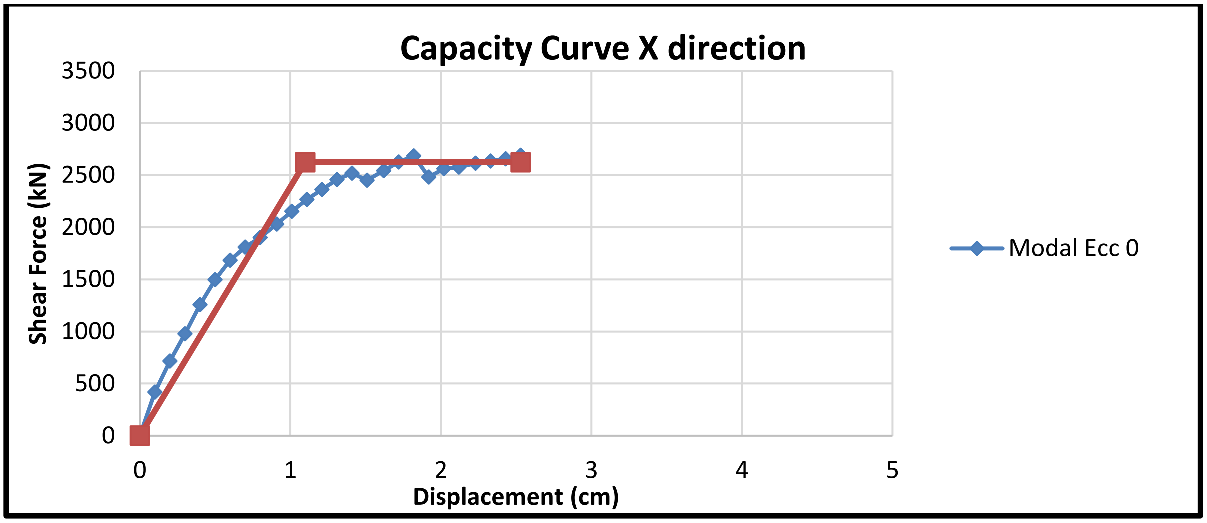

Figure 65: Capacity curve in x-direction C1A building

To proper compare different buildings and also for later use on spectrum analysis the capacity curves are normalized, where it is given in terms of shear force/weight of the building and top roof displacement/ height of the building.

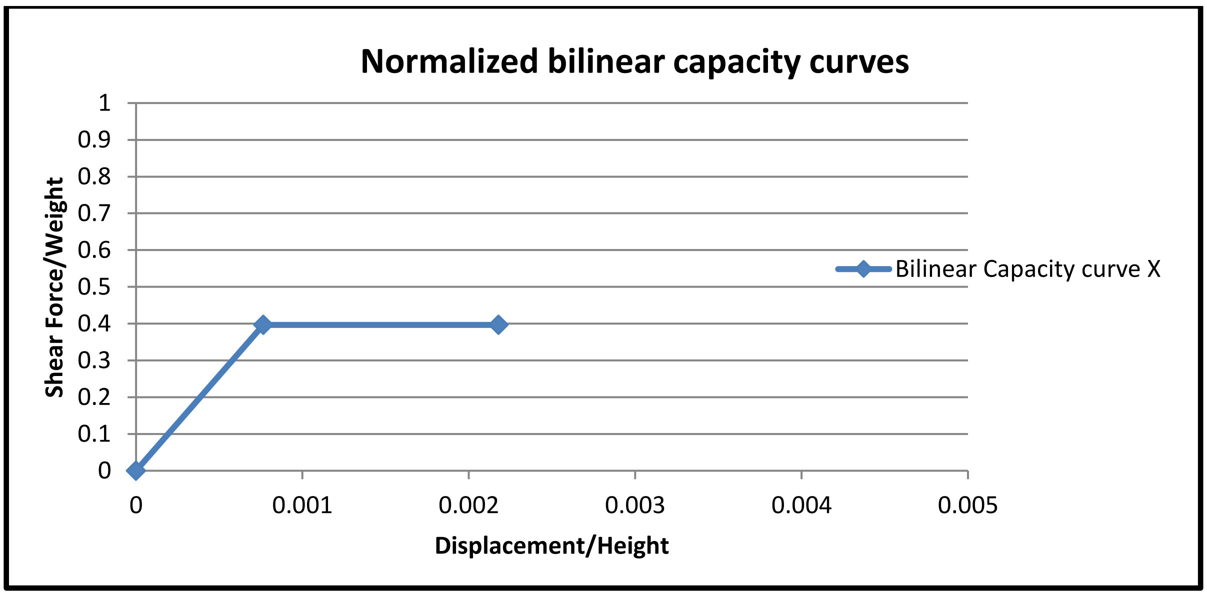

Figure 66: Normalized bilinear capacity curve C1A building

3muri allows step by step view of the MDOF under pushover analysis and the staic state of each pier and sprandel element. This allows generating a step by step failure mechanism for the building and even control the expected damage level on each wall. Following the procedure of 2.6.7, each limit damage state is associated to the strength and stiffness of the structure and drift capacity of each pier and sprandel element. For all the buildings in the sections below will be given the 24 pushover analysis cases, capacity curves in both x and y direction, normalized capacity curves in both direction, failure mechanism and the most loaded walls for each case. Also comparisons will be made on buildings with same plan but with interventions in first floors, or additional stories.

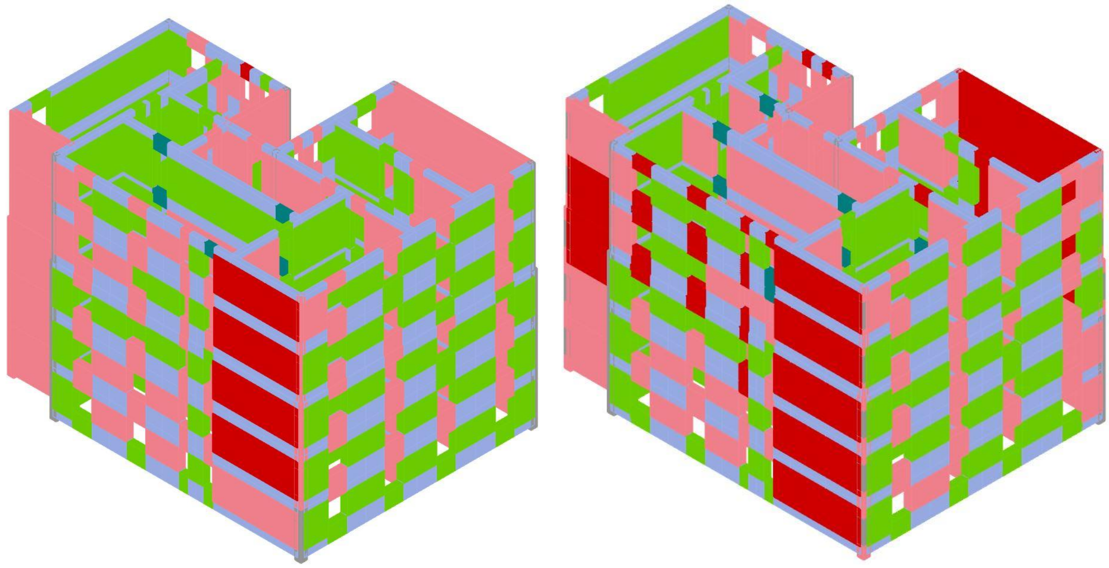

Figure 67: Failure mechanism of C1A and C1B buildings

5.2 Pushover analysis results of regular template buildings

The template building are modelled with 3muri software, according to their real dimensions. Only the load bearing walls are considered, while partition walls do not contribute in structural stiffness. But they are considered as additive static loads applied to each floor. Walls are considered as layered non-linear materials according to Turnsek-Cacovic approach as defined in EC-6 [3]. All the parameters are taken as defined in chapter 4. Foundations are considered pinned as the best approach to 3muri. For slab, the parameters are given for every building in the corresponding section below. A concrete line element is put at each level for load transmission and to approach real structure. In this section are represented 10 buildings that have no interevention comparing with each template and design.

5.2.1 Building of template A1

This building is symmetric and the seismic divide separates the two buildings from one another. So on modelling only half of the building, is considered.

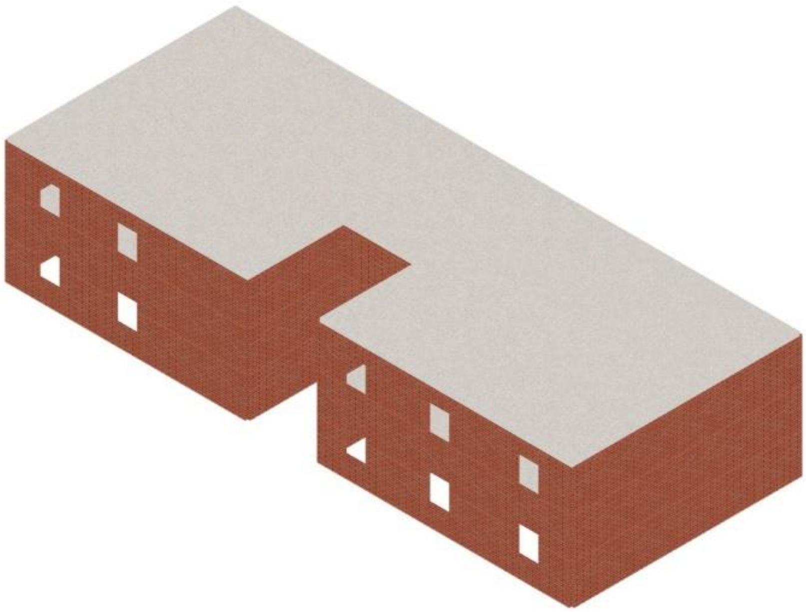

Figure 68: A1 building model

Loads are calculated as below:

-Slab 12cm	$0.12 * 21 * 1.1 = 2.77\text{kN/m}^2$
-Mortar 3cm	$0.03 * 19 * 1.2 = 0.57\text{kN/m}^2$
-Tiles 1cm	$0.01 * 22 * 1.2 = 0.26\text{kN/m}^2$
-Plaster 2cm	$0.02 * 18 * 1.2 = 0.43\text{kN/m}^2$
Sum	$= 4.03\text{kN/m}^2$
Addition load (Partition walls)	$= 1.0\text{kN/m}^2$
Probable live load	$= 2\text{kN/m}^2$

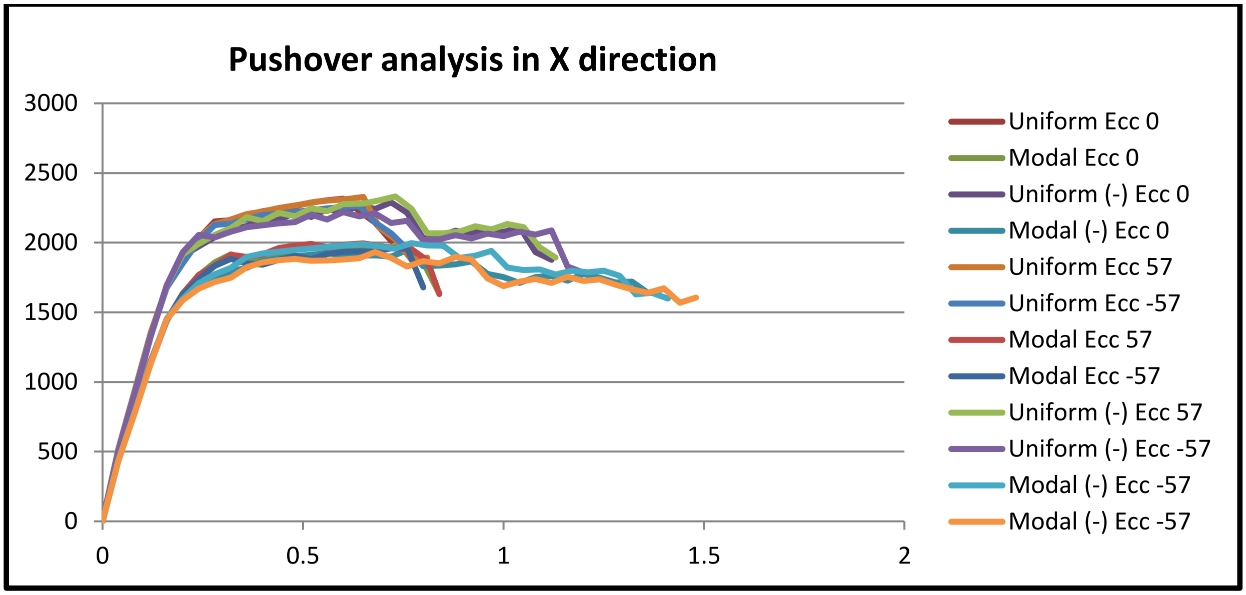

Figure 69: Pushover analysis in x-direction, 12 load patterns A1 building

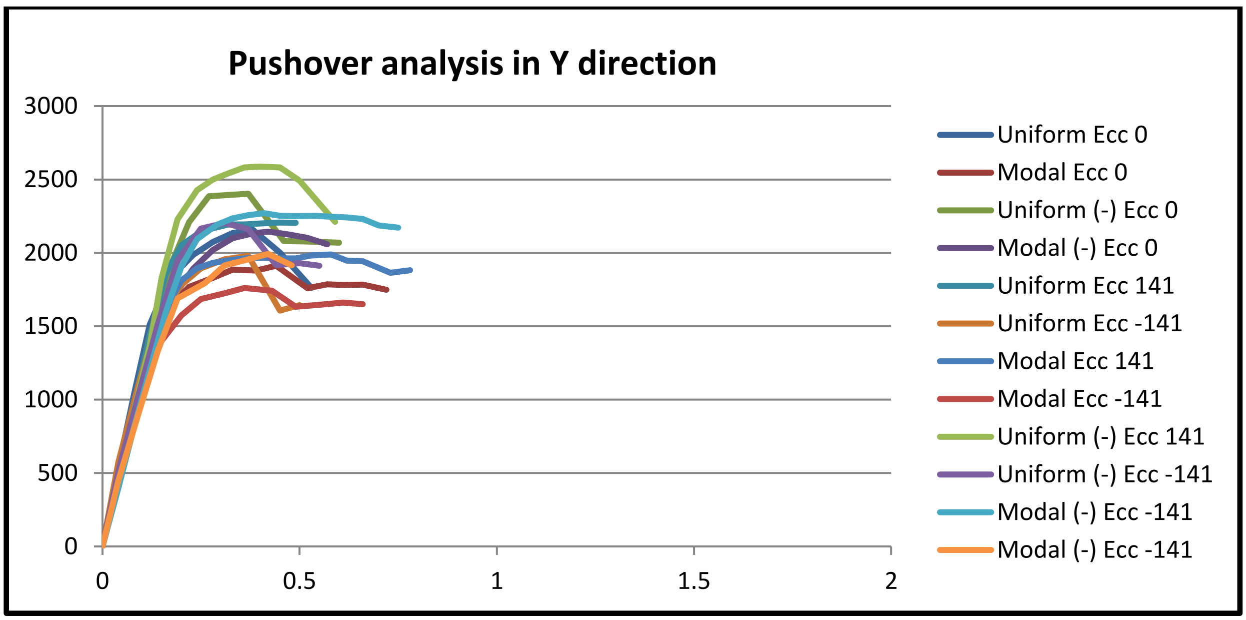

Figure 70: Pushover analysis in Y-direction, 12 load patterns A1 building

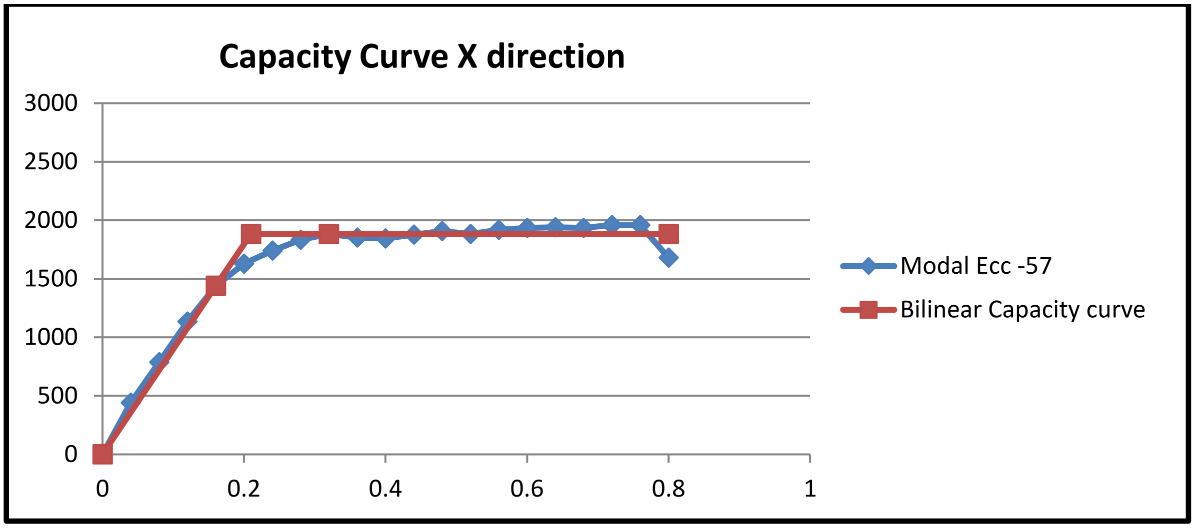

Figure 71: Capacity curve in x-direction, worst scenario and bilinear curve A1 building

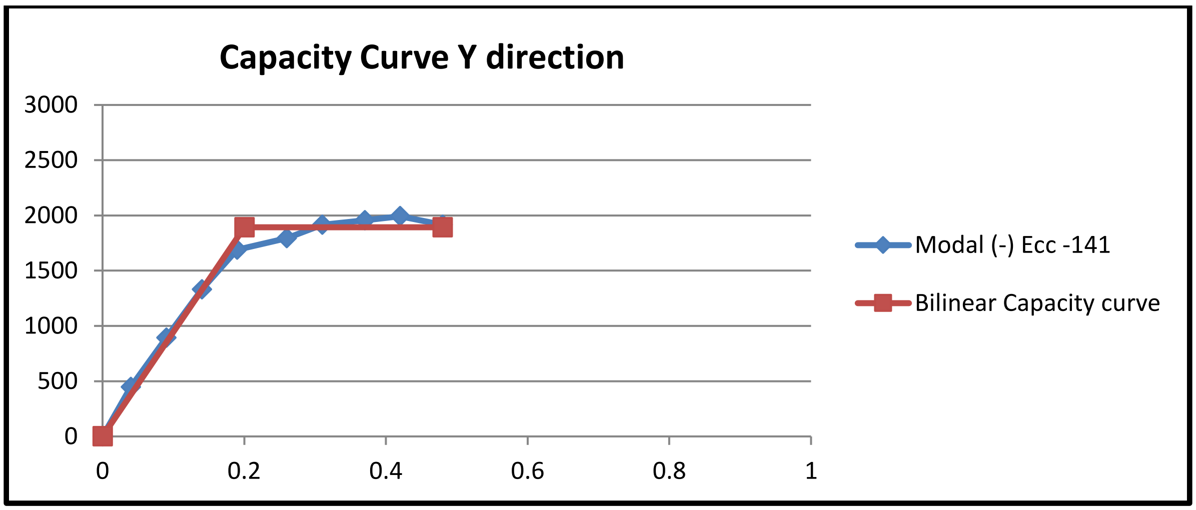

Figure 72: Capacity curve in y-direction, worst scenario and bilinear curve A1 building

Table 31: Pushover analysis parameters A1 building

Parameters	d_y^*	d_m^*	F_y^*	K^*	μ	F_y^*/W
x-direction	0.21cm	0.8cm	1883kN	8967kN/cm	3.80	0.712
y-direction	0.2cm	0.48cm	1893kN	9465kN/cm	2.4	0.716

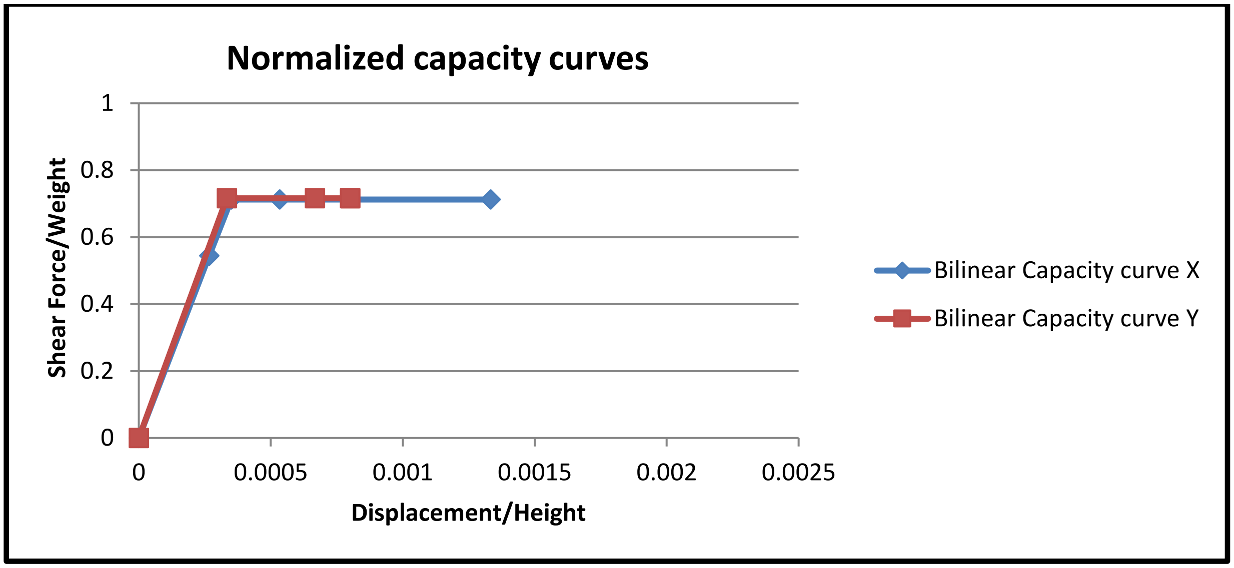

Figure 73: Normalized bilinear capacity curves of A1 building

Table 32: Period and mass participation of first 12 modes for building A1

Mode	T [s]	m_x [kg]	M_x [%]	m_y [kg]	M_y [%]	m_z [kg]	M_z [%]
1	0.10885	1173	0.24	446832	90.36	255	0.05
2	0.10371	1281	0.26	7911	1.60	50	0.01
3	0.09709	439155	88.80	1829	0.37	36	0.01
4	0.04538	6245	1.26	21998	4.45	40268	8.14
5	0.04361	9543	1.93	10876	2.20	221	0.45
6	0.04236	1577	0.32	1666	0.34	12257	2.48
7	0.04129	1787	0.36	684	0.14	11512	2.33
8	0.03984	8867	1.79	431	0.09	4551	0.92
9	0.03942	318	0.64	1785	0.36	171635	34.71
10	0.03768	7387	1.49	0	0.00	786	0.16
11	0.03700	16	0.00	59	0.01	5246	1.06
12	0.03597	6678	1.35	10	0.00	21546	4.36

5.2.2 Building of template A2

This building is symmetric but has no seismic divide, so its modelled as a single structure.

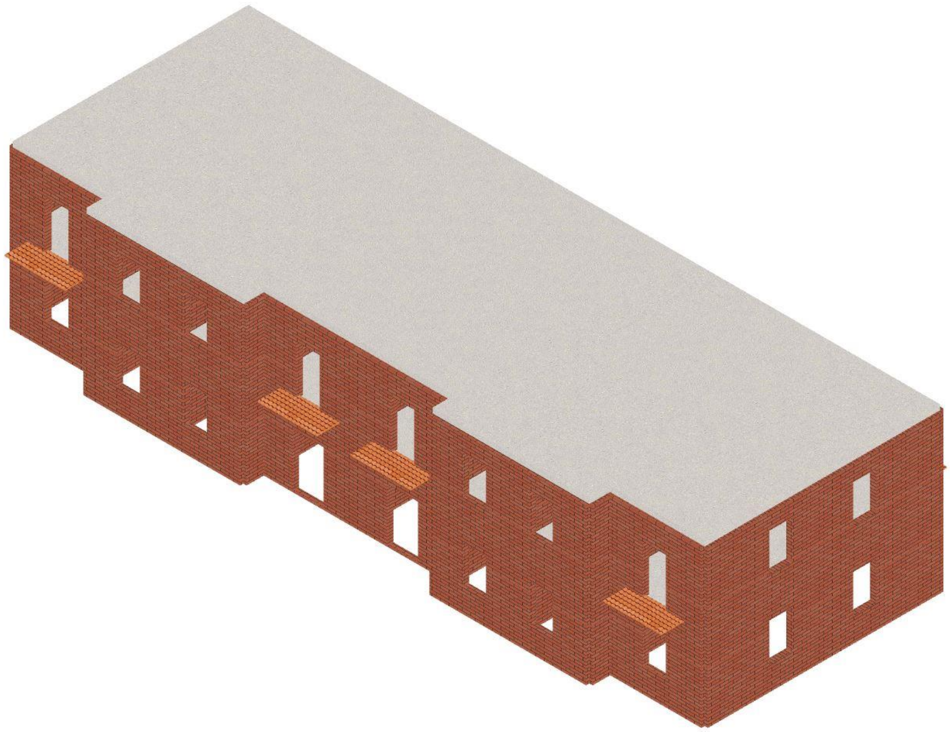

Figure 74: A2 building model

Loads are calculated as below:

-Slab 12cm	$0.12 * 21 * 1.1 = 2.77\text{kN/m}^2$
-Mortar 3cm	$0.03 * 19 * 1.2 = 0.57\text{kN/m}^2$
-Tiles 1cm	$0.01 * 22 * 1.2 = 0.26\text{kN/m}^2$
-Plaster 2cm	$0.02 * 18 * 1.2 = 0.43\text{kN/m}^2$
Sum	$= 4.03\text{kN/m}^2$
Addition load (Partition walls)	$= 1.0\text{kN/m}^2$
Probable live load	$= 2\text{kN/m}^2$

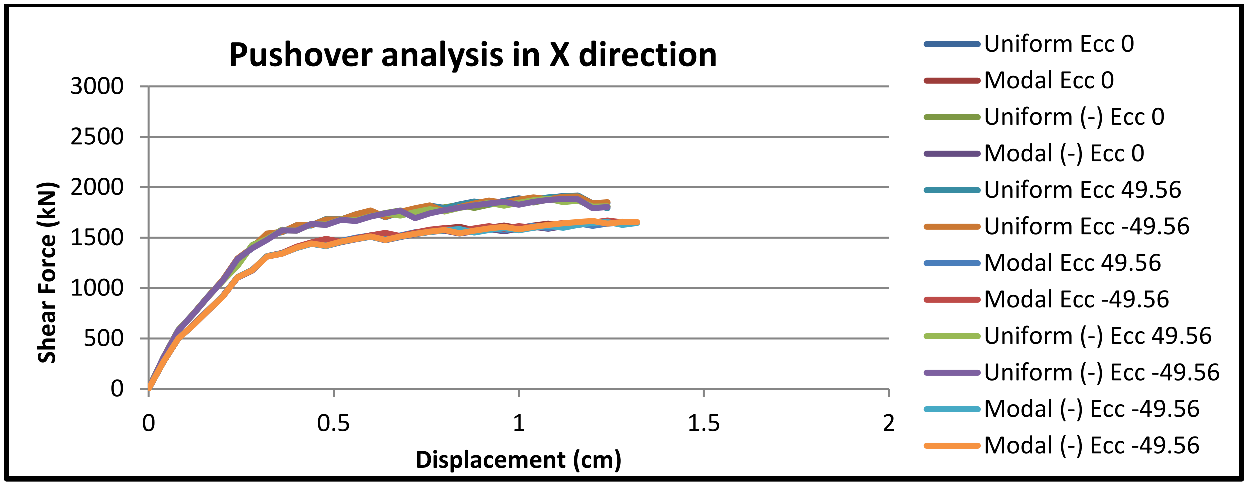

Figure 75: Pushover analysis in x-direction, 12 load patterns of A2 building

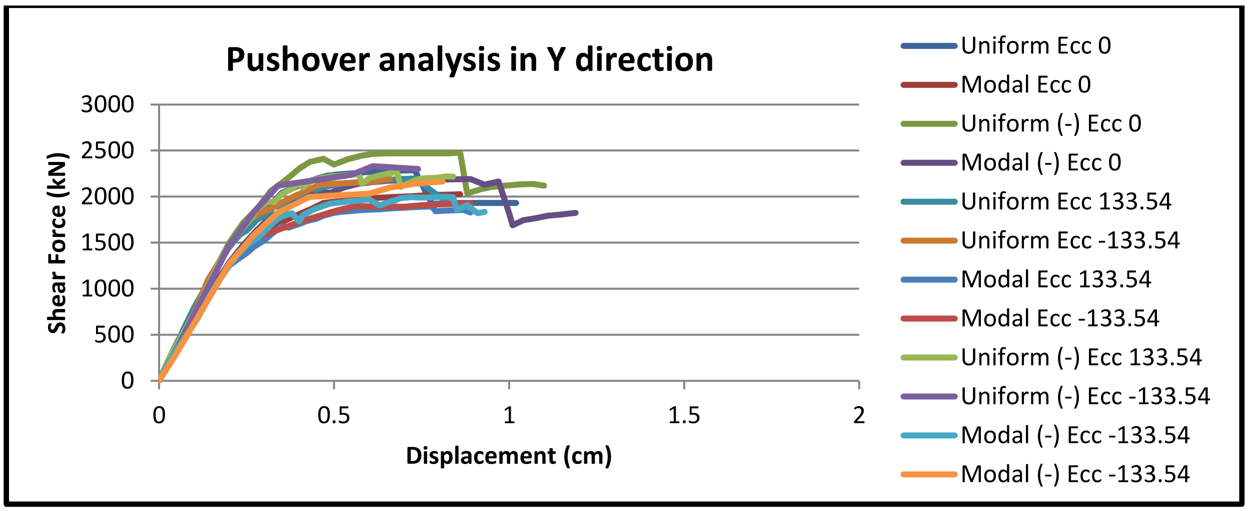

Figure 76: Pushover analysis in y-direction, 12 load patterns of A2 building

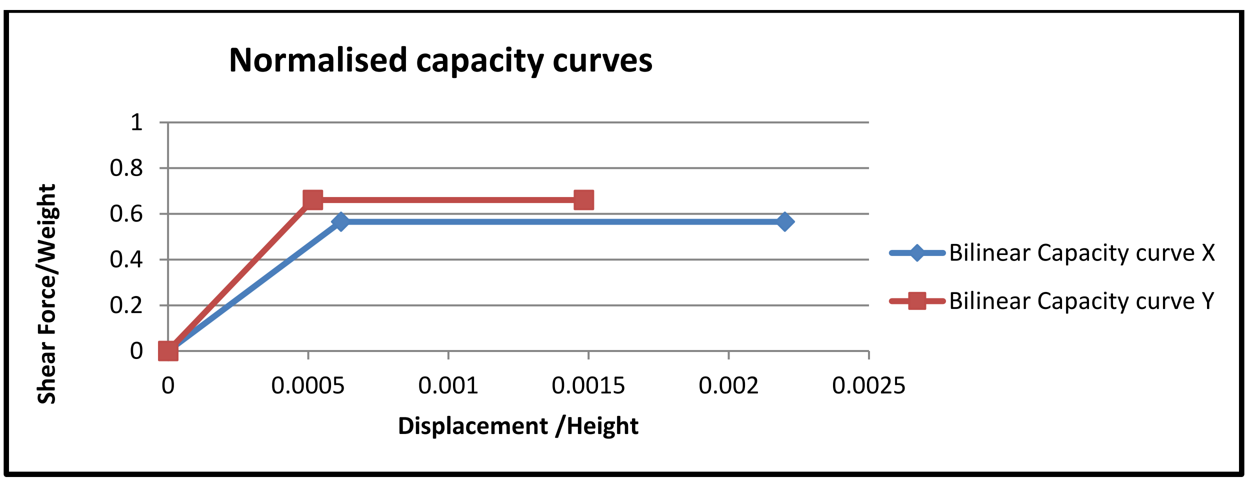

Figure 77: Normalised bilinear capacity curves of A2 building

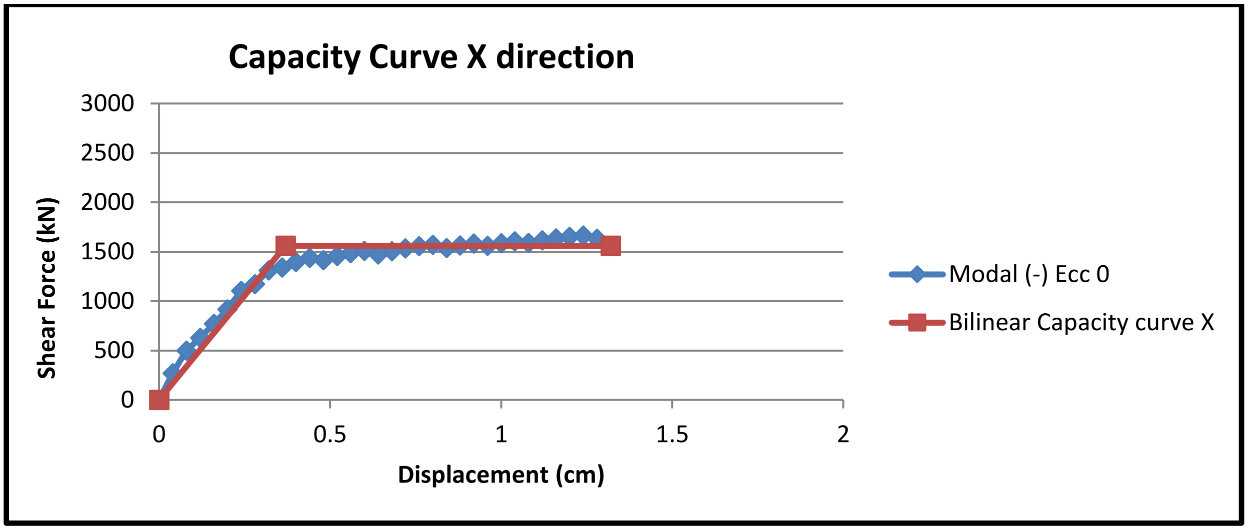

Figure 78: Capacity curve in x-dir, worst scenario and bilinear curve of A2 building

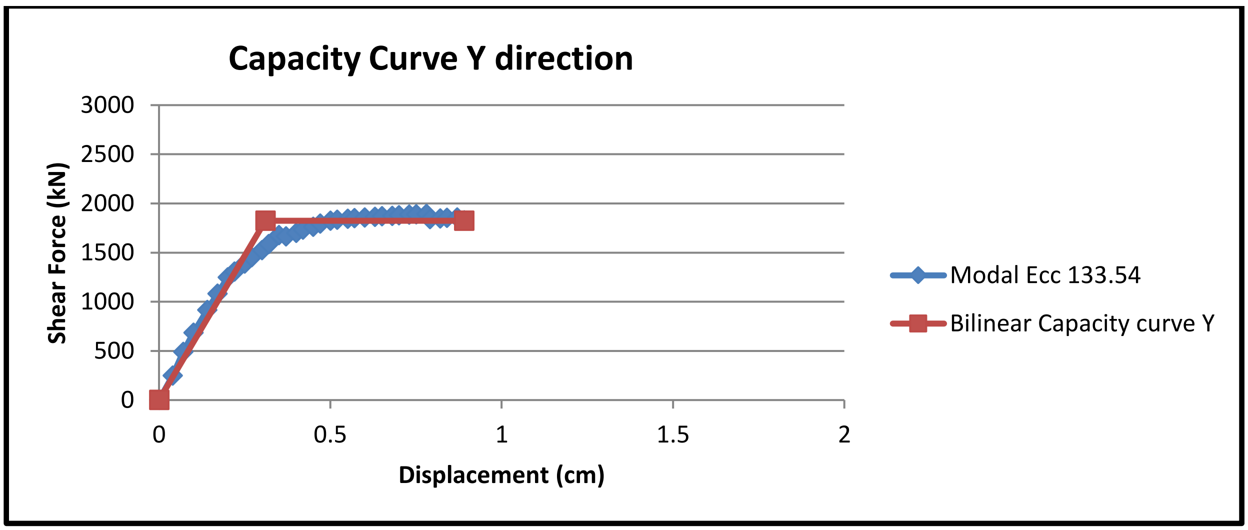

Figure 79: Capacity curve in y-dir, worst scenario and bilinear curve of A2 building

Table 33: Pushover analysis parameters A2 building

Load applied	d_y^*	d_m^*	F_y^*	K^*	μ	F_y^*/W
x-direction	0.37cm	1.32cm	1560kN	4218kN/cm	3.56	0.565
y-direction	0.31cm	0.89cm	1824kN	5883kN/cm	2.87	0.66

Table 34: Period and mass participation of first 12 modes for building A2

Mode	T [s]	m_x [kg]	M_x [%]	m_y [kg]	M_y [%]	m_z [kg]	M_z [%]
1	0,11810	467356	90,15	0	0,00	0	0,00
2	0,09965	0	0,00	46283	89,28	227	0,04
3	0,09053	2	0,00	433	0,08	3	0,00
4	0,04510	50629	9,77	4	0,00	13	0,00
5	0,03310	5	0,00	46456	8,96	8901	1,72
6	0,03081	24	0,00	1.431	0,28	16	0,00
7	0,02666	0	0,00	172	0,03	312164	60,22
8	0,02602	0	0,00	0	0,00	95	0,02
9	0,02543	0	0,00	262	0,05	6483	12,51
10	0,02527	0	0,00	17	0,00	8398	1,62
11	0,02437	1	0,00	25	0,00	21	0,00
12	0,02422	0	0,00	23	0,00	65	0,01

5.2.3 Building of template B1

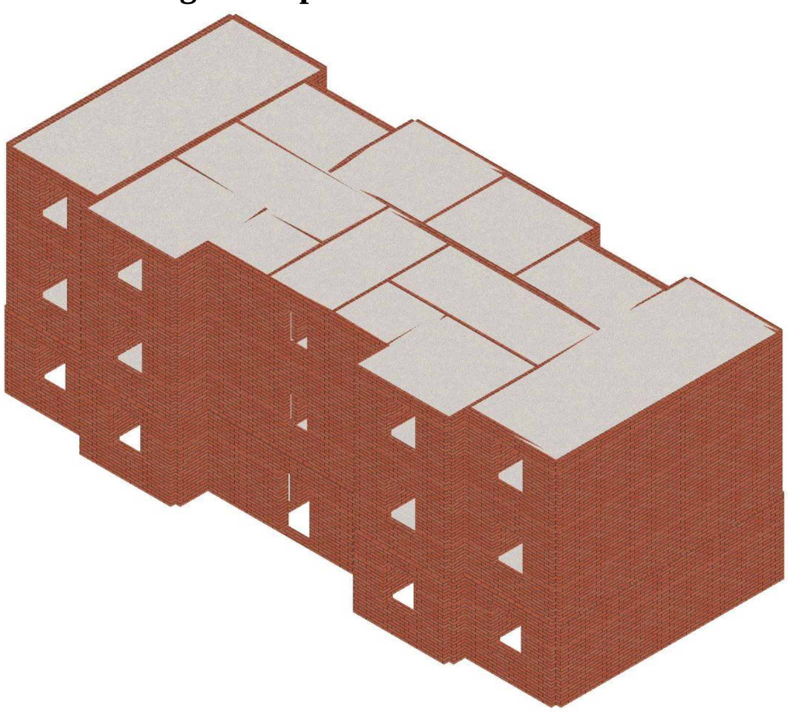

Figure 80: B1 building model

Loads are calculated as below:

-Slab 12cm $0.12 * 23 * 1.1 = 3.03\text{kN/m}^2$

-Mortar 3cm $0.03 * 20 * 1.2 = 0.72\text{kN/m}^2$

-Tiles 1cm $0.01 * 22 * 1.2 = 0.26\text{kN/m}^2$

-Plaster 2cm $0.02 * 18 * 1.2 = 0.43\text{kN/m}^2$

Sum $= 4.44\text{kN/m}^2$

Addition load (Partition walls) $= 1.2\text{kN/m}^2$

Probable live load $= 2\text{kN/m}^2$

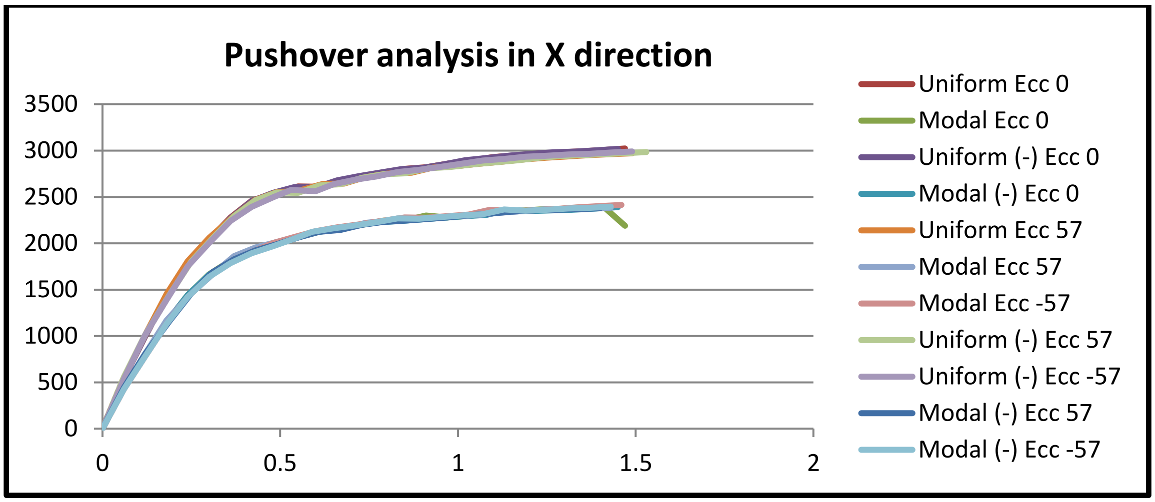

Figure 81: Pushover analysis in X-direction, 12 load patterns of B1 building

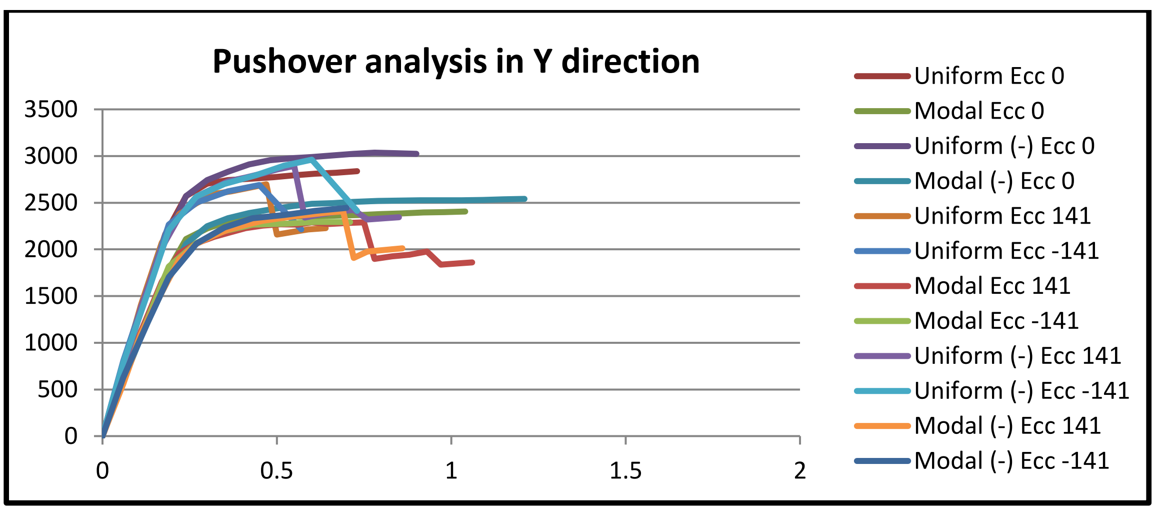

Figure 82: Pushover analysis in y-direction, 12 load patterns of B1 building

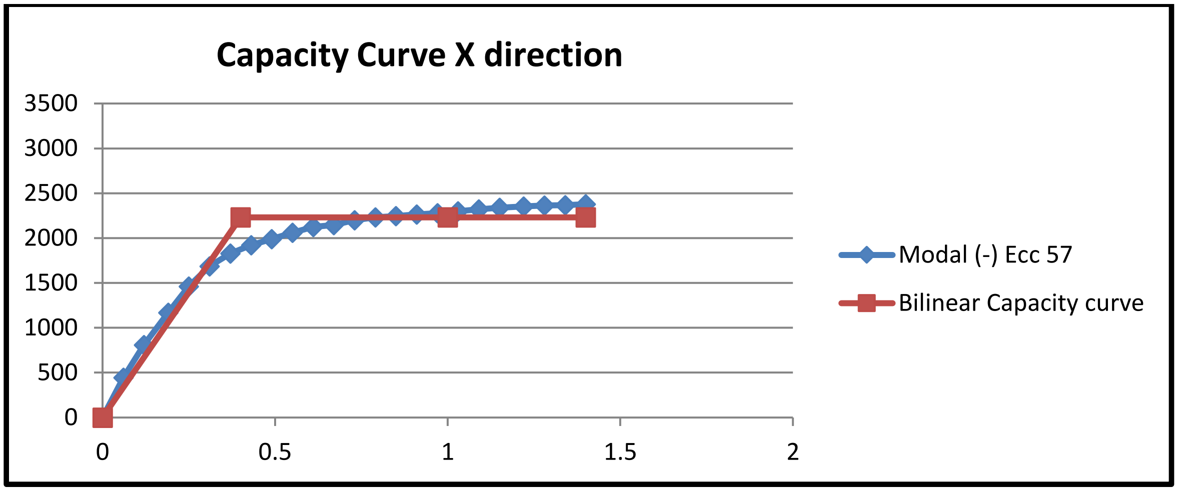

Figure 83: Capacity curve in x-direction of B1 building

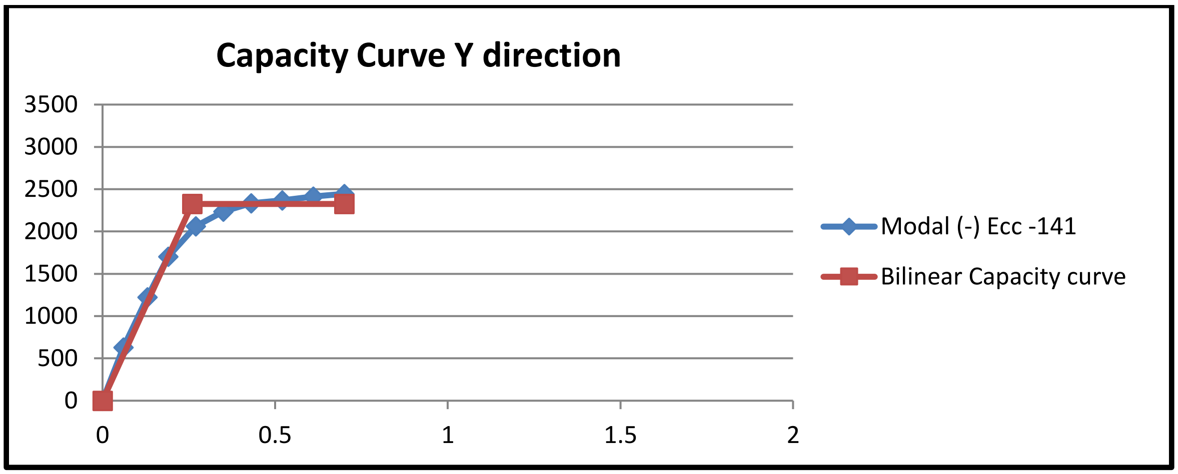

Figure 84: Capacity curve in y-direction of B1 building

Table 35: Pushover analysis parameters of B1 building

Load applied	d_y^*	d_m^*	F_y^*	K^*	μ	F_y^*/W
x-direction	0.4cm	1.4cm	2231kN	5713kN/cm	3.5	0.67
y-direction	0.26cm	0.7cm	2352kN	8943kN/cm	2.69	0.699

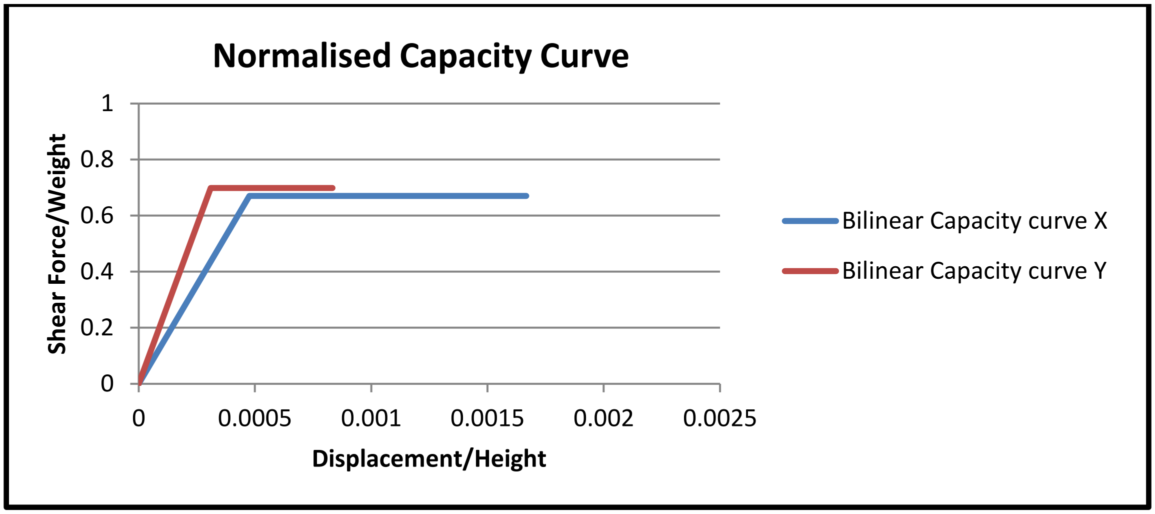

Figure 85: Normalised bilinear capacity curves of B1 building

Table 36: Period and mass participation of first 12 modes for building B1

Mode	T [s]	mx [kg]	Mx [%]	my [kg]	My [%]	mz [kg]	Mz [%]
1	0,13627	586152	81,43	0	0,00	0	0,00
2	0,13039	0	0,00	577699	80,25	15	0,00
3	0,11372	8.63	1,20	0	0,00	0	0,00
4	0,05159	93233	12,95	0	0,00	0	0,00
5	0,04898	0	0,00	115399	16,03	979	0,14
6	0,04405	1	0,00	984	0,14	149592	20,78
7	0,04376	7321	1,02	0	0,00	13	0,00
8	0,04298	867	0,12	0	0,00	0	0,00
9	0,03604	0	0,00	0	0,00	355006	49,32
10	0,03533	7736	1,07	0	0,00	0	0,00
11	0,03505	0	0,00	31	0,00	365 02	5,07
12	0,03489	0	0,00	0	0,00	4	0,00

5.2.4 Building of template B2

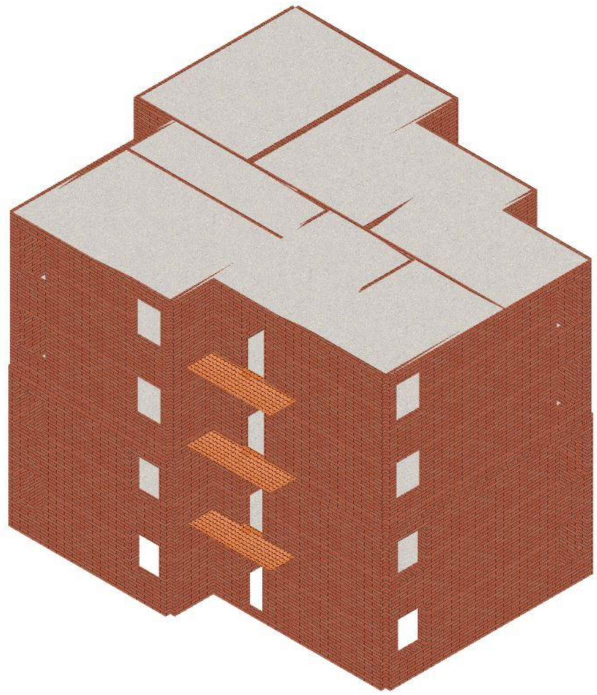

Figure 86: B2 building model

Slabs are modelled as reinforced concrete and masonry composite slabs as below:

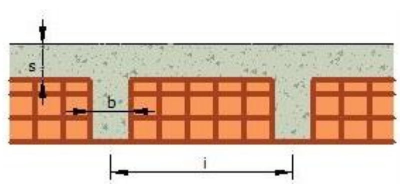

Figure 87: B2 building slabs

Slab parameters $\mathrm{b} = 10\mathrm{cm}, \mathrm{h} = 15\mathrm{cm}, \mathrm{i} = 50\mathrm{cm}, \mathrm{s} = 5\mathrm{cm}$, $\mathrm{E}_{\mathrm{conc}} = 15000\mathrm{N/mm}^2$

Addition load (Partition walls) $= 1.2\mathrm{kN/m}^2$

Probable live load $= 2\mathrm{kN/m}^2$

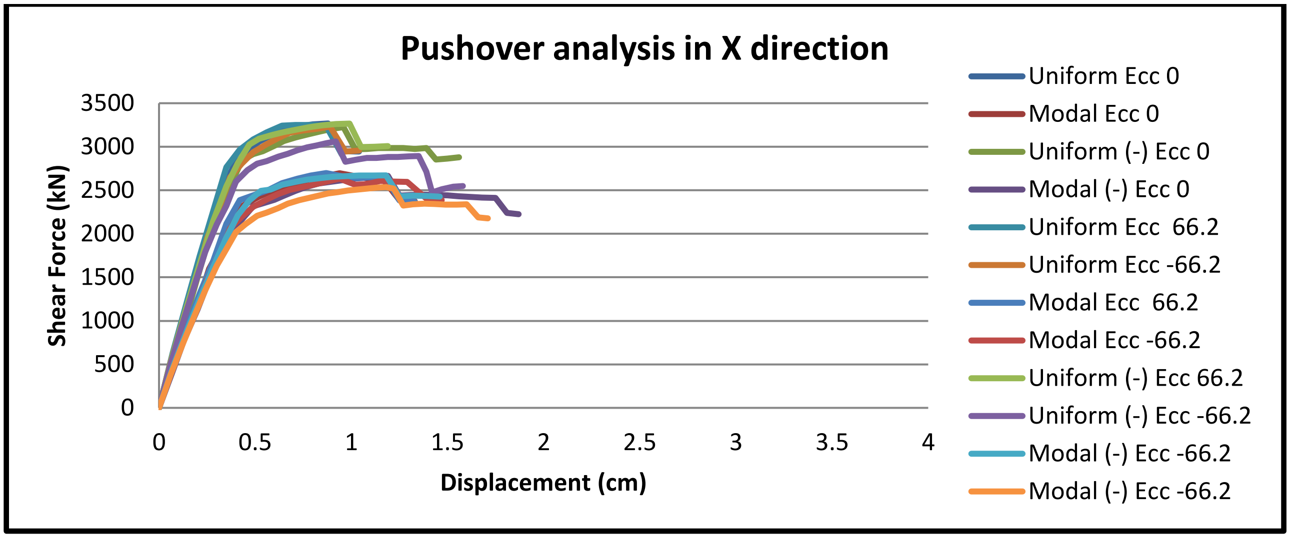

Figure 88: Pushover analysis in x-direction, 12 load patterns of B2 building

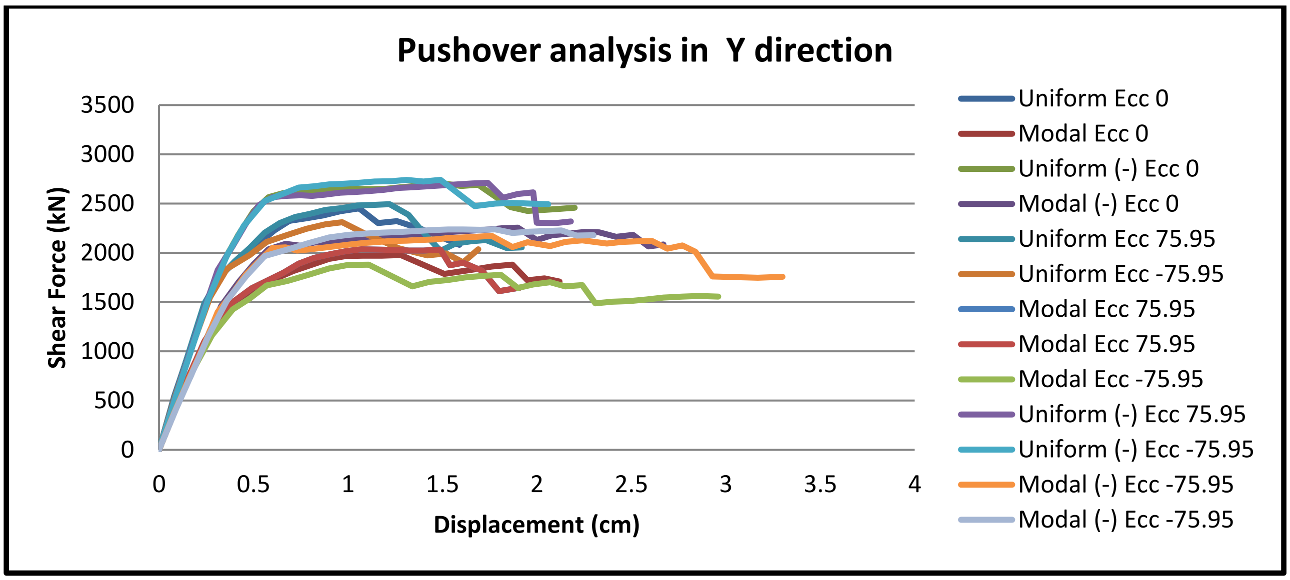

Figure 89: Pushover analysis in y-direction, 12 load patterns of B2 building

Table 37: Pushover analysis parameters of B2 building

Load applied	d_y^*	d_m^*	F_y^*	K^*	μ	F_y^*/W
x-direction	0.45cm	1.33cm	2571kN	5713kN/cm	2.96	0.663
y-direction	0.48cm	1.91cm	1898kN	3954kN/cm	3.97	0.489

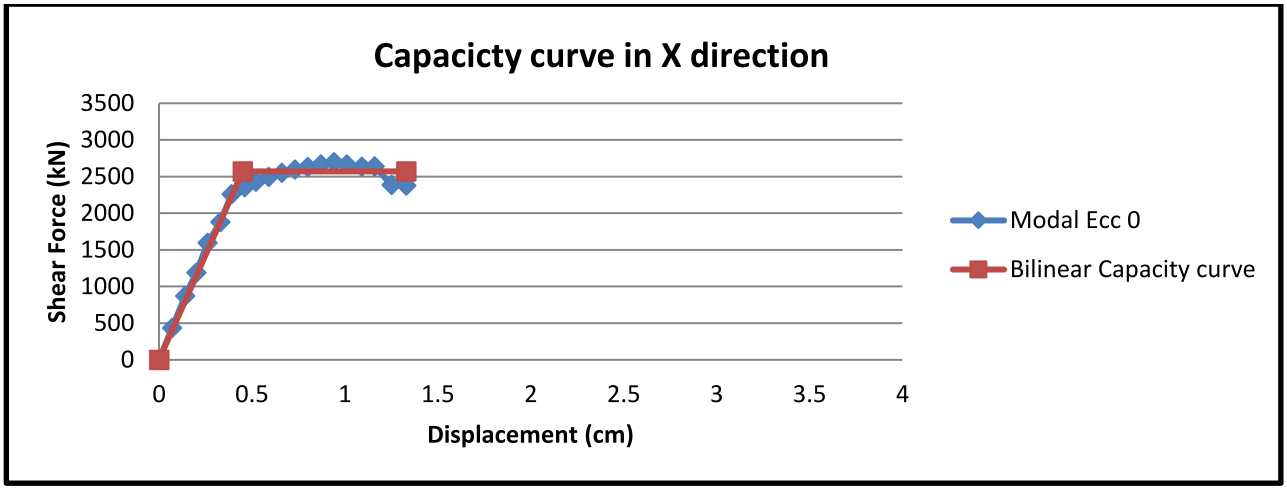

Figure 90: Pushover curve in x-direction of B2 building

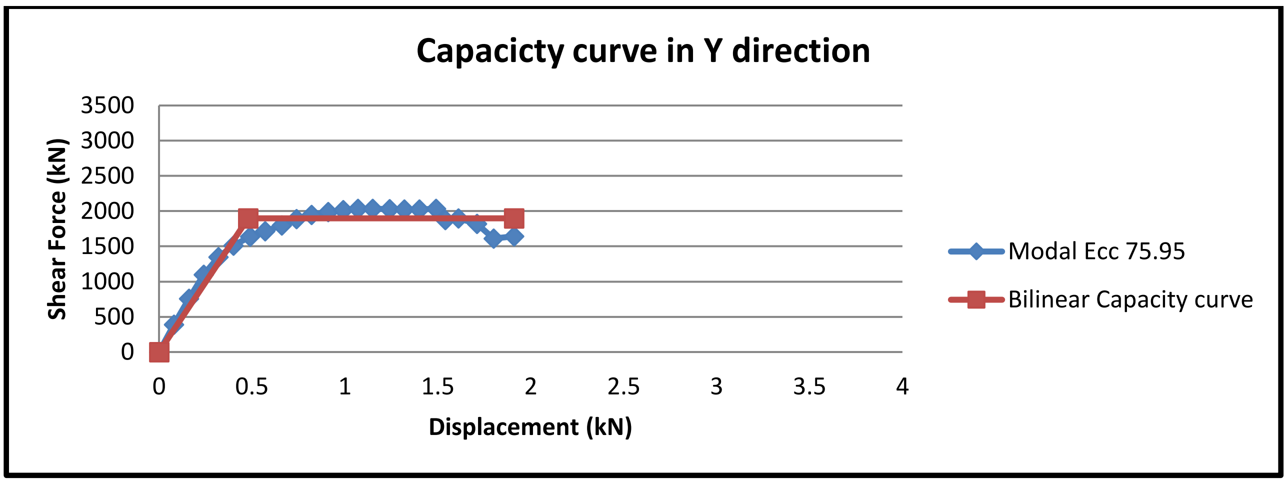

Figure 91: Pushover curve in y-direction of B2 building

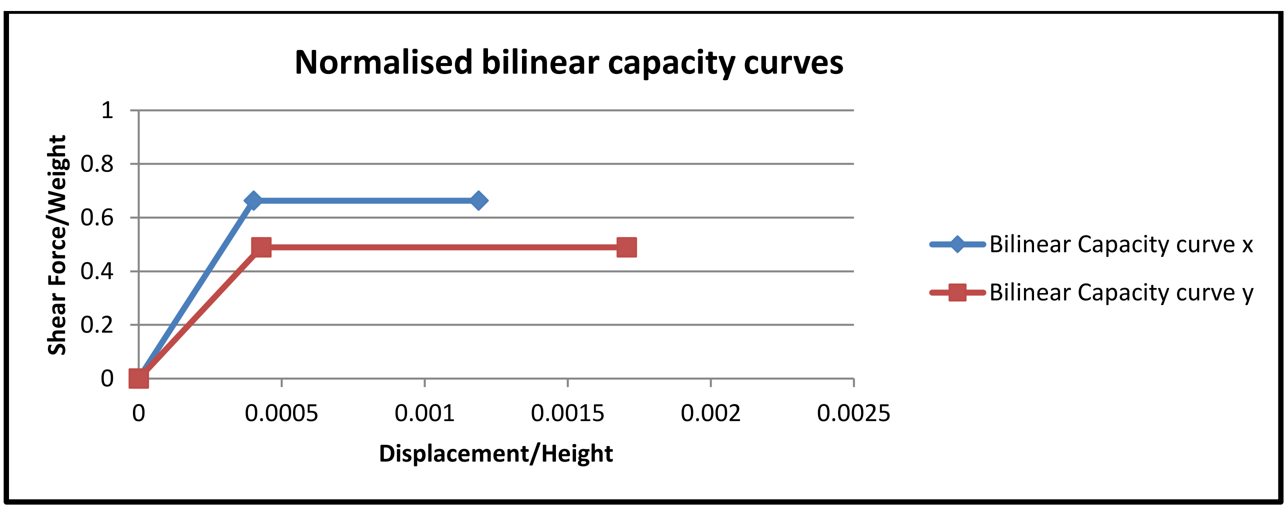

Figure 92: Normalised bilinear capacity curves of B2 building

Table 38: Period and mass participation of first 12 modes for building B2

Mode	T [s]	mx [kg]	Mx [%]	my [kg]	My [%]	mz [kg]	Mz [%]
1	0,18129	16371	1,80	623862	68,59	284	0,03
2	0,16622	638324	70,18	32127	3,53	40	0,00
3	0,14140	64136	7,05	25501	2,80	78	0,01
4	0,06565	6777	0,75	152532	16,77	2701	0,30
5	0,06216	138559	15,23	10914	1,20	1095	0,12
6	0,05391	4379	0,48	11306	1,24	20336	2,24
7	0,05100	74	0,01	220	0,02	581565	63,94
8	0,04765	107	0,01	2991	0,33	18851	2,07
9	0,04681	367	0,04	2835	0,31	3445	3,79
10	0,04538	1285	0,14	487	0,05	18313	2,01
11	0,04365	1294	0,14	111	0,12	42578	4,68
12	0,04067	347	0,04	584	0,06	6266	0,69

5.2.5 Building of template B3

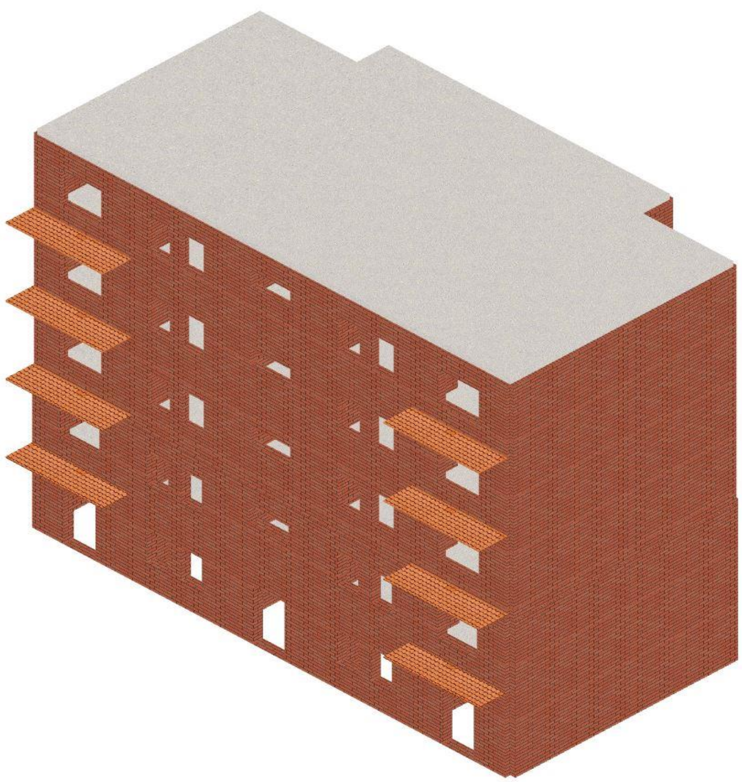

Figure 93: B3 building model

Loads are calculated as below:

-Slab 12cm $0.12 * 23 * 1.1 = 3.03\text{kN/m}^2$

-Mortar 3cm $0.03 * 20 * 1.2 = 0.72\text{kN/m}^2$

-Tiles 1cm $0.01 * 22 * 1.2 = 0.26\text{kN/m}^2$

-Plaster 2cm $0.02 * 18 * 1.2 = 0.43\text{kN/m}^2$

Sum $= 4.44\text{kN/m}^2$

Addition load (Partition walls) $= 1.2\text{kN/m}^2$

Probable live load $= 2\text{kN/m}^2$

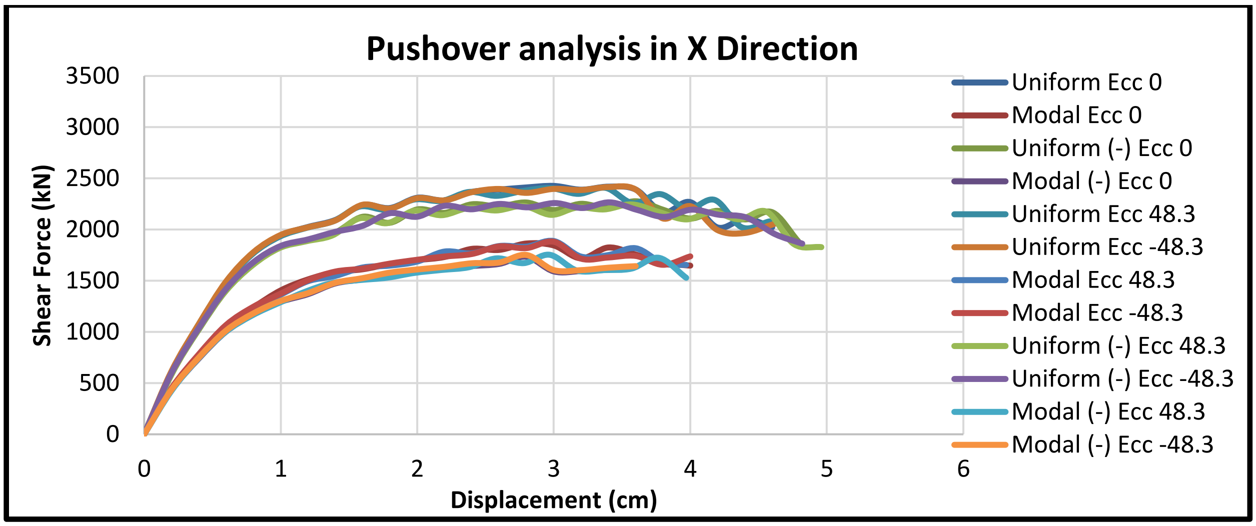

Figure 94: Pushover analysis in x-direction, 12 load patterns of B3 building

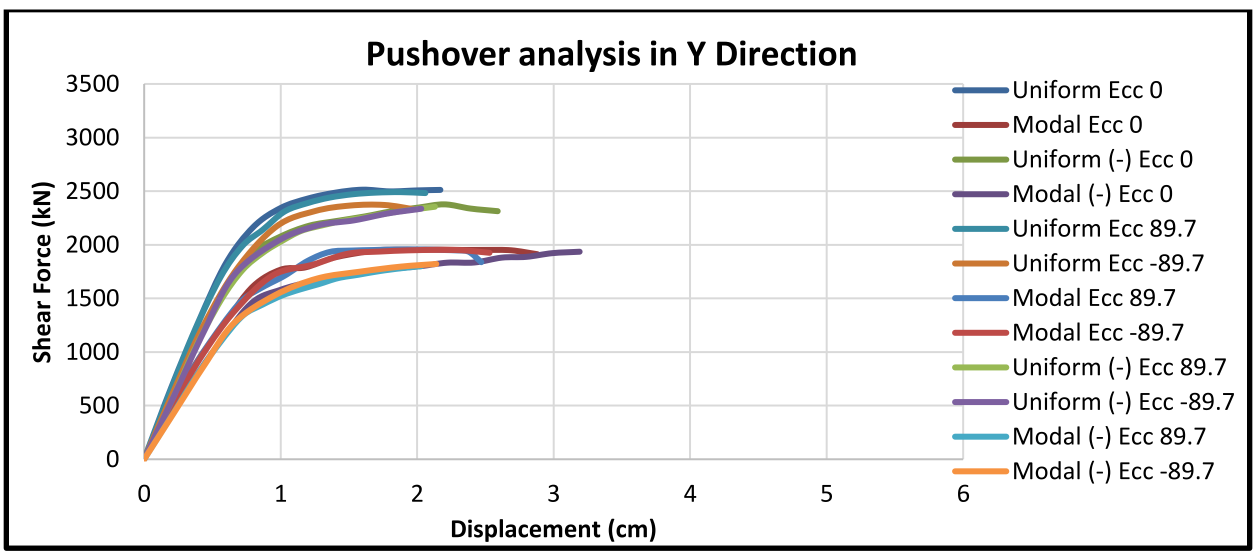

Figure 95: Pushover analysis in y-direction, 12 load patterns of B3 building

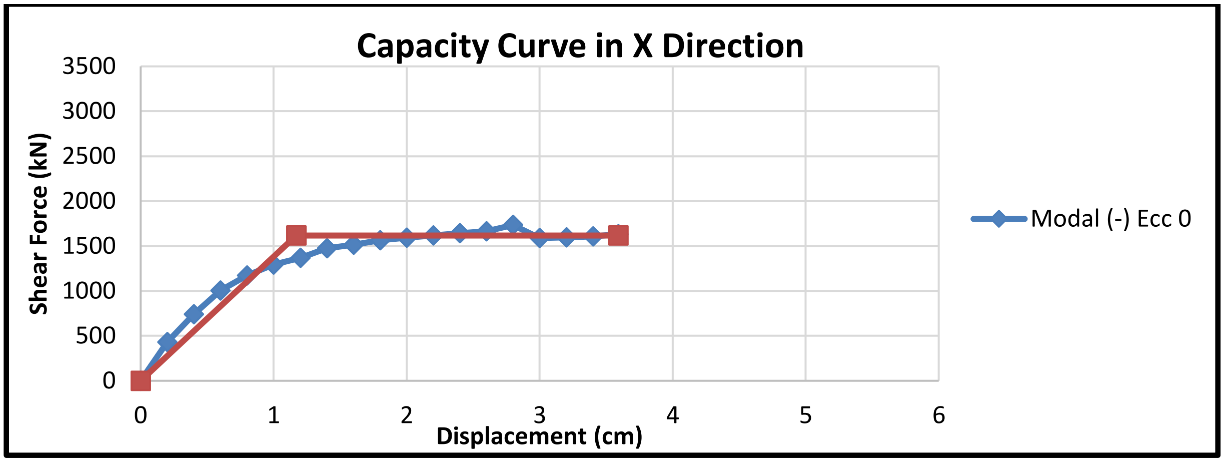

Figure 96: Capacity curve in x-direction of B3 building

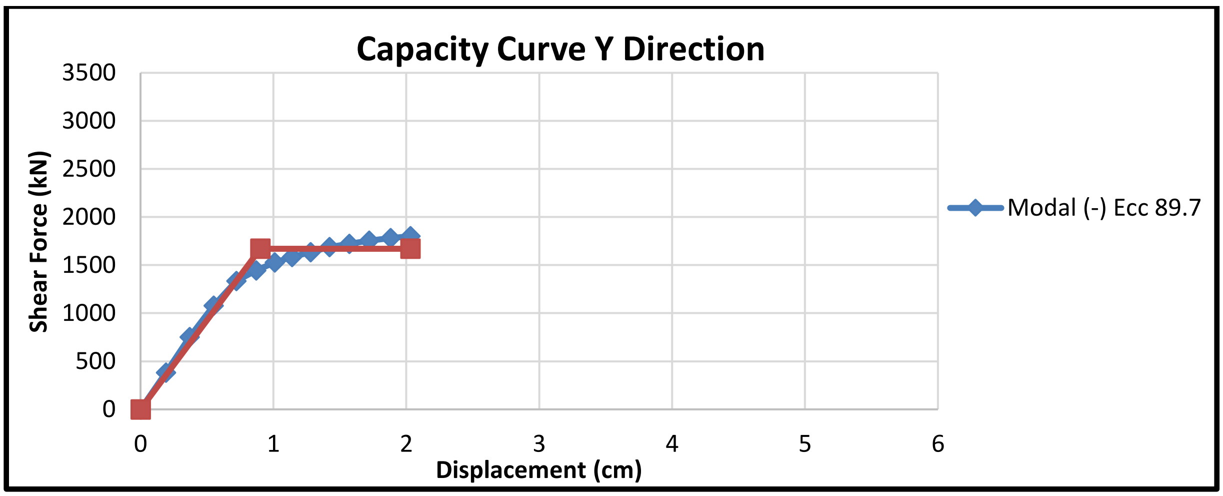

Figure 97: Capacity curve in y-direction of B3 building

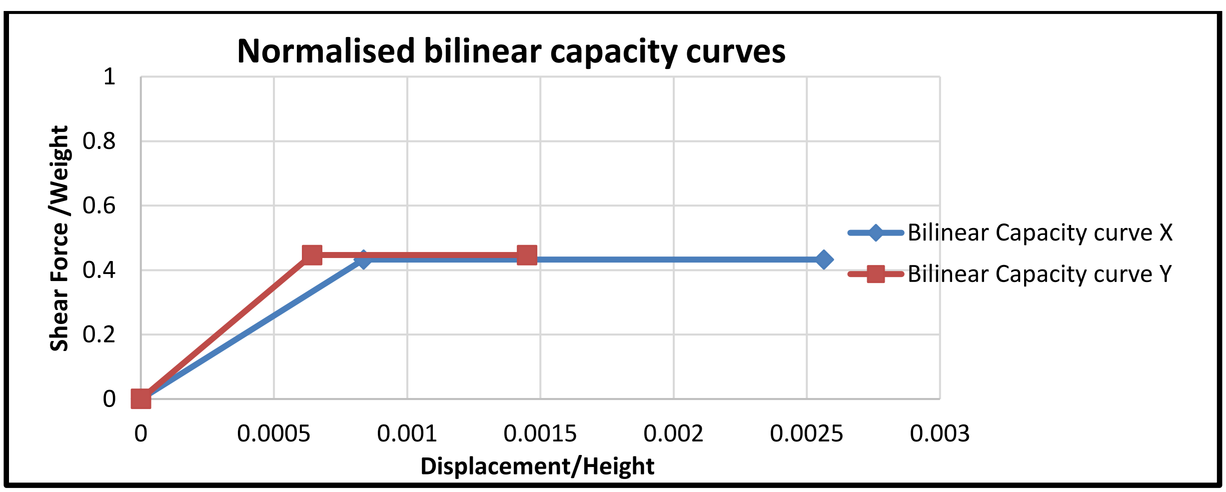

Figure 98: Normalised bilinear capacity curves of B3 building

Table 39: Pushover analysis parameters of B3 building

Load applied	d_y^*	d_m^*	F_y^*	K^*	μ	F_y^*/W
x-direction	1.17cm	3.59cm	1617kN	1382kN/cm	3.07	0.433
y-direction	0.9cm	2.03cm	1670kN	1856kN/cm	2.26	0.447

Table 40: Period and mass participation of first 12 modes for building B3

Mode	T [s]	mx [kg]	Mx [%]	my [kg]	My [%]	mz [kg]	Mz [%]
1	0,24388	75	0,01	679.317	72,74	252	0,03
2	0,23000	706.048	75,60	51	0,01	0	0,00
3	0,18980	3.867	0,41	438	0,05	0	0,00
4	0,08818	153	0,02	174.582	18,69	1.963	0,21
5	0,08750	143.598	15,38	159	0,02	3	0,00
6	0,07258	971	0,10	130	0,01	12	0,00
7	0,06347	11	0,00	211	0,02	740.266	79,26
8	0,05891	1.732	0,19	6	0,00	4.291	0,46
9	0,05413	4	0,00	2.167	0,23	2.548	0,27
10	0,05137	19	0,00	1.84	0,20	727	0,08
11	0,05019	42.44	4,54	3	0,00	31	0,00
12	0,04933	203	0,02	11.368	1,22	123	0,01

5.2.6 Building of template B4

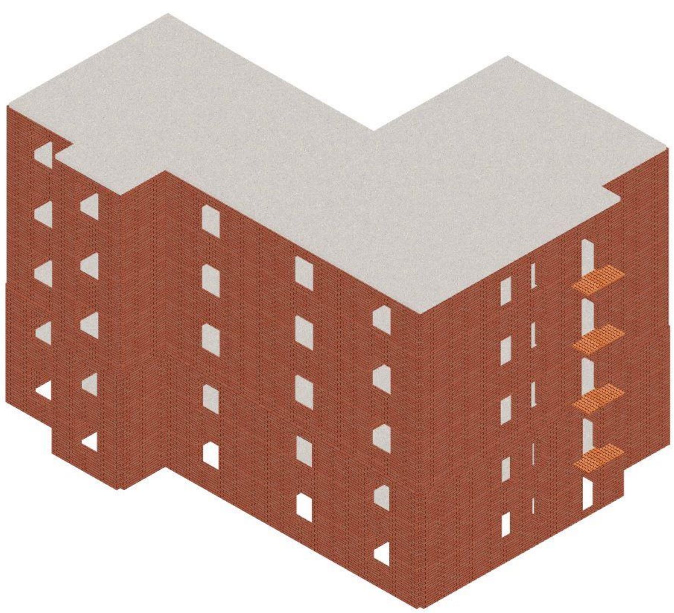

Figure 99: B4 building model

Slabs are modelled as reinforced concrete and masonry composite slabs as below:

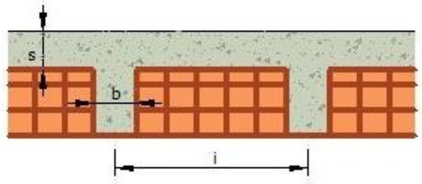

Figure 100: B4 building slabs

Slab parameters $b = 10cm, h = 15cm, i = 50cm, s = 5cm,\ E_{conc} = 15000N/mm^2$

Addition load (Partition walls) $= 1.3kN/m^2$

Probable live load $= 2kN/m^2$

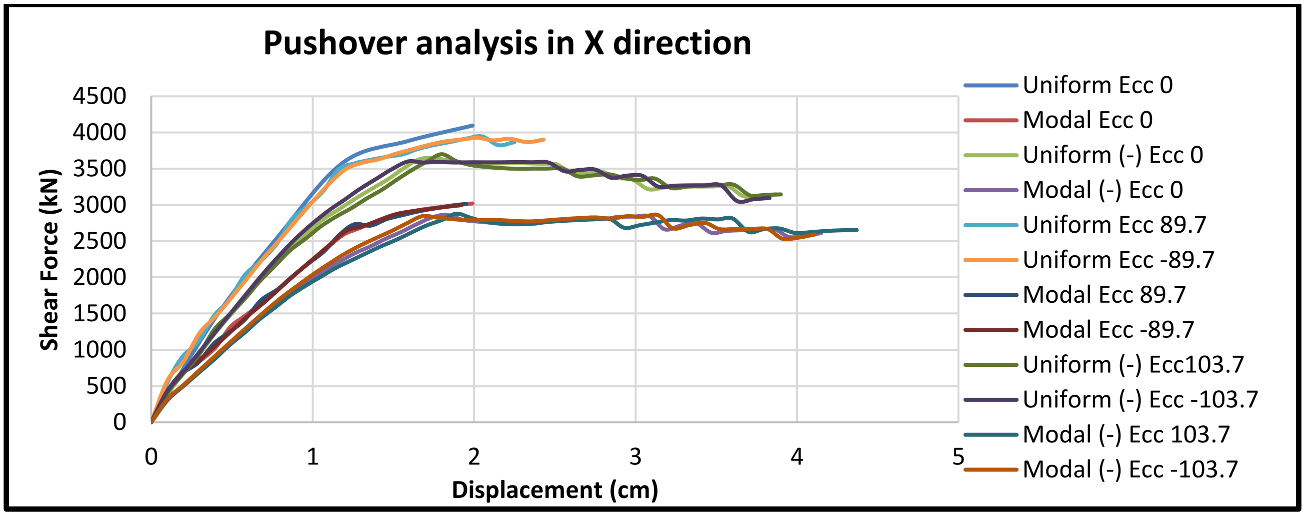

Figure 101: Pushover analysis in x-direction, 12 load patterns of B4 building

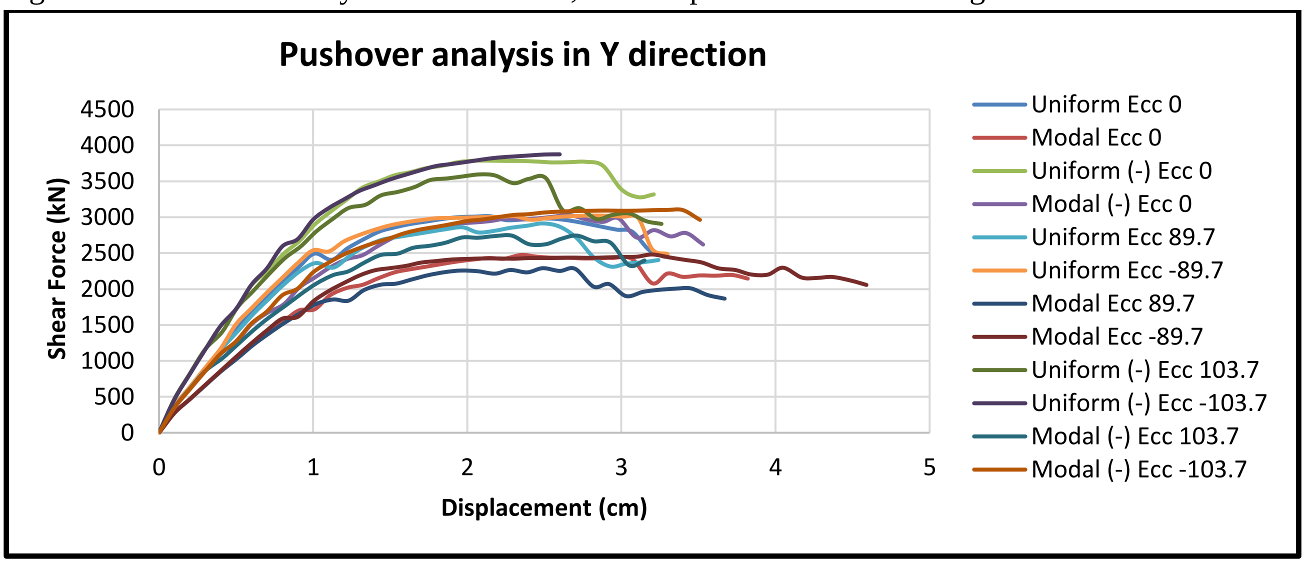

Figure 102: Pushover analysis in y-direction, 12 load patterns of B4 building

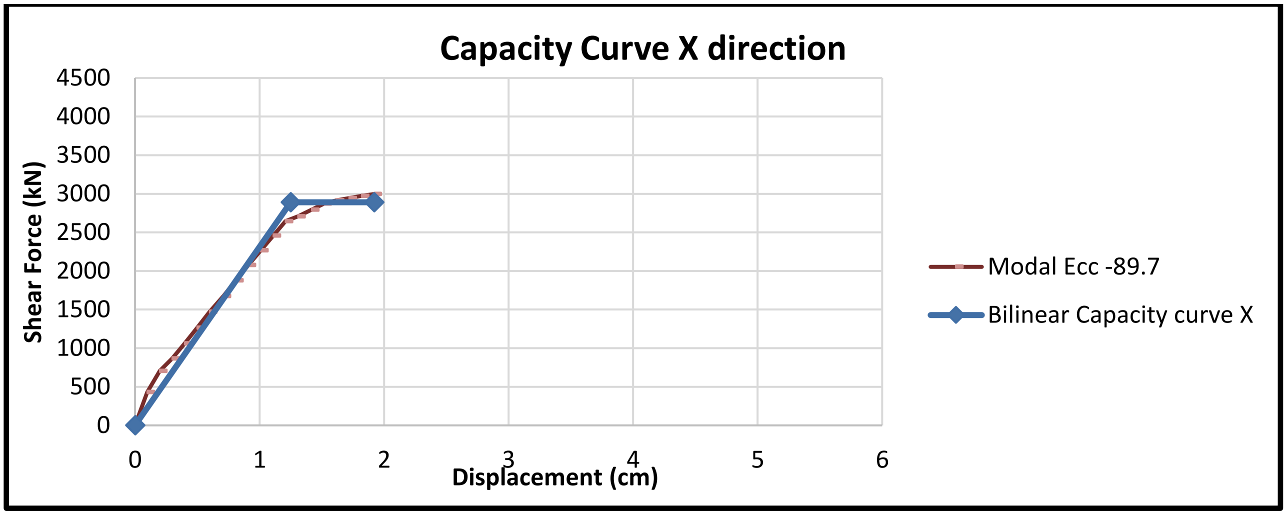

Figure 103: Capacity curve in y-direction of B4 building

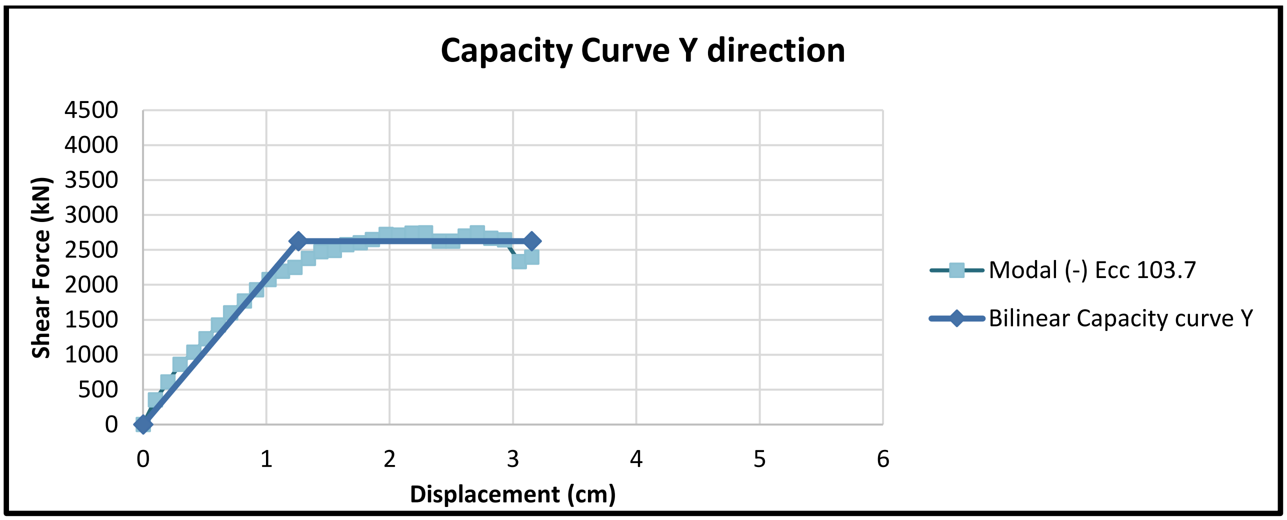

Figure 104: Capacity curve in y-direction of B4 building

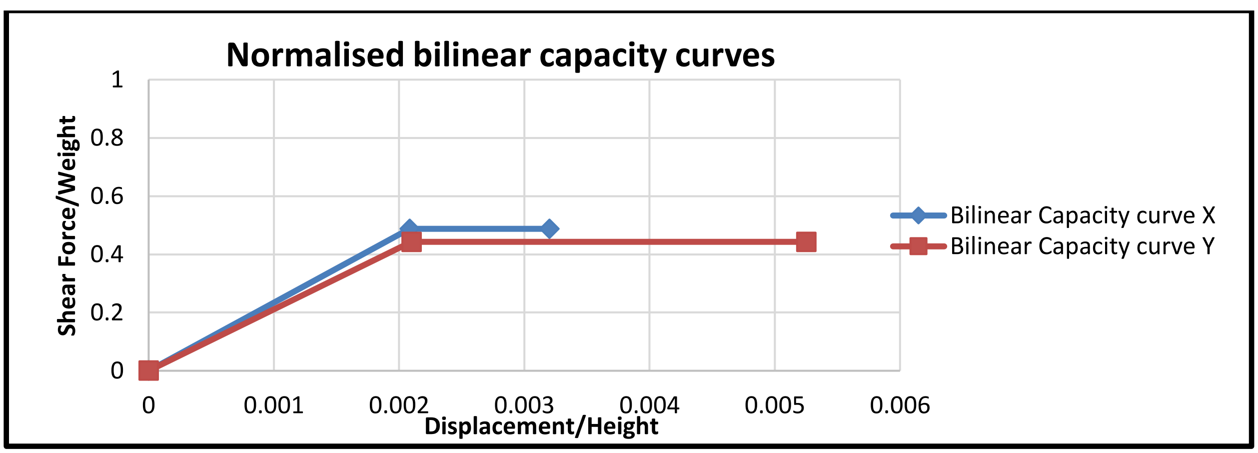

Figure 105: Normalised bilinear capacity curves of B4 building

Table 41: Pushover analysis parameters of B4 building

Load applied	d_y^*	d_m^*	F_y^*	K^*	μ	F_y^*/W
x-direction	1.25cm	1.92cm	2890kN	2312kN/cm	1.54	0.4876
y-direction	1.26cm	3.15cm	2625kN	2083kN/cm	2.5	0.4429

Table 42: Period and mass participation of first 12 modes for building B4

Mode	T [s]	mx [kg]	Mx [%]	my [kg]	My [%]	mz [kg]	Mz [%]
1	0.25938	64268	4,60	970987	69,49	13	0,00
2	0.23303	894028	63,98	58016	4,15	64	0,00
3	0.20304	101428	7,26	9068	0,65	66	0,00
4	0.09349	14444	1,03	242253	17,34	163	0,01
5	0.08745	205358	14,70	14202	1,02	1557	0,11
6	0.07753	11555	0,83	302	0,02	5845	0,42
7	0.06762	185	0,01	110	0,01	1063210	76,09
8	0.06506	1984	0,14	2407	0,17	24767	1,77
9	0.06099	116	0,01	264	0,02	356	0,03
10	0.05625	5501	0,39	6	0,00	2184	0,16
11	0.05542	372	0,03	2716	0,19	13521	0,97
12	0.05198	1186	0,08	32432	2,32	683	0,05

5.2.7 Building of template C1A

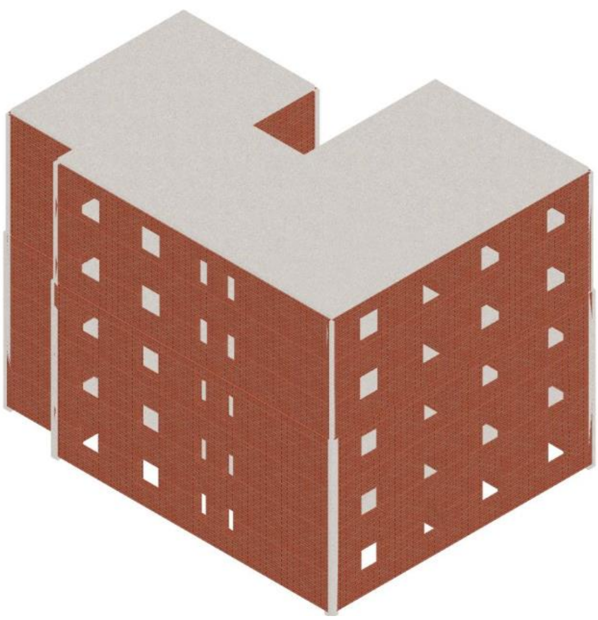

Figure 106: C1A building model

Loads are calculated as below:

-Slab 12cm	$0.12 * 25 * 1.1 = 3.3\text{kN/m}^2$
-Mortar 3cm	$0.03 * 18 * 1.2 = 0.65\text{kN/m}^2$
-Tiles 1cm	$0.01 * 22 * 1.2 = 0.26\text{kN/m}^2$
-Plaster 2cm	$0.02 * 18 * 1.2 = 0.43\text{kN/m}^2$
Sum	$= 4.64\text{kN/m}^2$
Addition load (Partition walls)	$= 1.3\text{kN/m}^2$
Probable live load	$= 2\text{kN/m}^2$

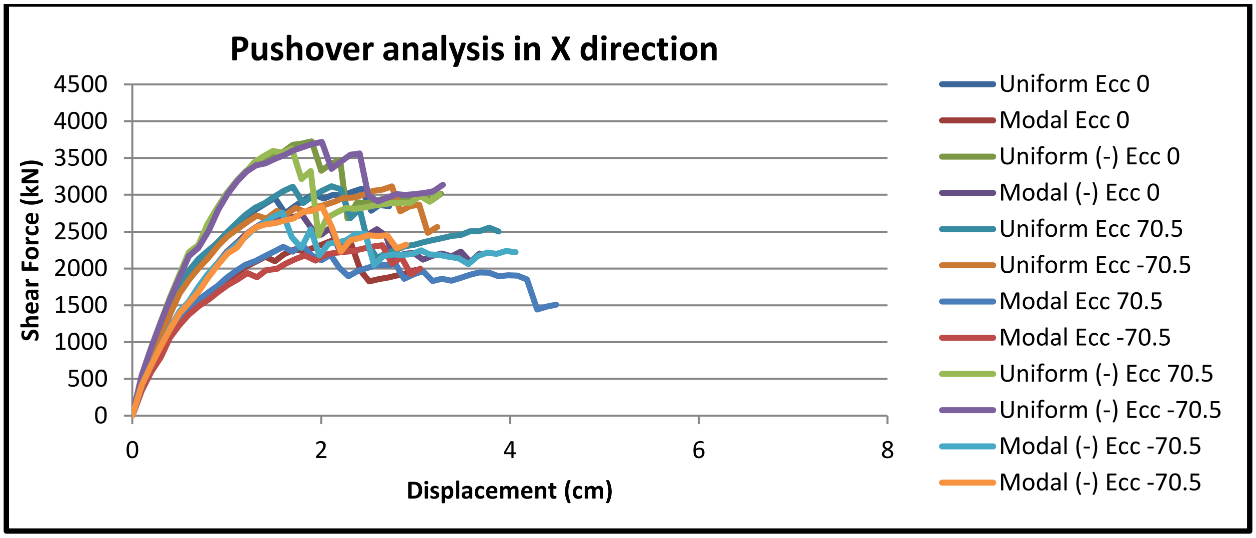

Figure 107: Pushover analysis in x-direction, 12 load patterns of C1A building

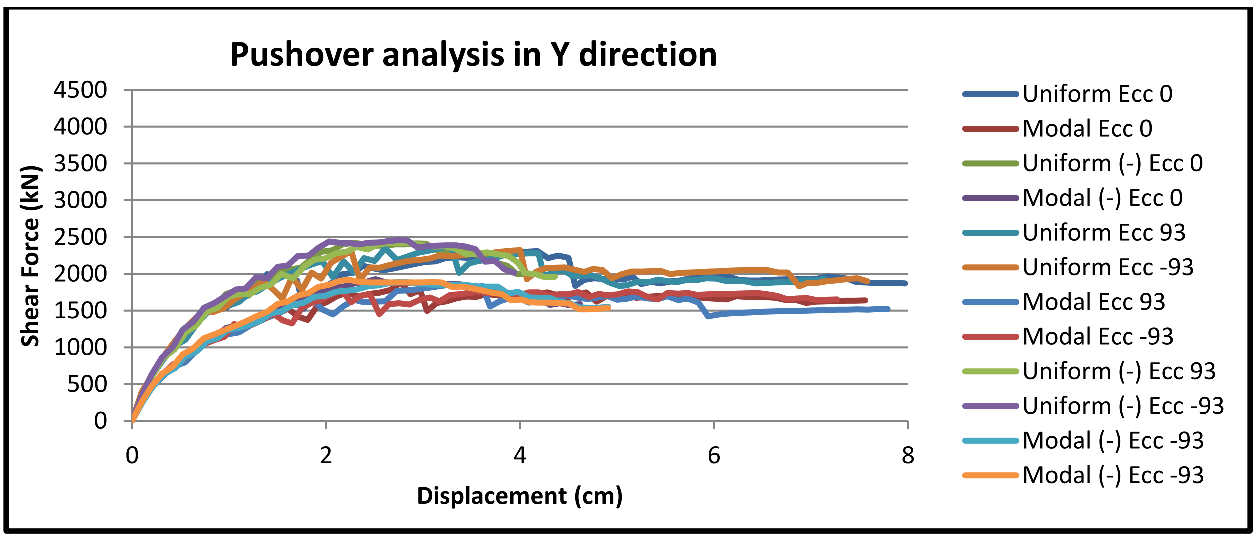

Figure 108: Pushover analysis in y-direction, 12 load patterns of C1A building

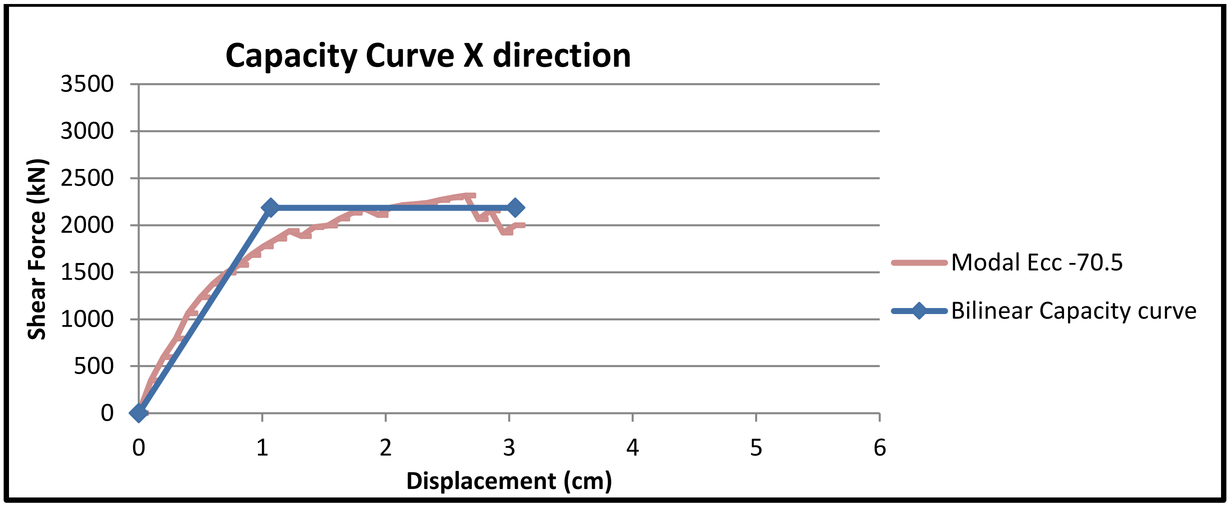

Figure 109: Capacity curve in x-direction of C1A building

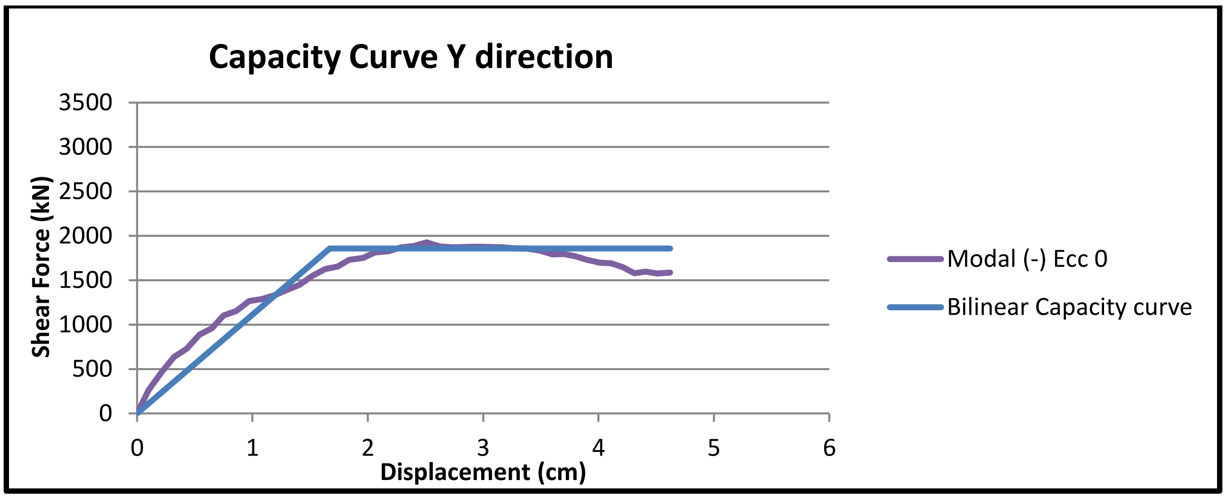

Figure 110: Capacity curve in y-direction of C1A building

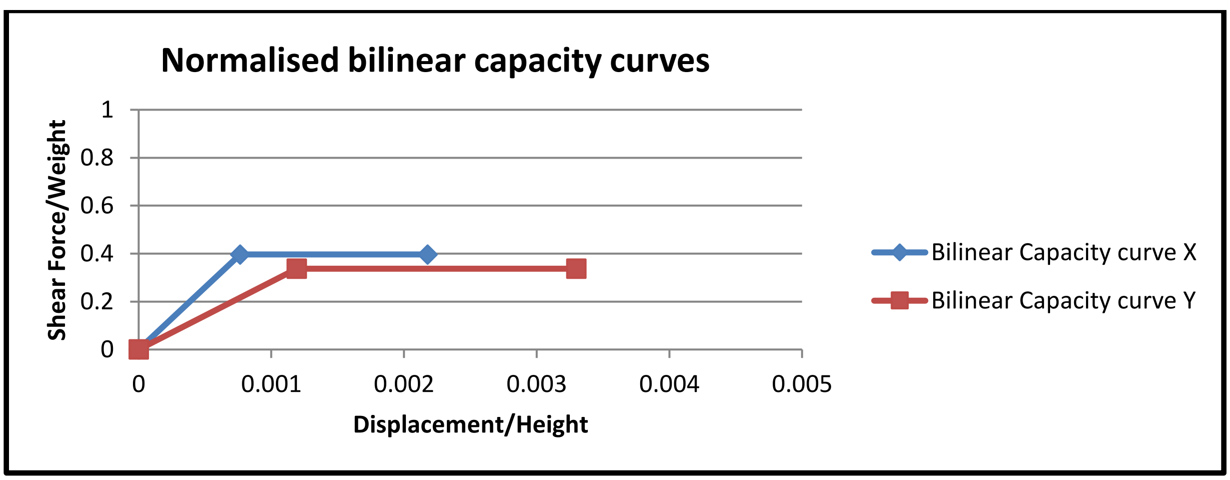

Figure 111: Normalised bilinear capacity curves of C1A building

Table 43: Pushover analysis parameters of C1A building

Load applied	d_y^*	d_m^*	F_y^*	K^*	μ	F_y^*/W
x-direction	1.07cm	3.05cm	2184kN	2042kN/cm	2.85	0.3965
y-direction	1.67cm	4.62cm	1857kN	1112kN/cm	2.76	0.3371

Table 44: Modal analysis parameters of building C1A

Mode	T [s]	mx [kg]	Mx [%]	my [kg]	My [%]	mz [kg]	Mz [%]
1	0,24719	332	0,03	978036	76,97	9	0,00
2	0,21997	978497	77,01	131	0,10	261	0,02
3	0,18609	24468	1,93	12082	0,95	711	0,06
4	0,09254	287	0,02	186406	14,67	0	0,00
5	0,08298	177083	13,94	531	0,04	10766	0,85
6	0,07251	358	0,03	5099	0,40	81817	6,44
7	0,06949	7151	0,56	199	0,02	250378	19,71
8	0,06151	201	0,02	32	0,00	19118	1,50
9	0,05878	256	0,02	0	0,00	445987	35,10
10	0,05489	22	0,00	1764	0,14	698	0,55
11	0,05313	316	0,02	41295	3,25	15772	1,24
12	0,05168	886	0,07	1393	0,11	49574	3,90

5.2.8 Building of template C1B

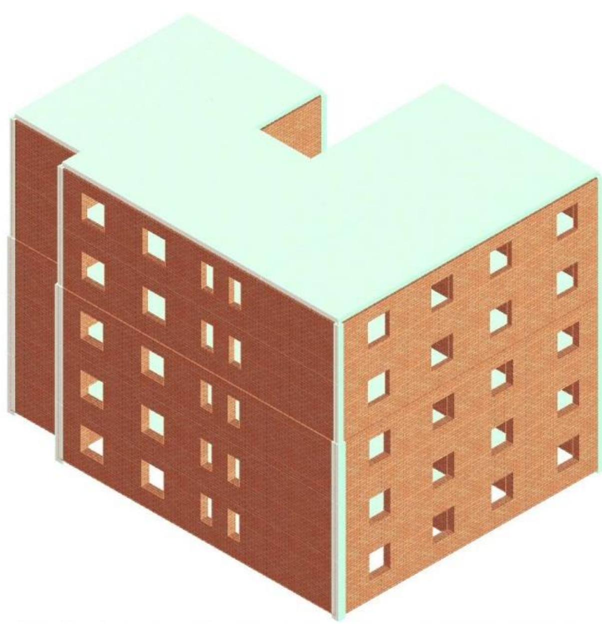

Figure 112: C1B building model

Loads are calculated as below:

-Slab 12cm	$0.12 * 25 * 1.1 = 3.3\text{kN/m}^2$
-Mortar 3cm	$0.03 * 18 * 1.2 = 0.65\text{kN/m}^2$
-Tiles 1cm	$0.01 * 22 * 1.2 = 0.26\text{kN/m}^2$
-Plaster 2cm	$0.02 * 18 * 1.2 = 0.43\text{kN/m}^2$
Sum	$= 4.64\text{kN/m}^2$
Addition load (Partition walls)	$= 1.3\text{kN/m}^2$
Probable live load	$= 2\text{kN/m}^2$

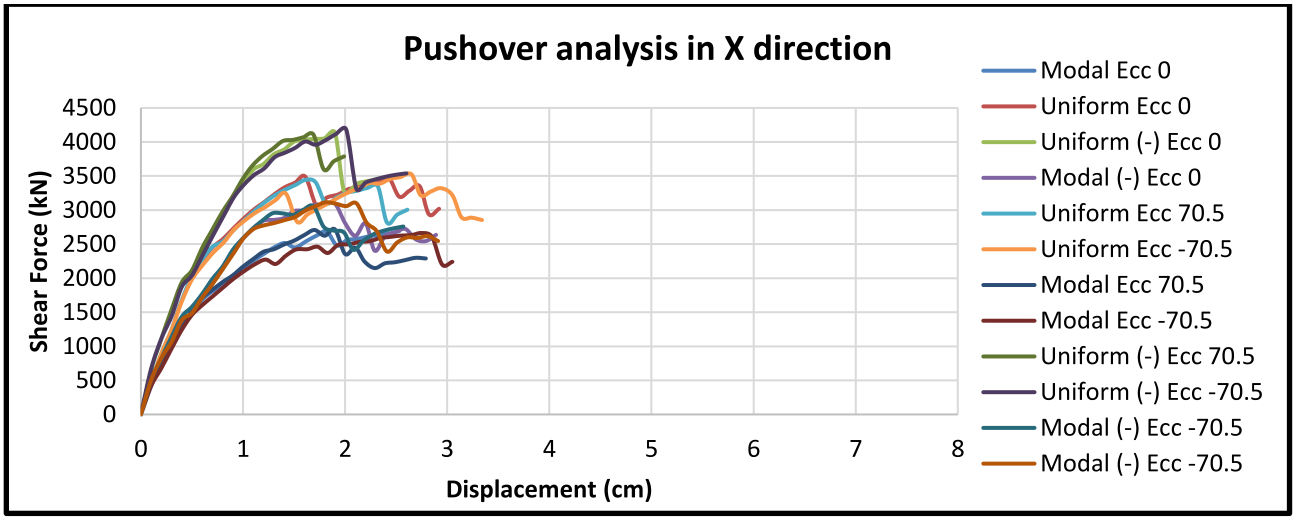

Figure 113: Pushover analysis for x-direction, 12 load patterns of C1B building

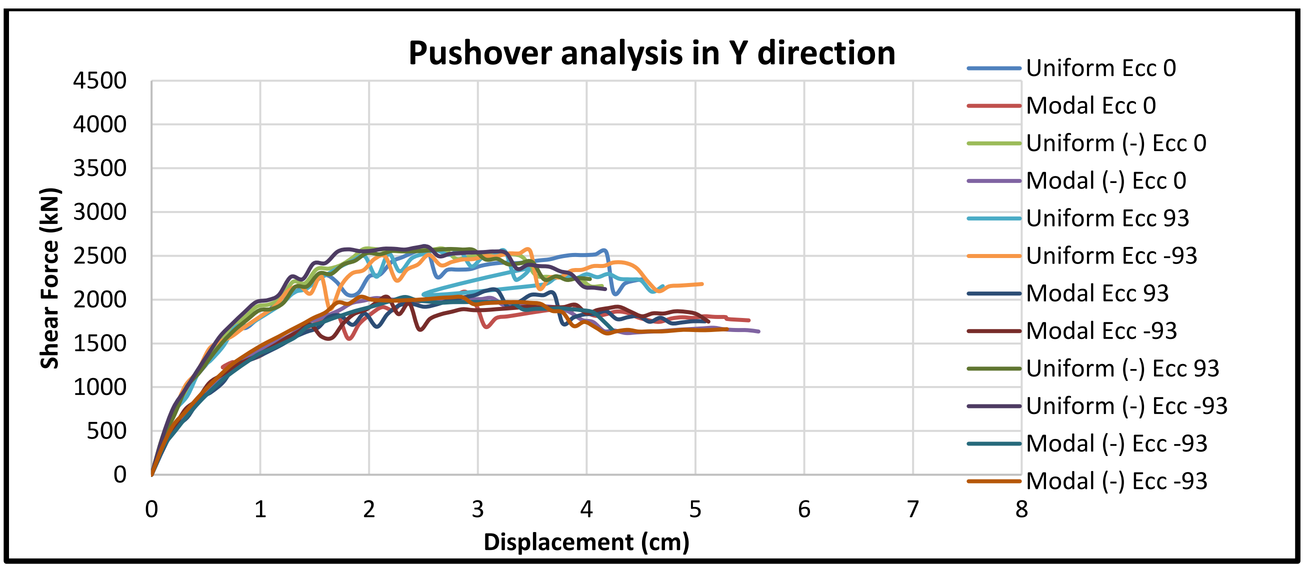

Figure 114: Pushover analysis for y-direction, 12 load patterns of C1B building

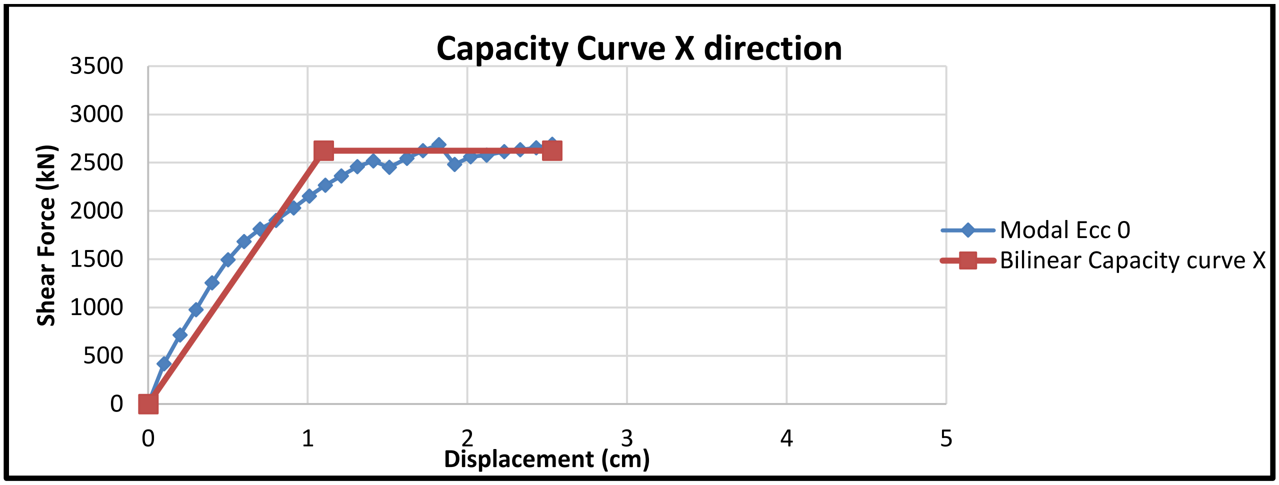

Figure 115: Capacity curve in x-direction of C1B building

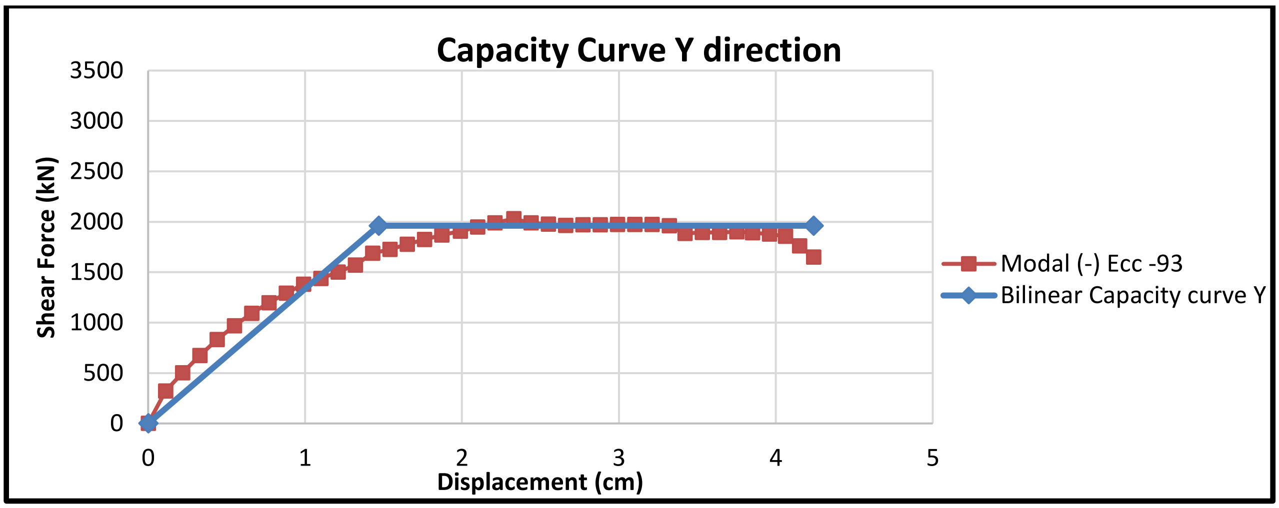

Figure 116: Capacity curve in y-direction of C1B building

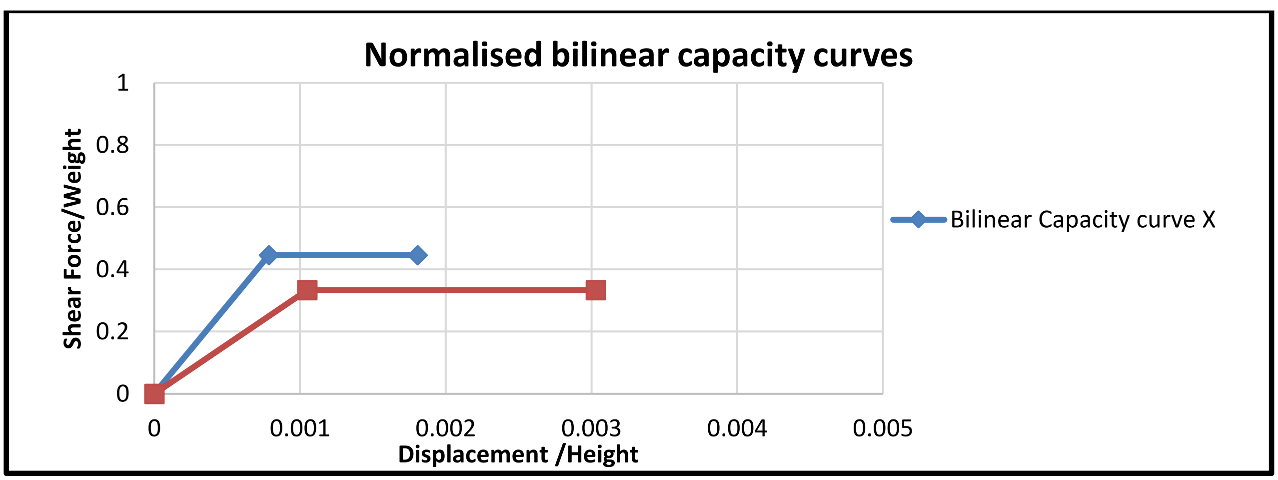

Figure 117: Normalised bilinear capacity curves of C1B building

Table 45: Pushover analysis parameters of C1B building

Load applied	d_y^*	d_m^*	F_y^*	K^*	μ	F_y^*/W
x-direction	1.1cm	2.53cm	2624kN	2385kN/cm	2.3	0.4461
y-direction	1.47cm	4.24cm	1961kN	1334kN/cm	2.88	0.3334

Table 46: Modal analysis parameters of C1B building

Mode	T [s]	mx [kg]	Mx [%]	my [kg]	My [%]	mz [kg]	Mz [%]
1	0,24409	410	0,03	1047848	77,11	9	0,00
2	0,21734	1043791	76,81	1.529	0,11	269	0,02
3	0,18419	29588	2,18	11.591	0,85	743	0,05
4	0,09155	376	0,03	199617	14,69	2	0,00
5	0,08202	189911	13,98	719	0,05	8887	0,65
6	0,07172	1606	0,12	5031	0,37	49336	3,63
7	0,06760	5638	0,41	15	0,00	312222	22,98
8	0,05966	182	0,01	44	0,00	20567	1,51
9	0,05716	229	0,02	1	0,00	492847	36,27
10	0,05361	1	0,00	6573	0,48	1.932	0,14
11	0,05253	412	0,03	36415	2,68	27.12	2,00
12	0,05119	0	0,00	8756	0,64	55313	4,07

5.2.9 Building of template C2

Figure 118: C2 building model

Loads are calculated as below:

-Slab 12cm	$0.12 * 25 * 1.1 = 3.3\text{kN/m}^2$
-Mortar 3cm	$0.03 * 18 * 1.2 = 0.65\text{kN/m}^2$
-Tiles 1cm	$0.01 * 22 * 1.2 = 0.26\text{kN/m}^2$
-Plaster 2cm	$0.02 * 18 * 1.2 = 0.43\text{kN/m}^2$
Sum	$= 4.64\text{kN/m}^2$
Addition load (Partition walls)	$= 1.3\text{kN/m}^2$
Probable live load	$= 2\text{kN/m}^2$

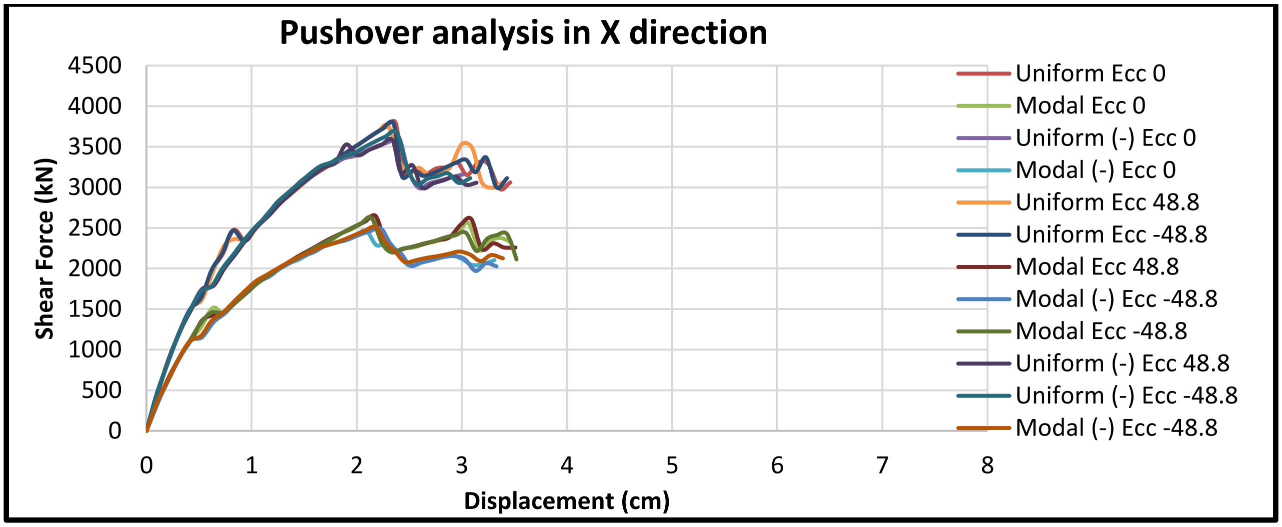

Figure 119: Pushover analysis in x-direction, 12 load patterns of C2 building

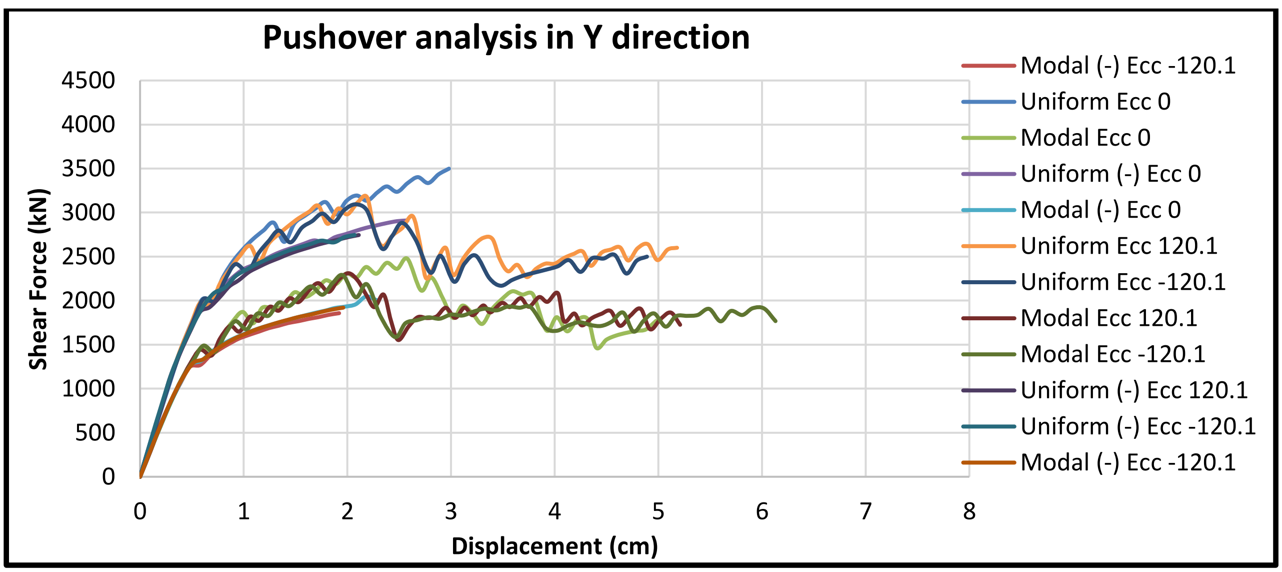

Figure 120: Pushover analysis in y-direction, 12 load patterns of C2 building

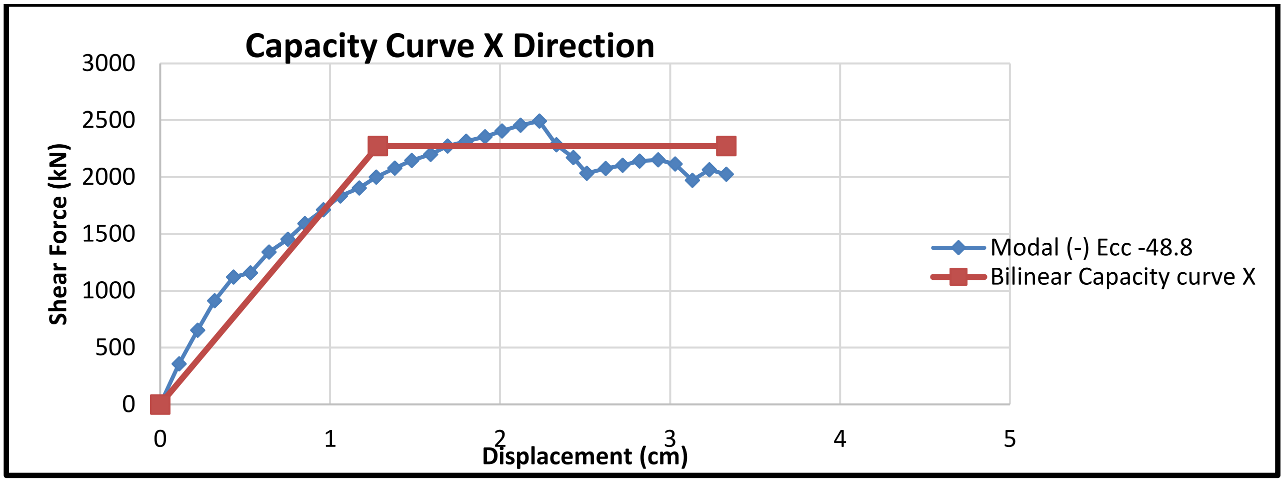

Figure 121: Capacity curve in x-direction of C2 building

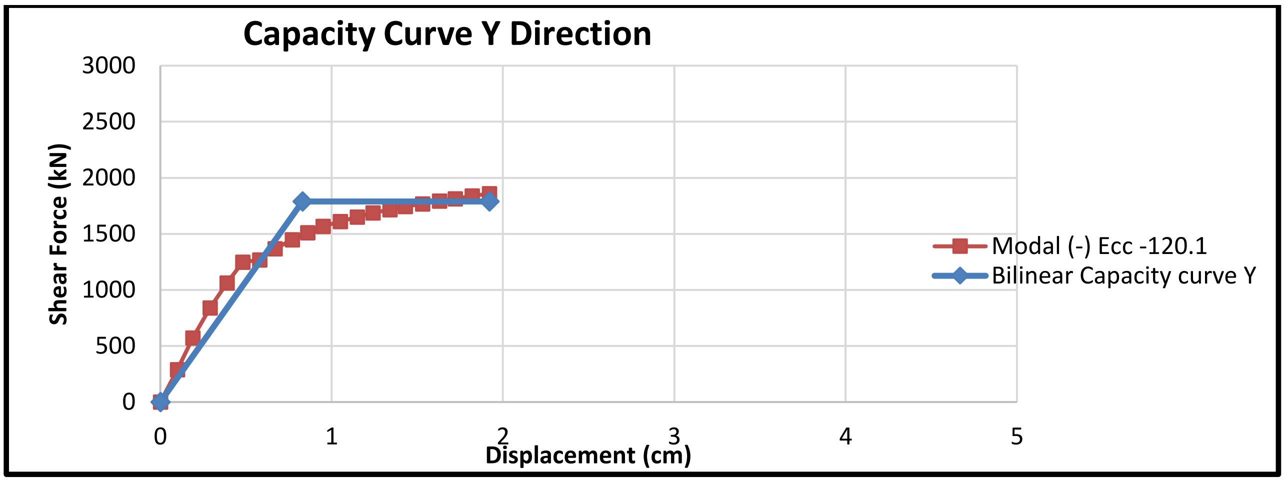

Figure 122: Capacity curve in y-direction of C2 building

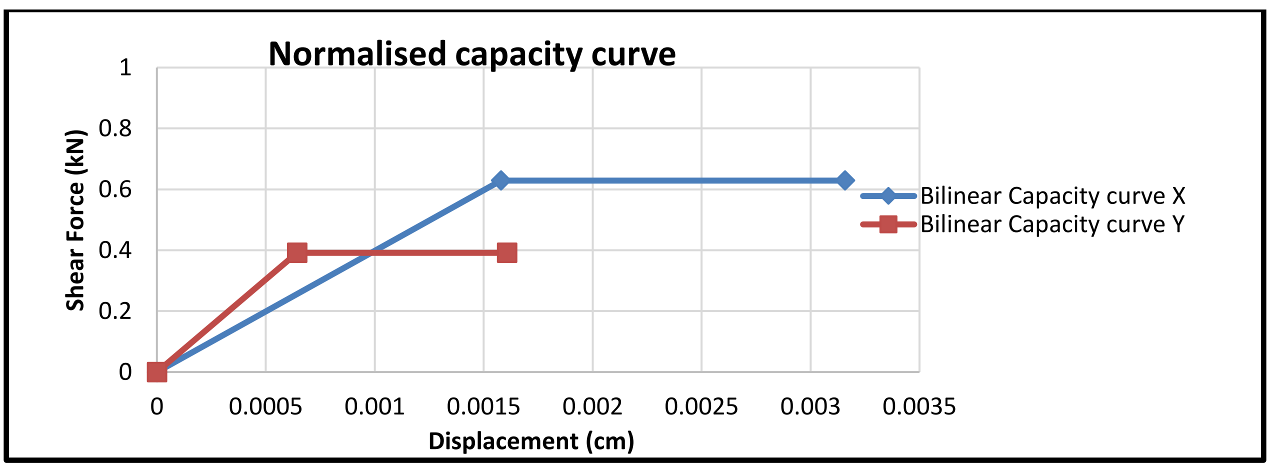

Figure 123: Normalised bilinear capacity curves of C2 building

Table 47: Pushover analysis parameters of C2 building

Load applied	d_y^*	d_m^*	F_y^*	K^*	μ	F_y^*/W
x-direction	2.21cm	4.42cm	3339kN	1510kN/cm	2	0.6287
y-direction	0.9cm	2.25cm	2079kN	2310daN/cm	2.5	0.3915

Table 48: Modal analysis parameters of C2 building

Mode	T [s]	mx [kg]	Mx [%]	my [kg]	My [%]	mz [kg]	Mz [%]
1	0,27895	0	0,00	952.557	75,96	2	0,00
2	0,24688	867.364	69,17	8	0,00	0	0,00
3	0,21812	103.639	8,26	69	0,01	0	0,00
4	0,10248	0	0,00	225.962	18,02	4	0,00
5	0,09049	179.742	14,33	1	0,00	1	0,00
6	0,08184	23.821	1,90	50	0,00	3	0,00
7	0,06441	1	0,00	45.479	3,63	0	0,00
8	0,05764	17.996	1,44	48	0,00	365.575	29,15
9	0,05708	25.25	2,01	1	0,00	329.61	26,29
10	0,05536	1.091	0,09	1.799	0,14	44.948	3,58
11	0,05400	20	0,00	1.283	0,10	104.477	8,33
12	0,05170	7.358	0,59	55	0,00	5.462	0,44

5.2.10 Building of template C3

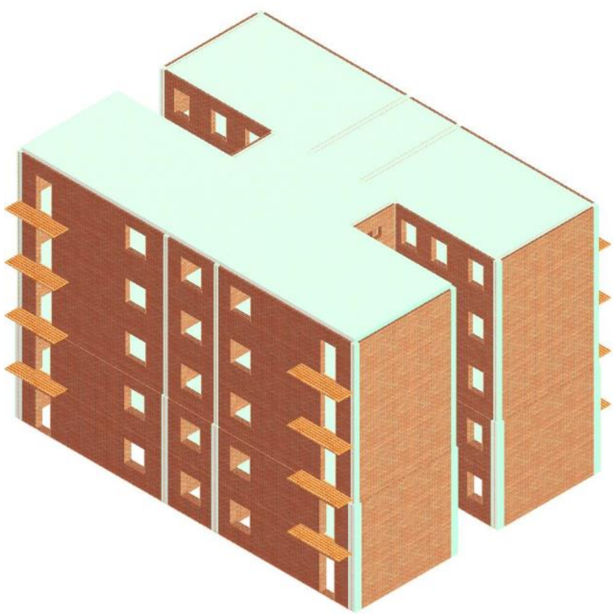

Figure 124: C3 building model

Loads are calculated as below:

-Slab 12cm $0.12 * 25 * 1.1 = 3.3\text{kN/m}^2$

-Mortar 3cm $0.03 * 18 * 1.2 = 0.65\text{kN/m}^2$

-Tiles 1cm $0.01 * 22 * 1.2 = 0.26\text{kN/m}^2$

-Plaster 2cm $0.02 * 18 * 1.2 = 0.43\text{kN/m}^2$

Sum $= 4.64\text{kN/m}^2$

Addition load (Partition walls) $= 1.3\text{kN/m}^2$

Probable live load $= 2\text{kN/m}^2$

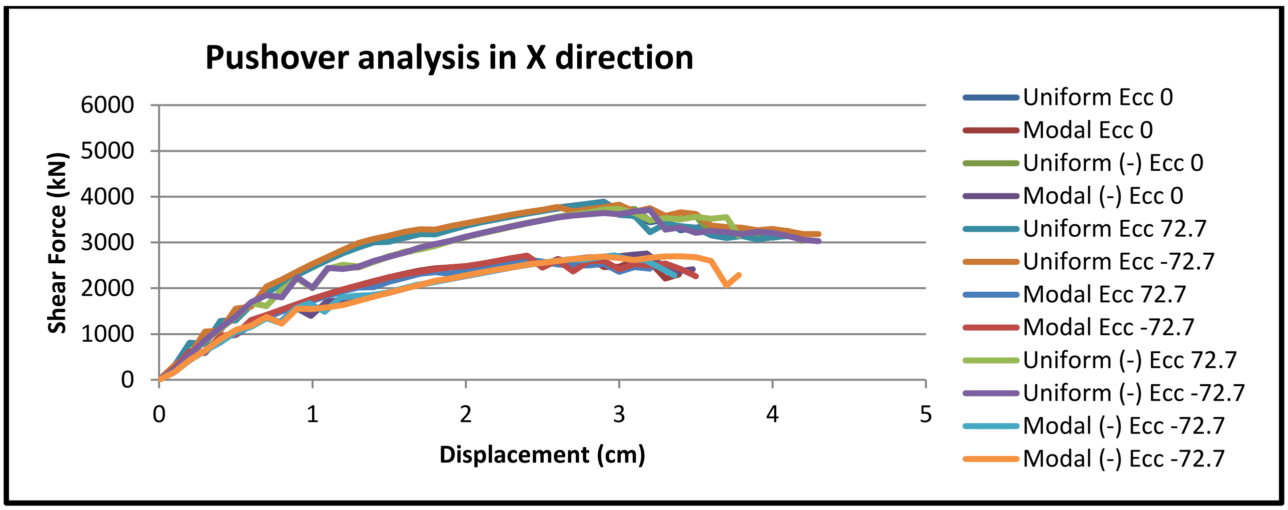

Figure 125: Pushover analysis for x-direction, 12 load patterns of C3 building

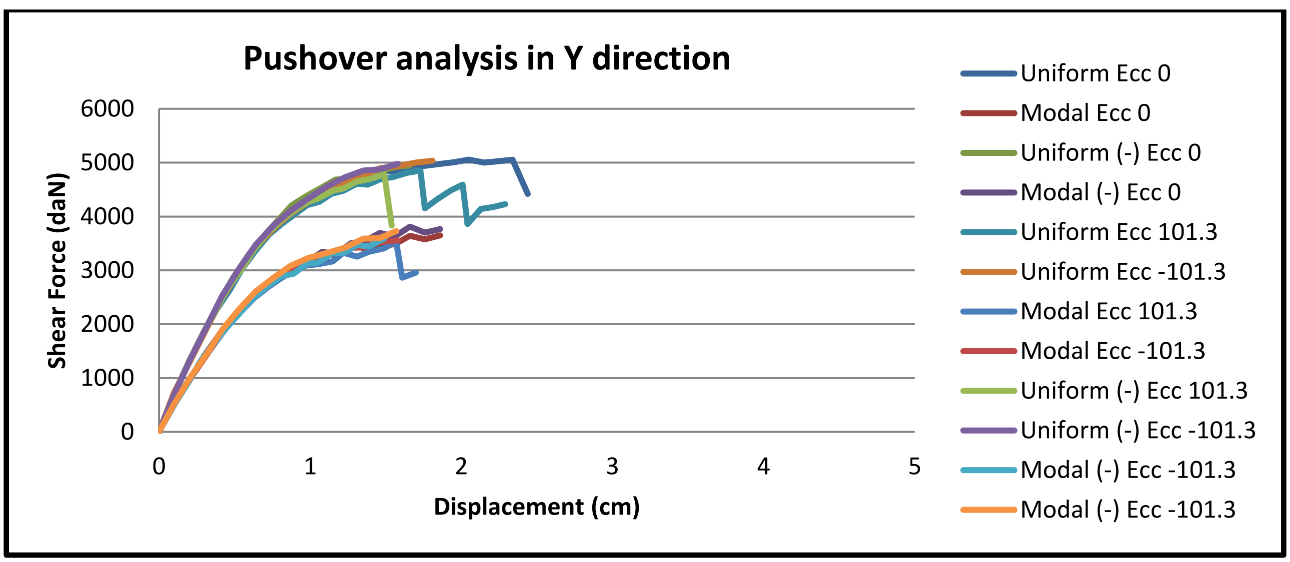

Figure 126: Pushover analysis for y-direction, 12 load patterns of C3 building

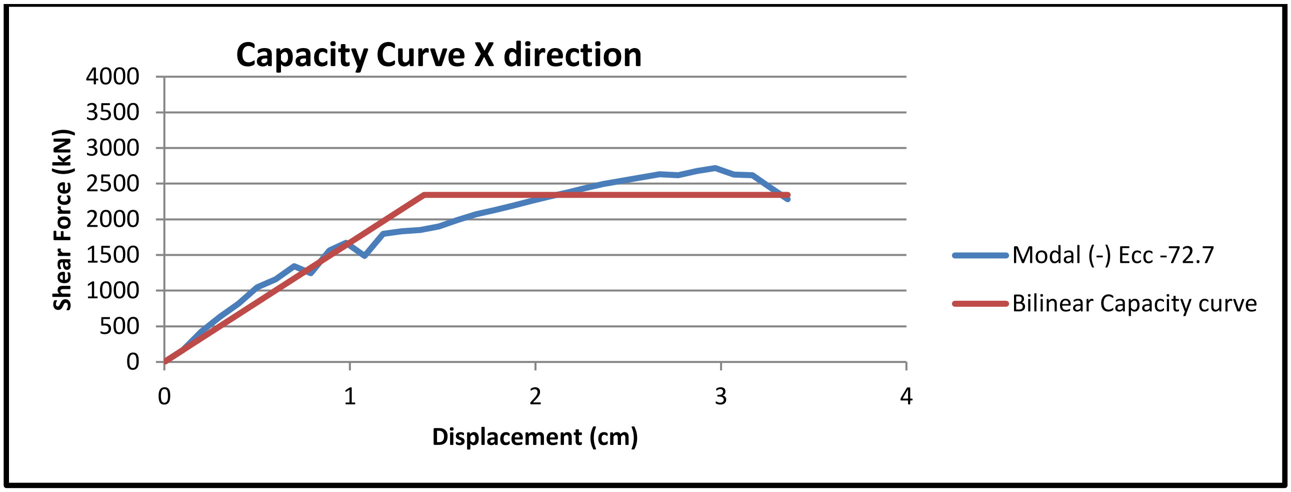

Figure 127: Capacity curve in x-direction of C3 building

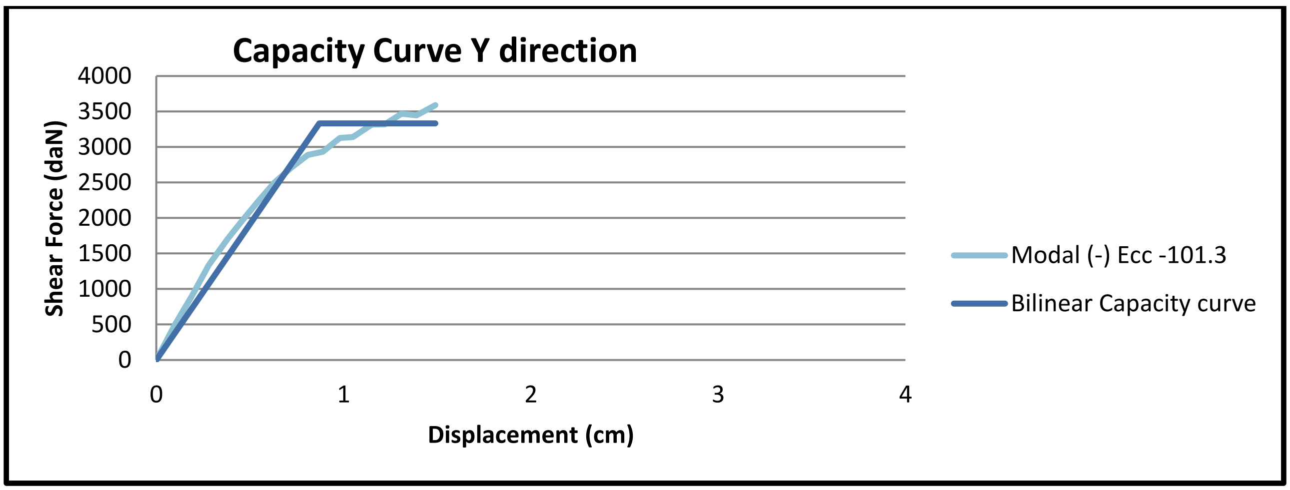

Figure 128: Capacity curve in y-direction of C3 building

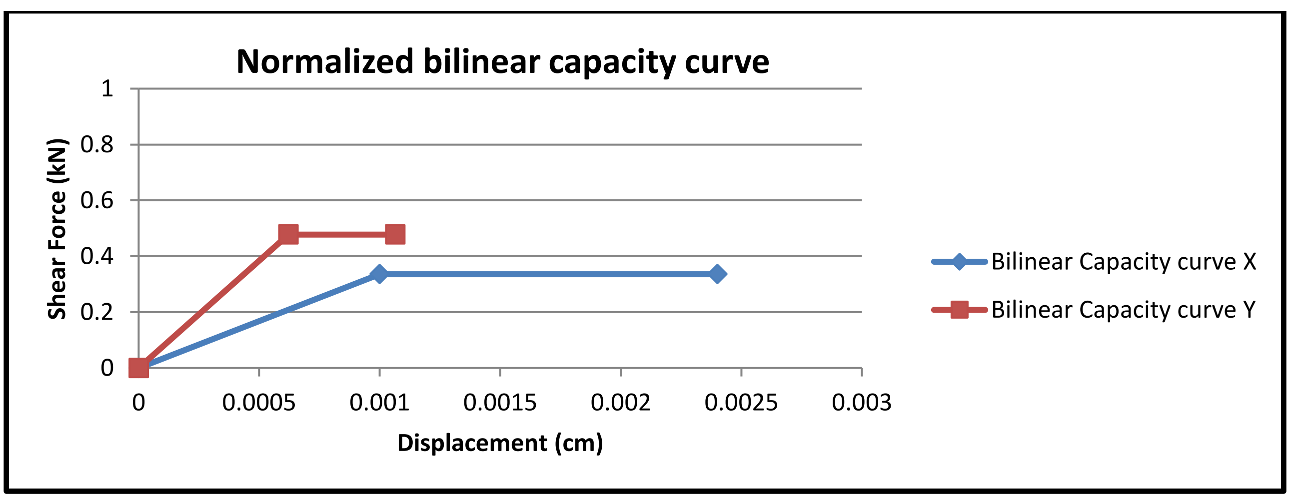

Figure 129: Normalized bilinear capacity curves of C3 building

Table 49: Pushover analysis parameters of C3 building

Load applied	d_y^*	d_m^*	F_y^*	K^*	μ	F_y^*/W
x-direction	1.41cm	3.36cm	2343kN	1673.6kN/cm	2.4	0.3357
y-direction	0.87cm	1.49cm	3333kN	3831daN/cm	1.72	0.4775

Table 50: Modal analysis parameters of building C3

Mode	**T [s]**	**mx [kg]**	**Mx [%]**	**my [kg]**	**My [%]**	**mz [kg]**	**Mz [%]**
1	0,24056	1277680	79,55	0	0,00	19	0,00
2	0,22071	1	0,00	1245019	77,51	0	0,00
3	0,20844	446	0,03	1454	0,09	0	0,00
4	0,09132	227878	14,19	1	0,00	109	0,01
5	0,08284	0	0,00	270177	16,82	0	0,00
6	0,07920	586	0,04	205	0,01	0	0,00
7	0,05744	13	0,00	5	0,00	571529	35,58
8	0,05658	59	0,00	646	0,04	207459	12,92
9	0,05640	122	0,01	1242	0,08	91861	5,72
10	0,05572	345	0,02	652	0,04	1684	0,10
11	0,05545	32	0,00	22	0,00	9262	0,58
12	0,05175	63425	3,95	0	0,00	299	0,02

5.3 Pushover analysis of buildings with intervention

Maybe for educational buildings and dormitories, that have been part of the state administration, some intervention on reinforcing and retrofitting in the structures are done, but for residential buildings especially the ones that are near main roads serious problems can be noticed. The subfloors were intended for magazines, with small openings, but due to commercial request for shops, stores etc, in many times interventions are done. Even though masonry structures work with shear walls, walls are demolished on the first floor and replace with two columns and a beam sustaining all the loads coming from above. This not only weakens the structure, but seriously affects seismic resistance. Examples like this, and of similar intervention on Albanian masonry structures are very widespread. Since lots of time has passed since the time of construction of these structures, all types of damage effects like physicals, chemicals, and from human intervention are present in these buildings. In this study two buildings with intervention of these type are analysed.

Another very wide spread intervention in Albanian building stock is the phenomenon of added stories. After the collapse of the communist regime in the 90s, because of the great demand in cities for housing, in many times stories were added in various buildings using light materials. These additions were done in a hurry and without design and projects during this time. But later at the 2000s due to the policies of the time, these additions were legalized and still exist nowadays. In this study 5 buildings with this intervention will be studied and compared with the design and project of original template.

5.3.1 Building with added stories

The buildings are modelled with the same assumption as in chapter VII. For the added floors the joints connections between the original stories and the added one are modelled as rigid joints because this interventions are done before many years and are consolidated. The walls are modelled as non-linear materials, with brick strength $f_b = 7.5\text{MPa}$, mortar strength $f_m = 5\text{MPa}$, density of wall $\rho_{wall} = 1200\,\text{kg/m}^3$, masonry strength $f_k = 2.5\text{MPa}$, shear strength $f_{vk} = 0.4$ and $f_{vk0} = 0.2$. Modulus of elasticity of masonry is taken as $E_m = 2500\text{MPa}$ and $G = 700\text{MPa}$. Those values represent the minimum requirements for masonry with hollow bricks and cement mortar as defined in KTP-89. The plan scheme of the added stories is assumed to be the same as the typical plan of the building. The slabs are modelled as rigid slabs because they are of reinforced concrete and with the above parameters:

Dead gravity loads $= 4\text{kN/m}^2$

Probable live load $= 2\text{kN/m}^2$

5.3.1.1 Building A1 with one added stories

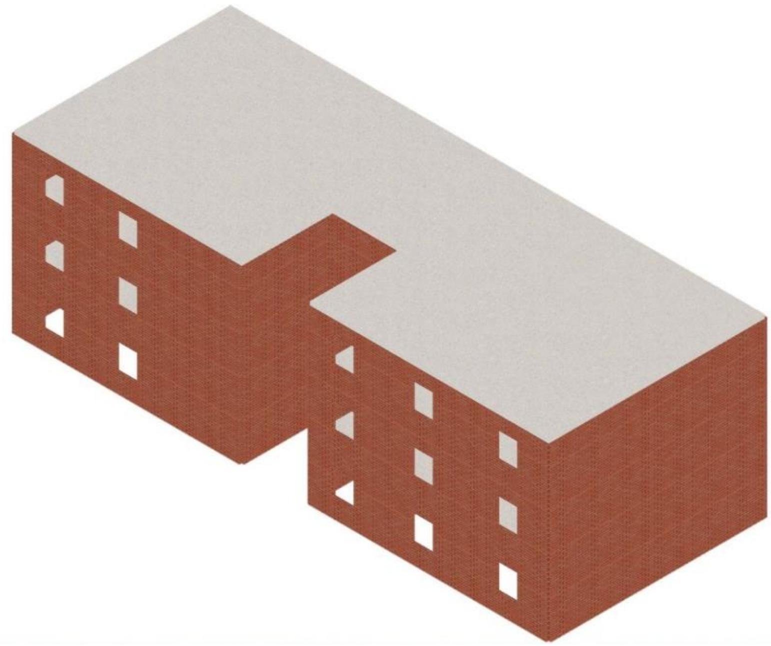

Figure 130: Building A1 with 1 story plus

Table 51: Pushover analysis parameters of A1 building with one added floor

Load applied	d_y^*	d_m^*	F_y^*	K^*	μ	F_y^*/W
x-direction	0.44cm	1.57cm	2022kN	4596kN/cm	3.56	0.5494
y-direction	0.42cm	0.78cm	2260kN	5381kN/cm	1.87	0.6141

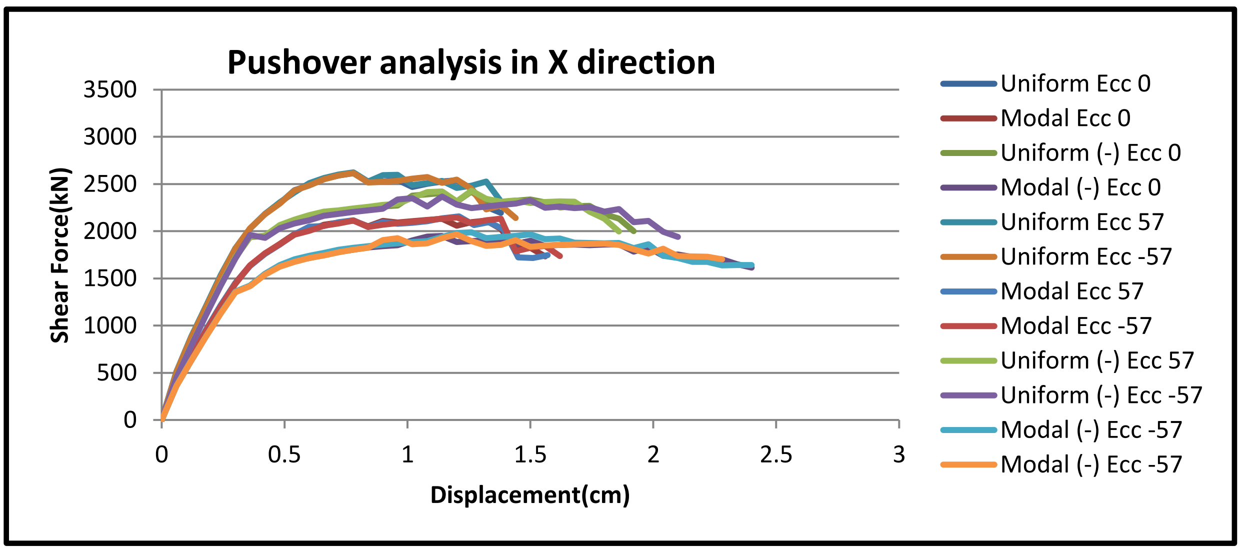

Figure 131: Pushover analysis for x-dir, 12 load patterns of building A1 three floors

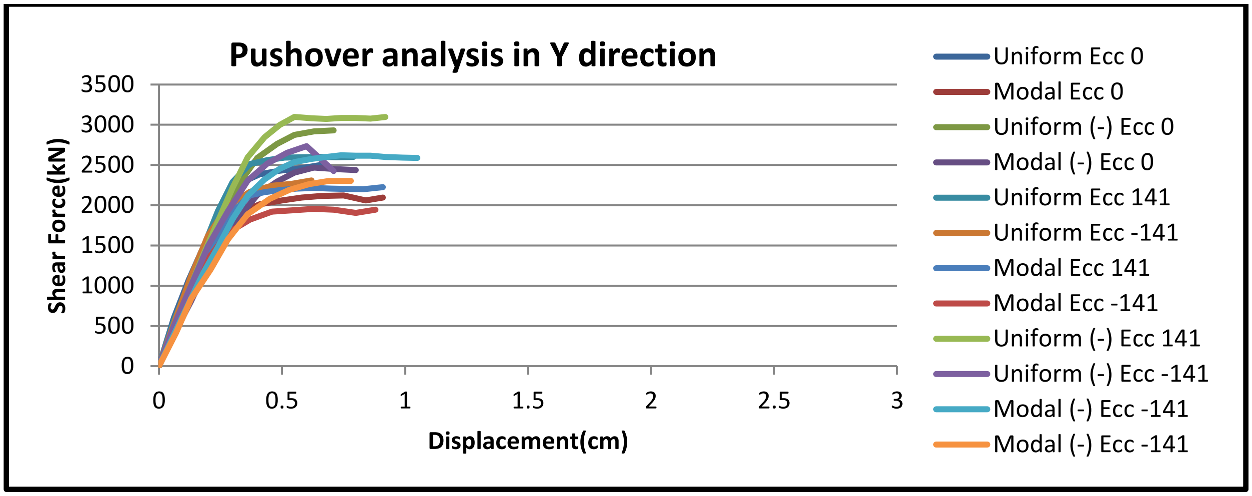

Figure 132: Pushover analysis for y-dir, 12 load patterns of building A1 three floors

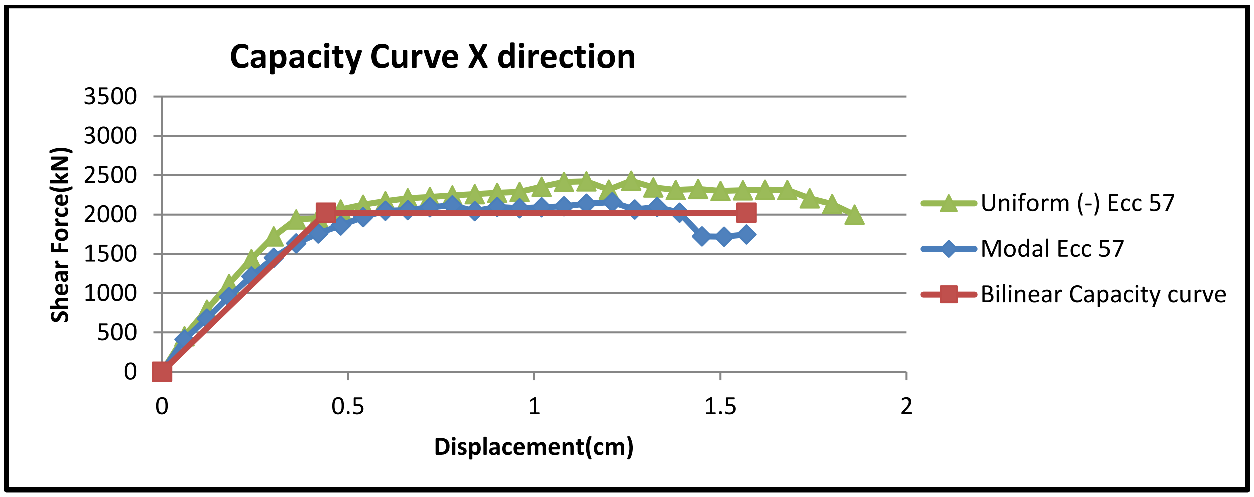

Figure 133: Capacity curve in x-dir of building A1 three floors

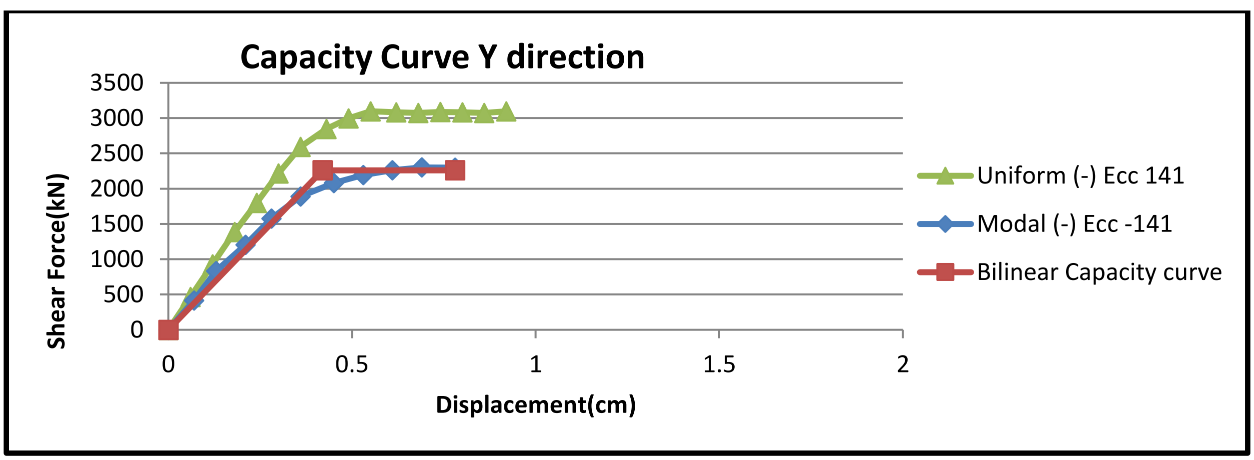

Figure 134: Capacity curve in y-dir of building A1 three floors

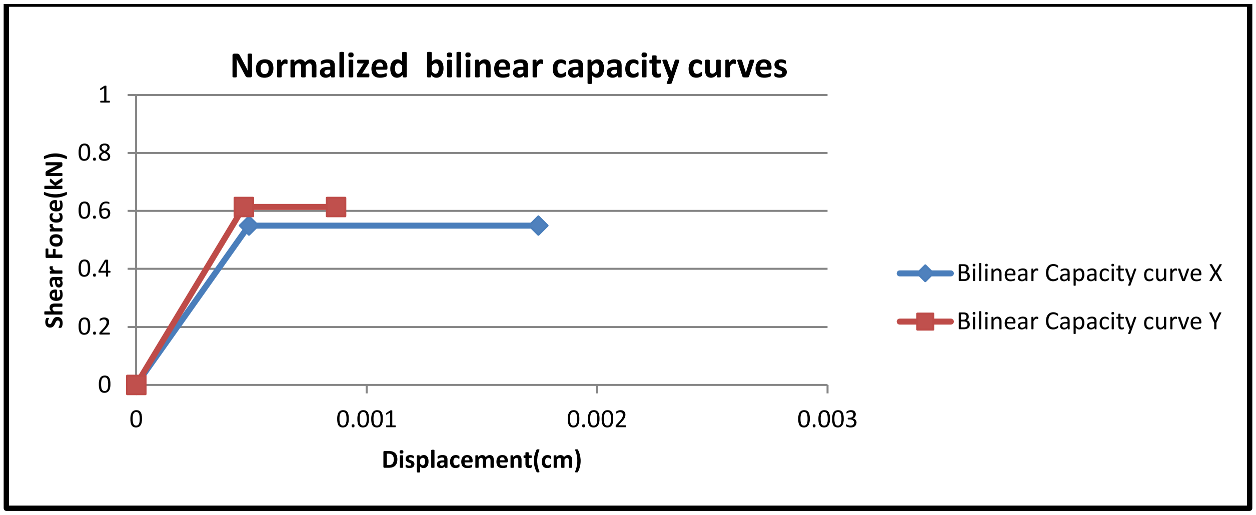

Figure 135: Normalized capacity curves for building A1 three stories

Table 52: Modal analysis parameters of building A1 three stories

Mode	T [s]	mx [kg]	Mx [%]	my [kg]	My [%]	mz [kg]	Mz [%]
1	0,15084	691	0,10	640.312	88,51	253	0,03
2	0,13834	3.895	0,54	5.581	0,77	13	0,00
3	0,12873	640.083	88,48	1.188	0,16	59	0,01
4	0,05427	5.389	0,75	50.459	6,98	81.789	11,31
5	0,05154	21.488	2,97	13.507	1,87	15.593	2,16
6	0,04794	14	0,00	1.21	0,17	289.193	39,98
7	0,04686	3.66	0,51	3.475	0,48	253.495	35,04
8	0,04493	1.946	0,27	1.145	0,16	4.794	0,66
9	0,04430	15.24	2,11	142	0,02	667	0,09
10	0,04180	23	0,00	124	0,02	0	0,00
11	0,04082	882	0,12	4.851	0,67	7.621	1,05
12	0,03819	27.109	3,75	0	0,00	481	0,07

5.3.1.2 Building A1 with two added stories

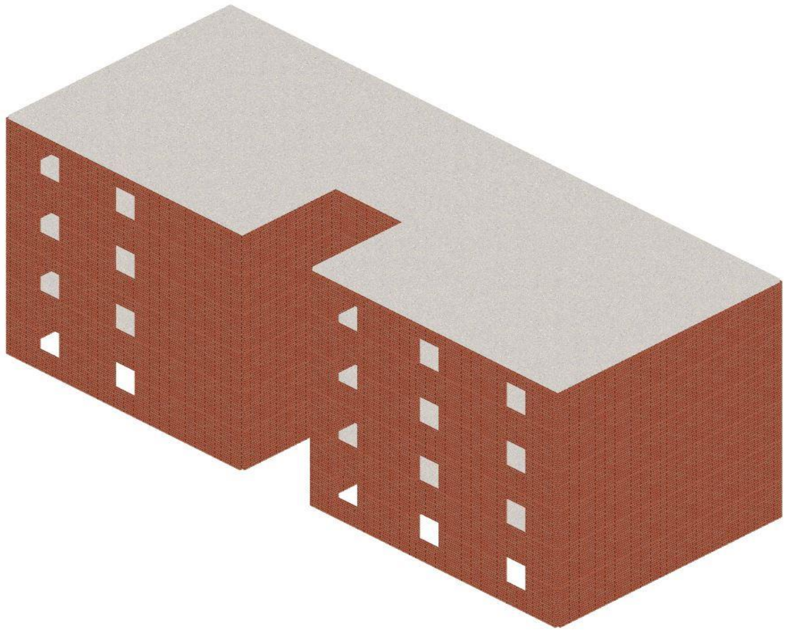

Figure 136: Building A1 with 2 additional stories

Table 53: Pushover analysis parameters of A1 building with two additional stories

Load applied	d_y^*	d_m^*	F_y^*	K^*	μ	F_y^*/W
x-direction	0.81cm	2.09cm	2201kN	2717kN/cm	2.5	0.4676
y-direction	0.52cm	1.17cm	1998kN	3842kN/cm	2.25	0.4245

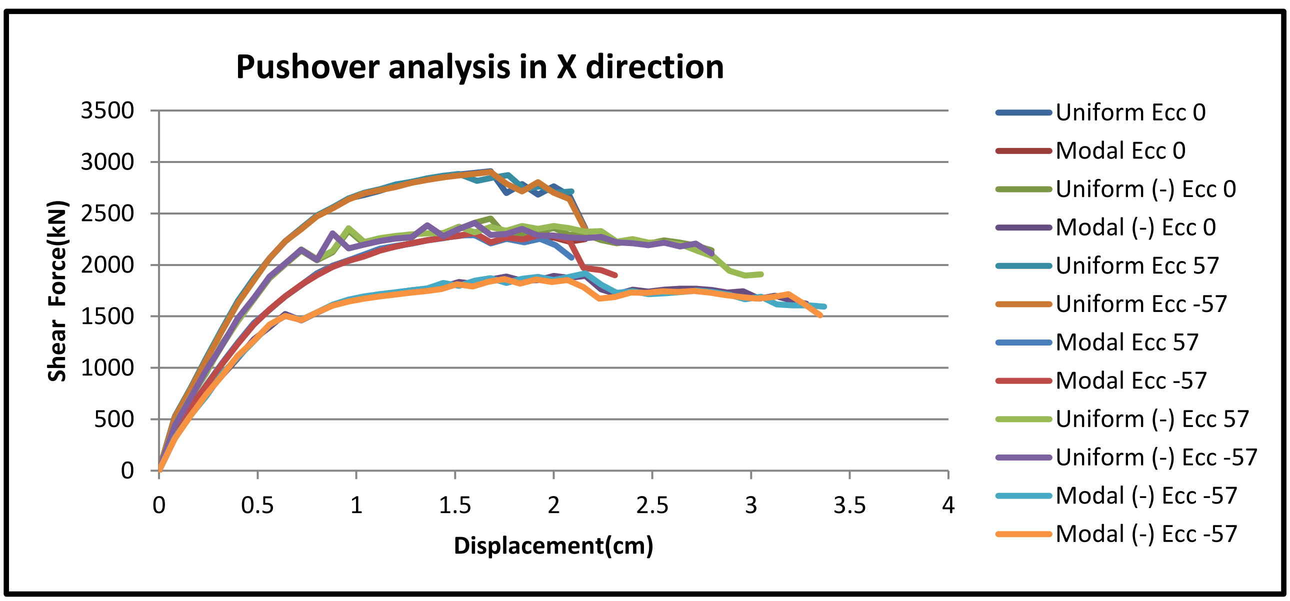

Figure 137: Pushover analysis in x-dir, 12 load patterns of building A1 four stories

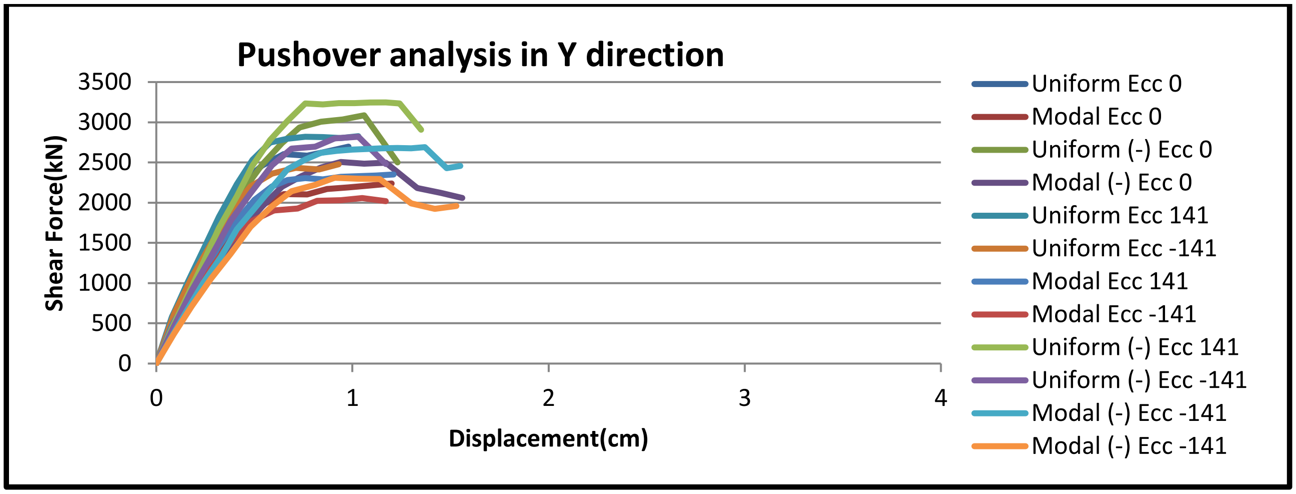

Figure 138: Pushover analysis in y-dir, 12 load patterns of building A1 four stories

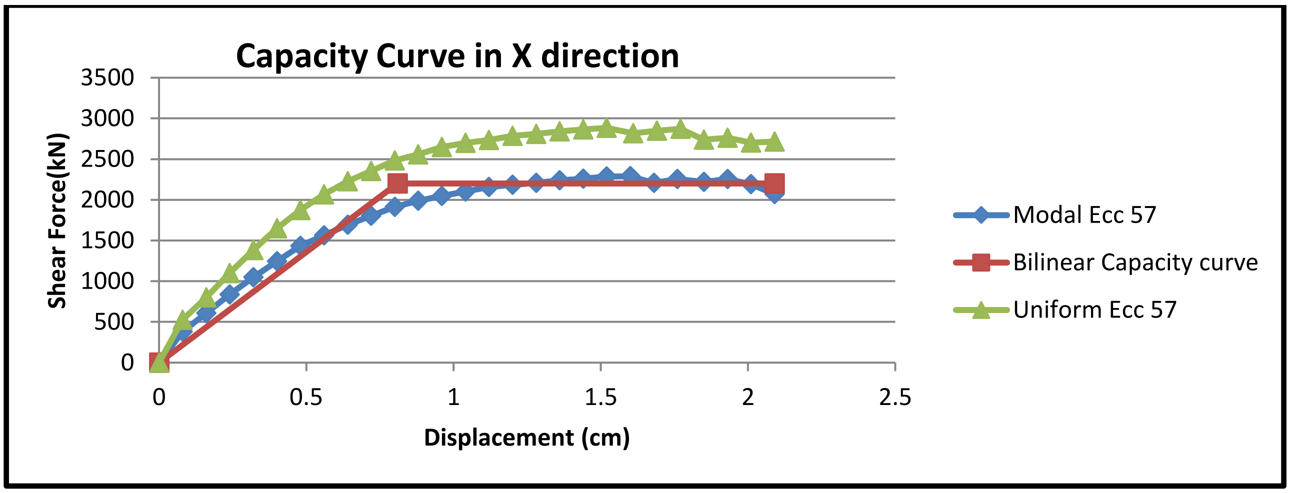

Figure 139: Capacity curve in x-dir of building A1 four stories

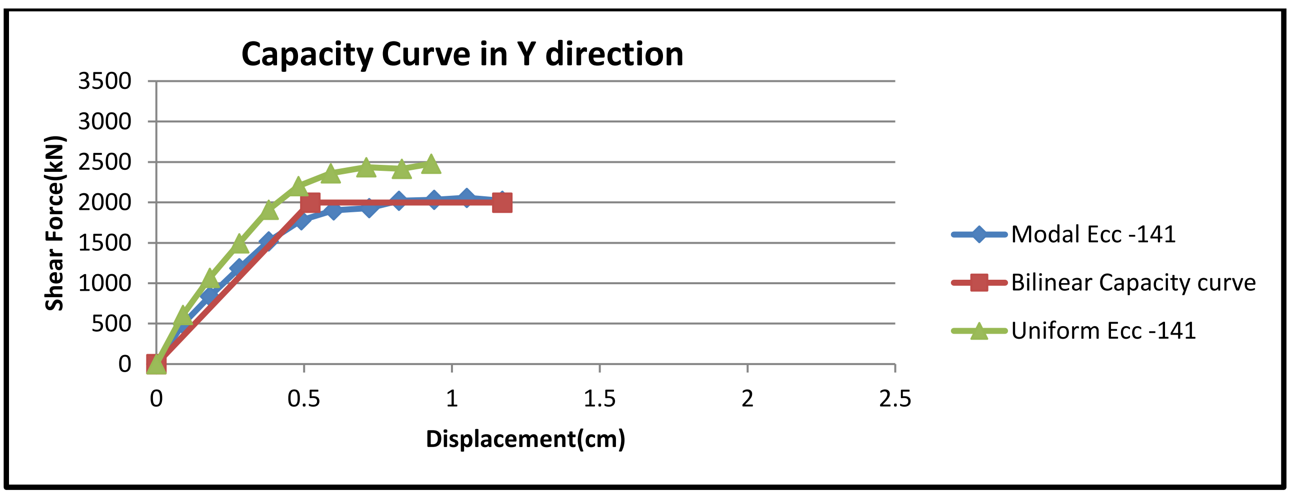

Figure 140: Capacity curve in y-dir of building A1 four stories

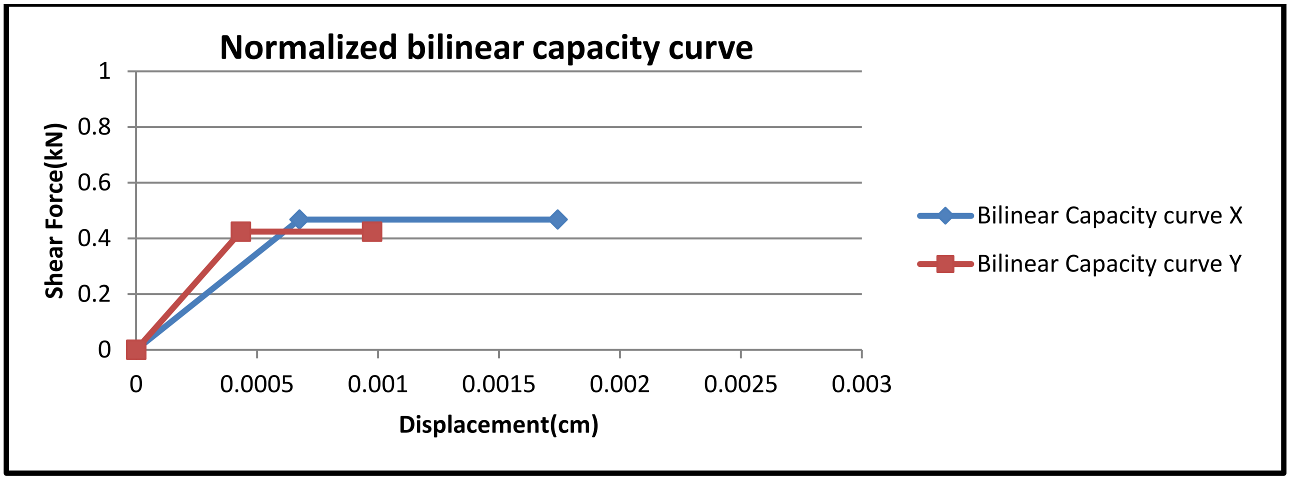

Figure 141: Normalized bilinear capacity curves of building A1 four stories

Table 54: Modal analysis parameters of building A1 four stories

Mode	T [s]	mx [kg]	Mx [%]	my [kg]	My [%]	mz [kg]	Mz [%]
1	0,19942	1.508	0,16	814.227	85,47	394	0,04
2	0,17872	451	0,05	36	0,00	5	0,00
3	0,16979	816.291	85,68	1.755	0,18	86	0,01
4	0,06964	3.792	0,40	100.689	10,57	51.979	5,46
5	0,06436	55.97	5,88	7.342	0,77	32.328	3,39
6	0,05963	1.074	0,11	117	0,01	78.063	8,19
7	0,05832	5.864	0,62	3.163	0,33	694.373	72,89
8	0,05385	20.684	2,17	126	0,01	269	0,03
9	0,05333	1.137	0,12	986	0,10	177	0,02
10	0,04682	956	0,10	12.838	1,35	2.474	0,26
11	0,04493	26.525	2,78	6	0,00	309	0,03
12	0,04342	559	0,06	171	0,02	679	0,07

5.3.1.3 Building B1 with one added story

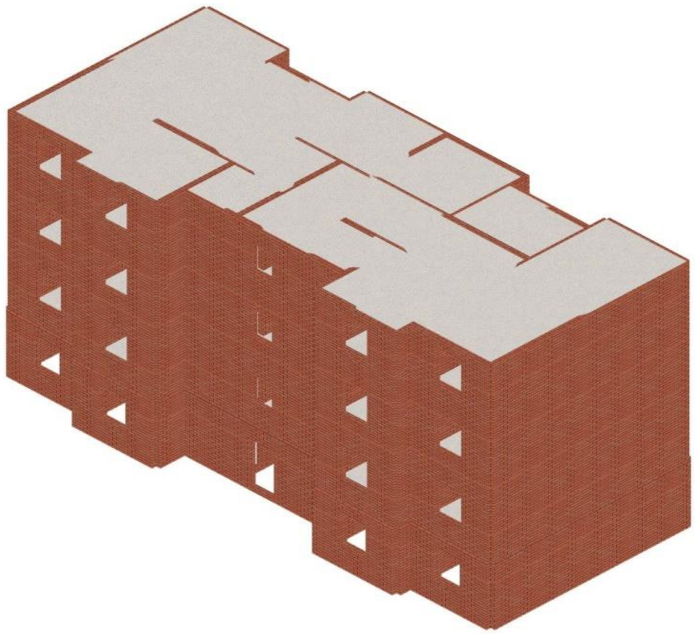

Figure 142: Building B1 with one additional story

Table 55: Pushover analysis parameters of building B1 with one additional story

Load applied	d_y^*	d_m^*	F_y^*	K^*	μ	F_y^*/W
x-direction	0.58cm	2.01cm	2257kN	3891kN/cm	3.46	0.5461
y-direction	0.4cm	1.04cm	2392kN	5980kN/cm	2.6	0.5788

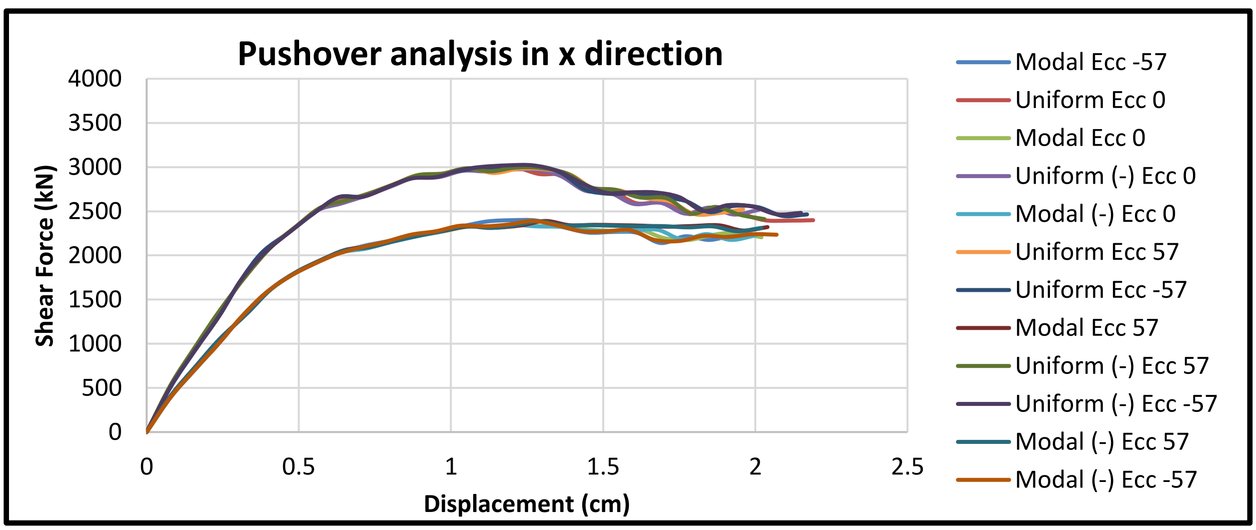

Figure 143: Pushover analysis in x-dir, 12 load patterns of B1 building with four stories

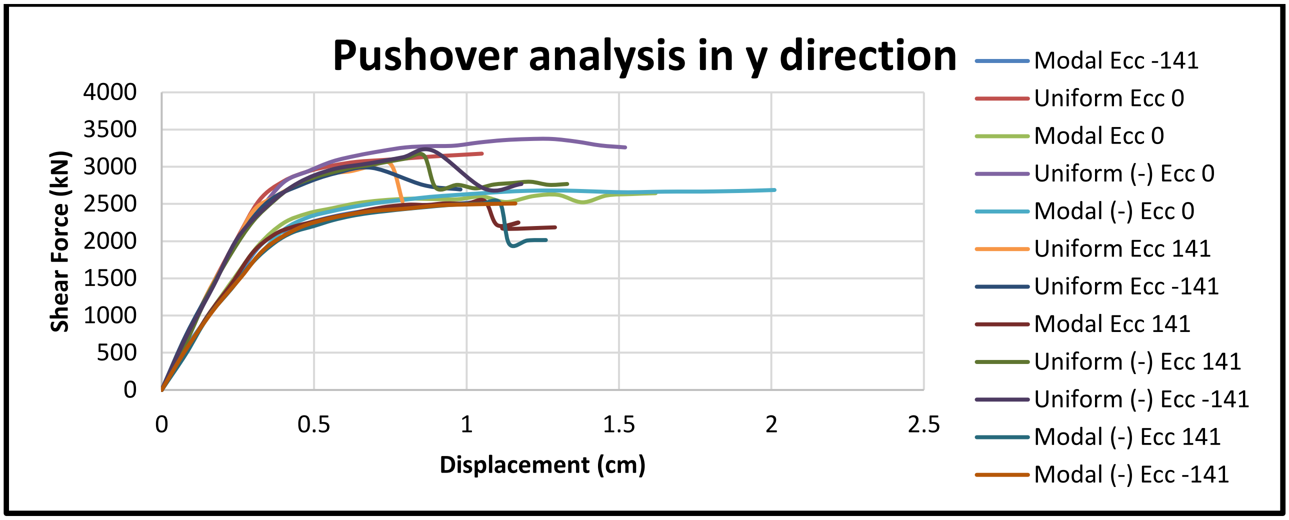

Figure 144: Pushover analysis in y-dir, 12 load patterns of B1 building with four stories

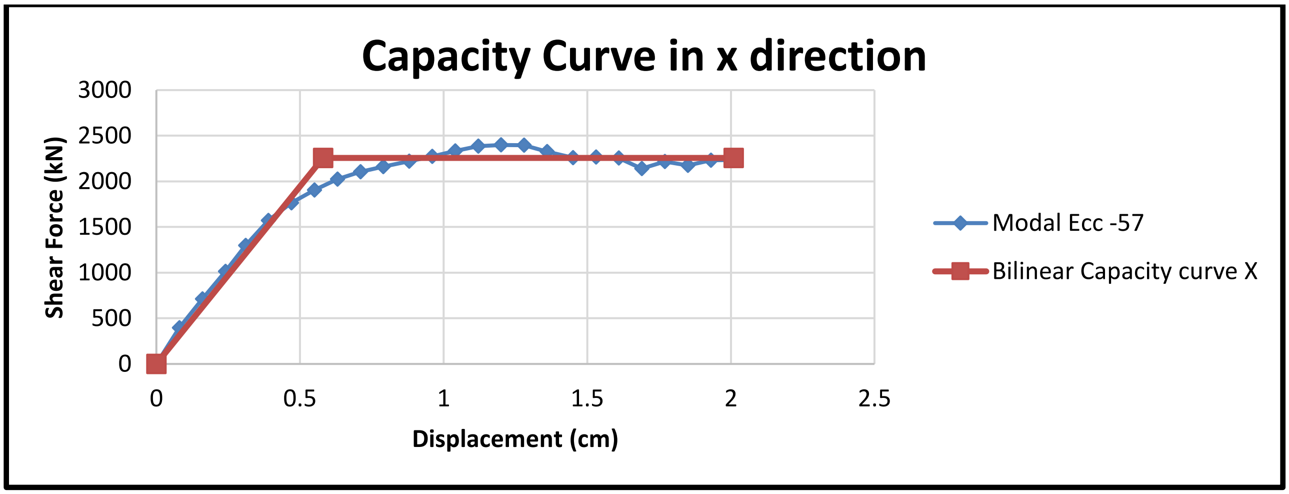

Figure 145: Capacity curve in x-dir of B1 building with four stories

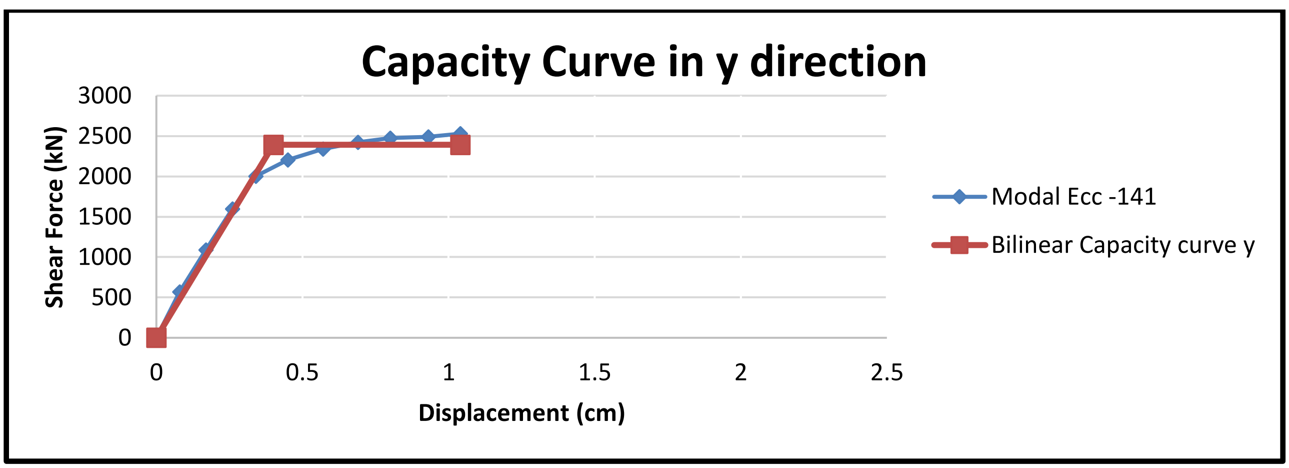

Figure 146: Capacity curve in y-dir of B1 building with four stories

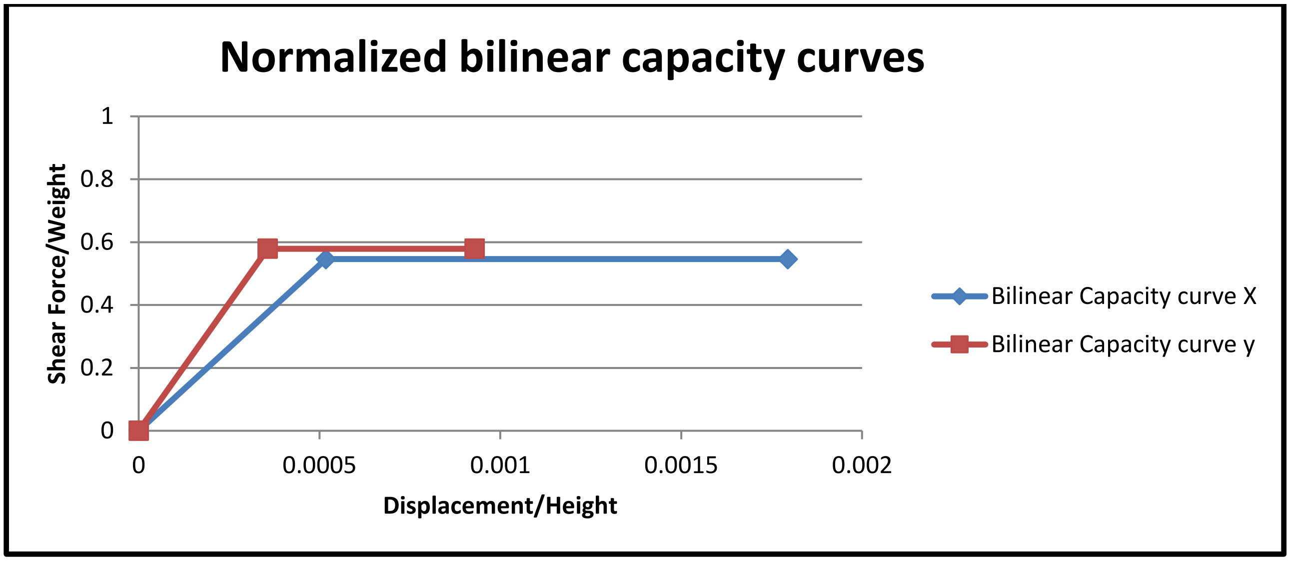

Figure 147: Normalized bilinear capacity curves of B1 building with four stories

Table 56: Modal analysis parameters of B1 building with four stories

Mode	T [s]	mx [kg]	Mx [%]	my [kg]	My [%]	mz [kg]	Mz [%]
1	0,17740	730863	78,70	0	0,00	0	0,00
2	0,17628	0	0,00	714297	76,91	10	0,00
3	0,15038	18.894	2,03	0	0,00	0	0,00
4	0,06397	119042	12,82	0	0,00	0	0,00
5	0,06174	0	0,00	159857	17,21	132	0,01
6	0,05413	2.866	0,31	0	0,00	0	0,00
7	0,05202	0	0,00	74	0,01	342172	36,84
8	0,05117	6644	0,72	0	0,00	0	0,00
9	0,04457	0	0,00	31	0,00	392282	42,24
10	0,04325	3892	0,42	0	0,00	0	0,00
11	0,04312	0	0,00	0	0,00	21236	2,29
12	0,04169	7498	0,81	0	0,00	0	0,00

5.3.1.4 Building C1B with one added story

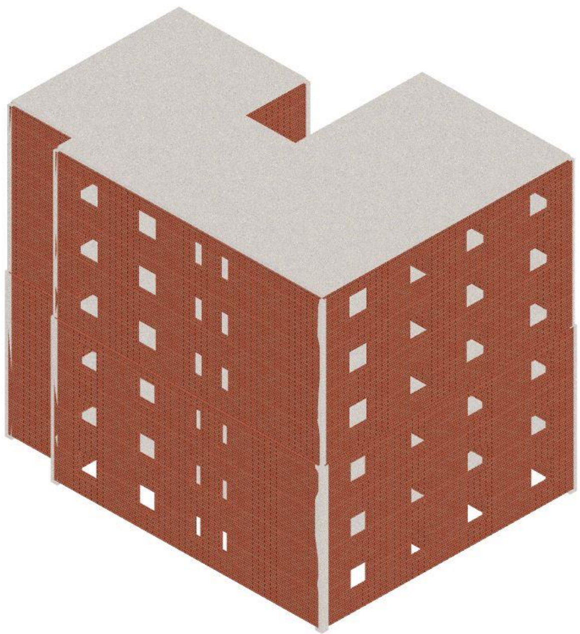

Figure 148: Building C1B with one additional story

Table 57: Pushover analysis parameters of building C1B with one additional story

Load applied	d_y^*	d_m^*	F_y^*	K^*	μ	F_y^*/W
x-direction	1.47cm	3.26cm	2503kN	1702kN/cm	2.22	0.3706
y-direction	2.06cm	5.24cm	2190kN	1063kN/cm	2.54	0.3243

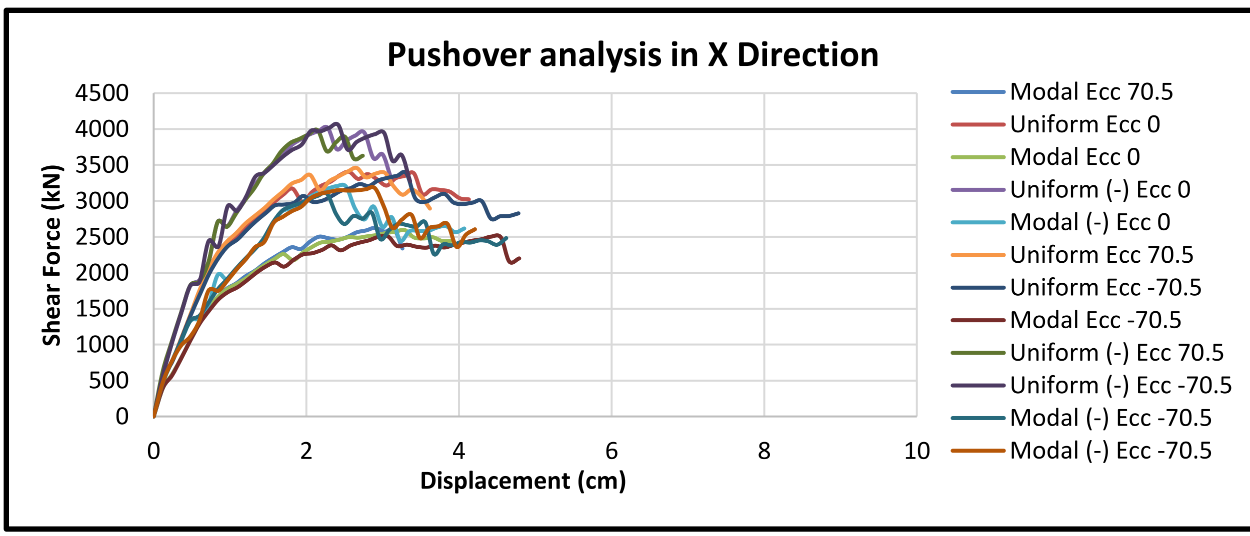

Figure 149: Pushover analysis in x-dir, 12 load patterns of building C1B six stories

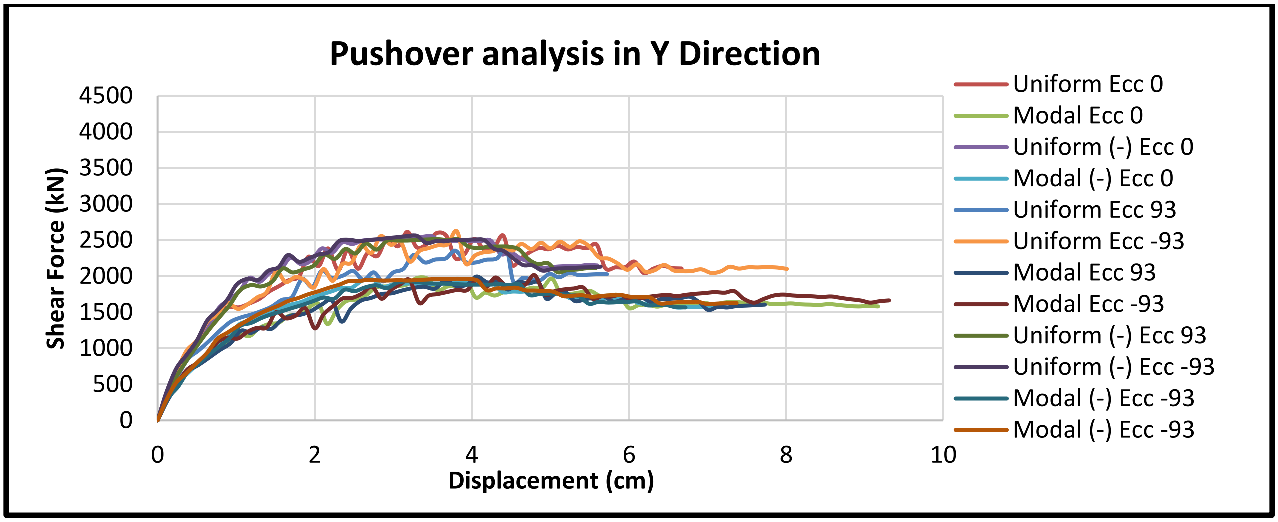

Figure 150: Pushover analysis in y-dir, 12 load patterns of building C1B six stories

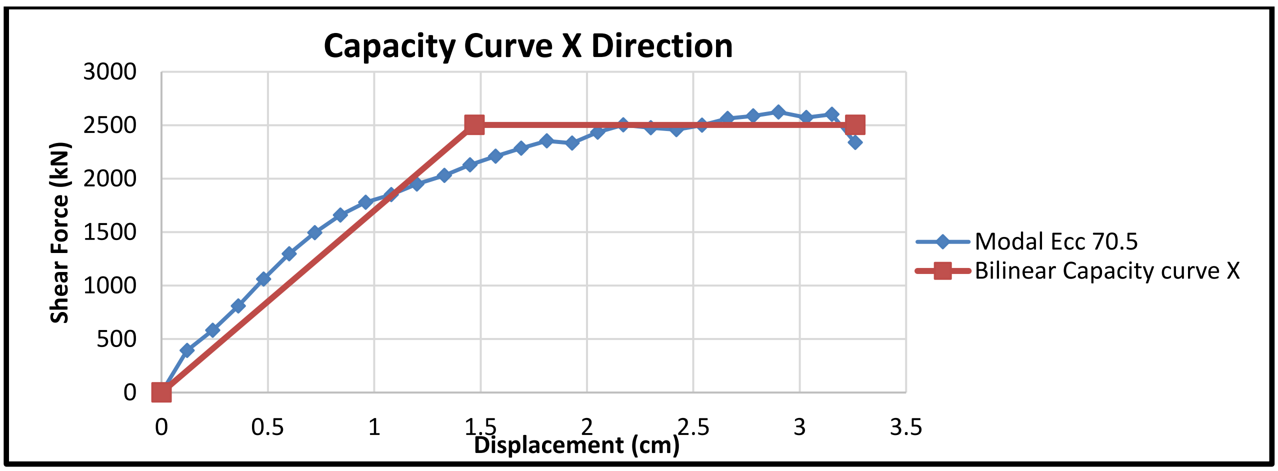

Figure 151: Capacity curve in x-dir of building C1B six stories

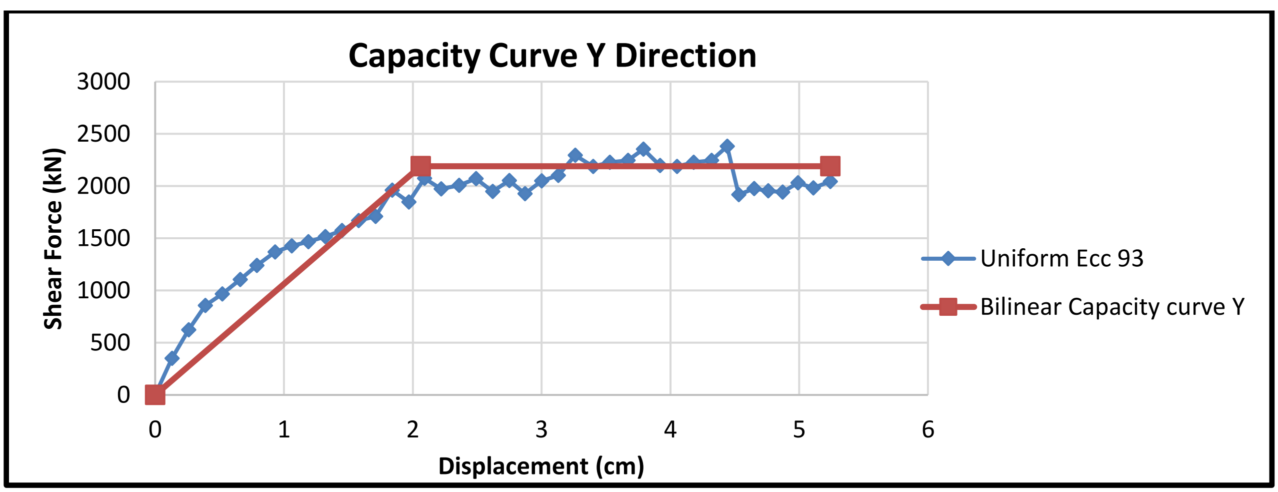

Figure 152: Capacity curve in y-dir of building C1B six stories

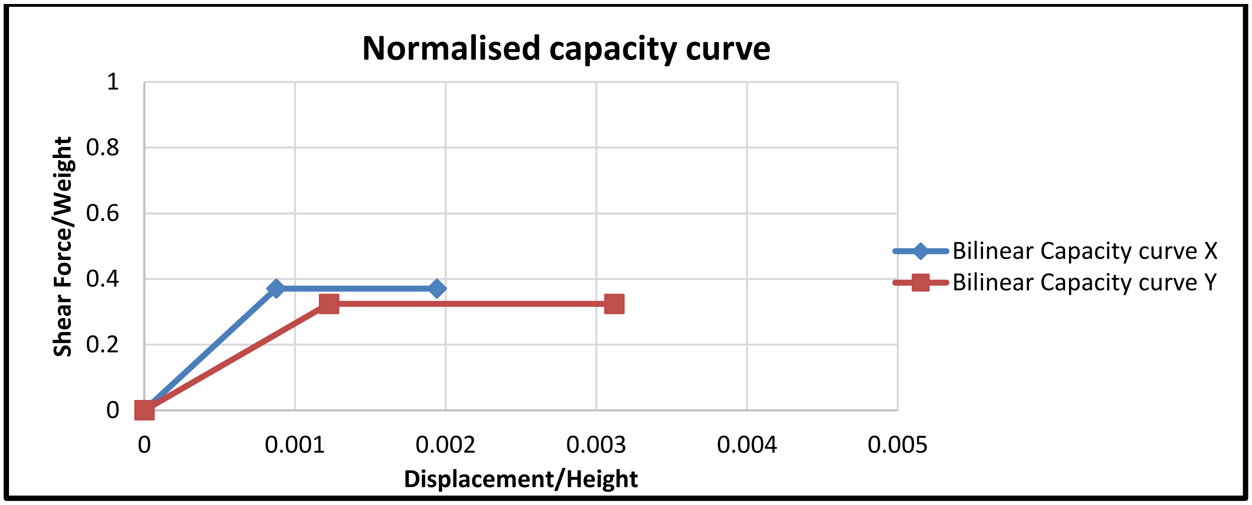

Figure 153: Normalized bilinear capacity curves of building C1B six stories

Table 58: Modal analysis parameters of building C1B six stories

Mode	T [s]	mx [kg]	Mx [%]	my [kg]	My [%]	mz [kg]	Mz [%]
1	0.30539	270	0.02	1181723	75.13	8	0
2	0.27175	1167694	74.23	1205	0.08	162	0.01
3	0.22716	37989	2.42	9381	0.6	622	0.04
4	0.11088	478	0.03	25802	16.4	3	0
5	0.09949	247710	15.75	926	0.06	2455	0.16
6	0.08572	4.608	0.29	3987	0.25	23670	1.5
7	0.07741	2442	0.16	57	0	647459	41.16
8	0.06817	2233	0.14	64	0	275435	17.51
9	0.06547	129	0.01	1144	0.73	144277	9.17
10	0.06352	42	0	19729	1.25	31.948	2.03
11	0.0605	246	0.02	22582	1.44	9.997	0.64
12	0.05808	2.85	0.18	7157	0.45	51925	3.3

5.3.1.5 Building C2 with one added story

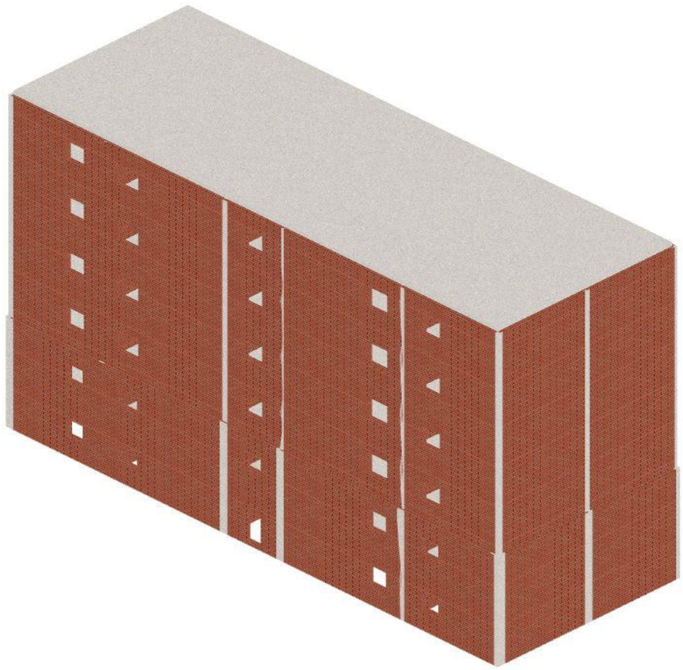

Figure 154: Building C2 with one additional story

Table 59: Pushover analysis parameters of building C2 with one additional story

Load applied	d_y^*	d_m^*	F_y^*	K^*	μ	F_y^*/W
x-direction	2.38cm	5.26cm	2543kN	1068kN/cm	2.2	0.4138
y-direction	1.05cm	2.62cm	1864kN	1775kN/cm	2.49	0.3033

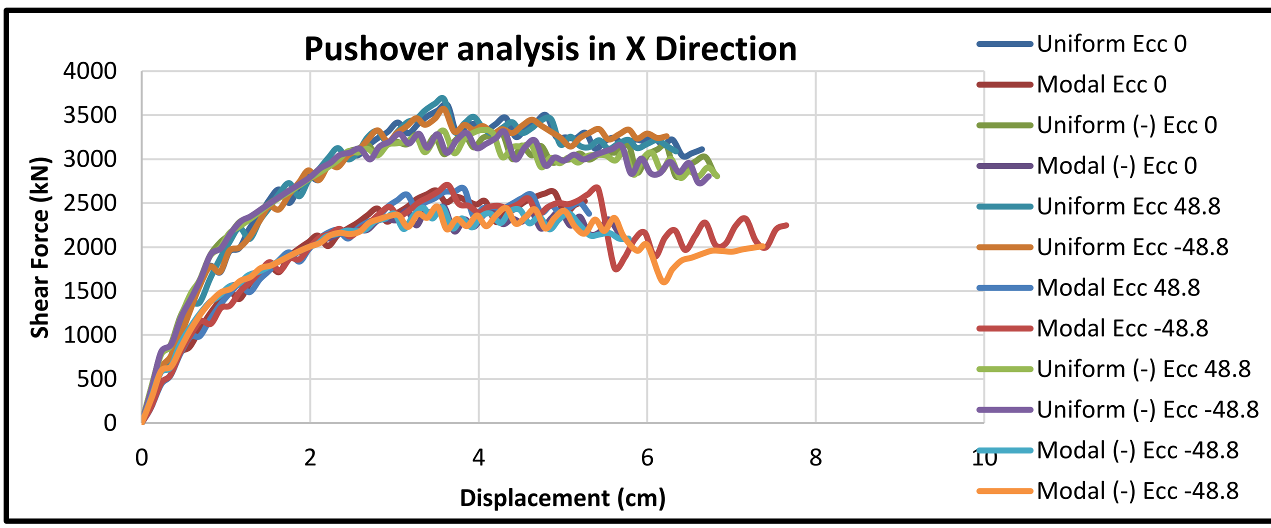

Figure 155: Pushover analysis in x-dir, 12 load patterns of building C2 six stories

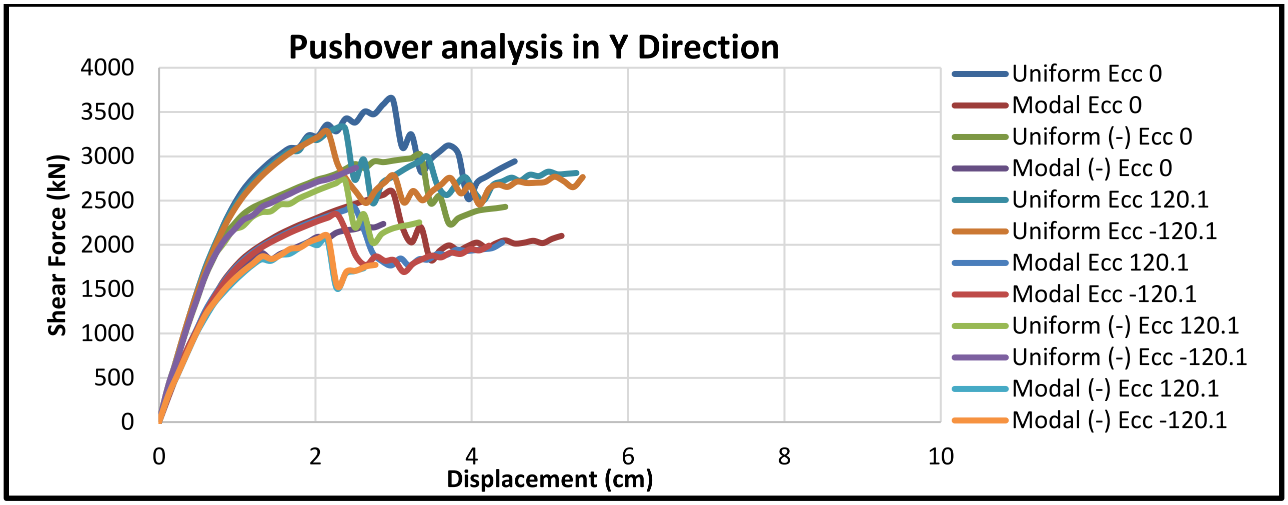

Figure 156: Pushover analysis in y-dir, 12 load patterns of building C2 six stories

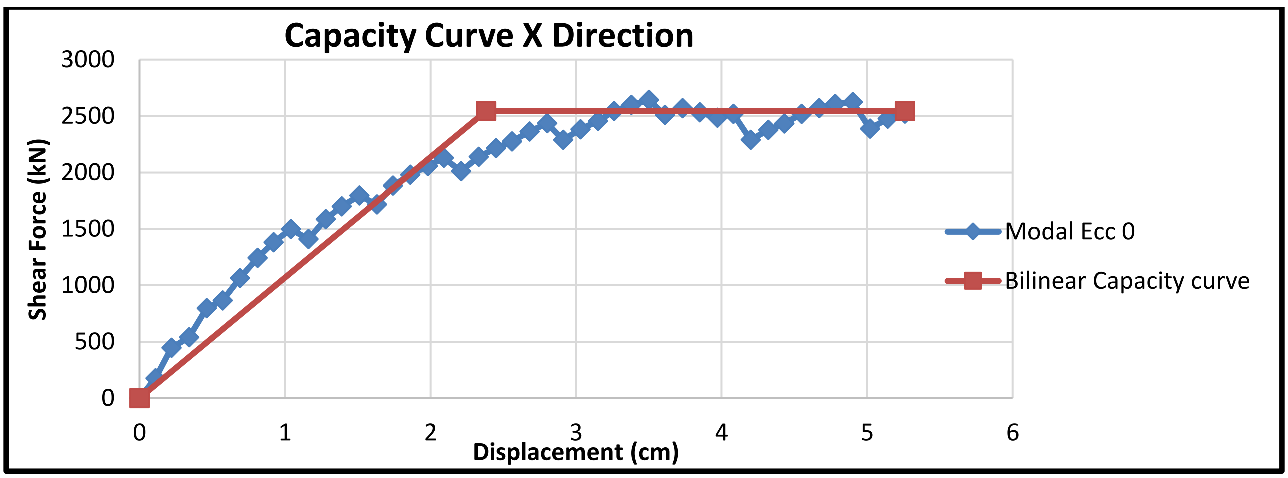

Figure 157: Capacity curve in x-dir of building C2 six stories

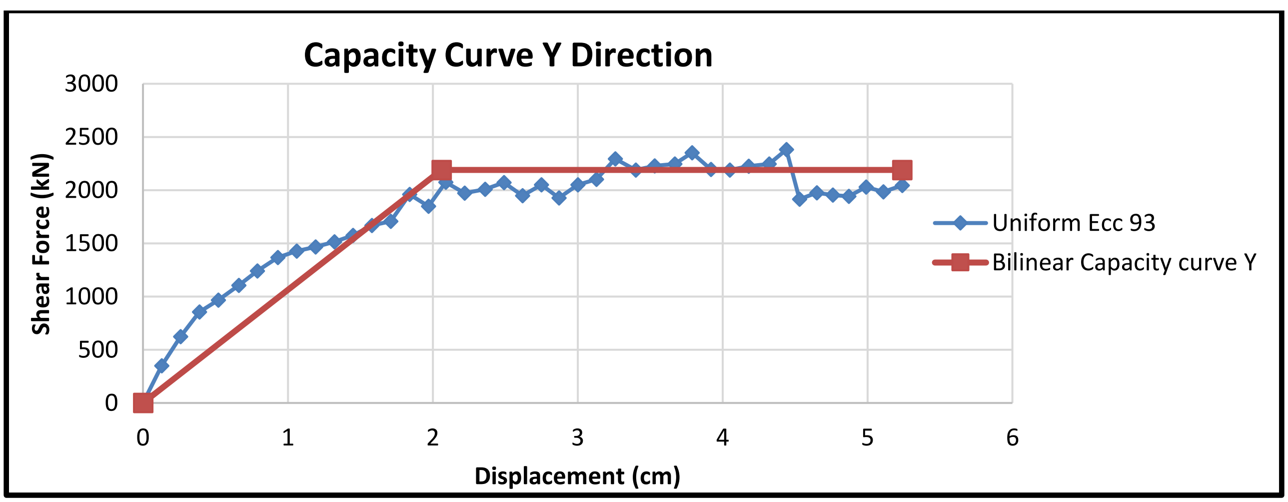

Figure 158: Capacity curve in y-dir of building C2 six stories

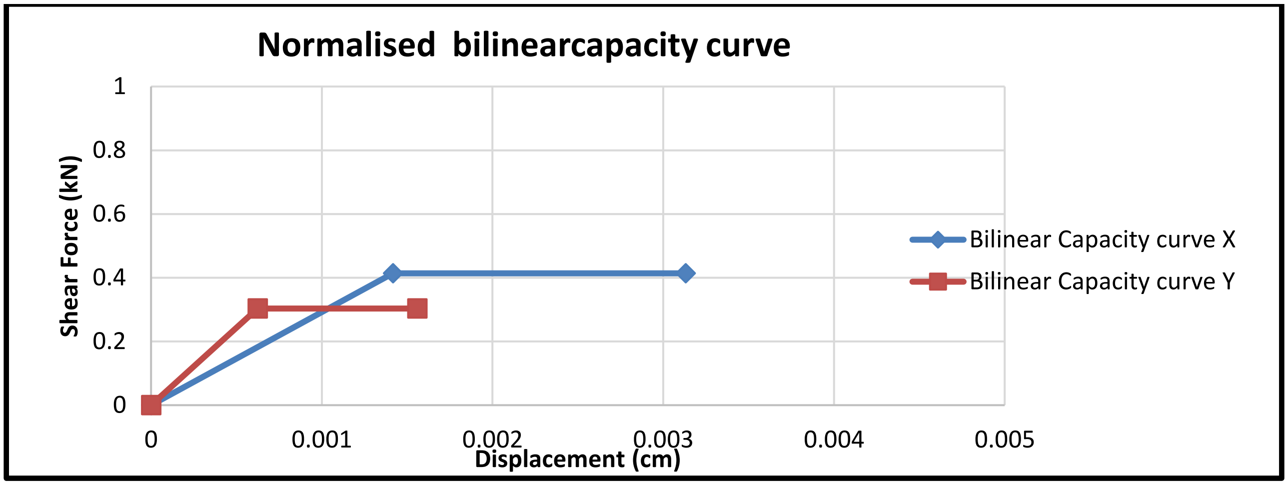

Figure 159: Normalized bilinear capacity curves of building C2 six stories

Table 60: Modal analysis parameters of building C2 six stories

Mode	T [s]	mx [kg]	Mx [%]	my [kg]	My [%]	mz [kg]	Mz [%]
1	0,34064	0	0,00	1086828	74,18	0	0,00
2	0,29524	989869	67,56	8	0,00	0	0,00
3	0,26086	133782	9,13	49	0,00	0	0,00
4	0,11873	1	0,00	267588	18,26	1	0,00
5	0,10279	20073	13,70	0	0,00	1	0,00
6	0,09312	31051	2,12	39	0,00	11	0,00
7	0,07277	8	0,00	69636	4,75	335	0,02
8	0,06659	1516	0,10	82	0,01	976549	66,65
9	0,06450	45228	3,09	114	0,01	69054	4,71
10	0,06151	11351	0,77	1.56	0,11	16.88	1,15
11	0,06027	161	0,01	6185	0,42	13354	0,91
12	0,05749	1692	1,15	49	0,00	2514	0,17

5.3.2 Pushover analysis of buildings with interventions in first floor

Two buildings are taken in consideration of template B3 and C1A. This templates are very popular and in the buildings stock have both variations with and without intervention.

5.3.2.1 Building B3 with intervention in first floor

In building B3, in one side of the first story, walls are replaced with reinforced concrete frame, with 5 openings as in the figure above.

Figure 160: B3 building with intervention on first floor.

Columns are of reinforced concrete C20/25 with dimensions (40*40)cm and steel reinforcement B400 with $A_s = A'_s = 12.56\text{cm}^2$ and stirrups φ8 every 15cm. Beams are also of reinforced concrete C20/25 with dimensions (30*50)cm and steel reinforcement B400 with $A_s = A'_s = 3.14\text{cm}^2$ and stirrups φ8 every 20cm.

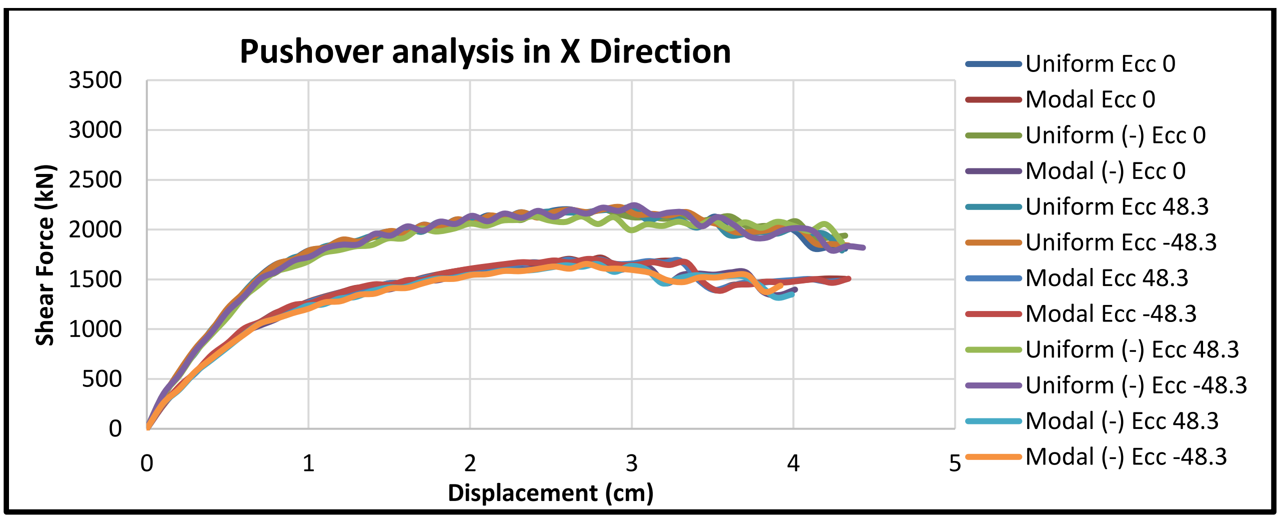

Figure 161: Pushover analysis for x-dir, 12 load patterns of building B3 with intervention

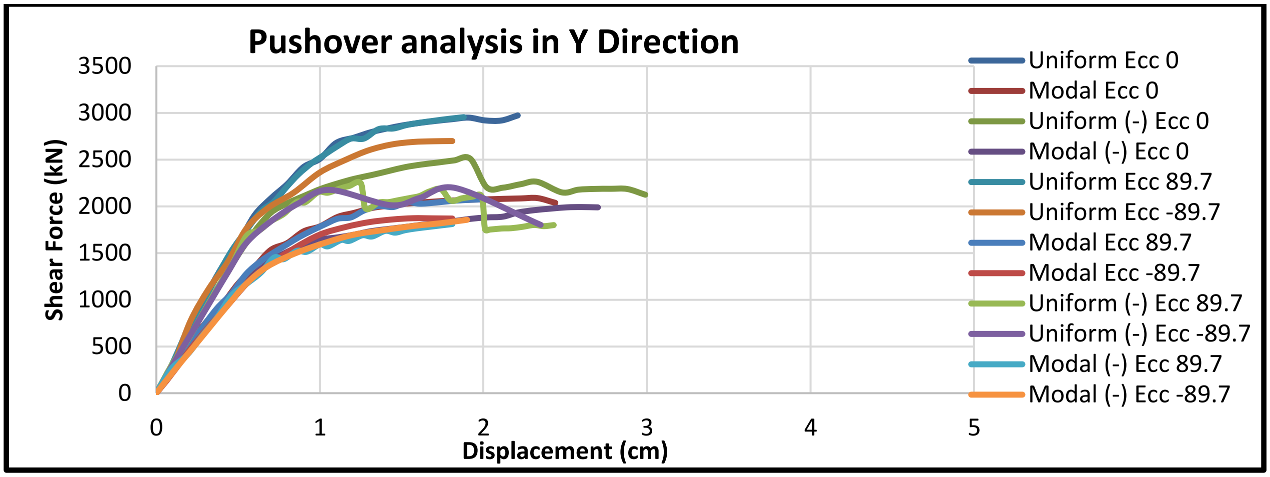

Figure 162: Pushover analysis for y-dir, 12 load patterns of building B3 with intervention

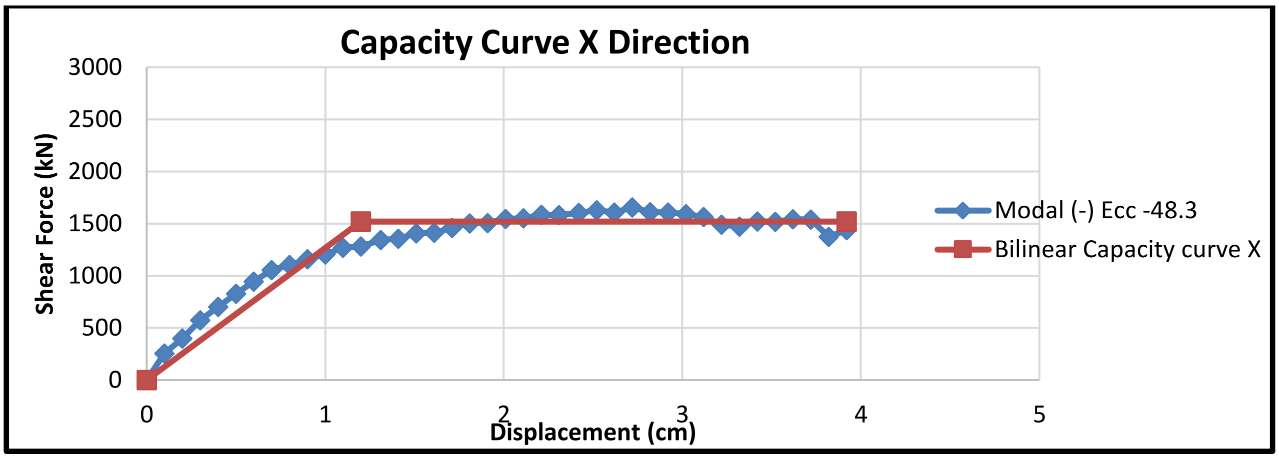

Figure 163: Capacity curve in x-dir of building B3 with intervention

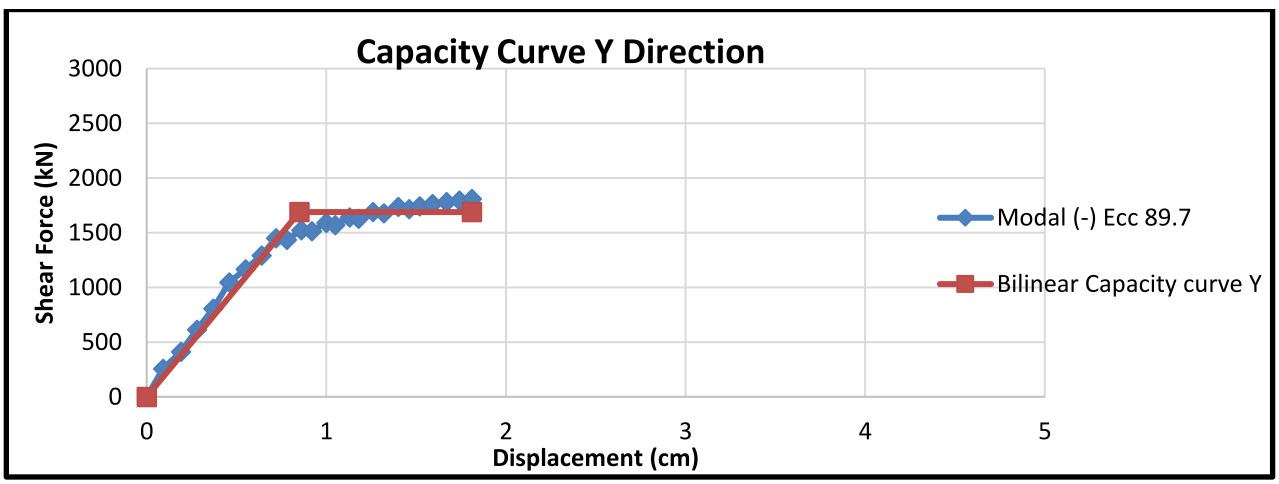

Figure 164: Capacity curve in y-dir of building B3 with intervention

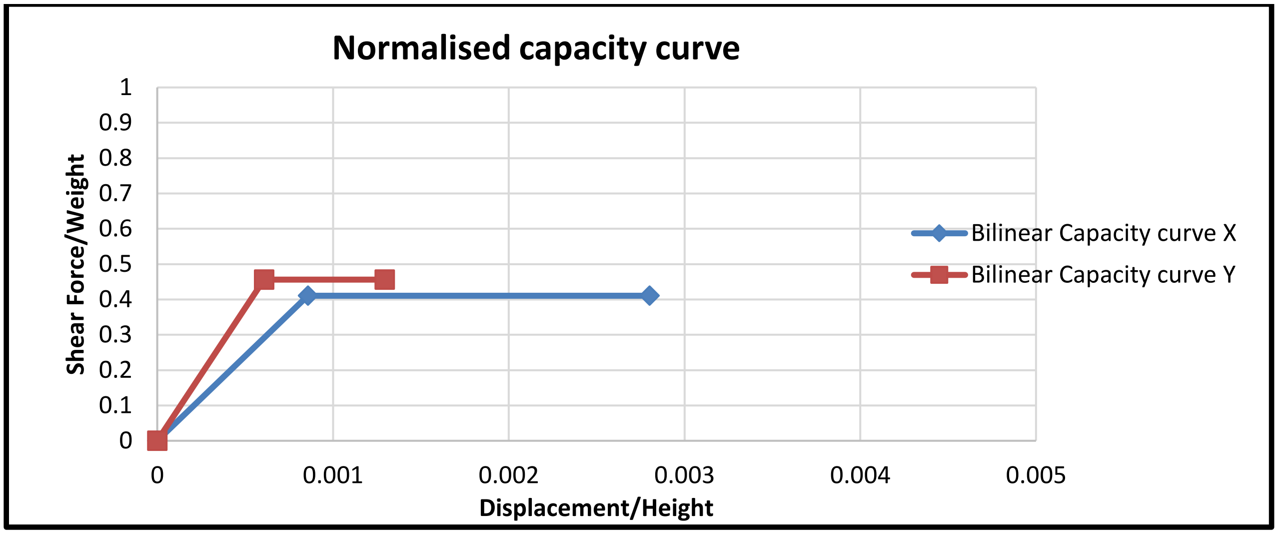

Figure 165: Normalized capacity curves of building B3 with intervention

Table 61: Pushover analysis parameters of B3 with intervention

Load applied	d_y^*	d_m^*	F_y^*	K^*	μ	F_y^*/W
x-direction	1.2cm	3.92cm	1520kN	1267kN/cm	3.27	0.4105
y-direction	0.85cm	1.81cm	1689kN	1987kN/cm	2.13	0.4561

Table 62: Modal analysis parameters of building B3 with intervention

Mode	T [s]	mx [kg]	Mx [%]	my [kg]	My [%]	mz [kg]	Mz [%]
1	0,23979	715.762	76,92	15.041	1,62	21	0,00
2	0,23676	17.051	1,83	656.711	70,57	684	0,07
3	0,19026	6.593	0,71	579	0,06	0	0,00
4	0,09111	131.298	14,11	105	0,01	15	0,00
5	0,08742	89	0,01	174.541	18,76	1.549	0,17
6	0,07333	281	0,03	151	0,02	2	0,00
7	0,06288	9	0,00	62	0,01	720.185	77,39
8	0,05837	2.109	0,23	3	0,00	4.305	0,46
9	0,05365	5	0,00	2.388	0,26	7.166	0,77
10	0,05176	38.105	4,09	16	0,00	44	0,00
11	0,05072	103	0,01	1.706	0,18	306	0,03
12	0,04904	28	0,00	5.717	0,61	118	0,01

5.3.2.2 Building C1A with intervention in first floor

In building C1B, in two sides of the first story, walls are replaced with reinforced concrete frame, with four openings as in the figure below.

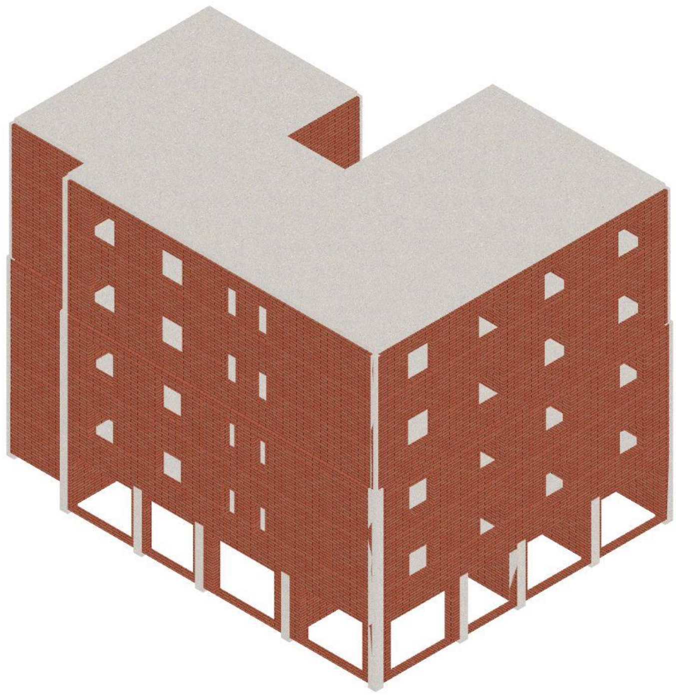

Figure 166: C1A building with intervention on first floor.

Columns are of reinforced concrete C20/25 with dimensions (40*40)cm and steel reinforcement B400 with $A_s = A_s' = 12.56\text{cm}^2$ and stirrups φ8 every 12cm. Beams are also of reinforced concrete C20/25 with dimensions (30*50)cm and steel reinforcement B400 with $A_s = A_s' = 3.14\text{cm}^2$ and stirrups φ8 every 20cm.

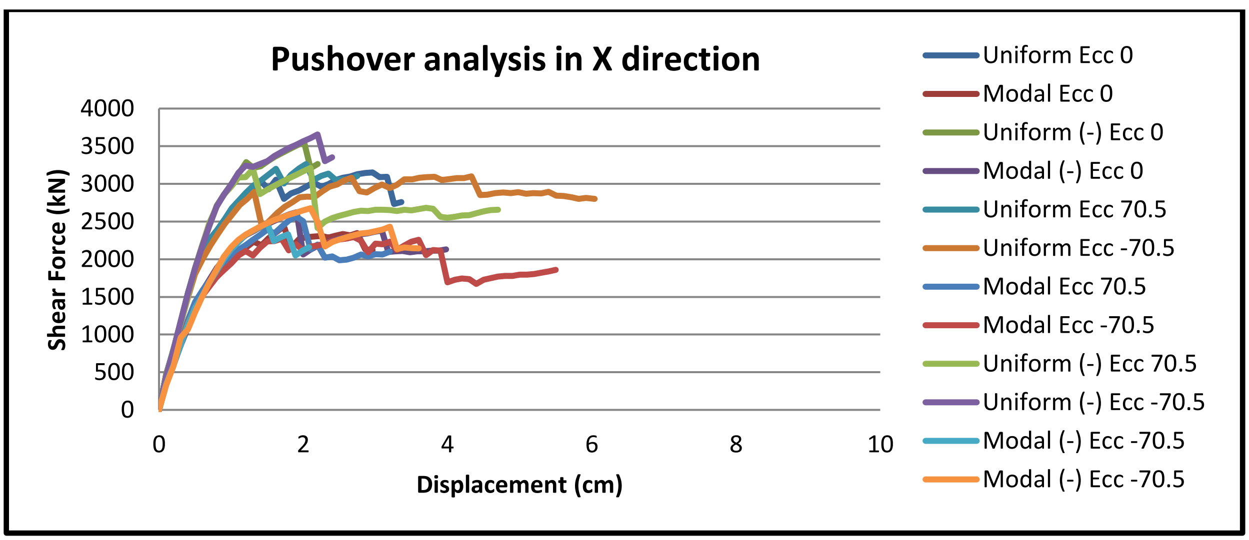

Figure 167: Pushover analysis for x-dir, 12 load patterns of building C1A with intervention

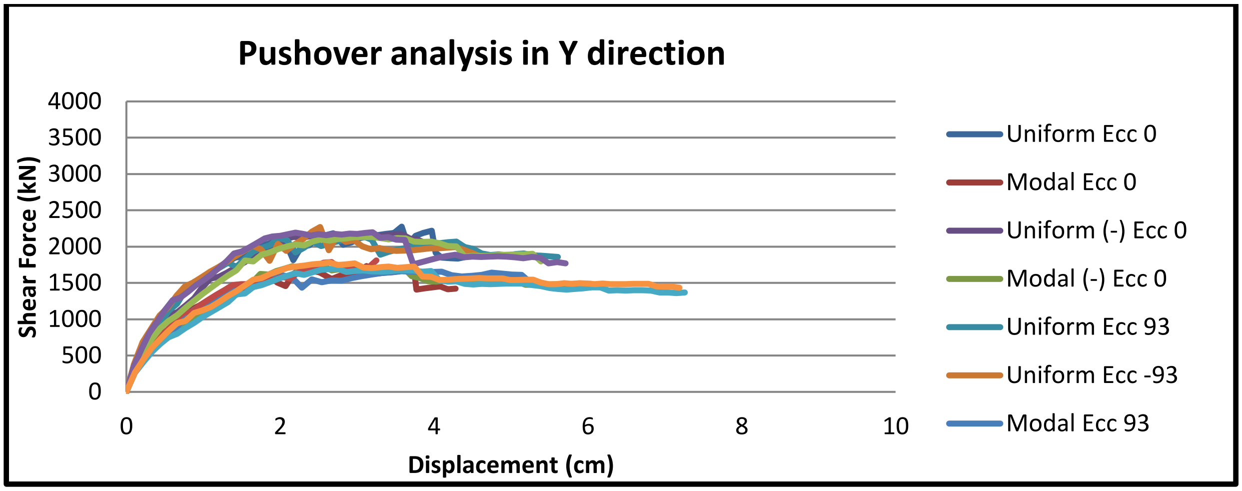

Figure 168: Pushover analysis for y-dir, 12 load patterns of building C1A with intervention

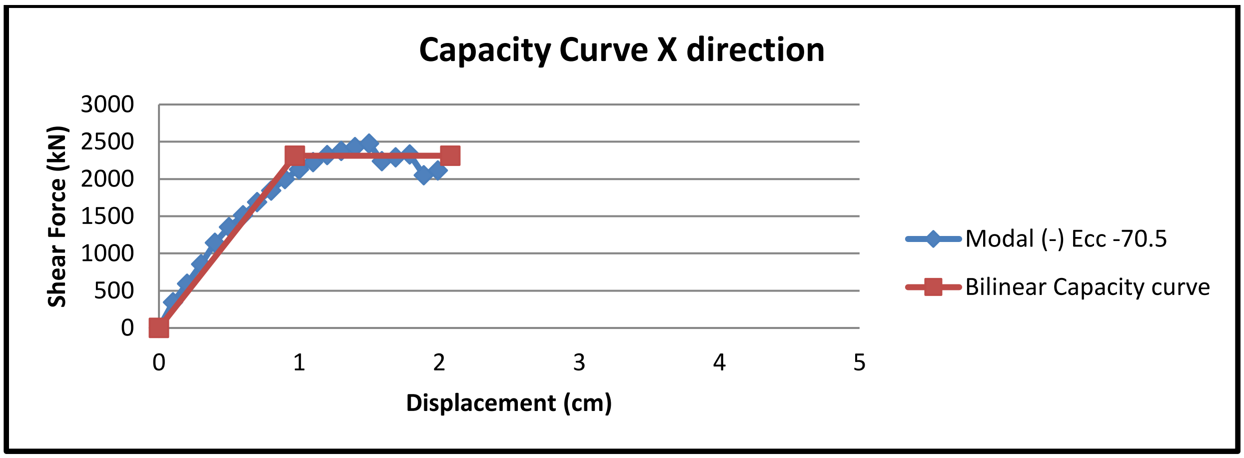

Figure 169: Capacity curve in x-dir of building C1A with intervention

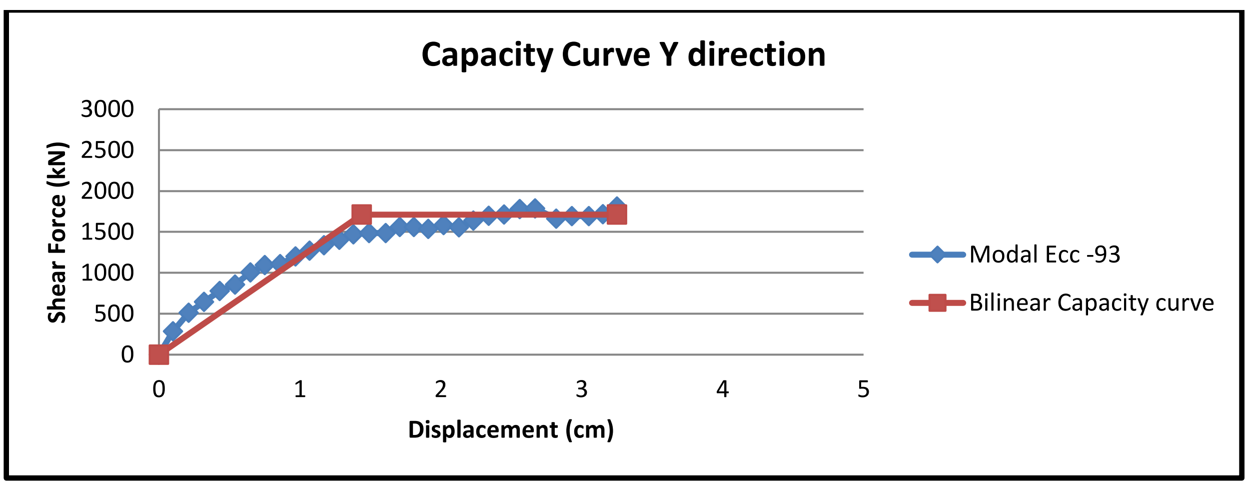

Figure 170: Capacity curve in y-dir of building C1A with intervention

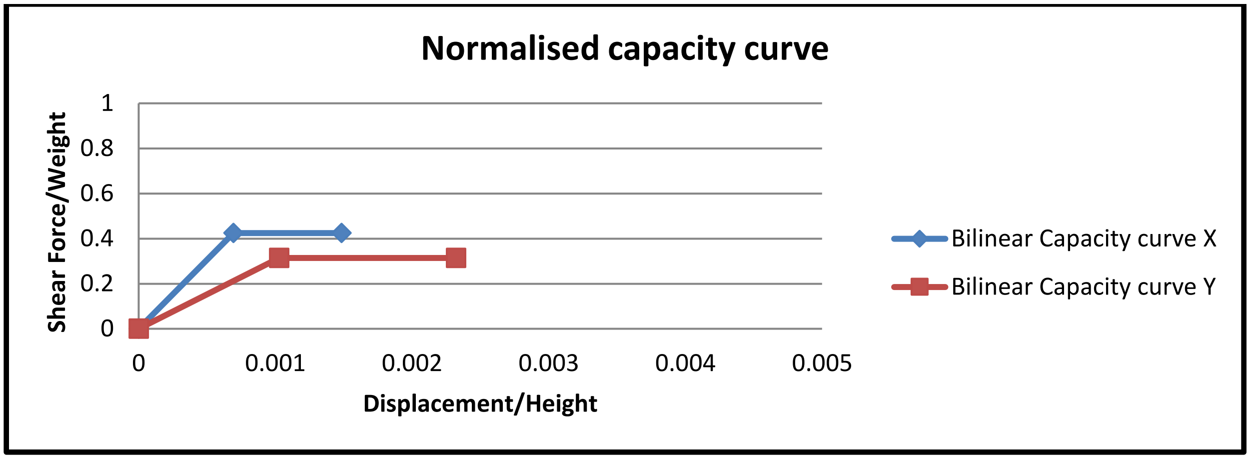

Figure 171: Normalized capacity curves of building C1A with intervention

Table 63: Pushover analysis parameters of building C1A with intervention

Load applied	d_y^*	d_m^*	F_y^*	K^*	μ	F_y^*/W
x-direction	0.97cm	2.08cm	2312kN	2384kN/cm	2.14	0.4244
y-direction	1.44cm	3.25cm	1711kN	1188kN/cm	2.25	0.3141

Table 64: Modal analysis parameters of building C1A with intervention

Mode	T [s]	mx [kg]	Mx [%]	my [kg]	My [%]	mz [kg]	Mz [%]
1	0,27337	12.31	0,97	909.234	71,74	3	0,00
2	0,22989	1.012.971	79,92	19.429	1,53	379	0,03
3	0,20144	16.013	1,26	105.368	8,31	204	0,02
4	0,09939	1	0,00	143.882	11,35	350	0,03
5	0,08629	156.406	12,34	1.911	0,15	11.602	0,92
6	0,07591	5.431	0,43	22.325	1,76	7.921	0,62
7	0,07001	2.843	0,22	2	0,00	312.822	24,68
8	0,06152	116	0,01	28	0,00	23.839	1,88
9	0,05753	123	0,01	6	0,00	451.776	35,64
10	0,05579	167	0,01	34.85	2,75	331	0,03
11	0,05397	269	0,02	2.903	0,23	5.356	0,42
12	0,05167	373	0,03	45	0,00	53.244	4,20

5.3.3 Pushover analysis of buildings with different projection conditions from template

In some cases, some templates have changes with the standard template for similar buildings. A2 template for example, is realized in some buildings, with a vertical opening in the middle of the building. This solution makes the two parts of the building perform independent from each other. Another case is of B2 building constructed in areas of mountainous climate, when all the perimeter walls from story 1 to 4 are with 38 cm width, not as the basic template of others buildings of this type with 38cm only on first floor.

5.3.3.1 Building A2 considering half building (seismic divide)

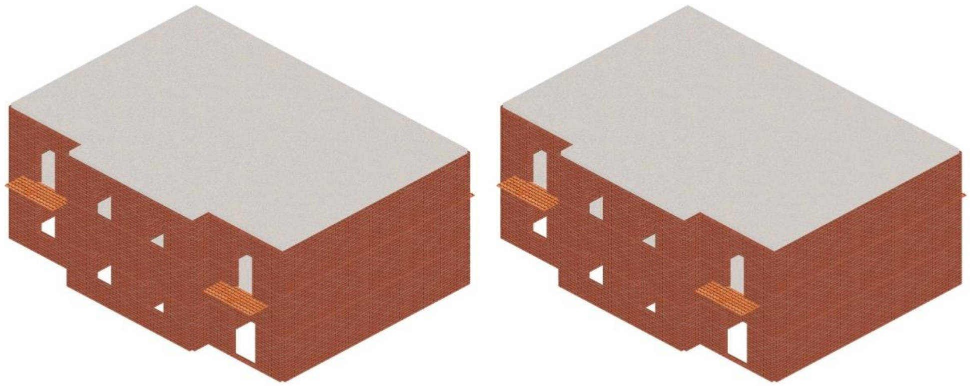

Figure 172: A2 building considering two independent halfs

Table 65: Pushover analysis parameters of building A2 considering two independent halfs

Load applied	d_y^*	d_m^*	F_y^*	K^*	μ	F_y^*/W
x-direction	0.34cm	1.25cm	822kN	2417kN/cm	3.67	0.595
y-direction	0.26cm	0.85cm	976kN	3753kN/cm	3.27	0.706

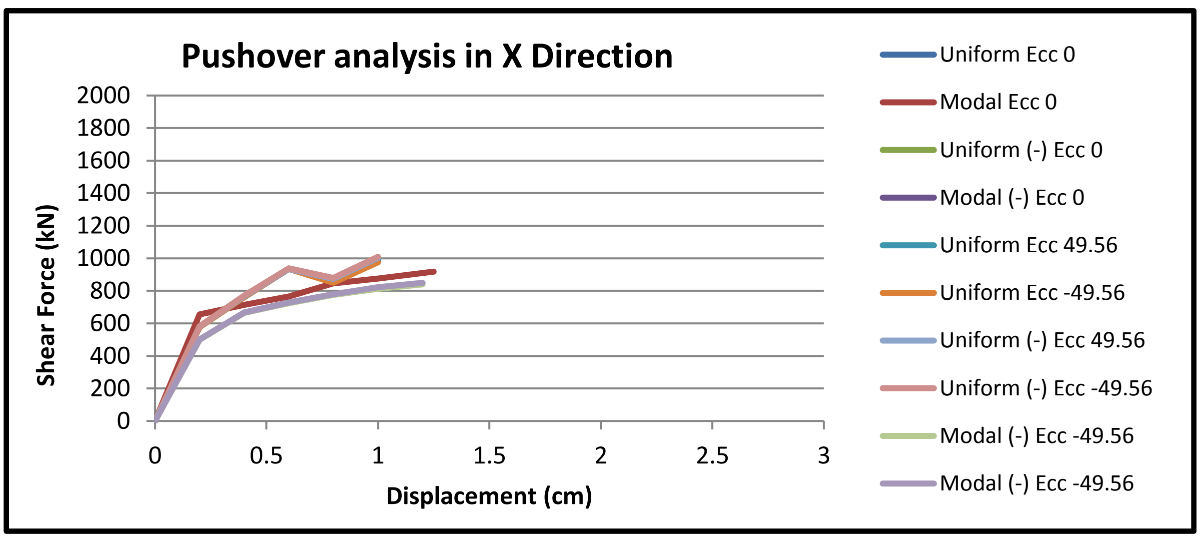

Figure 173: Pushover analysis for x-dir, 12 load patterns of building A2 considering two halves

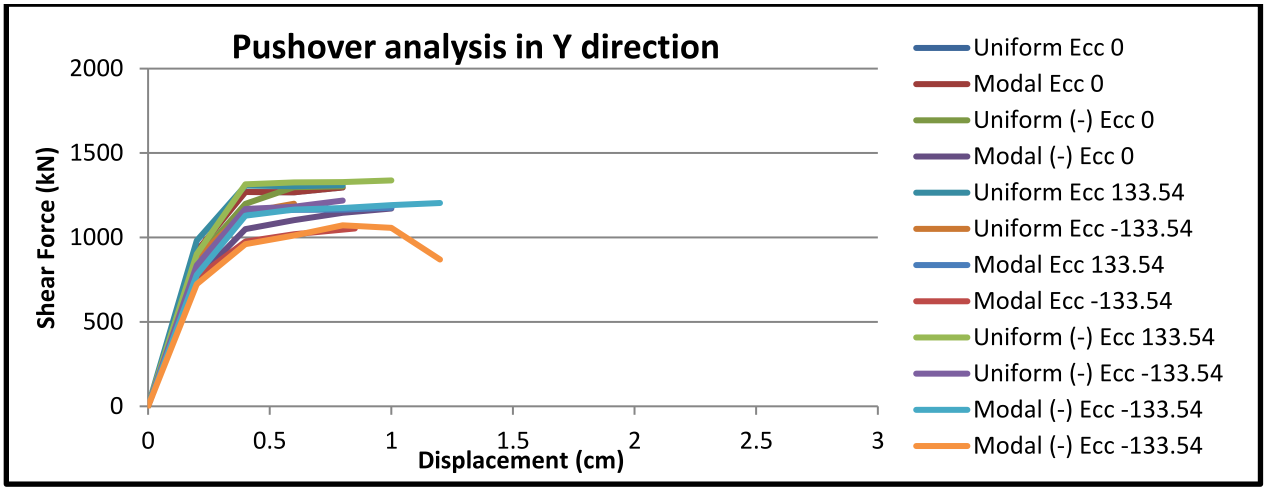

Figure 174: Pushover analysis for y-dir, 12 load patterns of building A2 considering two halves

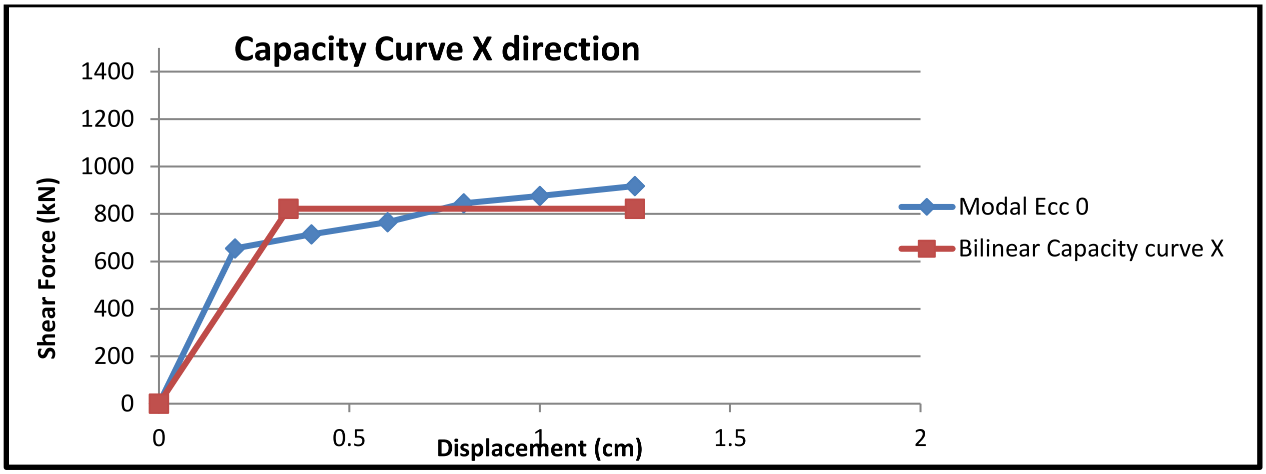

Figure 175: Capacity curve in x-dir of building A2 considering two halves

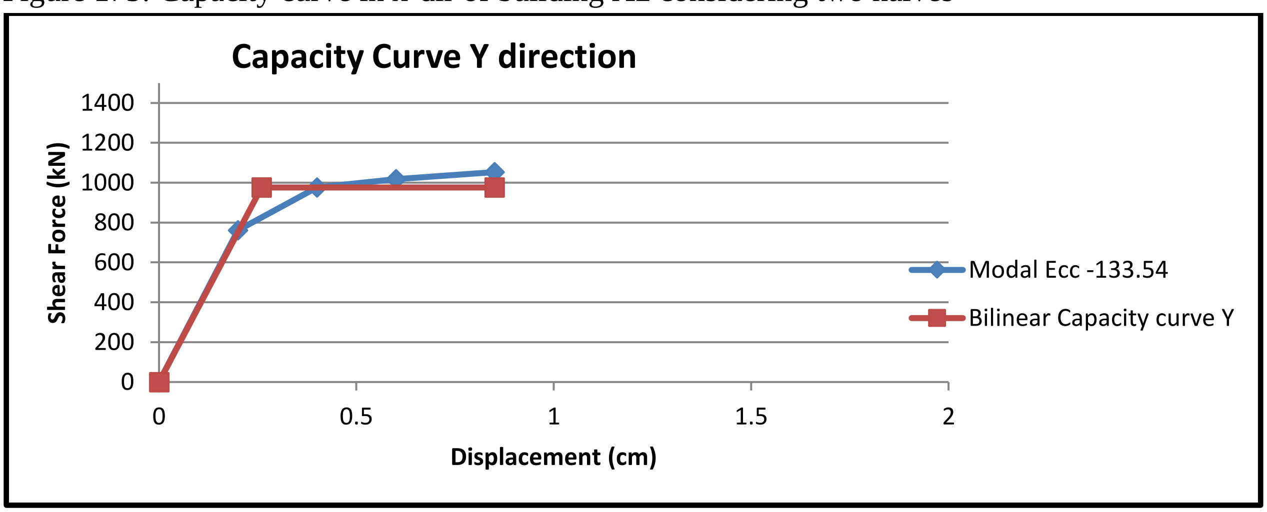

Figure 176: Capacity curve in y-dir of A2 building considering two halves

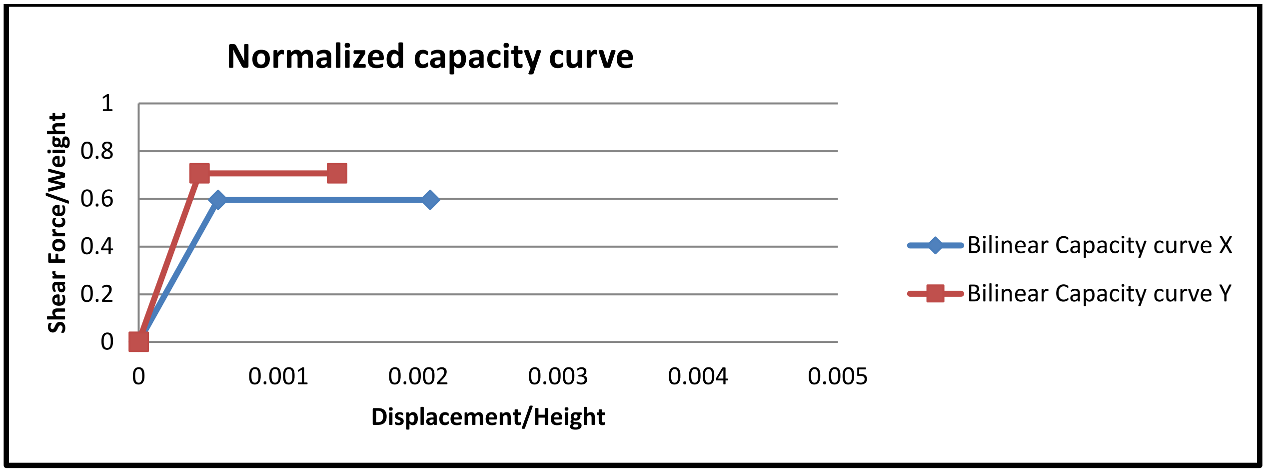

Figure 177: Normalized capacity curves of building A2 considering two independent halves

Table 66: Modal analysis parameters of building A2 considering two independent halves

Mode	T [s]	mx [kg]	Mx [%]	my [kg]	My [%]	mz [kg]	Mz [%]
1	0,11686	239.571	90,07	0	0,00	0,252	0,00
2	0,07522	132,251	0,05	67739	25,47	53,761	0,02
3	0,07033	54,356	0,02	168641	63,40	97,516	0,04
4	0,03496	26.025	9,78	4,287	0,00	1,701	0,00
5	0,02164	4,328	0,00	17550	6,60	5.046	1,90
6	0,02995	3,060	0,00	6517	2,45	2.962	1,11
7	0,02616	0,188	0,00	247	0,09	162.445	61,08
8	0,02515	0,440	0,00	97	0,04	10.071	3,79
9	0,02409	10,969	0,00	731	0,28	27,384	0,01
10	0,02374	1,419	0,00	1.504	0,57	3.026	1,14
11	0,02316	0,409	0,00	89,711	0,03	40.762	15,33
12	0,02268	0,703	0,00	26,396	0,01	574,513	0,22

5.3.3.2 Building B2 with 38 cm wall on all stories

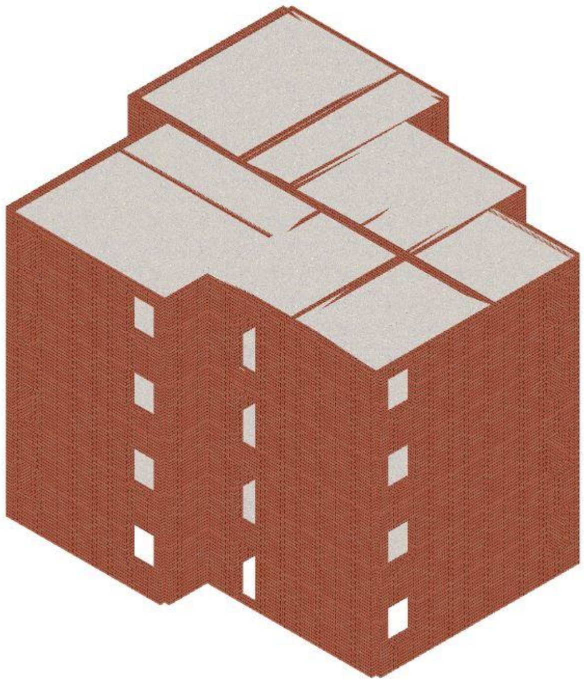

Figure 176: B2 building with 38cm walls

Table 67: Pushover analysis parameters of building B2 with 38cm walls

Load applied	d_y^*	d_m^*	F_y^*	K^*	μ	F_y^*/W
x-direction	0.45cm	1.33cm	2843kN	6317kN/cm	2.96	0.6545
y-direction	0.48cm	1.91cm	1945kN	4052kN/cm	3.97	0.4478

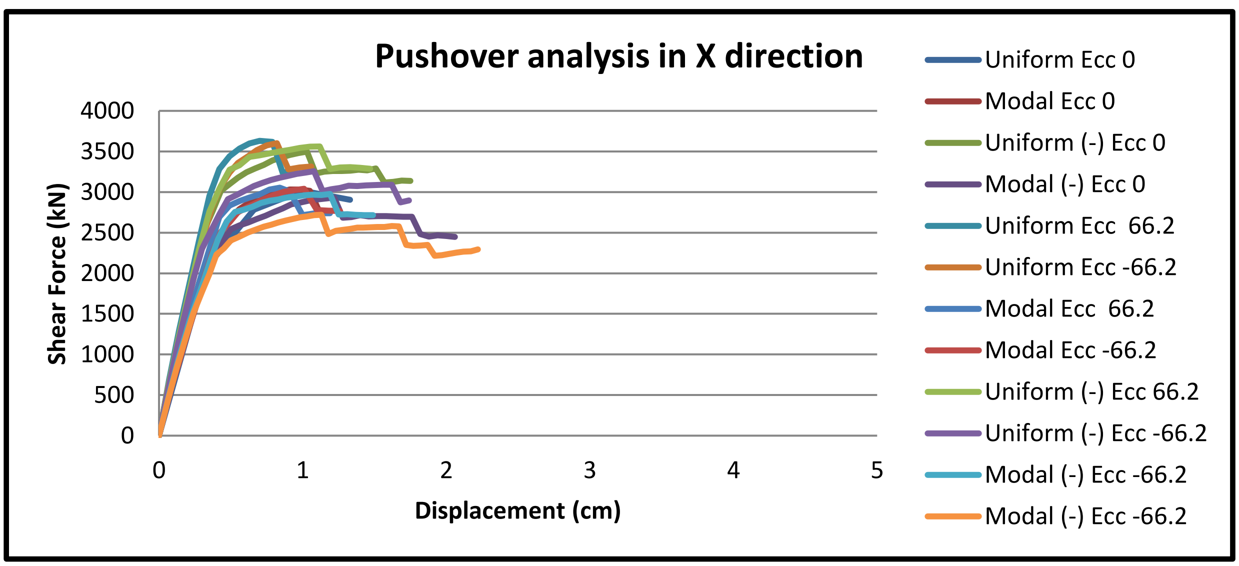

Figure 177: Pushover analysis for x-dir, 12 load patterns of building B2 with 38cm walls

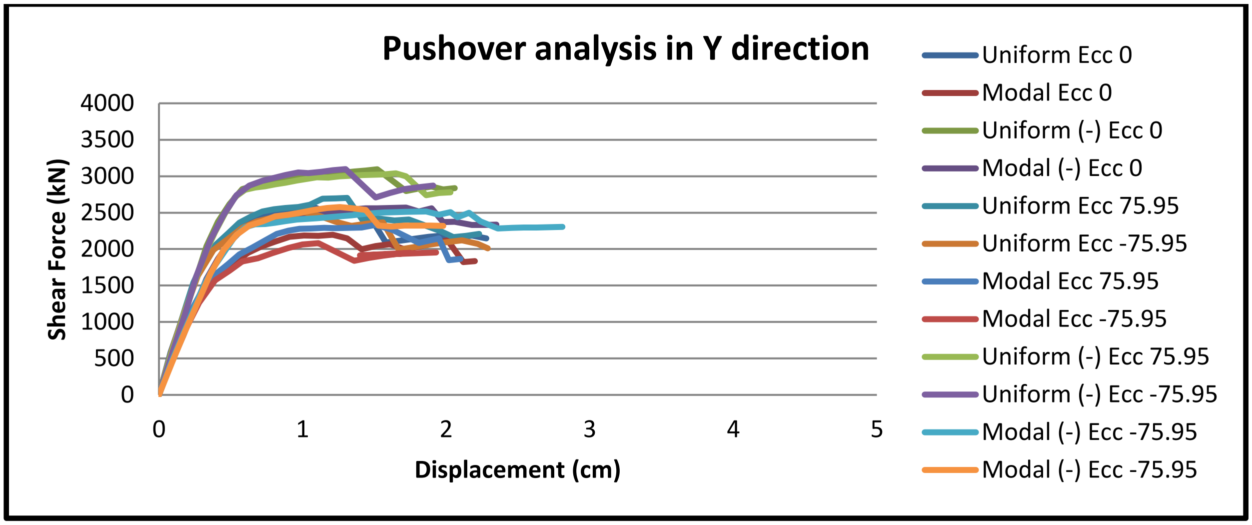

Figure 178: Pushover analysis for y-dir, 12 load patterns of building B2 with 38cm walls

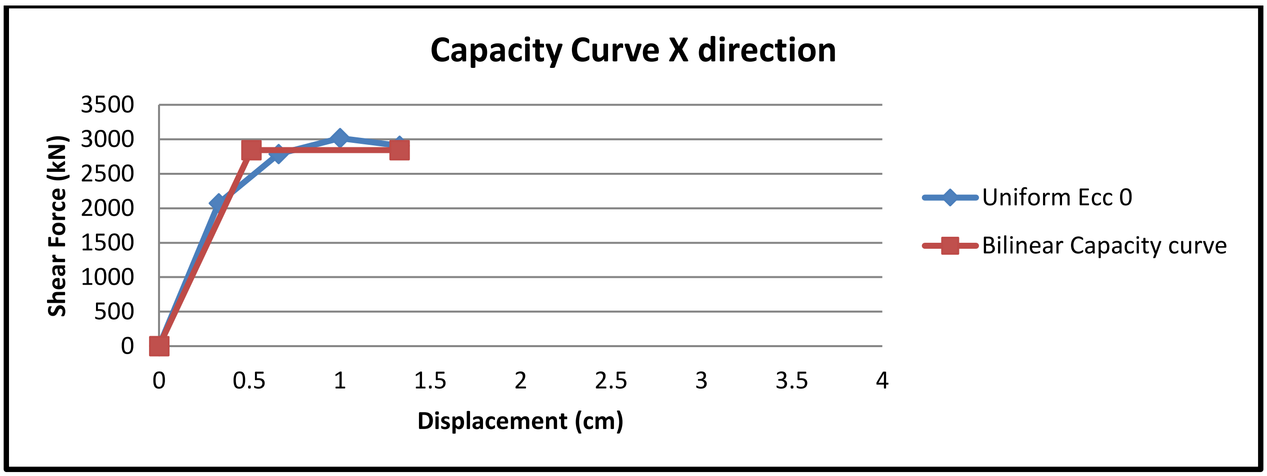

Figure 179: Capacity curve in x-dir of building B2 with 38cm walls

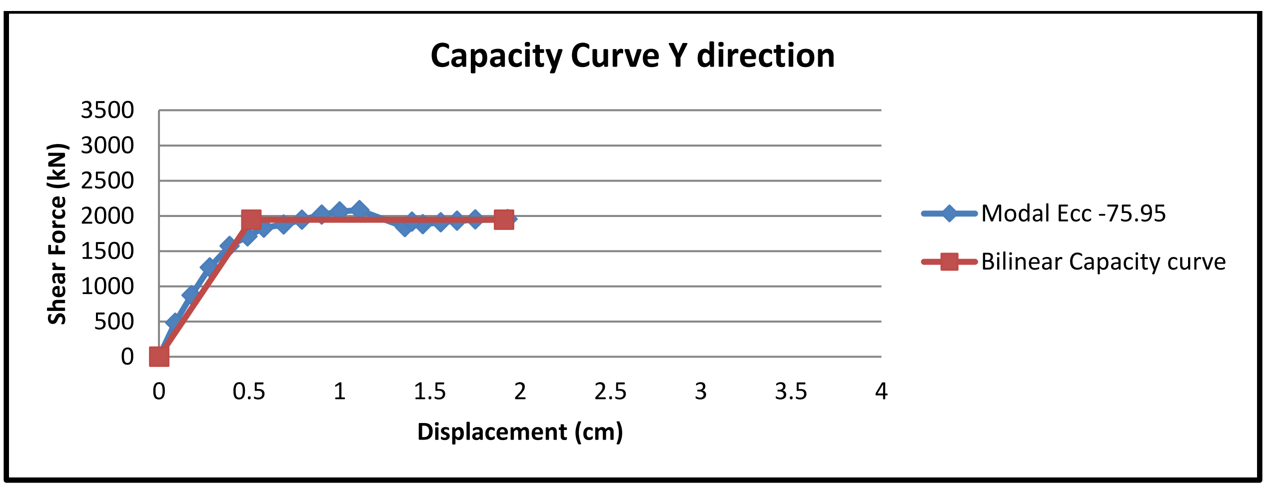

Figure 180: Capacity curve in y-dir of building B2 with 38cm walls

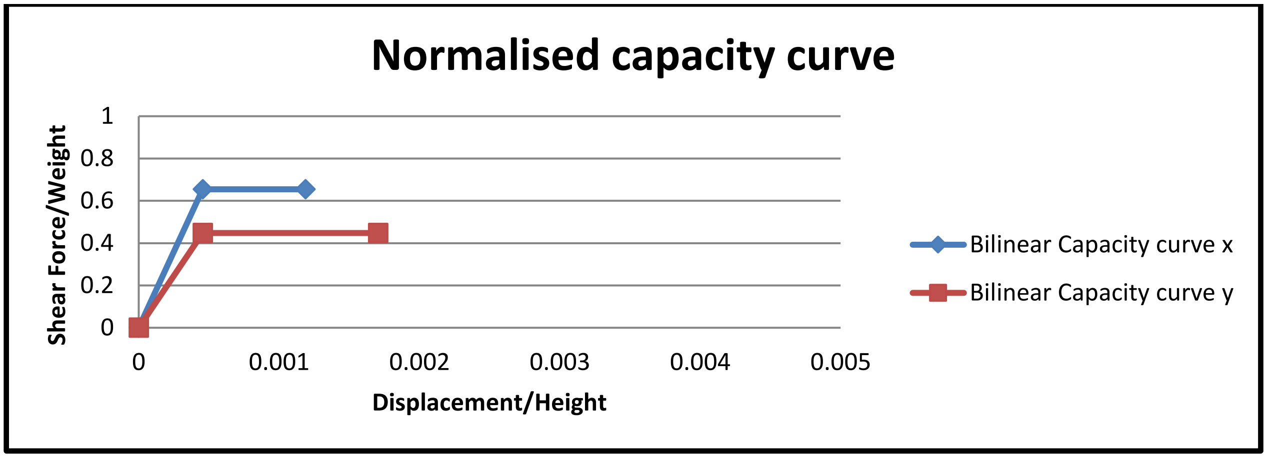

Figure 181: Normalized capacity curves of building B2 with 38 cm walls

Table 68: Modal analysis parameters of building B2 with 38cm walls

Mode	T [s]	mx [kg]	Mx [%]	my [kg]	My [%]	mz [kg]	Mz [%]
1	0,18644	10.625	1,03	769.506	74,79	297	0,03
2	0,17118	802.6	78,00	20.538	2,00	40	0,00
3	0,14498	47.331	4,60	28.685	2,79	85	0,01
4	0,06380	2.323	0,23	146.202	14,21	6.251	0,61
5	0,05959	121.16	11,78	4.642	0,45	4.552	0,44
6	0,05212	3.159	0,31	2.457	0,24	582.873	56,65
7	0,05118	869	0,08	2.399	0,23	219.404	21,32
8	0,04669	24	0,00	5.731	0,56	3.280,442	0,32
9	0,04614	1.849	0,18	5.145	0,50	26.736	2,60
10	0,04426	845	0,08	660	0,06	41.672	4,05
11	0,04325	4.056	0,39	1.082	0,11	7.308	0,71
12	0,03953	2	0,00	1.083	0,11	10.248	1,00

5.4 Interpretation of capacity curves

The capacity curve of the building, gives the basic parameters for all the later performed, spectrum based analysis, time history analysis and fragility analysis. Since the studied buildings are of different materials, height, era and template some interesting comparison can be done here. The buildings with intervention are compared with those of original project condition, giving a good view of what effect the intervention has on the capacity of the structure. Building of template C1 has four different cases: 5 story building with clay bricks, 5 story building with clay bricks with intervention on first floor, 5 story building with silicate bricks, 6 story building with silicate brick with one story added later on the building. A comparison among the capacity curves of these buildings with the same plan but with these changes gives a good view, how capacity is affected by the material of construction and interventions done on the building.

5.4.1 Comparison of C1 buildings with different brick materials

Template C1 is a good model for comparing pushover curves of a silicate and a clay masonry buildings. The silicate building has greater parameters of f_b f_m and f_k, but the bonding connection is stronger in clay-mortar comparing to silicate-mortar, when values of f_{vk} are almost the same for both buildings. This comes because mortar values are almost the same and even though the silicate building has stronger bricks 10MPa comparing to 7,5MPa, clay units bonds better, so the values are almost the same.

Table 69: Comparison of C1 buildings with different masonry material

		Building C1A (clay bricks)	Building C1B (silicate bricks)
Brick compressive strength	f_b	7.5MPa	10MPa
Mortar compressive strength	f_m	4.8MPa	5MPa
Masonry compressive strength	f_k	2.42MPa	2.97MPa
Shear strength of masonry	f_{vk}	0.36MPa	0.4MPa
Total weight	W	13202kN	14175kN
Max. Force (x-direction)	F_y^*	2184.6kN	2624kN
Max. Displacement (x-direction)	d_m^*	3.05 cm	2.53cm
Max. Force (y-direction)	F_y^*	1857kN	1961kN
Max. Displacement (y-direction)	d_m^*	4.62cm	4.24cm
Force/Weight (x-direction)	F_y^*/W	48.75%	39.65%
Displacement/Height (x-direction)	d_m^*/H	0.22%	0.18%
Force/Weight (y-direction)	F_y^*/W	33.7%	33.3%
Displacement/Height (y-direction)	d_m^*/H	0.33%	0.30%
Ductility index	μ_x	2.85	2.3
Ductility index	μ_y	2.76	2.88

The silicate masonry building has 10% more weight, because of the greater density of the brick elements. The maximum applied force is greater in the silicate building in both directions, but top roof displacement is greater in the clay building (in x-direction).

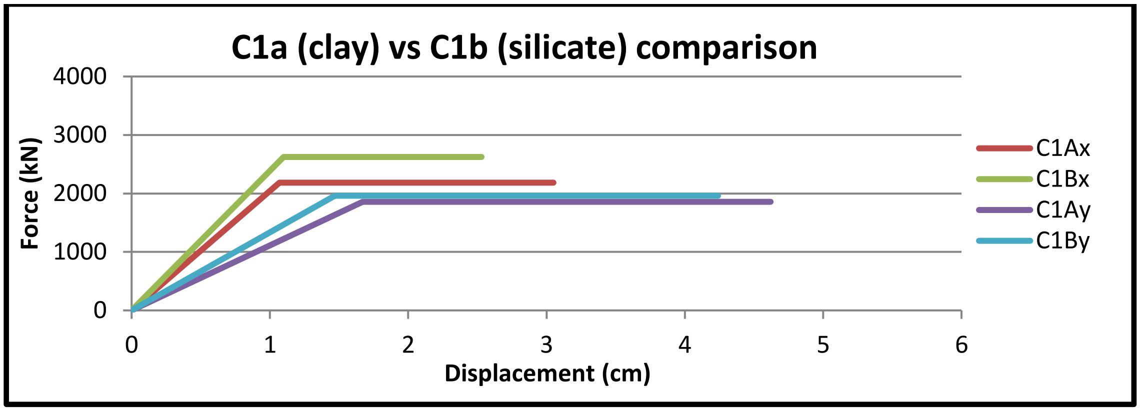

Figure 184: Comparison of capacity curve of C1 building with different materials

Also the ductility level is higher in the clay building, with the silicate building showing a more brittle behaviour, in x direction. For both buildings the displacement to height ratio is greater in the y-direction, because of the wall distribution in plan.A comparison between the two buildings failure mechanism on pushover analysis is shown below. From the failure scheme of the two building in x-direction, can be noted that the perimeter wall fails in both buildings in the upper floors from bending failure. [Bilgin H., Hysenlliu M., 2019]

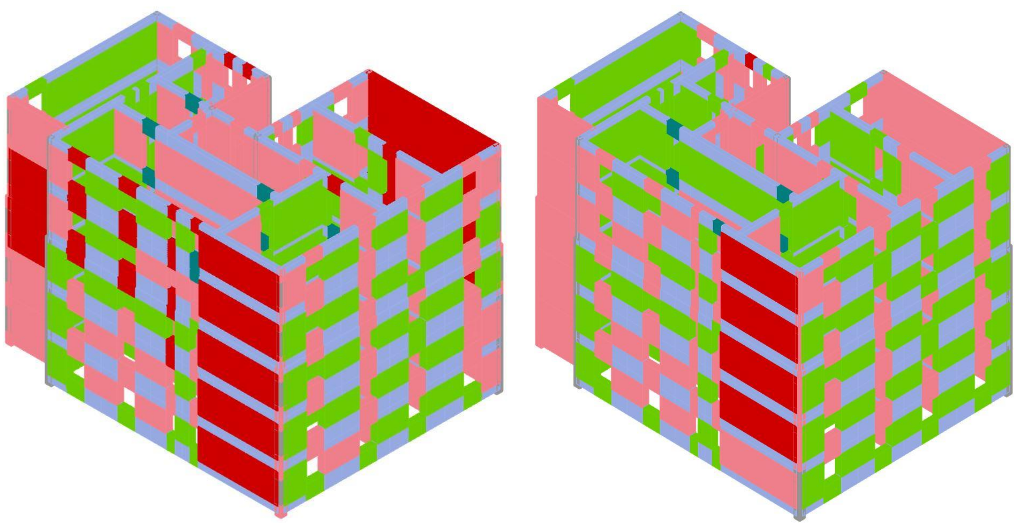

Figure 185: Failure mechanism of C1 (clay) and C1B(silicate) in pushover analysis

The failure mechanism shows more deformability of the first building. Failure is reached when all the right part of the perimeter wall fails in bending and also in the wall in the back part on upper levels. While in the silicate model the fail mechanism is reached before, and only on the front wall part in story 2 and above. The perimeter wall is taken in consideration, since it has the failure mechanism of both buildings. Below is shown the progression of the failure during pushover.

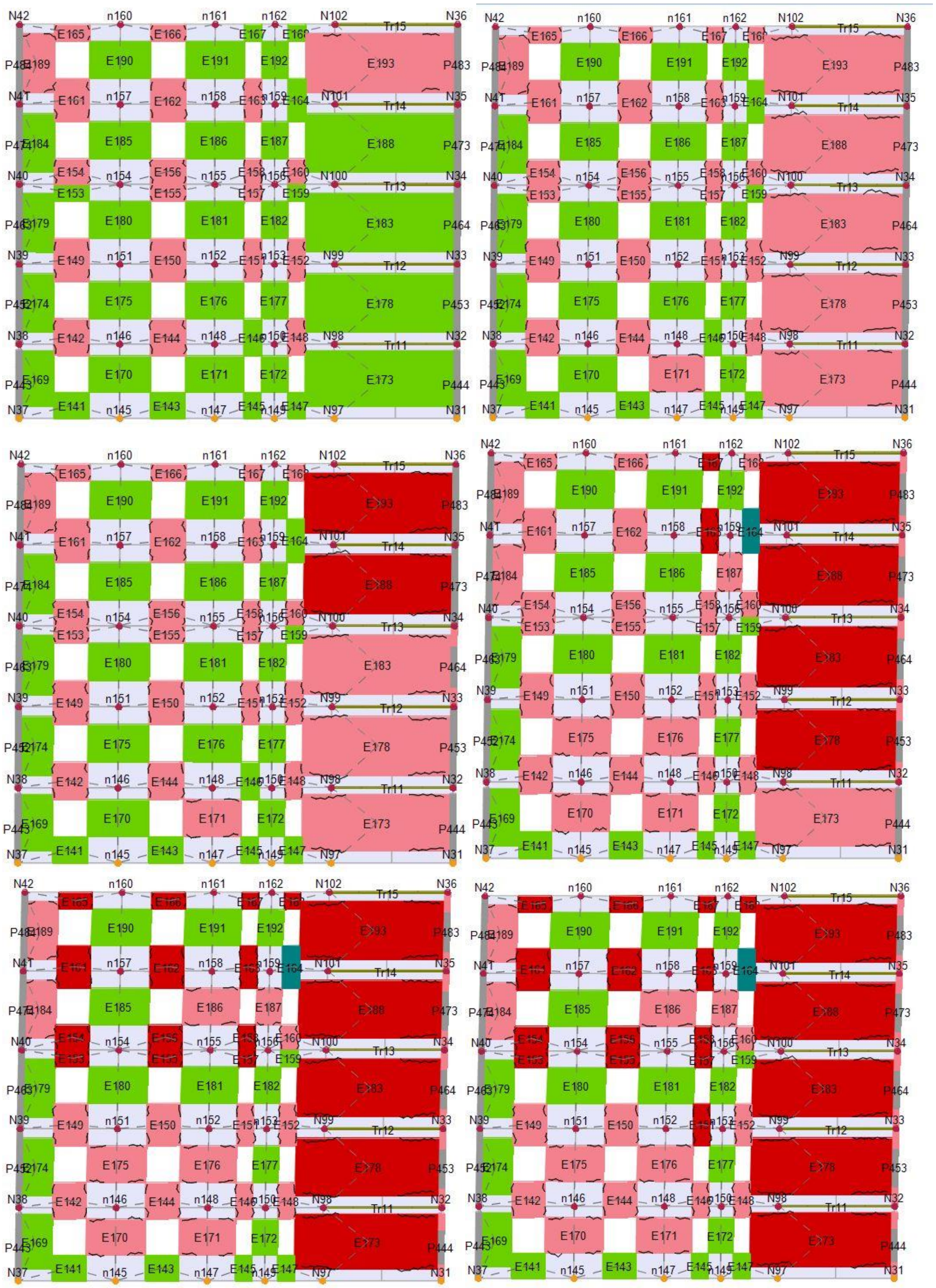

Figure 186: Perimeter wall failure mechanism C1A clay building step by step

The same wall is considered for the silicate building. As can be seen below the failure is more brittle and some parts of the same wall are undamaged in this scenario.

Figure 187: Perimeter wall failure mechanism C1B silicate building step by step

5.4.2 Comparison of buildings of same template with different nr. of stories

5.4.2.1 Buildings of template A1

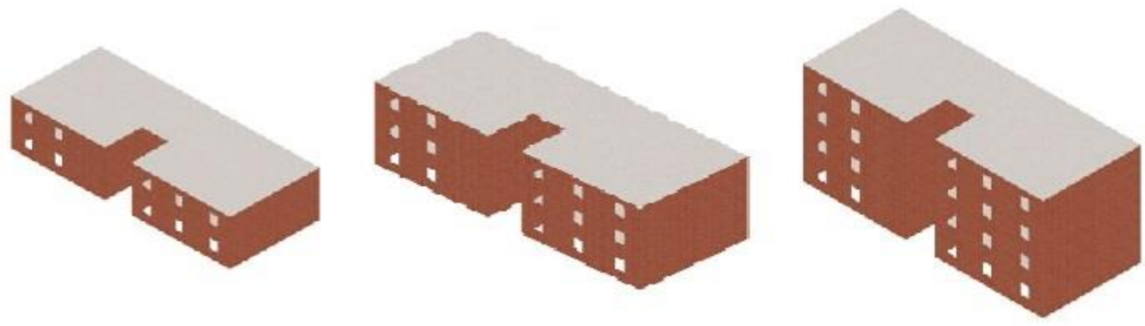

Figure 188: A1 buildings with different height

The template building A1 was designed for two stories. On the existing buildings in Tirana, The Moskat building all have two added stories, and the ones near Lana River, have one added story. If we compare the parameters from the pushover curves, the shear force / weight ratio significantly decteases in the two models with added stories, while the ductility index varies with the addition of stories, with the three story building showing more ductility.

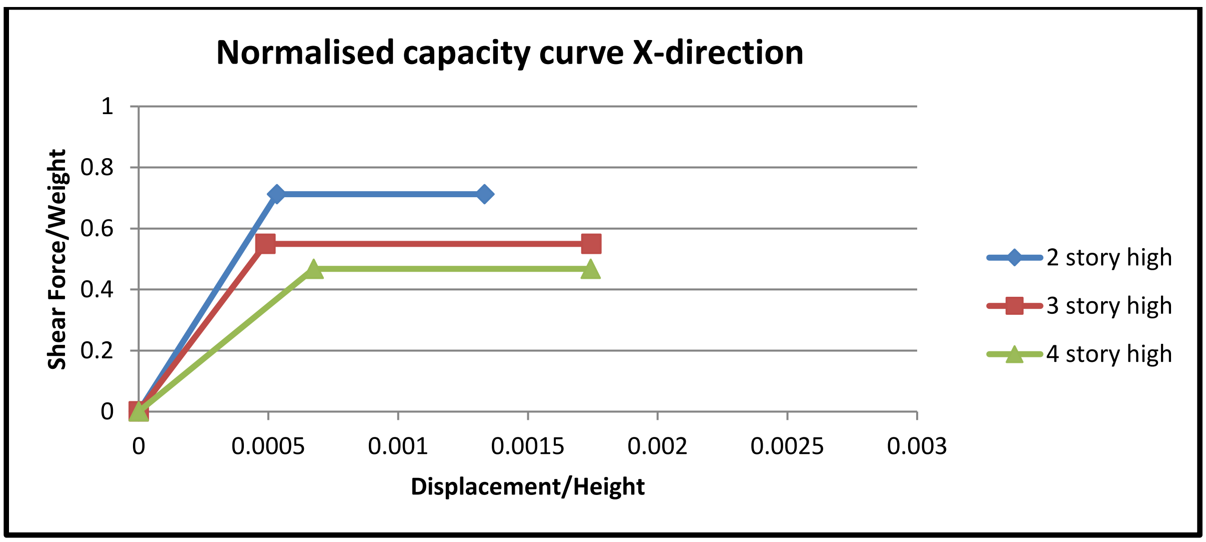

Figure 189: Normalised capacity curves in x-dir of A1 buildings with different height

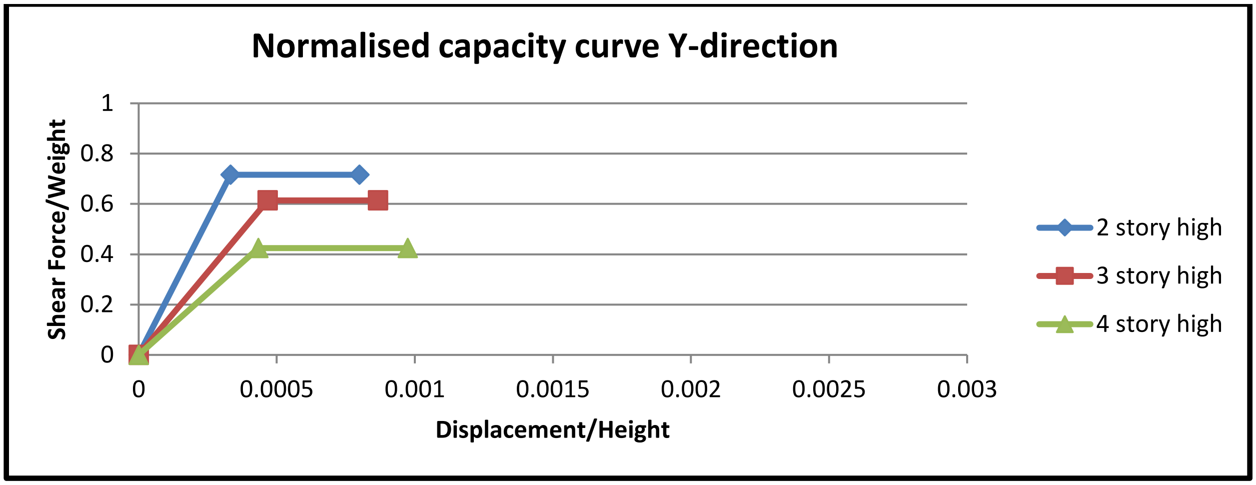

Figure 190: Normalised capacity curves in y-dir of A1 buildings with different height

Also the initial stiffness of the buildings decreases with height addition. If the fail mechanism are compared, in the buildings with more stories, in the upper stories walls have more from shear damage and some parts shear failure. Although the most damage still comes from bending failure in the lower parts of the inside walls of the buildings.

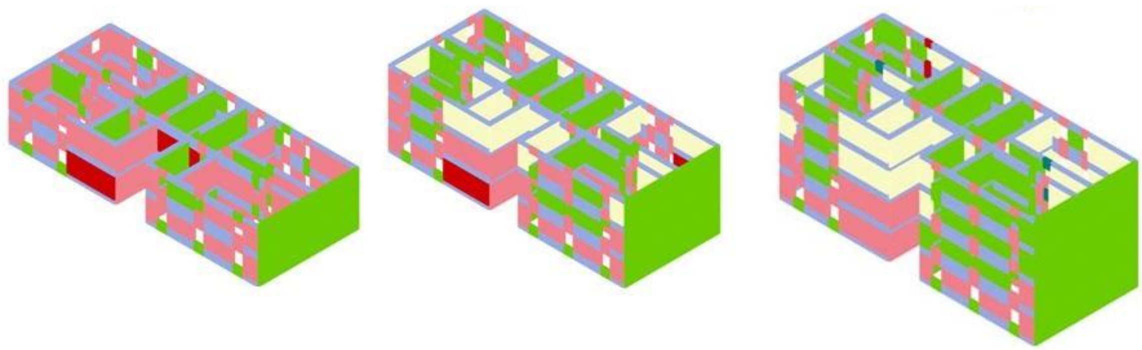

Figure 191: Failure mechanism of buildings A1 with different height

Table 70: Parameters of A1 template building with different heights

	Initial stiffness	Max Force/Weight	Yield Disp /Height	Max Disp /Height	Ductility index
A1x	5884	0.7122	0.000533	0.001333	2.5
A1x +1	4596	0.5494	0.000489	0.001744	3.57
A1x +2	2717	0.4676	0.000675	0.001741	2.58
A1y	9465	0.716	0.000333	0.0008	2.4
A1y +1	5381	0.6141	0.000467	0.000867	1.8
A1y +2	3842	0.4245	0.000433	0.000975	2.25

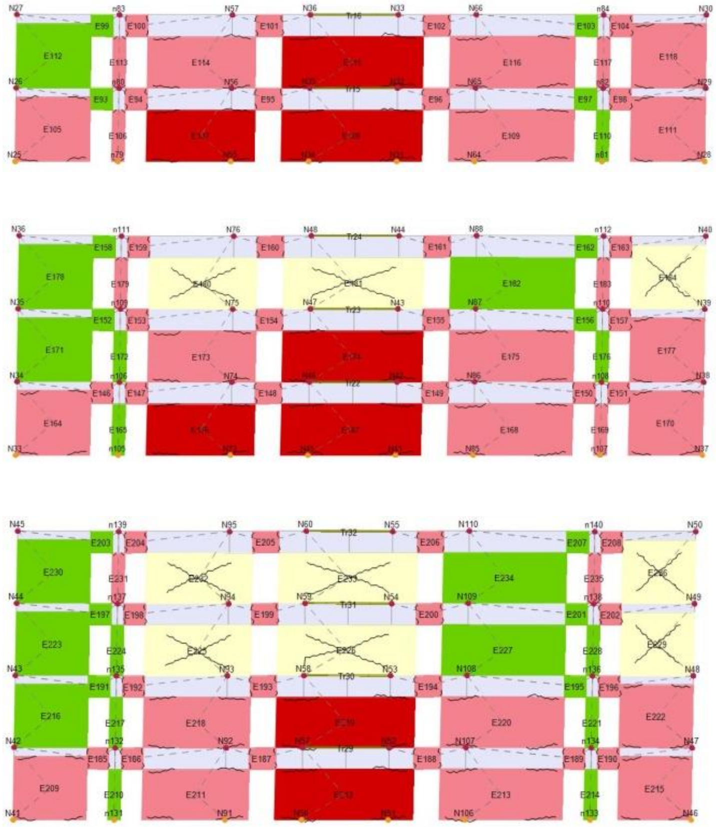

Figure192: Failure mechanism on most loaded wall in pushover analysis y-direction

5.4.2.2 Buildings of template B1

The template building B1 was designed for three stories, but as mentioned before, one floor was added in some buildings of this template, as in many cases in Albanian stock.

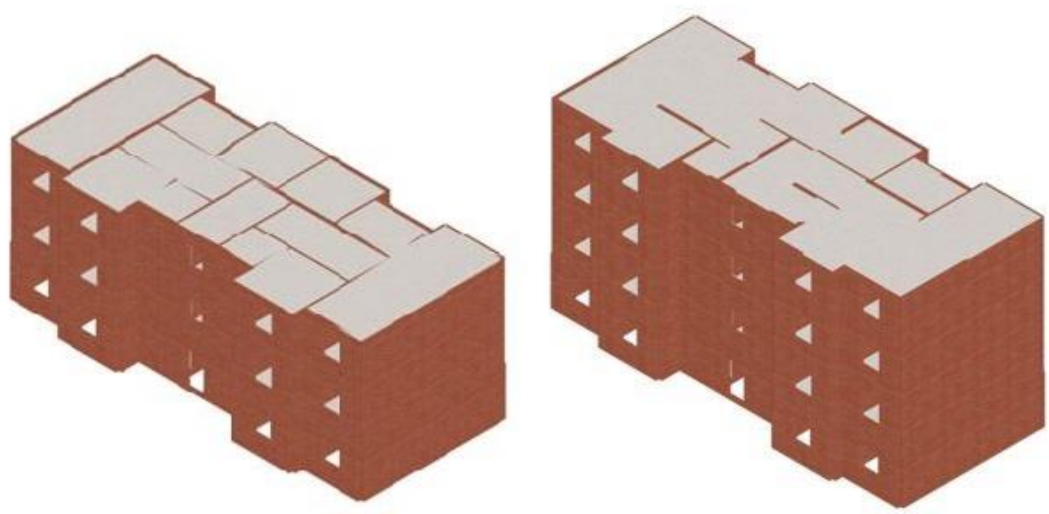

Figure 193: Buildings of template B1 with different height

For the 4 story building the shear force/weight ratio is lower than for the 3 story building in both direction at a ratio of 80%. The initial stiffness is also lower at a ratio of near 67% in both directions. The ductility levels also change but are almost the same in both buildings. The displacement/height ratio is increased for the 4 floor building.

Table 71: Parameters of B1 template building with different height

	Initial stiffness	Max Force/Weight	Yield Disp /Height	Max Disp /Height	Ductility index
B1x	5578	0.6704	0.000476	0.001667	3.500
B1x +1	3891	0.5461	0.000518	0.001795	3.466
B2y	8943	0.6987	0.000310	0.000833	2.692
B2y +1	5980	0.5788	0.000357	0.000929	2.6

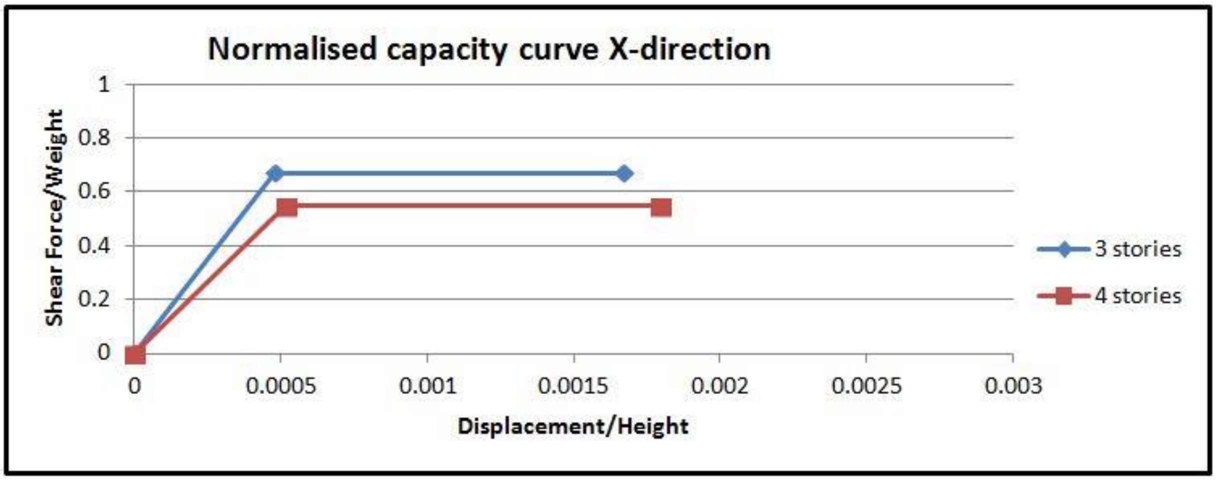

Figure 194: Normalised capacity curves in x-dir of B1 buildings with different heights

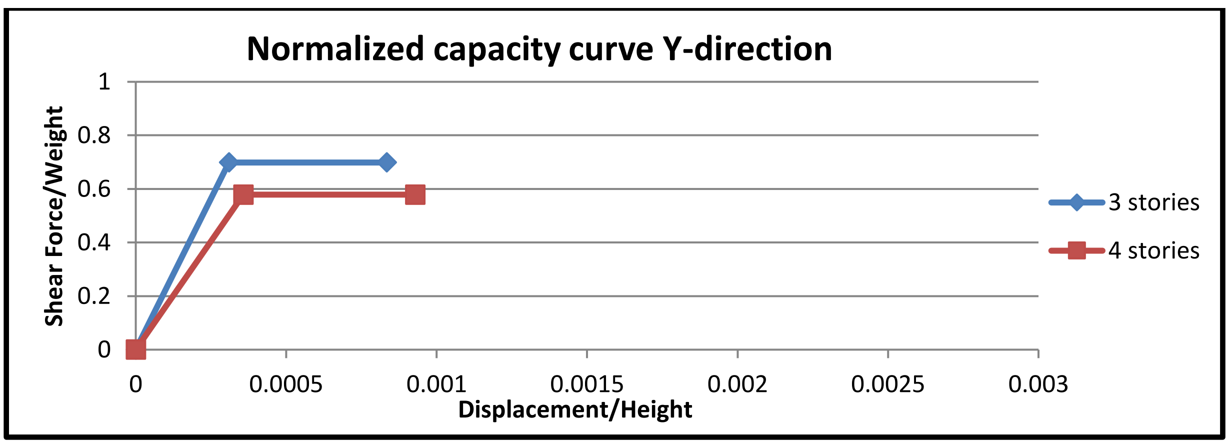

Figure 195:Normalised capacity curves in y-dir of B1 buildings with different height

If the failure mechanism are compared in both buildings, the most damaged is the perimeter wall in all wall levels in the y-direction load scenario. In the x direction the failure comes from bending failure of the walls in the first floor and is more distributed than first scenario.

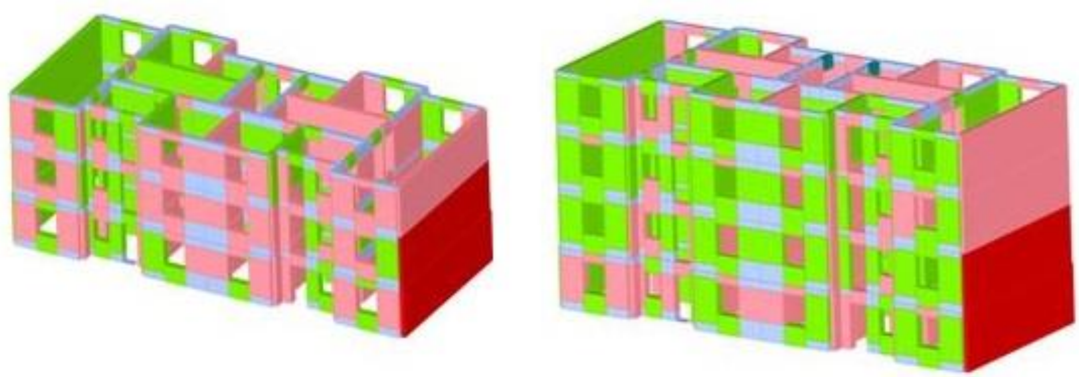

Figure 196:Failure mechanism in y-direction of B1 buildings with different height

5.4.2.3 Buildings of template C1B

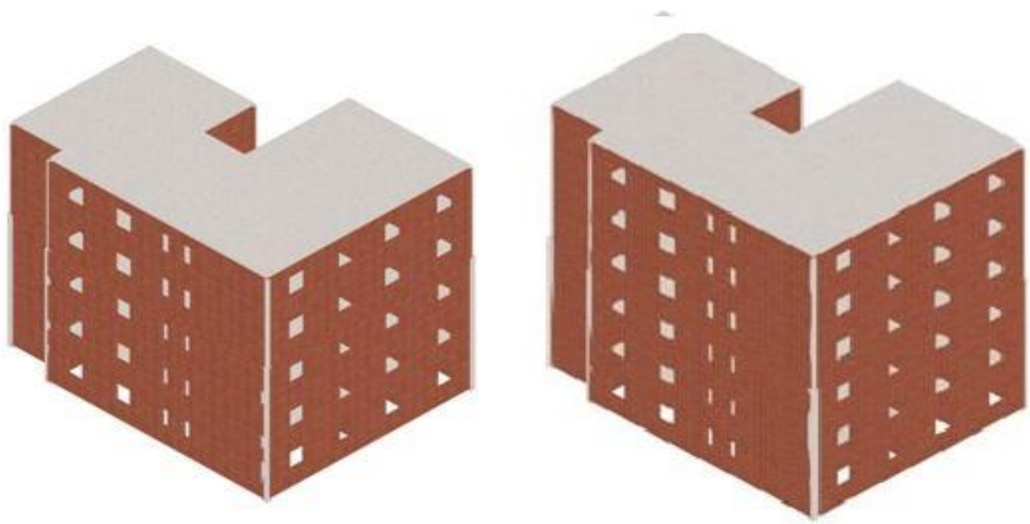

Figure 197: Buildings of template C1B with different heights

This template building is one of the most used in the country. As mentioned before it was designed both for clay brick and for silicate bricks. Since the silicate bricks were with higher strength, in many cases in these buildings one story is added. This examples are in Tirana and Vlore.

Table 72: Parameters of C1B template building with different height.

	Initial stiffness	Max Force/Weight	Yield Disp /Height	Max Disp /Height	Ductility index
C1Bx	2386	0.4461	0.000786	0.001807	2.3
C1Bx +1	1702	0.3706	0.000875	0.001940	2.217
C1By	1334	0.3334	0.001050	0.003029	2.885
C1By +1	1063	0.3243	0.001226	0.003119	2.543

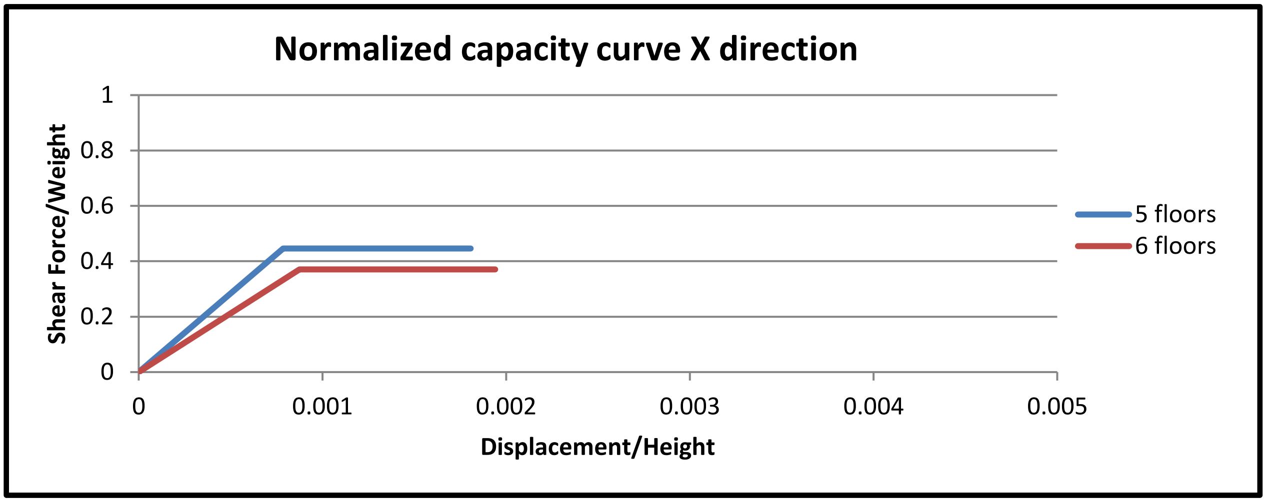

Figure 198:Normalized capacity curves in x-direction of C1B buildings with different height

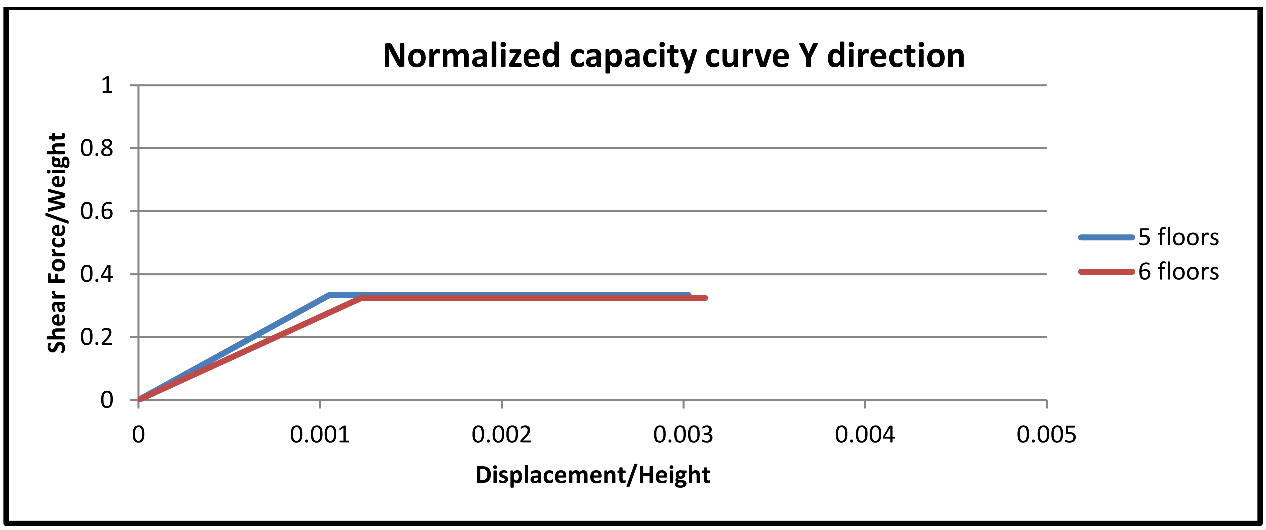

Figure 199:Normalized capacity curves in y-direction of C1B buildings with different height

Initial stiffness is reduced severely in both directions by 29% and 21% respectively, comparing to the original version. Also the shear force/weight is slightly reduced in x direction, but remains almost the same in y direction. The same can be noted for the ductility index. If we compare the failure mechanisms of both templates in y direction, can be noticed that failure comes from bending on the elements above windows in outside walls, but most damaged wall for the 5 floor building is inside wall in the left part of the building, and the outside wall on the left side for the 6 floor building. The added floor, suffers more from shear damage in this scenario.

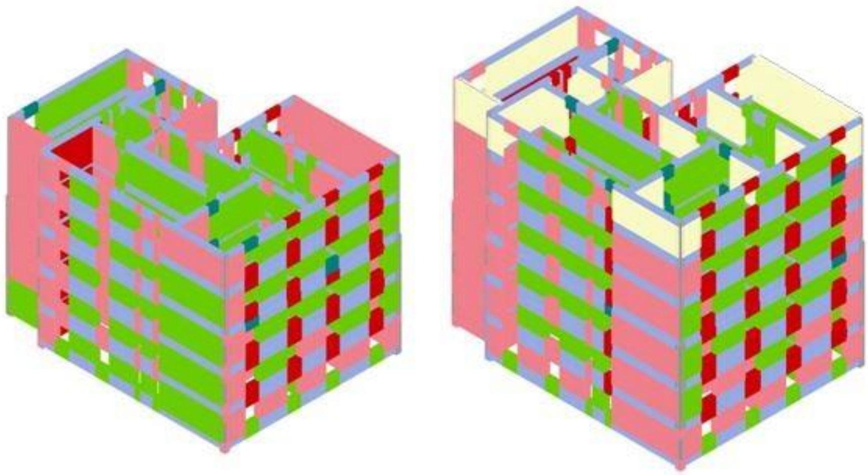

Figure 200:Failure mechanism in y-direction of C1B buildings with different height

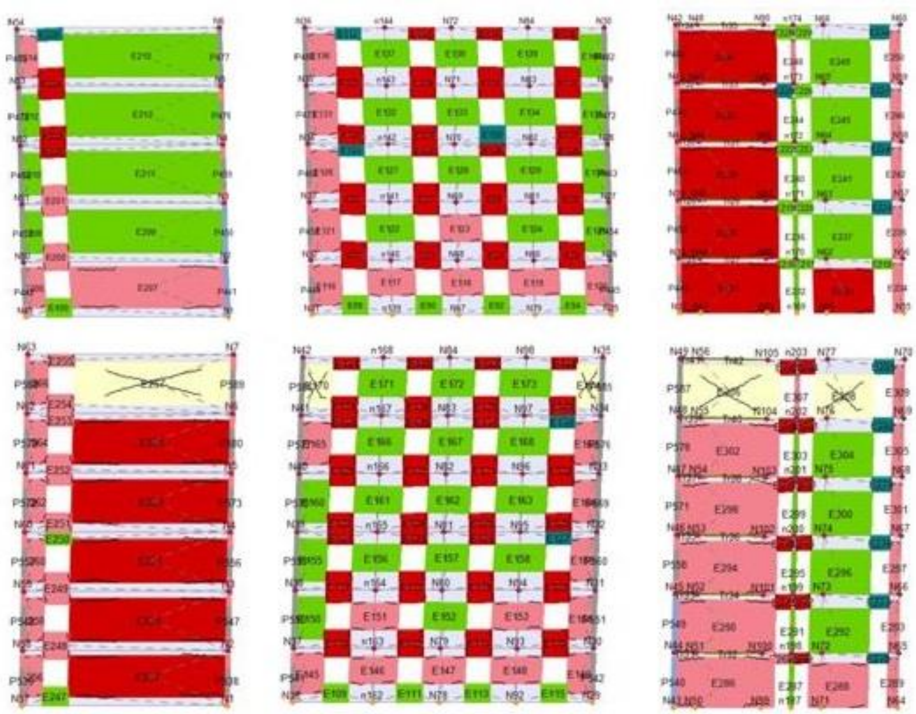

Figure 201: Failure mechanism of most damaged walls

5.4.2.4 Buildings of template C2

Buildings of this template also exist in both versions, with and without added stories.

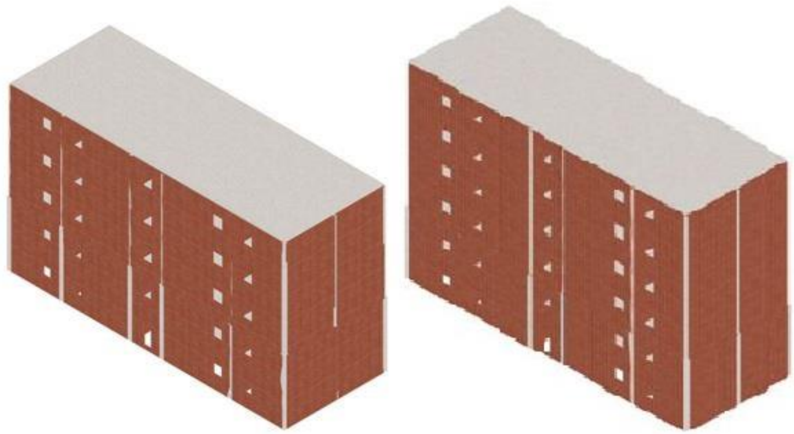

Figure 202: Buildings of template C2 with different heights

Table 73: Parameters of C2 template building with different height

	Initial stiffness	Max Force/Weight	Yield Disp /Height	Max Disp /Height	Ductility index
C2x	1510	0.6287	0.001579	0.003157	2
C2x +1	1069	0.4138	0.001417	0.003131	2.2
C2y	2310	0.3915	0.000642	0.001607	2.5
C2y +1	1775	0.3033	0.000625	0.001559	2.5

In this template building is viewed a great decrease in both stiffness and max force with the implementation of the added floor above. The ductility levels are almost the same for both buildings.

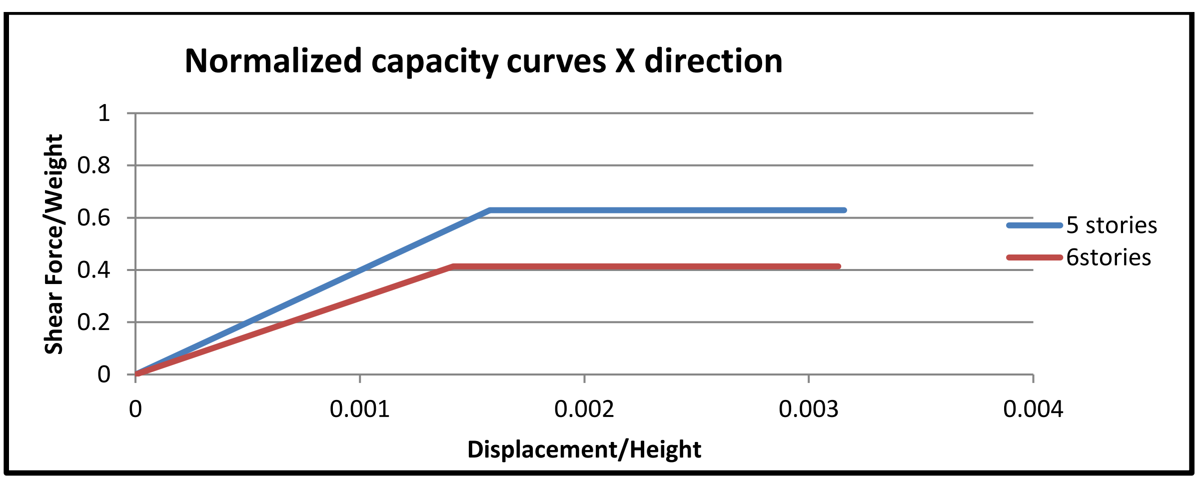

Figure 203:Normalized capacity curves in x-direction C2 buildings with different height

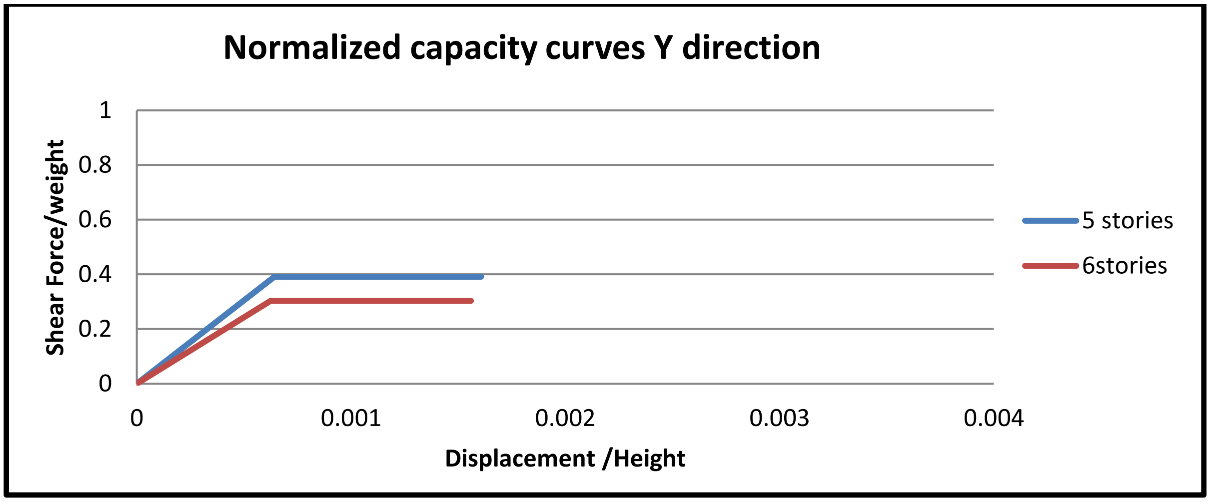

Figure 204: Normalized capacity curves in y-direction of C2 buildings with different height

If the failure mechanism of both buildings are similar and fail mostly from bending of the walls in the second and third floor. For this model is noted a high period of vibration of both modes. This comes from the template design with wide openings. This is done because this template as projected is done with slabs of reinforced concrete with pre-stressed reinforcement. The last floor of the building here suffers more from bending damage, not from shear damage as viewed in all other buildings with added floors.

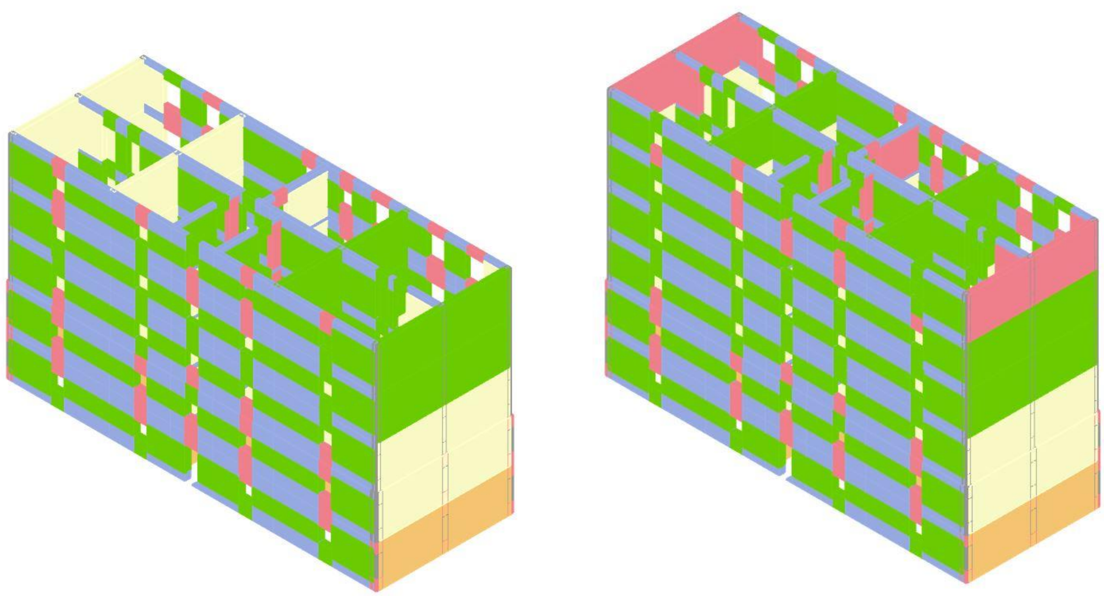

Figure 205: Failure scheme of both direction for building C2 with one added floor

5.4.4 Comparison of buildings with and without intervention

This type of interventions are made mostly in some buildings that are near main roads.

5.4.4.1 Buildings of template B3 with and without intervention

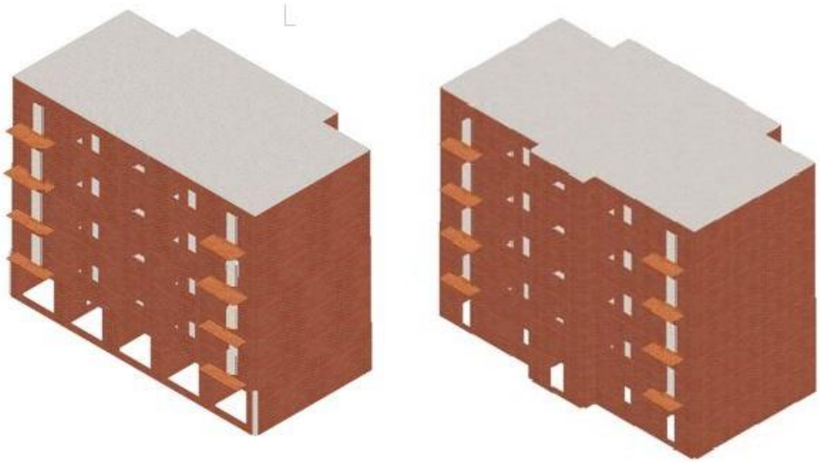

Figure 206: Buildings of template B3 with and without intervention

Table 74: Parameters of B3 template building with different height

	Initial stiffness	Max Force/Weight	Yield Disp /Height	Max Disp /Height	Ductility index
B3x	2041	0.4325	0.000764	0.002178	2.85
B3x +int	2385	0.4105	0.000693	0.001486	2.14
B3y	1112	0.4467	0.001193	0.0033	2.76
B3y +int	1188	0.4561	0.001029	0.002321	2.25

While comparing the pushover curves of both buildings, in the x direction is viewed a decrease in stiffness and max force, but a slightly increase in displacement and ductility. It must be sad that this value are very near and the change ratio is at levels of 8.35% for stiffness, 5.1% for max force, and 6% in ductility. These comes mostly because the demolished wall was in this direction, so the load bearing capacity has decreased. Meanwhile in y direction happens the opposite. Since the walls in this direction are the same, but also columns had been added in first floor, the stiffness and maximum force, slightly increases, while ductility levels remains almost the same, with some little decrease. The values of initial stiffness change at a ratio of 6.6%, the values of max force change at a ratio of 2.1% and the value of ductility at a ratio of 5.9%

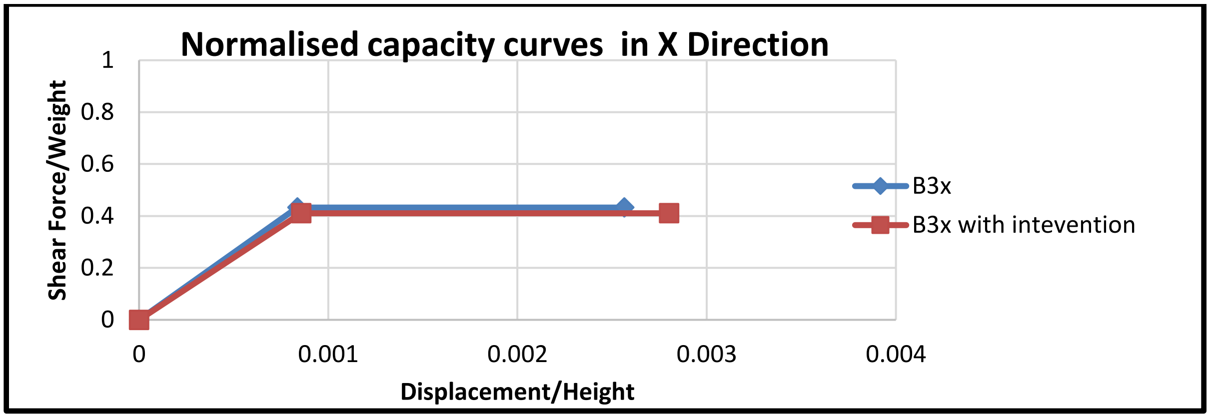

Figure 207:Normalised capacity curves in x-direction

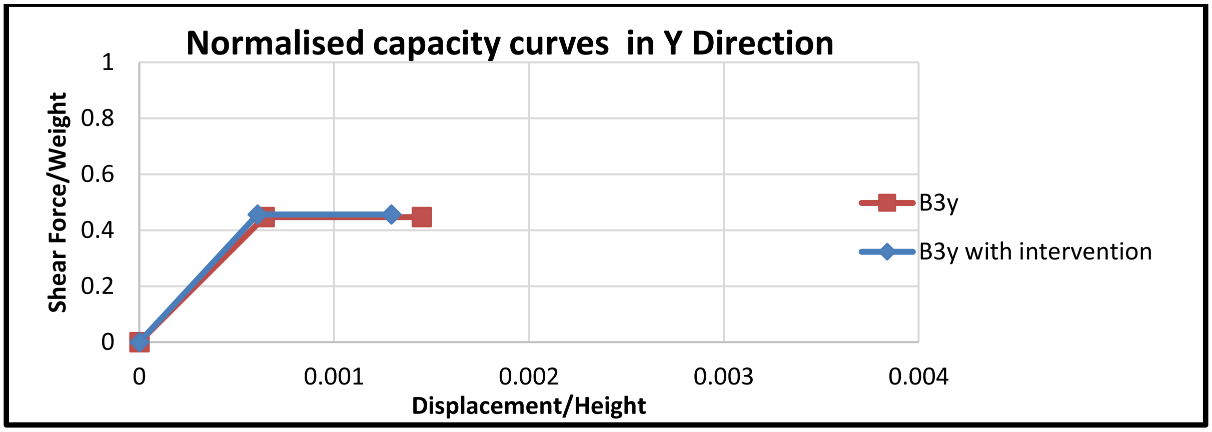

Figure 208: Normalised capacity curves in y-direction

If the fail mechanism are compared for both building are similar and in y-direction the most damaged are the perimeter walls and in x the inside walls, both from bending and shear damage.

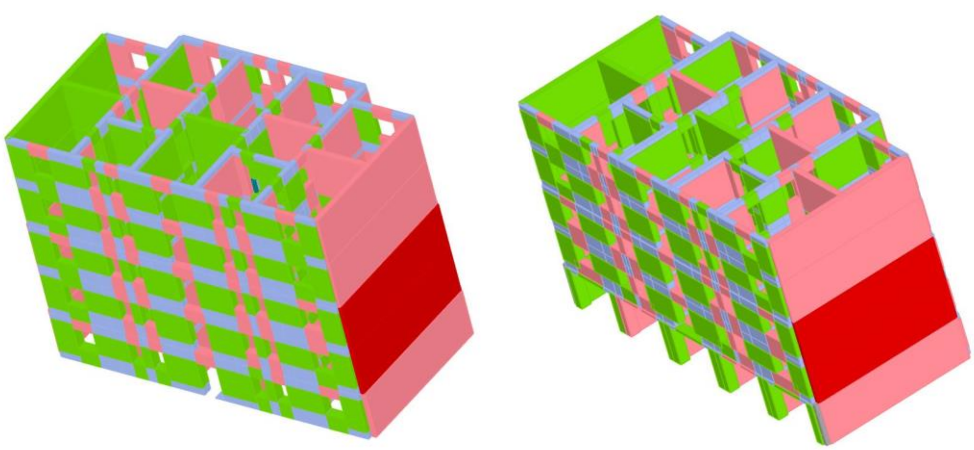

Figure 209: Failure mechanisms in y direction of B3 buildings

5.4.4.2 Buildings of template C1A with and without intervention

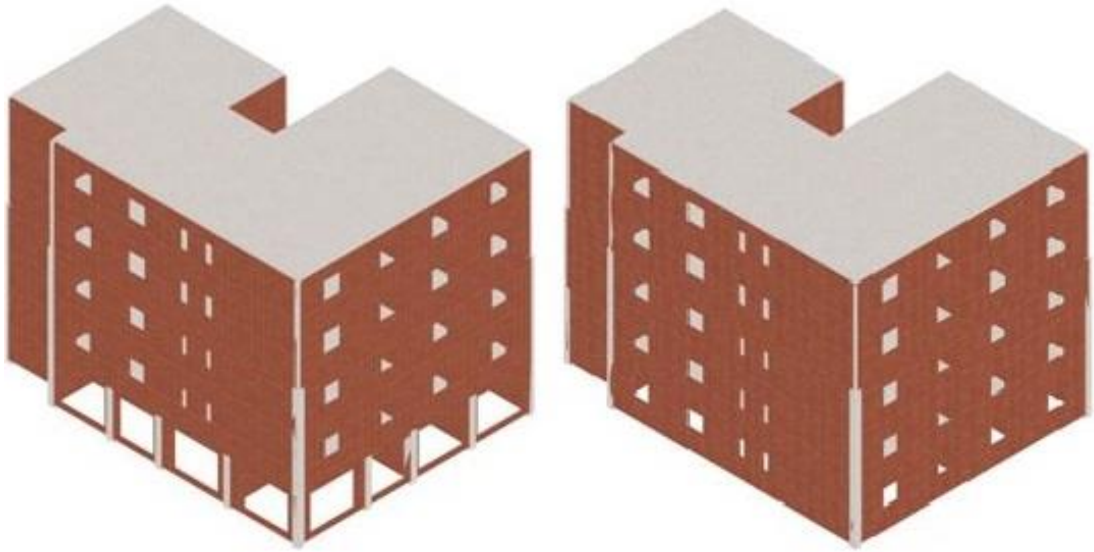

Figure 210: Buildings of template C1A with and without intervention

Table 75: Parameters of C1A buildings with and without intervention

	Initial stiffness	Max Force/Weight	Yield Disp /Height	Max Disp /Height	Ductility index
C1Ax	2031	0.3965	0.000835	0.002564	2.85
C1Ax +int	2385	0.4244	0.000857	0.002800	2.14
C1Ay	1857	0.3371	0.000642	0.001450	2.77
C1Ay +int	1711	0.3141	0.000607	0.001293	2.25

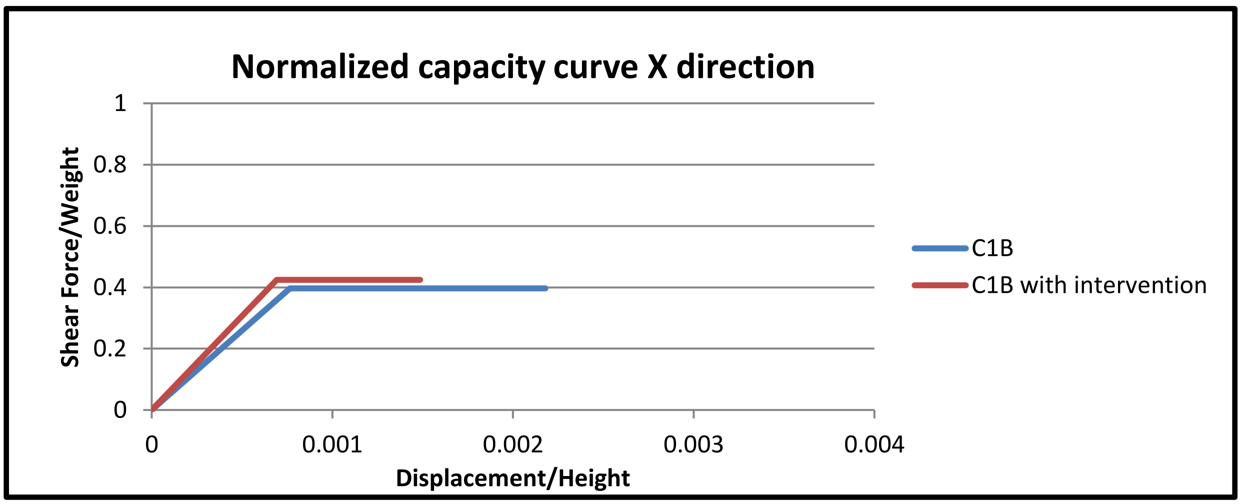

Figure 211:Normalized capacity curves in x-direction of C1A buildings

While comparing the pushover curves of both buildings, in the x direction is viewed a increase in stiffness and max force, but a slightly decrease in displacement and ductility. The change ratio is at level of 14.3% for stiffness, 5.5% for max force, and 24.7% in ductility. While in y direction the values of initial stiffness change at a ratio of 6.4%, the values of max force change at a ratio of 7.9% and the value of ductility at a ratio of 18.4%. In this pushover scenario all the parameters are decreased.

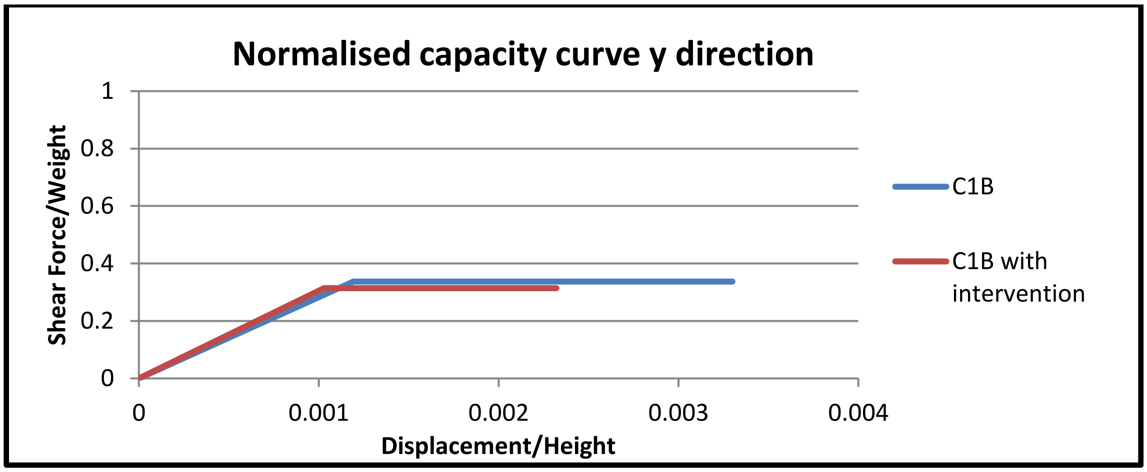

Figure 212:Normalized capacity curves in y-direction of C1A buildings

If the fail mechanism are compared for both building are similar but in y-direction one opening creates a weak point for the structure as shown in the figure above.

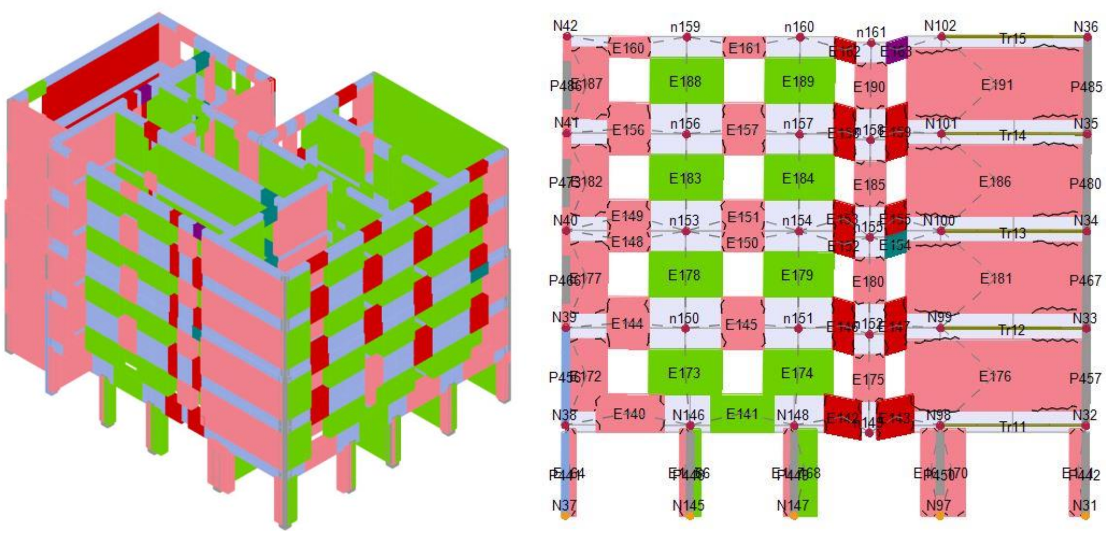

Figure 213: Failure mechanisms in y direction of building C1A with intervention

5.4.5 Comparison of buildings with different projection condition

Below are shown the differences in the capacity curves and fail mechanism of A2 template with and without seismic divide and B2 building with normal wall thickness and with 38cm wall on full height.

5.5.5.1 Buildings A2 comparison

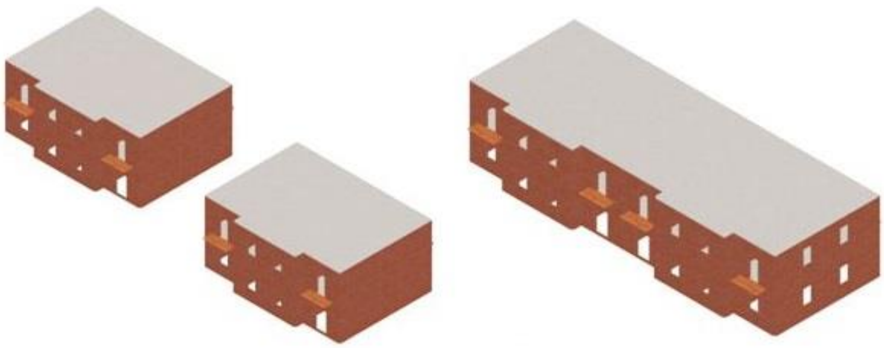

Figure 214: Buildings of template A2

Table 76: Parameters of A2 template buildings

	Initial stiffness	Max Force/Weight	Yield Disp /Height	Max Disp /Height	Ductility index
A2x	3012	0.565	0.000617	0.0022	3.57
A2x half	2417*2	0.595	0.000567	0.00208	3.67
A2y	5883	0.6604	0.000517	0.001483	2.87
A2y half	3753*2	0.7067	0.000433	0.001417	3.27

While comparing the pushover curves of both buildings, on both directions all the parameters increase when the template is divided in the middle.

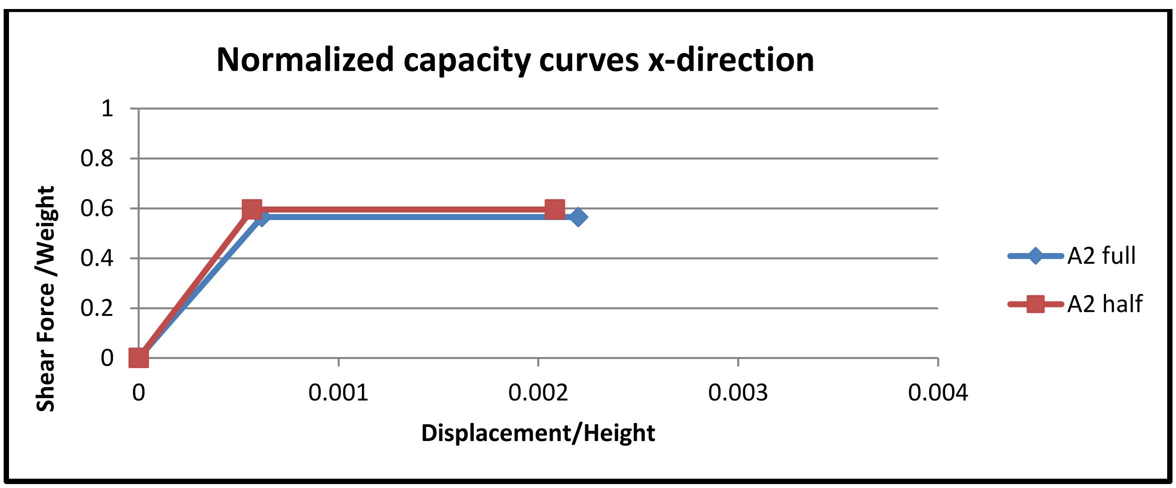

Figure 215:Normalized capacity curves in x-direction of A2 buildings

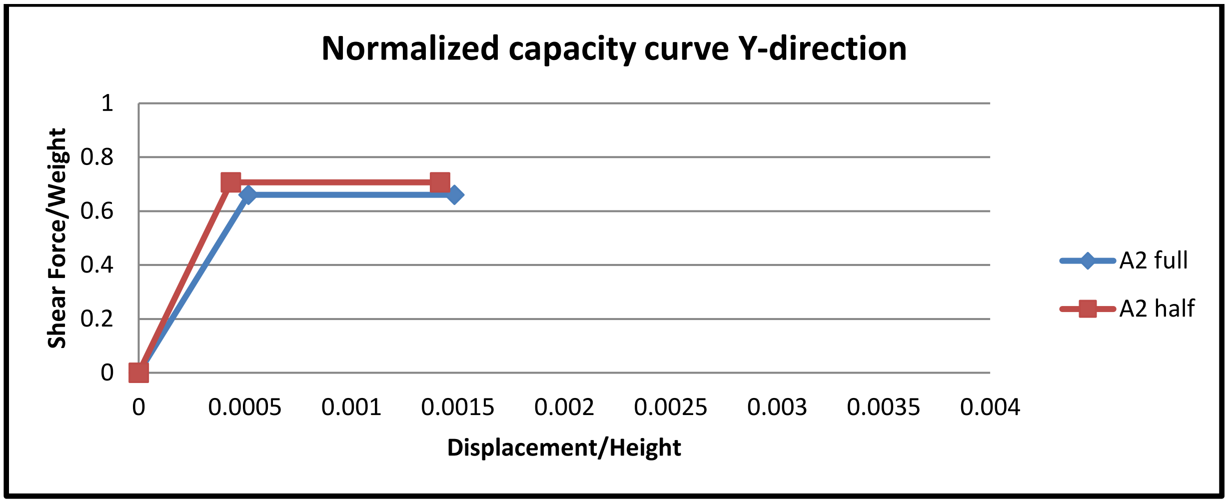

Figure 216:Normalised capacity curves in y-direction of A2 buildings

The fail mechanism are similar in x direction, but in y direction when building is considered with no opening, the walls in y-direction are severely damaged.

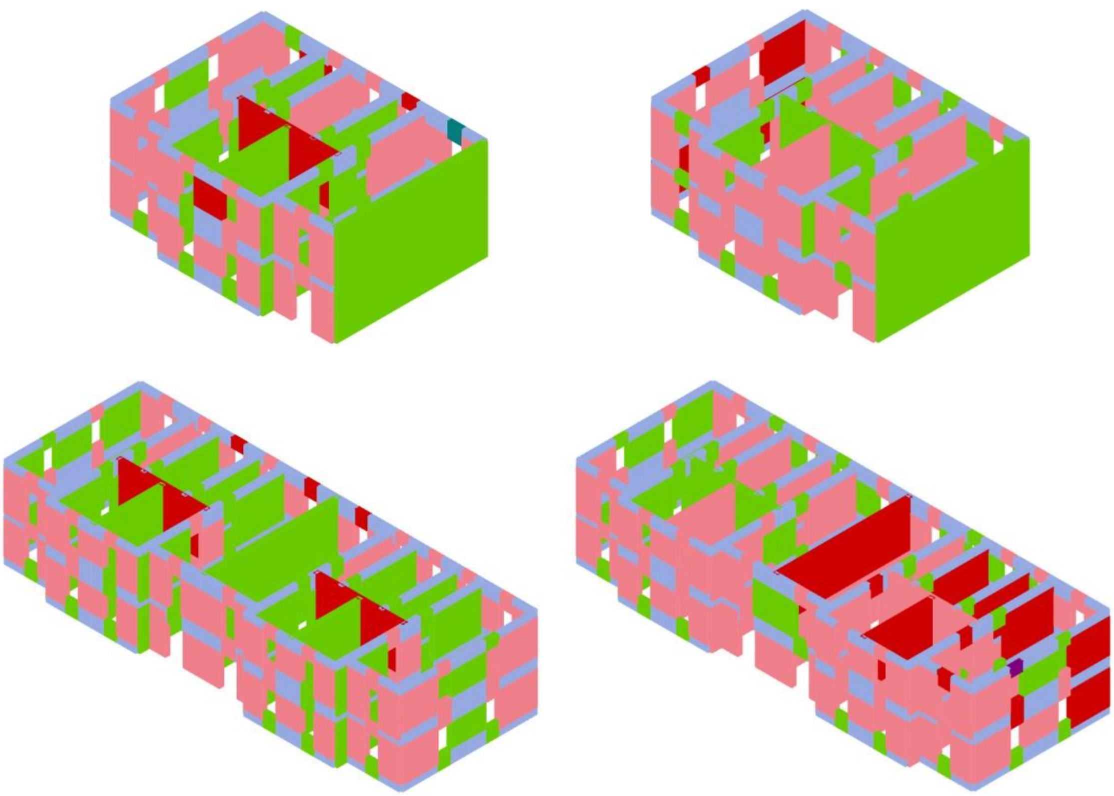

Figure 217: Failure mechanisms in y direction of building A2 with and without intervention

5.4.5.2 Buildings B2 comparison

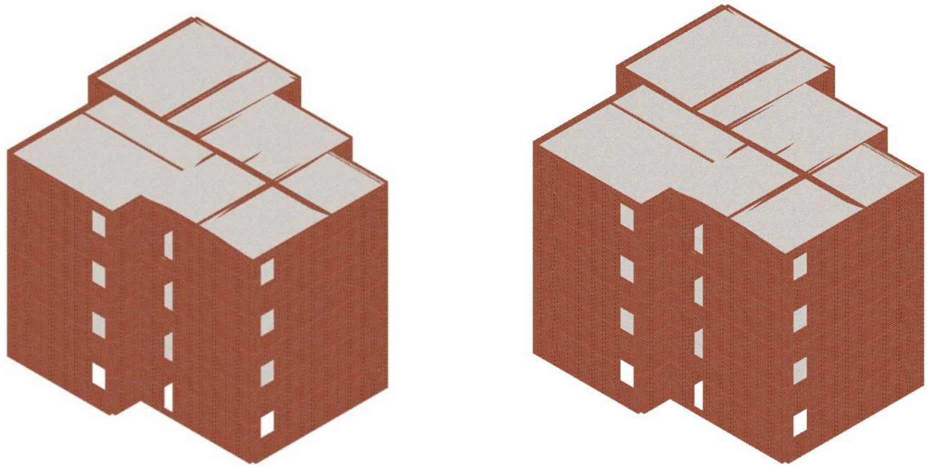

Figure 218: Buildings of template B2

Table 77: Parameters of B2 template buildings

	Initial stiffness	Max Force/Weight	Yield Disp /Height	Max Disp /Height	Ductility index
B2x	5714	0.663	0.000402	0.001187	2.95
B2x 38cm	6318	0.655	0.000454	0.001187	2.6
B2y	5883	0.489	0.000429	0.001705	3.97
B2y 38cm	3753*2	0.448	0.000455	0.001705	3.75

While comparing the pushover curves of both buildings, on both directions all the parameters decrease in the building with 38cm walls.

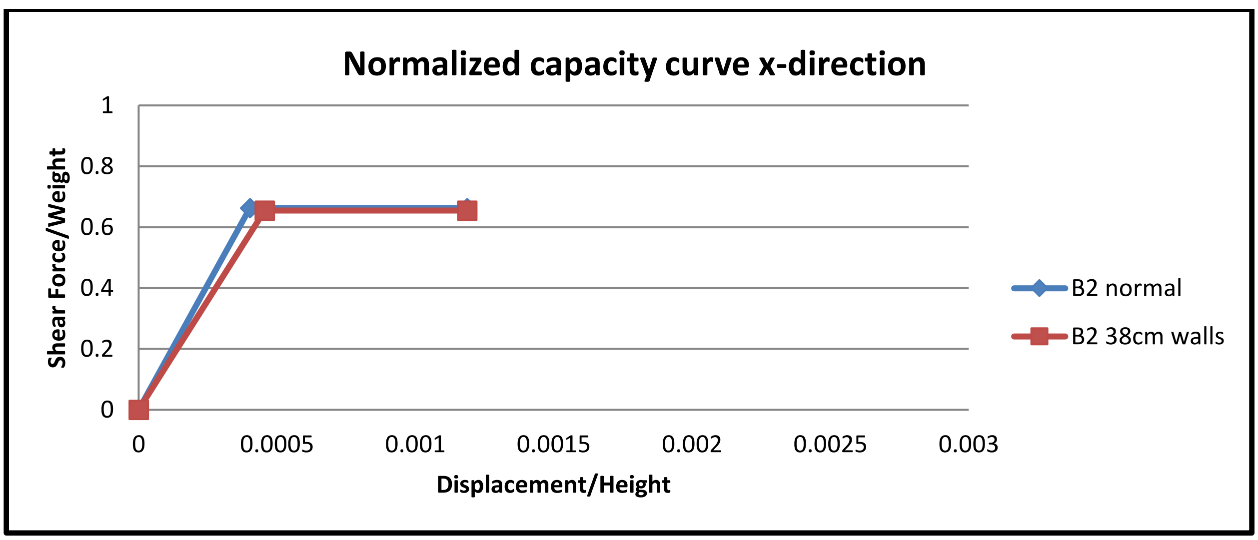

Figure 219:Normalized capacity curves in x-direction of B2 buildings

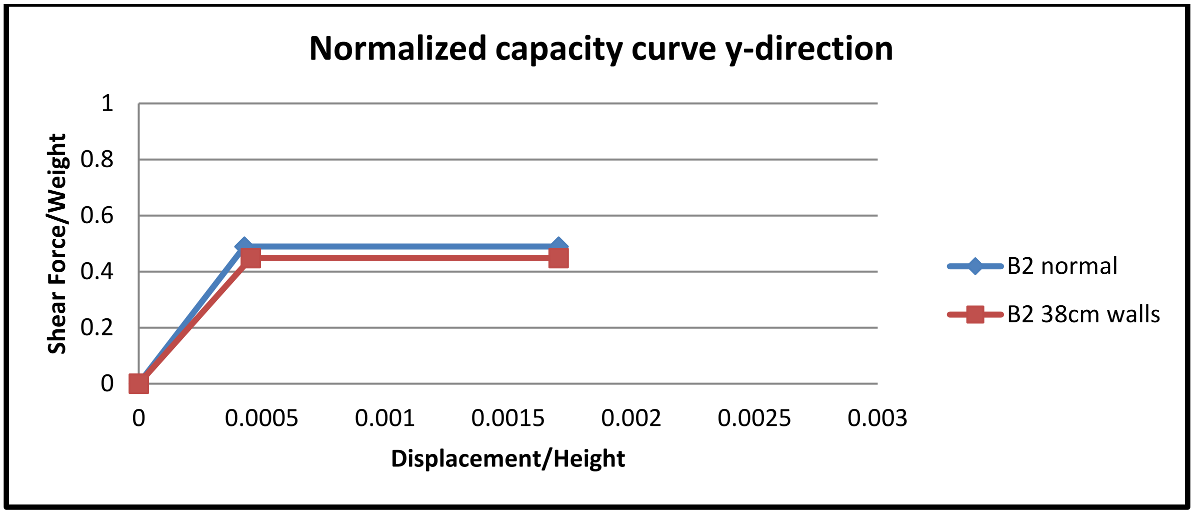

Figure 220:Normalized capacity curves in y-direction of B2 buildings

The fail mechanism are similar in both directions, but the model with 38cm walls has more bending damage on the perimeter walls, this because this walls masses are higher than the recommendations in the upper floors.

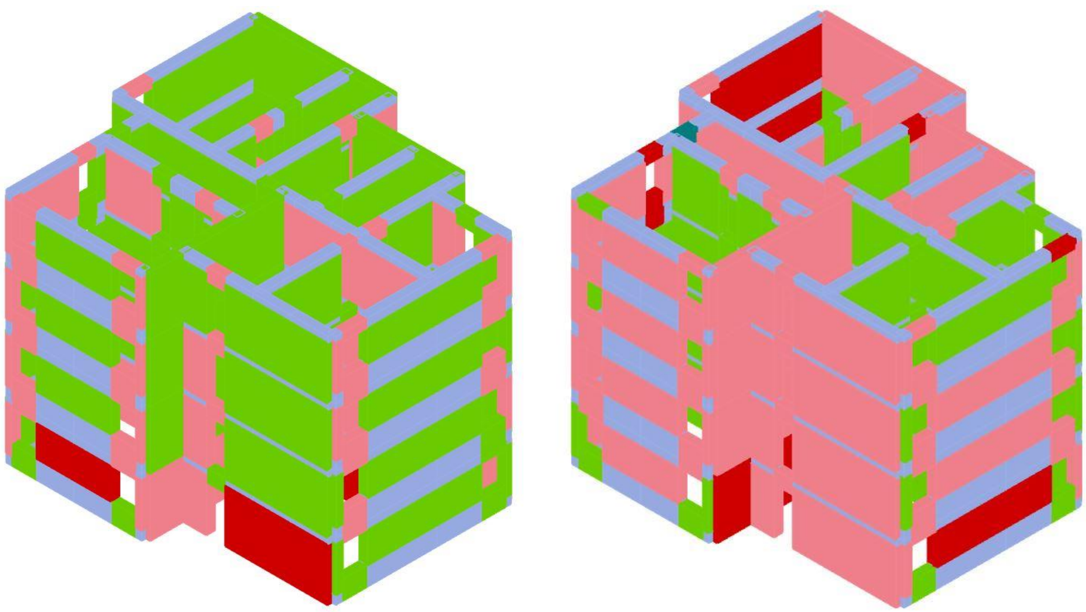

Figure 221: Failure mechanisms in both directions of building B2 with 38cm wall

5.5 Performance evaluation

Capacity evaluation of the investigated URM residential buildings is performed using EC-8 and N-2 guidancee.[Fajfar p. et al, 2005; EN1998, 2005] Three damage limit states levels, i.e., "Damage Limitation" (DL), the limit state "Significant Damage" (SD) and the limit state "Near Collapse" (NC) are considered as specified in this code and several other international guidelines such as FEMA-356 , ATC-40, and FEMA-440.[FEMA-356, 2000; FEMA-440, 2005; ATC-40, 1996] The performance of each building is evaluated by using the maximum pier shear and bending drift as given in chapter 3.4.6. So for DL state all the pier and sprandel are performing in elastic phase. On SD state pier shear failure is limited to δ_{SD} = 0.4% and for pier flexural failure to δ_{SD} = 0.8%. To obtain the NC drift capacity, the SD limits are multiplied by 4/3.

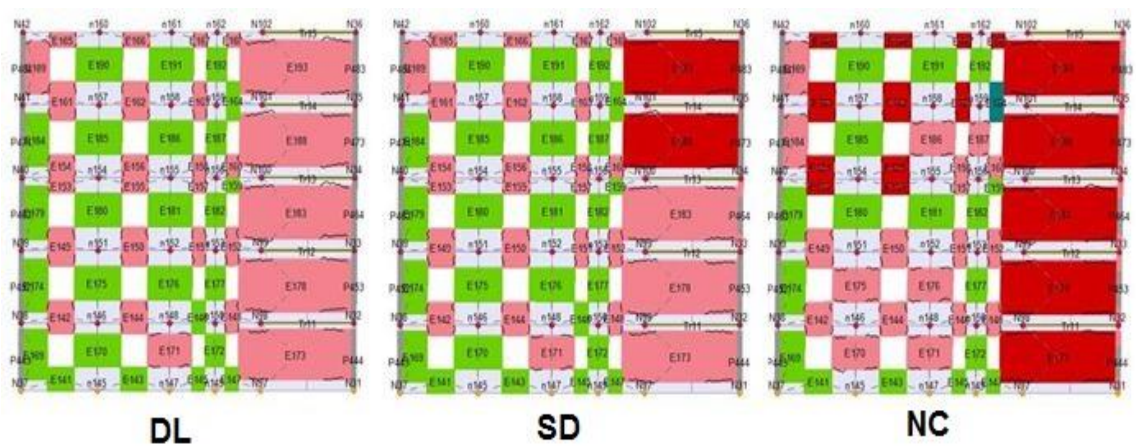

Figure 222: Wall model on each damage limit state

Pushover analysis data and criteria given above were used to determine global displacement drift ratio (defined as lateral displacement at roof level divided by building height) of each building corresponding to the performance levels considered. Table 77 lists global displacement drift ratios of each building.

Table 78: Global displacement drift capacities (%) of the investigated template buildings obtained from the pushover curves for the considered performance levels

Building	Direction	(Damage Limitation (DL)	Significant Damage (SD)	Near Collapse (NC)
		$\Delta_{roof}/H_{building}$		
A1	x	0.000283	0.001000	0.001333
	y	0.000267	0.000600	0.000800
A1 3fl	x	0.000378	0.001311	0.001744
	y	0.000356	0.000644	0.000867

A1 4fl	x	0.000517	0.001308	0.017417
	y	0.000317	0.000725	0.000975
A2	x	0.000500	0.001600	0.002133
	y	0.000383	0.000833	0.001100
A2 half	x	0.000583	0.001250	0.001667
	y	0.000333	0.000750	0.001000
B1	x	0.000357	0.001250	0.001667
	y	0.000226	0.000619	0.000833
B1 4fl	x	0.000393	0.001348	0.001795
	y	0.000259	0.000696	0.000929
B2	x	0.000250	0.000634	0.000848
	y	0.000304	0.001277	0.001705
B2 38cm	x	0.000259	0.000446	0.000589
	y	0.000304	0.001295	0.001723
B3	x	0.000579	0.001921	0.002564
	y	0.000443	0.001086	0.001450
B3 int	x	0.000614	0.002100	0.002800
	y	0.000407	0.000971	0.001293
B4	x	0.000679	0.001029	0.001371
	y	0.000643	0.001686	0.002250
C1A	x	0.000586	0.001614	0.002150
	y	0.000679	0.001750	0.002336
C1A int	x	0.000500	0.001114	0.001486
	y	0.000757	0.001743	0.002321
C1B	x	0.000557	0.001357	0.001807
	y	0.000743	0.002271	0.003029
C1B 6fl	x	0.000613	0.001458	0.001940
	y	0.000869	0.002762	0.003679
C2	x	0.000571	0.001607	0.002143
	y	0.000443	0.000943	0.001257
C2 6fl	x	0.001054	0.002345	0.003131
	y	0.000452	0.002262	0.003095
C3	x	0.000700	0.001929	0.002571
	y	0.000421	0.000964	0.001286

CHAPTER 6

PERFORMANCE EVALUATION

6.1 Spectrum based assessment

The spectrum approach for seismic design is a very useful and easy solution comparing to more complicated analysis as time history analysis or fragility analysis. It gives a limited solution, but its data is acceptable for most of the cases. Seismic loads in this approach are represented by the response spectrum function, which are derived from the time history records of earthquakes in a specific area. The Albanian code KTP-89 is still used as the legal code in Albania, but as reviewed earlier its values are lower compared to more updated EC8 [KTP-N2-89, 1989; EN1998, 2005]. The Albanian code is important considering, because the building analysed are all calculated with that code. Since the spectrum will be used for pushover analysis it will be adapted for this analysis. In calculation is used a elasto-plastic spectrum, which consists of elastic spectrum reduced with a ductility factor "q". Also the elastic response spectrum is reduced for an equivalent damping. If we compare elastic spectrum for the medium conditions of ground and seismicity:

Table 79: Medium conditions details from both codes.

	KTP-89	EC-8
Soil category	2	C
Seismic intensity	VIII	$0.2g = 1.96\,m/s^2$
Ductility	$\Psi = 1$	q =1

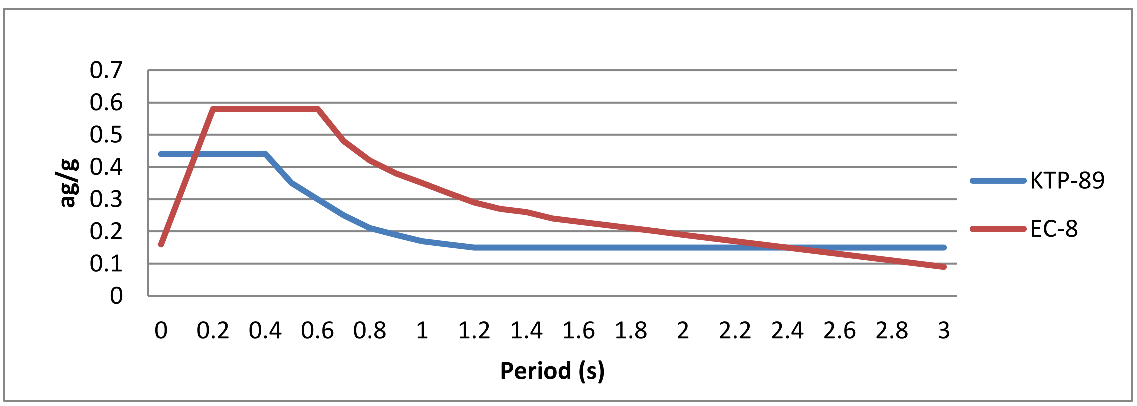

Figure 223: Elastic response spectrum for both buildings EC-8 (red) and KTP-89 (blue)

6.1.1 Demand spectrum and conversion in acceleration-displacement format

The calculation of the structures is based on N2 and EC-8 normative as given in section 2.1.3. [EN1998, 2005; NTC-40, 2008]. The building stock is calculated under type-1 maginitude spectra, since the expected magnitude is M > 5.5. Soil conditions are various among this buildings from B, C and D, but since the study is for the whole stock the ground type is choosen C. C typer refers to deep depostis of dense or medium dense sand, gravel or stiff clay with thickness from several tens of hundreds of meters. The spectrum parameters for this type are given in table 12, and are as below:

S=1.15 T_B=0.2s T_C=0.6s T_C=2.0s

According to EC-8 the behavior factor for URM varies from 1.5 to 2.5 but when the structure is in accordance with EN-1998-1. [EN-1998-1, 2004] But for masonry in accordance with EN1996 alone the recommended value is 1.5.[EN1996, 2005] Since Buildings of template A and B are prior KTP-78 this value is taken 1.5 for them, and for C buildings q is accepted 2, since the masonry has corner columns.

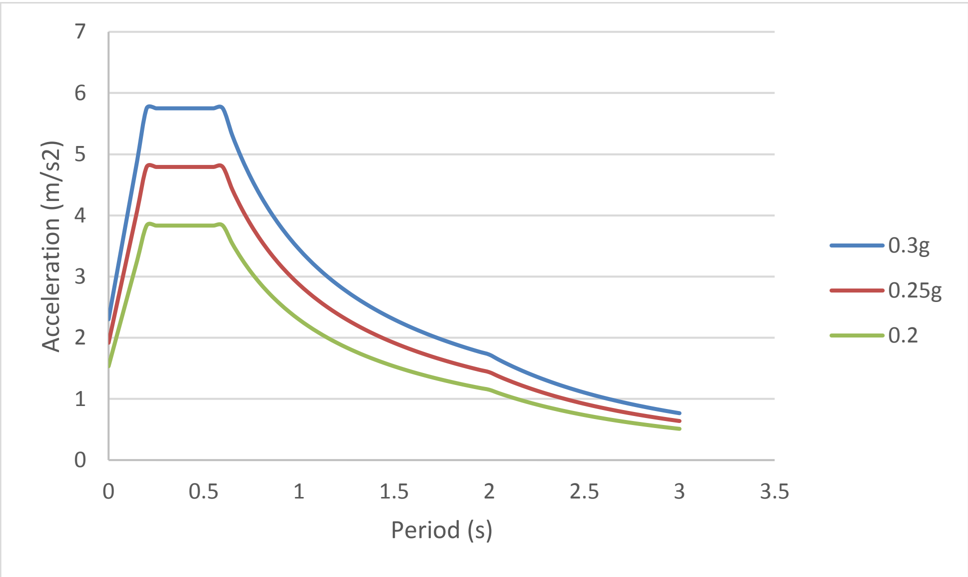

Figure 224: Inelastic spectrum Type-1 for ground C and different a_g levels

In N-2 method the elastic spectrum should be converted in acceleration-displacement format to compare with the building capacity in the same plot. [Fajfar p. et al, 2005; EN1998, 2005] This is done by following the procedure given in section 2.1.4 and following eqautions (22), (23), (24), (25), (26).

-Elastic spectrum in acc-disp format:

$S_{de} = \frac{T^2}{4\pi^2} S_{ae}$ (22)

-Determine inelastic spectra for constant ductilities

$S_a = \frac{S_{ae}}{R_\mu}$ (23), $S_d = \frac{\mu}{R_\mu} S_{de}$ (24)

$R_\mu = (\mu - 1)\frac{T}{T_C} + 1 \qquad T < T_C$ (25)

$R_\mu = \mu \qquad T \geq T_C$ (26)

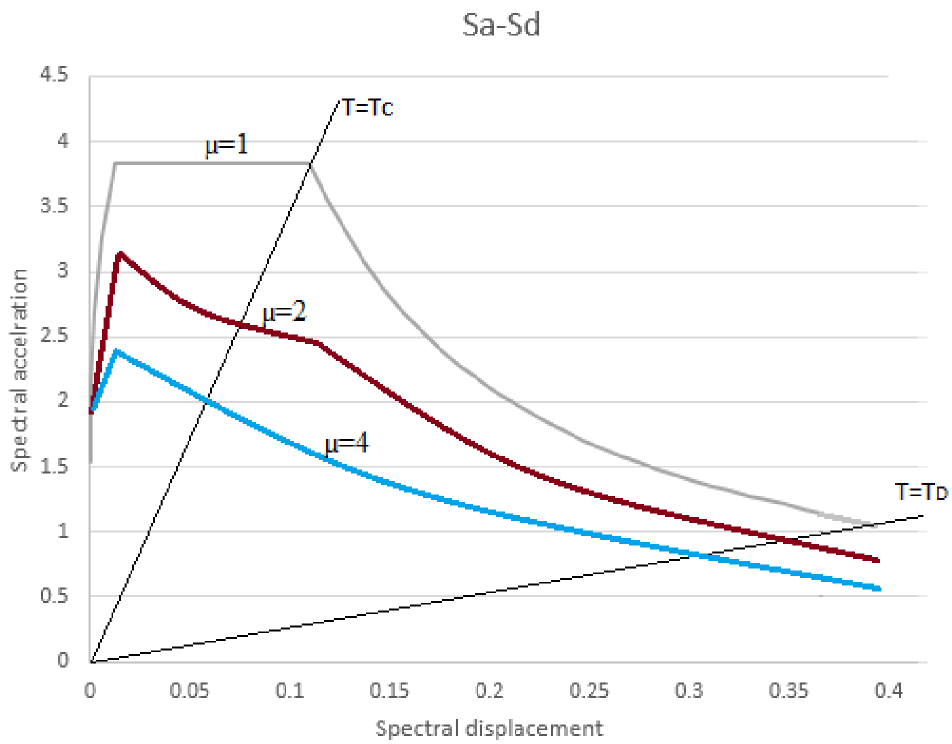

Figure 225: Elastic and inelastic spectrum in acceleration-displacement 0.2g

6.1.2 Conversion of building capacity in acceleration-displacement format

In chapter 5 the pushover analysis for all the buildings were presented in force-displacement (base shear force- top roof displacement) diagram. The capacity curves in both directions of the buildings were presented. In this section are shown the calcaluation made for B3 buildings to transform the capacity curve to acceleration-displacement format to proper compare with demand, as given in section 2.6.5. The N-2 method follows the steps as given below. [Fajfar p. et al, 2005; EN1998, 2005]

Determination of the mass m^* as given in equation (51)

$$m^* = \sum m_i \varphi_i = 478.3\ ton \quad (51)$$

-Then the MDOF quantities are transformed in SDOF quantities as given in equations (52), (53), (54):

$$d_* = \frac{\mathrm{d}}{\Gamma} \ (52) \quad F^* = \frac{V}{\Gamma} \ (53)$$

$$\Gamma = \frac{m^*}{\sum m_i {\varphi_i}^2} = 1.45 \quad (54)$$

-Determination of an approximate elasto-plastic force-displacement relationship

The capacity curve is bilinearized using equation (58) in section 2.6.5

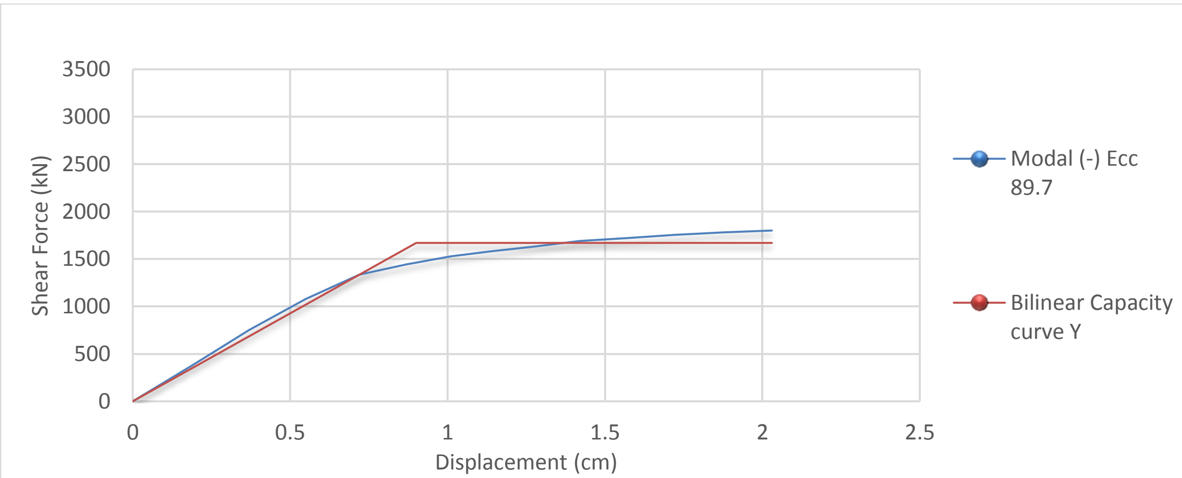

Figure 226: Capacity curve in y-direction of B3 building

-Determination of strength F_y^*, yield displacement D_y^* and period T^* as given in equations (52),(53) and (56)

$$d_y^* = \frac{d_y}{\Gamma} = \frac{0.01305m}{1.45} = 0.009m \qquad d_u^* = \frac{d_u}{\Gamma} = \frac{0.0509m}{1.45} = 0.0359m \qquad (52)$$

$$F^* = \frac{V}{\Gamma} = \frac{246.84kN}{1.45} = 170.23KN \qquad (53)$$

$$T^* = 2\pi\sqrt{\frac{\mathrm{m}^* D_y^*}{\mathrm{F}_y^*}} = 2 * 3.14 * \sqrt{\frac{478.3*0.009}{170.23}} = 0.319s \ (56)$$

$T^* = 0.319s$ $\qquad$ $\mathrm{F}_y^* = 1670kN$ $\qquad$ $D_y^* = 0.009m$

-Determination of capacity diagram acceleration versus displacement

$$S_{ay} = \frac{F^*}{m^*} = \frac{170.23}{478.3} = 0.356 \quad (76)$$

6.1.3 Seismic demand for SDOF model

-Determinitation of reduction factor R_μ

$$R_\mu = \frac{S_{ae}}{S_{ay}} = \frac{3.833}{0.356} = 10.7 \qquad (77)$$

-Determinations of displacement demands $S_d = D^*$

$$S_d = \frac{S_{de}}{R_\mu}\left(1 + (R_\mu - 1)\frac{T_C}{T^*}\right) \qquad T^* < T_C \qquad (78)$$

$$S_d = S_{de} \qquad T^* \geq T_C$$

Since for our building $T^* = 0.319s < 0.6s = T_C$

$$S_d = \frac{S_{de}}{R_\mu}\left(1 + (R_\mu - 1)\frac{T_C}{T^*}\right) = \frac{S_{de}}{10.7}\left(1 + (10.7 - 1)\frac{0.6}{0.312}\right) = 0.00989 * 1.83 = 0.0142$$

$where\ S_{de}$ is calculated from equation (22):

$$S_{de} = \frac{T^2}{4\pi^2} S_{ae} = 0.00914 \qquad (22) \qquad \text{for } T = T^* = 0.319s$$

For the MDOF model

$$D_t = \Gamma * S_d = 1.45 * 0.0142 = 0.0206 \qquad (79)$$

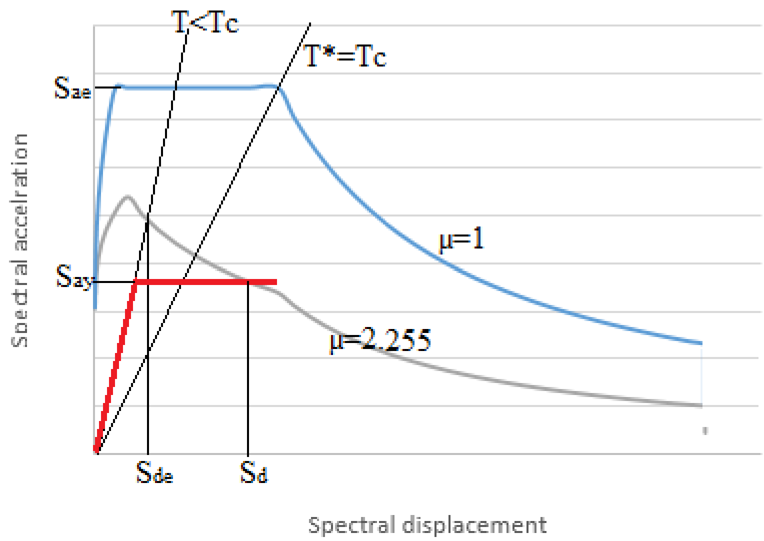

Figure 227: Determination of Dt for B3 building

If compared to the building capacity this levels refers to NC state of the building, so for the given ag level 0.2m/s^2. The procedure is automatically repeated by the software and for all the limit states are given the corresponding a_g values.

6.2 Results of spectrum based assessment

The drift ratio is the basic parameter for defining the performance points. For all buildings these limit state are calculated and by using the equivalent displacement method are compared with the EC spectra, giving a maximum a_g for each limit state. This process is generated automatically from 3muri software. Buildings are supposed to be in category C soil conditions with parameters:

S=1.15 T_B=0.2s T_C=0.6s T_C=2.0s

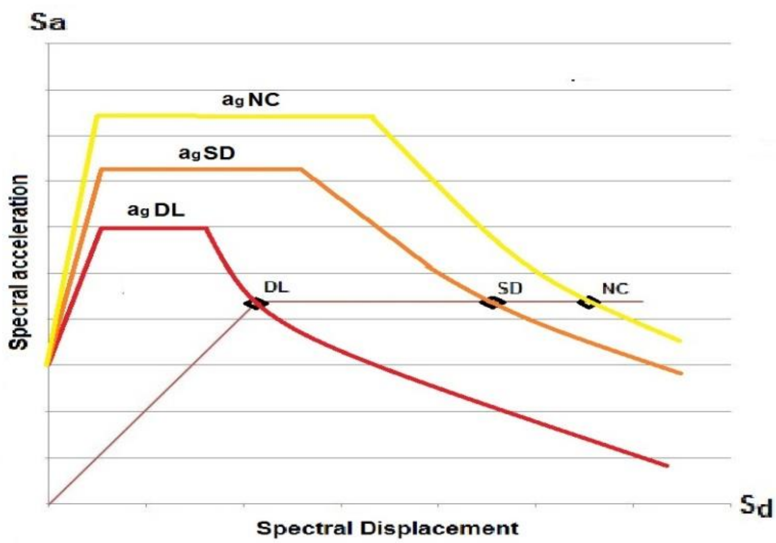

Figure 228: Simplified plot of the spectrum based assessment in 3muri

Below are shown the results for all buildings.

Table 80: Spectrum based analysis results for all buildings.

Building	Direction	d DL (cm)	d SD (cm)	d NC (cm)	ag DL (m/s2)	ag SD (m/s2)	ag NC (m/s2)	Hbuild (m)
A1	x	0.17	0.6	0.8	1.974	2.783	3.018	6
	y	0.16	0.36	0.48	2.046	2.699	2.731	6
A1 3fl	x	0.34	1.18	1.57	1.464	2.586	3.175	9
	y	0.32	0.58	0.78	1.577	1.948	2.18	9
A1 4fl	x	0.62	1.57	20.9	1.268	2.031	2.556	12
	y	0.38	0.87	1.17	1.167	1.628	1.978	12
A2	x	0.3	0.96	1.28	1.152	1.999	2.857	6

	y	0.23	0.5	0.66	1.823	2.163	2.623	6
A2 half	x	0.35	0.75	1	1.307	1.744	2.798	6
	y	0.2	0.45	0.6	2.166	2.68	3.007	6
B1	x	0.3	1.05	1.4	1.692	2.431	2.738	8.4
	y	0.19	0.52	0.7	1.839	2.126	2.621	8.4
B1 4fl	x	0.44	1.51	2.01	1.395	2.524	3.14	11.2
	y	0.29	0.78	1.04	1.515	2.112	2.514	11.2
B2	x	0.28	0.71	0.95	1.929	2.511	2.935	11.2
	y	0.34	1.43	1.91	1.288	2.506	3.113	11.2
B2 38cm	x	0.29	0.5	0.66	1.727	1.915	2.199	11.2
	y	0.34	1.45	1.93	1.128	2.049	2.286	11.2
B3	x	0.81	2.69	3.59	1.098	2.239	2.901	14
	y	0.62	1.52	2.03	1.16	1.699	2.134	14
B3 int	x	0.86	2.94	3.92	1.039	2.25	2.933	14
	y	0.57	1.36	1.81	1.179	1.656	2.063	14
B4	x	0.95	1.44	1.92	1.317	1.419	1.793	14
	y	0.9	2.36	3.15	1.197	2.025	2.614	14
C1A	x	0.82	2.26	3.01	1.182	2.035	2.618	14
	y	0.95	2.45	3.27	1.204	2.019	2.614	14
C1A int	x	0.7	1.56	2.08	1.088	1.558	1.976	14
	y	1.06	2.44	3.25	1.034	1.611	2.082	14
C1B	x	0.78	1.9	2.53	1.167	1.801	2.299	14
	y	1.04	3.18	4.24	1.067	2.081	2.708	14
C1B 6fl	x	1.03	2.45	3.26	1.116	1.747	2.263	16.8
	y	1.46	4.64	6.18	1.271	2.623	3.431	16.8
C2	x	0.8	2.25	3	1.56	2.653	3.363	14
	y	0.62	1.32	1.76	1.663	2.184	2.671	14
C2 6fl	x	1.77	3.94	5.26	1.459	2.29	2.987	16.8
	y	0.76	3.8	5.2	1.116	1.539	1.986	16.8
C3	x	0.98	2.7	3.6	1.004	2.722	3.563	14
	y	0.59	1.35	1.8	1.539	2.062	2.53	14

6.2.1 Results by building era

6.2.1.1 Buildings of A templates (before 1963 era)

A template buildings consists of building pre 63 era which are very old, but also have low height, so the building have higher values of P.G.A than other buildings. building with added stories have collapse point near 2m/s2 are very in risk.

Table 81: Performance of buildings from A template in different ag levels

Building	0.1g	0.12g	0.14g	0.16g	0.18g	0.2g	0.22g	0.24g	0.26g	0.28g	0.3g	0.32g
A1	DL	DL	DL	DL	DL	DL	SD	SD	SD	NC	-	-
A1 3fl	DL	DL	DL	DL	SD	SD	NC	-	-	-	-	-
A1 4fl	DL	DL	SD	SD	NC	NC	-	-	-	-	-	-
A2	DL	DL	SD	SD	SD	SD	NC	NC	NC	-	-	-
A2 half	DL	DL	SD	SD	SD	SD	NC	NC	NC	NC	-	-

Table 82: Buildings from A templates in each limit state for different ag levels

Building	0.1g	0.12g	0.14g	0.16g	0.18g	0.2g	0.22g	0.24g	0.26g	0.28g	0.3g	0.32g
% DL	100%	100%	40%	40 %	20%	20%	-	-	-	-	-	-
% SD	-	-	60%	60%	60%	60%	20%	20%	20%	-	-	-
% NC	-	-	-	-	20%	20%	60%	40%	40%	40%	-	-
% COLAPSE	-	-	-	-	-	-	20%	40%	40%	60%	100%	100%

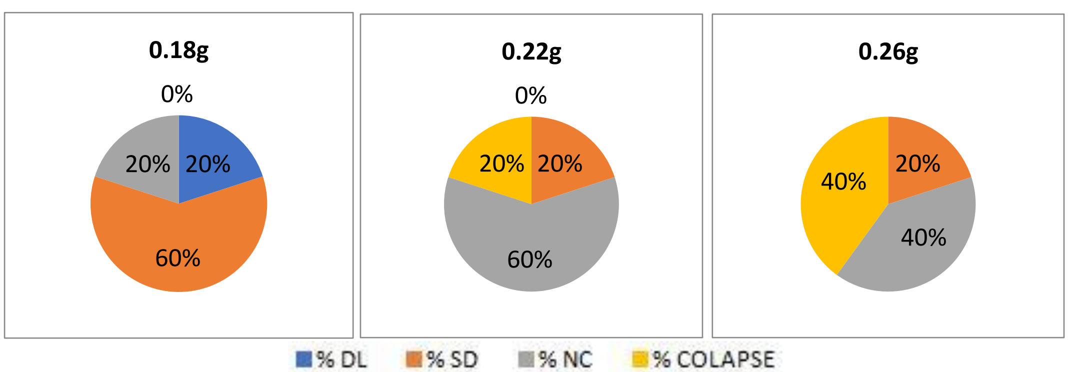

Figure 229: Percentage of buildings from A template in each limit state for ag levels

6.2.1.2 Buildings of B templates (1963-1978 era)

B template buildings consists of building of different height from 3 to 5 and of the era 63-78. In the higher buildings is viewed a higher risk and the a_g values are lower comparing to other buildings. In B1 template buildings if we compare the original template building with 3 stories and the one with 4 stories, the difference in a_g value is very small from 2.7 m/s^2 to 2.6m/s^2.

Meanwhile the B2 template building with wall thickness 38 cm in all floors comparing to the regular B2 has a high decrease in max a_g value from 2.8 m/s^2 to 2.2 m/s^2. In B3 template can be viewed that the intervention decreases the ag values but only from 2.1 m/s2 to 2 m/s^2. Meanwhile building from template B4 has a very low NC value of a_g=1.7m/s^2, concluding that these type are on a very high seismic hazard.

Table 83: Performance of buildings from B template in different ag levels

Building	0.1g	0.12g	0.14g	0.16g	0.18g	0.2g	0.22g	0.24g	0.26g	0.28g	0.3g	0.32g
B1	DL	DL	DL	DL	SD	SD	SD	SD	NC	-	-	-
B1 4fl	DL	DL	DL	SD	SD	SD	SD	NC	NC	-	-	-
B2	DL	DL	SD	SD	SD	SD	SD	SD	NC	NC	NC	-
B2 38cm	DL	DL	SD	SD	SD	SD	NC	-	-	-	-	-
B3	DL	DL	SD	SD	SD	SD	NC	-	-	-	-	-
B3 int	DL	DL	SD	SD	SD	NC	NC	-	-	-	-	-
B4	DL	DL	SD	NC	NC	-	-	-	-	-	-	-

Table 84: Percentage of buildings from B template in each limit state for ag levels

Building	0.1g	0.12g	0.14g	0.16g	0.18g	0.2g	0.22g	0.24g	0.26g	0.28g	0.3g	0.32g
% DL	100%	100%	29%	14%	-	-	-	-	-	-	-	-
% SD	-	-	71 %	71%	86%	43%	26%	29%	-	-	-	-
% NC	-	-	-	14%	14%	43%	53%	14%	43%	14%	14%	-
% COLAPSE	-	-	-	-	-	14 %	14%	57%	57%	86%	86%	100%

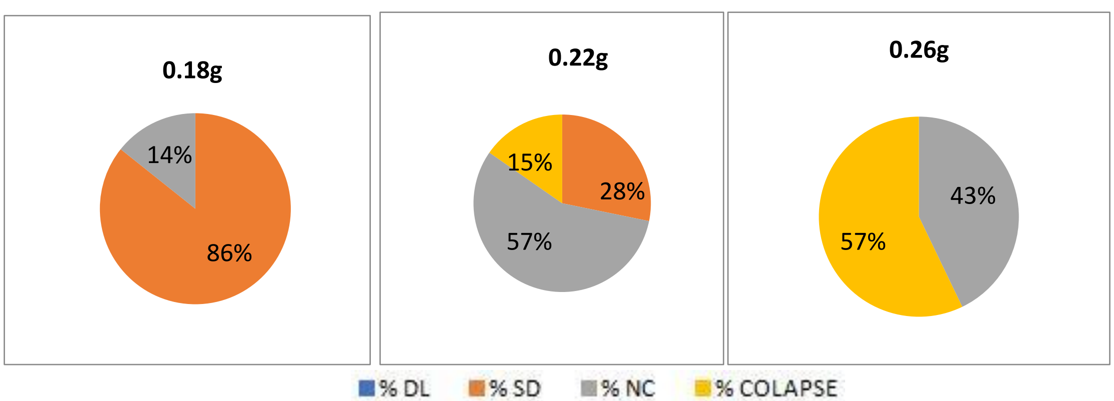

Figure 230: Percentage of buildings from B template in each limit state for a_g levels

6.2.1.3 Buildings of C templates (After 1978 era)

C template buildings consists of building of higher height of 5 and 6 floor and of 78 to 90 era. In C1 buildings we can see different variations, with clay builing having higher a_g =2.6m/s^2

but decreasing to a_g =2 m/s^2 with the interventions in the first floor. Meanwhile for the silicate buildings similar values are for NC a_g=2 m/s^2 on both 5 and 6 story building but this value is very low comparing to the seismic hazard on most of Albania. C2 and C3 buildings also have similar values of NC a_g =2.6 m/s^2 but C2 building with added floor has very lowered value of NC a_g =2 m/s^2. Comparing with all the others buildings, the buildings of these era have very low load bearing capacity.

Table 85: Performance of buildings from C template in different ag levels

Building	**0.1g**	**0.12g**	**0.14g**	**0.16g**	**0.18g**	**0.2g**	**0.22g**	**0.24g**	**0.26g**	**0.28g**	**0.3g**
C1A	DL	DL	SD	SD	SD	SD	NC	NC	NC	-	-
C1A int	DL	SD	SD	NC	NC	NC	-	-	-	-	-
C1B	DL	SD	SD	SD	SD	NC	NC	-	-	-	-
C1B 6fl	DL	SD	SD	SD	SD	NC	NC	-	-	-	-
C2	DL	DL	DL	SD	SD	SD	SD	NC	NC	-	-
C2 6fl	DL	SD	SD	NC	NC	NC	-	-	-	-	-
C3	DL	SD	SD	SD	SD	SD	NC	NC	NC	-	-

Table 86: Percentage of buildings from C template in each limit state for ag levels

Building	**0.1g**	**0.12g**	**0.14g**	**0.16g**	**0.18g**	**0.2g**	**0.22g**	**0.24g**	**0.26g**	**0.28g**	**0.3g**
% DL	100%	29%	14%	-	-	-	-	-	-	-	-
% SD		71 %	86%	71%	71%	43%	14%	-	-	-	-
% NC	-	-	-	29%	29%	57%	57%	43%	43%	-	-
% COLAPSE	-	-	-	-	-	-	29%	57%	57%	100%	100%

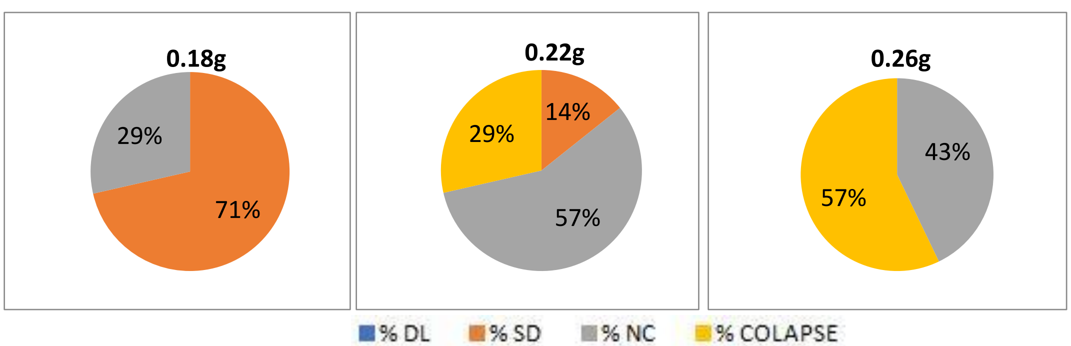

Figure 231: Percentage of buildings from C template in each limit state for ag levels

6.2.2 Results by building height

If we compare the results of spectrum analysis from height of the building, it can be easily concluded that especially 5 and 6 floor buildings have lower values of ag and in some templates especially the buildings with intervention or added stories have decreased value of ag. This puts these part of the stock on a higher seismic hazard comparing shorter buildings. Building C2 for example, in regular template has 5 stories with an NC a_g value near 2.6m/s^2, meanwhile the building with one added floor has no capacity to bear ag value higher then 2m/s^2.

Table 87: Percentage of buildings of different height in each limit state for ag levels

2 floors buildings	**0.14g**	**0.18g**	**0.22g**	**0.26g**	**0.3g**
% DL	33%	33%	-	-	-
% SD	66%	67%	33%	33%	-
% NC	-	-	67%	33%	-
% COLAPSE	-	-	-	33%	100%
3 floors buildings	**0.14g**	**0.18g**	**0.22g**	**0.26g**	**0.3g**
% DL	100%	-	-	-	-
% SD	-	100%	50%	-	-
% NC	-	-	50%	50%	-
% COLAPSE	-	-	-	50%	100%
4 floors buildings	**0.14g**	**0.18g**	**0.22g**	**0.26g**	**0.3g**
% DL	25%	-	-	-	-
% SD	75%	100%	50%	-	-
% NC	-	-	25%	50%	25%
% COLAPSE	-	-	25%	50%	75%
5 floors buildings	**0.14g**	**0.18g**	**0.22g**	**0.26g**	**0.3g**
% DL	13%	-	-	-	-
% SD	87%	75%	13%	-	-
% NC	-	25%	62%	38%	-
% COLAPSE	-	-	25%	62%	100%
6 floors buildings	**0.14g**	**0.18g**	**0.22g**	**0.26g**	**0.3g**
% DL	-	-	-	-	-
% SD	100%	50%	-	-	-
% NC	-	50%	50%	-	-
% COLAPSE	-	-	50%	100%	100%

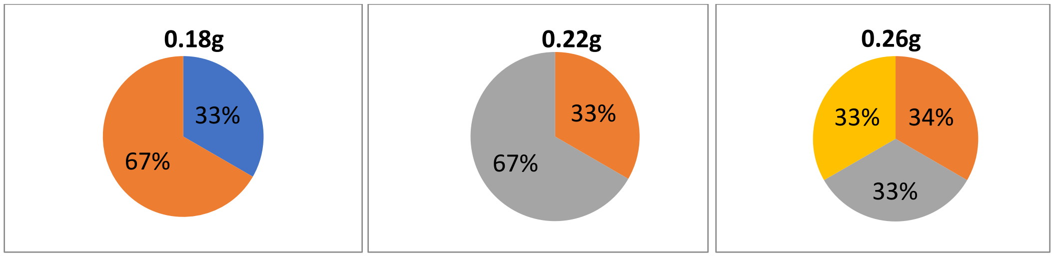

Figure 232: Percentage of buildings of 2 floors in each limit state for ag levels

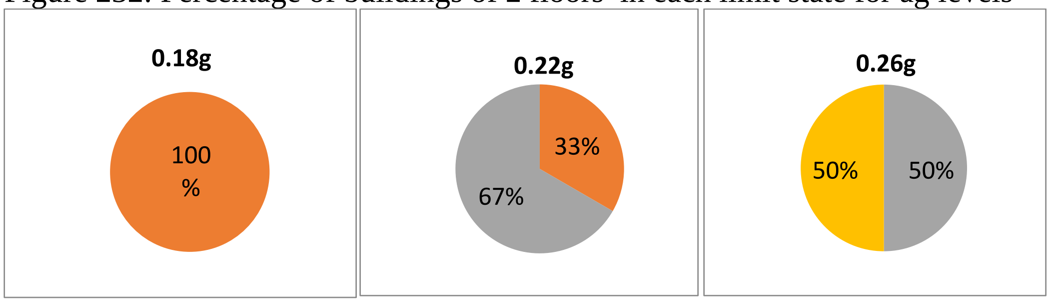

Figure 233: Percentage of buildings of 3 floors in each limit state for ag levels

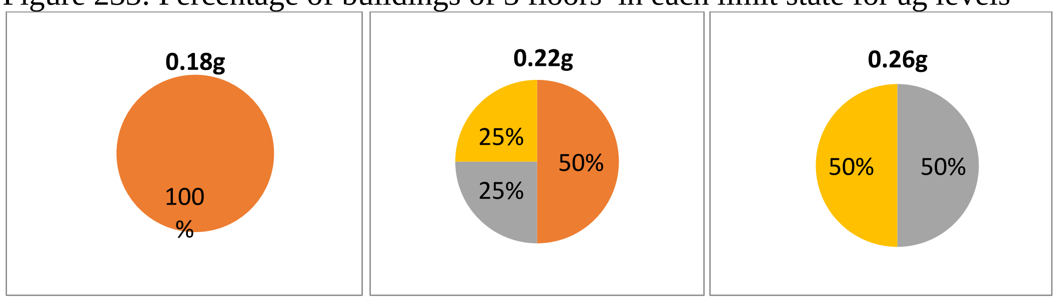

Figure 234: Percentage of buildings of 4 floors in each limit state for ag levels

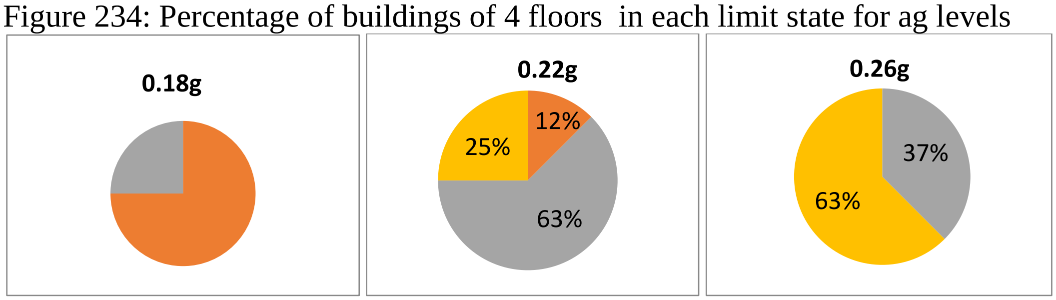

Figure 235: Percentage of buildings of 5 floors in each limit state for ag levels

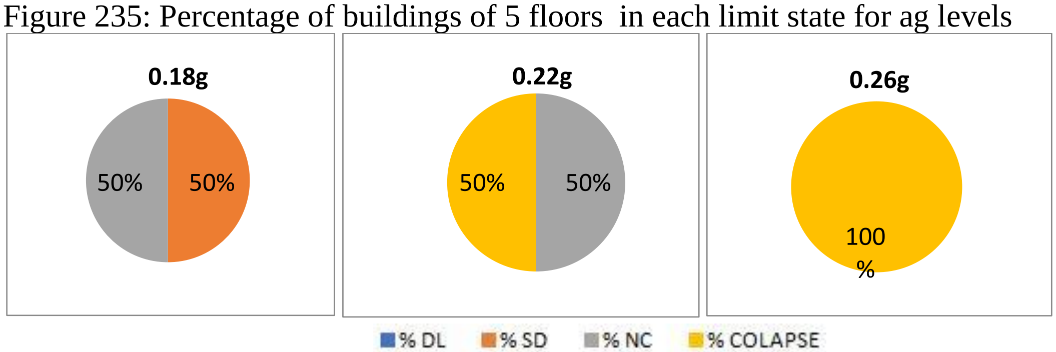

Figure 236: Percentage of buildings of 6 floors in each limit state for ag levels

6.2.3 Results by building materials used

If we compare the results of spectrum analysis from principal construction material can be viewed that clay building have more higher ag values. But the studied building of silicate masonry are mostly of 5 and 6 story, and because of this the maximum ag they can bear is lower. If we compare C1A and C1B buildings which have the same plan and height but are realized one with clay building and the other with silicate we can easily spot that the clay building has more capacity and performs better than the silicate building. The ag for the NC state for the clay building is near 0.26g meanwhile for the silicate building is near 0.22g. This mainly comes because the bonding between clay and mortar is stronger than between silicate and mortar, even though silicate bricks have higher compressive strength than clay bricks.

Table 88: Percentage of buildings in each limit state for different ag levels clay buildings

Building	0.1g	0.12g	0.14g	0.16g	0.18g	0.2g	0.22g	0.24g	0.26g	0.28g	0.3g	0.32g
% DL	100%	79%	36%	21%	7%	7 %	-	-	-	-	-	-
% SD	-	21%	64%	65%	71%	64%	29%	14%	7%	-	-	-
% NC	-	-	-	14%	22%	29%	50 %	36%	36%	7%	-	-
% COLAPSE	-	-	-	-	-	-	21%	50%	57%	93%	100%	100%

Table 89: Percentage of buildings in each limit state for different ag levels silicate buildings

Building	0.1g	0.12g	0.14g	0.16g	0.18g	0.2g	0.22g	0.24g	0.26g	0.28g	0.3g	0.32g
% DL	100%	60%	-	-	-	-	-	-	-	-	-	-
% SD	-	40%	100%	80%	80%	40%	20%	20%	-	-	-	-
% NC	-	-	-	20%	20 %	40%	60%	-	20%	20%	20%	-
% COLAPSE	-	-	-	-	-	20%	20%	80%	80%	80%	80%	100%

Table 90: Comparison of C1A and C1B buildings

Building	0.1g	0.12g	0.14g	0.16g	0.18g	0.2g	0.22g	0.24g	0.26g	0.28g	0.3g
C1A	DL	DL	SD	SD	SD	SD	NC	NC	NC	-	-
C1B	DL	SD	SD	SD	SD	NC	NC	-	-	-	-

Clay buildings vs silicate buildings

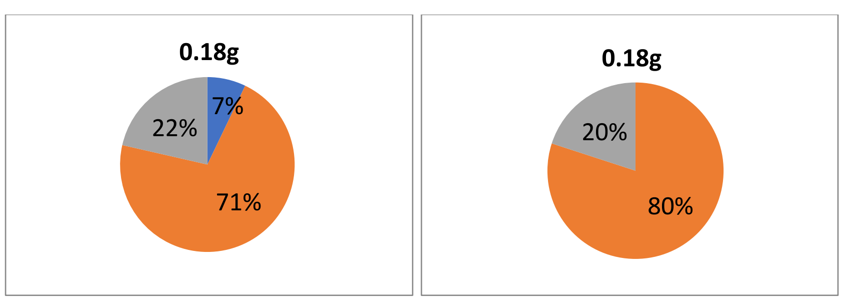

Figure 237: Percentage of buildings of different height in each limit state for ag levels

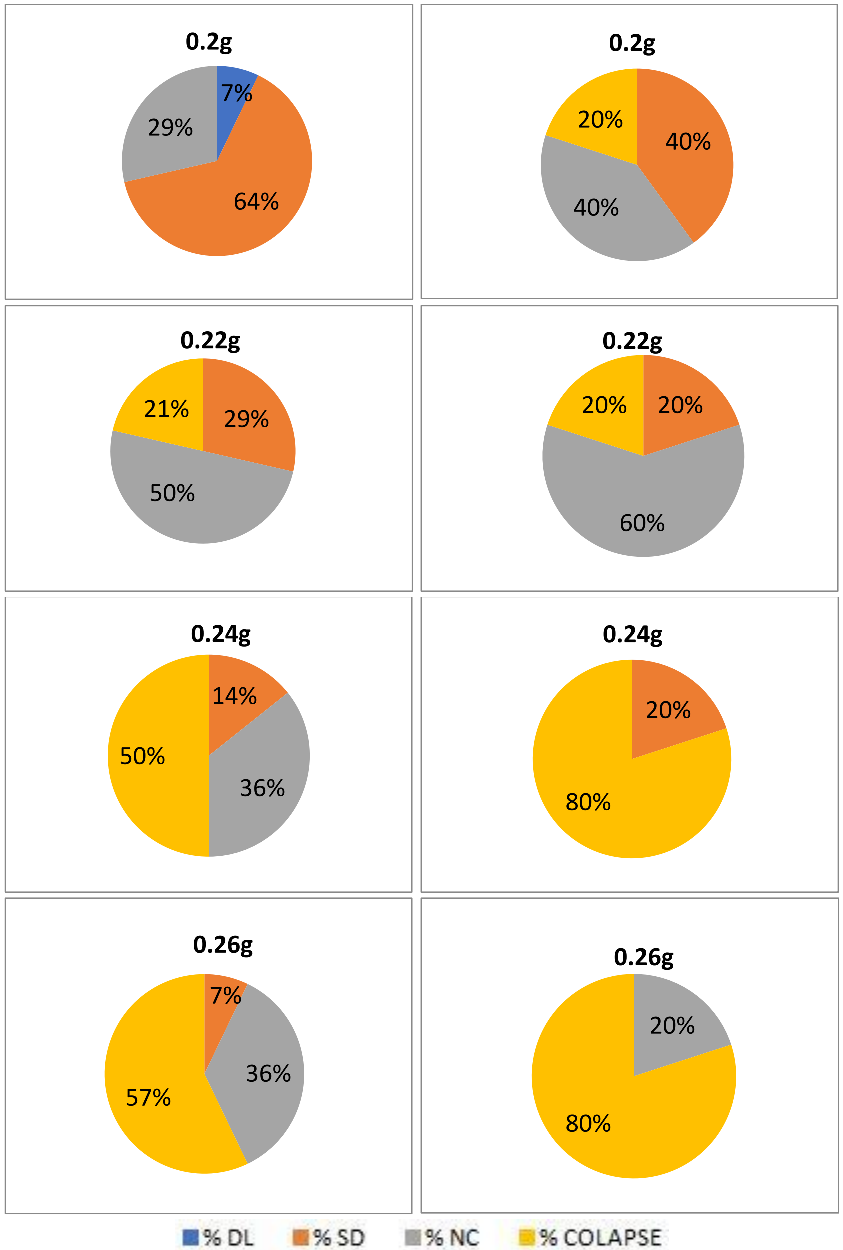

Figure 238: Percentage of buildings of different height in each limit state for ag levels

6.3 Time-history analysis

6.3.1 Equivalent Single degree of Freedom "ESDOF" Idealization of Building Response

The pushover curve of each building obtained from nonlinear static analysis was approximated with a bilinear curve using guidelines given in Eurocode 8. A typical example of pushover and idealized capacity curves is shown in Fig. 1. Yield and ultimate response points represent the idealized capacity curve. Yield strength coefficient, yield displacement and post-yield stiffness parameters describe “equivalent” SDOF models of buildings [58].

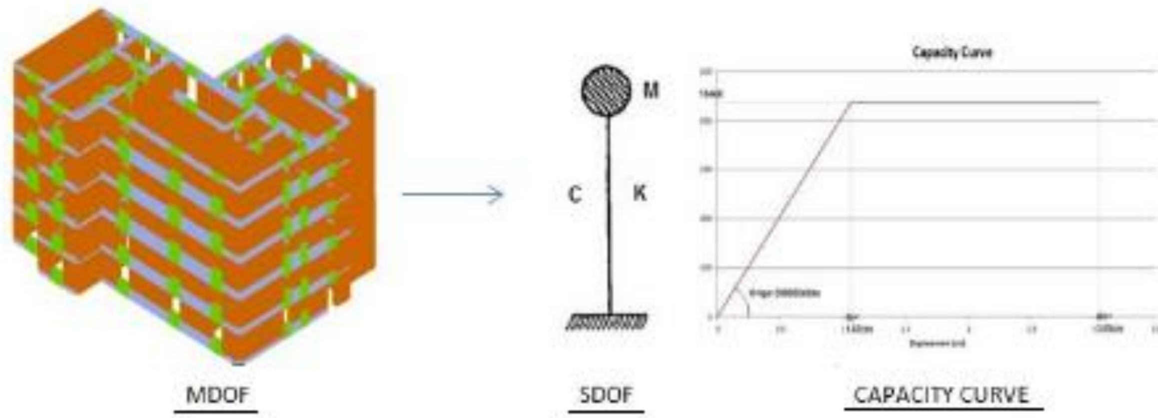

Figure 239: Idealization of MDOF to ESDOF for time history approach

FEMA-356 and ATC-40 [FEMA-356, 2000; ATC-40, 2005] provides guidance for “equivalent” SDOF representation of building capacity curve. While yield displacement representation of “equivalent” SDOF system is the same for both FEMA-356 and ATC-40 documents, yield strength coefficient representations differ. FEMA-440 [FEMA-356, 2000; FEMA-440, 2005; ATC-40, 2005] compared performance of both “equivalent” SDOF systems and recommends the use of ATC-40 representation. Thus, the capacity curve of each building generated for the first mode vector was converted to an “equivalent” SDOF system using ATC-40 representation in which yield displacement, Δy, and yield strength coefficients, Cy, are given by $\Delta_y = \frac{\Delta_{y,roof}}{\Gamma_1}$ (80) $C_y = \frac{S_a}{g} = \frac{V_{y,mdof}/W}{\alpha_1}$ (81) where:

$\Delta_{y\ roof}$: the roof displacement at yield,

PF1: the first (predominant) mode participation factor,

S_a: the pseudo-acceleration associated with yield of the “equivalent” SDOF system,

G: the acceleration of gravity,

V_y, MDOF: the base shear strength of the multi-degree-of-freedom (MDOF) system or building at global yield,

W: seismic weight of the MDOF system, and

α_1: the modal mass coefficient of the first mode.

Compared to N-2 method the approach on this code is similar with similar coefficients, where ɼ is equivalent of PF1. Dynamic analysis gives more similar results from both codes comparing to spectrum analysis, which is more code-dependent.

6.3.2 Nonlinear Dynamic Response History Analysis

The "equivalent" SDOF models of each investigated URM building were subjected to ground motion listed in Table 2-3 without any scaling to determine displacement demands. A total of 5548 "equivalent" SDOF nonlinear response history analyses were carried out using both "Utility Software for Earthquake Engineering program (USEE)" and "Computer Program for Nonlinear Dynamic Time History Analysis of Single- and Multi-Degree-of-Freedom Systems, (Nonlin 8.0)" [Inel M. et.al., 2001; Charney F. et.al., 2010]. As input on Nonlin 8.0 are given the weight of structure, yield stress SDOF and elastic stiffness.

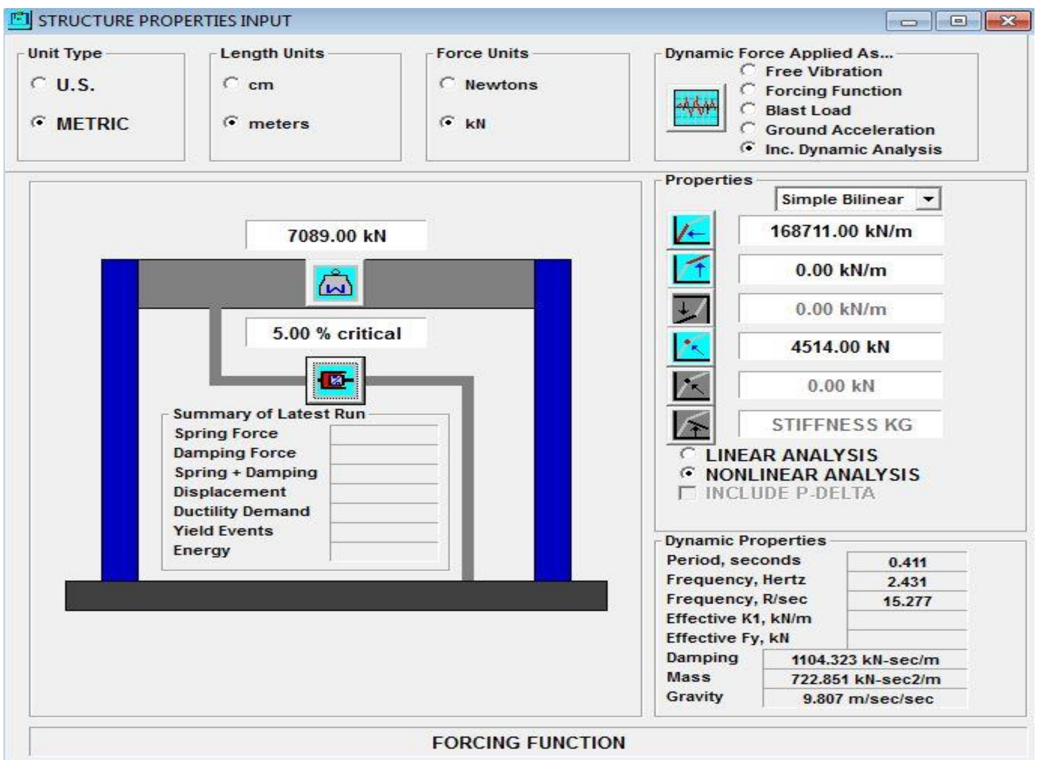

Figure 240: Parameter input for time history analysis of building

Nonlin 8.0 has also the full database of all the near-field and far-field and all the buildings are analyzed. Also all the parameters of the earthquakes can be checked as in the figure below:

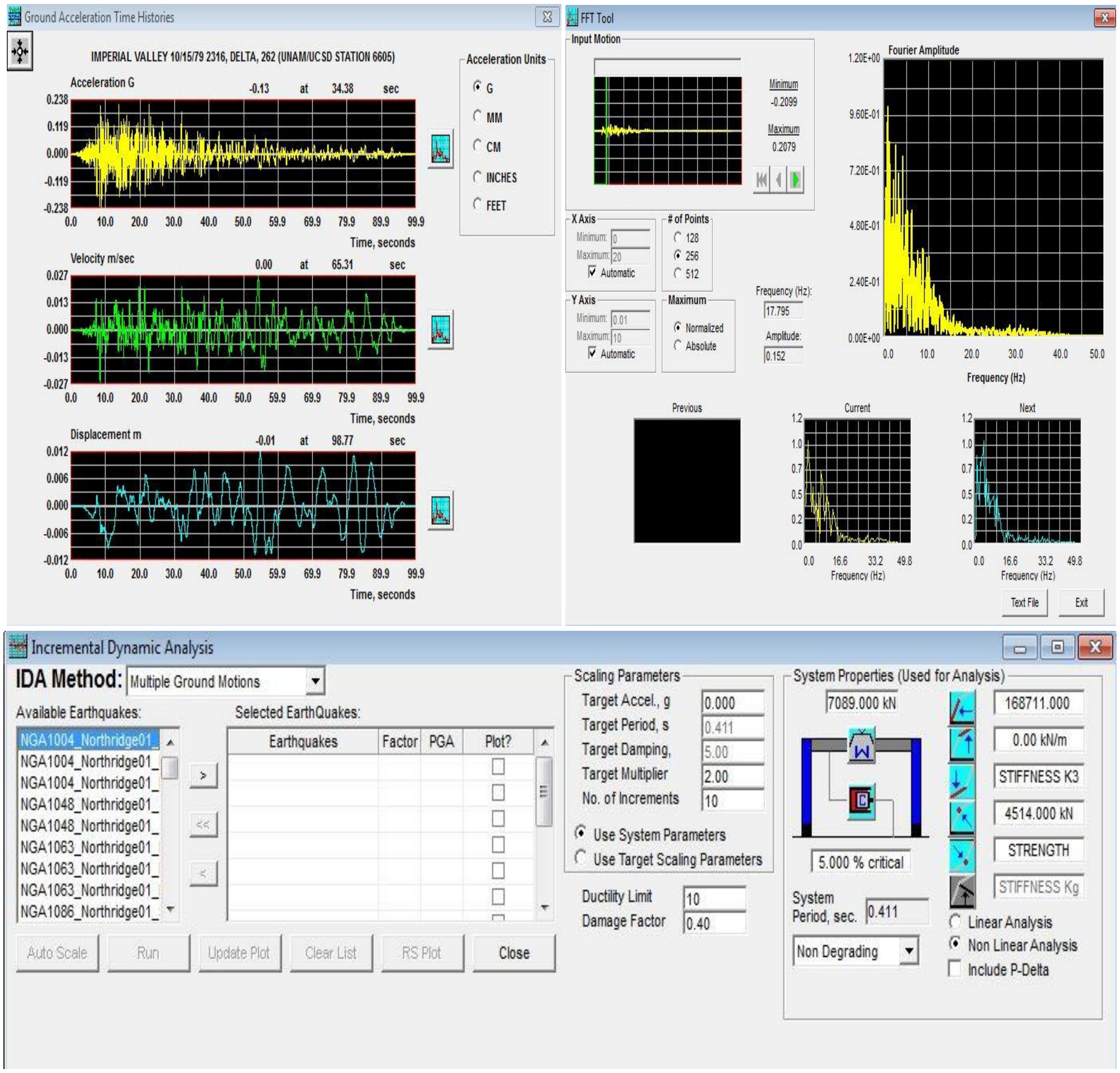

Figure 241: Seismic demand input for time history analysis Nonlin 8.0

The basic output are the time history plot of roof displacement vs time. This values are given for each earthquake for the SDOF system. The “equivalent” SDOF displacement demands were then converted into building displacement demands at the roof level multiplying by the first mode participation factor. Also for each analysis also are given the computed hysteresis plots of relative inertia, damping force, spring force to displacement and the energy plots under each seismic event. In the table below are shown the calculation of demand from time-history analysis, from demand of ESDOF in cm, converted demand*ϒ for MDOF and drift ratio of MDOF.

Table 91: Demand of A buildings and calculation of drift ratio

		Demand in cm		**A1 x**	**A1 y**	**A1 (3fl) x**	**A1 (3fl) y**	**A1 (4fl) x**	**A1 (4fl) y**	**A2 x**	**A2 y**	**A2 (half) x**	**A2 (half) y**
No	Year	Earthquake	Record and component	Dmd	Dmd	Dmd	Dmd	Dmd	Dmd	Dmd	Dmd	Dmd	Dmd
1	1971	San Fernando 2/9/1971	LA HOLLYWOOD STOR LOT, 090 (USGS STATION 135)	0.157	0.144	0.591	0.387	1.229	0.707	0.36	0.279	0.327	0.24
2	1971	San Fernando 2/9/1971	LA HOLLYWOOD STOR LOT, 180 (USGS STATION 135)	0.192	0.176	0.324	0.308	0.658	0.616	0.349	0.224	0.295	0.232
		Demand* Γ		**A1 x**	**A1 y**	**A1 (3fl) x**	**A1 (3fl) y**	**A1 (4fl) x**	**A1 (4fl) y**	**A2 x**	**A2 y**	**A2 (half) x**	**A2 (half) y**
No	Year	Earthquake	Record and component	Dmd	Dmd	Dmd	Dmd	Dmd	Dmd	Dmd	Dmd	Dmd	Dmd
1	1971	San Fernando 2/9/1971	LA HOLLYWOOD STOR LOT, 090 (USGS STATION 135)	0.196	0.177	0.756	0.495	1.598	0.926	0.446	0.346	0.405	0.298
2	1971	San Fernando 2/9/1971	LA HOLLYWOOD STOR LOT, 180 (USGS STATION 135)	0.240	0.216	0.415	0.394	0.855	0.807	0.433	0.278	0.366	0.288
		Drift ratio (demand/height)		**A1 x**	**A1 y**	**A1 (3fl) x**	**A1 (3fl) y**	**A1 (4fl) x**	**A1 (4fl) y**	**A2 x**	**A2 y**	**A2 (half) x**	**A2 (half) y**
No	Year	Earthquake	Record and component	Drift	Drift	Drift	Drift	Drift	Drift	Drift	Drift	Drift	Drift
1	1971	San Fernando 2/9/1971	LA HOLLYWOOD STOR LOT, 090 (USGS STATION 135)	0.033 %	0.030 %	0.084 %	0.055 %	0.133 %	0.077 %	0.074 %	0.058 %	0.068 %	0.050 %
2	1971	San Fernando 2/9/1971	LA HOLLYWOOD STOR LOT, 180 (USGS STATION 135)	0.040 %	0.036 %	0.046 %	0.044 %	0.071 %	0.067 %	0.072 %	0.046 %	0.061 %	0.048 %

6.3.3 Demand versus capacity calculation

After time-history analysis, for each building and analysis is made a comparison between the drift ratio (or displacement) of the demand and the capacity for all the three states DL, SD and NC. Below is shown this procedure for A buildings for the first two earthquakes. If the demand drift exceeds capacity drift in the table is written 1, if not 0. These tables are prepared for each building and earthquake, and are given in the appendix section.

Table 92: Demand and capacity of A buildings for first two earthquakes

	A1 x	A1 y	A1x (3fl)	A1y (3fl)	A1x (4fl)	A1y (4fl)	A2 x	A2 y	A2 (half) x	A2 (half) y
d DL	0.028%	0.027%	0.038%	0.036%	0.052%	0.032%	0.050%	0.038%	0.058%	0.033%
d SD	0.100%	0.060%	0.131%	0.064%	0.131%	0.073%	0.160%	0.083%	0.125%	0.075%
d NC	0.133%	0.080%	0.174%	0.087%	1.742%	0.098%	0.213%	0.110%	0.167%	0.100%
Eq1	0.033%	0.030%	0.084%	0.055%	0.133%	0.077%	0.074%	0.058%	0.068%	0.050%
Eq2	0.040%	0.036%	0.046%	0.044%	0.071%	0.067%	0.072%	0.046%	0.061%	0.048%

Table 93: Demand and capacity comparison of A buildings for first two earthquakes

		A1 x	A1 y	A1 (3fl) x	A1 (3fl) y	A1 (4fl) x	A1 (4fl) y	A2 x	A2 y	A2 (half) x	A2 (half) y
Earthquake	**Record and component**	DL	DL	DL	DL	DL	DL	DL	DL	DL	DL
San Fernando 2/9/1971	LA HOLLYWOOD STOR LOT, 090 (USGS STATION 135)	1	1	1	1	1	1	1	1	1	1
San Fernando 2/9/1971	LA HOLLYWOOD STOR LOT, 180 (USGS STATION 135)	1	1	1	1	1	1	1	1	1	1
Earthquake	**Record and component**	SD	SD	SD	SD	SD	SD	SD	SD	SD	SD
San Fernando 2/9/1971	LA HOLLYWOOD STOR LOT, 090 (USGS STATION 135)	0	0	0	0	1	1	0	0	0	0
San Fernando 2/9/1971	LA HOLLYWOOD STOR LOT, 180 (USGS STATION 135)	0	0	0	0	0	0	0	0	0	0
Earthquake	**Record and component**	NC	NC	NC	NC	NC	NC	NC	NC	NC	NC
San Fernando 2/9/1971	LA HOLLYWOOD STOR LOT, 090 (USGS STATION 135)	0	0	0	0	0	0	0	0	0	0
San Fernando 2/9/1971	LA HOLLYWOOD STOR LOT, 180 (USGS STATION 135)	0	0	0	0	0	0	0	0	0	0

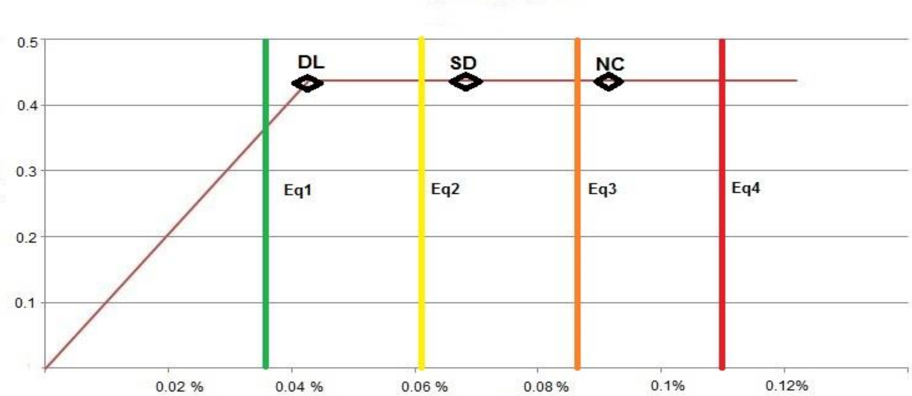

Figure 242: Demand versus capacity, graphical drift based comparison

6.3.4 Near field versus far field results

The results of each earthquake are plotted below and is given in % the ratio of exceeding each limit state for all the buildings. From the results of all buildings and templates can be concluded that the ratio of exceendance is higher for the near field results. The NC exceed ratio is 40% far far field, while 46% for near field result, also SD exceed ratio 62% for near field, while 57% for far field earthquakes.

Table 94: Ratio of exceedance for all building under each far field earthquakes

No	***Earthquake***	***Record***	***PGA (%g)***	***PGV (cm/s)***	***PGD (cm)***	***DL (% of exceedance)***	***SD (% of exceedance)***	***NC (% of exceedance)***
1	San Fernando 2/9/1971	LA HOLLYWOOD STOR LOT, 090 (USGS STATION 135)	0.21	18.93	12.42	100.00%	28.95%	0.00%
2	San Fernando 2/9/1971	LA HOLLYWOOD STOR LOT, 180 (USGS STATION 135)	0.174	14.87	6.32	100.00%	0.00%	0.00%
3	Friuli, Italy 5/6/1976	Tolmezzo, 000	0.351	22.03	4.11	100.00%	60.53%	34.21%
4	Friuli, Italy 5/6/1976	Tolmezzo, 270	0.315	30.80	5.09	97.37%	68.42%	52.63%
5	Imperial valley 10/15/1979	DELTA, 262 (UNAM/UCSD STATION 6605)	0.238	26.00	11.99	100.00%	42.11%	18.42%
6	Imperial valley 10/15/1979	DELTA, 352 (UNAM/UCSD STATION 6605)	0.351	33.02	19.03	100.00%	68.42%	18.42%
7	Imperial valley 10/15/1979	EL CENTRO ARRAY #11, 140 (USGS STATION 5058)	0.364	34.44	16.08	100.00%	76.32%	55.26%
8	Imperial valley 10/15/1979	EL CENTRO ARRAY #11, 230 (USGS STATION 5058)	0.38	42.14	18.63	100.00%	73.68%	60.53%
9	SuperstitionHills 02 11/24/87	EL CENTRO IMP CO CENTER, 000 (CDMG STATION 01	0.358	46.36	17.53	100.00%	52.63%	21.05%
10	SuperstitionHills 02 11/24/87	EL CENTRO IMP CO CENTER, 090 (CDMG STATION 01	0.258	40.87	20.1	84.21%	21.05%	5.26%

11	SuperstitionHills 02 11/24/87	POE, 270 (USGS STATION TEMP)	0.446	35.80	8.82	100.00%	55.26%	39.47%
12	SuperstitionHills 02 11/24/87	POE, 360 (USGS STATION TEMP)	0.3	32.80	11.28	100.00%	57.89%	31.58%
13	LOMA PRIETA 10/18/89	CAPITOLA, 000 (CDMG STATION 47125)	0.529	35.01	9.13	100.00%	89.47%	65.79%
14	LOMA PRIETA 10/18/89	CAPITOLA, 090 (CDMG STATION 47125)	0.443	29.21	5.49	100.00%	71.05%	57.89%
15	LOMA PRIETA 10/18/89	GILROY ARRAY #3, 000 (CDMG STATION 47381)	0.555	35.69	8.26	100.00%	97.37%	84.21%
16	LOMA PRIETA 10/18/89	GILROY ARRAY #3, 090 (CDMG STATION 47381)	0.367	44.67	19.33	100.00%	71.05%	39.47%
17	CAPE MENDOCINO 04/25/92	RIO DELL OVERPASS FF, 360 (CDMG STATION 89324)	0.549	42.00	19.55	100.00%	76.32%	57.89%
18	CAPE MENDOCINO 04/25/92	RIO DELL OVERPASS FF, 270	0.195	10.54	7.02	81.58%	0.00%	0.00%
19	LANDERS 7/23/92	COOLWATER, LN (SCE STATION 23)	0.283	25.64	13.71	94.74%	63.16%	50.00%
20	LANDERS 7/23/92	COOLWATER, TR (SCE STATION 23)	0.417	42.34	13.81	97.37%	60.53%	55.26%
21	LANDERS 06/28/92	YERMO FIRE STATION, 270 (CDMG STATION 22074)	0.245	51.44	43.85	81.58%	18.42%	0.00%
22	LANDERS 06/28/92	YERMO FIRE STATION, 360 (CDMG STATION 22074)	0.152	29.71	24.63	78.95%	18.42%	0.00%
23	NORTHRIDGE EQ 1/17/94	BEVERLY HILLS - 12520 MULH, 035 (USC STATION 90014	0.617	40.86	8.57	100.00%	89.47%	68.42%
24	NORTHRIDGE EQ 1/17/94	BEVERLY HILLS - 12520 MULH, 125 (USC STATION 90014	0.444	30.19	4.83	100.00%	84.21%	63.16%
25	NORTHRIDGE EQ 1/17/94	BEVERLY HILLS - 14145 MULH, 009 (USC STATION 90013	0.416	58.94	13.15	100.00%	65.79%	47.37%
26	NORTHRIDGE EQ 1/17/94	BEVERLY HILLS - 14145 MULH, 279 (USC STATION 90013	0.516	62.78	11.07	100.00%	81.58%	63.16%

27	NORTHRIDGE EQ 1/17/94	CANYON COUNTRY - W LOST CANYON, 000 (USC STATION 9	0.41	43.03	11.71	100.00%	63.16%	55.26%
28	NORTHRIDGE EQ 1/17/94	CANYON COUNTRY - W LOST CANYON, 270 (USC STATION 9	0.482	45.38	12.54	100.00%	89.47%	71.05%
29	KOBE 01/16/95	NISHI-AKASHI, 000	0.509	37.29	9.53	100.00%	76.32%	65.79%
30	KOBE 01/16/95	NISHI-AKASHI, 090	0.503	36.67	11.26	100.00%	73.68%	44.74%
31	KOBE 01/16/95	SHIN-OSAKA, 000	0.243	37.86	8.55	92.11%	23.68%	2.63%
32	KOBE 01/16/95	SHIN-OSAKA, 090	0.212	27.94	7.64	81.58%	28.95%	5.26%
33	KOCAELI 08/17/99	ARCELIK, 000 (KOERI)	0.219	17.69	13.65	76.32%	7.89%	2.63%
34	KOCAELI 08/17/99	ARCELIK, 090 (KOERI)	0.15	39.55	35.58	71.05%	0.00%	0.00%
35	KOCAELI 08/17/99	DUZCE, 180 (ERD)	0.312	58.88	44.13	92.11%	52.63%	36.84%
36	KOCAELI 08/17/99	DUZCE, 270 (ERD)	0.358	46.39	17.62	94.74%	60.53%	47.37%
37	CHI-CHI 09/20/99	CHY101, E	0.353	70.64	45.3	100.00%	42.11%	13.16%
38	CHI-CHI 09/20/99	CHY101, N	0.44	115.00	68.76	100.00%	60.53%	42.11%
39	CHI-CHI 09/20/99	TCU045, E	0.474	36.70	50.68	100.00%	65.79%	57.89%
40	CHI-CHI 09/20/99	TCU045, N	0.512	39.09	14.35	100.00%	65.79%	47.37%
41	DUZCE 11/12/99	BOLU, 000 (ERD)	0.728	56.49	23.07	100.00%	84.21%	68.42%
42	DUZCE 11/12/99	BOLU, 090 (ERD)	0.822	62.12	13.56	100.00%	84.21%	68.42%
43	IRAN_MANJIL 06/20/90	LONGITUDINAL COMP	0.515	43.26	14.92	100.00%	97.37%	78.95%
44	IRAN_MANJIL 06/20/90	TRANSVERSE COMP	0.496	55.55	20.83	100.00%	97.37%	81.58%
45	HECTOR MINE OCT 16, 1999	HEC, 000	0.266	28.58	22.54	92.11%	15.79%	2.63%
46	HECTOR MINE OCT 16, 1999	HEC, 090	0.337	41.75	13.96	100.00%	57.89%	50.00%
	TOTAL					96%	57%	40%

Table 95: Ratio of exceedance for all building under each near field earthquakes

No	Earthquake	Record	PGA (%g)	PGV (cm/s)	PGD (cm)	DL (% of exceendance)	SD (% of exceendance)	NC (% of exceendance)
1	IMPERIAL VALLEY 10/15/79	CHIHUAHUA, 012 (UNAM/UCSD STATION 6621)	0.27	24.85	9.13	89.47%	36.84%	10.53%
2	IMPERIAL VALLEY 10/15/79	CHIHUAHUA, 282 (UNAM/UCSD STATION 6621)	0.254	30.12	12.91	89.47%	34.21%	5.26%
3	IMPERIAL VALLEY 10/15/79	EL CENTRO ARRAY #6, 140 (CDMG STATION 942)	0.41	64.83	27.57	100.00%	60.53%	23.68%
4	IMPERIAL VALLEY 10/15/79	EL CENTRO ARRAY #6, 230 (CDMG STATION 942)	0.439	109.80	65.82	100.00%	60.53%	39.47%
5	IMPERIAL VALLEY 10/15/79	EL CENTRO ARRAY #7, 140 (USGS STATION 5028)	0.338	47.60	24.65	89.47%	36.84%	13.16%
6	IMPERIAL VALLEY 10/15/79	EL CENTRO ARRAY #7, 230 (USGS STATION 5028)	0.463	109.24	44.71	100.00%	60.53%	42.11%
7	IMPERIAL VALLEY 10/15/79	BONDS CORNER, 140 (USGS STATION 5054)	0.084	3.61	0.34	0.00%	0.00%	0.00%
8	IMPERIAL VALLEY 10/15/79	BONDS CORNER, 230 (USGS STATION 5054)	0.1	8.18	1.42	2.63%	2.63%	2.63%
9	IRPINIA EQ, 11/23/80	STURNO, 000	0.251	36.39	11.58	94.74%	57.89%	23.68%
10	IRPINIA EQ, 11/23/80	STURNO, 270	0.358	51.82	32.02	100.00%	71.05%	50.00%
11	NAHANNI, CANADA 12/23/85	SITE 1, 010	0.978	46.05	9.64	100.00%	100.00%	92.11%
12	NAHANNI, CANADA 12/23/85	SITE 1, 280	1.096	46.13	14.52	100.00%	100.00%	94.74%
13	NAHANNI, CANADA 12/23/85	SITE 1, UP	2.086	40.60	12.29	100.00%	92.11%	71.05%

14	NAHANNI, CANADA 12/23/85	SITE 2, 240	0.489	29.26	7.54	86.84%	39.47%	15.79%
15	NAHANNI, CANADA 12/23/85	SITE 2, 330	0.323	33.13	6.57	100.00%	15.79%	7.89%
16	SUPERSTITIO N HILLS 11/24/87	PTS, 225 (USGS STATION 5051)	0.455	112.00	52.83	100.00%	68.42%	50.00%
17	SUPERSTITIO N HILLS 11/24/87	PTS, 315 (USGS STATION 5051)	0.377	43.90	15.25	94.74%	52.63%	42.11%
18	LOMA PRIETA 10/18/89	BRAN, 000	0.481	55.74	11.69	100.00%	78.95%	65.79%
19	LOMA PRIETA 10/18/89	BRAN, 090	0.526	41.91	11.86	100.00%	92.11%	81.58%
20	LOMA PRIETA 10/18/89	CORRALITOS, 000 (CDMG STATION 57007)	0.644	55.16	10.82	100.00%	76.32%	63.16%
21	LOMA PRIETA 10/18/89	CORRALITOS, 090 (CDMG STATION 57007)	0.479	45.50	11.29	100.00%	68.42%	52.63%
22	LOMA PRIETA 10/18/89	SARATOGA ALOHA AVE, 000 (CDMG STATION 58065)	0.512	51.15	16.24	100.00%	65.79%	34.21%
23	LOMA PRIETA 10/18/89	SARATOGA ALOHA AVE, 090 (CDMG STATION 58065)	0.324	42.61	27.61	100.00%	63.16%	23.68%
24	ERZICAN 03/13/92	ERZICAN EAST-WEST COMP	0.496	64.30	21.92	100.00%	76.32%	63.16%
25	ERZICAN 03/13/92	ERZICAN - NORTH-SOUTH COMP	0.515	83.95	27.66	100.00%	63.16%	42.11%
26	CAPE MENDOCINO 04/25/92	CAPE MENDOCINO, 000 (CDMG STATION 89005)	1.497	125.57	39.74	100.00%	100.00%	97.37%
27	CAPE MENDOCINO 04/25/92	CAPE MENDOCINO, 090 (CDMG STATION 89005)	1.039	41.33	12.18	100.00%	86.84%	76.32%
28	CAPE MENDOCINO 04/25/92	PETROLIA, 000 (CDMG STATION 89156)	0.59	48.32	21.97	100.00%	73.68%	60.53%

29	CAPE MENDOCINO 04/25/92	PETROLIA, 090 (CDMG STATION 89156)	0.662	90.08	29.01	100.00%	76.32%	60.53%
30	LANDERS 6/28/92	LUCERNE, 260 (SCE STATION 24)	0.727	146.03	217.12	100.00%	86.84%	60.53%
31	LANDERS 6/28/92	LUCERNE, 345 (SCE STATION 24)	0.789	32.94	52.78	100.00%	78.95%	47.37%
32	NORTHRIDGE EARTHQUAKE	CA:LA;SEPULVEDA VA, BLD 40 GND; 270	0.749	78.10	13.39	100.00%	92.11%	71.05%
33	NORTHRIDGE EARTHQUAKE	CA:LA;SEPULVEDA VA, BLD 40 GND; 360	0.934	76.15	17.39	100.00%	100.00%	92.11%
34	NORTHRIDGE EQ 1/17/94	NORTHRIDGE - SATICOY, 090 (USC STATION 90003)	0.368	28.96	8.44	100.00%	68.42%	55.26%
35	NORTHRIDGE EQ 1/17/94	NORTHRIDGE - SATICOY, 180 (USC STATION 90003)	0.477	61.46	22.07	100.00%	78.95%	60.53%
36	NORTHRIDGE EQ 1/17/94	RINALDI RECEIVING STA, 228	0.825	160.33	29.62	100.00%	92.11%	78.95%
37	NORTHRIDGE EQ 1/17/94	RINALDI RECEIVING STA, 318	0.487	74.54	26.96	100.00%	86.84%	68.42%
38	NORTHRIDGE EQ 1/17/94	SYLMAR - HOSPITAL, 090 (CDMG STATION 24514)	0.604	78.37	16.82	100.00%	71.05%	55.26%
39	NORTHRIDGE EQ 1/17/94	SYLMAR - HOSPITAL, 360 (CDMG STATION 24514)	0.843	130.40	31.96	100.00%	92.11%	76.32%
40	KOCAELI 08/17/99	IZMIT, 090 (ERD)	0.22	29.78	17.13	89.47%	26.32%	18.42%
41	KOCAELI 08/17/99	IZMIT, 180 (ERD)	0.152	22.61	9.81	76.32%	18.42%	5.26%
42	KOCAELI 08/17/99	YARIMCA, 330 (KOERI)	0.349	62.16	50.98	86.84%	34.21%	15.79%
43	KOCAELI 08/17/99	YARIMCA, 060 (KOERI)	0.268	65.72	57.03	84.21%	36.84%	15.79%
44	CHI-CHI 09/20/99	TCU065, E	0.814	126.18	92.59	100.00%	81.58%	63.16%
45	CHI-CHI 09/20/99	TCU065, N	0.603	78.79	60.75	100.00%	65.79%	47.37%

46	CHI-CHI 09/20/99	TCU067, E	0.503	79.58	93.12	100.00%	60.53%	52.63%
47	CHI-CHI 09/20/99	TCU067, N	0.325	66.70	45.96	100.00%	60.53%	55.26%
48	CHI-CHI 09/20/99	TCU084, E	1.157	114.74	31.44	100.00%	97.37%	92.11%
49	CHI-CHI 09/20/99	TCU084, N	0.417	45.58	21.27	100.00%	60.53%	52.63%
50	CHI-CHI 09/20/99	TCU102, E	0.298	112.45	89.2	71.05%	18.42%	2.63%
51	CHI-CHI 09/20/99	TCU102, N	0.169	77.16	44.88	55.26%	2.63%	0.00%
52	DUZCE 11/12/99	DUZCE, 180 (ERD)	0.348	59.97	42.11	100.00%	60.53%	52.63%
53	DUZCE 11/12/99	DUZCE, 270 (ERD)	0.535	83.49	51.62	100.00%	71.05%	65.79%
54	DENALI ALASKA 11/03/02	PS10, 047	0.319	134.73	102.73	86.84%	47.37%	21.05%
55	DENALI ALASKA 11/03/02	PS10, 317	0.318	75.97	77.99	86.84%	15.79%	5.26%
						92%	62%	46%

6.4 Time-history analysis results comparison

As in the spectrum based analysis, the templates and their performance are compared from the era of construction, height of the building and principal brick material used for masonry.

6.4.1 Results by era of construction

By era of construction the buildings are divided in three section A, B and C reffering to the code was used on the era they were constructed.

6.4.1.1 Buildings of A templates (before 1963 era)

The building of A template perform well under near fault and far fault earthquakes, with only A1 building with 2 added floors, showing more than 30% exceendance for NC state on all analysis performed. It must be said that these buildings are of low height, so they show no great risk under the seismic risk, even though they are the oldest ones and they have materials with lower quality.

Table 96: Ratio of exceedance for A building under far field earthquakes

	A1 x	A1 y	A1x(3fl)	A1y(3fl)	A1x(4fl)	A1y(4fl)	A2 x	A2 y	A2x(half)	A2y(half)
DL	34	33	44	44	46	46	43	42	38	37
% DL	73.91%	71.74%	95.65%	95.65%	100.00%	100.00%	93.48%	91.30%	82.61%	80.43%
% DL		72.83%		95.65%		100.00%		92.39%		81.52%
SD	0	6	10	28	29	36	5	16	7	11
% SD	0.00%	13.04%	21.74%	60.87%	63.04%	78.26%	10.87%	34.78%	15.22%	23.91%
% SD		6.52%		41.30%		70.65%		22.83%		19.57%
NC	0	1	2	16	0	28	1	7	1	3
% NC	0.00%	2.17%	4.35%	34.78%	0.00%	60.87%	2.17%	15.22%	2.17%	6.52%
% NC		1.09%		19.57%		30.43%		8.70%		4.35%

Table 97: Ratio of exceedance for A building under near field earthquakes

	A1 x	A1 y	A1x(3fl)	A1y(3fl)	A1x(4fl)	A1y(4fl)	A2 x	A2 y	A2x(half)	A2y(half)
DL	40	40	51	48	53	52	49	48	42	42
% DL	72.73%	72.73%	92.73%	87.27%	96.36%	94.55%	89.09%	87.27%	76.36%	76.36%
% DL		72.73%		90.00%		95.45%		88.18%		76.36%
SD	8	14	14	31	41	42	13	21	17	17
% SD	14.55%	25.45%	25.45%	56.36%	74.55%	76.36%	23.64%	38.18%	30.91%	30.91%
% SD		20.00%		40.91%		75.45%		30.91%		30.91%
NC	5	9	7	24	0	37	9	15	11	10
% NC	9.09%	16.36%	12.73%	43.64%	0.00%	67.27%	16.36%	27.27%	20.00%	18.18%
% NC		12.73%		28.18%		33.64%		21.82%		19.09%

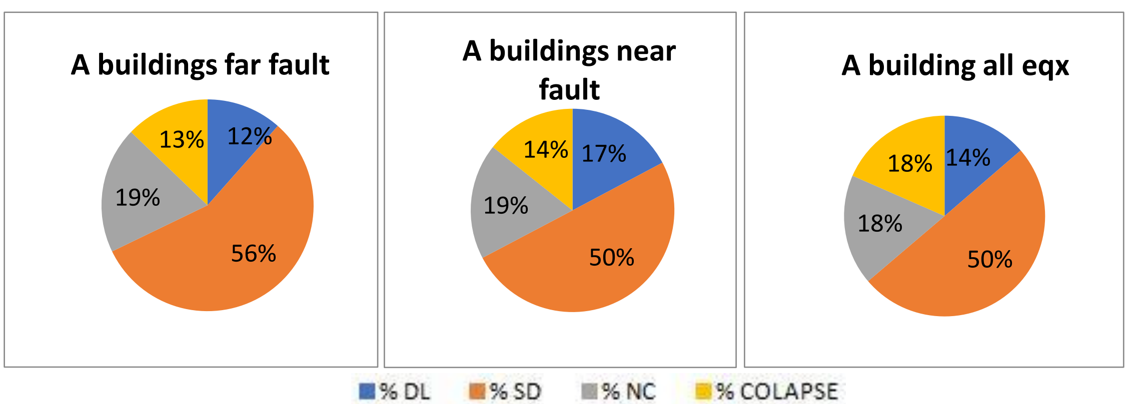

Figure 243: A buildings graphical results comparison

6.4.1.2 Buildings of B templates (1963-1978 era)

The building of B template perform differently under near fault and far fault earthquakes. Some buildings have higher risk, showing more than 40% exceendance for NC state on all analysis performed. This is noted in building of B3 and B4 template that are 5 story high. It also can be assumed that B3 with intervention has a highly increased seismic hazard compared with B3 without intervention. Building B4 in the other hand has a non regular plan, and the values of exceendance are very high.

Table 98: Ratio of exceedance for B building under far field earthquakes

	B1 x	B1 y	B1x(4fl)	B1y(4fl)	B2x	B2y	B2x(38cm)	B2y(38cm)	B3 x	B3 y	B3x int	B3y int	B4x	B4y
DL	43	41	46	46	46	46	46	46	45	46	45	46	44	45
% DL	93.48%	89.13%	100.00%	100.00%	100.00%	100.00%	100.00%	100.00%	97.83%	100.00%	97.83%	100.00%	95.65%	97.83%
% DL		91.30%		100.00%		100.00%		100.00%		98.91%		98.91%		96.74%
SD	3	9	13	19	24	14	36	15	31	37	28	37	41	34
% SD	6.52%	19.57%	28.26%	41.30%	52.17%	30.43%	78.26%	32.61%	67.39%	80.43%	60.87%	80.43%	89.13%	73.91%
% SD		13.04%		34.78%		41.30%		55.43%		73.91%		70.65%		81.52%
NC	0	3	4	8	10	6	26	10	21	30	20	30	35	24
% NC	0.00%	6.52%	8.70%	17.39%	21.74%	13.04%	56.52%	21.74%	45.65%	65.22%	43.48%	65.22%	76.09%	52.17%
% NC		3.26%		13.04%		17.39%		39.13%		55.43%		54.35%		64.13%

Table 99: Ratio of exceedance for B building under near field earthquakes

	B1 x	B1 y	B1x(4fl)	B1y(4fl)	B2x	B2y	B2x(38cm)	B2y(38cm)	B3x	B3y	B3x int	B3y int	B4x	B4y
DL	50	45	52	52	52	52	51	52	53	53	53	53	53	53
% DL	90.91%	81.82%	94.55%	94.55%	94.55%	94.55%	92.73%	94.55%	96.36%	96.36%	96.36%	96.36%	96.36%	96.36%
% DL		86.36%		94.55%		94.55%		93.64%		96.36%		96.36%		96.36%
SD	9	15	18	27	29	18	39	18	39	48	35	48	50	43
% SD	16.36%	27.27%	32.73%	49.09%	52.73%	32.73%	70.91%	32.73%	70.91%	87.27%	63.64%	87.27%	90.91%	78.18%
% SD		21.82%		40.91%		42.73%		51.82%		79.09%		75.45%		84.55%
NC	7	9	10	14	19	10	30	13	25	39	23	42	46	32
% NC	12.73%	16.36%	18.18%	25.45%	34.55%	18.18%	54.55%	23.64%	45.45%	70.91%	41.82%	76.36%	83.64%	58.18%
% NC		14.55%		21.82%		26.36%		39.09%		58.18%		59.09%		70.91%

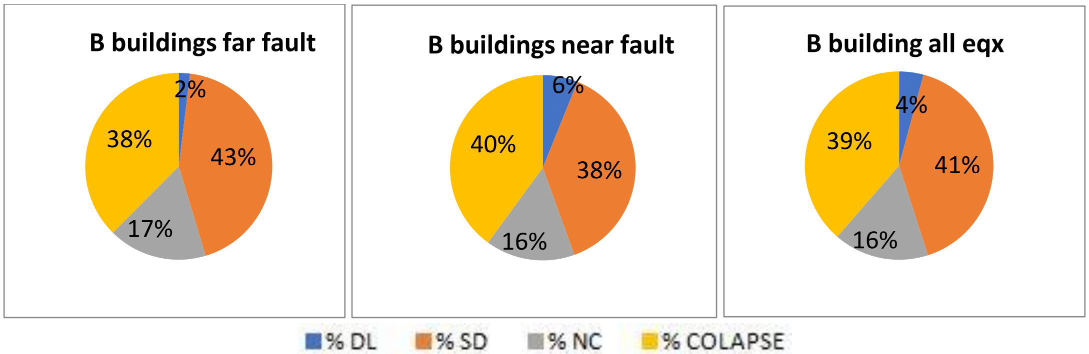

Figure 244:B buildings graphical results comparison

6.4.1.3 Buildings of C templates (After 1978 era)

The building of C template have very serious deficiency in performance under near fault and far fault earthquakes. In all this types is viewed an exceendance ratio higher then 40% for NC point. This comes because these buildings are calculated considering a lower seismic risk. 66% is the mean of the ratio of exceendance of NC point for all the buildings a very high value. So comparing to the other buildings constructed before 1978, although these building have higher values for material characteristics, they have lower seismic resistance and are more vulnerable to seismic hazard because they are taller and also the inerventions done in many buildings decrease the building capacity and increase the seismic hazard.

Table 100: Ratio of exceedance for C building under far field earthquakes

	C1A x	**C1A y**	**C1A int x**	**C1A int y**	**C1B x**	**C1B y**	**C1B (6fl) x**	**C1B (6fl) y**	**C2 x**	**C2 y**	**C2B (6fl) x**	**C2B (6fl) y**	**C3 x**	**C3 y**
DL	45	46	46	46	46	46	46	46	46	46	43	46	46	46
% DL	97.83%	100.00%	100.00%	100.00%	100.00%	100.00%	100.00%	100.00%	100.00%	100.00%	93.48%	100.00%	100.00%	100.00%
% DL		98.91%		100.00%		100.00%		100.00%		100.00%		96.74%		100.00%
SD	33	40	37	39	35	35	41	38	38	40	38	25	38	37
% SD	71.74%	86.96%	80.43%	84.78%	76.09%	76.09%	89.13%	82.61%	82.61%	86.96%	82.61%	54.35%	82.61%	80.43%
% SD		79.35%		82.61%		76.09%		85.87%		84.78%		68.48%		81.52%
NC	24	37	32	35	31	27	31	24	30	35	27	16	31	30
% NC	52.17%	80.43%	69.57%	76.09%	67.39%	58.70%	67.39%	52.17%	65.22%	76.09%	58.70%	34.78%	67.39%	65.22%
% NC		66.30%		72.83%		63.04%		59.78%		70.65%		46.74%		66.30%

Table 101: Ratio of exceedance for C building under near field earthquakes

	C1A x	C1A y	C1A int x	C1A int y	C1B x	C1B y	C1B (6fl) x	C1B (6fl) y	C2 x	C2 y	C2B (6fl) x	C2B (6fl) y	C3 x	C3 y
DL	53	53	54	53	53	53	53	53	53	53	53	53	53	53
% DL	96.36%	96.36%	98.18%	96.36%	96.36%	96.36%	96.36%	96.36%	96.36%	96.36%	96.36%	96.36%	96.36%	96.36%
% DL		96.36%		97.27%		96.36%		96.36%		96.36%		96.36%		96.36%
SD	43	51	49	50	46	44	49	44	47	49	46	29	49	48
% SD	78.18%	92.73%	89.09%	90.91%	83.64%	80.00%	89.09%	80.00%	85.45%	89.09%	83.64%	52.73%	89.09%	87.27%
% SD		85.45%		90.00%		81.82%		84.55%		87.27%		68.18%		88.18%
NC	31	46	40	44	37	35	40	29	39	46	33	16	39	43
% NC	56.36%	83.64%	72.73%	80.00%	67.27%	63.64%	72.73%	52.73%	70.91%	83.64%	60.00%	29.09%	70.91%	78.18%
% NC		70.00%		76.36%		65.45%		62.73%		77.27%		44.55%		74.55%

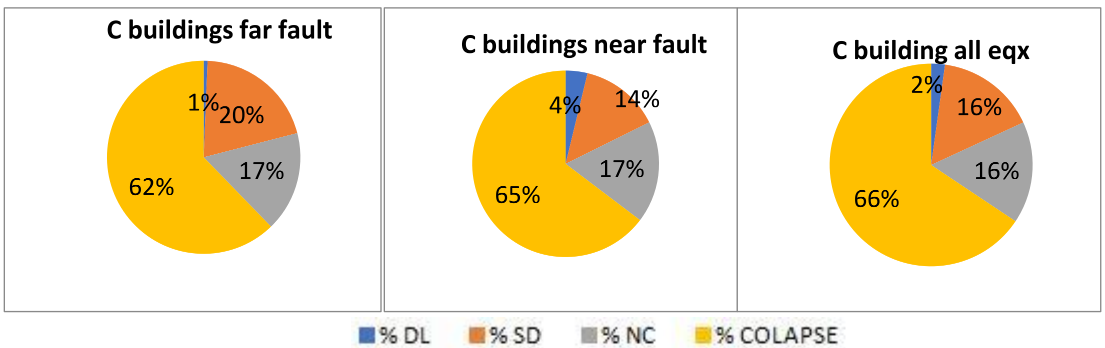

Figure 245: C buildings graphical results comparison

6.4.2 Results by building height

Table 102: Ratio of exceedance for buildings by height

`	**Far field results**			**Near field results**			**All earthquakes**		
	% DL	**% SD**	**% NC**	**% DL**	**% SD**	**% NC**	**% DL**	**% SD**	**% NC**
2fl buildings	82.25%	16.30%	4.71%	79.09%	27.27%	17.88%	80.53%	22.28%	11.88%
3fl buildings	93.48%	27.17%	11.41%	88.18%	31.36%	21.36%	90.59%	29.46%	16.83%
4fl buildings	100.00%	50.54%	25.00%	94.55%	52.73%	30.23%	97.03%	51.73%	27.85%
5fl buildings	99.18%	78.80%	64.13%	96.48%	83.98%	68.98%	97.71%	81.62%	66.77%
6fl buildings	98.37%	77.17%	53.26%	96.36%	76.36%	53.64%	97.28%	76.73%	53.47%

From the ratios of exceendance for all buildings can be easy spotted that buildings with height 5 and 6 have a higher risk under all earthquakes. Values of exceendance of Near

Collapse state are 66.77% and 53.47% for each, which is very high comparing to all others buildings. While height increases also increases the building vulnerability.

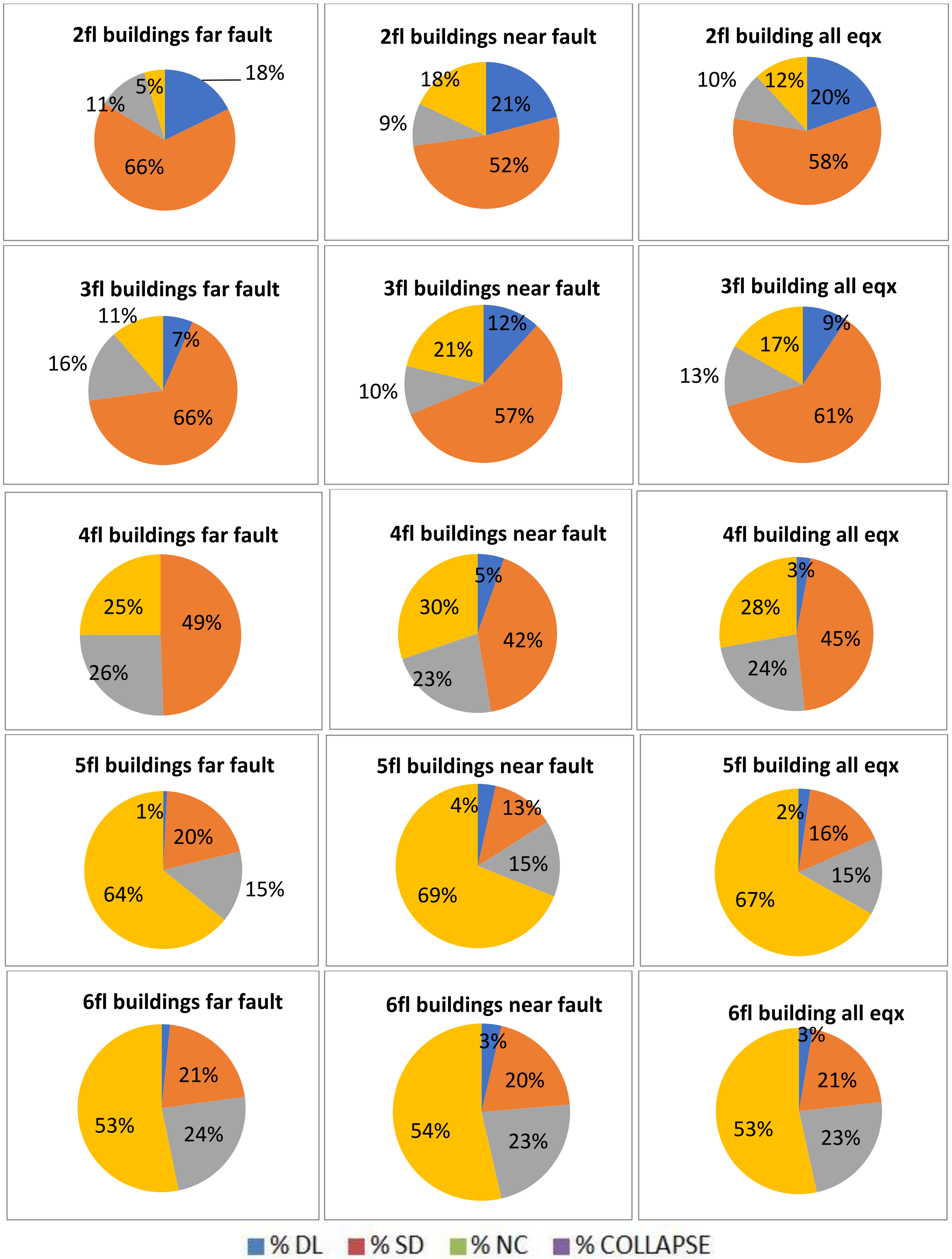

Figure 246: Graphical results comparison of buildings with different height

6.4.3 Results by material used

From the ratios of exceedance for all buildings can be easy spotted that buildings with height 5 and 6 have a higher risk under all earthquakes. If we compare the results of time history analysis from principal construction material can be viewed that clay building have lower ratios of exceedance compared to silicate buildings. But this happens because silicate masonry buildings are used for higher story buildings, with height 5 and 6 that have a higher risk under all earthquakes

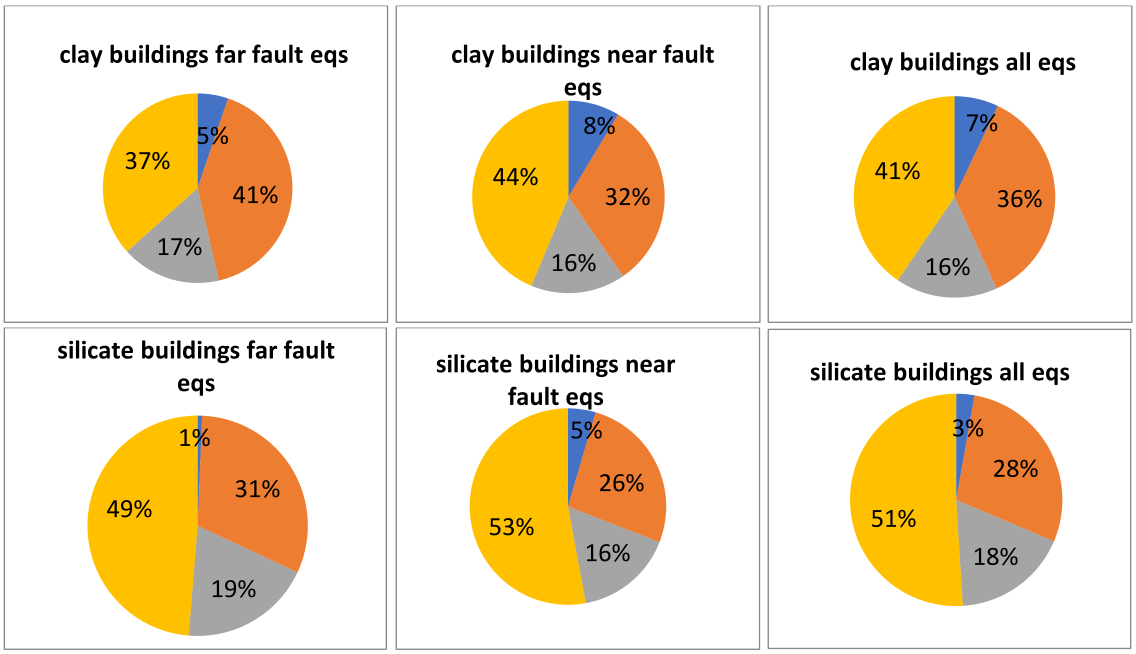

Figure 247: Graphical results comparison of buildings with clay and silicate masonry

Table 103: Ratio of exceedance for buildings by materials used

	Far fault earthquakes			Near fault earthquakes			All earthquakes		
	% DL	% SD	% NC	% DL	% SD	% NC	% DL	% SD	% NC
Clay masonry buildings	94.80%	53.57%	36.65%	91.36%	59.61%	43.70%	92.93%	56.86%	40.49%
Silicate masonry buildings	99.35%	68.04%	48.70%	95.45%	69.09%	52.91%	97.23%	68.61%	50.99%

6.4.4 Conclusions

The observed damages on masonry buildings during the past earthquakes worldwide were reported in many studies. [Decanni et al., 2004; Klinger, 2006; Kaplan et al., 2010; Bilgin and Korini, 2012; Moon et al, 2012; Penna et al, 2014; Amaryllis et al, 2014; Bilgin and Huta, 2016; Marotta et al, 2017;cSorrentino et al, 2018; Penna et al, 2019]. Hence, it is well known that the considerable amount of masonry buildings were damaged at various levels during recent earthquakes as mentioned above. Due to extremely high number of casualties and damaged buildings, these buildings were covered separately for several earthquakes such as for example in Emilia (Italy, 2012) and New Zealand (2010-2012), as documented for example in Penna et al, 2014, for the Emilia event and Dizhur et al, 2011, Senaldi et al, 2014 [Penna et al, 2014] for the Christchurch earthquakes. The observations from Tables 93 and 94 support high damaging property of 1985 Nahanni, 1989 Loma Prieta, 1990 Iran, 1992 Erzincan, 1992 Cape Mendocino, 1994 Northridge, 1999 Chile, 1999 Kocaeli and Duzce earthquakes for existing masonry buildings. Careful assessment of Table 93 and 94 supports the observed damages in the past earthquakes. Among one hundred one records considered herein, Loma Prieta, Cape Mendocino, Northridge, Düzce and Iran records have significant damaging effects with exceedance ratio of LS performance level greater than about 0.60 for far-fault records. Nahanni, Loma Prieta, Chile, Cape Mendocino and Northridge from near fault records have similar tendency with an exceedance ratio of 0.60. On the other hand Nahanni, Chile, Cape Mendocino and Northridge near fault records are extremely destructive with exceedance ratio of LS performance level greater than about 0.80. Similar observations are valid for CP level (Table 93) with smaller exceedance ratios. According to Albanian Code, residential buildings are expected to satisfy DL and SD performance levels under design and extreme earthquakes, corresponding to 10% and 2% probability of exceedance in 50 years, respectively.

CHAPTER 7

ADRIATIC SEA EARTHQUAKE 26/11/2019 AND DAMAGE EVALUATION ON MASONRY BUILDINGS

7.1 Adriatic sea earthquake 21/11/2019

On November 26, 2019, the central western part of Albania was hit by a strong earthquake. It was assessed as M_w 6.4 (Fig 246.). Its epicenter was located offshore north western Durrës, around 7 km north of the city and 30 km west from the capital city of Tirana. Its focal depth was about 10 km. Based on the focal plane solutions provided by several seismological institutes and observations; the main shock was generated by the activation of a NW-SE striking reverse fault. The main shock was felt in the neighboring Montenegro, Italy and Greece, especially in Corfu Island. In the space of three months, this was the second earthquake to strike the region.

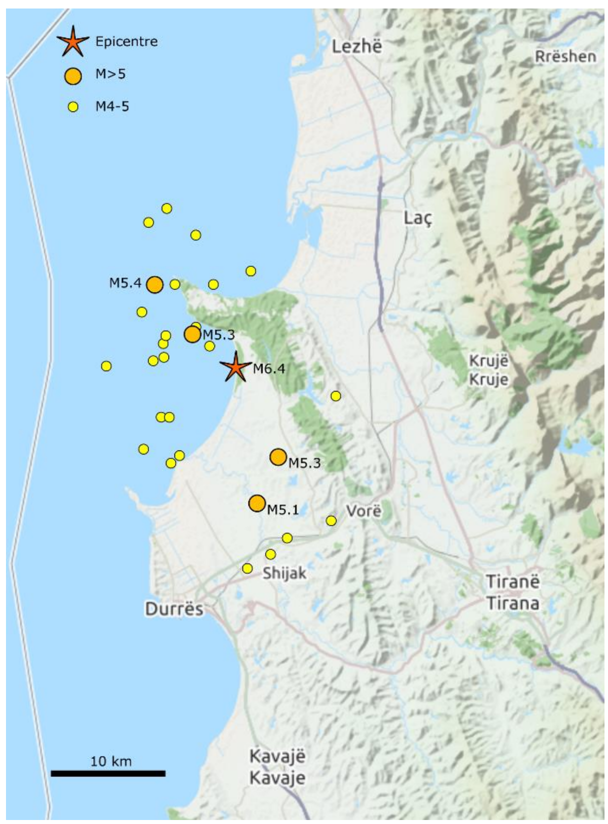

Figure 248: Location of epicenter and aftershocks of the 26 Novemember earthquake [CSEM-EMSC, 2019]

As regards the impact on the building stock, the main shock and the following aftershocks induced damage to buildings of Durrës, Tirana and several settlements of the broader area. The most earthquake-affected areas and the building damage was distributed along two ellipses, whose major axis is oriented generally NW-SE (Fig 247.). [Lekkas E. et.al., 2020]

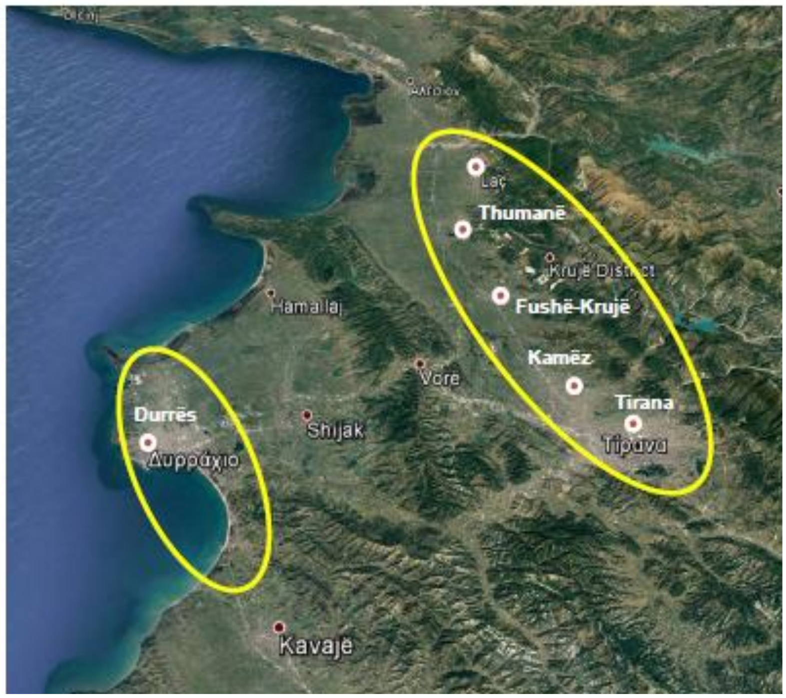

Figure 249: Earthquake-affected area during the November 26, 2019 Durres Earthquake [CSEM-EMSC, 2019]

The most affected areas are the Durres city and the Thumane town, while damage was also observed in Laç town, Fushe-Kruje town, Kamez, Vore and Tirana city. Based on the spatial distribution of the damage, two ellipses are formed, whose majot axis is oriented generally NW-SE directions. This direction coincides with the strike of the seismogenic fault as it is derived from the provided fault plane solutions. Moreover, these ellipses could be characterized as macrosesimic epicenters as a result of the interaction between the seismotectonic setting and the soil conditions and as outcome of of various conventions, reflections, refractions, directivity phenomena of seismic waves and resonance resulting in destruction in the earthquake-affected area.

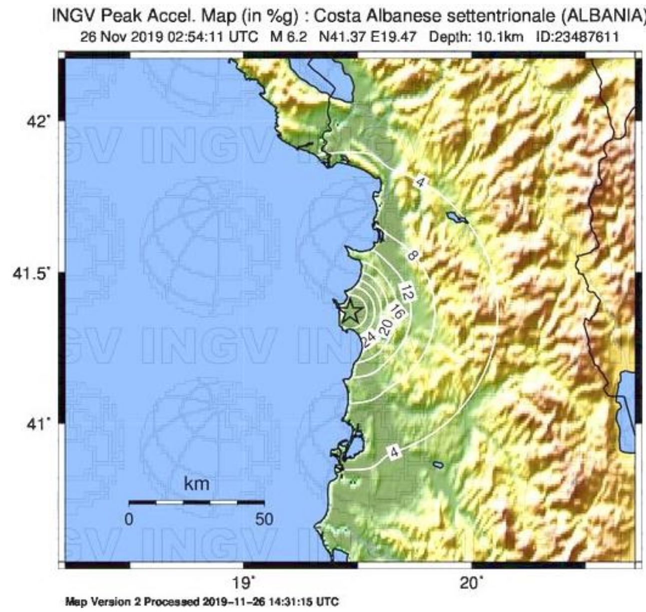

Figure 250: Peak ground acceleration map in (g %) [INGV, 2019]

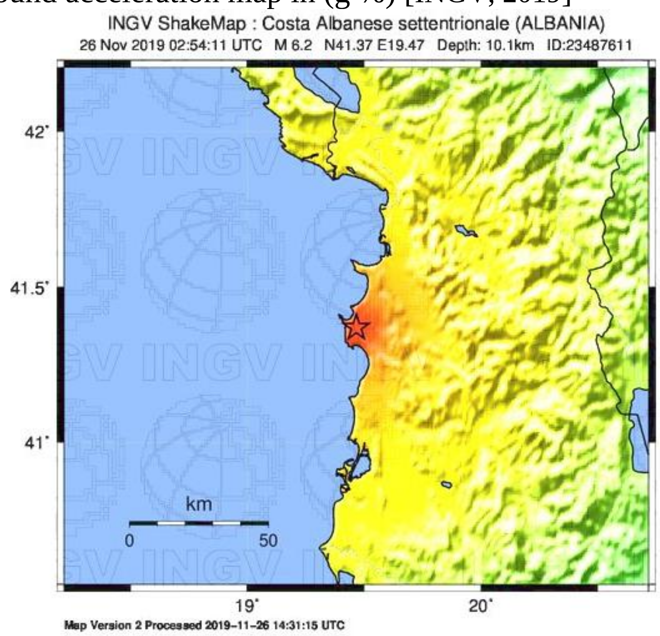

PERCEIVED SHAKING	Not felt	Weak	Light	Moderate	Strong	Very strong	Severe	Violent	Extreme
POTENTIAL DAMAGE	none	none	none	Very light	Light	Moderate	Mod./Heavy	Heavy	Very Heavy
PEAK ACC.(%g)	<0.06	0.2	0.8	2.0	4.8	12	29	70	>171
PEAK VEL.(cm/s)	<0.02	0.08	0.3	0.9	2.4	6.4	17	45	>120
INSTRUMENTAL INTENSITY	I	II–III	IV	V	VI	VII	VIII	IX	X+

Scale based upon Faenza and Michelini, 2010, 2011

Figure 251: Intensity Shake map of the 26 November Albania Earthquake [INGV, 2019]

The Mercalli intensity scale is based on the effects that the ground shaking produces and the reports by observers. Intensity Shake map of the 26 November Albania Earthquake [INGV, 2019] is shown in Fig 249. Fig 250. shows the distribution of peak ground acceleration expressed as percent of the acceleration of gravity (i.e., $g = 9.81\ m/s^2$). If the peak ground acceleration and intensity values are compared with the seismic zonation map of Albania, can be conluded that the resulted intensities from the earthquake under consideration, are within the limits specified in the Seismic Zonation Map from KTP-89. It is significant to note that the seismic zonation map in the seismic code of Albania compries zones based on observed seismic intensites and not on design accelerations. If these values are compared whith the probabilistic seismic hazard map for horizontal PGA, the values of these earthquake are typical for earthquake with 95 years of return period on the zone. But for this types of earthquakes according to EC-8 the building should perform in DL limit state. For many buildings especially in the zones like Vora or Thumane, in many buildings these damage limit state is exceeded. For Vora for example most of the unreiforced masonry buildings investigated have significant damage and near collapse in some cases. According to EC, signifaicant damage should occur for an earthquake with return period of 475 year.

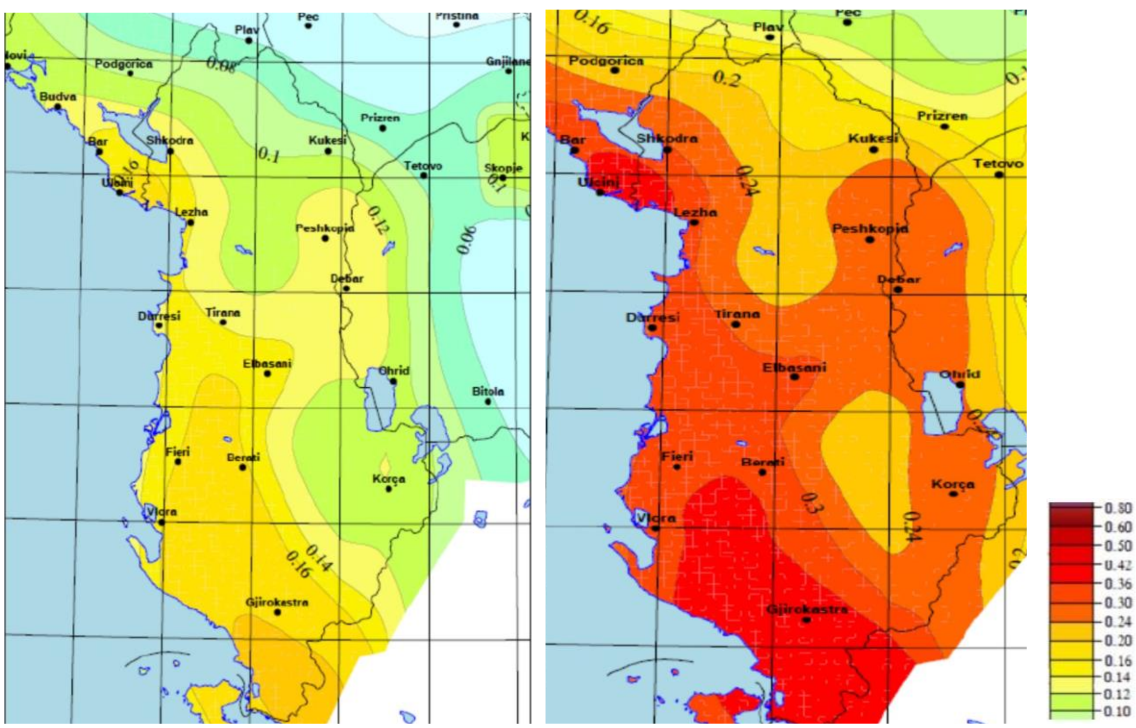

Figure 252: Probabilistic seismic hazard map for horizontal PGA, with return period of 95 years left and 475 years right [NATO SfP – 983054, 2009]

7.2 Caualities on Adriatic sea earthquake 21/11/2019

In Durres,two hotels and two apartment blocks have totally collapsed. Koder-Thumane was the hardest hit town from the earthquake where four buildings, including a five-story apartment block, collapsed. In the table above are shown the results of damage inspections done on the damaged building in Durres, Lezhe and Tirane by the Construction Institute of Albania. A total of 44582 building were inspected and as can be see below more then 1055 buildings in total were classified as DS4 and DS5, buildings that have serious damage on structural system.

Figure 253: Collapsed building in Durres beach right and collapsed ex-Kavaleshanca hotel in Durres

The unreiforced masonry structures with the load-bearing masonry walls suffered the most by the November 26, 2019 Durrës Earthquake due to reasons comprising, poor quality of construction, poor workmanship, old construction age, interventions made by people, the design code of the time – if ever was applied, lack of maintenance and inadequate repair after previous damaging seismic events. This type suffered not only non-structural damage but also structural damage including partial or total collapse of the load-bearing masonry walls.

As presented before the magnitude and ground acceleration of this earthquake are of an earthquake with return period of 95 years from the probabilistic seismic map. According to EC-8 on this types of earthquakes the buildings should perform on DL limit state. But in many occassions buildings have performed in SD and NC state and even collapsing in some part like Thumane, for example. Thumane was the most hardly hitted whith many old masonry buildings, done with volunteer work and poor workmanship. Buildings have collapsed and even caused victims among the inhabitants. Koder-Thumane city was very near the epicentre and the values of the peak groud accelerations on this zone are estimated to be around (25-28) %g. As shown in the chapter of spectrum based analysis most of the buildings have no capacity to bear such a strong ground motion. In Vora and Durres as can be seen on the shake ground map these values are lower around (20-22) %. Many buildings studied especially from Vora region, will be shown later on this study, have significant damage and even near collapse in some cases. This is also in accordance with the spectrum based analysis results for most of the stuided templates. Meanwhile in Tirana the peak ground acceleration values are low, because the epicentre is farther away comparing to Vore or Durres. Values here differ from (12-16) %g. Also the inspections done on most of the buildings are in damage limitation state mostly, and sometimes in significant damage phase.


Figure 254: Collapsed masonry building in Thumane

Figure 255: Building in Vore classified in NC state

The values of peak ground acceleration are a good estimatee, but it must be said that these values vary in many cases from soil conditions and site to source effects.

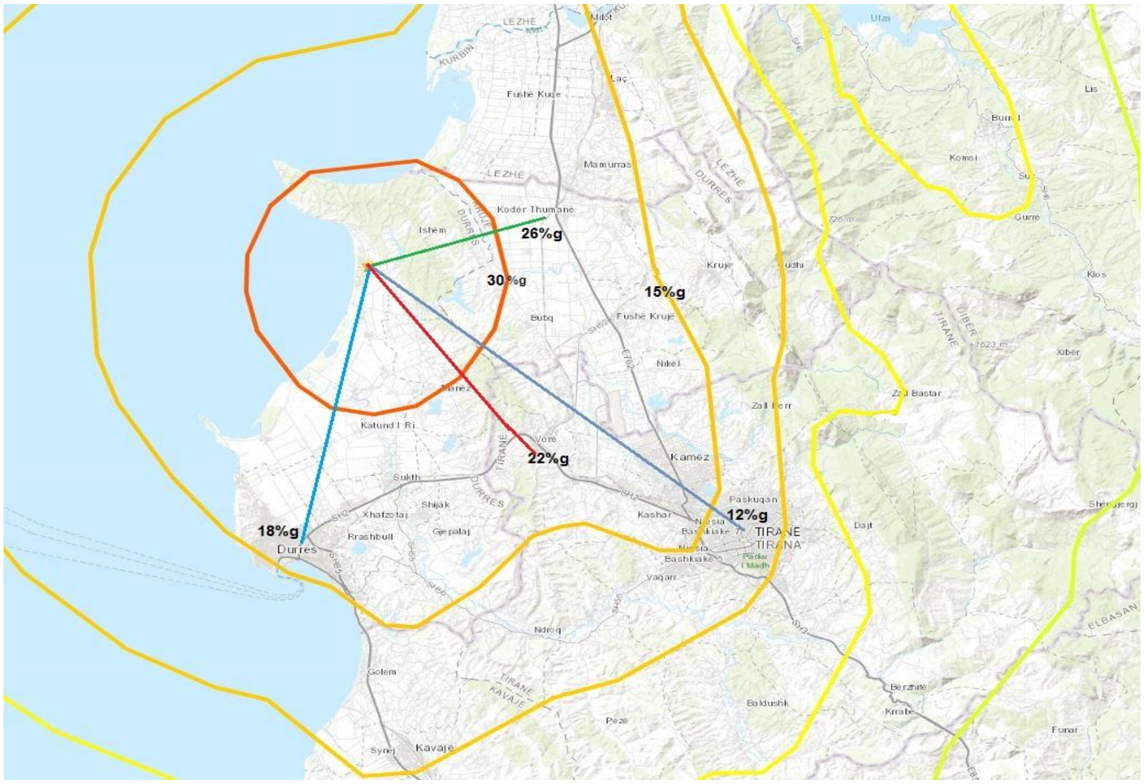

Figure 256: Map of estimated P.G.A during the strong motion sequence of the earthquake

Table 104: Estimated Peak Ground Acceleration by city

City	Estimated P.G.A
Thumane	(26-28)%g
Vore	(20-22)%g
Durres	(16-18)%g
Tirane	(10-16)%g

Table 105: Spectrum based analysis for all buildings

Building	0.12g	0.16g	0.2g	0.24g	0.26g	0.3g
% DL	73.68%	15.78%	5.26%	-	-	-
% SD	26.32%	68.42%	57.89%	15.79%	5.26%	-
% NC	-	15.80%	31.59%	26.32%	31.58%	5.26%
% COLLAPSE	-	-	5.26%	57.89%	63.16%	94.73%

According to spectrum based analysis, most of the URM buildings should be:

-in Tirana DL to SD - in Durres SD

-in Vore SD to NC phase -in Thumane NC to Collapse

7.3 Investigated buildings

7.3.1 Buildings in Thumane

The buildings of Thumane region have suffered an estimateed a_g around (26-28) %g during the strong motion earthquake sequence. For each building, the existing conditions of the structures are evaluated based on the detailed in-site inspections of the buildings by considering provisions of modern seismic guidlines (EC-8).

7.3.1.1 Collapsed 5 story building of template B2 in Thumane

The building had a plan similar to template B2 but the original B2 template has 4 stories, meanwhile this building had 5 stories. It was built in the early 60s, but not with proper workmanship, mostly by the inhabitants of the regions that built their own home. Also the material properties are very low and do not meet the conditions of today codes. Also very much degradation was observed even before the quake.

Figure 257: Collapsed building of template B2 plus one story in Thumane

After the first earthquake of 21 September 2019, this building was classified as uninhabitable and was damaged in structure but was not repaired and this led to total collapse after the 26 Novemeber 2019 earthquake sequence.

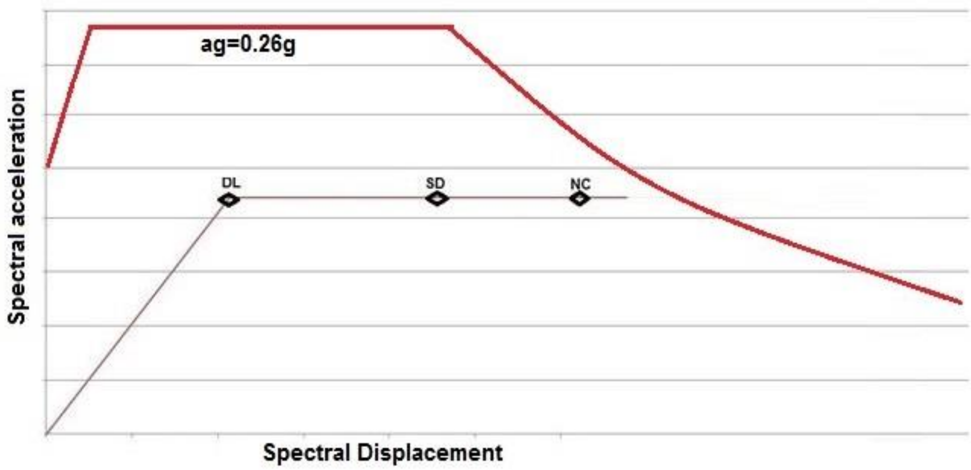

Figure 258: Demand of inelastic spectrum a_g = 0.26g versus capacity of the building

As seen from the photos, the building has totally collapsed because various wall elements have totally failed to bear horizontal loads. Damage was concentrated on one corner of the building. The fail mechanism is mostly dominated by torsion effects, but also from fail of slabs, that do not work as proper rigid diaphragms. If the capacity of the building templates B2 are compared with the estimated a_g=0.26g, and as seen from the figure the capacity curve doesnt intersect with the spectrum demand, meaning that the building has no capacity to bear such a high ground acceleration. This is also verified by the collapse of the building during the earthquake sequence.

Table 106: Comparison of a_g from earthquake estimate and spectrum based analysis result

Earthquake estimatee	a_g level	a_g DL	a_g SD	a_g NC
2.6-2.8 m/s^2	**B2 4floor**	1.288 m/s^2	2.506 m/s^2	2.935 m/s^2
	B2 intervention	1.128 m/s^2	1.915 m/s^2	2.199 m/s2
		Passed	Passed	Passed

7.3.1.2 Building of template A2 in Thumane

The building has a plan of template A2 but it has some added areas and balconies, and is building nr.7 located in street Rira in Thumane. It was built in the 1958, but not with proper workmanship, mostly by the inhabitants of the regions that built their own home. Also the material properties are very low and do not meet the conditions of today codes.

Figure 259: Building nr.7 in street "Rira" in Thumane of template A2

Much degradation was observed in the building even before the quake. After the first earthquake of 21 September 2019, this building has not been repaired, even though it had structural damage. As seen from the photos, the building has some serious deficiency. The mortar quality is very poor and this led to spall of mortar and separations all over the load bearing masonry. Damage was concentrated on the first floor walls, and especially in the corner parts, where spall of mortar and separation between masonry elements have occurred. Shear cracks in load bearig walls are up to 30 mm wide. This building is Near Collapse and strengthening of the building seems not efficient due to its probable high costs and consequently inefficient. These blocks should be demolished. [Papa Dh. Et.al., 2020]

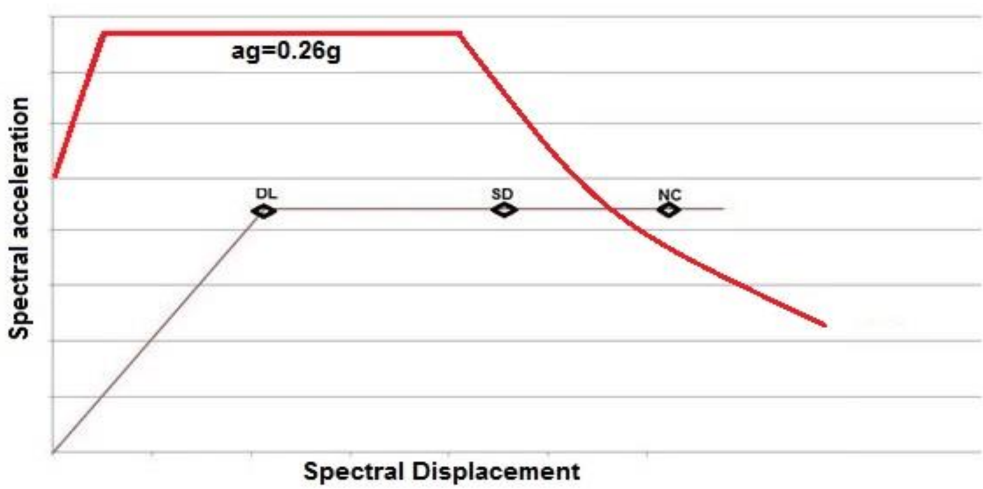

Figure 260: Demand of inelastic spectrum a_g =0.26g versus capacity of the building

If the capacity of the building templates A2 are compared with the estimated a_g=0.26g, and as seen from the figure the capacity curve intersects with the spectrum demand over SD point, meaning that the building has severe damage and is in NC phase. This is also verified by the observed damage of the building during the earthquake sequence.

Table 107: Comparison of a_g from earthquake estimate and spectrum based analysis result

Earthquake estimatee	**a_g DL**	**a_g SD**	**a_g NC**
2.6 - 2.8 m/s^2	1.307 m/s^2	2.148 m/s^2	2.88 m/s^2
	Passed	Passed	Not reached

7.3.1.3 Building of template A1 in Thumane

The building has a plan of template A1 but it has some added areas and balconies. Building nr.13 is located in street "Rira" in Thumane. It was built in the 1963, but not with proper workmanship, mostly by the inhabitants of the regions that built their own home. Also the material properties are very low and do not meet the conditions of today codes. Also very much degradation was observed even before the quake. After the first earthquake of 21 September 2019, this building has not been repaired, even though it had damage.

Figure 261: Building nr.13 in street "Rira" in Thumane of template A1

As seen from the photos, the building has some serious deficiency. The mortar quality is very poor and this led to cracks and separations all over the load bearing masonry. [Papa Dh. Et.al., 2020] Damage was concentrated on the second floor wall especially in the corner parts, where shear cracks have occurred. This cracks in load bearing walls are up to 30 mm wide However, this earthquake is considerably smaller than the design earthquake in Eurocode 8.

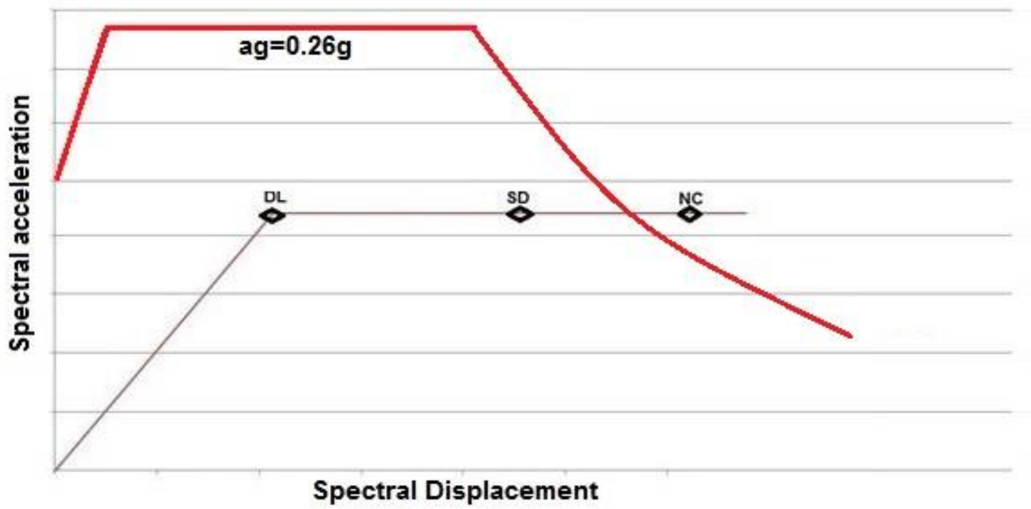

Figure 262: Demand of inelastic spectrum a_g=0.26g versus capacity of the building

If the capacity of the building templates A2 are compared with the estimated a_g=0.26g, and as seen from the figure the capacity curve intersects with the spectrum demand over SD point, meaning that the building has severe damage and is in NC phase. This is also verified by the observed damage of the building during the earthquake sequence. Strengthening of the building seems not efficient due to its probable high costs and consequently inefficient. These blocks should be demolished.

Table 108: Comparison of a_g from earthquake estimate and spectrum based analysis result

Earthquake estimatee	a_g DL	a_g SD	a_g NC
2.6 - 2.8 m/s^2	1.974 m/s^2	2.699 m/s^2	3.018 m/s^2
	Passed	Passed	Not reached

7.3.2 Buildings in Vore

The buildings investigated from Vora region have suffered an estimateed a_g around (20-22) %g during the strong motion earthquake sequence. For each building, the existing conditions of the structures are evaluated based on the detailed in-site inspections of the buildings by considering provisions of modern seismic guidlines (EC-8).

7.3.2.1 Building of template C1A in Vore

Building nr.5, which were damaged during the 26 November 2019 earthquake, have 5-story unreinforced masonry building constructed by using solid clay bricks. This buildingis of template C1A studied before on this study. The construction of the buildings was completed in 1981. Generally, they have regular plans in elevation supported by load bearing unreinforced masonry walls. The load bearing walls were formed by solid clay bricks and the partition walls with hollow bricks. This building underwent changes including some plaster renewals and paintings after the September 12, 2019 earthquake. For that reason, from the outer parts, damages are not clearly observed with visual inspection.

Figure 263: Buiding nr.5 in Vora region of template C1A

As seen from the photos, the material quality especially the mortar is very weak and could not prevent the segregation of the bricks. Damage was concentrated on the 1^{st}, 2^{nd} and 3^{rd} floors. Level of the damage on load bearing walls was severe whereas the partition walls were heavily damaged. Typical damage patterns like shear craks, spalling of mortar, separation of the load bearing wall segments especially over or under the openings are observed all over the first three floors and are shown in the figure below. On the upper floors, it was observed that the doors are not closed properly due to the possible drift concentrations on load bearing elements. According to the inspections and damage surveys done on the buildings, the buildings have serious deficiencies which do not meet the conditions stipulated in Eurocode 8. Especially, on the first 3 floors, severe damage patterns were observed on load bearing walls and very heavy damage was observed on partition walls. Shear cracks in load bearing walls are (25-30) mm wide. Material quality is extremely weak and caused degradation by time. Also, slab damages were observed on the lower stories of the building. Repairing or retrofitting of the buildings seem quite difficulty. [Bilgin H. et.al., 2020]

Figure 264:Typical damage patterns observed at several locations of the building nr.5 blocks

Figure 265: Heavy shear cracks (more than 3 cm separation) on load bearing walls and extensive damage on non- load bearing wall (left), serious damage observed on outer facade of the building in lower stories (right)

If we compare the spectrum analysis results of template C1A and the estimateed a_g level of the earthquake for Vora region, the performance of the building is on NC phase and slighly passing SD limit point.

Table 109: Comparison of a_g from earthquake estimate and spectrum based analysis result

Earthquake estimatee	**a_g DL**	**a_g SD**	**a_g NC**
2.0-2.2 m/s^2	1.182 m/s^2	2.019 m/s^2	2.614 m/s^2
	Passed	Passed	Not reached

In conclusion, during the 26 November 2019 earthquake, serious structural failures occurred in various parts of the structures causing heavy damages. However, this earthquake is considerably smaller than the design earthquake in Eurocode 8. Considering the actual damage status of the building, including the age, material quality as well as the low stiffness of the load bearing system, strengthening of the building seems not efficient due to its probable high costs and consequently inefficient. According to the opinion of our team, these blocks should be demolished. The inspected damage and performance are in accordance with the results of spectrum based analysis.

7.3.2.2 Building nr.11/1 in Vore

Figure 266: Buiding nr.11/1 in Vora region of template C2

Building nr.11/1 blocks, which were damaged during the 26 November 2019 earthquake, have 5-story unreinforced masonry building constructed by using solid clay bricks. This building is of template C2 studied before on this study. The construction of the buildings was completed in 1990. Generally, they have regular plans in elevation supported by load bearing unreinforced masonry walls. The load bearing walls were formed by solid clay bricks and the partition walls with hollow bricks. This building underwent changes including some plaster renewals and paintings after the September 12, 2019 earthquake. For that reason, from the outer parts, damages are not clearly observed with visual inspection.

Figure 267: Typical damage patterns observed at several locations of the building block 11/1

As seen from the photos, the material quality especially the mortar is very weak and could not prevent the spall of the bricks. Damage was concentrated on the 2nd and 3rd floors. Level of the damage on load bearing walls was moderate whereas the partition walls were heavily damaged. This building suffered not only non-structural damage but also very heavy structural damage with some separation on load bearing walls due to reasons comprising old construction age, poor quality of material and construction, poor workmanship, interventions made by people, the design code of the time- if ever was applied-lack of maintenance and inadequate repair after previous damaging seismic events. Typical damage patterns like spall of mortar and separations on the corners, spall of mortar and sprandel cracks near the window openings, partial collapse of partiotion walls are observedand are shown in the figures above. Shear cracks in load bearing walls are (25-30) mm wide.

If we compare the spectrum analysis results of template C2 and the estimateed a_g level of the earthquake for Vora region, the performance of the building is on NC phase and slighly passing SD limit point.

Table 110: Comparison of a_g from earthquake estimate and spectrum based analysis result

Earthquake estimatee	**a_g DL**	**a_g SD**	**a_g NC**
2.0-2.2 m/s^2	1.561 m/s^2	2.184 m/s^2	2.671 m/s^2
	Passed	Passed	Not reached

In conclusion, during the during the November 26, 2019 earthquake, shear cracks occurred in various parts of the structure causing moderate to heavy damages. However, this earthquake is considerably smaller than the design earthquake in Eurocode 8. Considering the actual damage status of the building; including the age, material quality as well as the low stiffness of the load bearing system, buildings could be retrofitted by taking the necessary measures, however the costs may be quite high. [Bilgin H. et.al. ,2020] The inspected damage and performance are in accordance with the results of spectrum based analysis.

7.3.2.3 Building nr.6 in Vore

Figure 268: Buiding nr.6 in Vora region of template C3

Building nr.6 blocks, which were damaged during the 26 November 2019 earthquake, have 5-story unreinforced masonry building constructed by using solid clay bricks. This building is of template C3 with some changes in plan. The construction of the buildings was completed in 1985. The load bearing walls were formed by solid clay bricks and the partition walls with hollow bricks. This building underwent changes including some plaster renewals and paintings after the September 12, 2019 earthquake. For that reason, from the outer parts, damages are not clearly observed with visual inspection. During the inspection inside the building, a considerable damage was observed at every story. We observed a 45^0 inclined serious shear crack on a number of walls on the first floor and second floors. Those cracks in load bearing walls are up to 30 mm wide. As seen from the photos, the material quality especially the mortar is very weak and could not prevent the segregation of the bricks. Damage was concentrated on the 2^{nd} and 3^{rd} floors. Level of the damage on load bearing walls was moderate-severe whereas the partition walls were heavily damaged.

Figure 269: Serious shear craks on load bearing walls and the piers of the building

Typical damage patterns like typical x shear cracks, spall of mortar and separations on the corners, spall of mortar and sprandel cracks near the window openings, shear craks on pier elements on the last story walls are observed and are shown in the figures below.

Figure 270: Heavy shear cracks on load bearing walls on the second floor

On the upper floors, it was observed that the doors are not closed properly due to the possible drift concentrations on load bearing elements. According to the inspections and damage surveys done on the building the building has serious deficiencies which do not meet the conditions stipulated in Eurocode 8. Especially, on the 2nd, 3rd and 4th floors moderate to severe damage was observed on load bearing walls and heavy damage was observed on partition walls. Material quality is very weak and caused degradation by time. Also, slab damages were observed on the lower stories of the building. Although some of the inappropriate situations can be removed by simple methods, some of them are quite serious and very difficult to remove for the building.

If we compare the spectrum analysis results of template C2 and the estimateed a_g level of the earthquake for Vora region, the performance of the building is on NC phase depending on soil conditions.

Table 111: Comparison of a_g from earthquake estimate and spectrum based analysis result

Earthquake estimatee	**a_g DL**	**a_g SD**	**a_g NC**
2.0-2.2 m/s^2	1.098 m/s^2	2.062 m/s^2	2.53 m/s^2
	Passed	Passed	Not reached

In conclusion, during the during the November 26, 2019 earthquake, serious structural cracks occurred in various parts of the structure causing moderate-heavy damage. Considering the actual damage status of the building, including the age, material quality as well as the low stiffness of the load bearing system, strengthening of the building may be costly and consequently inefficient.[Bilgin H. et.al. ,2020] The inspected damage and performance are in accordance with the results of spectrum based analysis.

7.3.3 Buildings in Tirana

The buildings from Tirana region have suffered an estimateed a_g around (12-16) %g during the strong motion earthquake sequence. For each building, the existing conditions of the structures are evaluated based on the detailed in-site inspections of the buildings by considering provisions of modern seismic guidlines (EC-8).

7.3.3.1 Building of template C1B near "Vasil Shanto" in Tirana

Building nr.3 is located near "Vasil Shanto" school at street "Preng Bib Doda". It was constructed in 1978 of C1B template and is 5 story of silicate brick masonry. In this area are 3 similar buildings of this template, built as as a block. Although this buildings have some added balconies, they have been well maintained. During the during the November 26, 2019 earthquake, light damage have occurred on this building types, mostly on non-structural elements. However, this earthquake is considerably smaller than the design earthquake in Eurocode 8. Considering the actual damage status of the building, including the age, material quality, strengthening of the building should be considered, because in this area are expected stronger earthquakes with a return period of 475 years, that can seriously risk the building.

Figure 271: Building nr.3 of C1B template near "Vasil Shanto"

Figure 272: Light damage patterns on non-structural elements

If the capacity of the building templates B2 are compared with the estimated a_g=0.12g, and as seen from the figure the capacity curve intersect with the spectrum demand, near the DL point, meaning that in this structure minor damage have occured. This is also verified by the observed damage on the building during the earthquake sequence.

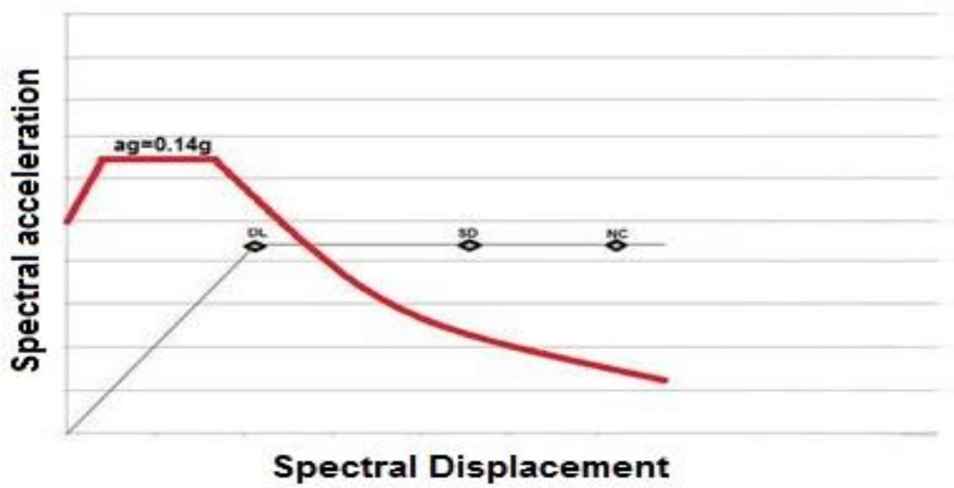

Figure 273: Demand of inelastic spectrum a_g = 0.14g versus capacity of the building

Table 112: Comparison of a_g from earthquake estimate and spectrum based analysis result

Earthquake estimatee	**a_g DL**	**a_g SD**	**a_g NC**
1.2-1.6 m/s^2	1.067 m/s^2	1.801 m/s^2	2.299 m/s^2
	Passed	Not reached	Not reached

7.3.3.2 Building of template C1B in Kombinat, Tirana

The building is located at street "Rruga e Qelqit" in Kombinat Tirana. It was constructed in 1978 of C1B template and is 5 story of silicate brick masonry. In this area are 4 similar buildings of this template, built as as a block. Although this buildings has some opening on first floor, but is well maintained. During the during the November 26, 2019 earthquake, light damage have occurred on load bearing walls and moderate damage on non- structural damage.

Figure 274: Building of C1B template at "Rruga e Qelqit", Kombinat

This building is in Significant Damage phase, but with repairable damage. However, this earthquake is considerably smaller than the design earthquake in Eurocode 8. Considering the actual damage status of the building, including the age, material quality, strengthening of the building should be considered, because in this area are expected stronger earthquakes with a return period of 475 years, that can seriously risk the building.

Figure 275: Light damage patterns on non-structural elements

If the capacity of the building templates B2 are compared with the estimated a_g=0.14g, and as seen from the figure the capacity curve intersect with the spectrum demand, near the DL point, meaning that in this structure minor damage have occured. This is also verified by the observed damage on the building during the earthquake sequence. [Bilgin H. et.al. ,2020]

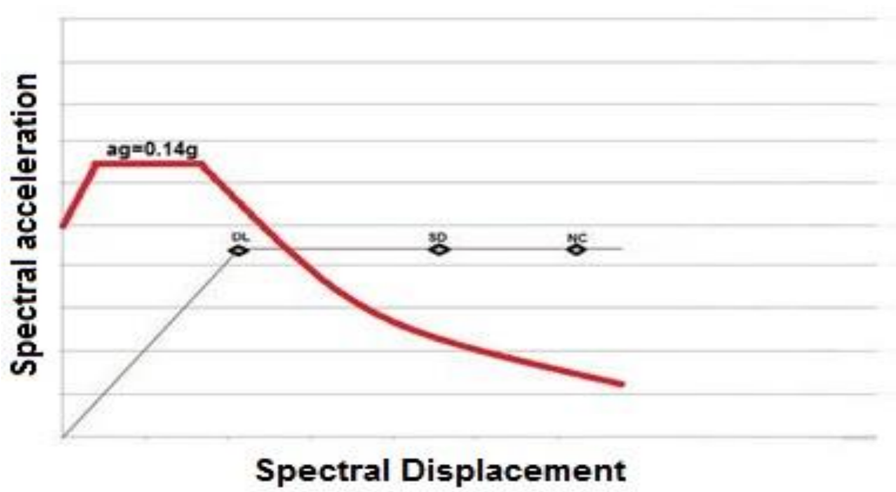

Figure 276: Demand of inelastic spectrum a_g=0.14g versus capacity of the building

Table 113: Comparison of a_g from earthquake estimate and spectrum based analysis result

Earthquake estimatee	**a_g DL**	**a_g SD**	**a_g NC**
1.2-1.6 m/s^2	1.067 m/s^2	1.801 m/s^2	2.299 m/s^2
	Passed	Not reached	Not reached

7.4 Conclusions

The results from the investigated buildings are in accordance with the spectrum analysis data from the earthquake.

The masonry buildings in Thumana region have suffered the most because they were more near the epicentre of the earthquake and the peak ground acceleration was felt (26-28) %g. Many masonry buildings in these region have collapsed and also many are classified in NC state by the observation and expertise of Construction Institute. These results are in accordance with spectrum based analysis for these level of ground acceler/ation.

The masonry buildings in Vora region have also suffered a lot from this earthquake because they were near the epicentre of the earthquake and the peak ground acceleration was felt (20-22)%g. Many masonry buildings in these region are classified in NC state by the observation and expertises of Construction Institute. 13 buildings in the center of Vora were classified in

NC state and are going to be demolished by the government because of high cost of repair. These results are in accordance with spectrum based analysis for these level of ground acceleration.

The masonry buildings in Tirana and Durres region have suffered not as much as the prior buildings because they were further the epicentre of the earthquake and the peak ground acceleration was felt (10-18) %g. Most of the masonry buildings in these region have performed well with light structural damage based on the observation and expertise of Construction Institute. But in some zones, like Kombinat for example, some masonry buildings have moderate to severe damage, this coming mostly because of the bad soil conditions of this zone and also from the degradation of the materials escpecially mortar. The soil conditions can amplify the felt ground acceleration many times. These results are in accordance with spectrum based analysis for these level of ground acceleration.

CHAPTER 8

RESULTS, CONCLUSION AND RECCOMENDATIONS FOR FURTHER STUDIES

The masonry building stock in Albania is designed with outdated codes, that take in consideration a lower seismic demand compared to EC-8. [KTP-63, 1963; KTP-78, 1978; KTP-N2-89, 1989]. Also, degradation of materials by time and interventions made on the original buildings have lowered the load bearing capacity of the structures. Within the scope of this study, nineteen masonry buildings from ten different types of template projects which were commonly used by the Ministry of Public Works and Settlement of Albanian Government in several parts of the country were selected to represent major percentage of residential buildings. These template designs were examined in order to contribute to the studies related to the evaluation and strengthening of existing masonry buildings located in high seismic regions of the country. Nonlinear static analysis methods and earthquake performance determination principles in Eurocode 8, Part 3 were used to analyze these projects. Seismic deformation capacities of each building were obtained by nonlinear static analyses. Nonlinear time-history analysis was used to predict the seismic displacement demands of the studied buildings by using "Equivalent Single Degree of Freedom System Approach" under the selected ground motions. The results of spectrum based, and time-history analysis show a high vulnerability of the masonry stock, and a highly expected damage, for this type of buildings under strong earthquake shakings. These results are verified by the investigations done on masonry buildings after 26.11.2019 Adriatic Sea earthquake.

The casualties from this earthquake where very high, with a total of 51 people killed in the earthquake, with about 3.000 injured and around 44.582 buildings affected by the earthquake and investigated later by Construction Institute of Albania. Although very high casualties, this earthquake parameters compared to probabilistic seismic hazard map of Albania for horizontal PGA, falls within the extents of an earthquake with the return period of 95 years. According to EC-8, for this type of earthquakes, the structure should perform in DL state. Many masonry structures not only have exceeded this state but in Thumane some have collapsed, in Vore and Durres many are in NC state, and some buildings in Tirana on SD stare. For an expected earthquake with a return period of 475 years, the peak ground acceleration values for cities like Durres, Shkodra, Korca and Elbasan are around 0.3g, while for cities like Gjirokaster, Sarande and part of Vlora even higher up to 0.4g. Considering that this cities have a high population of this buildings, and this buildings capacity are lower than 0.3g, the energetic potential is capable of creating a catastrophe at the national level.

According to the finding of this study all the buildings reach NC performance level for an earqauke level of 0.20-30g. So, the main factor affecting the safety of the building is its location, with buildings in higher risky seismic zones being more vulnerable. The second governing factor is the various interventions made on these buildings. These are very popular due to social and politic factors, during the 1990-2000s. Interventions made on first floor, like removing walls for opening façade of stores, or added additional stories significantly lowered the load bearing capacity of these buildings, and made them more vulnerable to seismic events. Another major factor is the era of construction. Although, for the time being, these buildings were constructed following specifications and regulations of KTP, the code deficiency have led to highly increases the vulnerability of these type of buildings. Especially buildings of templates A and B constructed in pre 1979 era, took into consideration a relatively low seismic demand. Time also implements another factor, such as degradation of material, especially encountered on mortar. Poor workmanship also plays its role here, where in some regions and hoods like Kombinat, the habitants of the buildings have participated as volunteer workers. Principal construction material also affects the vulnerability. From the analysis of this study, but also as a conclusion from the post-earthquake inspections of Construction Institute, silicate buildings were more damaged and had a worse performance comparing to clay buildings. The bonding between clay and mortar is better than silicate-mortar, giving so a greater value of f_{vk} shear strength of masonry. The confined masonry buildings are of the 1978 to 1990 era and have perimeter columns of C12/15 that increases lateral resistance of the shear walls, but this still high deficiency and vulnerability is viewed on this type. Buildings with higher height, for all these factors discussed and with the increased seismic demand from coming from height, show a higher vulnerability, comparing to shorter ones.

In this study the buildings were modeled using 3muri software package, that uses an equivalent frame macro-model approach. Non-linear pushover analysis was performed for all the cases, to evaluate the building capacity. The capacity of the each building was compared to seismic demand by following two different approaches: performance based assessment N-2 method and non-linear time-history analysis. For 8 buildings of the studied templates, that were subjected to earthquake ground motion of 26 Novemeber 2019, in-site inspections were made and the damage was compared to the results of prior analysis. Past earthquake reconnaissance team reports and the evidence of the observed structural damage and collapses have shown that damage to structures is increased under near field ground motions. This result was also observed from this study. Buildings subjected to near field ground motions, have shown a higher ratio of exceedance of SD and NC limit states, comparing to the results of far field earthquakes. If the performance-based assessment N-2 method is compared with the time history analysis, they show a good harmony with each other. In chapter VII the results of these two analyses have been compared with the real damage occurred during 26 November 2019 sequence, and for all the cases, they show a good correlation between the estimated PGA of the earthquake in the location, and the predicted damage from performance based assessment. During pushover analysis, failure mechanism for each template were presented, and in some investigated cases, the real damage has occurred in the predicted areas of the structure. It must be said that the earthquake hit direction, and the implemented load case of pushover analysis, from which these failure mechanisms have derived are not the same. But the failure mechanism shows the more vulnerable parts of the structure, and in the investigated damage in most of the cases has occurred in those areas.

The significance of the findings is further studied by examining the nonlinear behavior of selected buildings subjected to near and far-fault ground recordings. Findings regarding displacement capacities of residential buildings at different performance levels, weak points, causes of damages observed in past earthquakes and proposed solutions for buildings with insufficient earthquake performance are summarized below:

1. In the begging of this study, masonry buildings were classified based on era of construction, height of the building, principal material of construction and location of the building.
2. For the determination of the material characteristics of the selected masonry structures, destructive tests were made on bricks, mortars and brick pieces according to the relevant European norms [EN1052-1, EN1052-2, EN1052-3, EN1052-4 and EN1052-5]. Based on the results obtained from the laboratory test results, the material characteristics of the structures were determined. By examining the test results for the residential buildings, wall strengths were obtained to be used in earthquake analysis.
3. The material strengths in all residential buildings with pre-1989 projects were compared with the blueprints data and analytical models were prepared according to the findings obtained from the experimental results. It was observed that red clay and silicate clay bricks were commonly used in the residential buildings all over the country.
4. According to the analysis results, capacity curves obtained by pushover analysis reveal that URM building constructed by the red clay bricks performed better than the silicate bricked ones.
5. Based on the capacity evaluation; in contrast to the type of building constructed by clay masonry, silicate brick buildings showed stiffer and slightly stronger response. Yet, at similar values of in-plane, lateral drift, they exhibited more damage based on the analytical simulations. This observation was also monitored during the November 26, 2019 Durres Earthquake. Since the material is stiffer, the increased damage was not unforeseen, but the building also displayed a more brittle response during this earthquake. This appears to suggest that buildings built of calcium-silicate brick are more vulnerable to damage. Such observations were observed on wall specimens tested in northern Europe, as well [Korswagen et al., 2020]
6. When looking at the features of the examined residential buildings, they are generally rectangular in plan; It consists of quite long load bearing walls in one direction and lesser amount in the other direction. This has been found not only in the type projects in this study,

but also in many other residential buildings examined by the EPOKA University and Construction Institute [Bilgin and Korini, 2012; Bilgin and Huta, 2018; Act of expertise reports after November 26, 2019 Earthquake]. This practice caused the structures to have different seismic capacity values in both directions. For this reason, the ductility values of such structures in one direction become relatively low. In addition, for most of the projects that were constructed at that time, such applications have been made with the misconception that the long direction would have always better capacity. This situation was observed with a significant effect on both horizontal strength and displacement capacity in buildings with a lower wall ratio by examining the capacity curves.

7. In the performance evaluation of residential buildings, choices were made from the earthquakes that occurred in recent years and earthquake records reflecting various characteristics in FEMA P-752 (2013). In the nonlinear dynamic analysis of the structures, performance evaluations were made under each earthquake effect by using these earthquake records. To comparatively study influence of the far and near-fault earthquakes on the seismic behavior of the template designs, a total of 54 near-fault and 46 far-fault ground motions recorded on dense-to-firm soil sites were used for seismic performance evaluation.
8. For the studied template designs, the near-fault ground motions resulted in higher displacement demands compared to far-fault ones. This shows the damage potential of near-fault records due to the different relative or absolute energy exertion potential to the structural systems.
9. The main weakness of the residential buildings is the high displacement demands due their inadequate lateral load bearing capacities and stiffness under the considered earthquakes.
10. The impacts of near-fault ground motion characteristics on the seismic performance of low-story buildings are notable when compared with mid-rise ones.
11. A detailed examination of the exceedance ratio statistics showed that low-rise template designs perform better than mid-rise ones.
12. Analyses results showed that near-fault effects on the response of the masonry structures were more notable on the SD and NC limit states. For LD performance level, far-fault records gave more critical values. This could be justified with the frequency content of the records as a prominent issue.
13. In many modern earthquake codes of practice, the level of Life Safety performance is aimed in the design earthquake for residential buildings. The displacement demands of the selected earthquakes corresponding to the LD, CG and NC levels were calculated and the capacities of the residential buildings were compared to the capacities of the buildings. In a possible earthquake that will reflect the past earthquakes, LD is not satisfied for all buildings whereas SD level is not met in many residential buildings. Moreover, many of the investigated residential structures cannot meet the SD level and need to be reinforced first.
14. Analytical outcomes match the damage results observed in residential buildings in the 2019 Durres Earthquakes. Many housing structures were damaged in these earthquakes, especially due to poor material quality. (Bilgin and Hysenlliu, 2020; Hysenlliu et al, 2020; Act of expertise reports by Construction Institute).
15. The findings of this study support high damaging property of 1985 Nahanni, 1989 Loma Prieta, 1990 Iran, 1992 Erzincan, 1992 Cape Mendocino, 1994 Northridge, 1999 Chile, 1999 Kocaeli and Duzce earthquakes for the existing masonry buildings.

16. Considering the findings of this study together with the damage surveys done by the author together with a reconnaissance team after the 2019 Durres Eartquakes, it can be said that decision makers should be aware of the catastrophic nature of such brittle systems when weighing options for earthquake mitigation since a large inventory of the current building stock consist of such masonry and was built before the legislation of new guidelines.
17. The results of this current study were limited to number of the selected building configurations and a specific masonry typology.
18. For future studies, additional building typologies with the corresponding important parameters could also be explored in order to expand the findings of this study by considering more sophisticated modeling approaches.

The findings obtained in this study are believed to be used in the reinforcement studies to be carried out in order to increase the examined structures' performance levels defined in EC-8, Part 3. Such studies on common type projects will contribute to the study of many buildings at the same time.

REFERENCES

Aliaj Sh., "Harta e carjeve sizmo-tektonike të Shqipërisë në shkallë 1:200.000" IGJEUM, Tirana (2000)

Applied Technology Council, ATC-40. Seismic evaluation and retrofit of concrete buildings, Vols. 1 and 2. California, (1996)

Applied Technology Council, ATC-40. Seismic evaluation and retrofit of concrete buildings, Vols. 1 and 2. California, (1996).

Arkivi Teknik Qëndror I Ndërtimit, " Ndërtesa residenciale tip 58/2", Tiranë (2018)

Arkivi Teknik Qëndror I Ndërtimit, " Ndërtesa residenciale tip 63/1", Tiranë (2018)

Arkivi Teknik Qëndror I Ndërtimit, " Ndërtesa residenciale tip 69/3", Tiranë (2018)

Arkivi Teknik Qëndror I Ndërtimit, " Ndërtesa residenciale tip 72/1", Tiranë (2018)

Arkivi Teknik Qëndror I Ndërtimit, " Ndërtesa residenciale tip 72/3", Tiranë (2018)

Arkivi Teknik Qëndror I Ndërtimit, " Ndërtesa residenciale tip 77/5", Tiranë (2018)

Arkivi Teknik Qëndror I Ndërtimit, " Ndërtesa residenciale tip 83/3", Tiranë (2018)

Arkivi Teknik Qëndror I Ndërtimit, " Ndërtesa residenciale tip 83/10", Tiranë (2018)

Arkivi Teknik Qëndror I Ndërtimit, "Buletin Informativ nr.2", Tirane (1999)

Arkivi Teknik Qëndror I Ndërtimit, "Ndërtesa residenciale tip 40/1", Tiranë (2018)

Asteris P.G. Plevris V., "Handbook of research on seismic assessment and rehabilitation of historic structures ", Engineering science reference (2015)

ASTM C109, "Standard test method for sampling and testing grout masonry", ASTM, (2008) ASTM-C67, "Standart methods for sampling and testing brick and structural clay tile mortar" , ASTM, (2008)

Baballeku M., "Vlerësimi I dëmtimeve strukturore në ndërtesat tip të sistemit arsimor" , Universiteti Politeknik I Tiranës (2014)

Backes, H. P., Behavior of Masonry Under Tension in the Direction of the Bed Joints, PhD thesis, Aachen University of Technology, Aachen, Germany. (1985)

Bego M., "Skeda Arkitekturë" Tiranë (2009)

Beyer, K. (2013). Performance limits of brick masonry spandrels. 12th Canadian Masonry Symposium Vancouver, British Columbia, June 2-5, (2013)

Beyer, K., Dazio, A. (2012) "Quasi-static cyclic tests on masonry spandrels," Earthquake Spectra 18(3): 907-929.

Bilgin H. and Hysenlliu M. "Comparison of near and far-fault ground motion effects on low and mid-rise masonry buildings", Jounal of Building Engineering, DOI: 10.1016/j.jobe.2020.101248 http://ees.elsevier.com

Bilgin H., Bidaj A., Hysenlliu M., " Raport mbi analizën e performances strukturore të godinës Vorë", Instituti I Ndërtimit, (2020)

Bilgin H., Bidaj A., Hysenlliu M., " Raport mbi analizën e performances strukturore të godinës Vorë", Instituti I Ndërtimit, (2020)

Bilgin H., Bidaj A., Hysenlliu M., " Raport mbi analizën e performances strukturore të godinës nr.3 tek Vasil Shanto, Tiranë", Instituti I Ndërtimit, (2020)

Bilgin H., Bidaj A., Hysenlliu M., " Raport mbi analizën e performances strukturore të godinës nr.13 në Kombinat, Tiranë", Instituti I Ndërtimit, (2020)

Bilgin H., Bidaj A., Hysenlliu M., "Raport mbi analizën e performances strukturore të godinës nr.5 në Vorë", Instituti I Ndërtimit, (2020) Bilgin H., Huta E., "Earthquake performance assessment of low and mid-rise buildings: Emphasis on URM buildings in Albania", Earthquake and Structures vol.14 June (2018)

Binda L. Lualdi M. Saisi A. "Non-destructive testing techniques applied for diagnostic investigation: Syracuse Cathedral in Sicily,Italy"], International Journal of Architectural Heritage, (2007)

Capsulla C., Arigento L. and Maione A. in their study "Seismic safety assessment of a masonry building according to Italian guidelines on Cultural Heritage: simplified mechanical-based approach and pushover analysis", Naples (2016)

Cattari S., Camilletti D., Marino S., Lagomarsino S. (2015) Valutazione della risposta sismica di edifici in muratura irregolari in pianta e con solai flessibili, Atti del XVI Convegno ANIDIS 2015 “L’Ingegneria sismica in Italia”.

CEB-FIP Model Code 90, Final version published by Thomas Telford Ltd., London, (1993)

Charney F., Talwalkar R., Bowland A., Barngrover B., "Nonlin-eqt: A computer program for earthquake engineering education", Toronto, Ontario, Canada, (2010)

Construction Institute of Albania, "Report of investigation and casualities of 26 November earthquake", Tirane, 2020.

CSEM-EMSC, “M6.4 ALBANIA on November 26th 2019 at 02:54 UTC”, 2019 https://www.emsc-csem.org/Earthquake/262/M6-4-ALBANIA-on-November-26th-2019-at-02-54-UTC

Dizhur, D., Ingham, J., Moon, L., Griffith, M., Schultz, A., Senaldi, I., Magenes, G., Dickie, J., Lissel, S., Centeno, J., Ventura, C., Leite, J., Lourenco, P. “Performance of masonry buildings and churches in the 22 February 2011 Christchurch earthquake“. Bulletin of the New Zealand Society for Earthquake Engineering 44(4): 279-296., (2011).

Elnashi A.S., Di Sarno L., "Fundamentals of earthquake engineering", WILEY (2003)

EN 1052-1. Methods of test for masonry. Determination of compressive strength. (1998)

EN 1052-3. Methods of test for masonry. Determination of shear strength. (1998)

EN 1996-1. European masonry design code. (2005). “Design of masonry structures. Part 1: General rules for reinforced and unreinforced masonry structures”

EN 1996-2. European masonry design code. (2005). “Design of masonry structures. Part 1: General rules: Structural fire design”

EN 1996-3. European masonry design code. (2006). “Design of masonry structures. Part 1: Simplified calculation methods for unreinforced masonry structures”

EN 1998-1. European seismic design code. (2004). “Design of structures for earthquake resistance. Part 1: General rules, seismic actions and rules for buildings”

EN 1998-3. European seismic design code. (2005). “Design of structures for earthquake resistance. Part 3: Assessment and retrofitting of buildings”

EN 1998-5. European seismic design code. (2005). “Design of structures for earthquake resistance. Part 5: Foundations, retaining structures and geotechnical aspects”

European Seismological Commision, “Eurpean Macroseismic Scale 1998”, ESC Working group “Macroseismic Scales”, GeoForshungsZentrum Postdam, Germany, (1998)

Fajfar P., Eeri M., “A nonlinear analysis method for performance based design”, Earthquake Spectra, Vol. 16, No.3, August (2000)

Fajfar P., Marusic D., Perus I., “The extension of N2 method to asymmetric buildngs”, Proceedings of the 4th European workshop on the seismic behavior of irregular and complex structures, Thessaloniki (2005)

Federal Emergency Management Agency, FEMA-356. Prestandard and commentary for seismic rehabilitation of buildings, Washington (D.C); (2000)

Federal Emergency Management Agency, FEMA-356. Prestandard and commentary for seismic rehabilitation of buildings, Washington (D.C); 2000.

Federal Emergency Management Agency, FEMA-440. Improvement of nonlinear static seismic analysis procedures. Washington (D.C); (2005)

Federal Emergency Management Agency, FEMA-440. Improvement of nonlinear static seismic analysis procedures. Washington (D.C); 2005.

FEMA, 1997, NEHRP guidelines for the seismic rehabilitation of buildings, FEMA 273, and NEHRP Commentary on the guidelines for the seismic rehabilitation of buildings, FEMA 274, Federal Emergency Management Agency, Washington D.C.

Formisano A., Chieffo N., "Non-linear static analyses on an Italian masonry housing building through different calculation software packages, Internation Journal of Energy and enviroment, Vol.12, (2018)

Fundo A et.al., "Probabilistic seismic hazard assessment of Albania" Tirane (2012)

Galasco A., Lagomarsino S., Penna A. (2002) Analisi sismica non lineare a macroelementi di edifici in muratura, Atti del 10° Convegno Nazionale ANIDIS “L’ingegneria sismica in Italia”, Potenza-Matera

Galasco A., Lagomarsino S., Penna A. (2006) On the Use of Pushover Analysis for Existing Masonry Buildings, Proc. First European Conference on Earthquake Engineering and Seismology, 3-8 September 2006, Geneva, Switzerland – paper n. 1080.

Galasco A., Lagomarsino S., Penna A., Resemini S. (2004) Non-linear Seismic Analysis of Masonry Structures, Proc. 13th World Conference on Earthquake Engineering, Vancouver, 1-6 August, paper n. 843, 15 p

Graziotti, F., Penna, A. and Magenes, G. (2013). “Use of equivalent SDOF systems for the evaluation of displacement demand for masonry buildings”. Proc. of VEESD 2013, Vienna, Austria.

http://www.3muri.com , 3muri software package S.T.A. Data, C.so Raffaello, 1210126 Torino

Hysenlliu M. and Bidaj A. “Evaluation of capacity and seismic performance of brick masonry buildings with and without structural interventions”, International Symposium for Environmental Science and Engineering Research ISESER 2019 Konya, Turkey, (2019) http://www.iseser.com

Hysenlliu M. and Bidaj A. “Structural system on high rise buildings”, International Conference of Civil Engineering ICCE 2017 , Polytechnic University of Albania, Faculty of Civil Engineering, Tirane, Albania (2017) http://www.icce.al

Hysenlliu M. and Bilgin H. “The use of macro element approach for the seismic risk assessment of brick masonry buildings”, CRIT-RE-BUILT, (2019)

Hysenlliu M. and Gjini A. “Prism testing of most used templates of masonry structures in Albania”, International Student Conference of Civil Engineering ISCCE 2018 Polytechnic University of Albania, Faculty of Civil Engineering, Tirane, Albania (2018)

Hysenlliu M. Bidaj A. Bilgin H. “Analiza e performances e ndërtesave muraturë me dhe pa ndërhyrje”, “Buletini I Shkencave Teknike”, Universiteti Politeknik I Tiranës (2020)

Hysenlliu M. Bidaj A. Bilgin H. “Influence of material properties on the seismic response of masonry buildings”, Research on Engineering Structures & Materials http://Jresm.org (2019)

Hysenlliu M., Bidaj A, Bilgin H., “Influence of material properties on the seismic response of masonry buildings”, Research on Engineering Structures & Materials (2020) http://dx.doi.org/10.17515/resm2020.177st0120

ICOMOS, "Principles for the analysis, conservation and structural restoration of architectural heritage", ICOMOS 14th General Assembly, in Victoria Falls, Zimbawe (2003)

IGJEUM, "Tërmeti I Durrësit I 26 Nëntorit 2019", Tiranë (2020)

Ilaria Senaldi, Guido Magenes & Jason M. Ingham: “Damage Assessment of Unreinforced Stone Masonry Buildings After the 2010-2011 Canterbury Earthquakes”, International Journal of Architectural Heritage: Conservation, Analysis, and Restoration, (2014).

Inel M. Bretz E. , Black E., Aschheim M., Abrams D., "USEE 2001 : Utility Software for Earthquake Engineering Report and User's Manual" , University of Illinois, (2001)

Inel M., Ozmen H. B., Bilgin H., “Re-evaluation of building damage during recent earthquakes in Turkey”, Engineering Structures, 2008

INGV, “Characteristics of Adriatic sea earthquake 26.11.2019”, National Intitute of Geo-physics and Vulcanology, Italy, 2019
http://shakemap.rm.ingv.it/shake/23487611/intensity.html
http://shakemap.rm.ingv.it/shake/23487611/pga.html

INSTAT, "The population of Albania in 2001 - Main Results of the Population and Housing Census", INSTAT, November (2002).

K.Cika, "Llacet dhe betonet", Tiranë (1969)

Kalkan E., Kunnath S.K. "Effective cyclic energy as a measure of seismic demand" Journal of Earthquake Engineering, Vol.11 No.5 (2007)

Klingner, RE., “Behavior of masonry in the Northridge (US) and Tecoma´n–Colima (Mexico) earthquakes: Lessons learned, and changes in US design provisions.” Construction and Building Materials (20): 209-19. (2006)

KTP-63, "Kushti Teknik I Projektimit". Tirane (1963)

KTP-9-78, "Kushti Teknik I Projektimit". Tirane (1978)

KTP-N2-89, " Kushti Teknik I Projektimit ", Tirane. (1989)

Kunnath S., “Performance-Based Seismic Design and Evaluation of Building Structures”. Handbook of Structural Engineering Second Edition, (2005)

L.Gambarotta, S.Lagomarsino, "On dynamic response of masonry panels", in Gambarotta L. (ed) Proc.Nat.Conf. "Masonry mechanics between theory and practice" Messina,Italy (1996)

Lagomarsino S., Penna A., Galasco A., Cattari S. (2013) TREMURI Program: an equivalent frame model for the nonlinear seismic analysis of masonry buildings, Engineering Structures, 56

Lekkas E., Mavroulis S., Papa Dh., “ The Novemeber 26,2019 Mw 6.4 Durres (Albania) earthquake”, Newsletter of Enviromental, Disaster, and crises management strategies, National and Kapodistrian University of Athens, ISSN 2653-9454, (2020)

Lourenco P.B., Barros J.A., Oliveira J.A. "Shear testing of stack bonded masonry", Construction and Building Materials, 18, (2004)

M. Moon, Lisa & Dizhur, Dmytro & Ingham, Jason & Griffith, M. Seismic Performance of Masonry Buildings in the Christchurch Earthquakes 2010-2011: A Progress Report. (2012).

Marotta A, Sorrentino L, Liberatore D, Ingham JM. “Vulnerability assessment of unreinforced masonry churches following the 2010–2011 Canterbury (New Zealand) earthquake sequence.” J Earthq Eng 21(6):912–934, (2017).

Miranda E., (2000), “Inelastic displacement ratios for displacement-based earthquake resistant design”, Proceedings of the 12th World Conference on Earthquake Engineering, Auckland, New Zeland Society for Earthquake Engineering

Mouyiannou, Amaryllis & Penna, Andrea & Rota, Maria & Graziotti, Francesco & Magenes, Guido. “Implications of cumulated seismic damage on the seismic performance of unreinforced masonry buildings”. Bulletin of the New Zealand Society for Earthquake Engineering. 47. 157-170. (2014).

N.Kuka et.al “Seismic hazard assessment of Albania by spatially smoothed seismicity approach”, Tiranë (2003)

NATO SfP – 983054 "Harmonization of seismic hazard maps for the Western Balkan countries", BSHAP, (2007-2010).

NATO SfP Project No. 983054, “Harmonization of seismic hazard maps for the western Balkan countries”, ORFEUS, Institut d’Estudius Catalanas (2008)

NTC, "Miniserial decree of infrastructures and transportations, technical rules for construction", M.D. Offical Gazette of the Italian Republic n.28 (2008)

Panagiotis G. Asteris, Vasilis Sarhosis, Amin Mohebkhah, Vagelis Plevris. L.Papaloizou. Petros Komodromos, Jose V. Lemos., “Numerical modeling of historic masonry structures”, IGI Global, (2016)

Papa Dh., " Vlerësim I performancës strukturore të ndërtesës nr.7 në rrugën ‘Rira’, Thumanë", Construction Institute of Albania, (2020)

Papa Dh., "Vlerësim I performancës strukturore të ndërtesës nr.13 në rrugën ‘Rira’, Thumanë", Construction Institute of Albania, (2020)

Penna A, Morandi P, Rota M et al "Performance of masonry buildings during the Emilia 2012 earthquake." Bull Earthq Eng 12:2255–2273. (2014).

Penna A., Cattari S., Galasco A., Lagomarsino S. (2004) “Seismic Assessment of Masonry Structures by Non-linear Macro-element Analysis”, IV International Seminar on Structural Analysis of Historical Construction-Possibilities of Numerical and Experimental Techniques, Padova, 2004, Vol. 2

Penna A., Lagomarsino S., Galasco A. (2014) A nonlinear macro-element model for the seismic analysis of masonry buildings, Earthquake Engineering & Structural Dynamics, 43(2)

Penna, A., Calderini, C., Sorrentino, L. et al. Bull Earthquake Eng. “Damage to churches in the 2016 central Italy earthquakes”. (2019). https://doi.org/10.1007/s10518-019-00594-4

Petry, S., & Beyer, K. "Influence of boundary conditions and size effect on the drift capacity of URM walls" Engineering Structures, (2014)

R Marques, PB Lourenço (2014) Unreinforced and confined masonry buildings in seismic regions: Validation of macro-element models and cost analysis, Engineering Structures 64

Salat Z., “ Numerical Modelling of Out-of-Plane Behavior of Masonry Structural Members”, Thesis for: Advanced Masters in Structural Analysis of Monuments and Historical Constructions, DOI: 10.13140/RG.2.1.2115.8244/2 July (2015)

Salmanpour A.H. "Displacement Capacity of Structural Masonry" ETH ZURICH (2017)

Soric Z Bond and bond slip in reinforced masonry structures. Ph.D. Thesis, University of Colorado, Depart-ment of Civil, Environmental and Architectural Engineer-ing, Boulder, Colorado, USA (1987)

Sorrentino, L., Cattari, S., da Porto, F. et al. Bull Earthquake Eng .“Seismic behaviour of ordinary masonry buildings during the 2016 central Italy earthquakes” (2018).

Sulstarova et.al "Catalogue of historical earthquakes in Albania with Ms>4.5" Tiranë (2005)

Tomazevic M. "Earthquake-resistant design of masonry buildings" Innovation in structures and construction-Vol I, Imperial College Press (1999)

Tomazevic M., "Masonry materials and construction systems", Series on Innovation in Structures and Construction, (1999)

Tomazevic M., Lutman M., “Heritage Masonry Buildings in Urban Settlements and the Requirements of Eurocodes: Experience of Slovenia”, Internetional Journal of Architectural Heritage, (2007)

Turnsek V. and Cacovic F. "Some experimental results on the strength of brick masonry walls", Proc. 2nd int. brick masonry conf., Stroke-on-Trent (1971).

UNDP report, "Disaster risk assessment in Albania", Tirane (2003)

Vidic, T., Fajfar P., and Fischinger M., “Consistent inelastic design spectra: strength and displacement”, Earthquake Engineering and Structural Dynamics, (1994)

APPENDIX A

Comparison of the elastic seismic demands among KTP-78, KTP-89 and EC-8 for a typical building

<u>KTP-78</u>

Evaluating story weight

I. terrace

$g_{terr} = 450 * 1 = 450\, daN/m^2$

$p_{terr} = 280 * 0.8 = 224\, daN/m^2$

$q = g_{terr} + p_{terr} = 450 + 224 = 674\, daN/m^2$

II. story

$g_{story} = 445 * 1 = 445\, daN/m^2$

$p_{story} = 280 * 0.8 = 224\, daN/m^2$

$q = g_{story} + p_{story} = 445 + 224 = 669\, daN/m^2$

III. walls

t=25cm

wall $0.25 * 1800 * 1 * 1 * 1.15 = 517.5\, daN/m^2$

plaster $0.04 * 1800 * 1 * 1 * 1.2 = 86.4\, daN/m^2$

$g_{wall\ 25} = 517.5 + 86.4 = 604\, daN/m^2$

$g_{wall\ 25} = 604 * 2.81 = 1697\, daN/m$

t=38cm

wall $0.38 * 1800 * 1 * 1 * 1.15 = 786.6\, daN/m^2$

plaster $0.04 * 1800 * 1 * 1 * 1.2 = 86.4\, daN/m^2$

$g_{wall\ 38} = 786.6 + 86.4 = 873\, daN/m^2$

$g_{wall\ 38} = 873 * 2.81 = 2545\, daN/m$

t=51cm

wall $0.51 * 1800 * 1 * 1 * 1.15 = 1055.7\, daN/m^2$

plaster $0.04 * 1800 * 1 * 1 * 1.2 = 86.4\, daN/m^2$

$g_{wall\ 51} = 1055.7 + 86.4 = 1142.1\, daN/m^2$

$g_{wall\ 51} = 1142.1 * 2.81 = 3209\, daN/m$

IV. parapet

t=12cm

marble $0.2 * 0.02 * 1800 * 1.2 = 13.44\, daN/m^2$

wall $0.26 * 0.12 * 1800 * 1.15 = 149.04\, daN/m^2$

plaster $0.04 * 0.6 * 1 * 1800 * 1.2 = 51.84\, daN/m^2$

$g_{par} = 13.44 + 149.04 + 51.84 = 210\, daN/m$

$g_{par} = 210 * 1 = 210\, daN/m$

Surface of the story:

$S = 13.86m * 9.76m = 135.27m^2$

In our suppose, we will not take the stairs in consideration. The windows and doors are of different dimensions but we will accept 150cm*140cm for their dimension and a total of 10 windows and 9 doors.

Their weight will be considered negative in calculation

Doors

25cm: $0.25 * 2.1 * 1 * 1800 * 1.15 = 1086 daN$

38cm: $0.38 * 2.1 * 1 * 1800 * 1.15 = 1651daN$

51cm: $0.51 * 2.1 * 1 * 1800 * 1.15 = 2216daN$

Windows

25cm: $0.25 * 1.5 * 1.4 * 1800 * 1.15 = 1086.7daN$

38cm: $0.38 * 1.5 * 1.4 * 1800 * 1.15 = 1651.9daN$

51cm: $0.51 * 1.5 * 1.4 * 1800 * 1.15 = 2217daN$

Calculations

$Q_{parapet} = 2 * (13.6 + 9.5) * 210 = 9702daN$

$Q_{walls} = 2 * (13.6 + 9.5) * 1697 + (13.6 + 9.5 + 9.5) * 1697 - 9 * 1651 - 10 * 1086.7$

$Q_{walls} = 114055daN$

$Q_{walls} = 2 * (13.6 + 9.5) * 2545 + (13.6 + 9.5 + 9.5) * 1697 - 9 * 1086 - 10 * 1651.9 = Q_{walls} = 147580daN$ (for story 3 with 38cm wall on perimeter)

$Q_{walls} = 2 * (13.6 + 9.5) * 2545 + (13.6 + 9.5 + 9.5) * 2545 - 9 * 1486 - 10 * 1651.9 = Q_{walls} = 170653daN$ (for story 1 and 2 with 38cm wall on inside and perimeter)

$Q_{k5} = 9702daN + 0.5 * 114055daN + 135.27 * 674 = 157901daN$

$Q_{k4} = 0.5 * (114055daN + 114055daN) + 135.27 * 669 = 204550daN$

$Q_{k3} = 0.5 * (114055daN + 147580daN) + 135.27 * 669 = 221313daN$

$Q_{k2} = 0.5 * (147580daN + 170653daN) + 135.27 * 669 = 249612daN$

$Q_{k1} = 0.5 * (170653daN + 170653daN) + 135.27 * 669 = 261148daN$

$Q_{total} = 10945.2kN$

$E_{k5} = 0.025 * 1 * 0.45 * 2 * 157901 = 35.8kN$

$E_{k4} = 0.025 * 1 * 0.45 * 2 * 204550 = 46kN$

$E_{k3} = 0.025 * 1 * 0.45 * 2 * 221313 = 49.8kN$

$E_{k2} = 0.025 * 1 * 0.45 * 2 * 249612 = 56.2kN$

$E_{k1} = 0.025 * 1 * 0.45 * 2 * 261148 = 58{,}8kN$

$V_{base} = 35.8kN + 46kN + 49.8kN + 56.2kN + 58{,}8kN = 246.3kN$

$\frac{V_{base}}{Q_{total}} = \frac{246.3}{10945.2} = 0.0225$

<u>KTP-89</u>

Evaluating story weight

$g_{terr} = 450 * 0.9 = 405\, daN/m^2$

$p_{terr} = 280 * 0.4 = 112\, daN/m^2$

$q = g_{terr} + p_{terr} = 405 + 112 = 517\, daN/m^2$

II. story

$g_{story} = 445 * 0.9 = 401\, daN/m^2$

$p_{story} = 280 * 0.4 = 112\, daN/m^2$

$q = g_{story} + p_{story} = 401 + 112 = 513\, daN/m^2$

III. walls

t=25cm

wall $0.25 * 1800 * 1 * 1 * 1.15 = 517.5\, daN/m^2$

plaster $0.04 * 1800 * 1 * 1 * 1.2 = 86.4\, daN/m^2$

$g_{wall\ 25} = 517.5 + 86.4 = 604\, daN/m^2$

$g_{wall\ 25} = 604 * 2.81 = 1697\, daN/m$

t=38cm

wall $0.38 * 1800 * 1 * 1 * 1.15 = 786.6\, daN/m^2$

plaster $0.04 * 1800 * 1 * 1 * 1.2 = 86.4\, daN/m^2$

$g_{wall\ 38} = 786.6 + 86.4 = 873\ daN/m^2$

$g_{wall\ 38} = 873 * 2.81 = 2545\ daN/m$

t=51cm

wall $0.51 * 1800 * 1 * 1 * 1.15 = 1055.7\ daN/m^2$

plaster $0.04 * 1800 * 1 * 1 * 1.2 = 86.4\ daN/m^2$

$g_{wall\ 51} = 1055.7 + 86.4 = 1142.1\ daN/m^2$

$g_{wall\ 51} = 1142.1 * 2.81 = 3209\ daN/m$

IV. parapet

t=12cm

marble $0.2 * 0.02 * 1800 * 1.2 = 13.44\ daN/m^2$

wall $0.26 * 0.12 * 1800 * 1.15 = 149.04\ daN/m^2$

plaster $0.04 * 0.6 * 1 * 1800 * 1.2 = 51.84\ daN/m^2$

$g_{par} = 13.44 + 149.04 + 51.84 = 210\ daN/m$

$g_{par} = 210 * 1 = 280\ daN/m$

Surface of the story:

$S = 13.86m * 9.76m = 135.27m^2$

In our suppose, we will not take the stairs in consideration. The windows and doors are of different dimensions but we will accept 150cm*140cm for their dimension and a total of 10 windows and 9 doors.

Their weight will be considered negative in calculation

Doors

25cm: $0.25 * 2.1 * 0.9 * 1800 * 1.15 = 978daN$

38cm: $0.38 * 2.1 * 0.9 * 1800 * 1.15 = 1486daN$

51cm: $0.51 * 2.1 * 0.9 * 1800 * 1.15 = 1995daN$

Windows

25cm: $0.25 * 1.5 * 1.4 * 1800 * 1.15 = 1086.7daN$

38cm: $0.38 * 1.5 * 1.4 * 1800 * 1.15 = 1651.9daN$

51cm: $0.51 * 1.5 * 1.4 * 1800 * 1.15 = 2217daN$

Calculations

$Q_{parapet} = 8731daN$ $Q_{walls} = 114055daN$ (for story 4 and 5 with 25 cm wall)

$Q_{walls} = 2 * (13.6 + 9.5) * 2545 + (13.6 + 9.5 + 9.5) * 1697 - 9 * 978 - 10 * 1651.9 =$
$Q_{walls} = 147580daN$ (for story 3 with 38cm wall on perimeter)

$Q_{walls} = 2 * (13.6 + 9.5) * 2545 + (13.6 + 9.5 + 9.5) * 2545 - 9 * 1486 - 10 *$
$1651.9 = Q_{walls} = 170653daN$ (for story 1 and 2 with 38cm wall on inside and perimeter)

$Q_{k5} = 8731daN + 0.5 * 114055daN + 135.27 * 513 = 135151daN$

$Q_{k4} = 0.5 * (114055daN + 114055daN) + 135.27 * 513 = 183448daN$

$Q_{k3} = 0.5 * (114055daN + 147580daN) + 135.27 * 513 = 200211daN$

$Q_{k2} = 0.5 * (147580daN + 170653daN) + 135.27 * 513 = 228510daN$

$Q_{k1} = 0.5 * (170653daN + 170653daN) + 135.27 * 513 = 240046daN$

$Q_{total} = 9888.8kN$

$E_{k5} = 0.11 * 1 * 0.45 * 2 * 1.363 * 135151 = 182.4kN$

$E_{k4} = 0.11 * 1 * 0.45 * 2 * 1.091 * 183448 = 198.1kN$

$E_{k3} = 0.11 * 1 * 0.45 * 2 * 0.818 * 200211 = 162.1kN$

$E_{k2} = 0.11 * 1 * 0.45 * 2 * 0.545 * 228510 = 123.3kN$

$E_{k1} = 0.11 * 1 * 0.45 * 2 * 0.273 * 240046 = 64.9kN$

$V_{base} = 182.4kN + 198.1kN + 162.1kN + 123.3kN + 64.9kN = 730.8kN$

$$\frac{V_{base}}{Q_{total}} = \frac{730.8kN}{9888.8kN} = 0.0739$$

EUROCODE 8

Evaluating story weight

I. terrace

$g_{terr} = 450 * 1 = 450\,daN/m^2$

$p_{terr} = 280 * 0.3 = 84\,daN/m^2$

$q = g_{terr} + p_{terr} = 450 + 84 = 534\,daN/m^2$

II. story

$g_{story} = 445 * 1 = 445\,daN/m^2$

$p_{story} = 280 * 0.3 = 84\,daN/m^2$

$q = g_{story} + p_{story} = 445 + 84 = 529\,daN/m^2$

III. walls

t=25cm

wall $0.25 * 1800 * 1 * 1 * 1.15 = 517.5\,daN/m^2$

plaster $0.04 * 1800 * 1 * 1 * 1.2 = 86.4\,daN/m^2$

$g_{wall\,25} = 517.5 + 86.4 = 604\,daN/m^2$

$g_{wall\,25} = 604 * 2.81 = 1697\,daN/m$

t=38cm

wall $0.38 * 1800 * 1 * 1 * 1.15 = 786.6\,daN/m^2$

plaster $0.04 * 1800 * 1 * 1 * 1.2 = 86.4\,daN/m^2$

$g_{wall\,38} = 786.6 + 86.4 = 873\,daN/m^2$

$g_{wall\,38} = 873 * 2.81 = 2545\,daN/m$

t=51cm

wall $0.51 * 1800 * 1 * 1 * 1.15 = 1055.7\, daN/m^2$

plaster $0.04 * 1800 * 1 * 1 * 1.2 = 86.4\, daN/m^2$

$g_{wall\ 51} = 1055.7 + 86.4 = 1142.1\, daN/m^2$

$g_{wall\ 51} = 1142.1 * 2.81 = 3209\, daN/m$

IV. parapet

t=12cm

marble $0.2 * 0.02 * 1800 * 1.2 = 13.44\, daN/m^2$

wall $0.26 * 0.12 * 1800 * 1.15 = 149.04\, daN/m^2$

plaster $0.04 * 0.6 * 1 * 1800 * 1.2 = 51.84\, daN/m^2$

$g_{par} = 13.44 + 149.04 + 51.84 = 210\, daN/m$

$g_{par} = 210 * 0.9 = 189\, daN/m$

Surface of the story:

$S = 13.86m * 9.76m = 135.27m^2$

In our suppose, we will not take the stairs in consideration. The windows and doors are of different dimensions but we will accept 150cm*140cm for their dimension and a total of 10 windows and 9 doors.

Their weight will be considered negative in calculation

Doors

25cm: $0.25 * 2.1 * 0.9 * 1800 * 1.15 = 978daN$

38cm: $0.38 * 2.1 * 0.9 * 1800 * 1.15 = 1486daN$

51cm: $0.51 * 2.1 * 0.9 * 1800 * 1.15 = 1995daN$

Windows

25cm: $0.25 * 1.5 * 1.4 * 1800 * 1.15 = 1086.7daN$

38cm: $0.38 * 1.5 * 1.4 * 1800 * 1.15 = 1651.9 daN$

51cm: $0.51 * 1.5 * 1.4 * 1800 * 1.15 = 2217 daN$

Calculations

$Q_{parapet} = 2 * (13.6 + 9.5) * 210 = 9702 daN$

$Q_{walls} = 2 * (13.6 + 9.5) * 1697 + (13.6 + 9.5 + 9.5) * 1697 - 9 * 1651 - 10 * 1086.7$

$Q_{walls} = 114055 daN$ (for story 1 and 2 with 38cm wall on perimeter)

$Q_{walls} = 2 * (13.6 + 9.5) * 2545 + (13.6 + 9.5 + 9.5) * 1697 - 9 * 1086 - 10 * 1651.9 = Q_{walls} = 147580 daN$ (for story 3 with 38cm wall on perimeter)

$Q_{walls} = 2 * (13.6 + 9.5) * 2545 + (13.6 + 9.5 + 9.5) * 2545 - 9 * 1486 - 10 * 1651.9 = Q_{walls} = 170653 daN$ (for story 1 and 2 with 38cm wall on inside and perimeter)

$Q_{k5} = 9702 daN + 0.5 * 114055 daN + 135.27 * 517 = 136664 daN$

$Q_{k4} = 0.5 * (114055 daN + 114055 daN) + 135.27 * 513 = 183448 daN$

$Q_{k3} = 0.5 * (114055 daN + 147580 daN) + 135.27 * 513 = 200211 daN$

$Q_{k2} = 0.5 * (147580 daN + 170653 daN) + 135.27 * 513 = 228510 daN$

$Q_{k1} = 0.5 * (170653 daN + 170653 daN) + 135.27 * 513 = 240046 daN$

$Q_{total} = 9887 kN$

$$E_{k5} = 0.15 * 1 * \frac{2.5}{2.5} * 136664 = 205 kN$$

$$E_{k4} = 0.15 * 1 * \frac{2.5}{2.5} * 183448 = 275.2 kN$$

$$E_{k3} = 0.15 * 1 * \frac{2.5}{2.5} * 200211 = 300.3 kN$$

$$E_{k2} = 0.15 * 1 * \frac{2.5}{2.5} * 228510 = 342.76 kN$$

$$E_{k1} = 0.15 * 1 * \frac{2.5}{2.5} * 240046 = 360.1 kN$$

$V_{base} = 205kN + 275.2kN + 300.3kN + 342.76kN + 360.1kN = 1573.4kN$

$\frac{V_{base}}{Q_{total}} = \frac{1483.4kN}{9887kN} = 0.15$

Calculation of template building evaluating seismic demand from different height of buildings

Evaluating story weight

I. terrace

$g_{terr} = 450 * 0.9 = 405\, daN/m^2$

$p_{terr} = 280 * 0.4 = 112\, daN/m^2$

$q = g_{terr} + p_{terr} = 405 + 112 = 517\, daN/m^2$

II. story

$g_{story} = 445 * 0.9 = 401\, daN/m^2$

$p_{story} = 280 * 0.4 = 112\, daN/m^2$

$q = g_{story} + p_{story} = 401 + 112 = 513\, daN/m^2$

III. walls

t=25cm

wall $0.25 * 1800 * 1 * 1 * 1.15 = 517.5\, daN/m^2$

plaster $0.04 * 1800 * 1 * 1 * 1.2 = 86.4\, daN/m^2$

$g_{wall\ 25} = 517.5 + 86.4 = 604\, daN/m^2$

$g_{wall\ 25} = 604 * 2.81 = 1697\, daN/m$

t=38cm

wall $0.38 * 1800 * 1 * 1 * 1.15 = 786.6\, daN/m^2$

plaster $0.04 * 1800 * 1 * 1 * 1.2 = 86.4\, daN/m^2$

$g_{wall\ 38} = 786.6 + 86.4 = 873\ daN/m^2$

$g_{wall\ 38} = 873 * 2.81 = 2545\ daN/m$

t=51cm

wall $\quad 0.51 * 1800 * 1 * 1 * 1.15 = 1055.7\ daN/m^2$

plaster $0.04 * 1800 * 1 * 1 * 1.2 = 86.4\ daN/m^2$

$g_{wall\ 51} = 1055.7 + 86.4 = 1142.1\ daN/m^2$

$g_{wall\ 51} = 1142.1 * 2.81 = 3209\ daN/m$

IV. parapet

t=12cm

marble $\quad 0.2 * 0.02 * 1800 * 1.2 = 13.44\ daN/m^2$

wall $\quad 0.26 * 0.12 * 1800 * 1.15 = 149.04\ daN/m^2$

plaster $\quad 0.04 * 0.6 * 1 * 1800 * 1.2 = 51.84\ daN/m^2$

$g_{par} = 13.44 + 149.04 + 51.84 = 210\ daN/m$

$g_{par} = 210 * 0.9 = 189\ daN/m$

Surface of the story:

$S = 13.86m * 9.76m = 135.27m^2$

In our suppose, we will not take the stairs in consideration. The windows and doors are of different dimensions but we will accept 150cm*140cm for their dimension and a total of 10 windows and 9 doors.

Their weight will be considered negative in calculation

Doors

25cm: $0.25 * 2.1 * 0.9 * 1800 * 1.15 = 978daN$

38cm: $0.38 * 2.1 * 0.9 * 1800 * 1.15 = 1486daN$

51cm: $0.51 * 2.1 * 0.9 * 1800 * 1.15 = 1995daN$

Windows

25cm: $0.25 * 1.5 * 1.4 * 1800 * 1.15 = 1086.7daN$

38cm: $0.38 * 1.5 * 1.4 * 1800 * 1.15 = 1651.9daN$

51cm: $0.51 * 1.5 * 1.4 * 1800 * 1.15 = 2217daN$

<u>One floor building</u>

$Q_{parapet} = 2 * (13.6 + 9.5) * 189 = 8731daN$

$Q_{walls} = 2 * (13.6 + 9.5) * 1697 + (13.6 + 9.5 + 9.5) * 1697 - 9 * 978 - 10 * 1086.7$

$Q_{walls} = 114055daN$

$Q_{k1} = 8731daN + 0.5 * 114055daN + 135.27 * 513 = 135151daN$

$E_{k1} = 0.11 * 1 * 0.45 * 2 * 1 * 135151 = 112.98kN$

$\mathrm{V_{base}} = 112.98\mathrm{kN}$

<u>Two floors building</u>

$Q_{parapet} = 8731daN$ $Q_{walls} = 114055daN$

$Q_{k2} = 8731daN + 0.5 * 114055daN + 135.27 * 513 = 135151daN$

$Q_{k1} = 0.5 * (114055daN + 114055daN) + 135.27 * 513 = 183448daN$

$E_{k2} = 0.11 * 1 * 0.45 * 2 * 1.2 * 135151 = 135.58kN$

$E_{k1} = 0.11 * 1 * 0.45 * 2 * 0.6 * 183448 = 92.02kN$

$V_{base} = 135.58kN + 92.02kN = 227.6kN$

<u>Three floors building</u>

$Q_{parapet} = 8731daN$ $Q_{walls} = 114055daN$ (for story 2 and 3 with 25 cm wall)

$Q_{walls} = 2 * (13.6 + 9.5) * 2545 + (13.6 + 9.5 + 9.5) * 1697 - 9 * 978 - 10 * 1651.9 =$
$Q_{walls} = 147580daN$ (for story 1 with 38cm wall on perimeter)

$Q_{k3} = 8731daN + 0.5 * 114055daN + 135.27 * 513 = 135151daN$

$Q_{k2} = 0.5 * (114055daN + 114055daN) + 135.27 * 513 = 183448daN$

$Q_{k1} = 0.5 * (114055daN + 147580daN) + 135.27 * 513 = 200211daN$

$E_{k3} = 0.11 * 1 * 0.45 * 2 * 1.258 * 135151 = 142.13kN$

$E_{k2} = 0.11 * 1 * 0.45 * 2 * 0.857 * 183448 = 131.43kN$

$E_{k1} = 0.11 * 1 * 0.45 * 2 * 0.428 * 200211 = 71.63kN$

$V_{base} = 142.13kN + 131.43kN + 71.63kN = 345.2kN$

<u>Four floors building</u>

$Q_{parapet} = 8731daN$ $Q_{walls} = 114055daN$ (for story 3 and 4 with 25 cm wall)

$Q_{walls} = 2 * (13.6 + 9.5) * 2545 + (13.6 + 9.5 + 9.5) * 1697 - 9 * 978 - 10 * 1651.9 =$
$Q_{walls} = 147580daN$ (for story 2 with 38cm wall on perimeter)

$Q_{walls} = 2 * (13.6 + 9.5) * 2545 + (13.6 + 9.5 + 9.5) * 2545 - 9 * 1486 - 10 * 1651.9 = Q_{walls} = 170653daN$ (for story 1 with 38cm wall on inside and perimeter)

$Q_{k4} = 8731daN + 0.5 * 114055daN + 135.27 * 513 = 135151daN$

$Q_{k3} = 0.5 * (114055daN + 114055daN) + 135.27 * 513 = 183448daN$

$Q_{k2} = 0.5 * (114055daN + 147580daN) + 135.27 * 513 = 200211daN$

$Q_{k1} = 0.5 * (147580daN + 170653daN) + 135.27 * 513 = 228510daN$

$E_{k4} = 0.11 * 1 * 0.45 * 2 * 1.333 * 135151 = 150.61kN$

$E_{k3} = 0.11 * 1 * 0.45 * 2 * 1 * 183448 = 153.33kN$

$E_{k2} = 0.11 * 1 * 0.45 * 2 * 0.667 * 200211 = 111.64kN$

$E_{k1} = 0.11 * 1 * 0.45 * 2 * 0.333 * 228510 = 63.61kN$

$V_{base} = 150.61kN + 153.33kN + 111.64kN + 63.61kN = 479.2kN$

<u>Five floors building</u>

$Q_{parapet} = 8731daN$ $Q_{walls} = 114055daN$ (for story 4 and 5 with 25 cm wall)

$Q_{walls} = 2 * (13.6 + 9.5) * 2545 + (13.6 + 9.5 + 9.5) * 1697 - 9 * 978 - 10 * 1651.9 =$
$Q_{walls} = 147580 daN$ (for story 3 with 38cm wall on perimeter)

$Q_{walls} = 2 * (13.6 + 9.5) * 2545 + (13.6 + 9.5 + 9.5) * 2545 - 9 * 1486 - 10 * 1651.9 = Q_{walls} = 170653 daN$ (for story 1 and 2 with 38cm wall on inside and perimeter)

$Q_{k5} = 8731 daN + 0.5 * 114055 daN + 135.27 * 513 = 135151 daN$

$Q_{k4} = 0.5 * (114055 daN + 114055 daN) + 135.27 * 513 = 183448 daN$

$Q_{k3} = 0.5 * (114055 daN + 147580 daN) + 135.27 * 513 = 200211 daN$

$Q_{k2} = 0.5 * (147580 daN + 170653 daN) + 135.27 * 513 = 228510 daN$

$Q_{k1} = 0.5 * (170653 daN + 170653 daN) + 135.27 * 513 = 240046 daN$

$E_{k5} = 0.11 * 1 * 0.45 * 2 * 1.363 * 135151 = 154 kN$

$E_{k4} = 0.11 * 1 * 0.45 * 2 * 1.091 * 183448 = 167.31 kN$

$E_{k3} = 0.11 * 1 * 0.45 * 2 * 0.818 * 200211 = 136.91 kN$

$E_{k2} = 0.11 * 1 * 0.45 * 2 * 0.545 * 228510 = 104.11 kN$

$E_{k1} = 0.11 * 1 * 0.45 * 2 * 0.273 * 240046 = 54.78 kN$

$V_{base} = 154 kN + 167.31 kN + 136.91 kN + 104.11 kN + 54.78 kN = 617.1 kN$

<u>Six floors building</u>

$Q_{parapet} = 8731 daN$ $Q_{walls} = 114055 daN$ (for story 5 and 6 with 25 cm wall)

$Q_{walls} = 2 * (13.6 + 9.5) * 2545 + (13.6 + 9.5 + 9.5) * 1697 - 9 * 978 - 10 * 1651.9 =$
$Q_{walls} = 147580 daN$ (for story 4 with 38cm wall on perimeter)

$Q_{walls} = 2 * (13.6 + 9.5) * 2545 + (13.6 + 9.5 + 9.5) * 2545 - 9 * 1486 - 10 * 1651.9 = Q_{walls} = 170653 daN$ (for story 2 and 3 with 38cm wall on inside and perimeter)

$Q_{walls} = 2 * (13.6 + 9.5) * 3209 + (13.6 + 9.5 + 9.5) * 2545 - 9 * 1486 - 10 * 2217 =$
$Q_{walls} = 195679 daN$ (for story 1 with 51cm wall on perimeter)

$Q_{k6} = 8731 daN + 0.5 * 114055 daN + 135.27 * 513 = 135151 daN$

$$Q_{k5} = 0.5 * (114055daN + 114055daN) + 135.27 * 513 = 183448daN$$

$$Q_{k4} = 0.5 * (114055daN + 147580daN) + 135.27 * 513 = 200211daN$$

$$Q_{k3} = 0.5 * (147580daN + 170653daN) + 135.27 * 513 = 228510daN$$

$$Q_{k2} = 0.5 * (170653daN + 170653daN) + 135.27 * 513 = 240046daN$$

$$Q_{k1} = 0.5 * (170653daN + 195679daN) + 135.27 * 513 = 252559daN$$

$$E_{k6} = 0.11 * 1 * 0.45 * 2 * 1.385 * 135151 = 156.5kN$$

$$E_{k5} = 0.11 * 1 * 0.45 * 2 * 1.154 * 183448 = 176.7kN$$

$$E_{k4} = 0.11 * 1 * 0.45 * 2 * 0.923 * 200211 = 154.49kN$$

$$E_{k3} = 0.11 * 1 * 0.45 * 2 * 0.692 * 228510 = 132.20kN$$

$$E_{k2} = 0.11 * 1 * 0.45 * 2 * 0.462 * 240046 = 92.71kN$$

$$E_{k1} = 0.11 * 1 * 0.45 * 2 * 0.230 * 252559 = 48.56kN$$

$$V_{base} = 154kN + 167.31kN + 136.91kN + 104.11kN + 54.78kN = 761.42kN$$

Calculation of template building evaluating seismic demand from different height of buildings

5 story building under VII, VIII, IX scale earthquake

$Q_{k5} = 135151daN$ $\quad$ $Q_{k4} = 183448daN$ $\quad$ $Q_{k3} = 200211daN$

$Q_{k2} = 228510daN$ $\quad$ $Q_{k1} = 240046daN$

VII scale intensity

$$E_{k5} = 0.11 * 1 * 0.45 * 2 * 1.363 * 135151 = 182.4kN$$

$$E_{k4} = 0.11 * 1 * 0.45 * 2 * 1.091 * 183448 = 198.1kN$$

$$E_{k3} = 0.11 * 1 * 0.45 * 2 * 0.818 * 200211 = 162.1kN$$

$E_{k2} = 0.11 * 1 * 0.45 * 2 * 0.545 * 228510 = 123.3kN$

$E_{k1} = 0.11 * 1 * 0.45 * 2 * 0.273 * 240046 = 64.9kN$

$V_{base} = 182.4kN + 198.1kN + 162.1kN + 123.3kN + 64.9kN = 730.81kN$

VIII scale intensity

$E_{k5} = 0.22 * 1 * 0.45 * 2 * 1.363 * 135151 = 364.7kN$

$E_{k4} = 0.22 * 1 * 0.45 * 2 * 1.091 * 183448 = 396.3kN$

$E_{k3} = 0.22 * 1 * 0.45 * 2 * 0.818 * 200211 = 324.3kN$

$E_{k2} = 0.22 * 1 * 0.45 * 2 * 0.545 * 228510 = 246.6kN$

$E_{k1} = 0.22 * 1 * 0.45 * 2 * 0.273 * 240046 = 129.7kN$

$V_{base} = 364.7kN + 396.3kN + 324.3kN + 246.6kN + 129.7kN = 1461.6kN$

IX scale intensity

$E_{k5} = 0.36 * 1 * 0.45 * 2 * 1.363 * 135151 = 596.8kN$

$E_{k4} = 0.36 * 1 * 0.45 * 2 * 1.091 * 183448 = 648.5kN$

$E_{k3} = 0.36 * 1 * 0.45 * 2 * 0.818 * 200211 = 530.6kN$

$E_{k2} = 0.36 * 1 * 0.45 * 2 * 0.545 * 228510 = 403.5kN$

$E_{k1} = 0.36 * 1 * 0.45 * 2 * 0.273 * 240046 = 212.3kN$

$V_{base} = 596.8kN + 648.5kN + 530.6kN + 403.5kN + 212.3kN = 2391.7kN$

APPENDIX B

Geometrical properties of studied buildings (plan view, facade, elevation view

Building A1 (template 40/1)

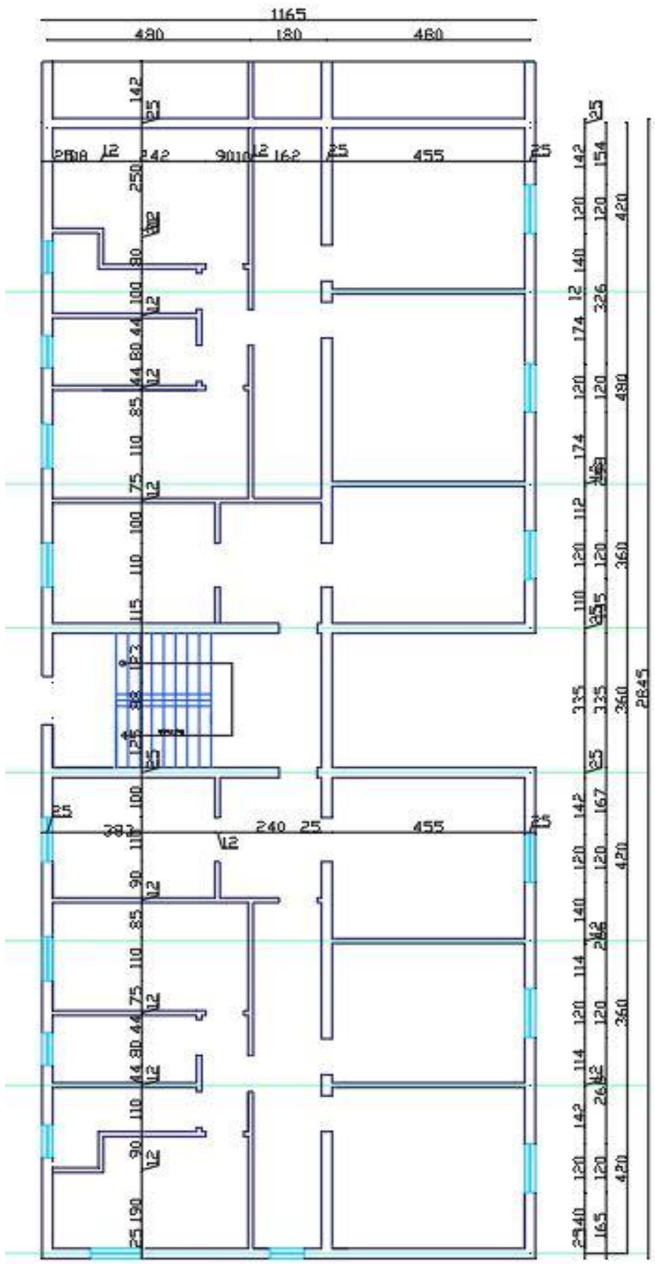

Figure 277:Plan view of building A1

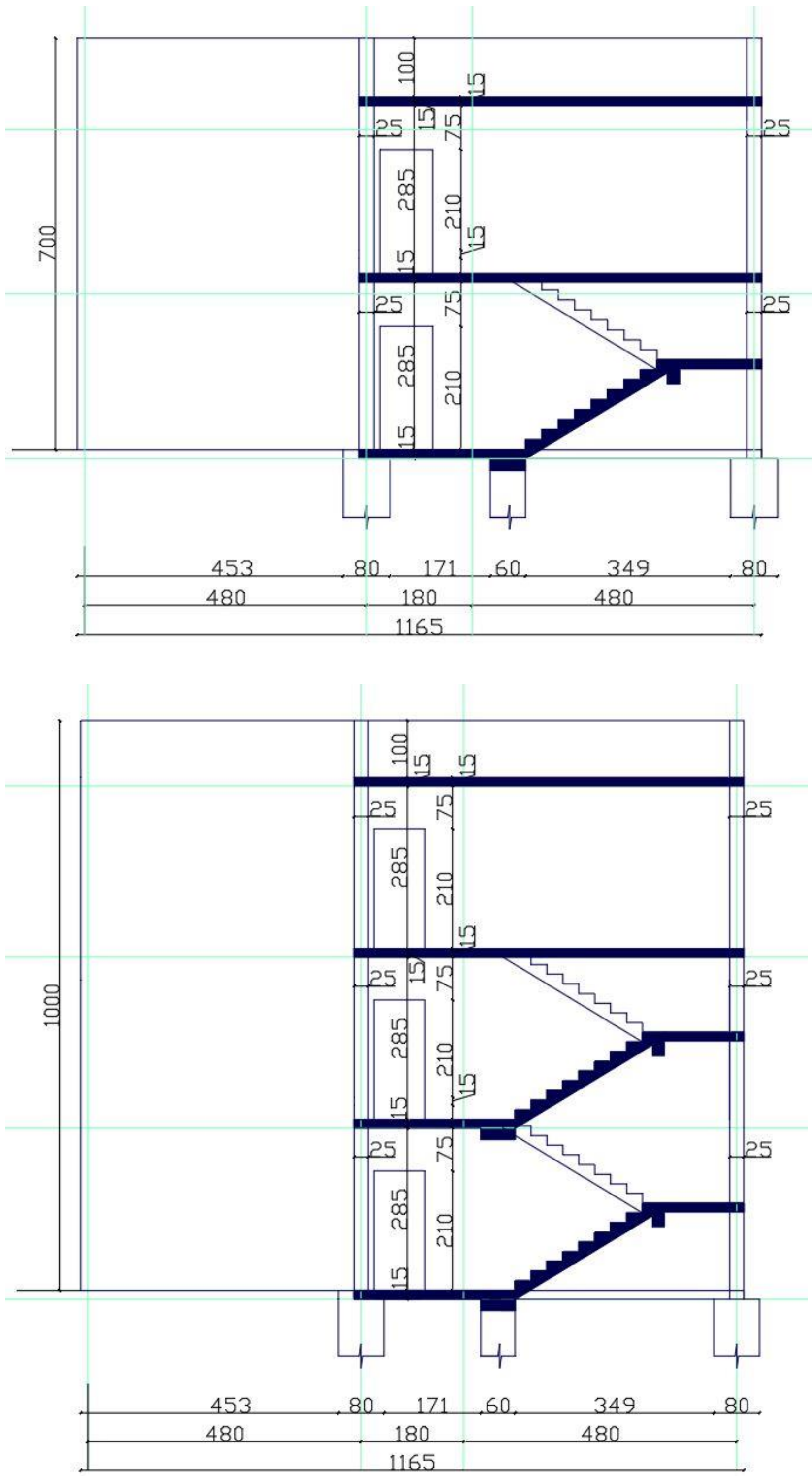

Figure 278: Elevation view of building A1 for original building and building with one added story

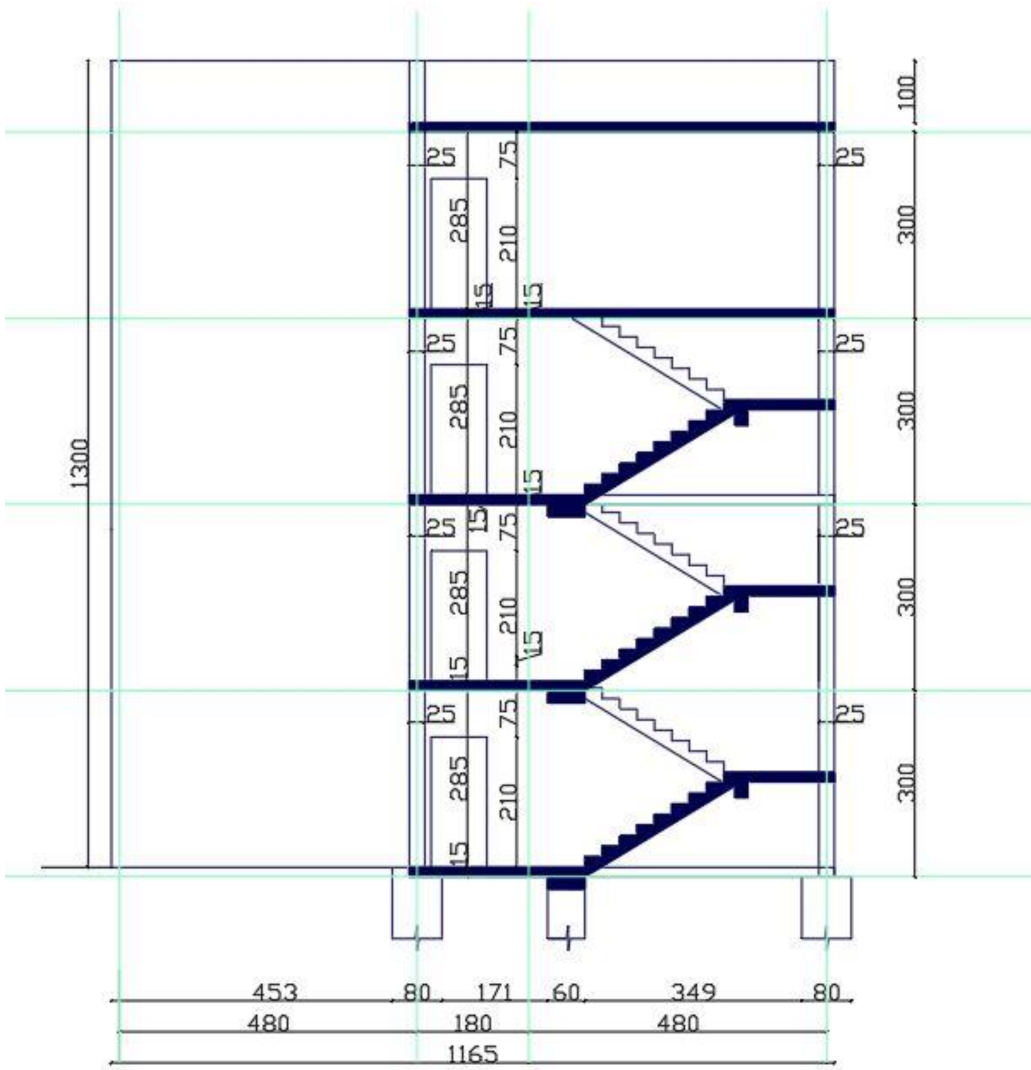

Figure 279: Elevation view of building A1 with two story added

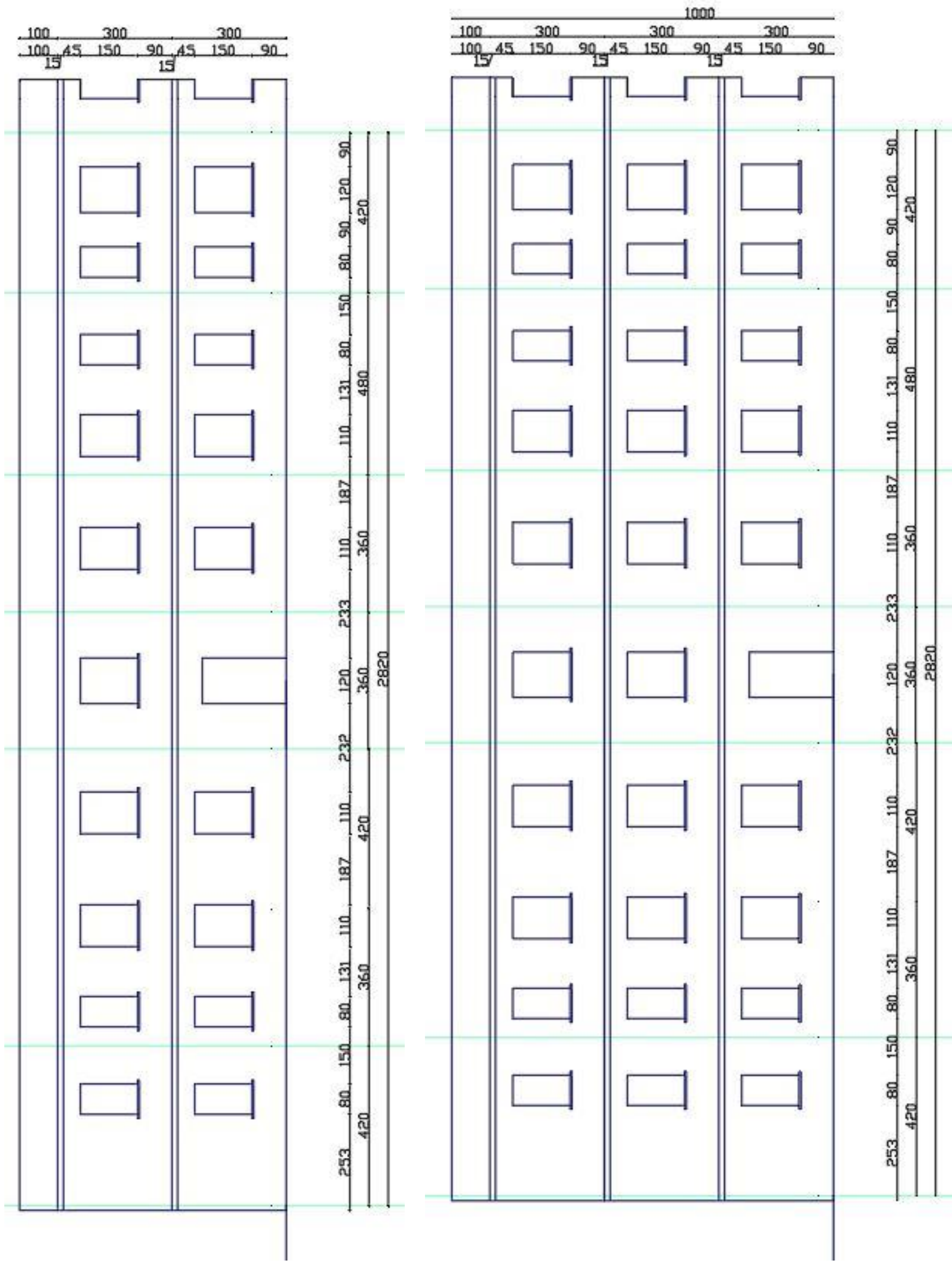

Figure 280:Facade view of building A1 for original building and plus one story building

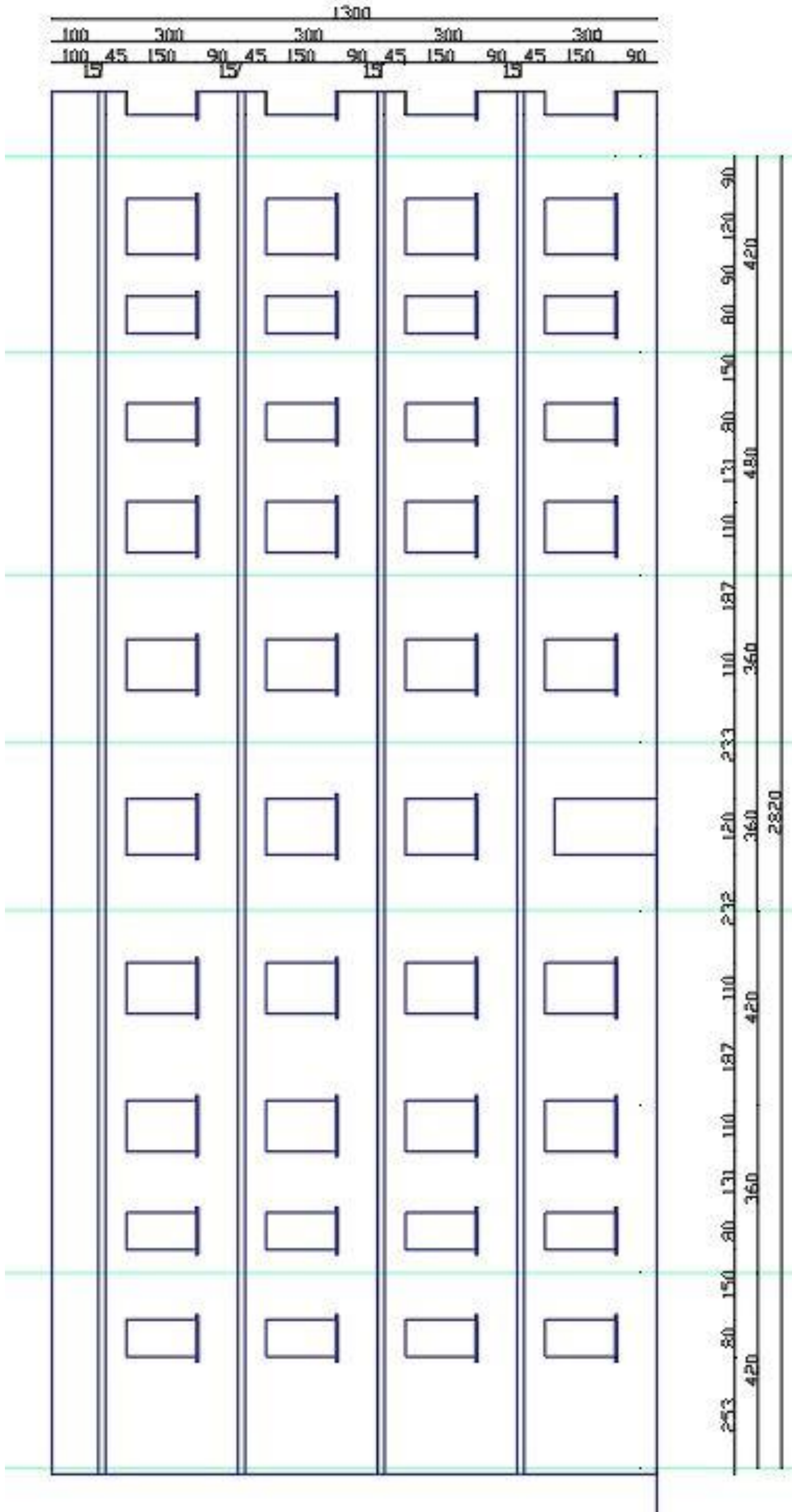

Figure 281:Facade view of building A1 for building with plus two stories

Building A2 (template 58/2)

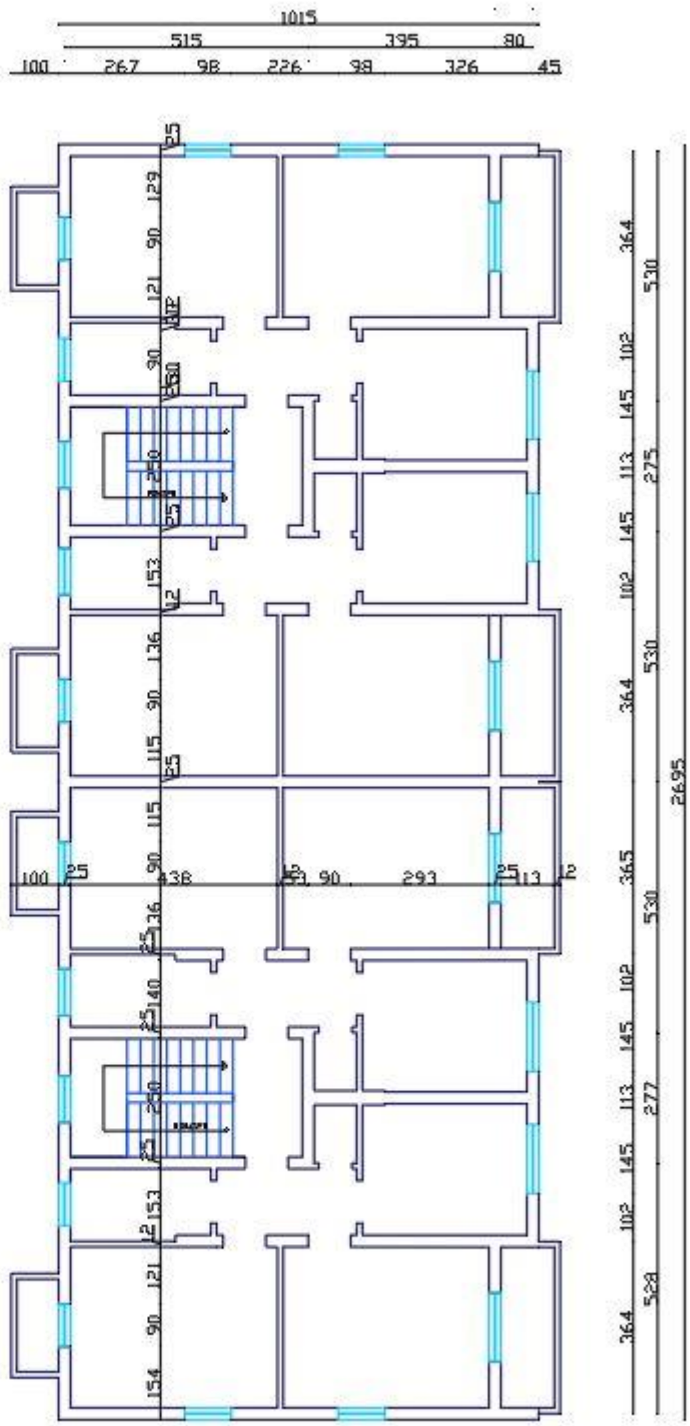

Figure 282: Plan view of building A2

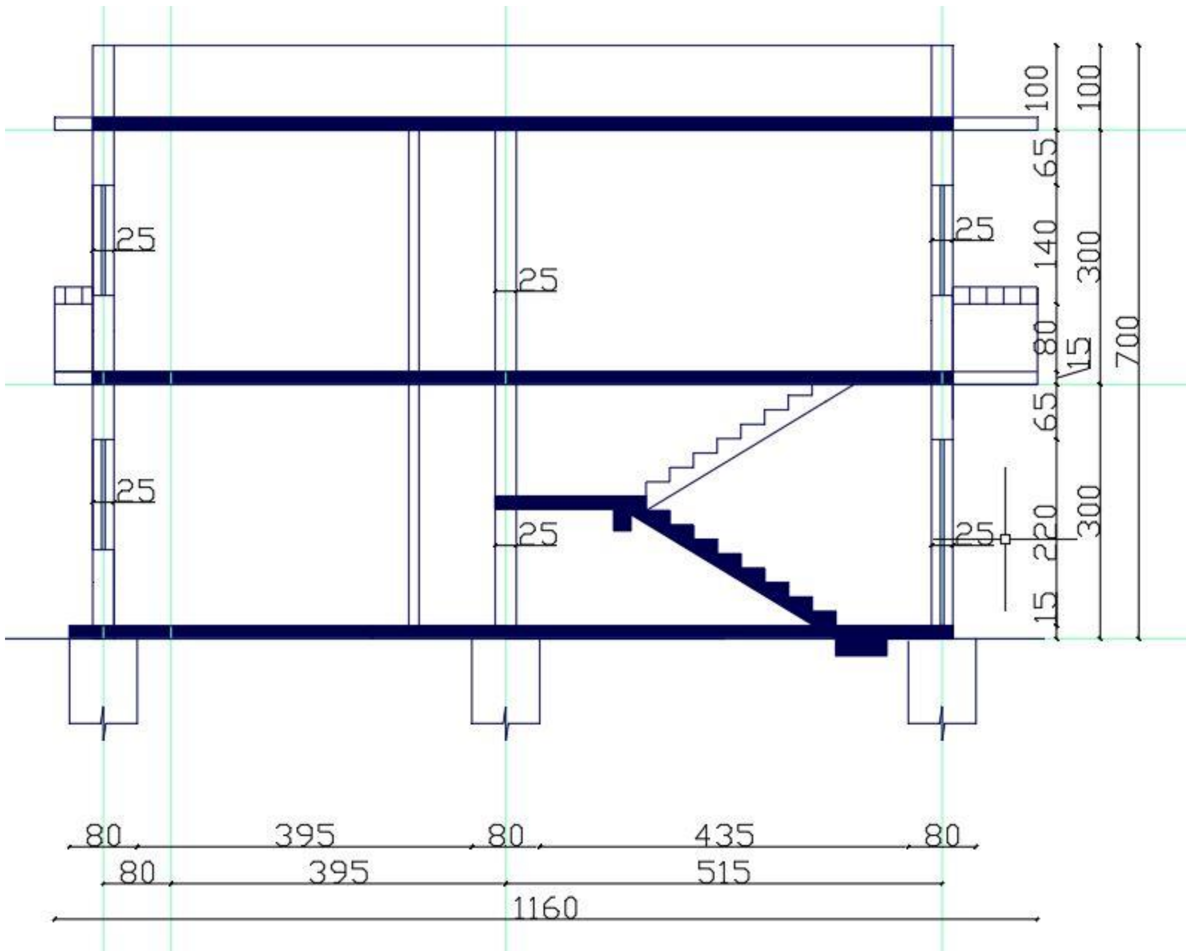

Figure 283 : Elevation view of building A2

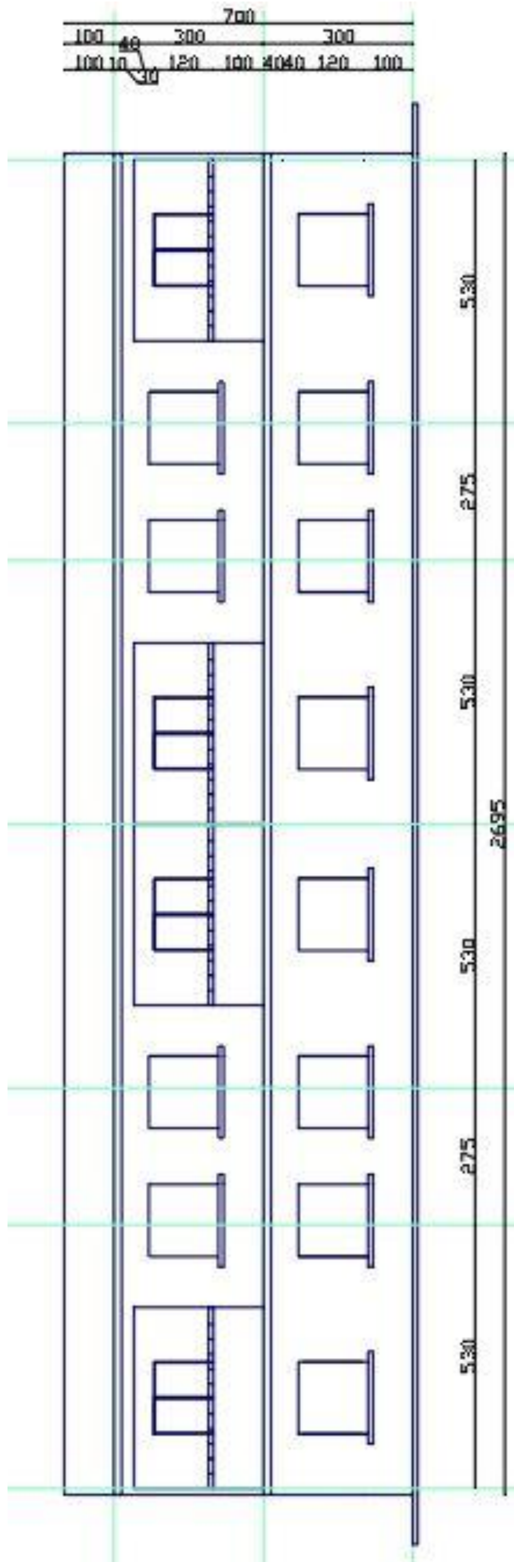

Figure 284: Facade view of building A2

Building B1 (template 63/1)

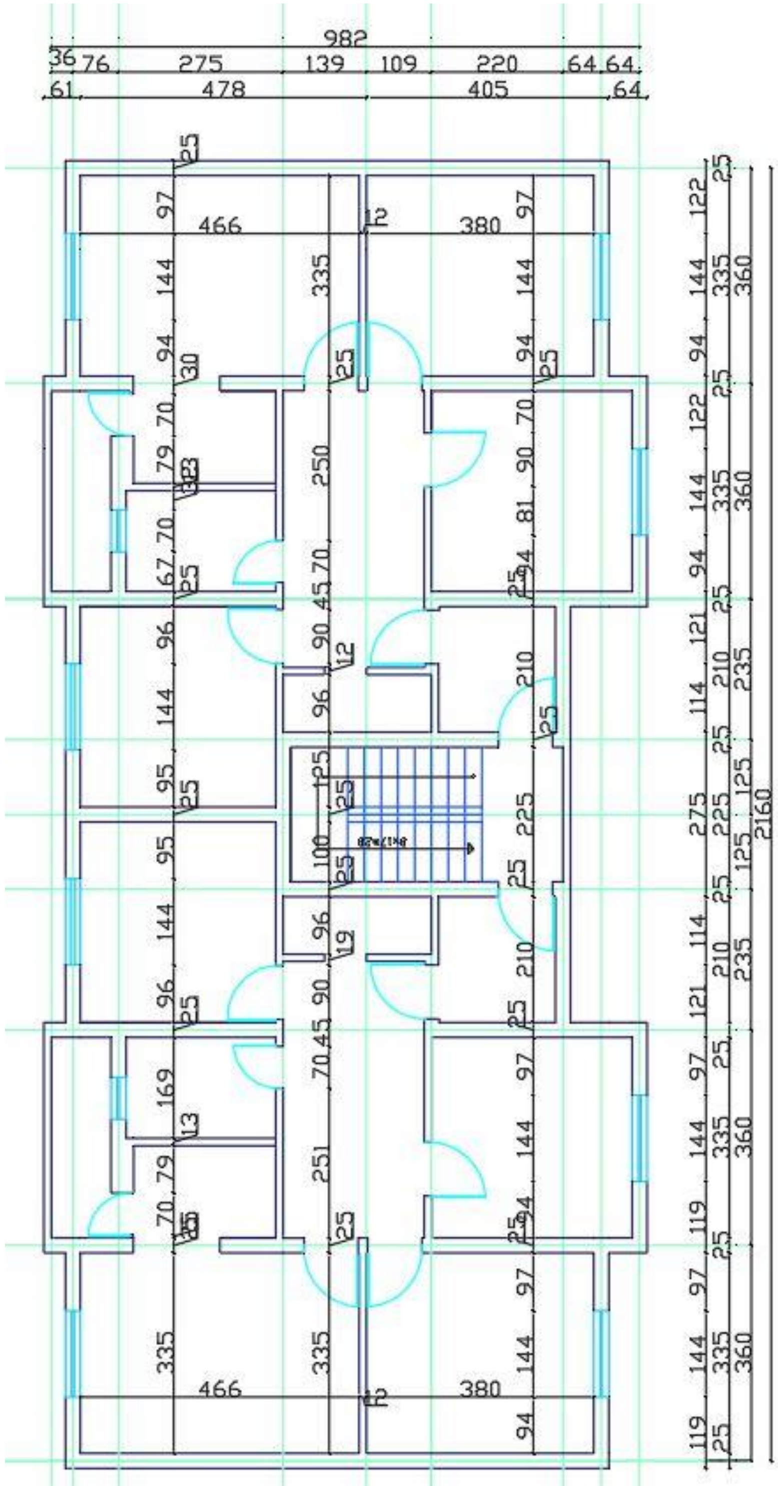

Figure 257:Plan view of building B1

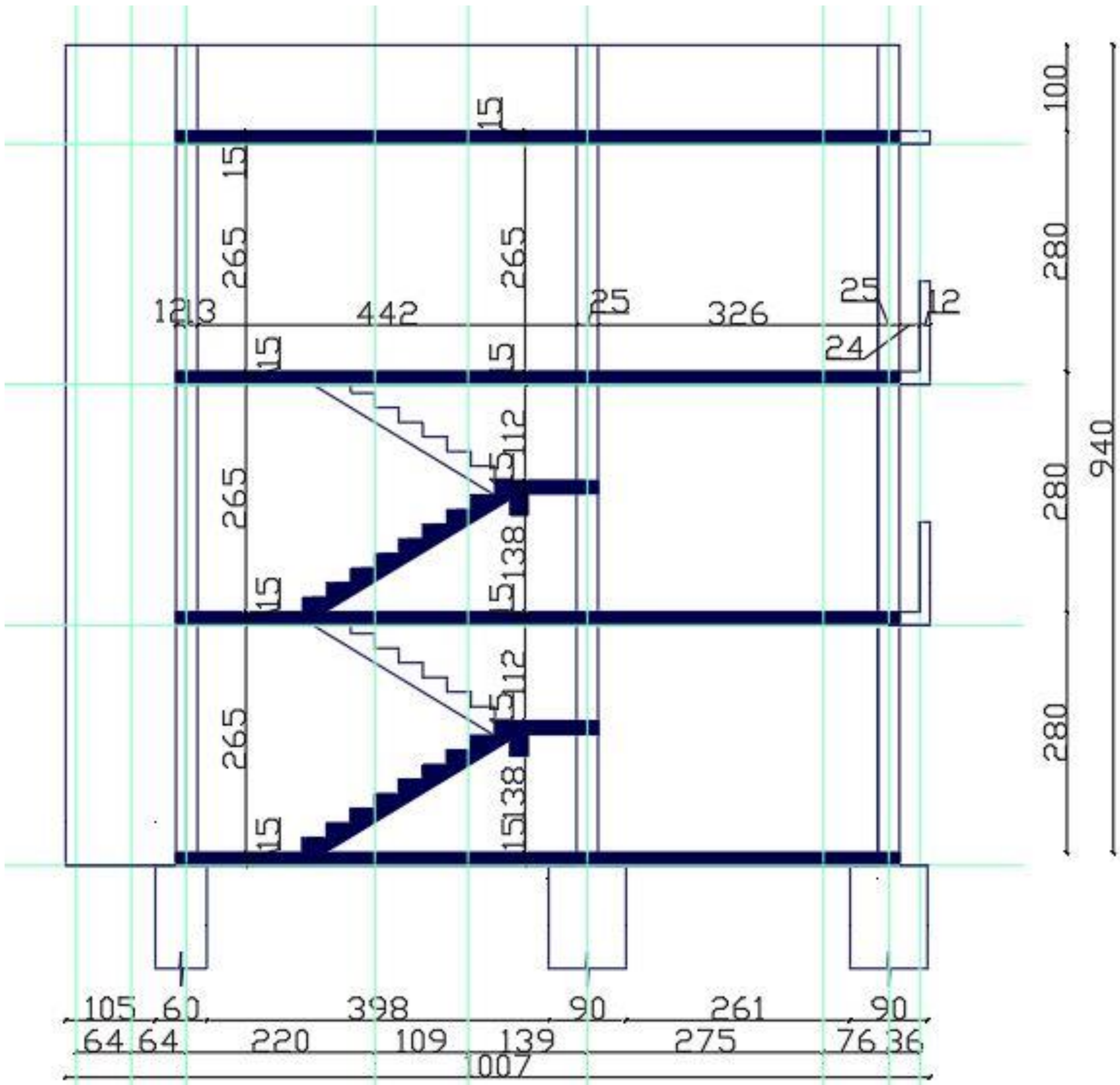

Figure 286: Elevation view of building B1

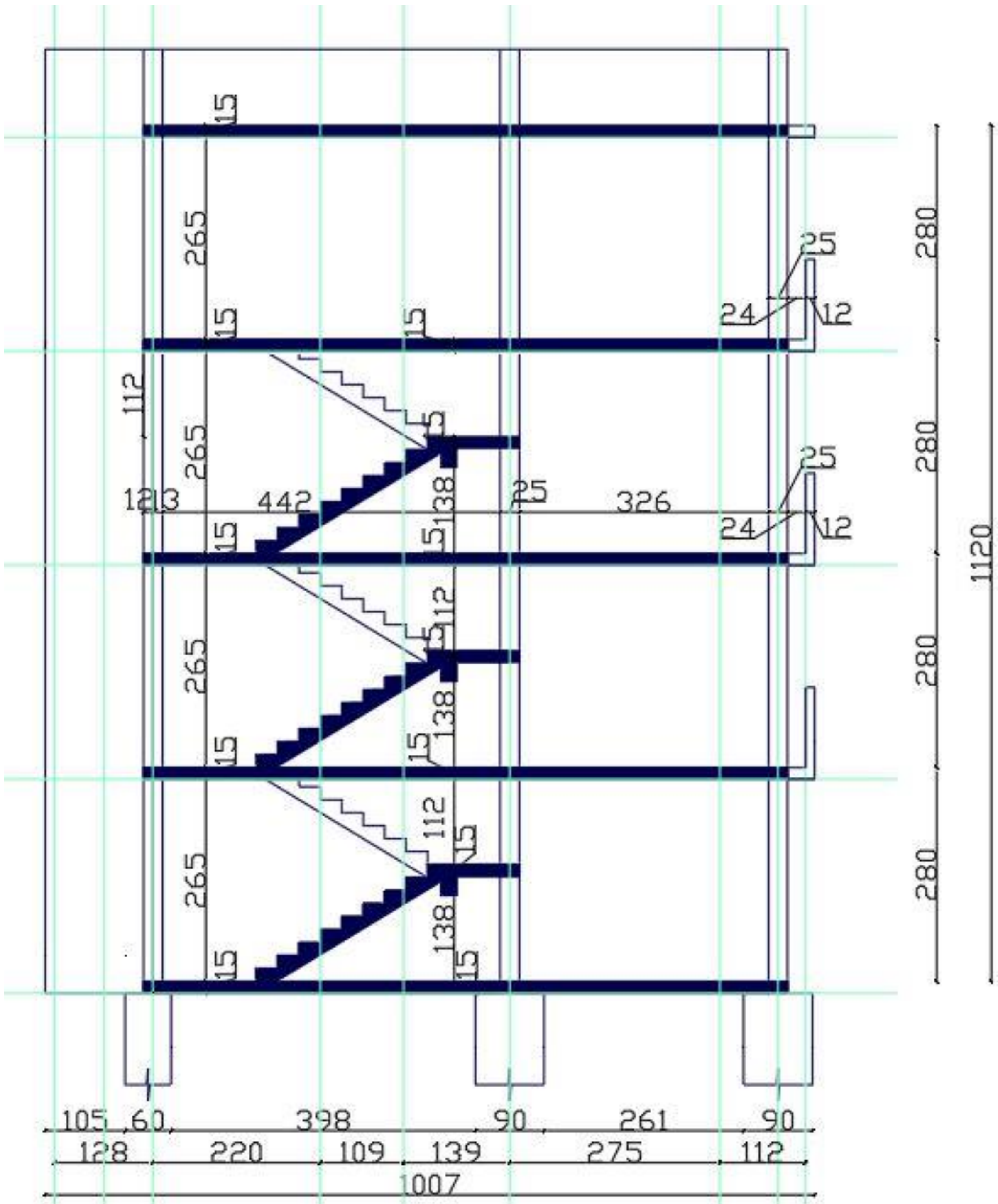

Figure 287: Elevation view of B1 building with one added floor

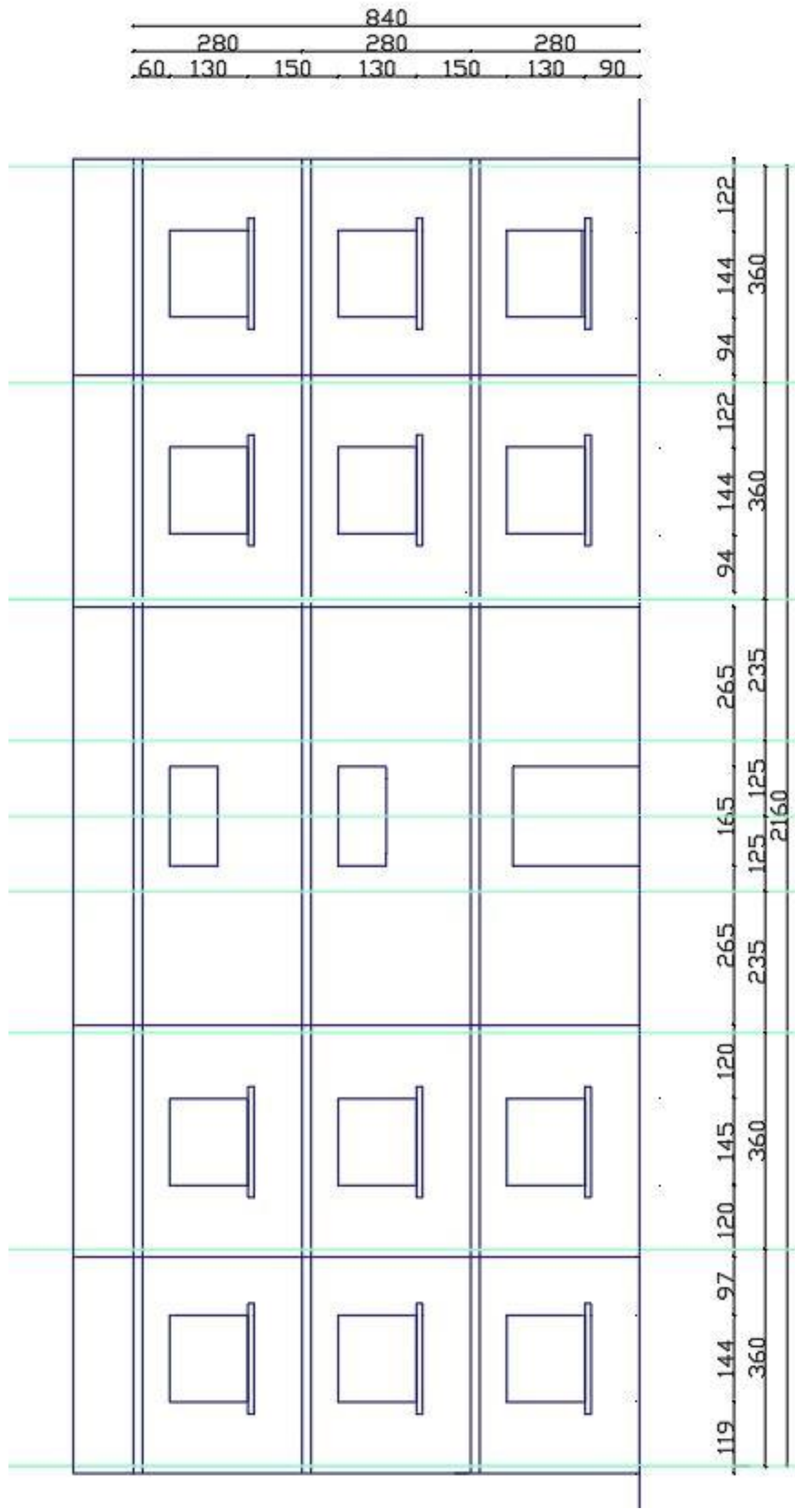

Figure 288: Facade view of building B1

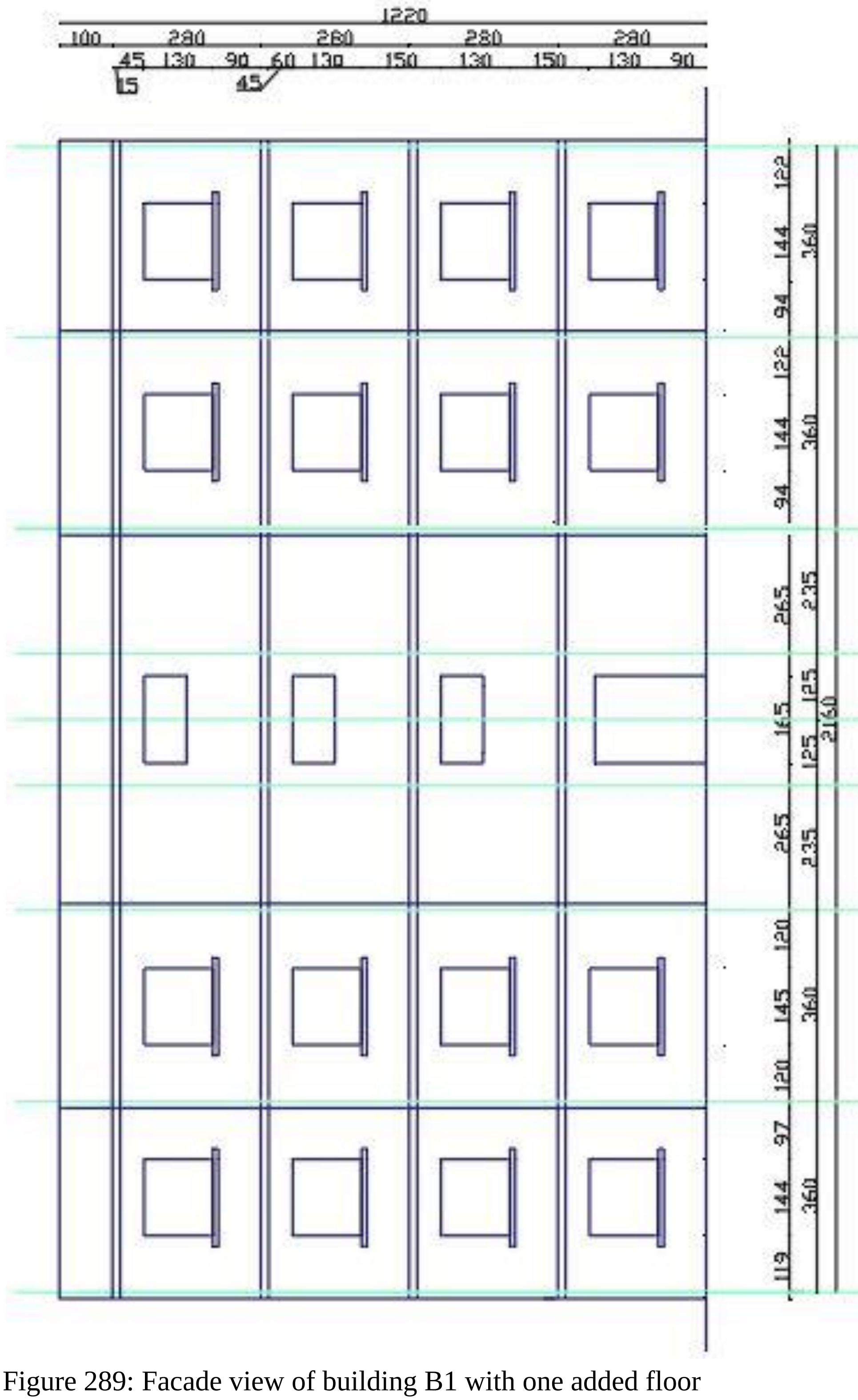

Figure 289: Facade view of building B1 with one added floor

Building B2 (69/3)

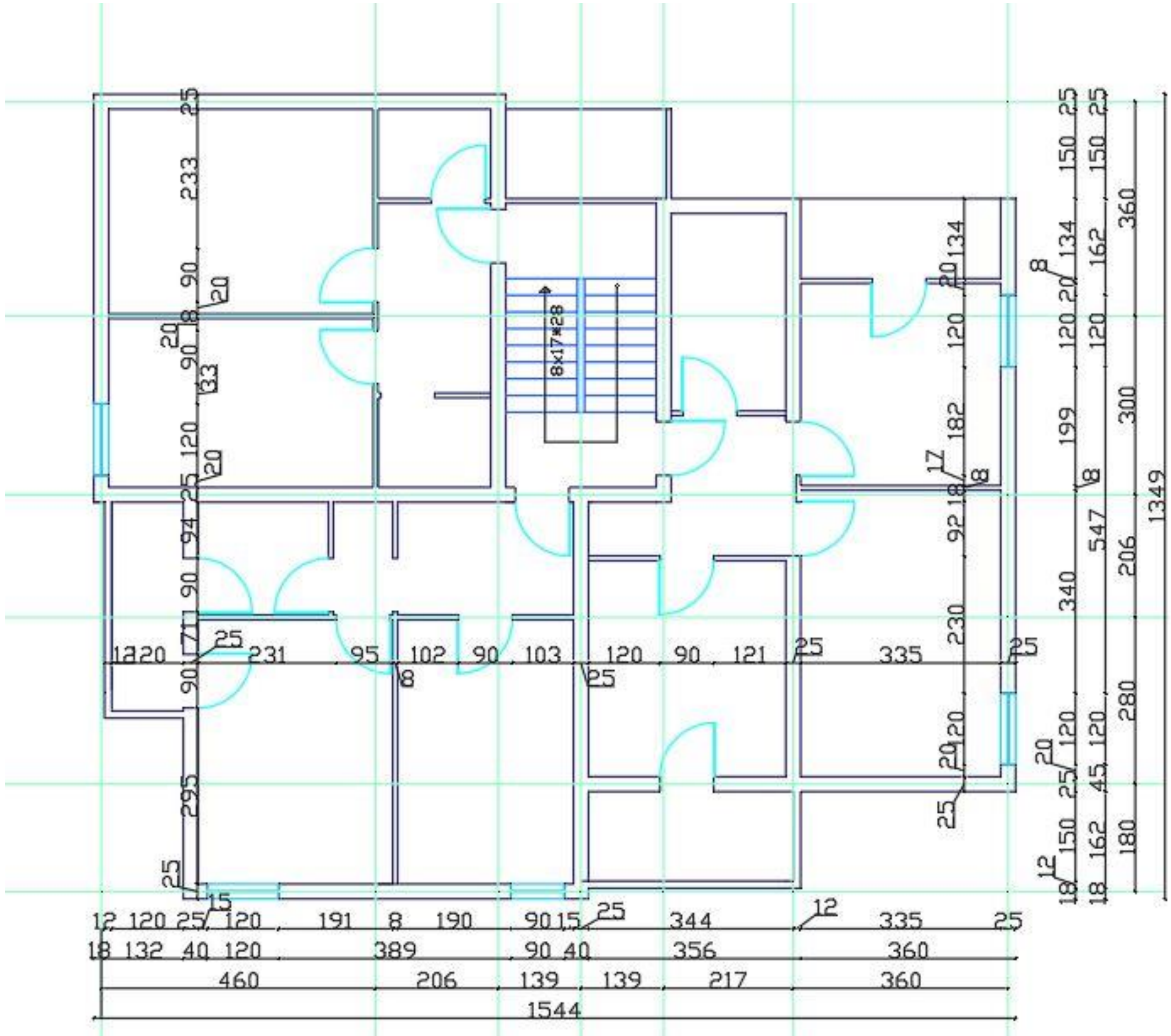

Figure 290: Plan view of building B2

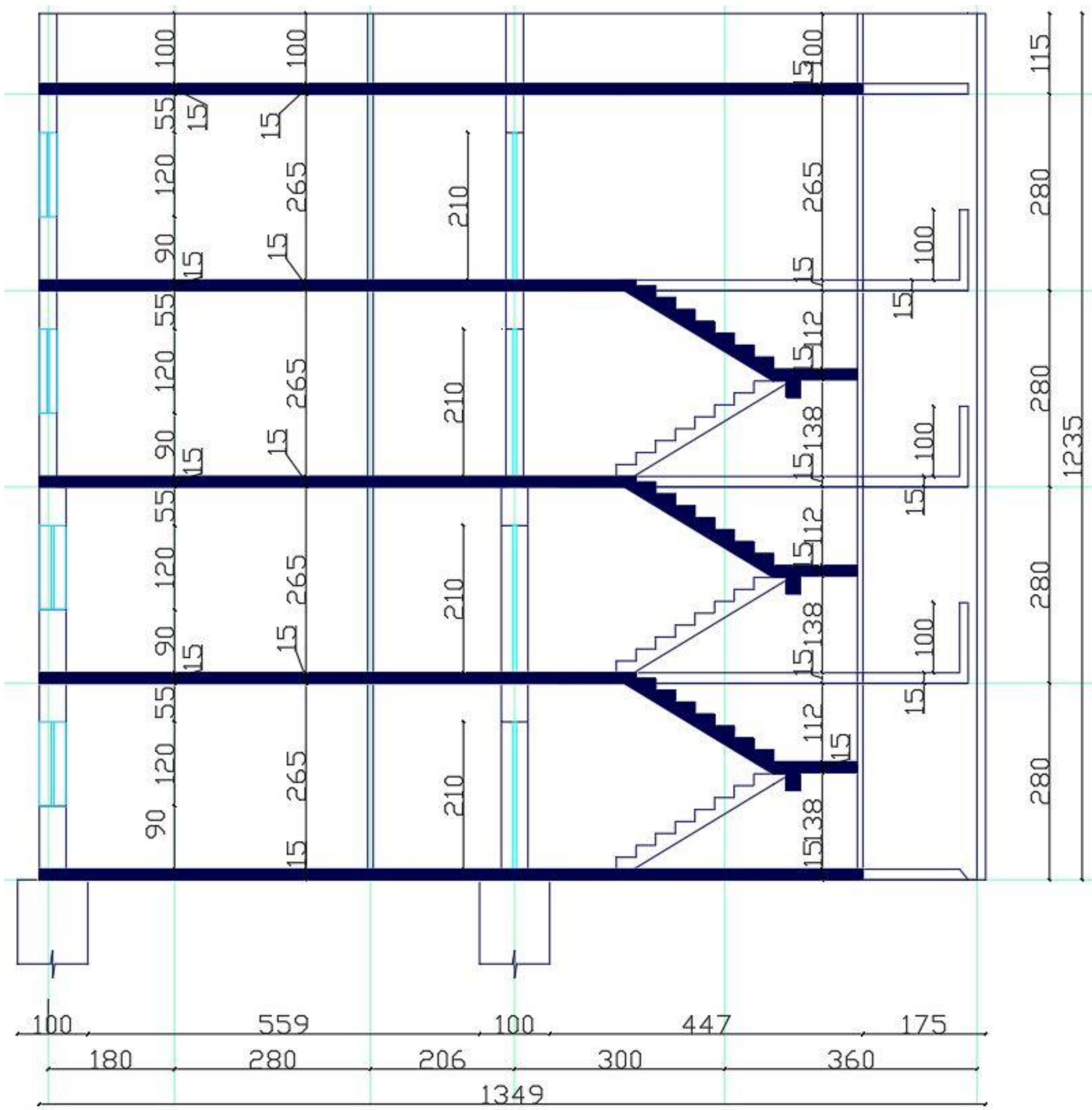

Figure 290: Elevation view of building B2

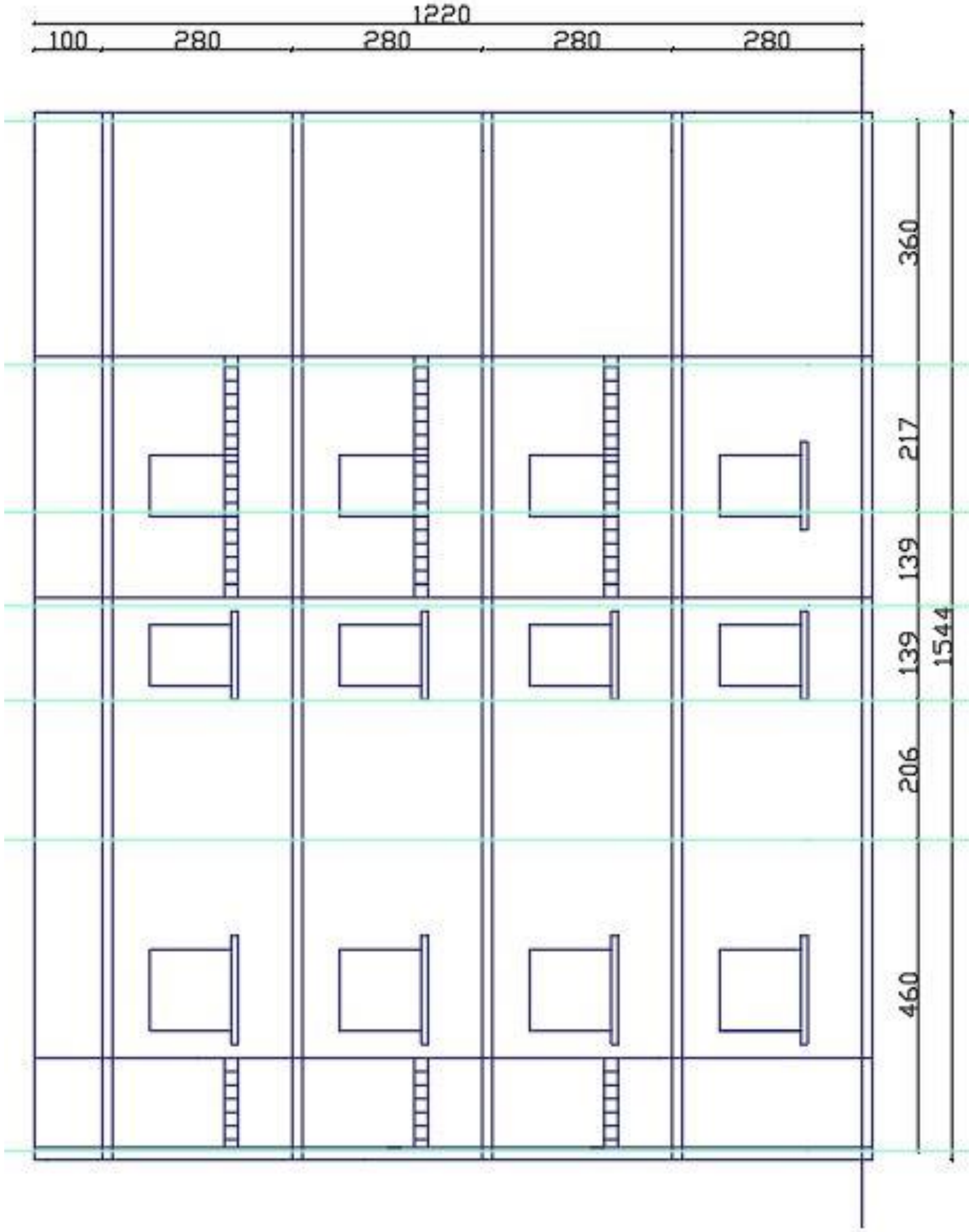

Figure 291: Facade view of building B2

Building B3 (72/1)

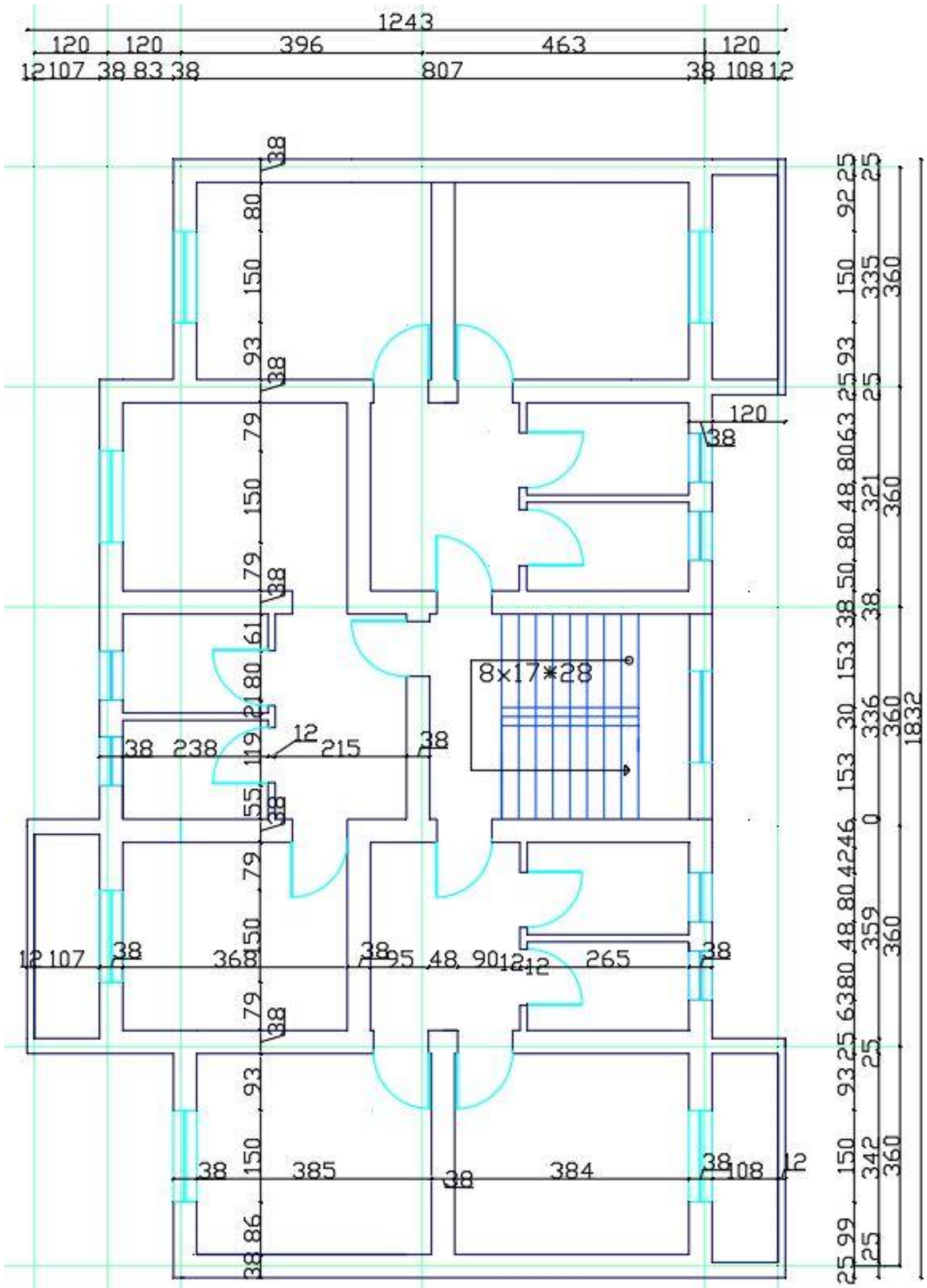

Figure 292:Plan view of building B3

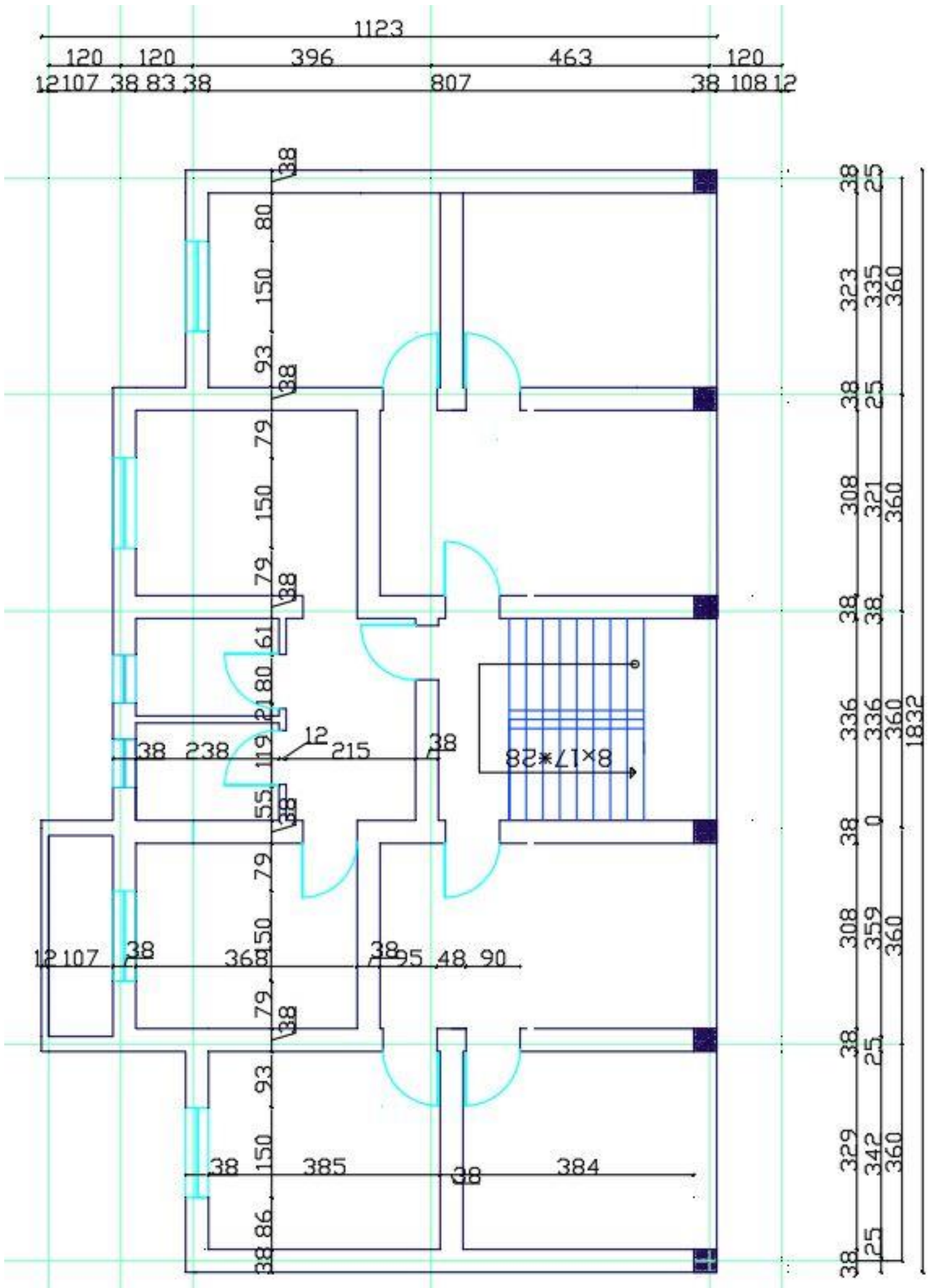

Figure 293: Plan view of building B3 with intervention

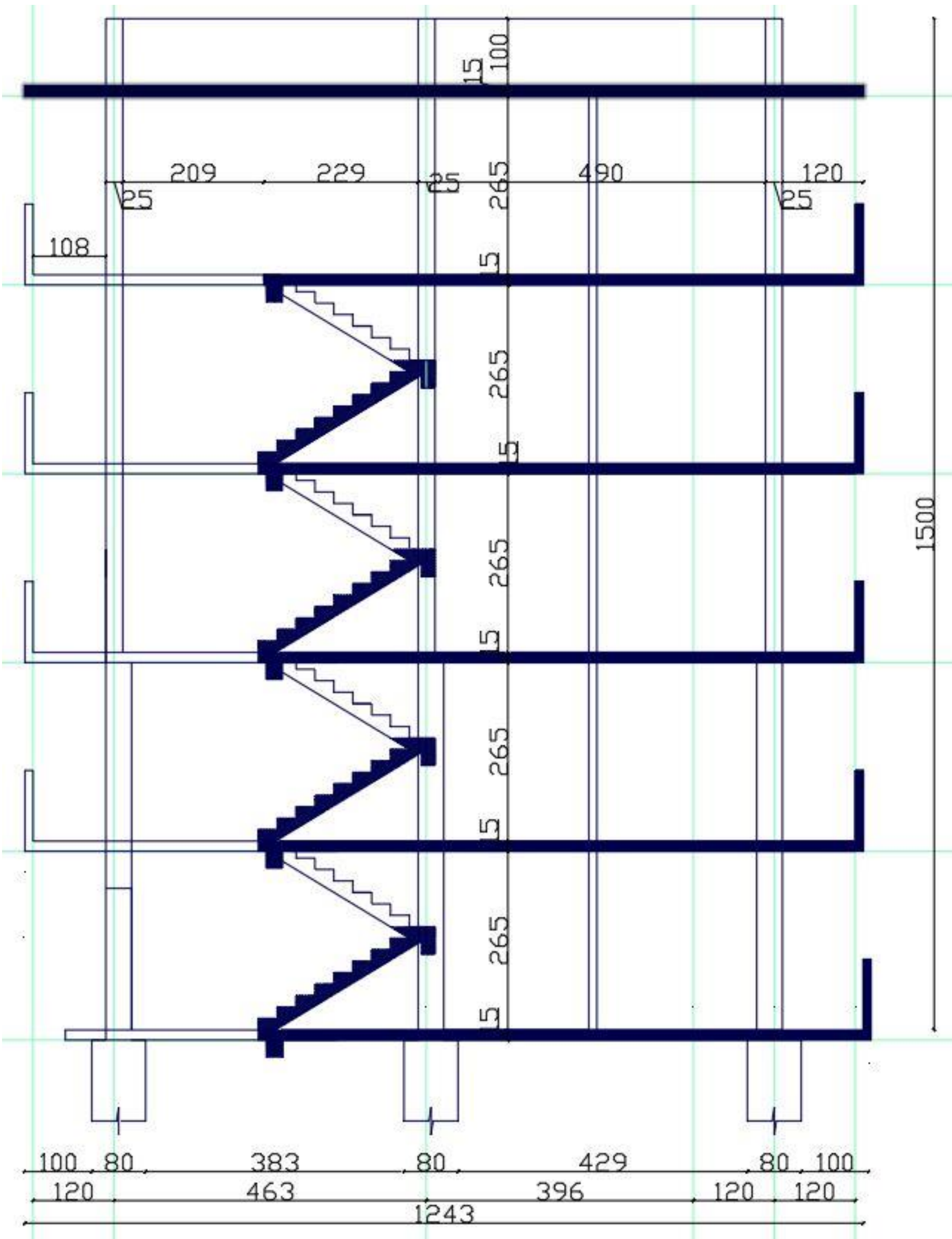

Figure 294: Elevation view of building B3

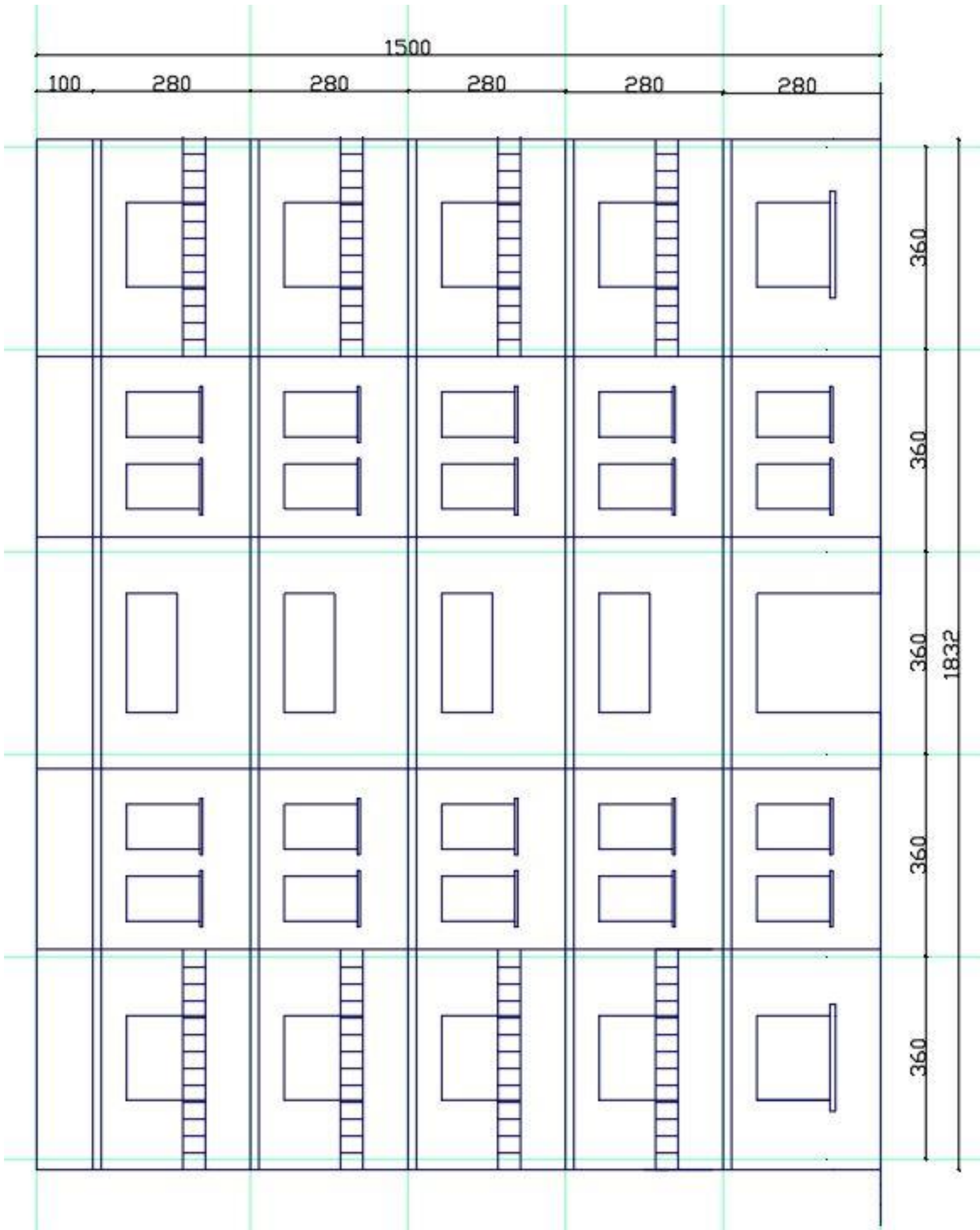

Figure 295: Facade view of building B3

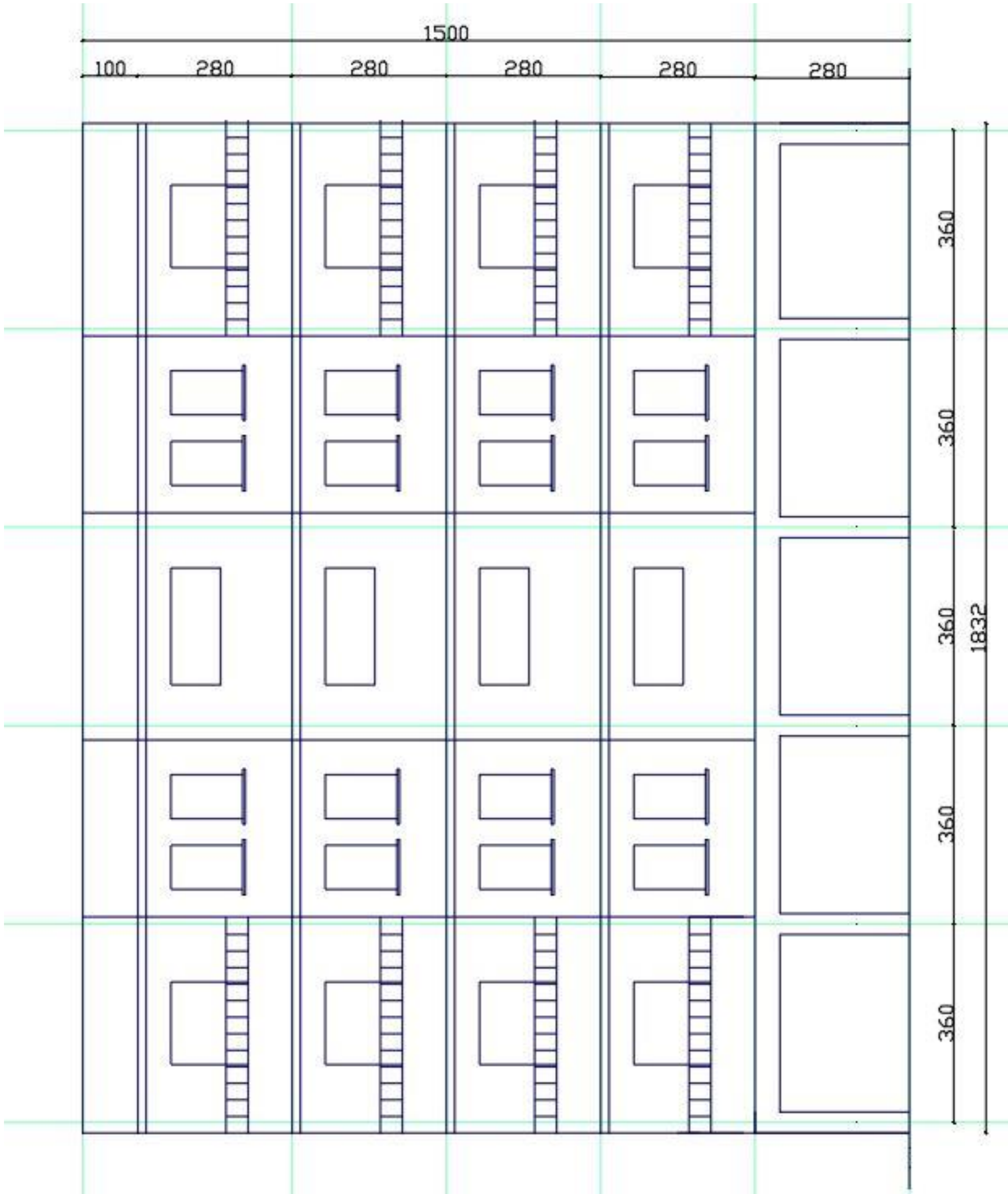

Figure 296: Facade view of building B3 with intervention

Building B4 (72/3)

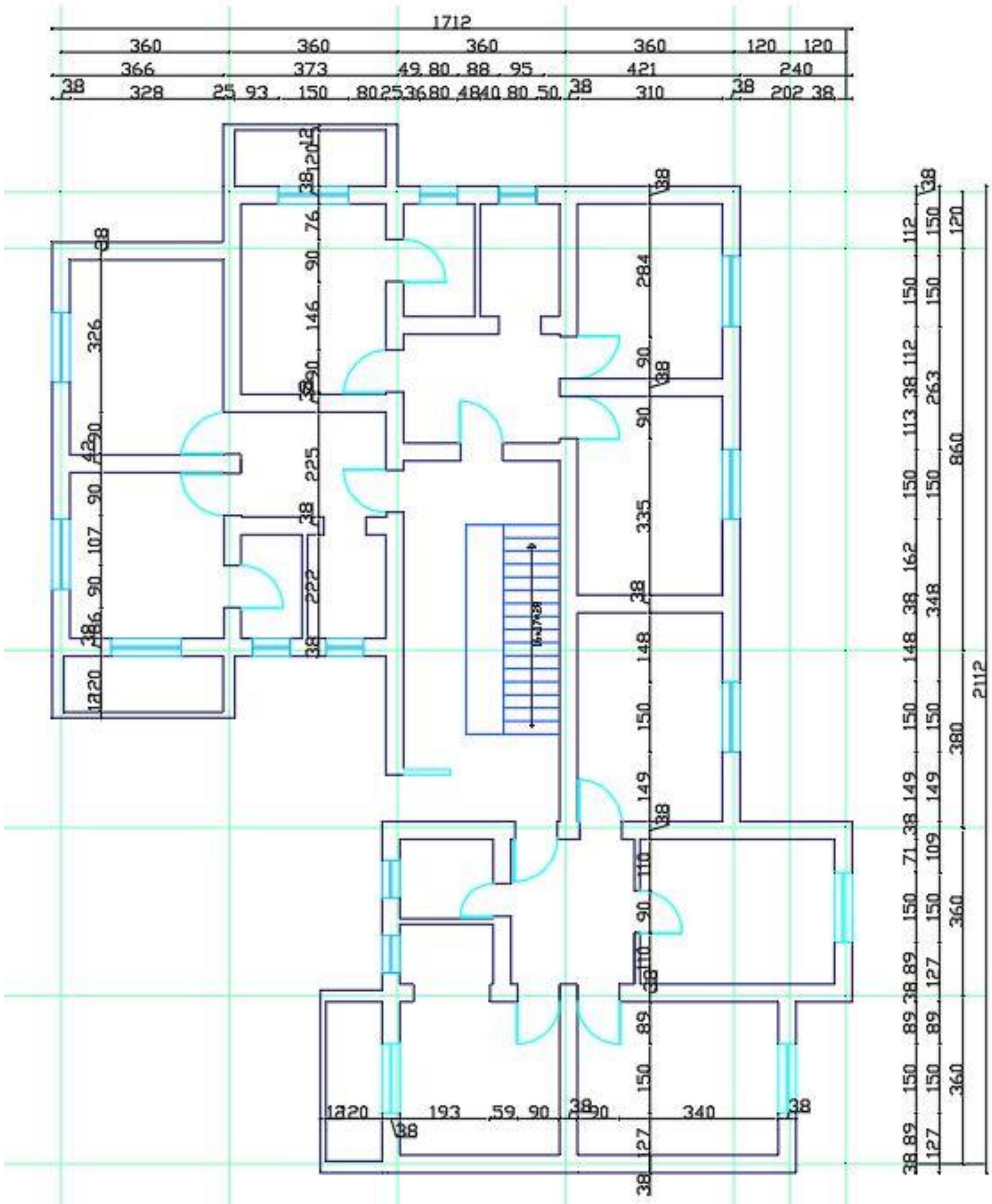

Figure 297: Plan view of building B4

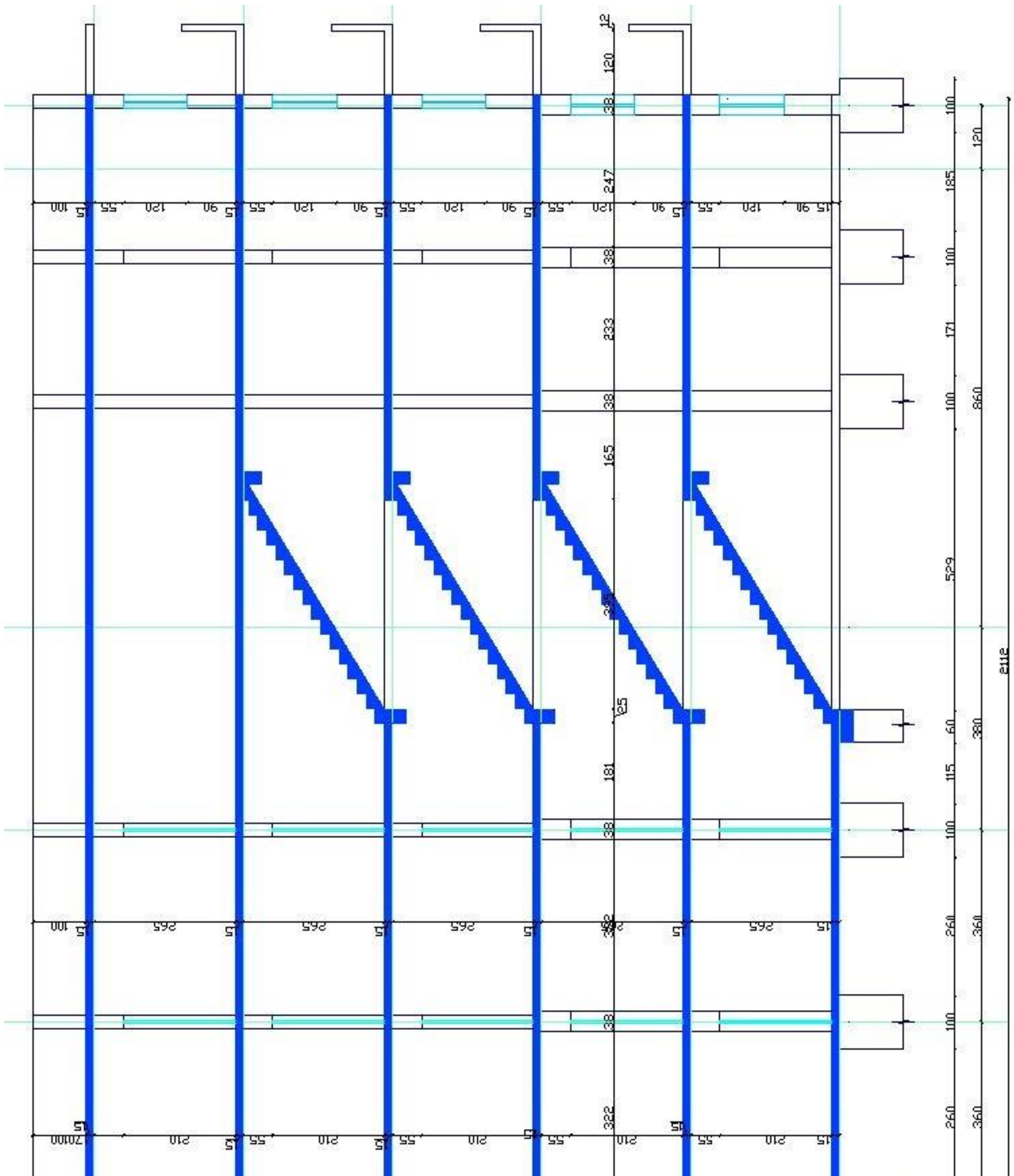

Figure 298: Elevation view of building B4

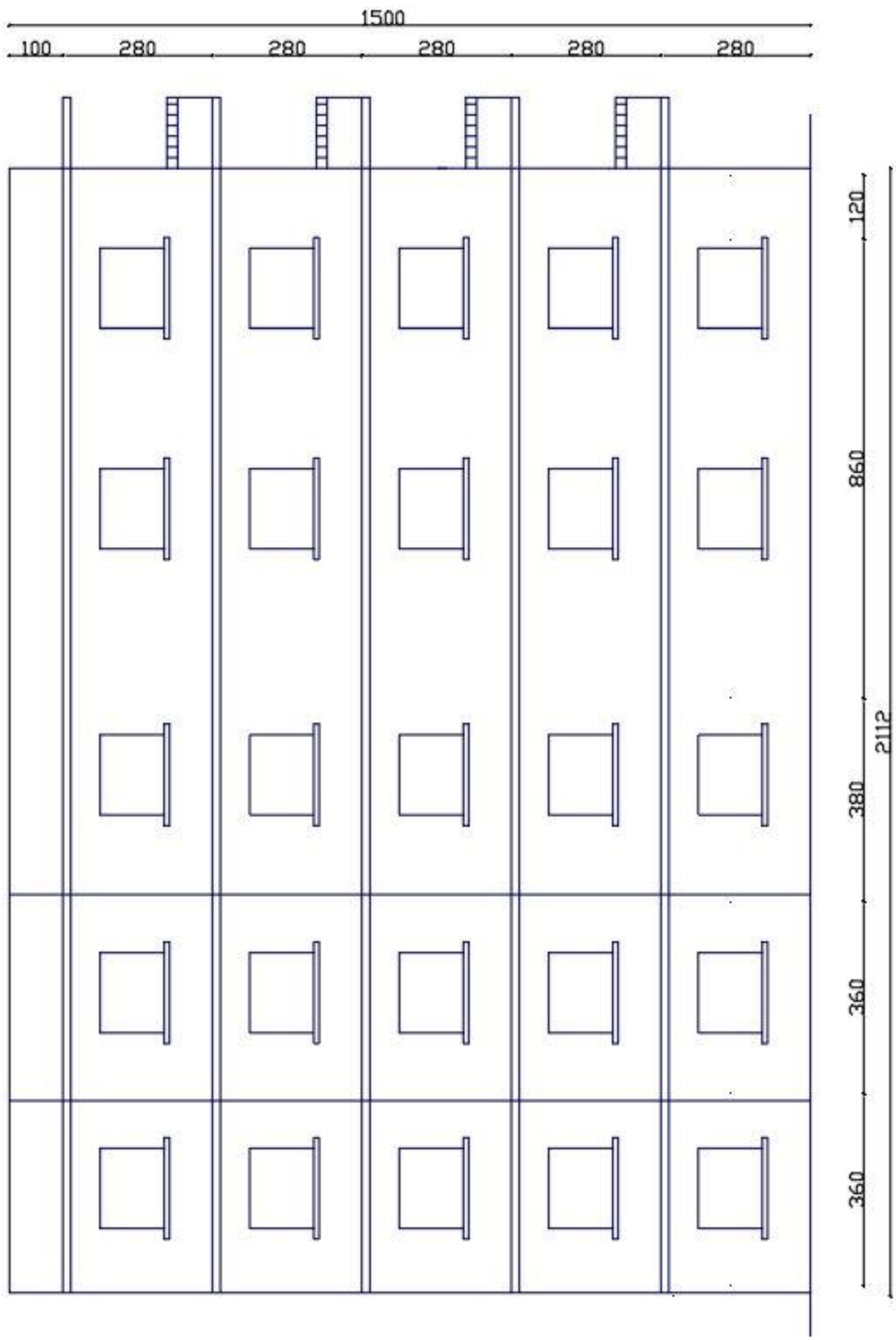

Figure 299: Facade view of building B4

Building C1 (77/5)

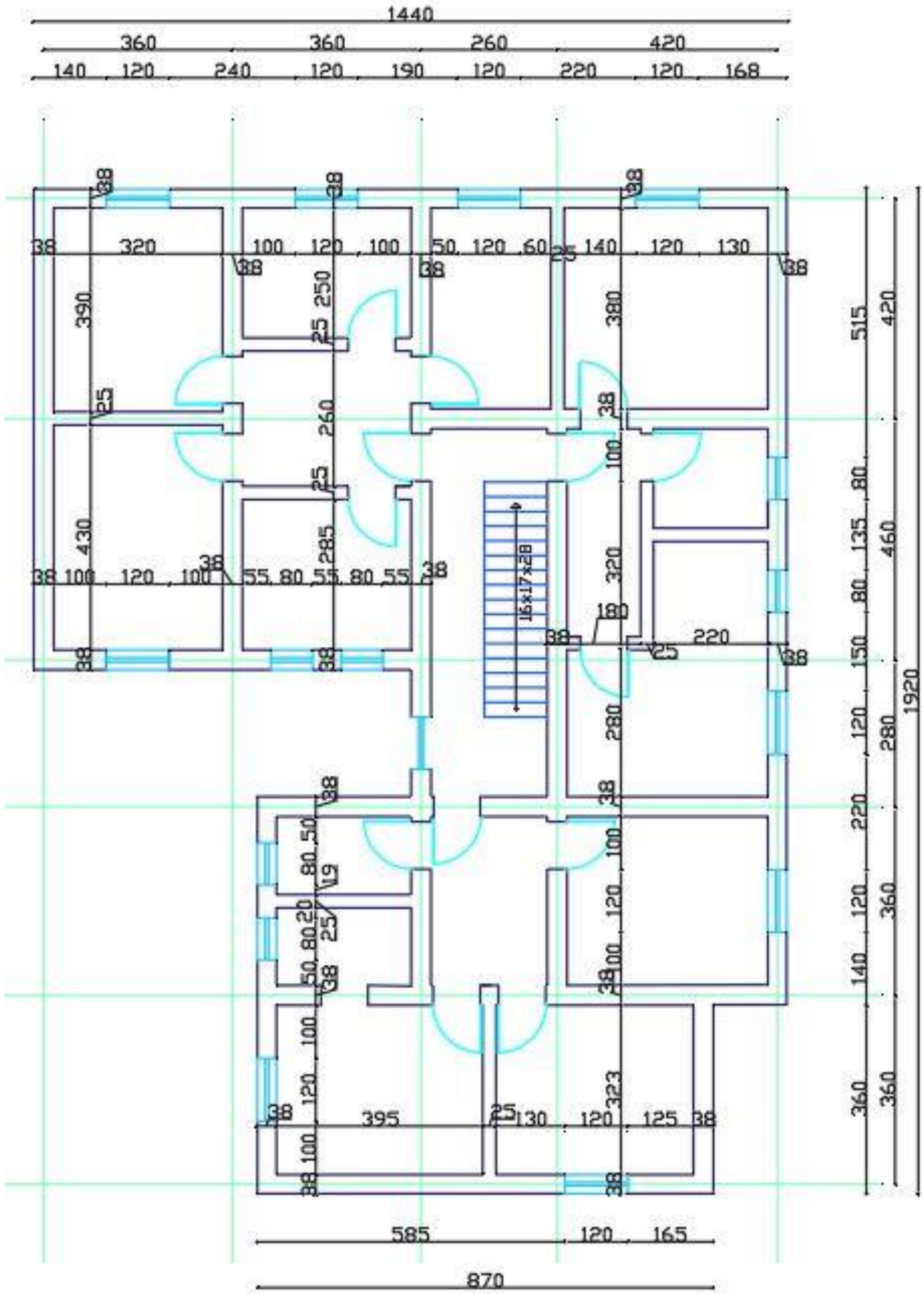

Figure 300: Plan view of buildings C1 (C1A and C1B)

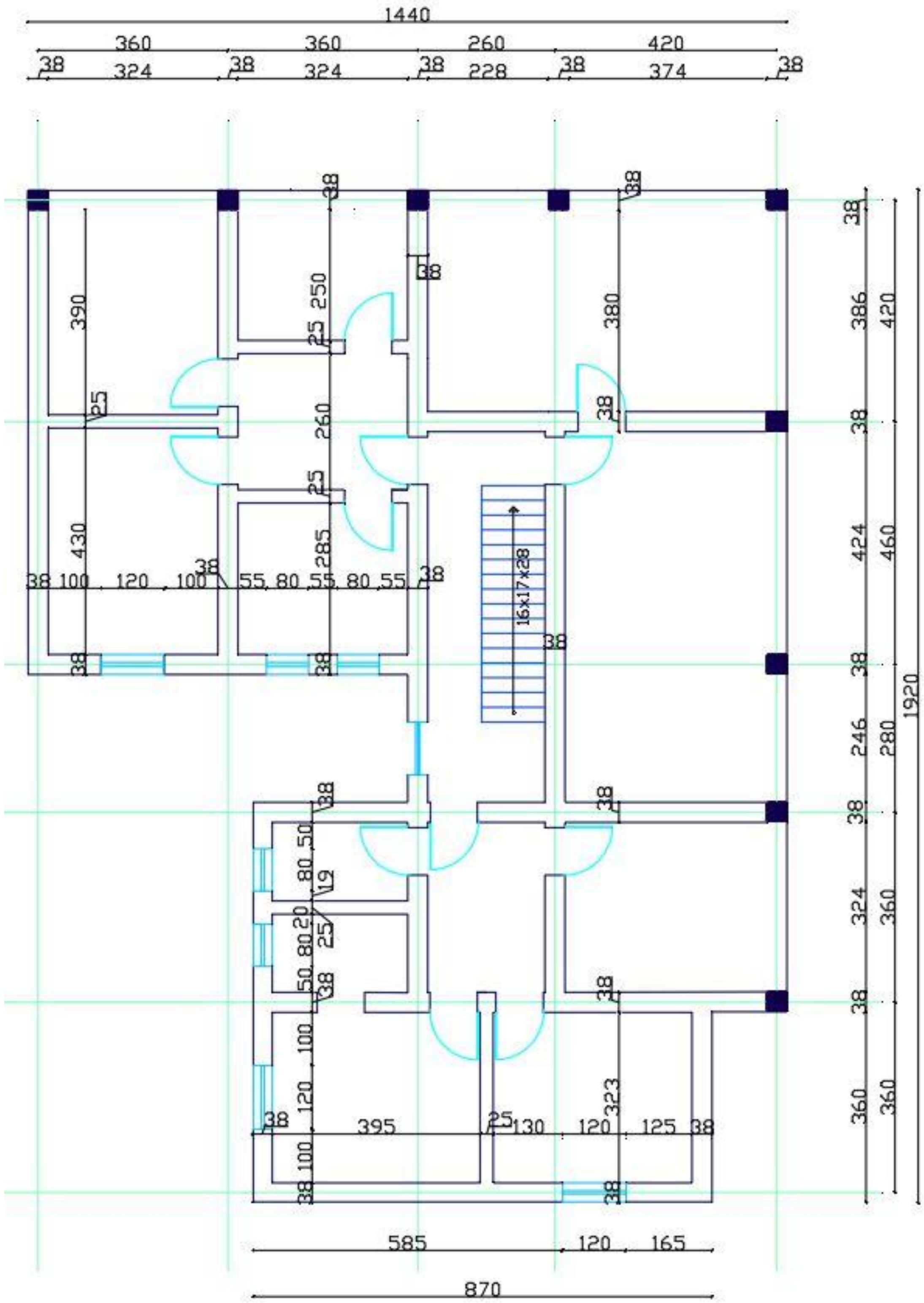

Figure 301: Plan view of first floor of building C1A with intervention

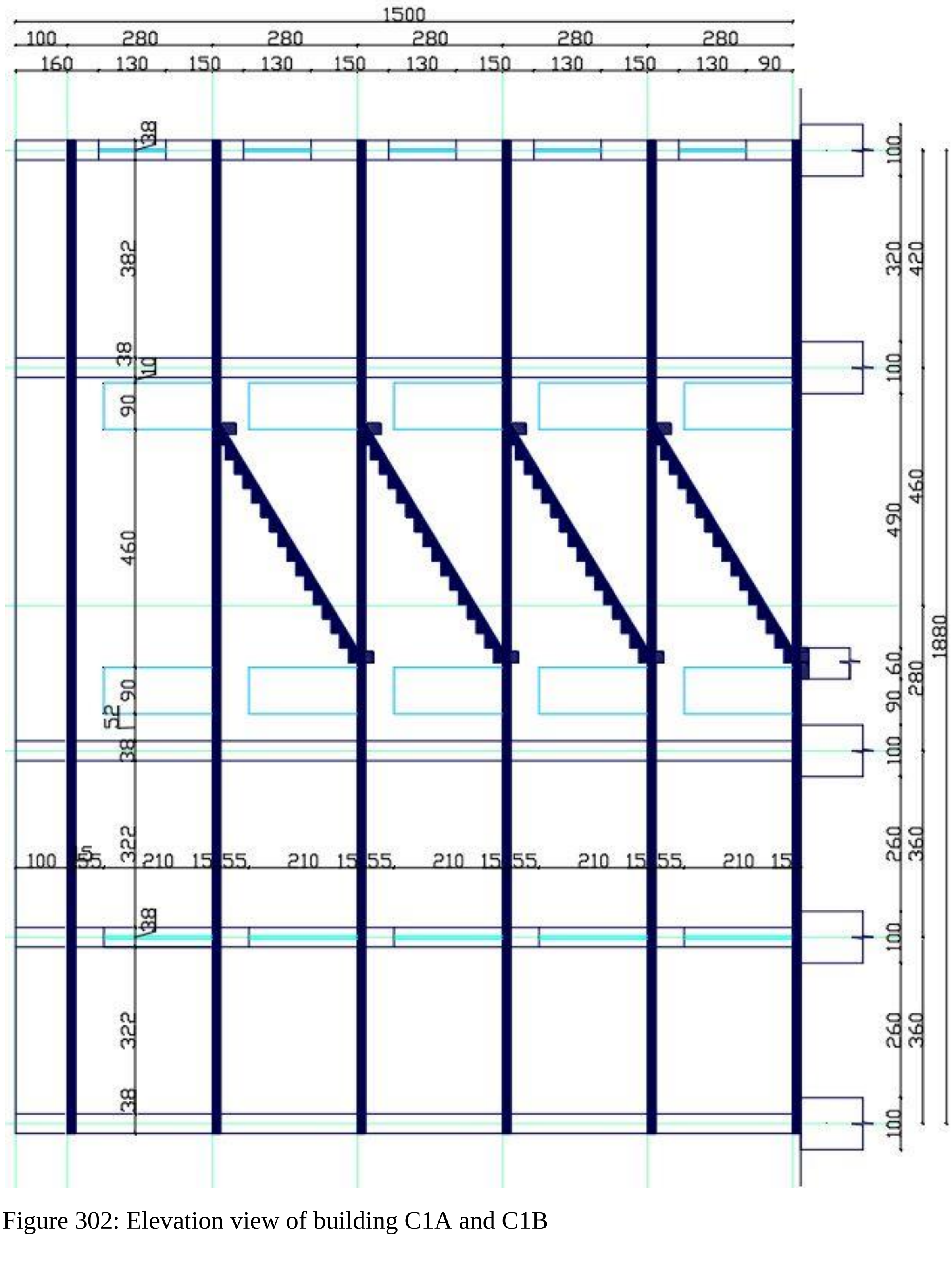

Figure 302: Elevation view of building C1A and C1B

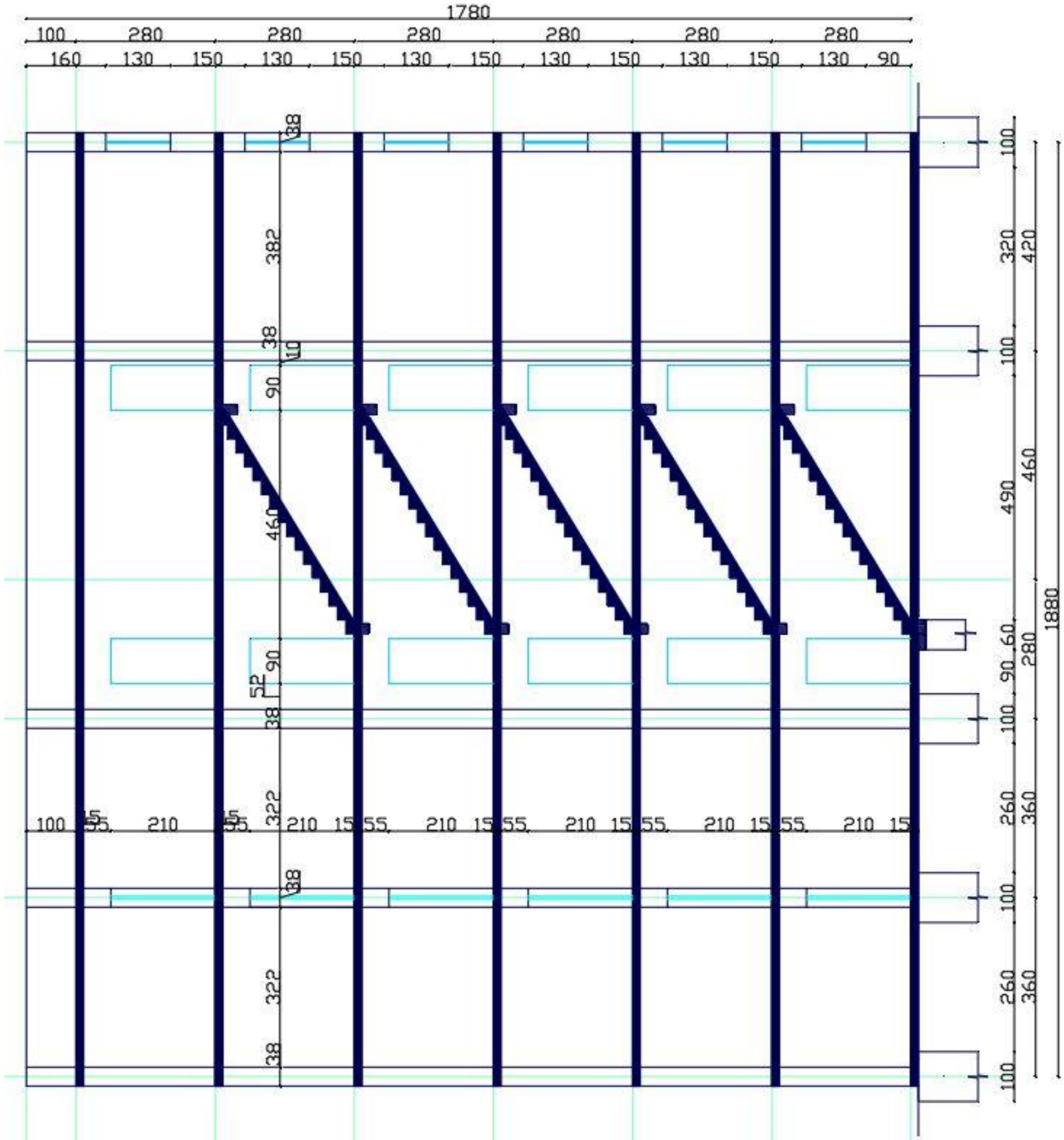

Figure 303: Elevation view of building C1B with one added floor

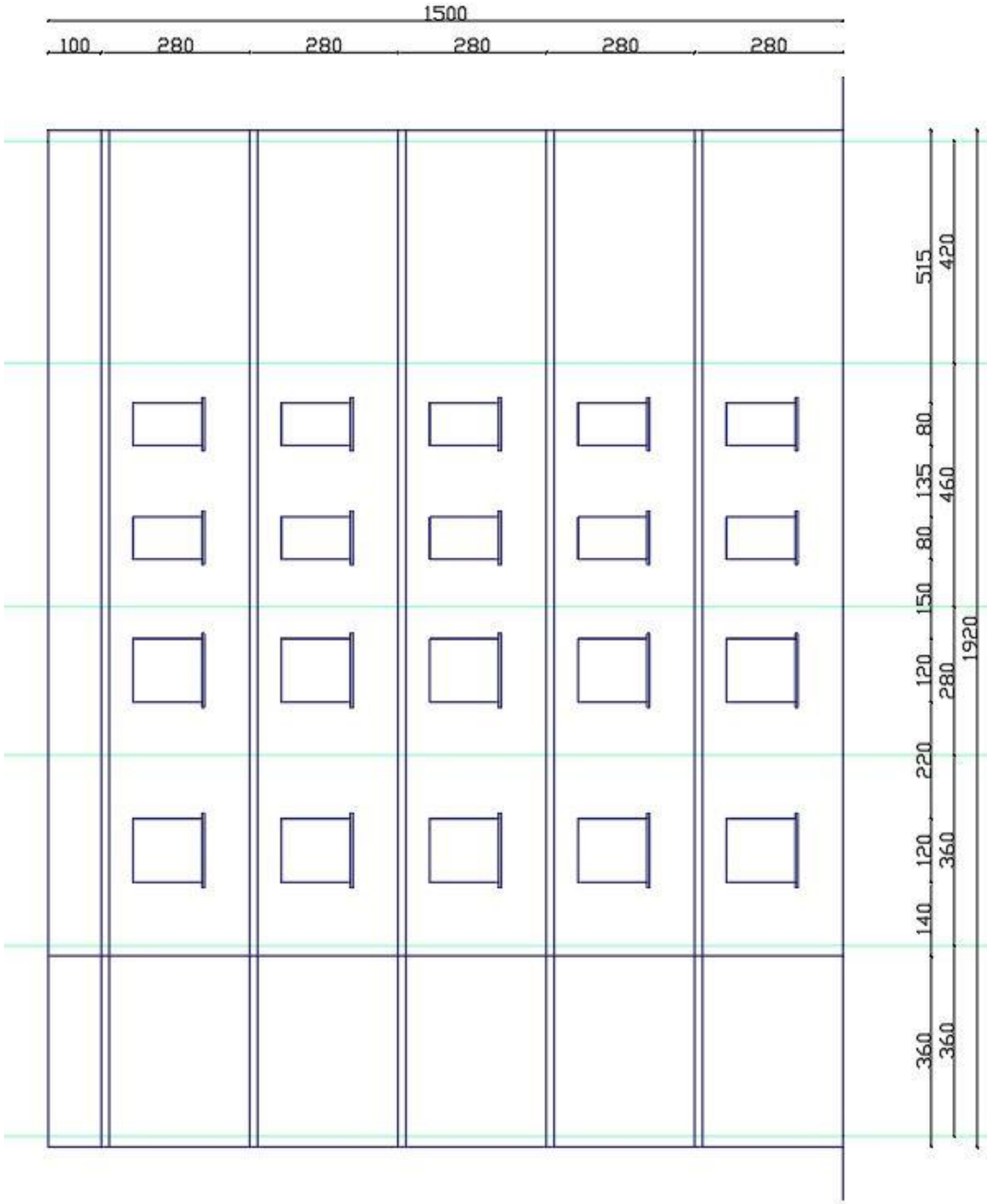

Figure 304: Facade view of building C1 (C1A and C1B)

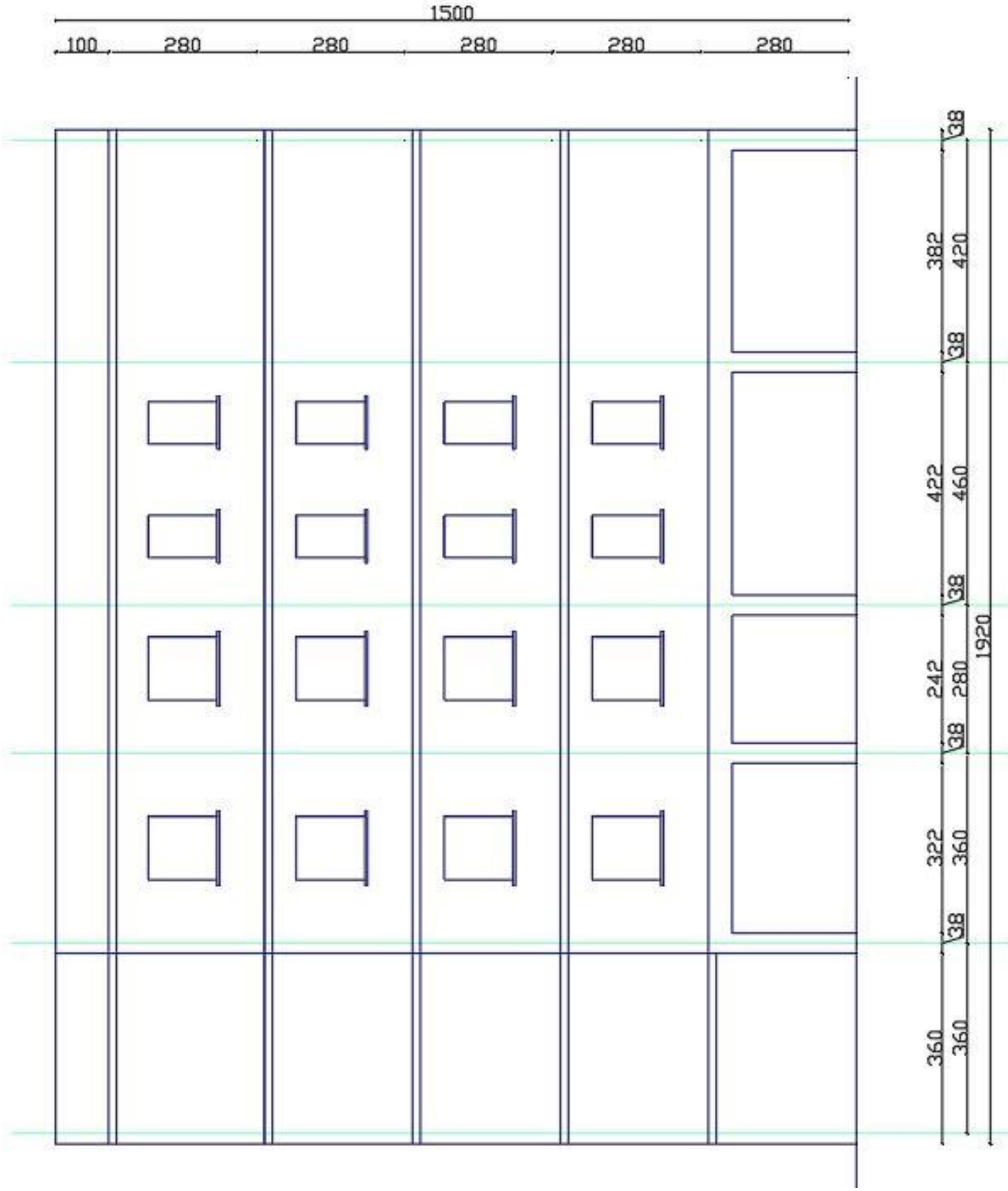

Figure 305: Facade view of building C1A building with intervention

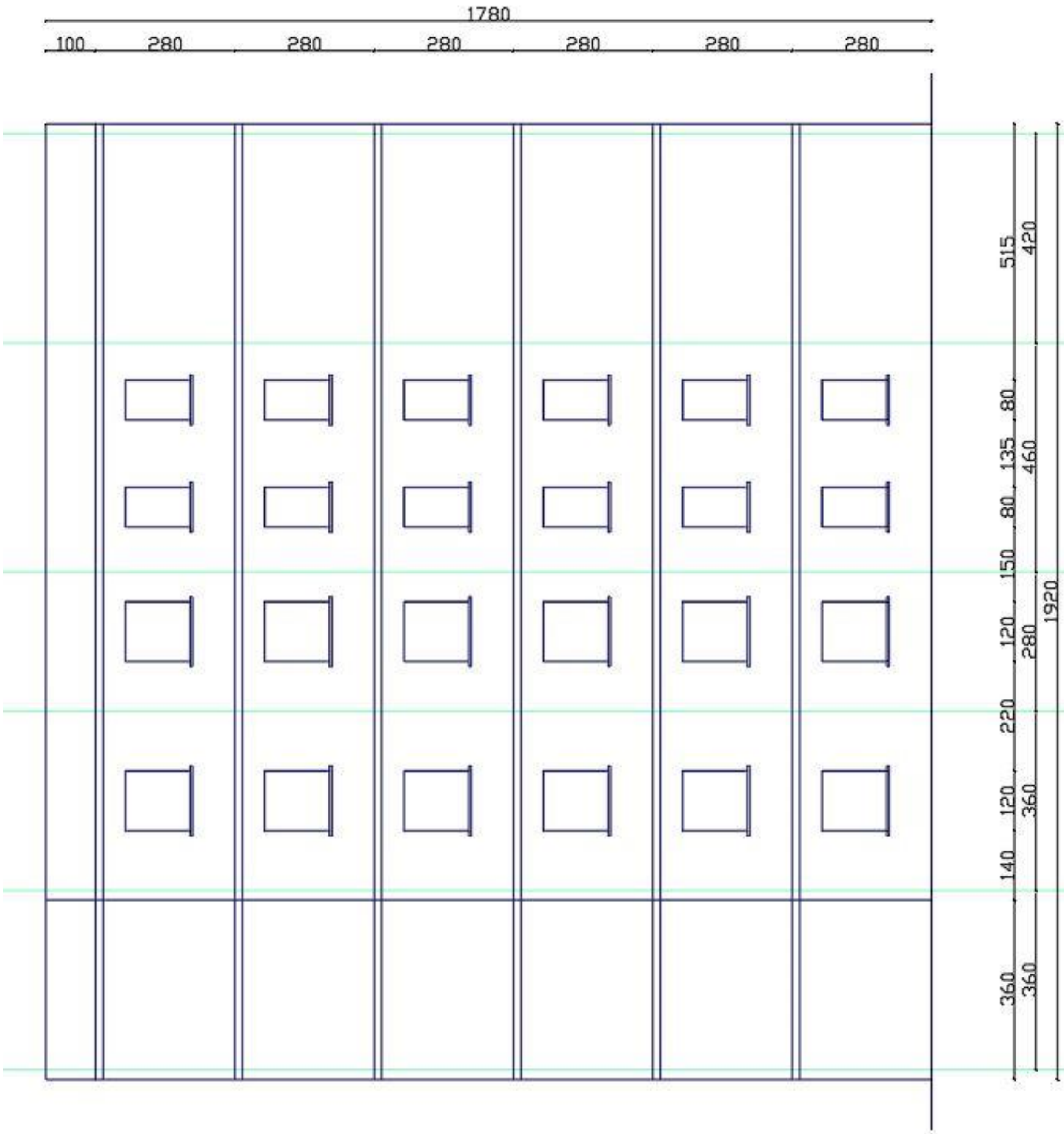

Figure 306: Facade view of building C1B building with one added floor

Building C2 (83/3)

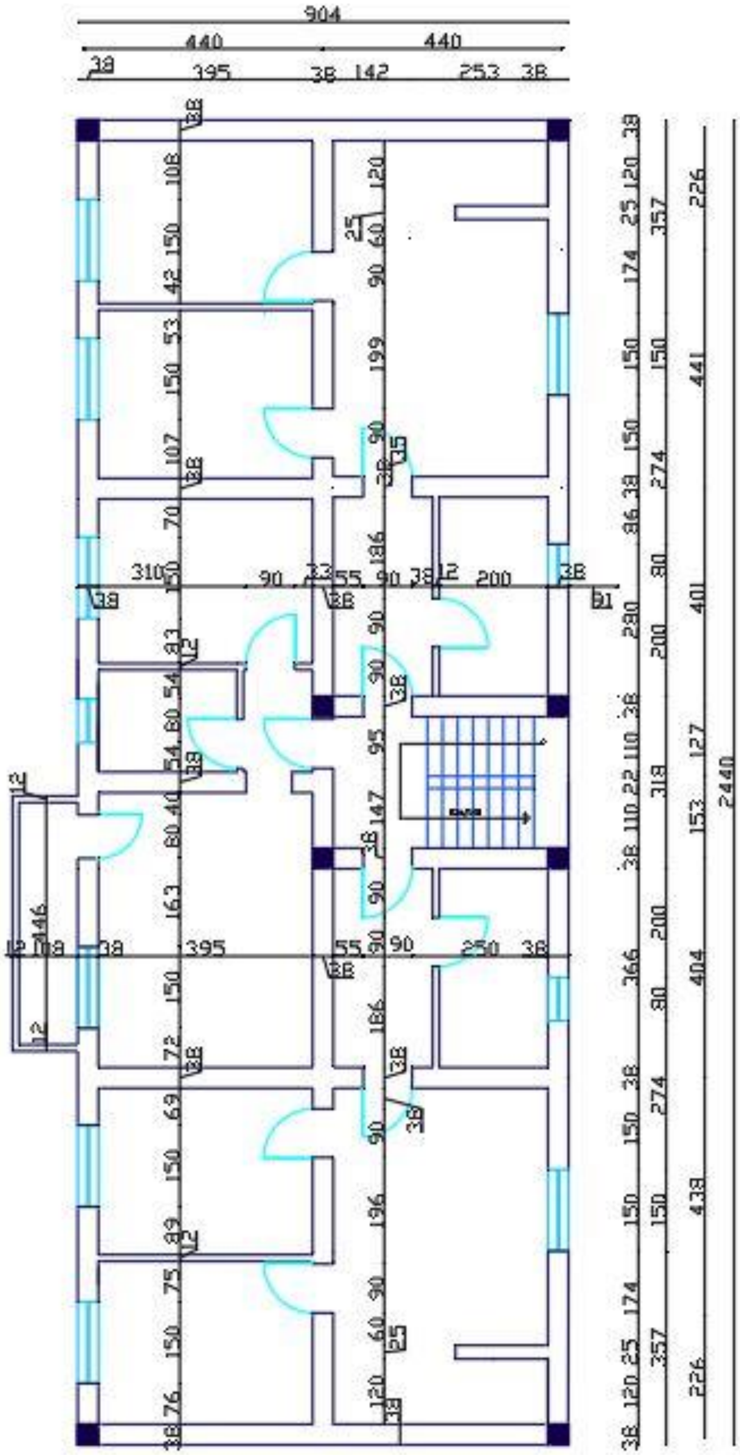

Figure 307: Plan view of building C2

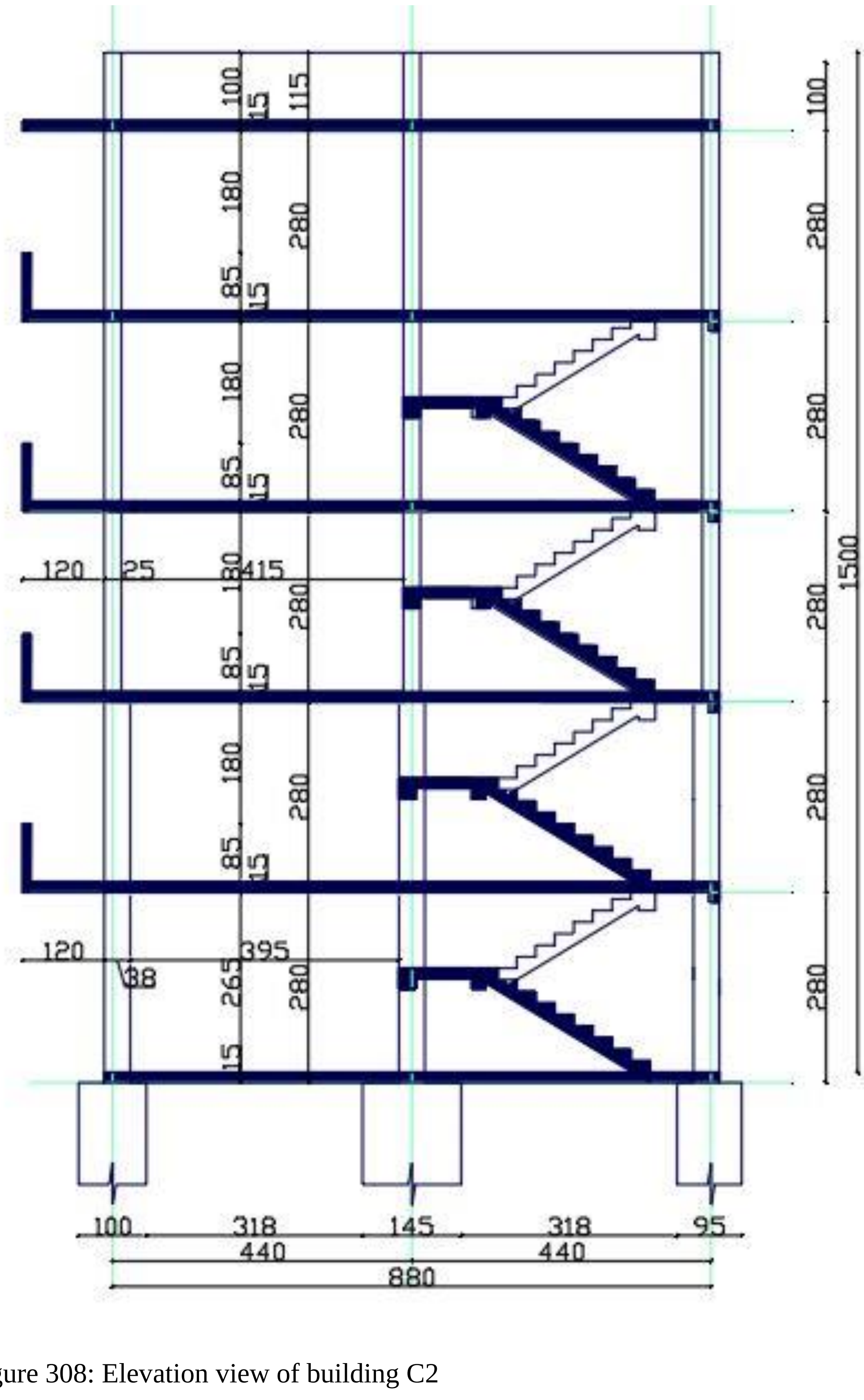

Figure 308: Elevation view of building C2

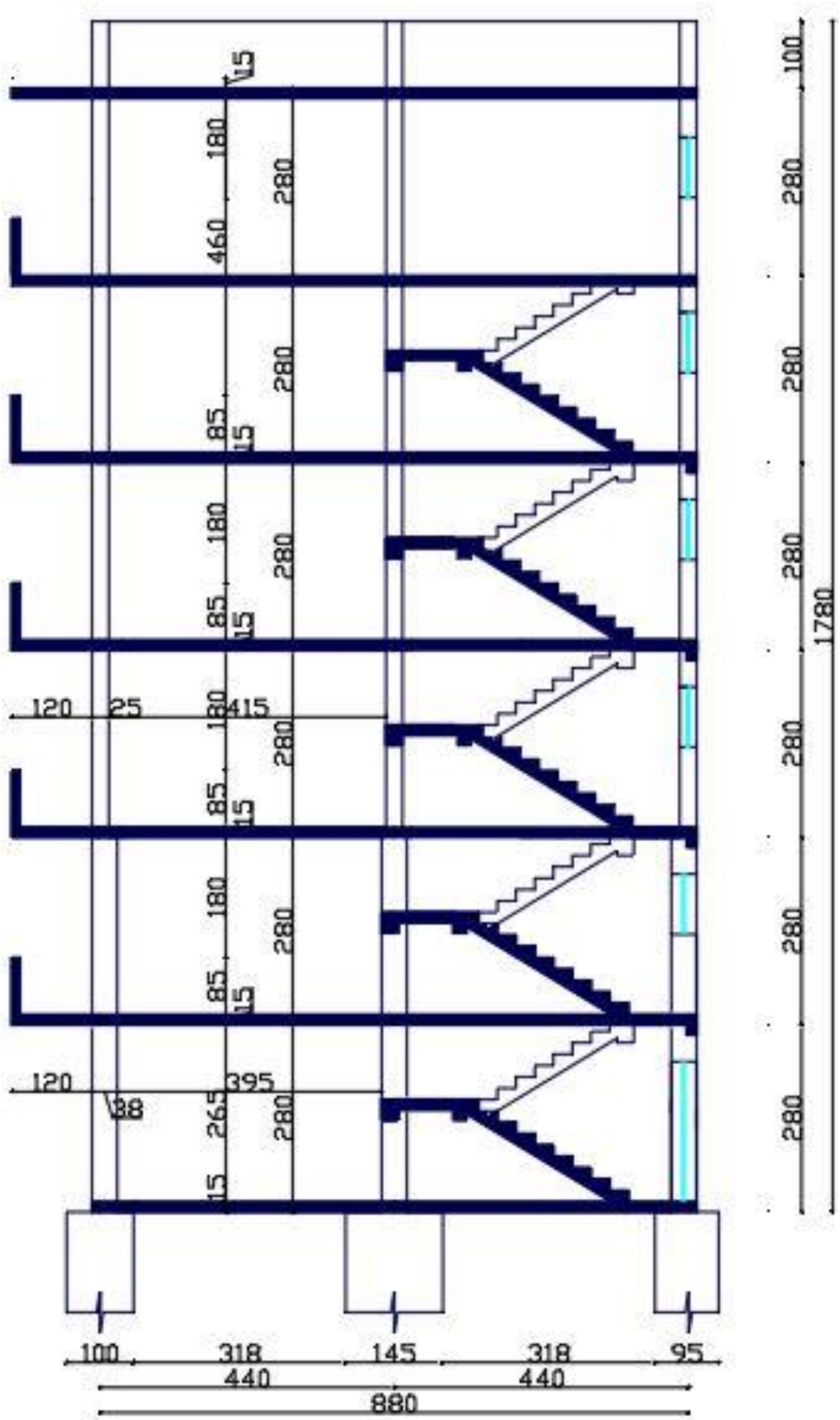

Figure 309: Elevation view of building C2 with one added floor

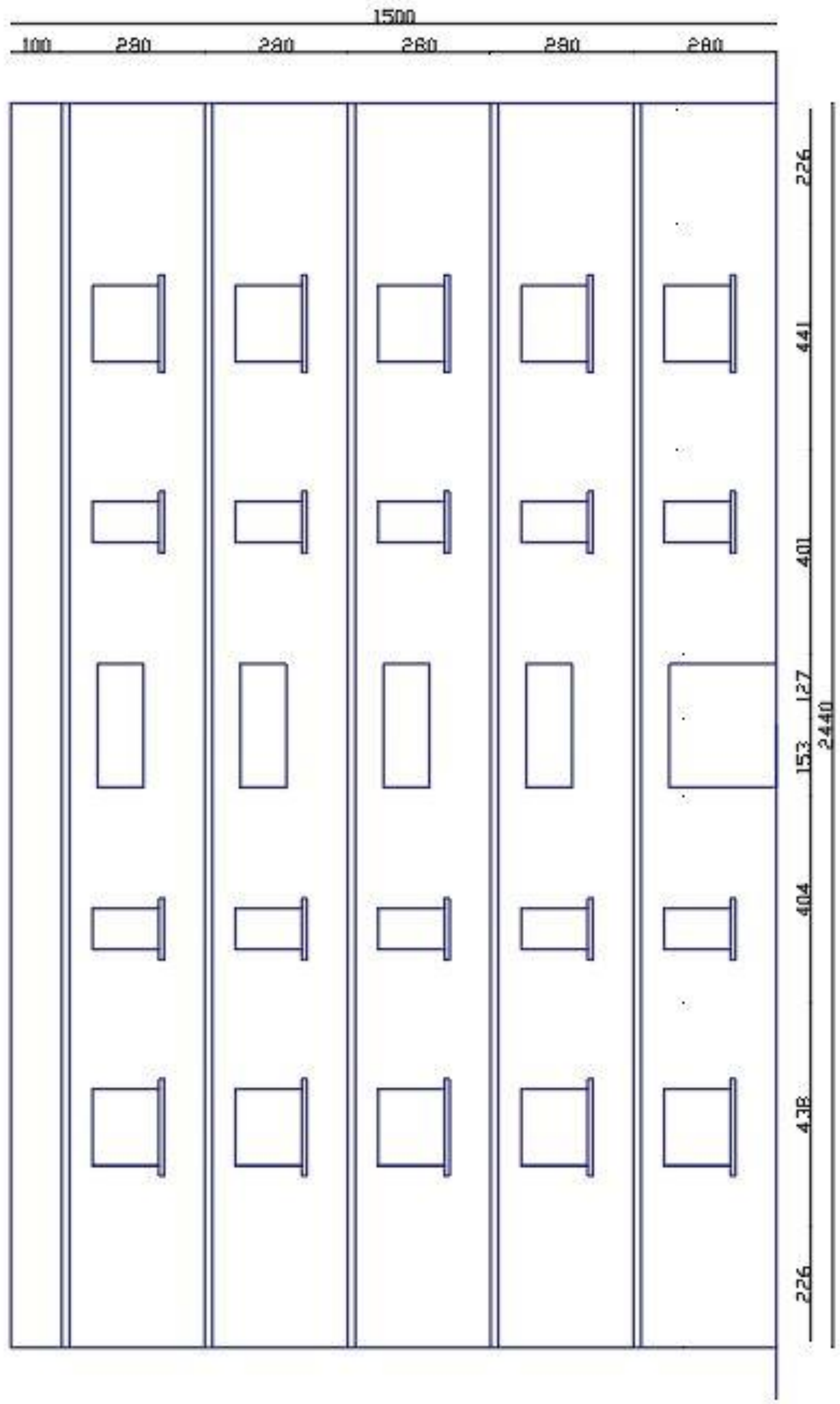

Figure 310: Facade view of building C2

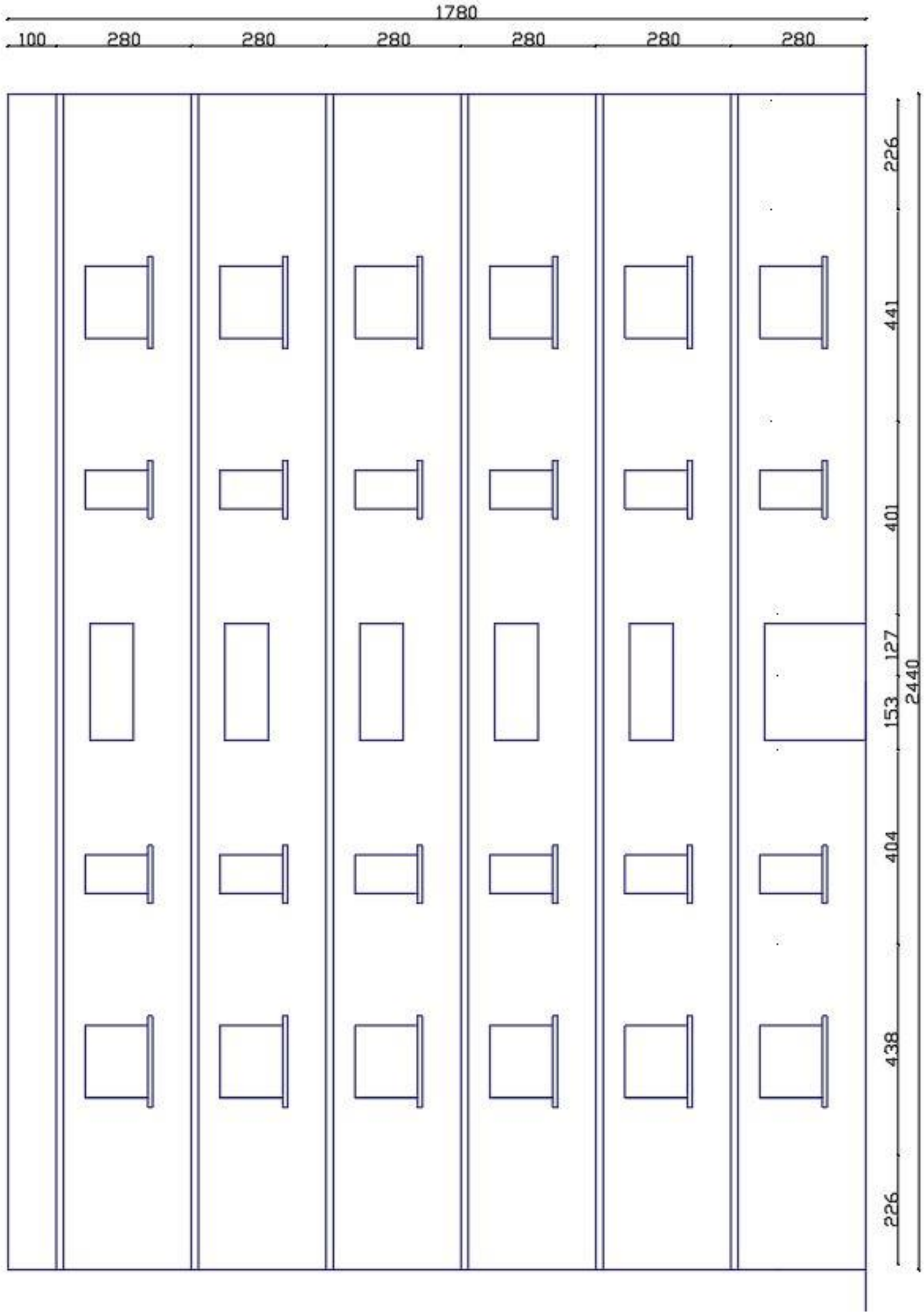

Figure 311: Facade view of building C2 with one added floor

Building C3 (template 83/10)

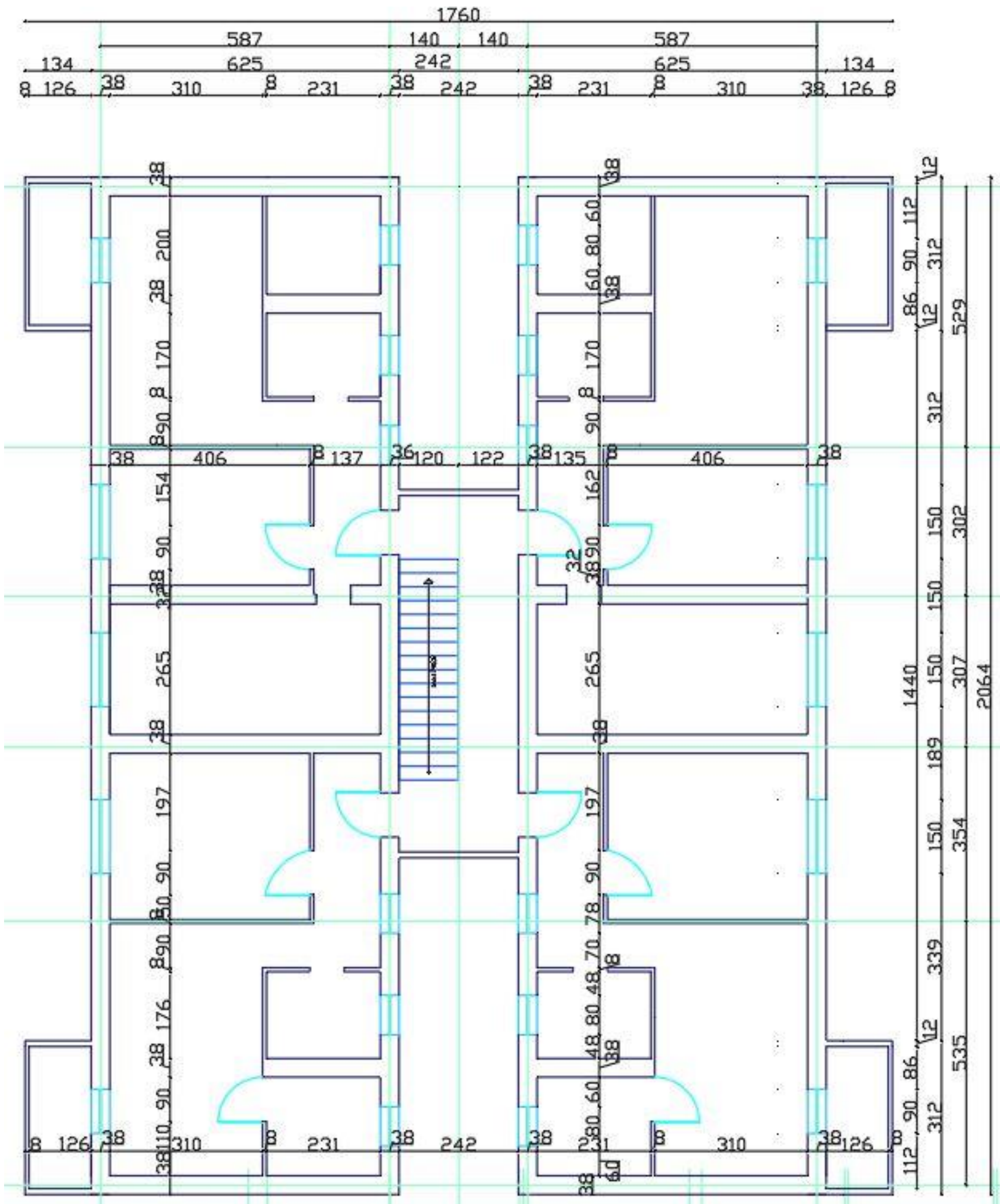

Figure 312: Plan view of building C3

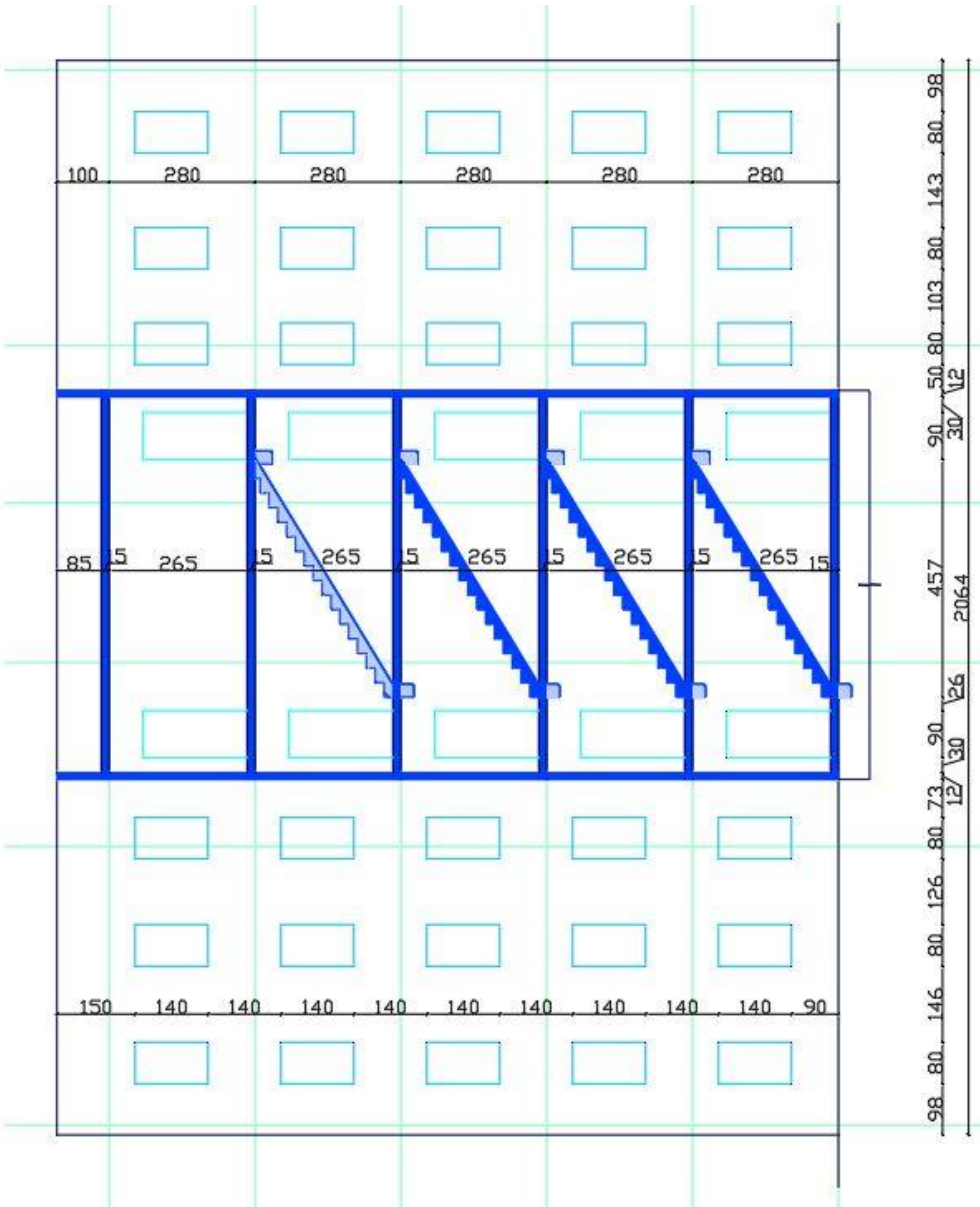

Figure 313: Elevation view of building C3

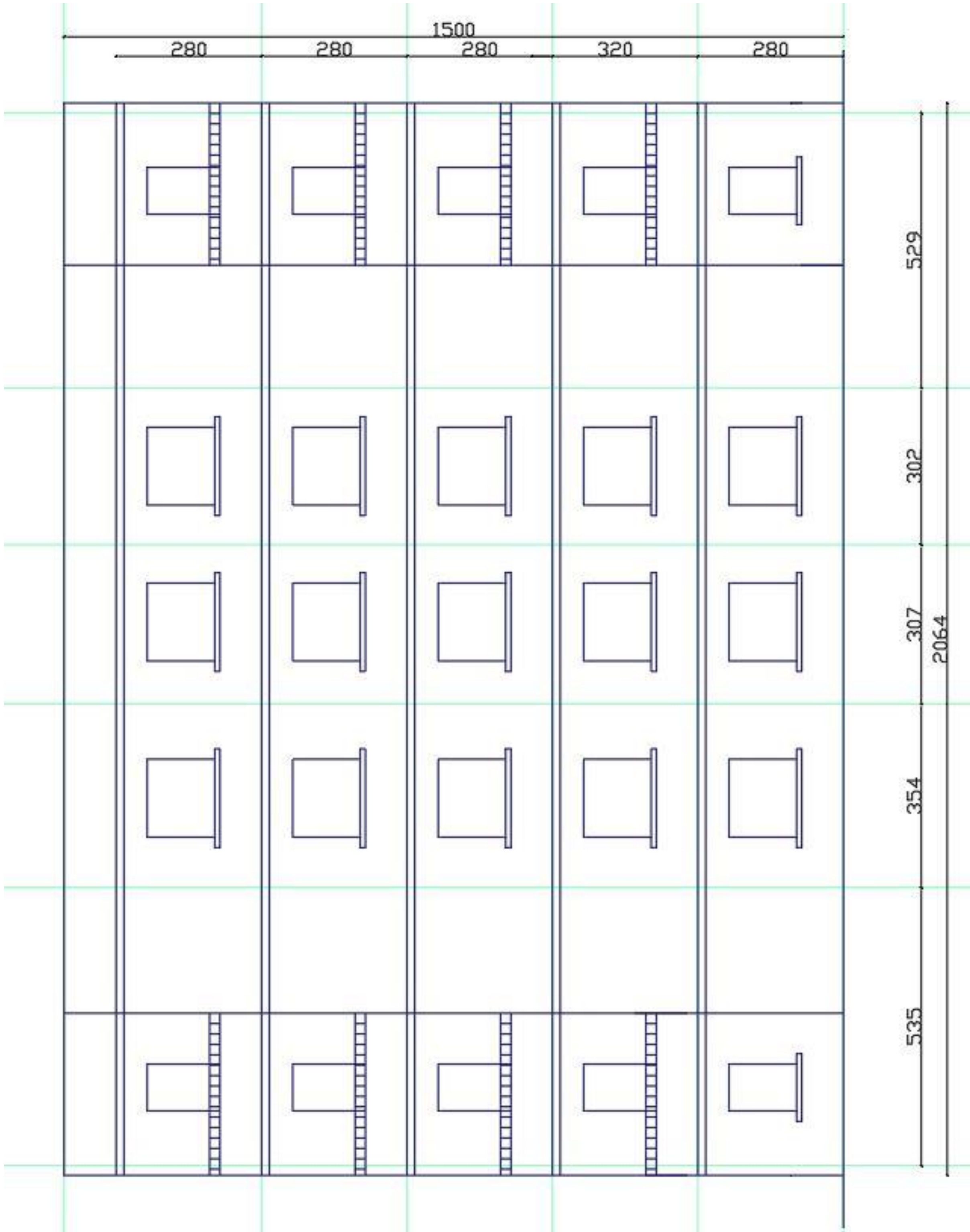

Figure 314: Facade view of building C3

APPENDIX C

Material characteristics of template designs

Test results for Building A1 (40/1)

Table 114: Compressive test of solid bricks of A1 building

Compressive test of solid bricks (clay bricks)								
Sample	**Sample dimensions**				**Fracture force (kN)**	**Compressive strength (MPa)**	**Sample weight m (gr)**	**Sample density (kg/m^3)**
	Length L(mm)	**Width B(mm)**	**Height H(mm)**	**Area A(mm^2)**				
1	247	120	65	14820	72.3	4.88	2864	1486.557
2	246	118	64	14514	73.1	5.04	3100	1668.648
3	247	119	66	14696.5	74.2	5.05	2980	1536.132
4	248	119	64	14756	72.9	4.94	3012	1594.69
5	250	119	66	14875	75.7	5.09	2856	1454.545
				Average		5		1548

Table 115: Brick density and water absorption tests of A1 building

Tensile flexural test of solid bricks (clay bricks)						
Sample	**Sample dimensions**				**Fracture force W (kN)**	**Tensile strength (MPa)**
	Length L(mm)	**Width B(mm)**	**Height H(mm)**	**Area A(mm^2)**		
1	247	120	65	7800	8.6	1.102564
2	246	118	64	7552	8.3	1.099047
3	247	119	66	7854	8.9	1.133181
4	248	119	64	7616	8.2	1.076681
5	250	119	66	7854	9.1	1.158645
				Average		1.11

Table 116:Tensile flexural test of solid bricks of A1 building

Compressive and tensile flexural test of mortar samples								
Sample	**Compressive test**				**Flexural tensile strength**			
	Dimensions LxBxH (mm^3)	**Area A (mm^2)**	**Fracture Force F (kN)**	**Compressive strength (MPa)**	**Dimensions LxBxH (mm^3)**	**Area A (mm^2)**	**Fracture Force F (kN)**	**Tensile strength (MPa)**
1	50x50x50	2500	6.35	2.54	160x40x40	1600	0.7	0.44
2	50x50x50	2500	5.75	2.3	160x40x40	1600	0.9	0.56
3	50x50x50	2500	5.65	2.26	160x40x40	1600	0.7	0.44
4	50x50x50	2500	5.55	2.22	160x40x40	1600	0.6	0.38
5	50x50x50	2500	5.45	2.18	160x40x40	1600	0.5	0.31
6	50x50x50	2500	5.85	2.34	160x40x40	1600	0.9	0.56
		Average		2.3		**Average**		0.45

Table 117:Compressive test of mortar samples of A1 building

Compressive test of masonry prism samples									
Sample	**Sample dimensions**				**Fracture force W (kN)**	**Compressive strength R (MPa)**	**Prism ratio H/B**	**Correlation factor n**	**Compressive strength f_k (MPa)**
	Length L(mm)	**Width B(mm)**	**Height H(mm)**	**Area A(mm^2)**					
1	248	242	401	60016	95.7	1.595	1.657	0.904	1.442
2	249	242	401	60258	95.5	1.586	1.657	0.904	1.434
3	250	240	401	60000	94.5	1. 575	1.67	0.908	1.43
4	249	240	400	59760	93.8	1.57	1.667	0.907	1.424
5	248	241	403	59768	95.03	1.59	1.672	0.908	1.452
							Average		1.437

Table 118:Triplet test of the samples with and without compressive test of A1 building

Triplet test of masonry samples						
Sample	**Sample dimensions**				**Fracture force Q (kN)**	**Shear strength fv (MPa)**
	Length L(mm)	**Width B(mm)**	**Height H(mm)**	**Area A(mm^2)**		
1	202	119	250	29750	9.2	0.154202
2	201	119	250	29512	9	0.153348
3	200	119	249	29382	8.8	0.145296
				Average		0.15
1'	201	119	250	29750	18.4	0.31
2'	199	118	250	29880	16.8	0.28
3'	200	119	250	29750	19	0.32
				Average		0.3

Test results for building A2 (58/2)

Table 119: Compressive test of solid bricks of A2 building

Compressive test of solid bricks (clay bricks)								
Sample	**Sample dimensions**				**Fracture force (kN)**	**Compressive strength (MPa)**	**Sample weight m (gr)**	**Sample density (kg/m^3)**
	Length L(mm)	**Width B(mm)**	**Height H(mm)**	**Area A(mm^2)**				
1	250	118	65	14750	102.9	6.98	3123	1628.68
2	246	120	65	14760	104.4	7.08	3222	1679.17
3	247	119	64	14696	103.9	7.07	3345	1778.17
4	246	119	63	14637	103.5	7.07	3412	1850.06
5	250	119	65	14875	104.8	7.05	3321	1717.39
				Average		7		1730

Table 120:Tensile flexural test of solid clay bricks of A2 building

Tensile flexural test of solid bricks (clay bricks)						
Sample	Sample dimensions				Fracture force W (kN)	Tensile strength (MPa)
	Length L(mm)	Width B(mm)	Height H(mm)	Area A(mm^2)		
1	250	118	65	7670	11.5	1.50
2	246	120	65	7800	10.6	1.36
3	247	119	64	7616	11.9	1.56
4	246	119	63	7497	12.6	1.68
5	250	119	65	7735	11.1	1.44
				Average		1.51

Table 121: Compressive and tensile flexural test of mortar samples of A2 building

Compressive and tensile flexural test of mortar samples								
Sample	**Compressive test**				**Flexural tensile strength**			
	Dimensions LxBxH (mm^3)	**Area A (mm^2)**	**Fracture Force F (kN)**	**Compressive strength (MPa)**	**Dimensions LxBxH (mm^3)**	**Area A (mm^2)**	**Fracture Force F (kN)**	**Tensile strength (MPa)**
1	50x50x50	2500	5.5	2.2	160x40x40	1600	0.8	0.5
2	50x50x50	2500	5	2	160x40x40	1600	0.8	0.5
3	50x50x50	2500	5.3	2.12	160x40x40	1600	0.7	0.4375
4	50x50x50	2500	5.9	2.36	160x40x40	1600	1	0.625
5	50x50x50	2500	5.1	2.04	160x40x40	1600	0.8	0.5
6	50x50x50	2500	5.3	2.12	160x40x40	1600	0.7	0.4375
		Average		2.13		**Average**		0.5

Table 122: Compressive test of masonry prism samples of A2 building

Compressive test of masonry prism samples									
Sample	**Sample dimensions**				**Fracture force W (kN)**	**Compressive strength R (MPa)**	**Prism ratio H/B**	**Correlation factor n**	**Compressive strength f_k (MPa)**
	Length L(mm)	**Width B(mm)**	**Height H(mm)**	**Area A(mm^2)**					
1	249	243	402	60507	122.6	2.026	1.654	0.903	1.81
2	247	243	400	60021	124.8	2.079	1.646	0.901	1.87
3	250	244	401	61000	123.7	2.028	1.643	0.9	1.82
4	248	242	403	60016	123	2.05	1.665	0.906	1.85
5	250	244	403	61000	123.5	2.024	1.652	0.902	1.82
							Average		1.84

Table 123: Triplet test of the samples with and without compressive test of A2 building

Triplet test of masonry samples						
Sample	**Sample dimensions**				**Fracture force Q (kN)**	**Shear strength fv (MPa)**
	Length L(mm)	**Width B(mm)**	**Height H(mm)**	**Area A(mm^2)**		
1	201	120	250	30000	10.1	0.168333
2	200	118	248	29264	9.7	0.165733
3	200	120	249	29880	10.2	0.170683
				Average		0.169
1'	200	118	248	29264	20.3	0.346843
2'	202	119	250	29750	19.2	0.322689
3'	200	120	250	30000	18.7	0.311667
				Average		0.327

Test results for building B1 (63/1)

Table 124: Compressive test of solid bricks of B1 building

Compressive test of solid bricks (clay bricks)								
Sample	Sample dimensions				Fracture force (kN)	Compressive strength (MPa)	Sample weight m (gr)	Sample density (kg/m^3)
	Length L(mm)	Width B(mm)	Height H(mm)	Area A(mm^2)				
1	245	120	65	14700	105.5	7.177	3203	1676.09
2	246	119	64	14637	106.4	7.269	3456	1844.64
3	247	118	66	14573	105	7.205	3543	1841.83
4	247	120	64	14820	106.4	7.179	3654	1926.24
5	249	118	65	14691	105.9	7.208	3354	1756.18
				Average		7.2		1809

Table 125: Tensile flexural test of solid clay bricks of B1 building

Tensile flexural test of solid bricks (clay bricks)						
Sample	Sample dimensions				Fracture force W (kN)	Tensile strength (MPa)
	Length L(mm)	Width B(mm)	Height H(mm)	Area A(mm^2)		
1	245	120	65	7800	12.8	1.64
2	246	119	64	7616	12.7	1.67
3	247	118	66	7788	12.9	1.66
4	247	120	64	7680	13.3	1.73
5	249	118	65	7670	13.8	1.8
				Average		1.7

Table 126: Compressive and tensile flexural test of mortar samples of B1 building

Compressive and tensile flexural test of mortar samples								
Sample	**Compressive test**				**Flexural tensile strength**			
	Dimensions LxBxH (mm^3)	**Area A (mm^2)**	**Fracture Force F (kN)**	**Compressive strength (MPa)**	**Dimensions LxBxH (mm^3)**	**Area A (mm^2)**	**Fracture Force F (kN)**	**Tensile strength (MPa)**
1	50x50x50	2500	5.2	2.08	160x40x40	1600	0.7	0.4375
2	50x50x50	2500	5.1	2.04	160x40x40	1600	0.9	0.5625
3	50x50x50	2500	5.9	2.36	160x40x40	1600	0.8	0.5
4	50x50x50	2500	5.9	2.36	160x40x40	1600	0.9	0.5625
5	50x50x50	2500	5.7	2.28	160x40x40	1600	0.7	0.4375
6	50x50x50	2500	5.6	2.24	160x40x40	1600	0.8	0.5
		Average		2.23		**Average**		0.5

Table 127:Compressive test of masonry prism samples of B1 building

Compressive test of masonry prism samples									
Sample	**Sample dimensions**				**Fracture force W (kN)**	**Compressive strength R (MPa)**	**Prism ratio H/B**	**Correlation factor n**	**Compressive strength f_k (MPa)**
	Length L(mm)	**Width B(mm)**	**Height H(mm)**	**Area A(mm^2)**					
1	247	240	400	59280	127.3	2.147	1.667	0.907	1.947
2	249	243	403	60507	124.6	2.059	1.658	0.904	1.862
3	250	242	401	60500	123.6	2.043	1.657	0.904	1.846
4	250	244	403	61000	125.7	2.060	1.651	0.902	1.859
5	246	243	402	59778	124.2	2.078	1.654	0.903	1.876
							Average		1.87

Table 128: Triplet test of the samples with and without compressive test of B1 building

Triplet test of masonry samples						
Sample	**Sample dimensions**				**Fracture force Q (kN)**	**Shear strength fv (MPa)**
	Length L(mm)	**Width B(mm)**	**Height H(mm)**	**Area A(mm^2)**		
1	201	120	249	29880	9.9	0.165663
2	202	118	250	29500	10.3	0.174576
3	202	118	249	29382	10.7	0.182084
				Average		0.174
1'	200	118	250	29500	20.2	0.342373
2'	202	119	250	29750	21	0.352941
3'	200	120	250	30000	20.1	0.335
				Average		0.34

Test results for Building B2 (69/3)

Table 129: Compressive test of solid silicate bricks of B2 building

Compressive test of solid bricks (silicate bricks)								
Sample	**Sample dimensions**				**Fracture force (kN)**	**Compressive strength (MPa)**	**Sample weight m (gr)**	**Sample density (kg/m^3)**
	Length L(mm)	**Width B(mm)**	**Height H(mm)**	**Area A(mm^2)**				
1	249	118	65	14691	108.6	7.392	3898	2041.02
2	246	119	65	14637	108.5	7.412	4007	2105.83
3	247	119	64	14696	107.6	7.321	4123	2191.74
4	246	120	65	14760	107.4	7.276	4105	2139.36
5	250	120	65	15000	107.5	7.167	3943	2022.05
				Average		7.3		2100

Table 130: Tensile flexural test of solid silicate bricks of B2 building

Tensile flexural test of solid bricks (silicate bricks)						
Sample	**Sample dimensions**				**Fracture force W (kN)**	**Tensile strength (MPa)**
	Length L(mm)	**Width B(mm)**	**Height H(mm)**	**Area $A(mm^2)$**		
1	249	118	65	7670	14.2	1.851
2	246	119	65	7735	14.9	1.926
3	247	119	64	7616	15.9	2.088
4	246	120	65	7800	14.5	1.859
5	250	120	65	7800	14.1	1.807
				Average		1.9

Table 131: Compressive and tensile flexural test of mortar samples of B2 building

Compressive and tensile flexural test of mortar samples								
Sample	**Compressive test**				**Flexural tensile strength**			
	Dimensions LxBxH (mm^3)	**Area A (mm^2)**	**Fracture Force F (kN)**	**Compressive strength (MPa)**	**Dimensions LxBxH (mm^3)**	**Area A (mm^2)**	**Fracture Force F (kN)**	**Tensile strength (MPa)**
1	50x50x50	2500	5.5	2.2	160x40x40	1600	1	0.625
2	50x50x50	2500	6	2.4	160x40x40	1600	1.1	0.6875
3	50x50x50	2500	6	2.4	160x40x40	1600	1	0.625
4	50x50x50	2500	5.9	2.36	160x40x40	1600	0.9	0.5625
5	50x50x50	2500	6.1	2.44	160x40x40	1600	1.1	0.6875
6	50x50x50	2500	5.7	2.28	160x40x40	1600	0.9	0.5625
		Average		2.35		**Average**		0.63

Table 132: Compressive test of masonry prism samples of B2 building

Compressive test of masonry prism samples									
Sample	**Sample dimensions**				**Fracture force W (kN)**	**Compressive strength R (MPa)**	**Prism ratio H/B**	**Correlation factor n**	**Compressive strength f_k (MPa)**
	Length L(mm)	**Width B(mm)**	**Height H(mm)**	**Area A(mm^2)**					
1	248	243	401	60264	127.3	2.112	1.65	0.902	1.905
2	249	243	400	60507	125.4	2.072	1.646	0.901	1.867
3	250	242	402	60500	123.6	2.043	1.66	0.905	1.849
4	248	240	402	59520	123.7	2.078	1.675	0.909	1.889
5	250	242	400	60500	128	2.116	1.653	0.903	1.910
							Average		1.88

Table 133: Triplet test of the samples with and without compressive test of B2 building

Triplet test of masonry samples						
Sample	**Sample dimensions**				**Fracture force Q (kN)**	**Shear strength fv (MPa)**
	Length L(mm)	**Width B(mm)**	**Height H(mm)**	**Area A(mm^2)**		
1	202	119	248	29512	11.7	0.198
2	200	120	250	30000	11.4	0.19
3	199	118	248	29264	10.4	0.177
				Average		0.189
1'	201	119	249	29631	21.3	0.359
2'	200	120	250	30000	20.4	0.34
3'	201	120	248	29760	20	0.336
				Average		0.345

Test results for building B3 (72/1)

Table 134: Compressive test of solid bricks of B3 building

Compressive test of solid bricks (clay bricks)								
Sample	**Sample dimensions**				**Fracture force (kN)**	**Compressive strength (MPa)**	**Sample weight m (gr)**	**Sample density (kg/m^3)**
	Length L(mm)	**Width B(mm)**	**Height H(mm)**	**Area A(mm^2)**				
1	245	119	65	29155	103.2	7.08	3123	1647.96
2	248	120	65	29760	112.5	7.56	3242	1675.97
3	250	118	65	29500	105.2	7.13	3450	1799.22
4	249	118	64	29382	104.9	7.14	3321	1766.07
5	250	120	64	30000	110.8	7.39	3145	1638.02
				Average		7.25		1705

Table 135: Tensile flexural test of solid clay bricks of B3 building

Tensile flexural test of solid bricks (clay bricks)						
Sample	**Sample dimensions**				**Fracture force W (kN)**	**Tensile strength (MPa)**
	Length L(mm)	**Width B(mm)**	**Height H(mm)**	**Area A(mm^2)**		
1	245	119	65	7735	13.4	1.73
2	248	120	65	7800	12.6	1.62
3	250	118	65	7670	12.9	1.68
4	249	118	64	7552	14.3	1.8
5	250	120	64	7680	12.1	1.58
				Average		1.7

Table 136: Compressive and tensile flexural test of mortar samples of B3 building

Compressive and tensile flexural test of mortar samples								
Sample	Compressive test				Flexural tensile strength			
	Dimensions LxBxH (mm^3)	Area A (mm^2)	Fracture Force F (kN)	Compressive strength (MPa)	Dimensions LxBxH (mm^3)	Area A (mm^2)	Fracture Force F (kN)	Tensile strength (MPa)
1	50x50x50	2500	5.5	2.84	160x40x40	1600	0.8	0.5
2	50x50x50	2500	6.2	2.6	160x40x40	1600	1.1	0.69
3	50x50x50	2500	6.3	2.68	160x40x40	1600	1	0.63
4	50x50x50	2500	5.9	2.28	160x40x40	1600	0.9	0.56
5	50x50x50	2500	6	2.4	160x40x40	1600	1.1	0.69
6	50x50x50	2500	6.1	2.44	160x40x40	1600	1	0.62
		Average		2.4		**Average**		0.62

Table 137: Compressive test of masonry prism samples of B3 building

Compressive test of masonry prism samples									
Sample	Sample dimensions				Fracture force W (kN)	Compressive strength R (MPa)	Prism ratio H/B	Correlation factor n	Compressive strength f_k (MPa)
	Length L(mm)	Width B(mm)	Height H(mm)	Area A(mm^2)					
1	250	241	400	60250	128.3	2.13	1.66	0.905	1.93
2	249	243	400	60507	126.4	2.09	1.65	0.901	1.88
3	248	242	402	60016	125.6	2.09	1.66	0.905	1.89
4	248	241	403	59768	128.7	2.15	1.67	0.908	1.96
5	246	242	400	59532	123	2.07	1.65	0.902	1.87
							Average		1.9

Table 138: Triplet test of the samples with and without compressive test of B3 building

Triplet test of masonry samples						
Sample	Sample dimensions				Fracture force	Shear strength
	Length L(mm)	Width B(mm)	Height H(mm)	Area A(mm^2)	Q (kN)	fv (MPa)
1	200	119	248	29512	10.8	0.18
2	200	120	250	30000	10.3	0.17
3	202	120	250	30000	11.4	0.19
				Average		0.18
1'	199	119	250	29750	22.3	0.37
2'	199	118	249	29382	20.1	0.34
3'	201	120	248	29760	20.5	0.34
				Average		0.35

Test results for building B4 (72/3)

Table 139: Compressive test of solid bricks of B4 building

Compressive test of solid bricks (silicate bricks)								
Sample	Sample dimensions				Fracture force	Compressive strength	Sample weight	Sample density
	Length L(mm)	Width B(mm)	Height H(mm)	Area A(mm^2)	(kN)	(MPa)	m (gr)	(kg/m^3)
1	250	119	65	14875	109.7	7.37	4112	2126.4
2	250	118	66	14750	107.5	7.29	4231	2173.1
3	249	118	65	14940	109.3	7.44	4056	2123.7
4	249	119	67	14875	110.4	7.45	3614	1820.4
5	248	119	65	14756	108.7	7.37	4046	2109.2
				Average		7.38		2070

Table 140: Tensile flexural test of solid bricks of B4 building

Tensile flexural test of solid bricks (silicate bricks)						
Sample	**Sample dimensions**				**Fracture force W (kN)**	**Tensile strength (MPa)**
	Length L(mm)	**Width B(mm)**	**Height H(mm)**	**Area $A(mm^2)$**		
1	250	119	65	7735	12.3	1.59
2	250	118	66	7788	13.5	1.73
3	249	118	65	7670	11.4	1.48
4	249	119	67	7973	14.6	1.83
5	248	119	65	7735	12.7	1.64
				Average		1.66

Table 141: Compressive test of mortar samples of B4 building

Compressive and tensile flexural test of mortar samples								
Sample	**Compressive test**				**Flexural tensile strength**			
	Dimensions LxBxH (mm^3)	**Area A (mm^2)**	**Fracture Force F (kN)**	**Compressive strength (MPa)**	**Dimensions LxBxH (mm^3)**	**Area A (mm^2)**	**Fracture Force F (kN)**	**Tensile strength (MPa)**
1	50x50x50	2500	11.3	4.52	160x40x40	1600	1.4	0.88
2	50x50x50	2500	11.8	4.72	160x40x40	1600	1.5	0.94
3	50x50x50	2500	12.2	4.88	160x40x40	1600	1.5	0.94
4	50x50x50	2500	12.5	5	160x40x40	1600	1.6	1
5	50x50x50	2500	12.1	4.8	160x40x40	1600	1.6	1
6	50x50x50	2500	12.3	4.92	160x40x40	1600	1.4	0.88
		Average		4.8		**Average**		0.95

Table 142: Compressive strength of masonry prism samples of B4 building

Compressive test of masonry prism samples									
Sample	Sample dimensions				Fracture force W (kN)	Compressive strength R (MPa)	Prism ratio H/B	Correlation factor n	Compressive strength f_k (MPa)
	Length L(mm)	Width B(mm)	Height H(mm)	Area A(mm^2)					
1	249	241	401	60009	159.2	2.653	1.664	0.906	2.403
2	248	241	401	59768	161.2	2.697	1.664	0.906	2.443
3	248	244	402	60512	163.4	2.7	1.648	0.901	2.439
4	249	243	400	60507	157.8	2.608	1.646	0.9	2.35
5	250	241	400	59527	156.7	2.632	1.659	0.905	2.382
							Average		2.402

Table 143: Triplet test of the samples with and without compressive test of B4 building

Triplet test of masonry samples						
Sample	Sample dimensions				Fracture force Q (kN)	Shear strength fv (MPa)
	Length L(mm)	Width B(mm)	Height H(mm)	Area A(mm^2)		
1	201	120	249	29880	11.6	0.205
2	200	120	250	30000	11	0.218
3	202	120	249	29880	12.4	0.198
				Average		0.207
1'	200	118	248	29264	21.2	0.362
2'	200	119	250	29750	22.3	0.375
3'	200	120	250	30000	22.2	0.37
				Average		0.37

Test results for building C1A (77/5)

Table 144: Compressive test of solid bricks of C1A building

Compressive test of solid bricks (clay bricks)								
Sample	**Sample dimensions**				**Fracture force (kN)**	**Compressive strength (MPa)**	**Sample weight m (gr)**	**Sample density (kg/m³)**
	Length L(mm)	**Width B(mm)**	**Height H(mm)**	**Area A(mm²)**				
1	249	120	65	15000	109.5	7.33	3750	1930
2	250	120	64	14756	112.2	7.48	3300	1718
3	249	120	65	14940	112.4	7.52	3210	1652
4	250	119	65	14940	113.3	7.61	3495	1807
5	250	119	66	14756	111.2	7.47	3384	1723
				Average		7.48		1766

Table 145: Brick density and water absorption tests of C1A building

Tensile flexural test of solid bricks (clay bricks)						
Sample	**Sample dimensions**				**Fracture force W (kN)**	**Tensile strength (MPa)**
	Length L(mm)	**Width B(mm)**	**Height H(mm)**	**Area A(mm²)**		
1	249	120	65	7800	12.2	1.56
2	250	120	64	7680	12.9	1.68
3	249	120	65	7800	13.4	1.72
4	250	119	65	7735	14.7	1.90
5	250	119	66	7854	13.1	1.66
				Average		1.71

Table 146: Tensile flexural test of solid bricks of C1A building

Compressive and tensile flexural test of mortar samples								
Sample	Compressive test				Flexural tensile strength			
	Dimensions LxBxH (mm^3)	Area A (mm^2)	Fracture Force F (kN)	Compressive strength (MPa)	Dimensions LxBxH (mm^3)	Area A (mm^2)	Fracture Force F (kN)	Tensile strength (MPa)
1	50x50x50	2500	12.5	5	160x40x40	1600	1.8	1.13
2	50x50x50	2500	12.7	5.08	160x40x40	1600	1.7	1.06
3	50x50x50	2500	11.3	4.52	160x40x40	1600	1.6	1
4	50x50x50	2500	12.5	5	160x40x40	1600	1.7	1.06
5	50x50x50	2500	12.3	4.92	160x40x40	1600	1.8	1.13
6	50x50x50	2500	11.2	4.48	160x40x40	1600	1.7	1.06
		Average		4.8		**Average**		1.08

Table 147: Compressive test of mortar samples of C1A building

Compressive test of masonry prism samples									
Sample	Sample dimensions				Fracture force W (kN)	Compressive strength R (MPa)	Prism ratio H/B	Correlation factor n	Compressive strength f_k (MPa)
	Length L(mm)	Width B(mm)	Height H(mm)	Area A(mm^2)					
1	249	242	400	60258	163.4	2.712	1.653	0.903	2.448
2	250	242	402	60500	159.1	2.63	1.661	0.905	2.380
3	249	241	401	60009	160.7	2.678	1.664	0.906	2.426
4	250	243	401	60750	162.4	2.673	1.650	0.902	2.411
5	250	241	401	60250	161.4	2.679	1.664	0.906	2.427
							Average		2.419

Table 148: Triplet test of the samples with and without compressive test of C1A building

Triplet test of masonry samples						
Sample	**Sample dimensions**				**Fracture force Q (kN)**	**Shear strength fv (MPa)**
	Length L(mm)	**Width B(mm)**	**Height H(mm)**	**Area A(mm²)**		
1	202	119	250	29750	12.1	0.203
2	201	119	250	29750	11.9	0.2
3	200	119	249	29631	11.2	0.189
				Average		0.198
1'	201	119	250	29750	21.1	0.355
2'	199	118	250	29500	21.5	0.364
3'	200	119	250	29750	21.4	0.36
				Average		0.36

Test results for building C1B (77/5 type 2)

Table 149: Compressive test of solid silicate bricks of C1B building

Compressive test of solid bricks (silicate bricks)								
Sample	**Sample dimensions**				**Fracture force (kN)**	**Compressive strength (MPa)**	**Sample weight m (gr)**	**Sample density (kg/m³)**
	Length L(mm)	**Width B(mm)**	**Height H(mm)**	**Area A(mm²)**				
1	249	120	65	14940	153.8	10.29	4120	2121
2	250	119	64	14875	150.7	10.13	4007	2104
3	247	118	65	14573	147.3	10.1	3967	2093
4	246	119	64	14637	143.4	9.80	3943	2022
5	250	120	64	15000	150.2	10.01	4105	2191
				Average		10.06		2106

Table 150: Tensile flexural test of solid silicate bricks of C1B building

Tensile flexural test of solid bricks (silicate bricks)						
Sample	**Sample dimensions**				**Fracture force W (kN)**	**Tensile strength (MPa)**
	Length L(mm)	**Width B(mm)**	**Height H(mm)**	**Area A(mm^2)**		
1	249	120	65	8160	19.2	2.46
2	250	119	64	7497	20.4	2.67
3	247	118	65	8040	19.9	2.59
4	246	119	65	7800	20.9	2.74
5	250	120	65	7854	19.4	2.48
				Average		2.59

Table 151: Compressive and tensile flexural test of mortar samples of C1B building

Compressive and tensile flexural test of mortar samples								
Sample	**Compressive test**				**Flexural tensile strength**			
	Dimensions LxBxH (mm^3)	**Area A (mm^2)**	**Fracture Force F (kN)**	**Compressive strength (MPa)**	**Dimensions LxBxH (mm^3)**	**Area A (mm^2)**	**Fracture Force F (kN)**	**Flex tensile strength (MPa)**
1	50x50x50	2500	12.1	4.84	160x40x40	1600	1.7	1.06
2	50x50x50	2500	12.4	4.96	160x40x40	1600	1.8	1.13
3	50x50x50	2500	13.2	5.28	160x40x40	1600	1.7	1.06
4	50x50x50	2500	12.7	5.08	160x40x40	1600	1.6	1
5	50x50x50	2500	12.5	5	160x40x40	1600	1.5	0.94
6	50x50x50	2500	12.8	5.12	160x40x40	1600	1.3	0.81
		Average		5.06		**Average**		1

Table 152: Compressive test of masonry prism samples of C1B building

Compressive test of masonry prism samples									
Sample	**Sample dimensions**				**Fracture force W (kN)**	**Compressive strength R (MPa)**	**Prism ratio H/B**	**Correlation factor n**	**Compressive strength f_k (MPa)**
	Length L(mm)	**Width B(mm)**	**Height H(mm)**	**Area $A(mm^2)$**					
1	249	243	402	60507	201.1	3.324	1.654	0.904	3.00
2	249	243	404	60507	203.2	3.358	1.663	0.906	3.04
3	250	244	403	61000	201.4	3.302	1.652	0.903	2.97
4	250	244	402	61000	200.9	3.293	1.652	0.903	2.97
5	250	244	403	61000	203.3	3.333	1.652	0.903	3.01
							Average		3

Table 153: Triplet test of the samples with and without compressive test of C1B building

Triplet test of masonry samples						
Sample	**Sample dimensions**				**Fracture force Q (kN)**	**Shear strength fv (MPa)**
	Length L(mm)	**Width B(mm)**	**Height H(mm)**	**Area $A(mm^2)$**		
1	201	120	249	29880	13.4	0.224
2	201	120	249	29880	12.8	0.214
3	202	120	250	30000	13.7	0.228
				Average		0.222
1'	200	120	250	29750	23.4	0.393
2'	199	119	250	30000	24.3	0.405
3'	200	120	250	30000	24.1	0.402
				Average		0.40

Test results for Building C2 (83/3)

Table 154: Compressive test of solid bricks of C2 building

Compressive test of solid bricks (clay bricks)								
Sample	**Sample dimensions**				**Fracture force (kN)**	**Compressive strength (MPa)**	**Sample weight m (gr)**	**Sample density (kg/m³)**
	Length L(mm)	**Width B(mm)**	**Height H(mm)**	**Area A(mm²)**				
1	245	120	64	14700	111.1	7.31	3689	1960
2	246	119	65	14637	119.4	7.76	3423	1798
3	247	120	65	14820	117.5	7.67	3890	2019
4	246	118	64	14514	122.3	8.01	3567	1920
5	250	117	65	14625	113.9	7.34	3750	1972
				Average		7.60		1934

Table 155: Tensile flexural test of solid clay bricks of C2 building

Tensile flexural test of solid bricks (clay bricks)						
Sample	**Sample dimensions**				**Fracture force W (kN)**	**Tensile strength (MPa)**
	Length L(mm)	**Width B(mm)**	**Height H(mm)**	**Area A(mm²)**		
1	246	120	64	8160	14.2	1.84
2	250	119	65	7497	15.8	2.04
3	248	118	65	8040	15.2	1.94
4	249	117	64	7800	16.1	2.13
5	249	119	65	7854	13.9	1.82
				Average		1.82

Table 156: Compressive and tensile flexural test of mortar samples of C2 building

Compressive and tensile flexural test of mortar samples								
Sample	**Compressive test**				**Flexural tensile strength**			
	Dimensions LxBxH (mm^3)	**Area A (mm^2)**	**Fracture Force F (kN)**	**Compressive strength (MPa)**	**Dimensions LxBxH (mm^3)**	**Area A (mm^2)**	**Fracture Force F (kN)**	**Tensile strength (MPa)**
1	50x50x50	2500	7.1	2.84	160x40x40	1600	0.9	0.57
2	50x50x50	2500	6.5	2.6	160x40x40	1600	1.2	0.75
3	50x50x50	2500	6.7	2.68	160x40x40	1600	1.2	0.75
4	50x50x50	2500	5.7	2.28	160x40x40	1600	1	0.63
5	50x50x50	2500	6.3	2.52	160x40x40	1600	1.1	0.65
6	50x50x50	2500	6.4	2.54	160x40x40	1600	0.9	0.57
		Average		2.57		**Average**		0.65

Table 157: Compressive test of masonry prism samples of C2 building

Compressive test of masonry prism samples									
Sample	**Sample dimensions**				**Fracture force W (kN)**	**Compressive strength R (MPa)**	**Prism ratio H/B**	**Correlation factor n**	**Compressive strength f_k (MPa)**
	Length L(mm)	**Width B(mm)**	**Height H(mm)**	**Area A(mm^2)**					
1	250	243	400	60750	130.3	2.144	1.646	0.904	1.932
2	248	241	404	59768	127.3	2.130	1.676	0.899	1.936
3	249	244	403	60756	136.7	2.250	1.651	0.902	2.030
4	250	244	402	61000	127	2.081	1.647	0.901	1.876
5	250	243	403	60750	129.8	2.137	1.658	0.904	1.932
							Average		1.942

Table 158: Triplet test of the samples with and without compressive test of C2 building

Triplet test of masonry samples						
Sample	**Sample dimensions**				**Fracture force Q (kN)**	**Shear strength fv (MPa)**
	Length L(mm)	**Width B(mm)**	**Height H(mm)**	**Area $A(mm^2)$**		
1	200	120	250	30000	11.9	0.201
2	202	120	250	30000	10.5	0.176
3	201	119	250	29750	11.8	0.179
				Average		0.185
1'	200	120	249	29880	21.3	0.258
2'	199	119	250	29750	21.8	0.371
3'	200	120	249	29880	20.2	0.342
				Average		0.35

Test results for Building C3 (83/10)

Table 159: Compressive test of solid bricks of C3 building

Compressive test of solid bricks (clay bricks)								
Sample	**Sample dimensions**				**Fracture force (kN)**	**Compressive strength (MPa)**	**Sample weight m (gr)**	**Sample density (kg/m^3)**
	Length L(mm)	**Width B(mm)**	**Height H(mm)**	**Area $A(mm^2)$**				
1	250	120	68	15000	103.2	6.88	3543	1816
2	248	119	63	14756	114.3	7.74	3438	1792
3	249	120	67	14940	119	7.97	3759	1965
4	249	120	65	14940	113.8	7.62	3566	1836
5	248	119	66	14756	114.7	7.77	3789	1975
				Average		7.55		1877

Table 160: Tensile flexural test of solid bricks of C3 building

Tensile flexural test of solid bricks (clay bricks)						
Sample	**Sample dimensions**				**Fracture force W (kN)**	**Tensile strength (MPa)**
	Length L(mm)	**Width B(mm)**	**Height H(mm)**	**Area A(mm^2)**		
1	250	120	68	8160	14.3	1.75
2	248	119	63	7497	15.6	2.08
3	249	120	67	8040	13.4	1.67
4	249	120	65	7800	14.1	1.80
5	248	119	66	7854	14.7	1.87
				Average		1.85

Table 161: Compressive test of mortar samples of C3 building

Compressive and tensile flexural test of mortar samples								
Sample	**Compressive test**				**Flexural tensile strength**			
	Dimensions LxBxH (mm^3)	**Area A (mm^2)**	**Fracture Force F (kN)**	**Compressive strength (MPa)**	**Dimensions LxBxH (mm^3)**	**Area A (mm^2)**	**Fracture Force F (kN)**	**Tensile strength (MPa)**
1	50x50x50	2500	12.2	4.88	160x40x40	1600	1.9	1.18
2	50x50x50	2500	12.1	4.84	160x40x40	1600	1.8	1.11
3	50x50x50	2500	13	5.2	160x40x40	1600	2	1.25
4	50x50x50	2500	12.8	5.12	160x40x40	1600	2.1	1.31
5	50x50x50	2500	12.9	5.16	160x40x40	1600	2	1.25
6	50x50x50	2500	13.9	5.56	160x40x40	1600	1.6	1
		Average		5.12		**Average**		1.18

Table 162: Compressive strength of masonry prism samples of C3 building

Compressive test of masonry prism samples									
Sample	Sample dimensions				Fracture force W (kN)	Compressive strength R (MPa)	Prism ratio H/B	Correlation factor n	Compressive strength f_k (MPa)
	Length L(mm)	Width B(mm)	Height H(mm)	Area A(mm^2)					
1	250	243	403	60750	168.4	2.772	1.658	0.904	2.507
2	249	244	400	60756	171.4	2.866	1.639	0.899	2.576
3	250	244	401	61000	160	2.623	1.643	0.9	2.361
4	249	244	402	60756	167.4	2.755	1.647	0.901	2.483
5	250	243	403	60750	165.6	2.726	1.658	0.904	2.465
							Average		2.479

Table 163: Triplet test of the samples with and without compressive test of C3 building

Triplet test of masonry samples						
Sample	Sample dimensions				Fracture force Q (kN)	Shear strength fv (MPa)
	Length L(mm)	Width B(mm)	Height H(mm)	Area A(mm^2)		
1	200	120	250	30000	12.3	0.205
2	202	120	250	30000	13.1	0.218
3	201	119	250	29750	11.8	0.198
				Average		0.207
1'	200	120	249	29880	23.3	0.389
2'	199	119	250	29750	24.5	0.411
3'	200	120	249	29880	22.1	0.369
				Average		0.39

APPENDIX D

Failure mechanism of template buildings in pushover analysis

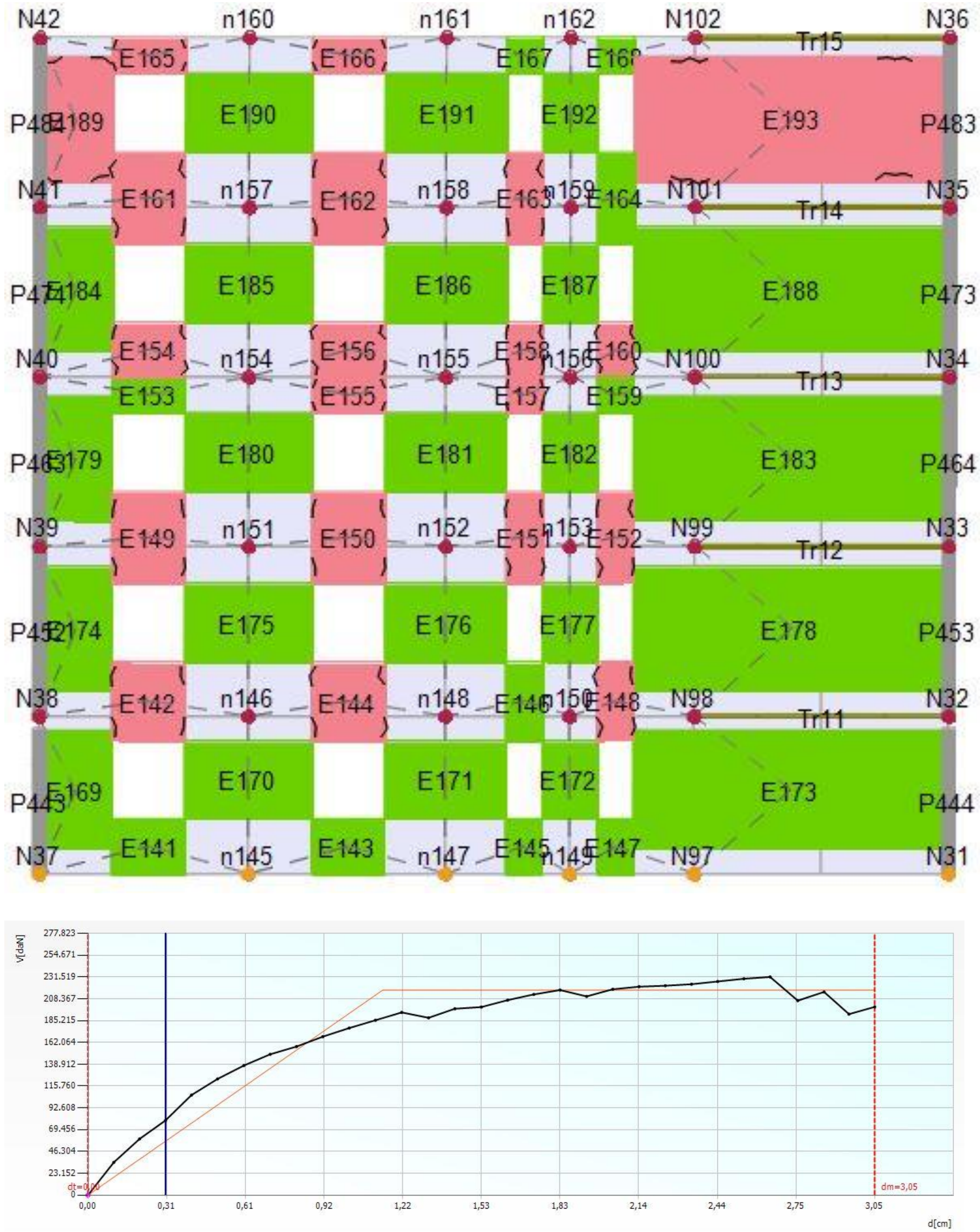

Figure 315: Wall damage on C1A clay building, pushover scenario step 1/6

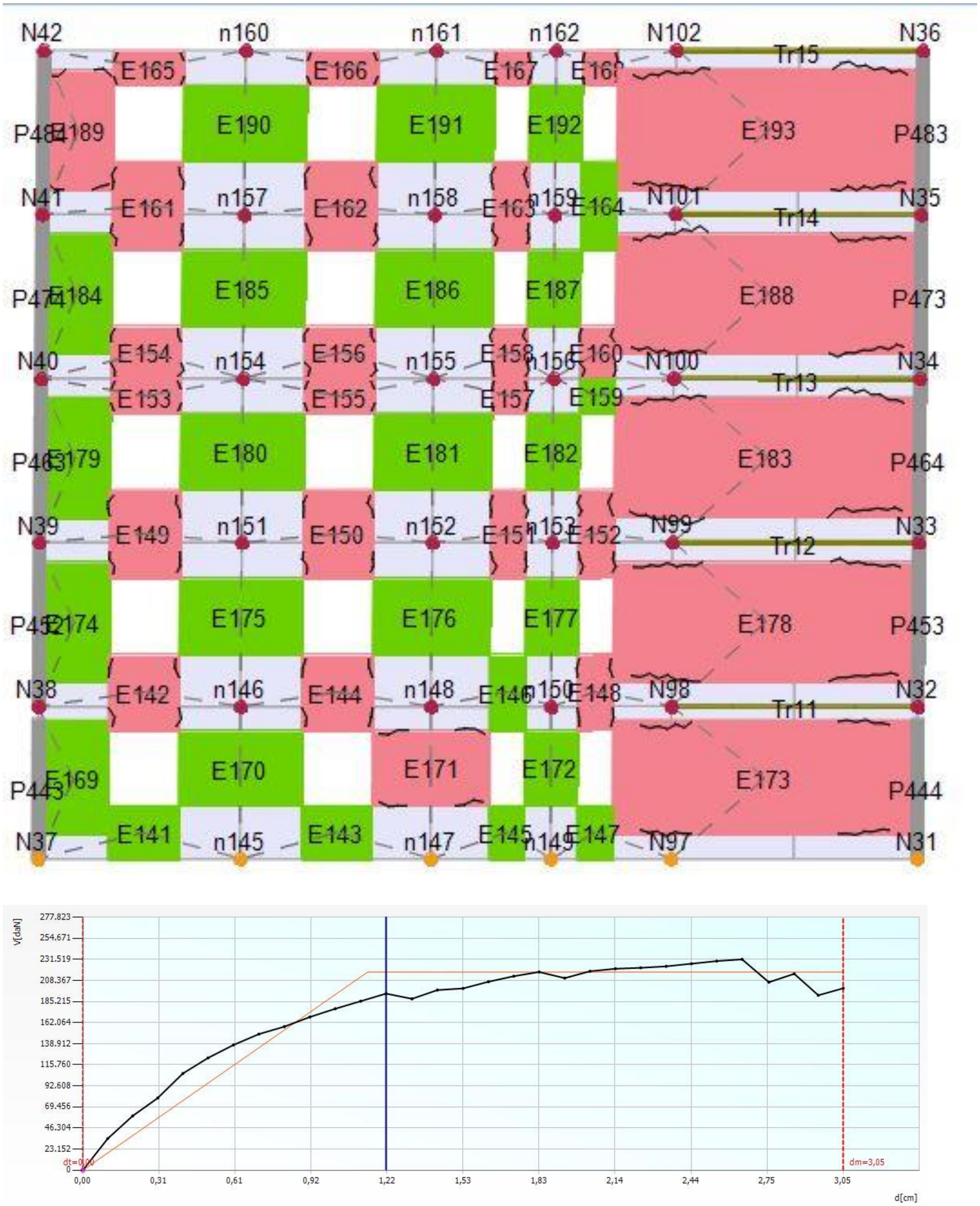

Figure 316: Wall damage on C1A clay building, pushover scenario step 2/6

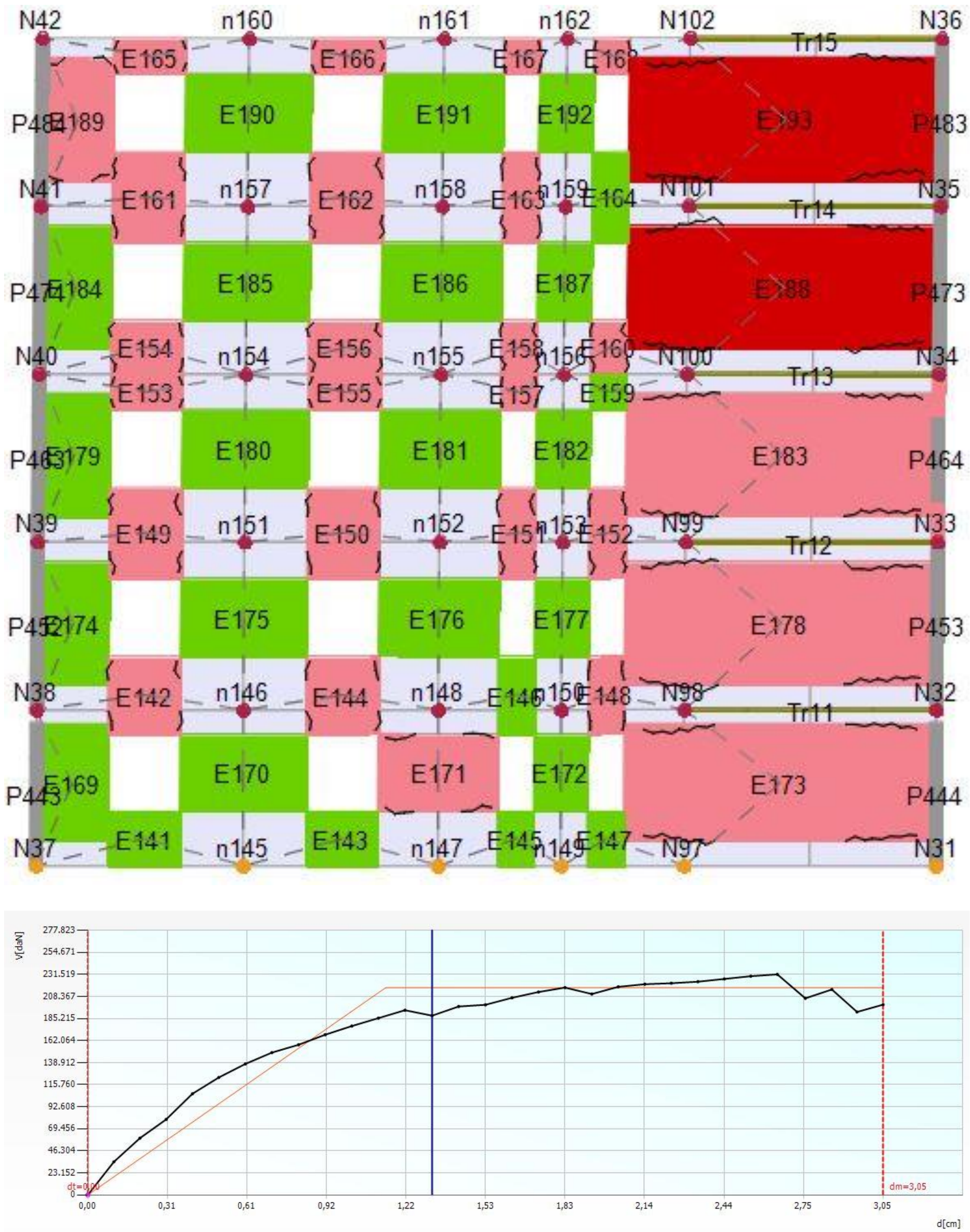

Figure 317: Wall damage on C1A clay building, pushover scenario step 3/6

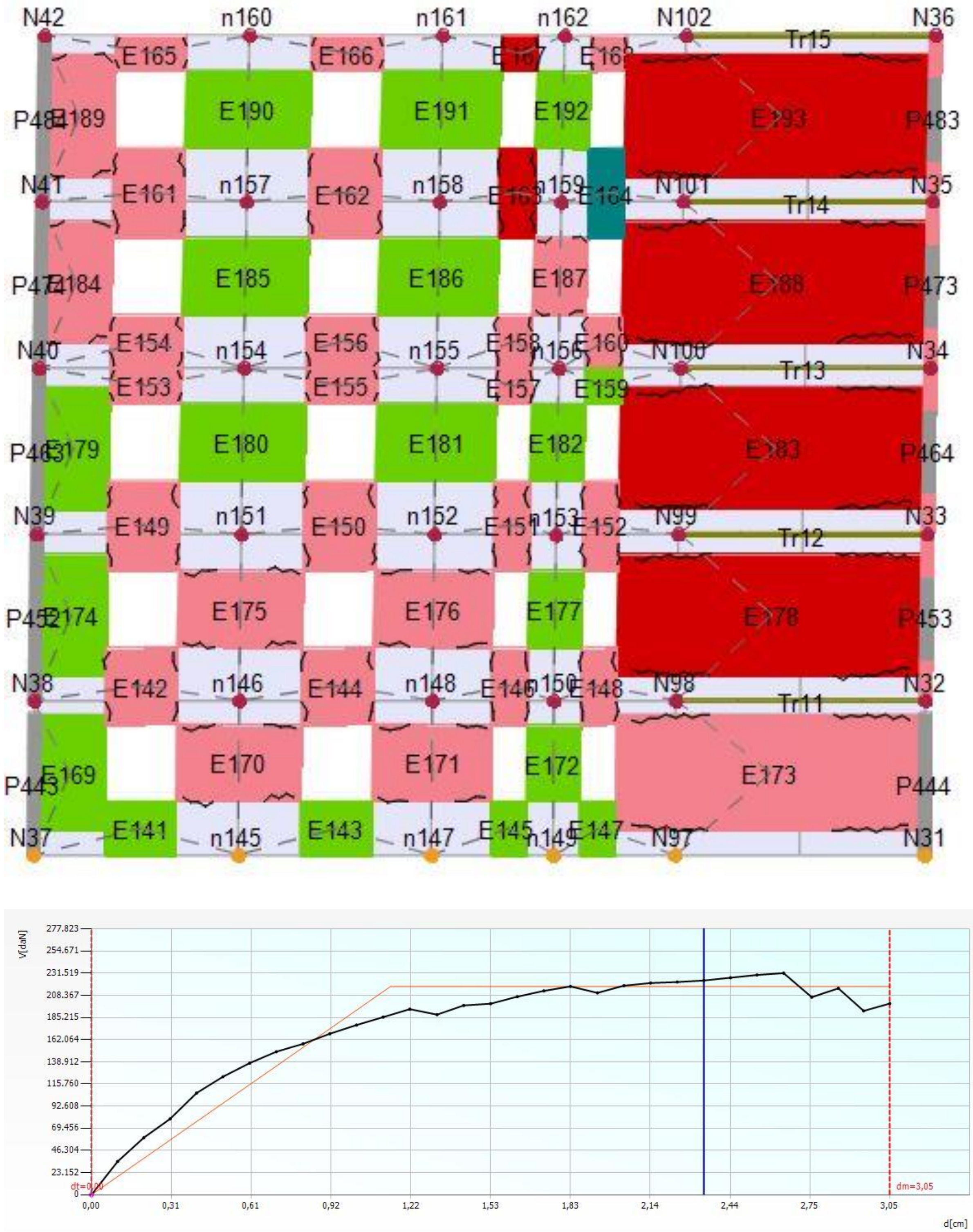

Figure 318: Wall damage on C1A clay building, pushover scenario step 4/6

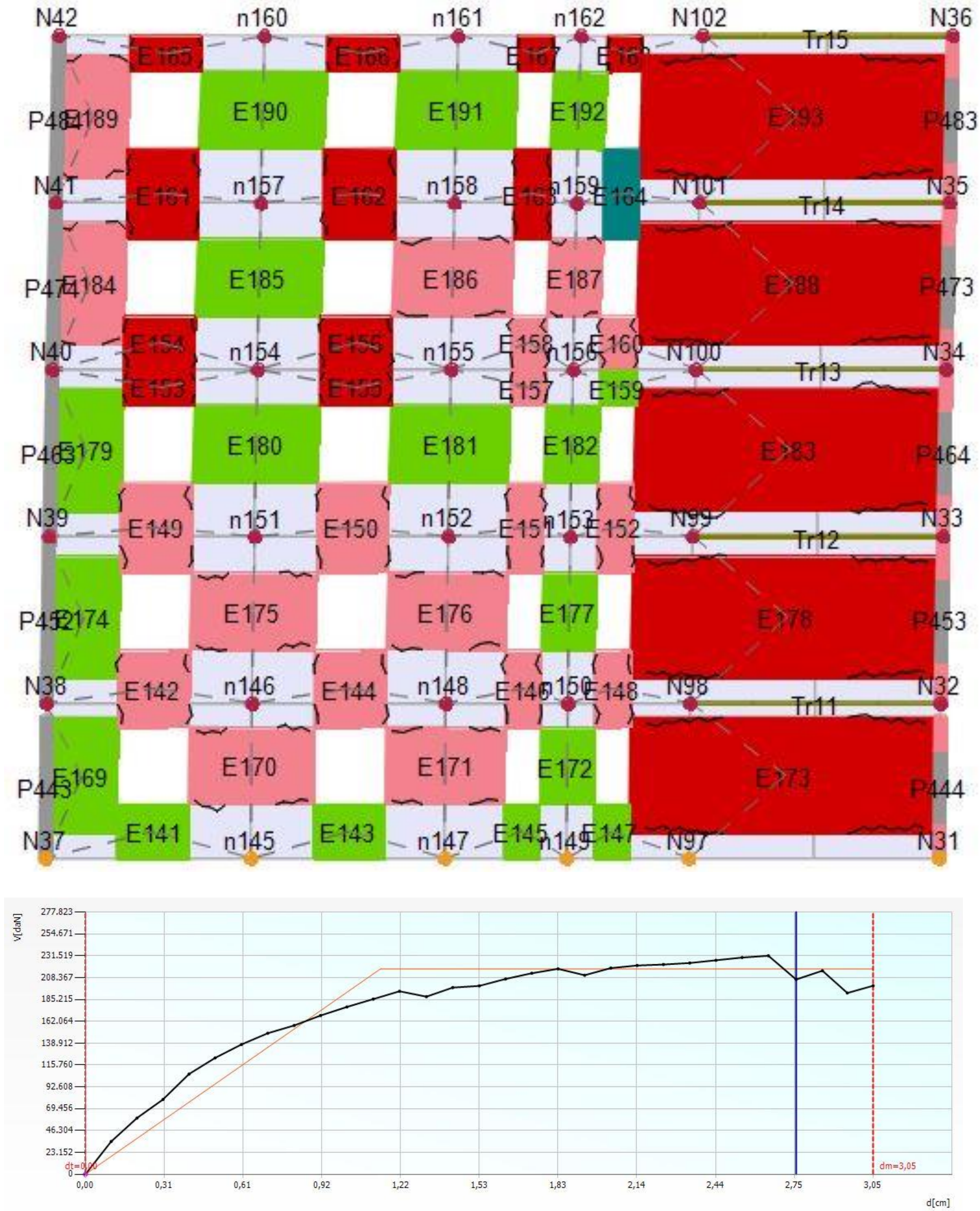

Figure 319: Wall damage on C1A clay building, pushover scenario step 5/6

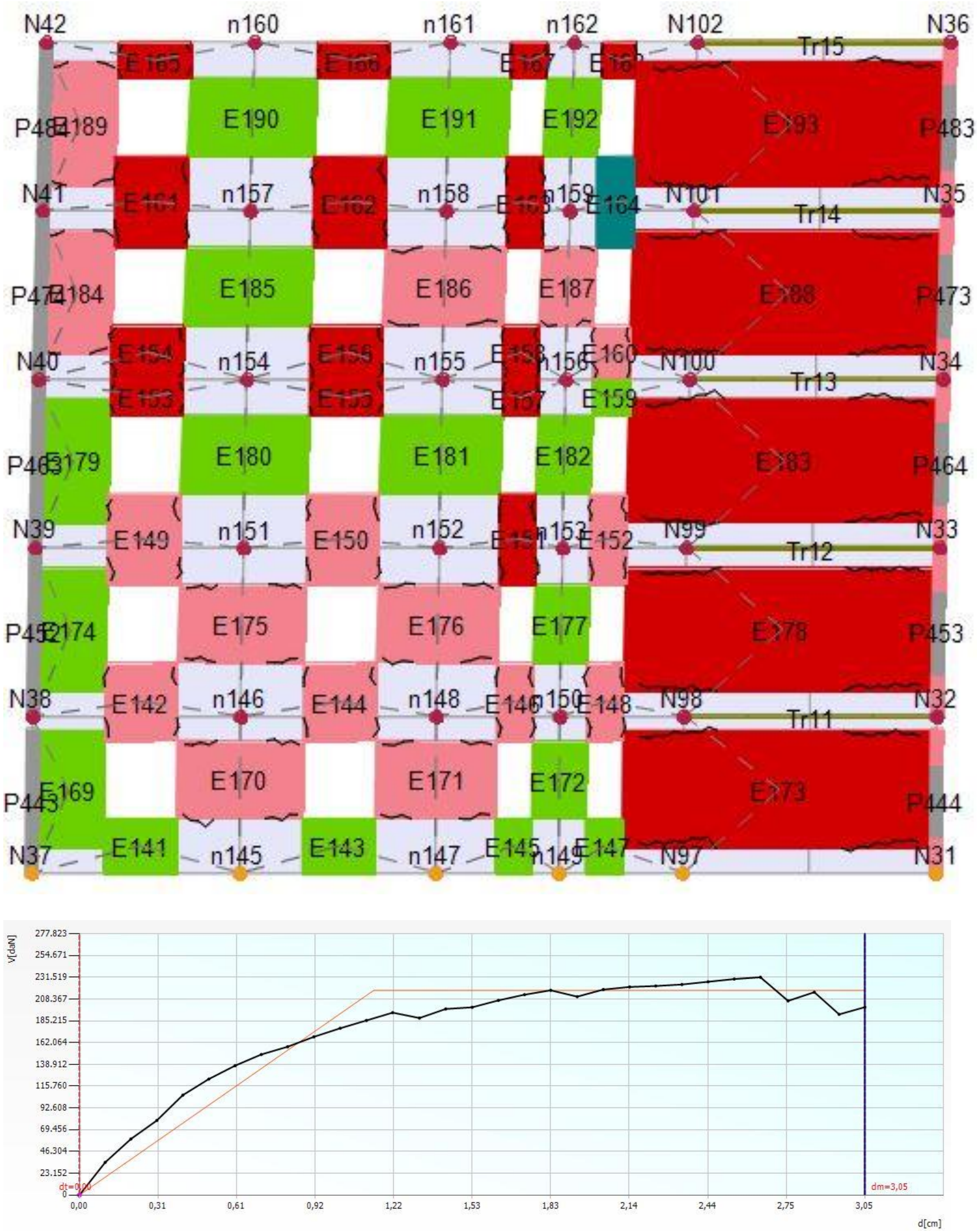

Figure 320: Wall damage on C1A clay building failure mechanism, pushover scenario step 6/6

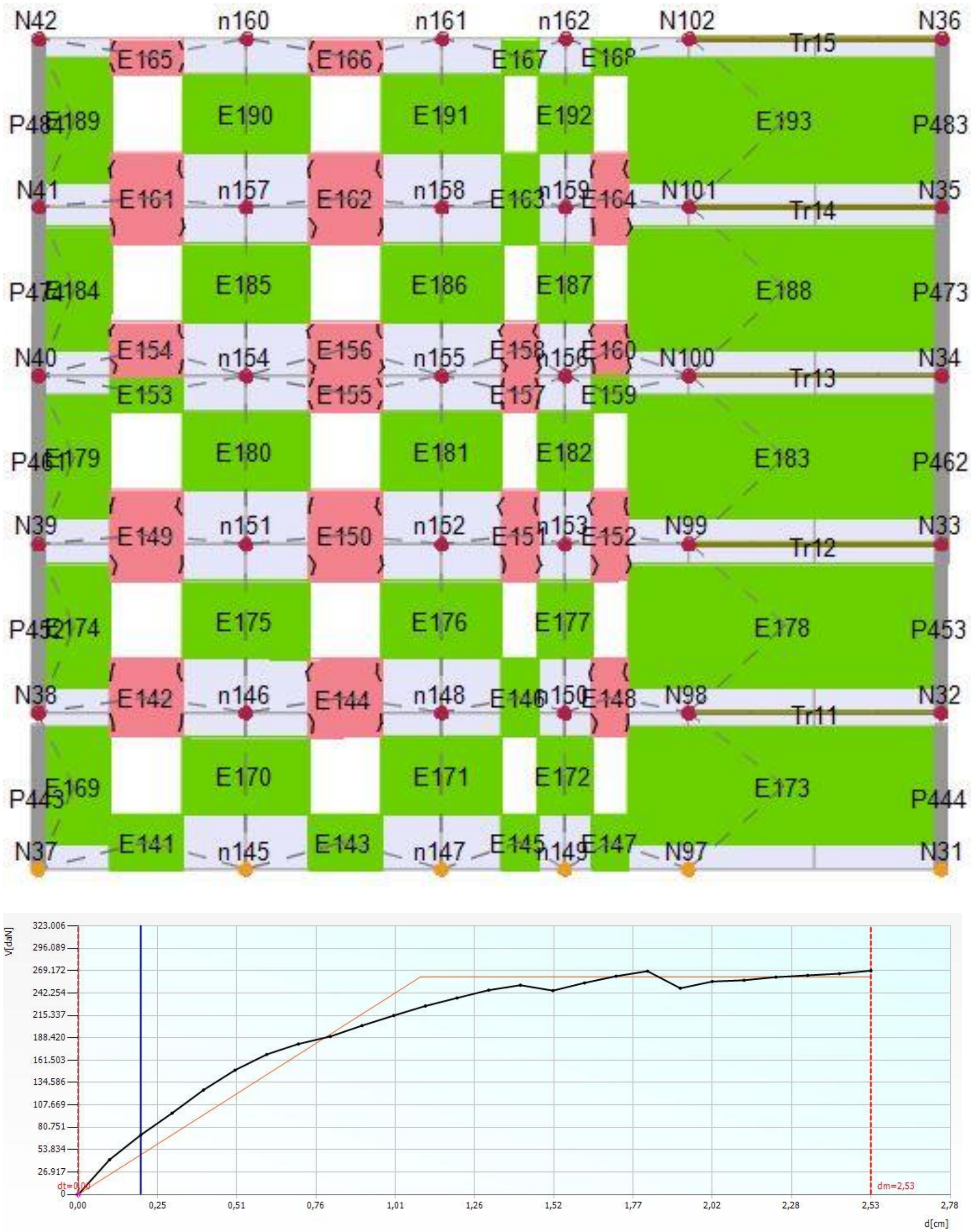

Figure 321: Wall damage on C1' silicate building, pushover scenario step 1/6

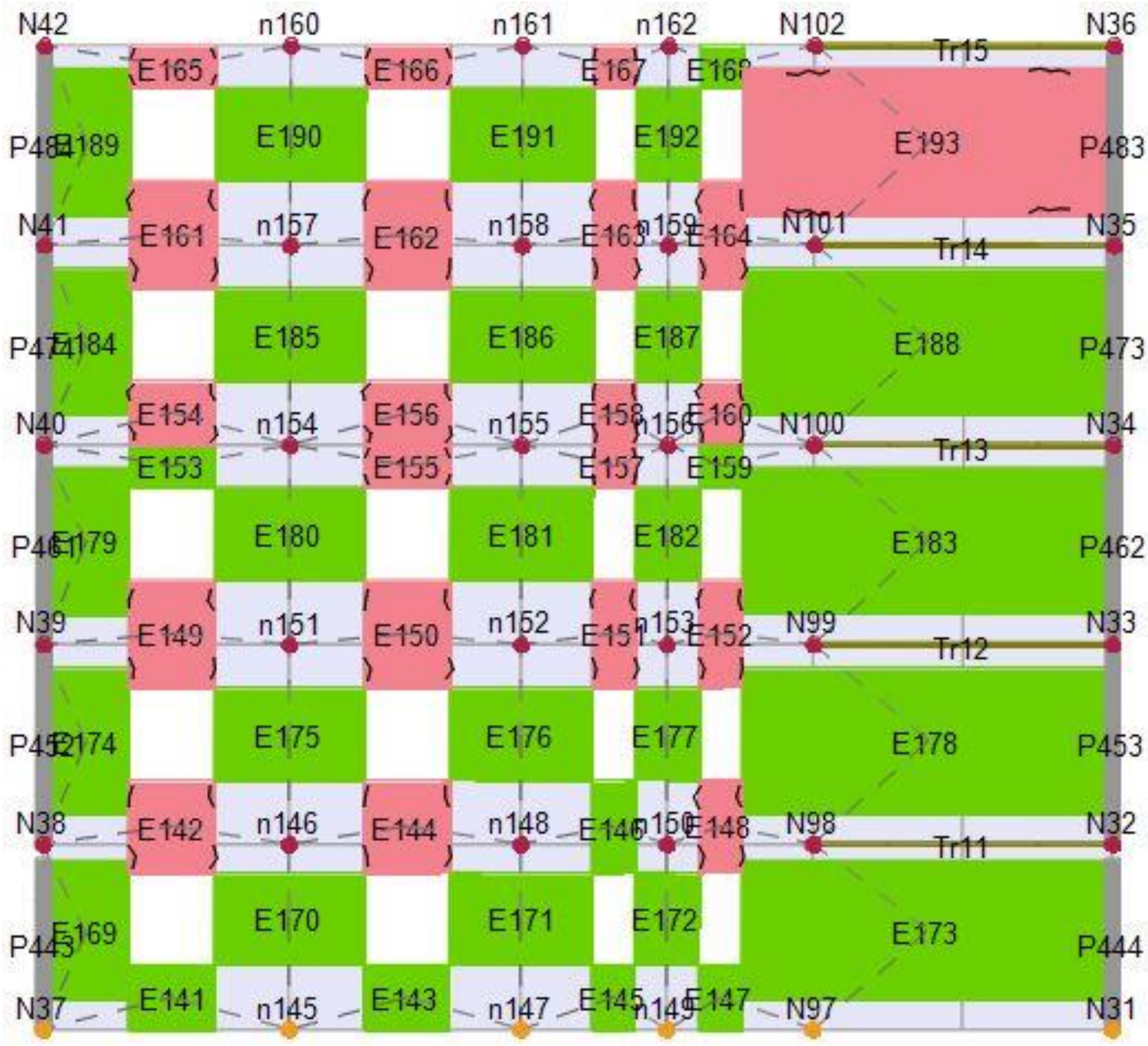

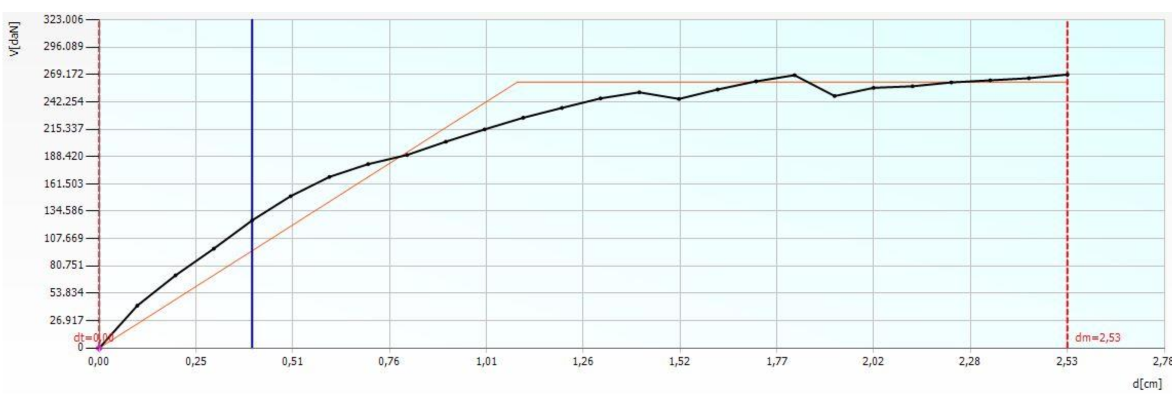

Figure 322: Wall damage on C1B silicate building, pushover scenario step 2/6

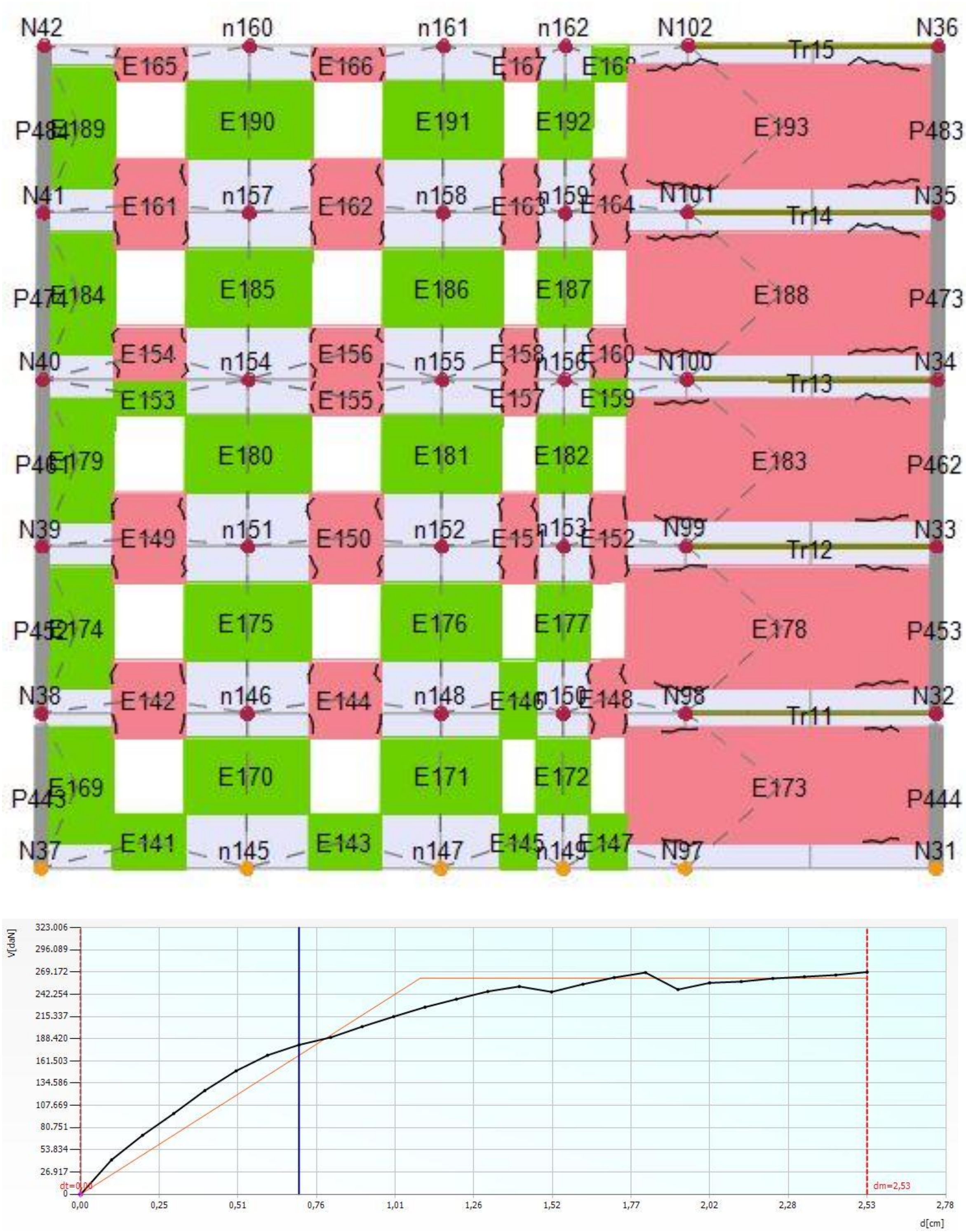

Figure 323: Wall damage on C1B silicate building, pushover scenario step 3/6

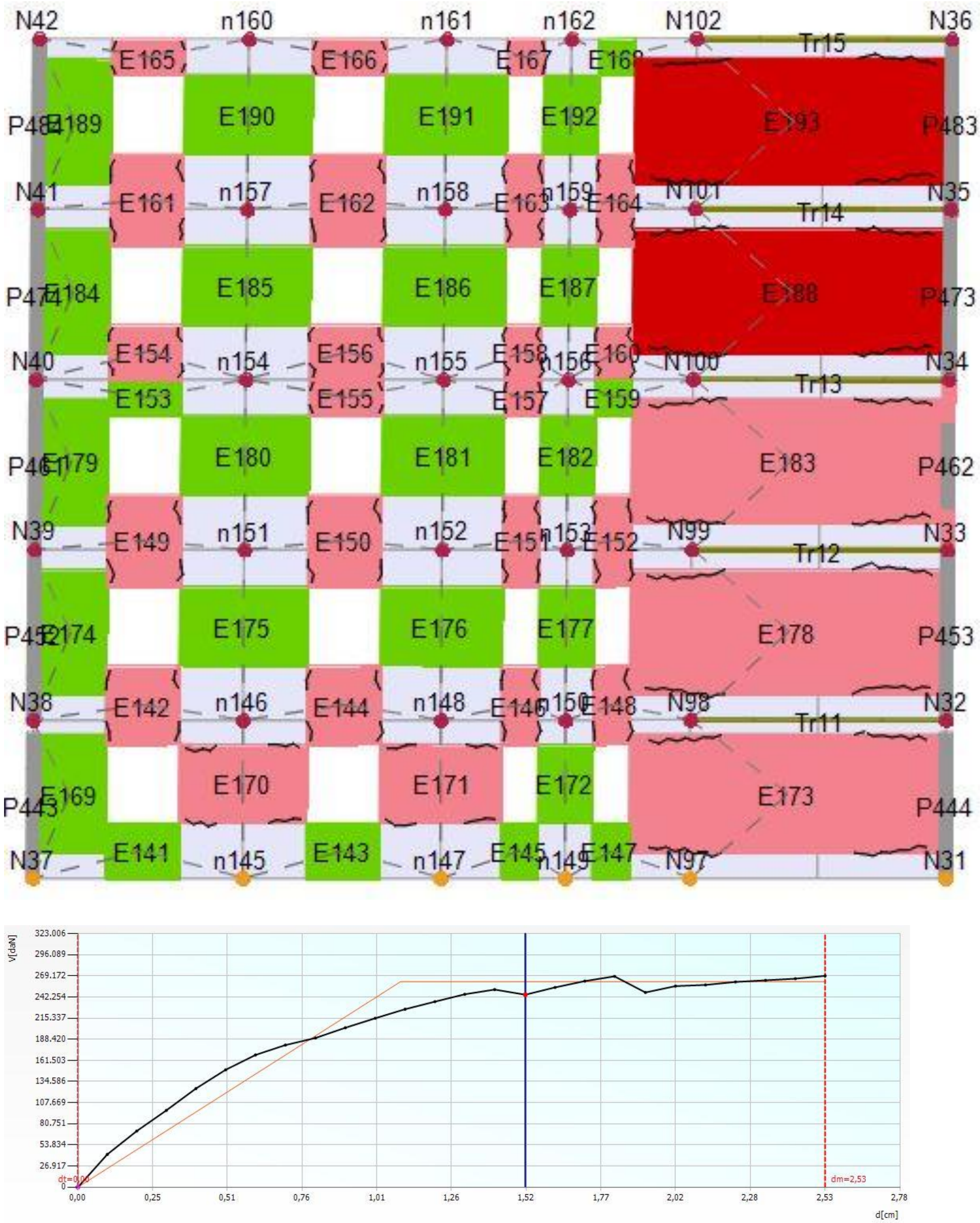

Figure 324: Wall damage on C1B silicate building, pushover scenario step 4/6

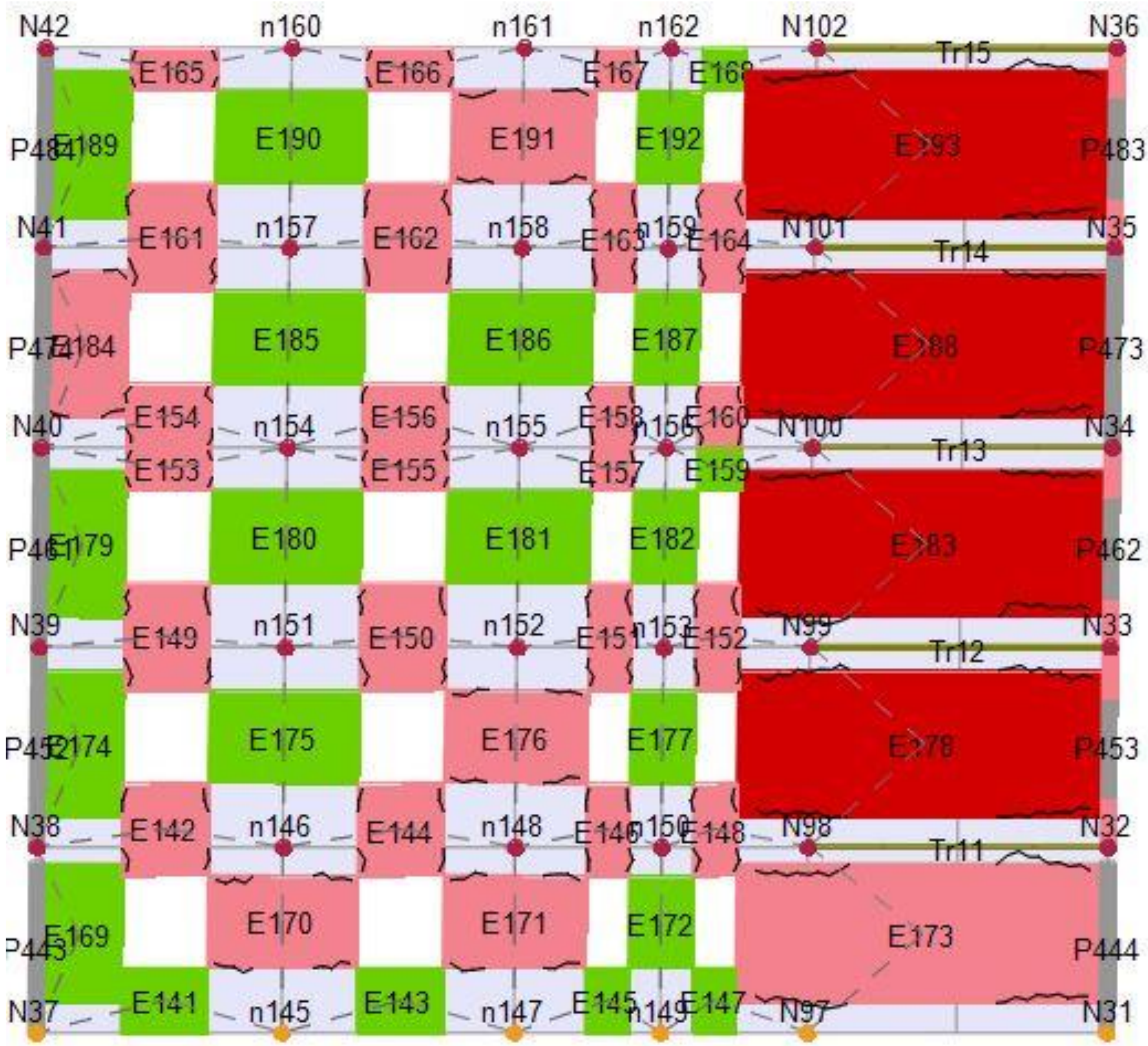

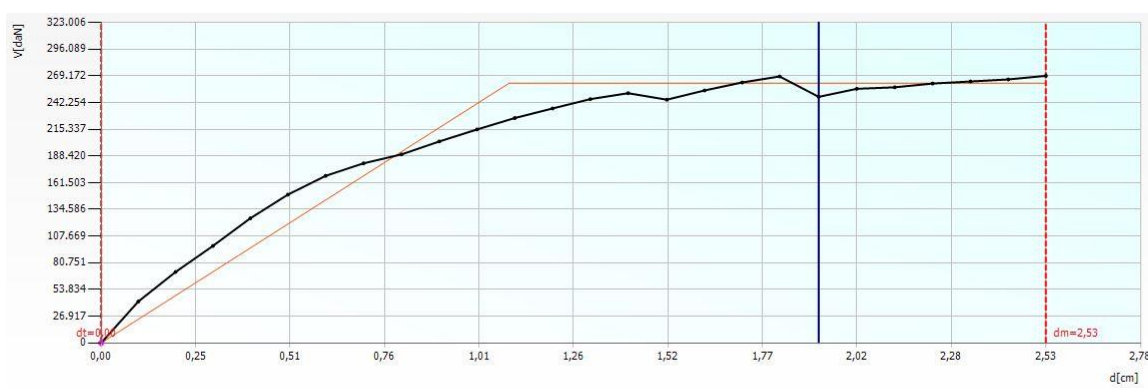

Figure 325: Wall damage on C1B silicate building, pushover scenario step 5/6

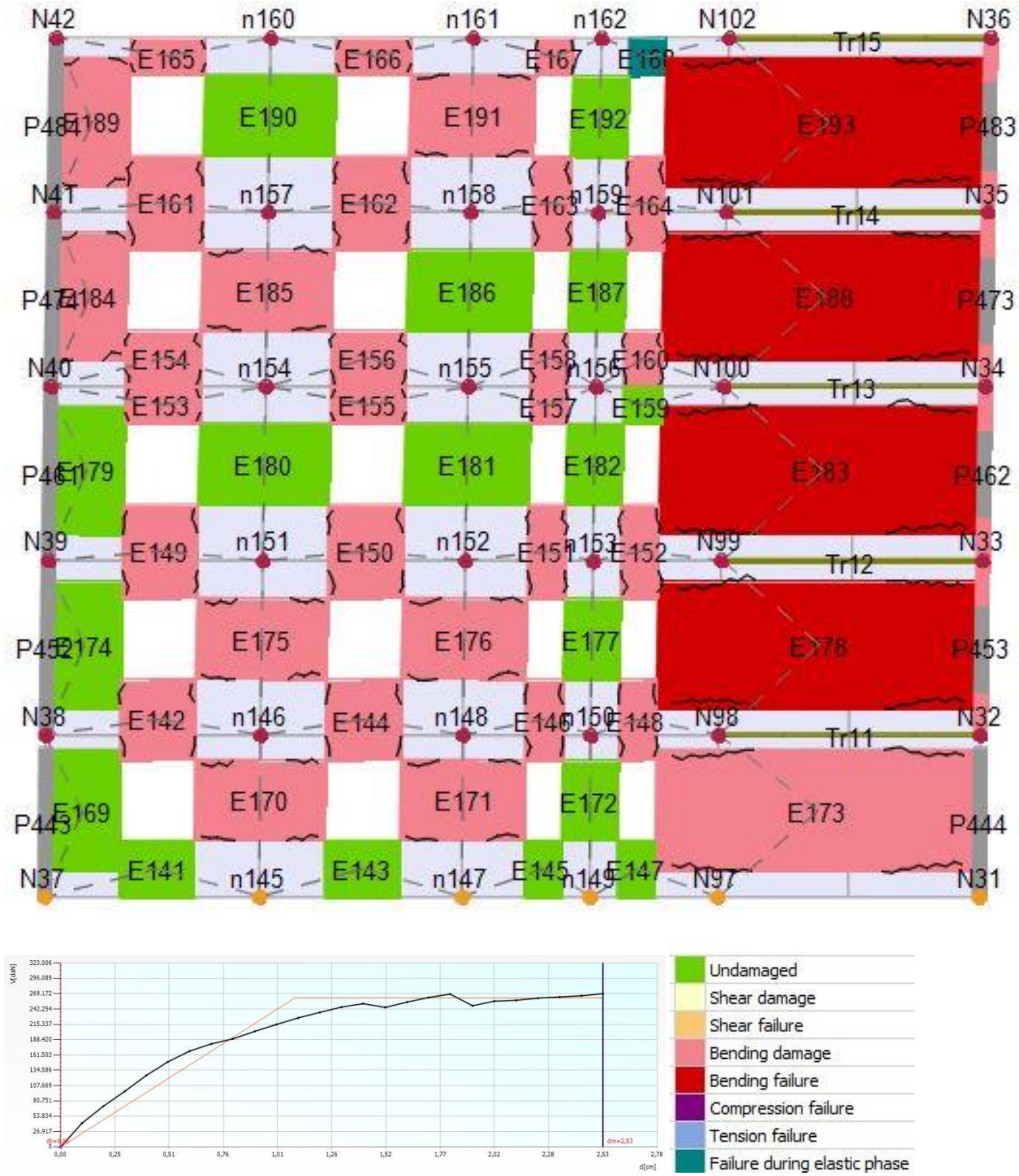

Figure 326: Wall damage on C1B silicate building, failure mechanism pushover scenario step 6/6

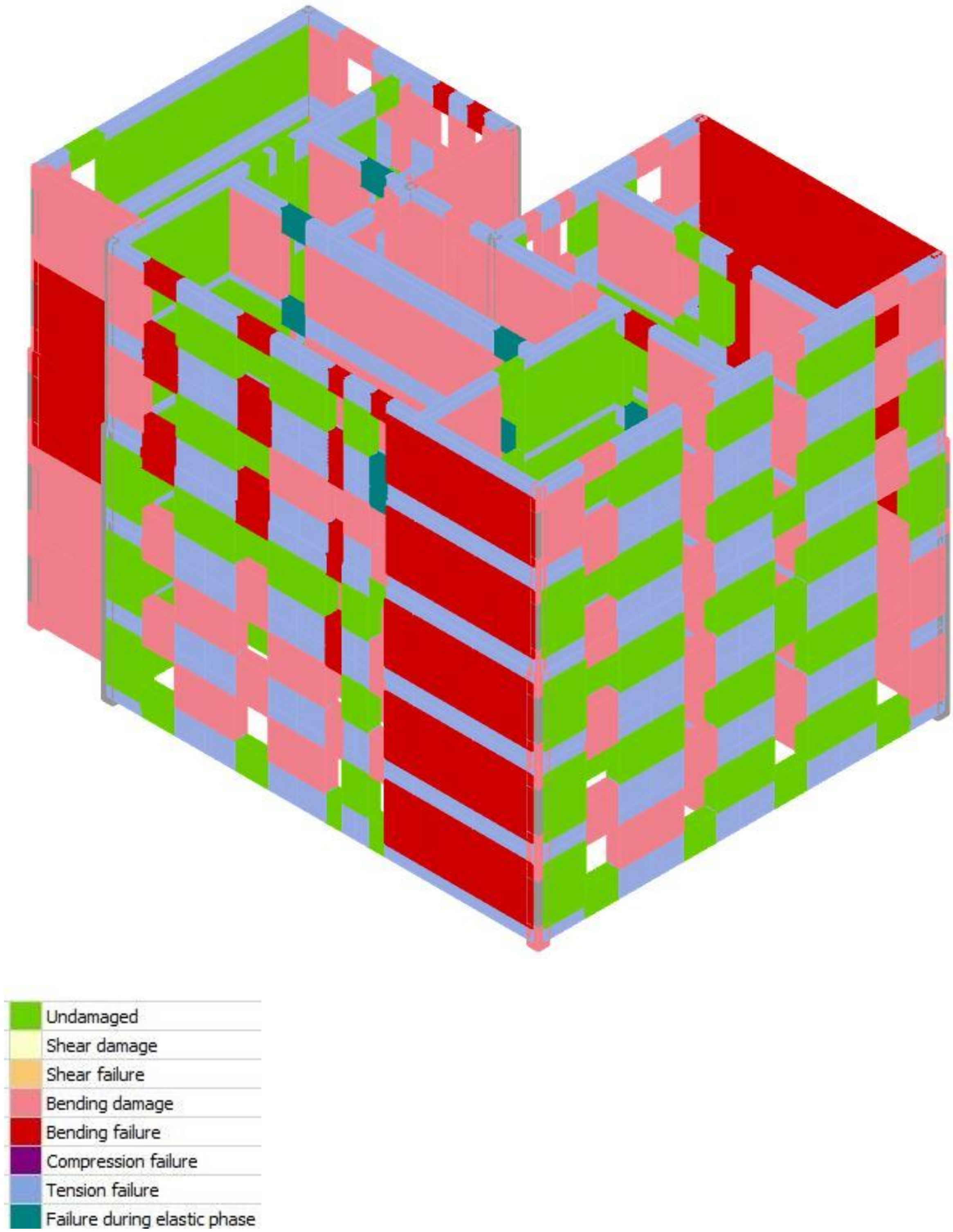

Figure 327: Failure mechanism pushover scenario, C1A clay building

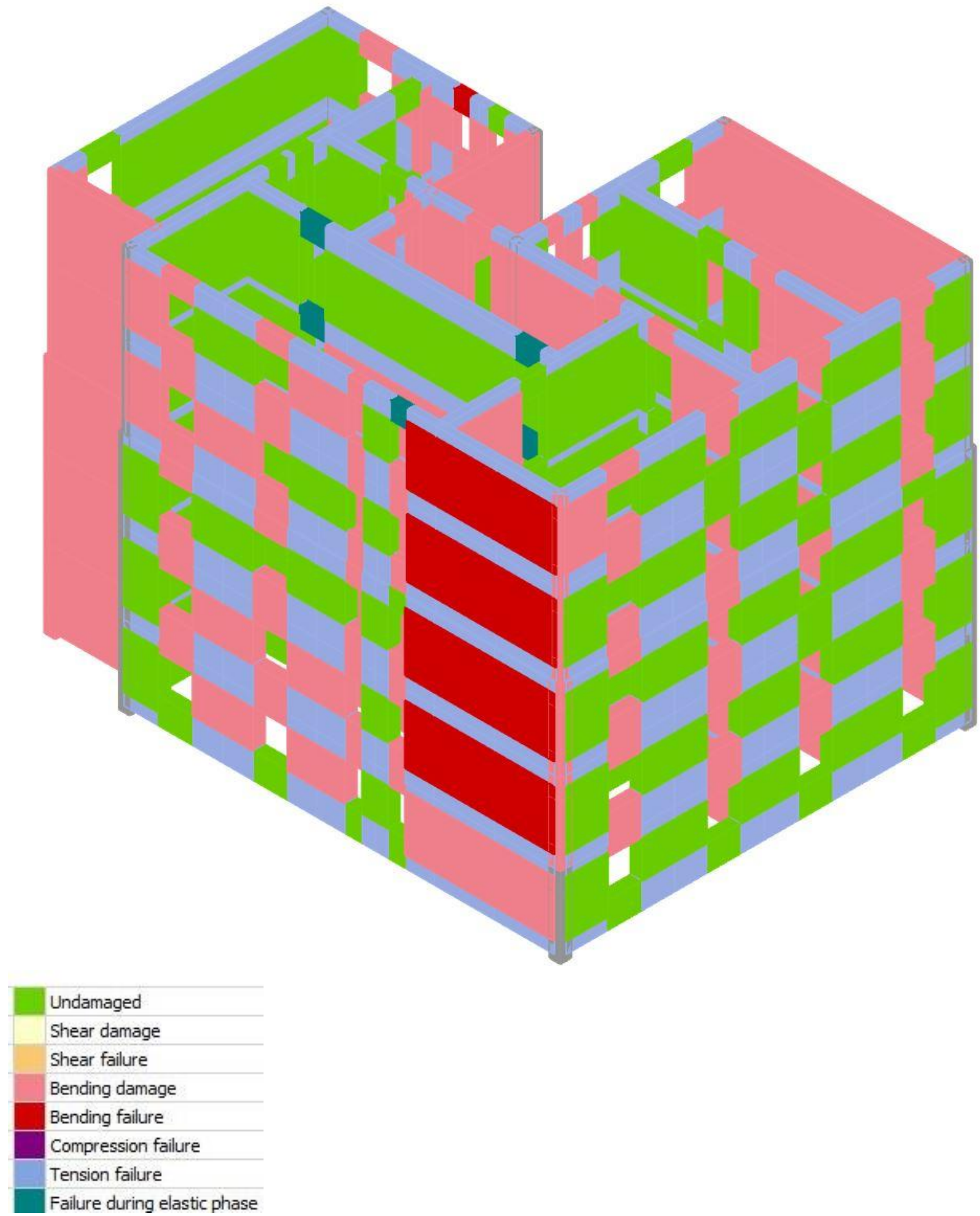

Figure 328: Failure mechanism pushover scenario, C1B silicate building

APPENDIX E

Spectrum analysis full parameters

Table 164: Spectrum analysis parameters A template buildings

Building	A1		A1 3fl		A1 4fl		A2		A2 half	
Dir	x	y	x	y	x	y	x	y	x	y
Vy (kN)	191.947	192.966	206.12	230.38	224.36	203.67	159.02	185.93	83.792	99.49
Dy (m)	0.0021	0.002	0.0044	0.0042	0.0081	0.0052	0.0037	0.0031	0.0034	0.0026
dm (m)	0.008	0.0048	0.0157	0.0078	0.0209	0.0117	0.0132	0.0089	0.0125	0.0085
k (t/m)	91403.3	96483	46845.5	54852.4	27698.8	39167.3	42978.4	59977.4	24644.7	38265.4
T_1 (s)	0.1037	0.1089	0.1508	0.1451	0.199	0.199	0.09965	0.1181	0.11686	0.0752
ɼ	1.25	1.23	1.28	1.28	1.3	1.31	1.24	1.24	1.24	1.24
α	0.625	0.643	0.622	0.629	0.619	0.609	0.643	0.653	0.64	0.647
Wsist (ton)	269.59	269.59	375.146	375.146	479.81	479.81	281.45	281.45	140.826	140.826
H_{build} (m)	6	6	9	9	12	12	6	6	6	6
Cy	0.712	0.7157	0.5494	0.6141	0.4676	0.4245	0.5650	0.6606	0.5950	0.7065
Cy*	1.1392	1.1132	0.8833	0.9763	0.7554	0.6970	0.8787	1.0117	0.9296	1.0919
dy*	0.0017	0.0016	0.0034	0.0033	0.0062	0.0039	0.0029	0.0025	0.0027	0.0021
dy*	0.168	0.162	0.3438	0.3281	0.6231	0.3969	0.2984	0.25	0.2742	0.2097
Teq (s)	0.125	0.124	0.205	0.19	0.304	0.248	0.222	0.162	0.247	0.143

Table 165: Spectrum analysis parameters B template buildings part one

Building	B1		B1 4fl		B2		B2 38cm	
Dir	x	y	x	y	x	y	x	y
Vy (kN)	227.42	239.76	230.0714	243.8328	262.0795	193.476	289.8063	198.2671
Dy (m)	0.004	0.0026	0.0058	0.004	0.0045	0.0048	``	0.0048
dm (m)	0.014	0.007	0.00201	0.00104	0.0133	0.0191	0.0133	0.0191
k (t/m)	56855	92215.38	39667.48	60958.21	58239.89	40307.51	64401.4	41305.64
T_1 (s)	0.13039	0.13627	0.1774	0.1763	0.18129	0.16622	0.17118	0.18644
ɼ	1.32	1.34	1.34	1.38	1.38	1.4	1.33	1.35
α	0.558	0.544	0.551	0.521	0.53	0.503	0.588	0.556
Wsist (ton)	339.43	339.43	421.3	421.3	395.3	395.3	442.8	442.8
H_{build} (m)	8.4	8.4	11.2	11.2	11.2	11.2	11.2	11.2
Cy	0.670006	0.706361	0.546099	0.578763	0.662989	0.489441	0.654486	0.447758
Cy*	1.200727	1.298457	0.991105	1.110869	1.250922	0.973044	1.113071	0.805319
dy*	0.00303	0.00194	0.004328	0.002899	0.003261	0.003429	0.003383	0.003556
dy*	0.30303	0.19403	0.432836	0.289855	0.326087	0.342857	0.338346	0.355556
Teq (s)	0.18	0.14	0.24	0.186	0.16	0.222	0.174	0.24

Table 166: Spectrum analysis parameters B template buildings part two

Building	B3		B3 int		B4	
Dir	x	y	x	y	x	y
Vy (kN)	164.8318	170.2345	154.9439	172.1713	294.5973	270.3364
Dy (m)	0.0117	0.009	0.012	0.0085	0.0125	0.0126
dm (m)	0.0359	0.0203	0.0392	0.0181	0.0192	0.0315
k (t/m)	14088.19	18914.94	12911.99	20255.44	23567.79	21455.27
T_1 (s)	0.24388	0.23	0.23979	0.23676	0.23303	0.25938
ɼ	1.42	1.45	1.41	1.44	1.39	1.4
α	0.499	0.474	0.525	0.474	0.517	0.503
Wsist (ton)	380.7	380.7	377.47	377.47	604.2	604.2
H_{build} (m)	14	14	14	14	14	14
Cy	0.43297	0.447162	0.41048	0.456119	0.487583	0.447429
Cy*	0.867676	0.943379	0.781867	0.962276	0.9431	0.88952
dy*	0.008239	0.006207	0.008511	0.005903	0.008993	0.009
dy*	0.823944	0.62069	0.851064	0.590278	0.899281	0.9
Teq (s)	0.377	0.319	0.403	0.304	0.366	0.377

Table 167: Spectrum analysis parameters C template buildings part one

Building	C1A		C1A int		C1B		C1B 6fl	
Dir	x	y	x	y	x	y	x	y
Vy (kN)	222.63	189.2966	235.6779	174.4139	267.4822	199.8981	255.1478	223.2416
Dy (m)	0.0107	0.0167	0.0097	0.0144	0.011	0.0147	0.0147	0.0206
dm (m)	0.0305	0.0462	0.0208	0.0325	0.0253	0.0424	0.0326	0.0524
k (t/m)	20806.54	11335.13	24296.69	12112.07	24316.56	13598.51	17356.99	10836.97
T1 (s)	0.21997	0.24719	0.22989	0.27337	0.21734	0.24409	0.27175	0.3059
ɼ	1.38	1.4	1.39	1.36	1.41	1.41	1.41	1.41
α	0.536	0.529	0.564	0.57	0.536	0.526	0.521	0.516
W_{sist} (ton)	561.49	561.49	555.3	555.3	599.6	599.6	688.4	688.4
H_{build} (m)	14	14	14	14	14	14	16.8	16.8
Cy	0.396499	0.337133	0.424415	0.314089	0.446101	0.333386	0.370639	0.324291
Cy*	0.739736	0.637302	0.75251	0.551034	0.832278	0.633813	0.711399	0.62847
dy*	0.007754	0.011929	0.006978	0.010588	0.007801	0.010426	0.010426	0.01461
dy*	0.775362	1.192857	0.697842	1.058824	0.780142	1.042553	1.042553	1.460993
Teq (s)	0.364	0.386	0.353	0.502	0.337	0.465	0.444	0.537

Table 168: Spectrum analysis parameters C template buildings part two

Building	C2		C2 6fl		C3	
Dir	x	y	x	y	x	y
Vy (kN)	340.367	211.9266	259.2253	190.0102	238.8379	339.7554
Dy (m)	0.0221	0.009	0.0238	0.0105	0.0141	0.0087
dm (m)	0.0442	0.0225	0.0526	0.0262	0.0336	0.0149
k (t/m)	15401.22	23547.4	10891.82	18096.21	16938.86	39052.34
T_1 (s)	0.24688	0.27895	0.29524	0.34054	0.24056	0.22071
Γ	1.37	1.39	1.34	1.38	1.42	1.44
α	0.533	0.529	0.541	0.513	0.524	0.508
Wsist (ton)	541.3	541.3	626.45	626.45	711.5	711.5
H_{build} (m)	14	14	16.8	16.8	14	14
Cy	0.628795	0.391514	0.4138	0.303313	0.335682	0.47752
Cy*	1.179729	0.740102	0.764881	0.591253	0.640615	0.94
dy*	0.016131	0.006475	0.017761	0.007609	0.00993	0.006042
dy*	1.613139	0.647482	1.776119	0.76087	0.992958	0.604167
Teq (s)	0.385	0.301	0.556	0.421	0.481	0.263

Time history analysis

Table 169: Demand of A template buildings (in cm) under far field earthquakes (SDOF system)

	Earthquake	Record and component	A1 x	A1 y	A1 (3fl) x	A1 (3fl) y	A1 (4fl) x	A1 (4fl) y	A2 x	A2 y	A2 (½)x	A2 (½)y
1	San Fernando 2/9/1971	LA HOLLYWOOD STOR LOT, 090	0.157	0.144	0.591	0.387	1.229	0.707	0.36	0.279	0.327	0.24
2	San Fernando 2/9/1971	LA HOLLYWOOD STOR LOT, 180	0.192	0.176	0.324	0.308	0.658	0.616	0.349	0.224	0.295	0.232
3	San Fernando 2/9/1971	LA HOLLYWOOD STOR LOT, UP	0.079	0.086	0.092	0.09	0.158	0.25	0.082	0.091	0.1	0.081
4	Friuli, Italy 5/6/1976	Tolmezzo, 000	0.169	0.168	0.541	0.418	1.712	0.934	0.428	0.341	0.401	0.21
5	Friuli, Italy 5/6/1976	Tolmezzo, 270	0.145	0.126	0.593	0.628	1.239	0.87	0.613	0.381	0.461	0.201

6	Friuli, Italy 5/6/1976	Tolmezzo, UP	0.196	0.179	0.61	0.54	0.66	0.732	0.479	0.339	0.404	0.22
7	Imperial valley 10/15/1979	DELTA, 262 (UNAM/UCSD STATION 6605)	0.183	0.17	0.531	0.354	0.96	0.618	0.359	0.299	0.379	0.226
8	Imperial valley 10/15/1979	DELTA, 352 (UNAM/UCSD STATION 6605)	0.239	0.243	0.666	0.594	1.237	0.758	0.574	0.429	0.536	0.472
9	Imperial valley 10/15/1979	DELTA, DWN (UNAM/UCSD STATION 6605)	0.095	0.085	0.207	0.185	0.372	0.28	0.187	0.157	0.172	0.134
10	Imperial valley 10/15/1979	EL CENTRO ARRAY #11, 140 (USGS STATION 5058)	0.214	0.189	1.041	0.767	1.865	1.36	0.689	0.292	0.487	0.253
11	Imperial valley 10/15/1979	EL CENTRO ARRAY #11, 230 (USGS STATION 5058)	0.146	0.148	1.155	0.747	2.002	1.49	0.663	0.311	0.516	0.22
12	Imperial valley 10/15/1979	EL CENTRO ARRAY #11, UP (USGS STATION 5058)	0.104	0.095	0.207	0.249	0.433	0.441	0.233	0.226	0.209	0.148
13	SuperstitionHills 02 11/24/87	EL CENTRO IMP CO CENTER, 000 (CDMG STATION 01	0.161	0.141	0.716	0.512	1.191	0.975	0.495	0.378	0.488	0.25
14	SuperstitionHills 02 11/24/87	EL CENTRO IMP CO CENTER, 090 (CDMG STATION 01	0.108	0.102	0.438	0.324	0.931	0.614	0.298	0.166	0.245	0.134
15	SuperstitionHills 02 11/24/87	EL CENTRO IMP CO	0.119	0.109	0.212	0.193	0.369	0.283	0.21	0.169	0.21	0.136

		CENTER, UP (CDMG STATION 01										
16	SuperstitionHills 02 11/24/87	POE, 270 (USGS STATION TEMP)	0.161	0.153	0.602	0.513	1.08	0.797	0.478	0.3	0.467	0.224
17	SuperstitionHills 02 11/24/87	POE, 360 (USGS STATION TEMP)	0.173	0.159	0.618	0.453	1.1	1.053	0.435	0.438	0.423	0.317
18	LOMA PRIETA 10/18/89	CAPITOLA, 000 (CDMG STATION 47125)	0.361	0.305	0.806	0.673	2.895	2.582	0.617	0.561	0.636	0.452
19	LOMA PRIETA 10/18/89	CAPITOLA, 090 (CDMG STATION 47125)	0.259	0.241	0.782	0.538	1.169	1.048	0.529	0.554	0.536	0.417
20	LOMA PRIETA 10/18/89	CAPITOLA, UP (CDMG STATION 47125)	0.47	0.394	1.289	1.081	1.048	1.136	0.963	0.701	0.913	0.603
21	LOMA PRIETA 10/18/89	GILROY ARRAY #3, 000 (CDMG STATION 47381)	0.437	0.401	1.196	0.939	1.802	2.22	0.908	0.634	0.747	0.633
22	LOMA PRIETA 10/18/89	GILROY ARRAY #3, 090 (CDMG STATION 47381)	0.296	0.265	0.77	0.745	1.43	1.652	0.713	0.49	0.653	0.354
23	LOMA PRIETA 10/18/89	GILROY ARRAY #3, UP (CDMG STATION 47381)	0.239	0.209	0.294	0.27	0.784	0.372	0.272	0.339	0.261	0.371
24	CAPE MENDOCINO 04/25/92	RIO DELL OVERPASS FF, 360 (CDMG	0.199	0.192	0.935	0.608	3.49	1.765	0.569	0.351	0.448	0.288

		STATION 89324)										
25	CAPE MENDOCINO 04/25/92	RIO DELL OVERPASS FF, UP (CDMG STATION 89324)	0.114	0.111	0.418	0.322	0.824	0.544	0.279	0.196	0.234	0.121
26	CAPE MENDOCINO 04/25/92	RIO DELL OVERPASS FF, 270	0.114	0.111	0.418	0.322	0.824	0.544	0.279	0.196	0.234	0.121
27	LANDERS 7/23/92	COOLWATER, LN (SCE STATION 23)	0.12	0.114	0.684	0.457	1.803	0.947	0.432	0.33	0.35	0.195
28	LANDERS 7/23/92	COOLWATER, TR (SCE STATION 23)	0.15	0.134	0.472	0.38	1.518	1.028	0.353	0.232	0.277	0.172
29	LANDERS 7/23/92	COOLWATER, UP (SCE STATION 23)	0.137	0.147	0.31	0.283	0.916	0.608	0.285	0.245	0.256	0.149
30	LANDERS 06/28/92	YERMO FIRE STATION, 270 (CDMG STATION 22074)	0.092	0.08	0.355	0.271	0.932	0.559	0.247	0.181	0.223	0.13
31	LANDERS 06/28/92	YERMO FIRE STATION, 360 (CDMG STATION 22074)	0.116	0.095	0.36	0.255	0.823	0.699	0.229	0.147	0.215	0.108
32	LANDERS 06/28/92	YERMO FIRE STATION, UP (CDMG STATION 22074)	0.086	0.071	0.26	0.283	0.5	0.391	0.177	0.112	0.155	0.094
33	NORTHRIDGE EQ 1/17/94	BEVERLY HILLS - 12520 MULH, 035 (USC STATION 90014	0.327	0.293	0.892	0.778	3.181	1.808	0.644	0.457	0.667	0.428

34	NORTHRIDGE EQ 1/17/94	BEVERLY HILLS - 12520 MULH, 125 (USC STATION 90014	0.258	0.224	1.02	0.65	3.094	1.405	0.604	0.505	0.579	0.37
35	NORTHRIDGE EQ 1/17/94	BEVERLY HILLS - 12520 MULH, UP (USC STATION 90014)	0.238	0.239	0.786	0.681	1.129	1.063	0.64	0.348	0.495	0.23
36	NORTHRIDGE EQ 1/17/94	BEVERLY HILLS - 14145 MULH, 009 (USC STATION 90013	0.15	0.134	0.791	0.643	2.118	1.106	0.626	0.438	0.545	0.276
37	NORTHRIDGE EQ 1/17/94	BEVERLY HILLS - 14145 MULH, 279 (USC STATION 90013	0.224	0.196	0.952	0.751	2.368	1.619	0.747	0.499	0.602	0.328
38	NORTHRIDGE EQ 1/17/94	BEVERLY HILLS - 14145 MULH, UP (USC STATION 90013)	0.235	0.215	0.685	0.48	1.723	1.207	0.42	0.369	0.402	0.275
39	NORTHRIDGE EQ 1/17/94	CANYON COUNTRY - W LOST CANYON, 000 (USC STATION 9	0.215	0.198	0.566	0.454	1.314	1.597	0.446	0.32	0.398	0.278
40	NORTHRIDGE EQ 1/17/94	CANYON COUNTRY - W LOST CANYON, 270	0.258	0.24	1.014	0.865	1.952	2.198	0.938	0.573	0.53	0.394

		(USC STATION 9										
41	NORTHRIDGE EQ 1/17/94	CANYON COUNTRY - W LOST CANYON, UP (USC STATION 90	0.177	0.165	0.539	0.472	0.908	0.582	0.467	0.302	0.396	0.263
42	KOBE 01/16/95	NISHI-AKASHI, 000	0.192	0.187	0.681	0.594	1.933	2.039	0.558	0.353	0.422	0.262
43	KOBE 01/16/95	NISHI-AKASHI, 090	0.234	0.212	0.87	0.529	1.746	1.706	0.503	0.409	0.529	0.297
44	KOBE 01/16/95	NISHI-AKASHI, V	0.219	0.217	0.956	0.689	1.622	1.366	0.602	0.328	0.448	0.234
45	KOBE 01/16/95	SHIN-OSAKA, 000	0.097	0.085	0.402	0.345	0.823	0.505	0.309	0.224	0.304	0.143
46	KOBE 01/16/95	SHIN-OSAKA, 090	0.107	0.09	0.262	0.228	0.634	0.559	0.234	0.211	0.225	0.16
47	KOBE 01/16/95	SHIN-OSAKA, V	0.029	0.027	0.1	0.092	1.622	0.172	0.09	0.056	0.066	0.043
48	KOCAELI 08/17/99	ARCELIK, 000 (KOERI)	0.094	0.082	0.509	0.532	0.597	0.54	0.485	0.236	0.351	0.144
49	KOCAELI 08/17/99	ARCELIK, 090 (KOERI)	0.097	0.083	0.264	0.242	0.722	0.44	0.236	0.169	0.249	0.129
50	KOCAELI 08/17/99	ARCELIK, DWN (KOERI)	0.053	0.053	0.157	0.129	0.234	0.195	0.119	0.084	0.109	0.058
51	KOCAELI 08/17/99	DUZCE, 180 (ERD)	0.117	0.114	0.488	0.34	1.175	0.625	0.339	0.199	0.271	0.164
52	KOCAELI 08/17/99	DUZCE, 270 (ERD)	0.129	0.121	0.502	0.426	1.835	0.861	0.397	0.313	0.361	0.231
53	KOCAELI 08/17/99	DUZCE, UP (ERD)	0.27	0.256	0.361	0.298	0.651	0.458	0.267	0.25	0.268	0.219
54	CHI-CHI 09/20/99	CHY101, E	0.157	0.155	0.684	0.657	0.993	0.794	0.623	0.288	0.46	0.251
55	CHI-CHI 09/20/99	CHY101, N	0.236	0.225	0.562	0.444	1.32	0.701	0.412	0.307	0.388	0.259
56	CHI-CHI 09/20/99	CHY101, Vertical	0.134	0.119	0.219	0.278	0.614	0.414	0.288	0.247	0.282	0.17
57	CHI-CHI 09/20/99	TCU045, E	0.187	0.172	0.679	0.525	1.963	0.939	0.498	0.308	0.368	0.25

58	CHI-CHI 09/20/99	TCU045, N	0.18	0.17	0.64	0.522	1.926	0.959	0.495	0.334	0.418	0.247
59	CHI-CHI 09/20/99	TCU045, Vertical	0.201	0.186	0.298	0.248	0.517	0.443	0.239	0.227	0.19	0.191
60	DUZCE 11/12/99	BOLU, 000 (ERD)	0.25	0.231	0.991	0.647	3.729	2.154	0.578	0.412	0.5	0.363
61	DUZCE 11/12/99	BOLU, 090 (ERD)	0.324	0.303	0.848	0.768	1.695	1.226	0.78	0.589	0.728	0.447
62	DUZCE 11/12/99	BOLU, UP (ERD)	0.144	0.141	0.458	0.378	0.817	0.534	0.317	0.217	0.286	0.174
63	IRAN_MANJIL 06/20/90	LONGITUDINAL COMP	0.377	0.346	1.345	1.041	1.724	1.667	1.277	0.734	1.072	0.539
64	IRAN_MANJIL 06/20/90	TRANSVERSE COMP	0.391	0.363	1.401	0.895	2.842	2.239	0.781	0.648	0.772	0.743
65	IRAN_MANJIL 06/20/90	VERTICAL COMP	0.473	0.503	0.94	0.937	1.897	1.472	0.874	0.715	0.757	0.531
66	HECTOR MINE OCT 16, 1999	HEC, 000	0.121	0.113	0.543	0.425	1.112	0.943	0.436	0.241	0.412	0.155
67	HECTOR MINE OCT 16, 1999	HEC, 090	0.162	0.154	0.687	0.415	1.323	1.239	0.391	0.227	0.288	0.202
68	HECTOR MINE OCT 16, 1999	HEC, VER	0.113	0.118	0.312	0.251	0.796	0.363	0.248	0.177	0.217	0.15

Table 170: Demand of B template buildings (in cm) under far field earthquakes (SDOF system) part one

	Earthquake	**Record and component**	**B1 x**	**B1 y**	**B1 (4fl)x**	**B1 (4fl)y**	**B2 x**	**B2 y**	**B2x (38cm)**	**B2y (38cm)**
1	San Fernando 2/9/1971	LA HOLLYWOOD STOR LOT, 090	0.352	0.24	0.62	0.397	0.376	0.641	0.392	0.619
2	San Fernando 2/9/1971	LA HOLLYWOOD STOR LOT, 180	0.328	0.232	0.457	0.308	0.317	0.414	0.303	0.464
3	San Fernando 2/9/1971	LA HOLLYWOOD STOR LOT, UP	0.089	0.081	0.187	0.093	0.087	0.163	0.091	0.19
4	Friuli, Italy 5/6/1976	Tolmezzo, 000	0.418	0.21	0.732	0.415	0.42	0.614	0.416	0.747
5	Friuli, Italy 5/6/1976	Tolmezzo, 270	0.526	0.201	0.677	0.629	0.627	0.607	0.628	0.681

6	Friuli, Italy 5/6/1976	Tolmezzo, UP	0.414	0.22	0.549	0.549	0.531	0.516	0.545	0.559
7	Imperial valley 10/15/1979	DELTA, 262 (UNAM/UCSD STATION 6605)	0.388	0.226	0.539	0.355	0.352	0.541	0.355	0.54
8	Imperial valley 10/15/1979	DELTA, 352 (UNAM/UCSD STATION 6605)	0.56	0.456	0.617	0.596	0.591	0.694	0.595	0.614
9	Imperial valley 10/15/1979	DELTA, DWN (UNAM/UCSD STATION 6605)	0.183	0.134	0.247	0.188	0.186	0.239	0.187	0.254
10	Imperial valley 10/15/1979	EL CENTRO ARRAY #11, 140 (USGS STATION 5058)	0.56	0.254	1.203	0.901	0.847	1.152	0.889	1.249
11	Imperial valley 10/15/1979	EL CENTRO ARRAY #11, 230 (USGS STATION 5058)	0.548	0.22	1.165	0.763	0.727	0.958	0.753	1.114
12	Imperial valley 10/15/1979	EL CENTRO ARRAY #11, UP (USGS STATION 5058)	0.217	0.148	0.414	0.249	0.248	0.424	0.249	0.413
13	SuperstitionHills02 11/24/87	EL CENTRO IMP CO CENTER, 000 (CDMG STATION 01	0.505	0.25	0.927	0.522	0.506	0.91	0.517	0.94
14	SuperstitionHills02 11/24/87	EL CENTRO IMP CO CENTER, 090 (CDMG STATION 01	0.263	0.134	0.549	0.33	0.319	0.495	0.327	0.553
15	SuperstitionHills02 11/24/87	EL CENTRO IMP CO CENTER, UP (CDMG STATION 01	0.217	0.136	0.245	0.193	0.197	0.271	0.192	0.239
16	SuperstitionHills02 11/24/87	POE, 270 (USGS STATION TEMP)	0.473	0.224	0.716	0.524	0.505	0.609	0.519	0.728
17	SuperstitionHills02 11/24/87	POE, 360 (USGS STATION TEMP)	0.448	0.317	1.02	0.466	0.443	0.824	0.459	0.951

18	LOMA PRIETA 10/18/89	CAPITOLA, 000 (CDMG STATION 47125)	0.738	0.446	1.462	0.689	0.661	1.304	0.681	1.807
19	LOMA PRIETA 10/18/89	CAPITOLA, 090 (CDMG STATION 47125)	0.533	0.417	0.8	0.537	0.538	0.825	0.538	0.814
20	LOMA PRIETA 10/18/89	CAPITOLA, UP (CDMG STATION 47125)	1.198	0.588	1.424	1.225	1.179	1.586	1.201	1.487
21	LOMA PRIETA 10/18/89	GILROY ARRAY #3, 000 (CDMG STATION 47381)	1.049	0.598	1.834	1.094	1.243	1.686	1.096	1.974
22	LOMA PRIETA 10/18/89	GILROY ARRAY #3, 090 (CDMG STATION 47381)	0.639	0.354	1.444	0.748	0.734	1.147	0.745	1.532
23	LOMA PRIETA 10/18/89	GILROY ARRAY #3, UP (CDMG STATION 47381)	0.251	0.371	0.346	0.266	0.271	0.314	0.268	0.354
24	CAPE MENDOCINO 04/25/92	RIO DELL OVERPASS FF, 360 (CDMG STATION 89324)	0.486	0.288	1.126	0.621	0.6	1.1	0.615	1.204
25	CAPE MENDOCINO 04/25/92	RIO DELL OVERPASS FF, UP (CDMG STATION 89324)	0.214	0.121	0.405	0.336	0.312	0.431	0.329	0.409
26	CAPE MENDOCINO 04/25/92	RIO DELL OVERPASS FF, 270	0.214	0.121	0.405	0.336	0.312	0.431	0.329	0.409
27	LANDERS 7/23/92	COOLWATER, LN (SCE STATION 23)	0.376	0.196	0.981	0.466	0.451	0.95	0.461	0.913
28	LANDERS 7/23/92	COOLWATER, TR (SCE STATION 23)	0.286	0.172	0.726	0.385	0.376	0.574	0.383	0.754
29	LANDERS 7/23/92	COOLWATER, UP (SCE STATION 23)	0.259	0.149	0.489	0.282	0.284	0.463	0.282	0.493
30	LANDERS 06/28/92	YERMO FIRE STATION, 270	0.224	0.13	0.435	0.274	0.269	0.417	0.273	0.436

		(CDMG STATION 22074)								
31	LANDERS 06/28/92	YERMO FIRE STATION, 360 (CDMG STATION 22074)	0.218	0.108	0.504	0.259	0.251	0.43	0.257	0.512
32	LANDERS 06/28/92	YERMO FIRE STATION, UP (CDMG STATION 22074)	0.17	0.094	0.464	0.208	0.197	0.466	0.205	0.454
33	NORTHRIDGE EQ 1/17/94	BEVERLY HILLS - 12520 MULH, 035 (USC STATION 90014	0.665	0.463	1.626	0.771	0.76	1.361	0.77	1.456
34	NORTHRIDGE EQ 1/17/94	BEVERLY HILLS - 12520 MULH, 125 (USC STATION 90014	0.616	0.37	1.41	0.662	0.64	1.443	0.656	1.557
35	NORTHRIDGE EQ 1/17/94	BEVERLY HILLS - 12520 MULH, UP (USC STATION 90014)	0.561	0.23	1.225	0.677	0.685	1.174	0.677	1.116
36	NORTHRIDGE EQ 1/17/94	BEVERLY HILLS - 14145 MULH, 009 (USC STATION 90013	0.565	0.276	1.036	0.648	0.64	1	0.646	1.071
37	NORTHRIDGE EQ 1/17/94	BEVERLY HILLS - 14145 MULH, 279 (USC STATION 90013	0.679	0.328	1.212	0.726	0.705	1.166	0.718	1.344
38	NORTHRIDGE EQ 1/17/94	BEVERLY HILLS - 14145 MULH, UP (USC STATION 90013)	0.394	0.275	1.223	0.493	0.47	0.986	0.486	1.231
39	NORTHRIDGE EQ 1/17/94	CANYON COUNTRY - W LOST CANYON, 000 (USC STATION 9	0.423	0.278	0.899	0.462	0.451	0.683	0.458	0.959
40	NORTHRIDGE EQ 1/17/94	CANYON COUNTRY - W	0.612	0.394	1.47	0.779	0.775	1.28	0.775	1.707

		LOST CANYON, 270 (USC STATION 9								
41	NORTHRIDGE EQ 1/17/94	CANYON COUNTRY - W LOST CANYON, UP (USC STATION 90	0.429	0.263	0.601	0.469	0.474	0.556	0.471	0.603
42	KOBE 01/16/95	NISHI-AKASHI, 000	0.464	0.262	1.853	0.605	0.588	1.395	0.6	1.853
43	KOBE 01/16/95	NISHI-AKASHI, 090	0.523	0.297	1.118	0.537	0.524	1.048	0.533	1.293
44	KOBE 01/16/95	NISHI-AKASHI, V	0.494	0.234	1.213	0.709	0.673	1.117	0.699	1.439
45	KOBE 01/16/95	SHIN-OSAKA, 000	0.323	0.143	0.422	0.352	0.339	0.406	0.349	0.429
46	KOBE 01/16/95	SHIN-OSAKA, 090	0.232	0.16	0.427	0.225	0.229	0.36	0.226	0.435
47	KOBE 01/16/95	SHIN-OSAKA, V	0.078	0.043	0.155	0.093	0.092	0.146	0.093	0.155
48	KOCAELI 08/17/99	ARCELIK, 000 (KOERI)	0.384	0.144	0.581	0.54	0.525	0.669	0.536	0.568
49	KOCAELI 08/17/99	ARCELIK, 090 (KOERI)	0.249	0.13	0.344	0.244	0.241	0.368	0.243	0.345
50	KOCAELI 08/17/99	ARCELIK, DWN (KOERI)	0.114	0.058	0.194	0.132	0.127	0.211	0.13	0.196
51	KOCAELI 08/17/99	DUZCE, 180 (ERD)	0.286	0.164	0.507	0.339	0.341	0.532	0.34	0.513
52	KOCAELI 08/17/99	DUZCE, 270 (ERD)	0.371	0.231	0.721	0.435	0.42	0.63	0.431	0.734
53	KOCAELI 08/17/99	DUZCE, UP (ERD)	0.25	0.219	0.383	0.304	0.294	0.374	0.301	0.387
54	CHI-CHI 09/20/99	CHY101, E	0.519	0.251	0.666	0.663	0.651	0.652	0.66	0.671
55	CHI-CHI 09/20/99	CHY101, N	0.398	0.259	0.805	0.456	0.434	0.741	0.45	0.806
56	CHI-CHI 09/20/99	CHY101, Vertical	0.29	0.17	0.41	0.274	0.281	0.38	0.276	0.415
57	CHI-CHI 09/20/99	TCU045, E	0.409	0.25	1.023	0.529	0.52	0.952	0.527	1.049
58	CHI-CHI 09/20/99	TCU045, N	0.44	0.247	0.773	0.528	0.517	0.725	0.525	0.781

59	CHI-CHI 09/20/99	TCU045, Vertical	0.21	0.191	0.439	0.249	0.247	0.404	0.248	0.44
60	DUZCE 11/12/99	BOLU, 000 (ERD)	0.512	0.364	1.922	0.665	0.635	1.828	0.656	2.27
61	DUZCE 11/12/99	BOLU, 090 (ERD)	0.692	0.437	0.972	0.759	0.747	0.907	0.756	0.993
62	DUZCE 11/12/99	BOLU, UP (ERD)	0.285	0.174	0.619	0.39	0.368	0.584	0.384	0.619
63	IRAN_MANJIL 06/20/90	LONGITUDINAL COMP	0.995	0.541	1.336	1.332	1.41	1.383	1.329	1.509
64	IRAN_MANJIL 06/20/90	TRANSVERSE COMP	0.997	0.594	1.458	0.901	0.989	1.675	0.904	1.947
65	IRAN_MANJIL 06/20/90	VERTICAL COMP	0.88	0.55	1.189	0.908	1.029	1.093	0.898	1.282
66	HECTOR MINE OCT 16, 1999	HEC, 000	0.433	0.155	0.744	0.434	0.42	0.63	0.429	0.756
67	HECTOR MINE OCT 16, 1999	HEC, 090	0.318	0.202	1	0.418	0.412	0.779	0.416	1.039
68	HECTOR MINE OCT 16, 1999	HEC, VER	0.233	0.15	0.379	0.253	0.249	0.369	0.252	0.38

Table 171: Demand of B template buildings (in cm) under far field earthquakes (SDOF system) part two

	Earthquake	**Record and component**	**B3x**	**B3y**	**B3x int**	**B3y int**	**B4x**	**B4y**
1	San Fernando 2/9/1971	LA HOLLYWOOD STOR LOT, 090	1.331	1.115	1.542	1.221	1.223	1.432
2	San Fernando 2/9/1971	LA HOLLYWOOD STOR LOT, 180	0.88	0.766	0.848	0.703	0.846	0.837
3	San Fernando 2/9/1971	LA HOLLYWOOD STOR LOT, UP	0.256	0.158	0.322	0.159	0.22	0.293
4	Friuli, Italy 5/6/1976	Tolmezzo, 000	2.125	1.867	2.304	2.128	1.944	2.198
5	Friuli, Italy 5/6/1976	Tolmezzo, 270	2.329	1.41	2.924	1.335	2.071	2.504
6	Friuli, Italy 5/6/1976	Tolmezzo, UP	1.634	0.822	1.579	0.668	1.627	1.607

7	Imperial valley 10/15/1979	DELTA, 262 (UNAM/UCSD STATION 6605)	1.595	1.117	1.752	1.02	1.587	1.727
8	Imperial valley 10/15/1979	DELTA, 352 (UNAM/UCSD STATION 6605)	1.932	1.342	1.748	1.145	1.976	1.786
9	Imperial valley 10/15/1979	DELTA, DWN (UNAM/UCSD STATION 6605)	0.672	0.449	0.723	0.393	0.676	0.697
10	Imperial valley 10/15/1979	EL CENTRO ARRAY #11, 140 (USGS STATION 5058)	2.593	2.487	2.605	2.21	2.419	2.761
11	Imperial valley 10/15/1979	EL CENTRO ARRAY #11, 230 (USGS STATION 5058)	2.868	2.501	2.758	2.371	2.698	3.414
12	Imperial valley 10/15/1979	EL CENTRO ARRAY #11, UP (USGS STATION 5058)	0.498	0.504	0.515	0.5	0.472	0.512
13	SuperstitionHills02 11/24/87	EL CENTRO IMP CO CENTER, 000 (CDMG STATION 01	1.789	1.214	1.727	1.303	1.682	1.792
14	SuperstitionHills02 11/24/87	EL CENTRO IMP CO CENTER, 090 (CDMG STATION 01	1.009	0.896	1.085	0.914	0.968	1.06
15	SuperstitionHills02 11/24/87	EL CENTRO IMP CO CENTER, UP (CDMG STATION 01	0.459	0.414	0.493	0.428	0.4	0.484
16	SuperstitionHills02 11/24/87	POE, 270 (USGS STATION TEMP)	1.854	1.603	2.008	1.346	1.708	1.936
17	SuperstitionHills02 11/24/87	POE, 360 (USGS STATION TEMP)	2.176	1.081	2.467	0.987	2.032	2.403
18	LOMA PRIETA 10/18/89	CAPITOLA, 000 (CDMG STATION 47125)	3.601	3.707	3.72	3.156	3.677	3.821

19	LOMA PRIETA 10/18/89	CAPITOLA, 090 (CDMG STATION 47125)	2.614	1.478	2.856	1.406	2.324	3.017
20	LOMA PRIETA 10/18/89	CAPITOLA, UP (CDMG STATION 47125)	1.481	1.229	1.788	1.156	1.323	1.653
21	LOMA PRIETA 10/18/89	GILROY ARRAY #3, 000 (CDMG STATION 47381)	3.051	2.439	3.412	2.016	2.781	3.174
22	LOMA PRIETA 10/18/89	GILROY ARRAY #3, 090 (CDMG STATION 47381)	2.457	2.124	1.935	1.625	2.65	2.167
23	LOMA PRIETA 10/18/89	GILROY ARRAY #3, UP (CDMG STATION 47381)	1.01	1.044	0.987	0.983	1.054	0.997
24	CAPE MENDOCINO 04/25/92	RIO DELL OVERPASS FF, 360 (CDMG STATION 89324)	3.623	4.223	4.42	3.791	3.7	3.937
25	CAPE MENDOCINO 04/25/92	RIO DELL OVERPASS FF, UP (CDMG STATION 89324)	0.73	0.779	0.704	0.852	0.801	0.704
26	CAPE MENDOCINO 04/25/92	RIO DELL OVERPASS FF, 270	0.73	0.779	0.704	0.852	0.801	0.704
27	LANDERS 7/23/92	COOLWATER, LN (SCE STATION 23)	2.997	1.994	2.998	1.925	2.75	3.06
28	LANDERS 7/23/92	COOLWATER, TR (SCE STATION 23)	3.501	1.802	3.214	1.627	3.35	3.702
29	LANDERS 7/23/92	COOLWATER, UP (SCE STATION 23)	1.322	0.883	1.352	0.826	1.217	1.363
30	LANDERS 06/28/92	YERMO FIRE STATION, 270 (CDMG STATION 22074)	1.197	0.898	1.352	0.869	1.057	1.29
31	LANDERS 06/28/92	YERMO FIRE STATION, 360	1.133	1.082	1.206	0.896	1.093	1.181

		(CDMG STATION 22074)						
32	LANDERS 06/28/92	YERMO FIRE STATION, UP (CDMG STATION 22074)	0.509	0.503	0.524	0.484	0.518	0.497
33	NORTHRIDGE EQ 1/17/94	BEVERLY HILLS - 12520 MULH, 035 (USC STATION 90014	3.2	2.713	4.107	2.712	2.869	3.503
34	NORTHRIDGE EQ 1/17/94	BEVERLY HILLS - 12520 MULH, 125 (USC STATION 90014	3.269	2.752	3.452	2.855	3.715	3.46
35	NORTHRIDGE EQ 1/17/94	BEVERLY HILLS - 12520 MULH, UP (USC STATION 90014)	1.31	1.071	1.296	1.126	1.212	1.344
36	NORTHRIDGE EQ 1/17/94	BEVERLY HILLS - 14145 MULH, 009 (USC STATION 90013	2.076	2.095	1.939	2.201	2.09	2.015
37	NORTHRIDGE EQ 1/17/94	BEVERLY HILLS - 14145 MULH, 279 (USC STATION 90013	3.166	2.558	3.28	2.119	3.102	3.111
38	NORTHRIDGE EQ 1/17/94	BEVERLY HILLS - 14145 MULH, UP (USC STATION 90013)	1.39	1.674	1.549	1.789	1.376	1.482
39	NORTHRIDGE EQ 1/17/94	CANYON COUNTRY - W LOST CANYON, 000 (USC STATION 9	3.225	1.515	3.668	1.407	2.769	3.302
40	NORTHRIDGE EQ 1/17/94	CANYON COUNTRY - W LOST CANYON, 270 (USC STATION 9	3.881	2.031	4.123	1.865	3.505	3.935

41	NORTHRIDGE EQ 1/17/94	CANYON COUNTRY - W LOST CANYON, UP (USC STATION 90	0.916	0.864	0.908	0.828	0.955	0.891
42	KOBE 01/16/95	NISHI-AKASHI, 000	3.327	2.38	3.101	2.359	3.376	3.464
43	KOBE 01/16/95	NISHI-AKASHI, 090	2.306	2.203	2.478	1.739	2.414	2.178
44	KOBE 01/16/95	NISHI-AKASHI, V	2.356	2.386	2.137	2.186	2.601	2.238
45	KOBE 01/16/95	SHIN-OSAKA, 000	1.452	0.828	1.592	0.831	1.259	1.553
46	KOBE 01/16/95	SHIN-OSAKA, 090	1.204	0.823	0.623	0.662	1.166	1.306
47	KOBE 01/16/95	SHIN-OSAKA, V	0.262	0.249	0.289	0.207	0.24	0.278
48	KOCAELI 08/17/99	ARCELIK, 000 (KOERI)	0.564	0.623	0.591	0.647	0.584	0.577
49	KOCAELI 08/17/99	ARCELIK, 090 (KOERI)	0.637	0.701	0.728	0.715	0.597	0.689
50	KOCAELI 08/17/99	ARCELIK, DWN (KOERI)	0.286	0.26	0.315	0.247	0.289	0.292
51	KOCAELI 08/17/99	DUZCE, 180 (ERD)	2.311	1.375	2.8	1.221	2.403	2.537
52	KOCAELI 08/17/99	DUZCE, 270 (ERD)	2.838	2.899	3.77	2.547	2.595	3.181
53	KOCAELI 08/17/99	DUZCE, UP (ERD)	0.936	0.629	1.009	0.663	0.901	0.96
54	CHI-CHI 09/20/99	CHY101, E	1.569	1.593	1.698	1.237	1.507	1.593
55	CHI-CHI 09/20/99	CHY101, N	1.973	1.732	2.439	1.424	2.011	2.136
56	CHI-CHI 09/20/99	CHY101, Vertical	1.068	0.568	1.187	0.622	0.968	1.146
57	CHI-CHI 09/20/99	TCU045, E	3.25	2.238	3.821	2.001	3.067	3.404
58	CHI-CHI 09/20/99	TCU045, N	2.118	1.776	2.319	1.647	1.983	2.214
59	CHI-CHI 09/20/99	TCU045, Vertical	1.045	0.599	1.114	0.526	0.992	1.076
60	DUZCE 11/12/99	BOLU, 000 (ERD)	4.922	3.146	4.331	2.883	5.353	4.758

61	DUZCE 11/12/99	BOLU, 090 (ERD)	4.081	1.835	5.367	1.755	3.206	4.385
62	DUZCE 11/12/99	BOLU, UP (ERD)	1.175	0.955	1.075	0.929	1.165	1.135
63	IRAN_MANJIL 06/20/90	LONGITUDINAL COMP	3.046	2.305	3.502	2.138	2.669	3.328
64	IRAN_MANJIL 06/20/90	TRANSVERSE COMP	3.123	2.266	4.288	2.202	2.993	3.792
65	IRAN_MANJIL 06/20/90	VERTICAL COMP	2.515	2.376	2.321	2.016	2.646	2.361
66	HECTOR MINE OCT 16, 1999	HEC, 000	1.322	0.95	1.47	0.973	1.274	1.374
67	HECTOR MINE OCT 16, 1999	HEC, 090	2.624	1.693	2.569	1.538	2.515	2.609
68	HECTOR MINE OCT 16, 1999	HEC, VER	0.759	0.846	0.689	0.898	0.799	0.713

Table 172: Demand of C template buildings (in cm) under far field earthquakes (SDOF system) part one

	Earthquake	**Record and component**	**C1Ax**	**C1Ay**	**C1Ax int**	**C1Ay int**	**C1Bx**	**C1By**	**C1Bx (6fl)**	**C1By (6fl)**
1	San Fernando 2/9/1971	LA HOLLYWOOD STOR LOT, 090	1.328	1.582	1.216	1.742	1.216	1.772	1.81	1.917
2	San Fernando 2/9/1971	LA HOLLYWOOD STOR LOT, 180	0.88	1.607	0.805	1.702	0.77	1.58	1.187	2.005
3	San Fernando 2/9/1971	LA HOLLYWOOD STOR LOT, UP	0.255	0.378	0.195	0.371	0.199	0.401	0.379	0.413
4	Friuli, Italy 5/6/1976	Tolmezzo, 000	2.072	3.195	1.767	2.87	1.828	2.901	2.913	4.215
5	Friuli, Italy 5/6/1976	Tolmezzo, 270	2.394	5.214	1.536	5.195	1.875	4.338	3.444	6.285
6	Friuli, Italy 5/6/1976	Tolmezzo, UP	1.634	0.772	1.331	0.885	1.568	0.971	1.242	0.764
7	Imperial valley 10/15/1979	DELTA, 262 (UNAM/UCSD STATION 6605)	1.591	3.283	1.386	3.085	1.528	2.806	2.515	4.188

8	Imperial valley 10/15/1979	DELTA, 352 (UNAM/UCSD STATION 6605)	1.937	2.988	1.679	2.62	1.834	2.376	2.1	3.996
9	Imperial valley 10/15/1979	DELTA, DWN (UNAM/UCSD STATION 6605)	0.672	0.642	0.554	0.687	0.654	0.675	0.69	0.826
10	Imperial valley 10/15/1979	EL CENTRO ARRAY #11, 140 (USGS STATION 5058)	2.55	3.982	2.397	3.766	2.409	3.427	2.945	3.337
11	Imperial valley 10/15/1979	EL CENTRO ARRAY #11, 230 (USGS STATION 5058)	2.711	4.382	2.51	4.284	2.76	3.378	3.266	5.486
12	Imperial valley 10/15/1979	EL CENTRO ARRAY #11, UP (USGS STATION 5058)	0.498	0.61	0.479	0.528	0.448	0.486	0.447	0.531
13	SuperstitionHills02 11/24/87	EL CENTRO IMP CO CENTER, 000 (CDMG STATION 01	1.788	3.223	1.435	2.531	1.635	2.329	2.302	4.022
14	SuperstitionHills02 11/24/87	EL CENTRO IMP CO CENTER, 090 (CDMG STATION 01	1.008	3.117	0.817	2.552	0.907	2.316	2.192	3.55
15	SuperstitionHills02 11/24/87	EL CENTRO IMP CO CENTER, UP (CDMG STATION 01	0.458	0.6	0.313	0.639	0.358	0.613	0.51	1.105
16	SuperstitionHills02 11/24/87	POE, 270 (USGS STATION TEMP)	1.851	5.022	1.647	4.535	1.629	4.831	3.992	5.245
17	SuperstitionHills02 11/24/87	POE, 360 (USGS STATION TEMP)	2.009	3.783	1.684	3.783	1.992	2.934	2.703	3.696
18	LOMA PRIETA 10/18/89	CAPITOLA, 000 (CDMG STATION 47125)	2.929	5.898	4.445	6.169	3.838	4.797	3.985	5.182
19	LOMA PRIETA 10/18/89	CAPITOLA, 090 (CDMG STATION 47125)	2.566	4.246	1.861	3.493	2.063	3.823	3.575	4.756

20	LOMA PRIETA 10/18/89	CAPITOLA, UP (CDMG STATION 47125)	1.476	1.748	1.344	1.607	1.275	1.594	1.575	1.445
21	LOMA PRIETA 10/18/89	GILROY ARRAY #3, 000 (CDMG STATION 47381)	3.53	4.506	2.419	4.627	2.796	4.811	5.321	6.654
22	LOMA PRIETA 10/18/89	GILROY ARRAY #3, 090 (CDMG STATION 47381)	2.284	2.456	2.027	2.043	2.463	1.832	1.921	4.564
23	LOMA PRIETA 10/18/89	GILROY ARRAY #3, UP (CDMG STATION 47381)	1.01	1.501	1.076	1.422	1.088	1.379	1.11	1.424
24	CAPE MENDOCINO 04/25/92	RIO DELL OVERPASS FF, 360 (CDMG STATION 89324)	3.929	6.932	3.274	7.028	3.662	6.418	5.446	8.304
25	CAPE MENDOCINO 04/25/92	RIO DELL OVERPASS FF, UP (CDMG STATION 89324)	0.73	1.12	0.799	1.109	0.837	1.134	1.024	1.175
26	CAPE MENDOCINO 04/25/92	RIO DELL OVERPASS FF, 270	0.73	1.12	0.799	1.109	0.837	1.134	1.024	1.175
27	LANDERS 7/23/92	COOLWATER, LN (SCE STATION 23)	2.375	3.184	2.169	3.057	2.359	2.964	3.107	4.456
28	LANDERS 7/23/92	COOLWATER, TR (SCE STATION 23)	3.081	5.858	2.357	5.926	2.975	5.58	4.179	5.836
29	LANDERS 7/23/92	COOLWATER, UP (SCE STATION 23)	1.32	1.211	0.98	0.96	1.106	0.817	0.78	1.165
30	LANDERS 06/28/92	YERMO FIRE STATION, 270 (CDMG STATION 22074)	1.194	2.005	0.86	2.016	0.98	1.997	1.855	3.439
31	LANDERS 06/28/92	YERMO FIRE STATION, 360 (CDMG STATION 22074)	1.132	1.901	0.963	1.699	1.047	1.813	1.886	2.818

32	LANDERS 06/28/92	YERMO FIRE STATION, UP (CDMG STATION 22074)	0.509	0.915	0.551	0.926	0.519	0.962	0.898	0.872
33	NORTHRIDGE EQ 1/17/94	BEVERLY HILLS - 12520 MULH, 035 (USC STATION 90014	3.686	3.949	2.593	3.405	2.625	3.814	4.11	3.918
34	NORTHRIDGE EQ 1/17/94	BEVERLY HILLS - 12520 MULH, 125 (USC STATION 90014	3.388	3.155	3.281	3.462	3.908	3.517	3.369	4.451
35	NORTHRIDGE EQ 1/17/94	BEVERLY HILLS - 12520 MULH, UP (USC STATION 90014)	1.307	1.195	1.171	1.041	1.197	0.971	0.978	1.246
36	NORTHRIDGE EQ 1/17/94	BEVERLY HILLS - 14145 MULH, 009 (USC STATION 90013	2.08	3.765	2.004	3.547	2.062	3.733	3.368	8.277
37	NORTHRIDGE EQ 1/17/94	BEVERLY HILLS - 14145 MULH, 279 (USC STATION 90013	3.444	5.95	3.112	5.964	3.327	5.313	5.538	6.828
38	NORTHRIDGE EQ 1/17/94	BEVERLY HILLS - 14145 MULH, UP (USC STATION 90013)	1.388	2.844	1.47	2.725	1.442	2.473	1.643	3.93
39	NORTHRIDGE EQ 1/17/94	CANYON COUNTRY - W LOST CANYON, 000 (USC STATION 9	3.331	5.089	2.181	5.869	2.662	5.106	4.794	5.809
40	NORTHRIDGE EQ 1/17/94	CANYON COUNTRY - W LOST CANYON, 270 (USC STATION 9	4.152	5.822	3.035	5.397	3.407	4.693	3.776	6.26
41	NORTHRIDGE EQ 1/17/94	CANYON COUNTRY - W LOST CANYON,	0.917	1.755	0.899	1.674	0.945	1.6	1.374	1.66

		UP (USC STATION 90								
42	KOBE 01/16/95	NISHI-AKASHI, 000	2.499	6.568	2.416	6.855	3.01	7.042	5.005	8.039
43	KOBE 01/16/95	NISHI-AKASHI, 090	2.173	4.362	2.294	4.921	2.35	4.591	4.367	5.854
44	KOBE 01/16/95	NISHI-AKASHI, V	2.392	3.34	2.28	2.702	2.679	2.567	2.36	3.836
45	KOBE 01/16/95	SHIN-OSAKA, 000	1.449	2.636	0.966	2.162	1.116	2.178	2.07	4.056
46	KOBE 01/16/95	SHIN-OSAKA, 090	1.204	2.814	1.176	2.464	1.145	2.486	2.209	3.759
47	KOBE 01/16/95	SHIN-OSAKA, V	0.261	0.472	0.275	0.442	0.249	0.428	0.478	0.74
48	KOCAELI 08/17/99	ARCELIK, 000 (KOERI)	0.564	1.214	0.571	0.989	0.605	0.858	0.761	1.36
49	KOCAELI 08/17/99	ARCELIK, 090 (KOERI)	0.636	0.937	0.634	0.915	0.561	0.916	0.985	1.114
50	KOCAELI 08/17/99	ARCELIK, DWN (KOERI)	0.286	0.616	0.284	0.557	0.295	0.525	0.482	0.749
51	KOCAELI 08/17/99	DUZCE, 180 (ERD)	2.336	3.855	1.549	4.489	1.855	4.29	3.374	4.261
52	KOCAELI 08/17/99	DUZCE, 270 (ERD)	3.109	4.253	3.162	4.631	2.695	4.769	4.453	4.221
53	KOCAELI 08/17/99	DUZCE, UP (ERD)	0.935	0.774	0.717	0.761	0.859	0.818	0.959	0.781
54	CHI-CHI 09/20/99	CHY101, E	1.568	2.28	1.494	2.038	1.505	2.023	1.986	2.985
55	CHI-CHI 09/20/99	CHY101, N	1.971	4.458	2.167	3.485	2.075	3.246	3.238	6.458
56	CHI-CHI 09/20/99	CHY101, Vertical	1.065	0.87	0.735	0.757	0.903	0.746	0.879	1.541
57	CHI-CHI 09/20/99	TCU045, E	3.486	5.999	3.227	6.012	3.208	5.308	4.774	6.665
58	CHI-CHI 09/20/99	TCU045, N	2.12	4.364	1.784	5.061	1.876	4.785	4.359	5.958
59	CHI-CHI 09/20/99	TCU045, Vertical	1.044	1.831	0.785	1.706	0.931	1.717	1.642	2.668
60	DUZCE 11/12/99	BOLU, 000 (ERD)	4.678	5.575	4.908	5.276	5.322	5.752	4.504	7.586
61	DUZCE 11/12/99	BOLU, 090 (ERD)	4.323	9.274	2.259	9.873	3.029	8.451	7.286	11.194

62	DUZCE 11/12/99	BOLU, UP (ERD)	1.175	1.179	1.009	1.086	1.097	0.985	0.748	1.178
63	IRAN_MANJIL 06/20/90	LONGITUDINAL COMP	3.041	3.785	2.351	3.841	2.545	3.631	3.404	3.951
64	IRAN_MANJIL 06/20/90	TRANSVERSE COMP	3.294	4.743	2.489	4.35	2.861	4.074	4.253	6.706
65	IRAN_MANJIL 06/20/90	VERTICAL COMP	2.176	2.978	2.407	2.975	2.315	2.884	2.697	3.249
66	HECTOR MINE OCT 16, 1999	HEC, 000	1.321	1.627	1.086	1.492	1.21	1.475	1.502	2.607
67	HECTOR MINE OCT 16, 1999	HEC, 090	2.709	4.093	2.051	3.394	2.452	3.61	3.046	6.988
68	HECTOR MINE OCT 16, 1999	HEC, VER	0.761	1.806	0.786	1.485	0.809	1.254	0.875	1.823

Table 1: Demand of C template buildings (in cm) under far field earthquakes (SDOF system) part two

	Earthquake	**Record and component**	**C2 x**	**C2 y**	**C2Bx (6fl)**	**C2By (6fl)**	**C3x**	**C3y**
1	San Fernando 2/9/1971	LA HOLLYWOOD STOR LOT, 090	2.072	1.221	1.74	2.06	1.798	1.213
2	San Fernando 2/9/1971	LA HOLLYWOOD STOR LOT, 180	0.891	0.797	1.669	0.902	1.368	0.677
3	San Fernando 2/9/1971	LA HOLLYWOOD STOR LOT, UP	0.373	0.194	0.326	0.375	0.404	0.154
4	Friuli, Italy 5/6/1976	Tolmezzo, 000	2.75	1.761	3.721	2.824	2.938	1.915
5	Friuli, Italy 5/6/1976	Tolmezzo, 270	3.037	1.558	6.503	3.09	3.932	1.317
6	Friuli, Italy 5/6/1976	Tolmezzo, UP	1.479	1.353	0.754	1.492	1.094	0.659
7	Imperial valley 10/15/1979	DELTA, 262 (UNAM/UCSD STATION 6605)	2.032	1.404	4.02	1.934	2.617	1.001
8	Imperial valley 10/15/1979	DELTA, 352 (UNAM/UCSD STATION 6605)	1.631	1.676	3.557	1.589	2.251	1.172

9	Imperial valley 10/15/1979	DELTA, DWN (UNAM/UCSD STATION 6605)	0.715	0.561	0.806	0.718	0.678	0.393
10	Imperial valley 10/15/1979	EL CENTRO ARRAY #11, 140 (USGS STATION 5058)	2.765	2.398	3.66	2.359	3.085	2.217
11	Imperial valley 10/15/1979	EL CENTRO ARRAY #11, 230 (USGS STATION 5058)	3.653	2.564	4.443	2.591	3.231	2.362
12	Imperial valley 10/15/1979	EL CENTRO ARRAY #11, UP (USGS STATION 5058)	0.391	0.479	0.674	0.385	0.474	0.483
13	SuperstitionHills02 11/24/87	EL CENTRO IMP CO CENTER, 000 (CDMG STATION 01	1.88	1.456	3.707	1.823	2.293	1.282
14	SuperstitionHills02 11/24/87	EL CENTRO IMP CO CENTER, 090 (CDMG STATION 01	1.861	0.821	3.617	1.784	2.216	0.916
15	SuperstitionHills02 11/24/87	EL CENTRO IMP CO CENTER, UP (CDMG STATION 01	0.613	0.312	0.903	0.609	0.519	0.414
16	SuperstitionHills02 11/24/87	POE, 270 (USGS STATION TEMP)	3.282	1.638	6.595	3.286	4.521	1.259
17	SuperstitionHills02 11/24/87	POE, 360 (USGS STATION TEMP)	2.744	1.711	4.171	2.62	2.747	1.008
18	LOMA PRIETA 10/18/89	CAPITOLA, 000 (CDMG STATION 47125)	5.612	4.395	4.881	4.113	4.361	3.175
19	LOMA PRIETA 10/18/89	CAPITOLA, 090 (CDMG STATION 47125)	4.031	1.882	4.542	2.937	3.476	1.322
20	LOMA PRIETA 10/18/89	CAPITOLA, UP (CDMG STATION 47125)	1.893	1.343	1.49	1.92	1.463	1.132

21	LOMA PRIETA 10/18/89	GILROY ARRAY #3, 000 (CDMG STATION 47381)	3.692	2.469	6.625	5.516	5.142	1.989
22	LOMA PRIETA 10/18/89	GILROY ARRAY #3, 090 (CDMG STATION 47381)	1.931	2.052	3.676	1.903	1.843	1.556
23	LOMA PRIETA 10/18/89	GILROY ARRAY #3, UP (CDMG STATION 47381)	0.84	1.081	1.456	0.805	1.283	0.936
24	CAPE MENDOCINO 04/25/92	RIO DELL OVERPASS FF, 360 (CDMG STATION 89324)	4.843	3.239	8.894	5.463	6.118	3.636
25	CAPE MENDOCINO 04/25/92	RIO DELL OVERPASS FF, UP (CDMG STATION 89324)	0.793	0.81	1.093	0.773	1.126	0.852
26	CAPE MENDOCINO 04/25/92	RIO DELL OVERPASS FF, 270	0.793	0.81	1.093	0.773	1.126	0.852
27	LANDERS 7/23/92	COOLWATER, LN (SCE STATION 23)	3.131	2.176	4.219	3.065	3.131	1.82
28	LANDERS 7/23/92	COOLWATER, TR (SCE STATION 23)	4.151	2.375	6.736	5.58	5.213	1.58
29	LANDERS 7/23/92	COOLWATER, UP (SCE STATION 23)	0.93	0.991	1.082	0.967	0.722	0.872
30	LANDERS 06/28/92	YERMO FIRE STATION, 270 (CDMG STATION 22074)	1.59	0.867	2.944	1.581	1.918	0.878
31	LANDERS 06/28/92	YERMO FIRE STATION, 360 (CDMG STATION 22074)	1.634	0.955	2.533	1.561	1.908	0.855
32	LANDERS 06/28/92	YERMO FIRE STATION, UP (CDMG STATION 22074)	0.81	0.548	0.908	0.789	0.979	0.486

33	NORTHRIDGE EQ 1/17/94	BEVERLY HILLS - 12520 MULH, 035 (USC STATION 90014	3.963	2.522	4.351	3.96	4.314	2.661
34	NORTHRIDGE EQ 1/17/94	BEVERLY HILLS - 12520 MULH, 125 (USC STATION 90014	3.881	3.263	3.396	3.996	3.592	3.088
35	NORTHRIDGE EQ 1/17/94	BEVERLY HILLS - 12520 MULH, UP (USC STATION 90014)	1.065	1.17	1.309	1.073	0.94	1.113
36	NORTHRIDGE EQ 1/17/94	BEVERLY HILLS - 14145 MULH, 009 (USC STATION 90013	2.235	2.032	5.508	2.306	4.145	2.131
37	NORTHRIDGE EQ 1/17/94	BEVERLY HILLS - 14145 MULH, 279 (USC STATION 90013	3.186	3.111	7.034	4.787	5.469	2.129
38	NORTHRIDGE EQ 1/17/94	BEVERLY HILLS - 14145 MULH, UP (USC STATION 90013)	1.47	1.473	3.463	1.411	2.036	1.753
39	NORTHRIDGE EQ 1/17/94	CANYON COUNTRY - W LOST CANYON, 000 (USC STATION 9	3.948	2.268	5.033	5.023	5.46	1.363
40	NORTHRIDGE EQ 1/17/94	CANYON COUNTRY - W LOST CANYON, 270 (USC STATION 9	3.594	3.104	6.254	4.215	4.228	1.857
41	NORTHRIDGE EQ 1/17/94	CANYON COUNTRY - W LOST CANYON, UP (USC STATION 90	1.274	0.901	1.722	1.261	1.494	0.837
42	KOBE 01/16/95	NISHI-AKASHI, 000	4.219	2.487	8.476	4.378	6.346	2.312

43	KOBE 01/16/95	NISHI-AKASHI, 090	3.581	2.328	6.702	3.482	4.22	1.68
44	KOBE 01/16/95	NISHI-AKASHI, V	1.935	2.242	4.278	1.855	2.501	1.936
45	KOBE 01/16/95	SHIN-OSAKA, 000	1.704	0.97	3.371	1.63	2.148	0.836
46	KOBE 01/16/95	SHIN-OSAKA, 090	1.944	1.183	3.433	1.906	2.41	0.643
47	KOBE 01/16/95	SHIN-OSAKA, V	0.443	0.274	0.578	0.432	0.448	0.199
48	KOCAELI 08/17/99	ARCELIK, 000 (KOERI)	0.72	0.577	1.255	0.717	0.76	0.641
49	KOCAELI 08/17/99	ARCELIK, 090 (KOERI)	0.956	0.626	1.032	0.937	0.952	0.724
50	KOCAELI 08/17/99	ARCELIK, DWN (KOERI)	0.406	0.288	0.652	0.408	0.5	0.242
51	KOCAELI 08/17/99	DUZCE, 180 (ERD)	3.727	1.568	3.932	3.157	3.643	1.221
52	KOCAELI 08/17/99	DUZCE, 270 (ERD)	4.607	3.164	4.253	3.7	5.163	2.451
53	KOCAELI 08/17/99	DUZCE, UP (ERD)	1.178	0.73	0.68	1.182	0.856	0.665
54	CHI-CHI 09/20/99	CHY101, E	2.048	1.475	2.581	1.982	1.86	1.104
55	CHI-CHI 09/20/99	CHY101, N	3.253	2.186	5.262	3.919	2.937	1.371
56	CHI-CHI 09/20/99	CHY101, Vertical	1.019	0.75	1.309	1.035	0.791	0.622
57	CHI-CHI 09/20/99	TCU045, E	4.566	3.291	6.373	4.803	5.187	1.957
58	CHI-CHI 09/20/99	TCU045, N	3.362	1.748	5.254	3.839	4.762	1.632
59	CHI-CHI 09/20/99	TCU045, Vertical	1.366	0.796	2.409	1.348	1.722	0.521
60	DUZCE 11/12/99	BOLU, 000 (ERD)	4.763	5.041	7.033	3.806	5.619	3.006
61	DUZCE 11/12/99	BOLU, 090 (ERD)	5.219	2.364	9.56	7.788	8.214	1.761
62	DUZCE 11/12/99	BOLU, UP (ERD)	0.648	1.012	1.175	0.659	0.889	0.909
63	IRAN_MANJIL 06/20/90	LONGITUDINAL COMP	4.053	2.369	3.874	3.113	3.572	2.116

64	IRAN_MANJIL 06/20/90	TRANSVERSE COMP	3.715	2.48	5.739	4.723	4.252	2.277
65	IRAN_MANJIL 06/20/90	VERTICAL COMP	2.639	2.402	2.905	2.485	2.773	1.922
66	HECTOR MINE OCT 16, 1999	HEC, 000	1.551	1.094	2.341	1.583	1.486	1.03
67	HECTOR MINE OCT 16, 1999	HEC, 090	2.832	2.05	5.092	2.714	3.219	1.5
68	HECTOR MINE OCT 16, 1999	HEC, VER	0.879	0.772	1.804	0.418	1.033	0.89

Table 174: Demand of A template buildings (in cm) under near field earthquakes (SDOF system)

	Earthquake	**Record and component**	**A1 x**	**A1 y**	**A1x (3fl)**	**A1y (3fl)**	**A1x (4fl)**	**A1y (4fl)**	**A2x**	**A2 y**	**A2 (½)x**	**A2 (½)y**
1	IMPERIAL VALLEY	CHIHUAHUA, 012 (UNAM/UCSD STATION 6621)	0.134	0.112	0.392	0.278	1.432	0.756	0.272	0.223	0.22	0.155
2	IMPERIAL VALLEY	CHIHUAHUA, 282 (UNAM/UCSD STATION 6621)	0.118	0.11	0.346	0.266	0.88	0.549	0.264	0.225	0.236	0.147
3	IMPERIAL VALLEY	CHIHUAHUA, DWN (UNAM/UCSD STATION 6621)	0.143	0.142	0.302	0.283	0.353	0.365	0.273	0.176	0.247	0.16
4	IMPERIAL VALLEY	EL CENTRO ARRAY #6, 140 (CDMG STATION 942)	0.357	0.34	0.474	0.379	1.379	0.821	0.342	0.262	0.292	0.333
5	IMPERIAL VALLEY	EL CENTRO ARRAY #6, 230 (CDMG STATION 942)	0.175	0.171	0.444	0.425	1.584	0.938	0.426	0.362	0.437	0.237
6	IMPERIAL VALLEY	EL CENTRO ARRAY #6, UP (CDMG STATION 942)	2.395	2.398	2.683	2.586	2.772	3.28	2.849	3.163	2.816	2.775
7	IMPERIAL VALLEY	EL CENTRO ARRAY #7, 140 (USGS STATION 5028)	0.123	0.117	0.406	0.307	1.138	0.663	0.298	0.186	0.252	0.154

8	IMPERIAL VALLEY	EL CENTRO ARRAY #7, 230 (USGS STATION 5028)	0.159	0.151	0.502	0.415	1.361	0.896	0.402	0.248	0.383	0.237
9	IMPERIAL VALLEY	EL CENTRO ARRAY #7, UP (USGS STATION 5028)	0.36	0.339	0.406	0.382	0.677	0.442	0.361	0.361	0.365	0.397
10	IMPERIAL VALLEY	BONDS CORNER, 140 (USGS STATION 5054)	0.05	0.047	0.132	0.099	0.15	0.15	0.09	0.059	0.066	0.064
11	IMPERIAL VALLEY	BONDS CORNER, 230 (USGS STATION 5054)	0.045	0.043	0.16	0.127	0.237	0.213	0.118	0.073	0.098	0.058
12	IMPERIAL VALLEY	BONDS CORNER, UP (USGS STATION 5054)	0.024	0.025	0.078	0.072	0.055	0.078	0.078	0.051	0.098	0.03
13	IRPINIA EQ / ITALY	STURNO, 000	0.119	0.113	0.442	0.405	1.019	0.706	0.388	0.249	0.344	0.17
14	IRPINIA EQ / ITALY	STURNO, 270	0.178	0.172	0.946	0.737	1.568	1.096	0.668	0.379	0.47	0.297
15	IRPINIA EQ / ITALY	STURNO, UP	0.147	0.14	0.274	0.211	0.522	0.557	0.197	0.172	0.147	0.124
16	NAHANNI, CANADA	SITE 1, 010	0.754	0.657	2.512	1.717	2.432	2.71	1.843	1.054	1.073	0.654
17	NAHANNI, CANADA	SITE 1, 280	0.673	0.696	1.397	1.172	4.283	2.308	1.07	0.772	1.036	0.562
18	NAHANNI, CANADA	SITE 1, UP	1.582	1.651	3.099	2.571	1.426	2.084	2.428	0.883	1.35	1.144
19	NAHANNI, CANADA	SITE 2, 240	0.154	0.159	0.296	0.249	1.259	0.534	0.243	0.176	0.224	0.135
20	NAHANNI, CANADA	SITE 2, 330	0.173	0.16	0.355	0.253	0.665	0.573	0.261	0.293	0.285	0.231

21	SUPERSTITION HILLS	PTS, 225 (USGS STATION 5051)	0.169	0.164	0.652	0.629	1.785	0.837	0.637	0.32	0.558	0.243
22	SUPERSTITION HILLS	PTS, 315 (USGS STATION 5051)	0.128	0.13	0.489	0.354	1.366	1.055	0.334	0.221	0.291	0.204
23	LOMA PRIETA	BRAN, 000	0.232	0.228	0.834	0.709	2.786	1.247	0.756	0.778	0.699	0.401
24	LOMA PRIETA	BRAN, 090	0.371	0.326	1.074	1.07	2.34	2.31	1.193	0.872	1.079	0.601
25	LOMA PRIETA	BRAN, UP	0.423	0.407	0.703	0.501	2.047	1.176	0.507	0.576	0.64	0.485
26	LOMA PRIETA	CORRALITOS, 000 (CDMG STATION 57007)	0.236	0.224	0.956	0.745	2.944	1.849	0.714	0.419	0.547	0.29
27	LOMA PRIETA	CORRALITOS, 090 (CDMG STATION 57007)	0.189	0.169	0.78	0.697	1.793	1.308	0.675	0.403	0.501	0.295
28	LOMA PRIETA	CORRALITOS, UP (CDMG STATION 57007)	0.288	0.272	0.86	0.664	1.827	1.486	0.603	0.328	0.45	0.335
29	LOMA PRIETA	SARATOGA ALOHA AVE, 000 (CDMG STATION 58065)	0.29	0.252	0.92	0.733	1.212	1.039	0.681	0.423	0.679	0.346
30	LOMA PRIETA	SARATOGA ALOHA AVE, 090 (CDMG STATION 58065)	0.173	0.167	0.812	0.575	0.801	1.495	0.546	0.367	0.534	0.259
31	LOMA PRIETA	SARATOGA ALOHA AVE, UP (CDMG STATION 58065)	0.205	0.211	0.367	0.287	0.499	0.36	0.263	0.242	0.265	0.22
32	ERZICAN TURKEY	ERZICAN EAST-WEST COMP	0.197	0.186	0.856	0.586	2.252	1.816	0.566	0.354	0.49	0.29
33	ERZICAN TURKEY	ERZICAN - NORTH-SOUTH COMP	0.196	0.185	0.636	0.477	1.433	0.987	0.453	0.333	0.395	0.261

34	ERZICAN TURKEY	ERZICAN -UP COMP	0.159	0.148	0.36	0.383	0.751	0.523	0.421	0.236	0.344	0.205
35	CAPE MENDOCINO	CAPE MENDOCINO, 000 (CDMG STATION 89005)	2.399	2.381	4.613	4.386	8.16	7.504	4.532	4.032	4.202	3.398
36	CAPE MENDOCINO	CAPE MENDOCINO, 090 (CDMG STATION 89005)	0.634	0.629	1.079	0.936	2.066	1.562	0.804	0.921	0.819	0.859
37	CAPE MENDOCINO	CAPE MENDOCINO, UP (CDMG STATION 89005)	0.488	0.449	1.113	1.091	0.97	1.037	1.135	0.811	0.841	0.697
38	CAPE MENDOCINO	PETROLIA, 000 (CDMG STATION 89156)	0.26	0.226	0.812	0.534	1.337	1.105	0.49	0.542	0.478	0.398
39	CAPE MENDOCINO	PETROLIA, 090 (CDMG STATION 89156)	0.337	0.305	0.913	0.734	1.405	0.914	0.728	0.483	0.586	0.366
40	CAPE MENDOCINO	PETROLIA, UP (CDMG STATION 89156)	0.099	0.106	0.309	0.246	0.63	0.55	0.235	0.201	0.234	0.167
41	LANDERS 6/28/92	LUCERNE, 260 (SCE STATION 24)	0.911	0.884	0.748	0.659	2.442	2.298	0.728	0.678	0.832	0.896
42	LANDERS 6/28/92	LUCERNE, 345 (SCE STATION 24)	0.544	0.642	0.919	0.948	1.604	1.317	1.111	0.638	0.904	0.527
43	LANDERS 6/28/92	LUCERNE, UP (SCE STATION 24)	0.395	0.411	0.439	0.629	0.693	0.675	0.598	0.455	0.533	0.486
44	NORTHRIDGE EARTHQUAKE	CA:LA;SEPULVEDA VA, BLD 40 GND; 270	0.309	0.283	1.118	1.046	2.789	2.832	0.999	0.508	0.624	0.392
45	NORTHRIDGE EARTHQUAKE	CA:LA;SEPULVEDA VA, BLD 40 GND; 360	0.518	0.498	2.064	1.772	5.649	5.917	1.61	1.705	1.425	1.086

46	NORTHRIDGE EARTHQUAKE	CA:LA;SEPULVEDA VA, BLD 40 GND; UP	0.347	0.308	0.841	0.632	1.32	1.119	0.55	0.418	0.504	0.309
47	NORTHRIDGE EARTHQUAKE	NORTHRIDGE - SATICOY, 090 (USC STATION 90003)	0.18	0.176	0.858	0.696	1.427	1.119	0.653	0.333	0.514	0.207
48	NORTHRIDGE EARTHQUAKE	NORTHRIDGE - SATICOY, 180 (USC STATION 90003)	0.258	0.233	0.974	0.631	1.601	1.324	0.615	0.376	0.545	0.326
49	NORTHRIDGE EARTHQUAKE	RINALDI RECEIVING STA, 228	0.275	0.261	1.714	1.035	9.399	6.782	1.248	0.514	0.792	0.422
50	NORTHRIDGE EARTHQUAKE	RINALDI RECEIVING STA, 318	0.29	0.279	1.002	0.697	2.414	2.661	0.777	0.584	0.802	0.328
51	NORTHRIDGE EARTHQUAKE	RINALDI RECEIVING STA, UP	0.555	0.588	2.019	1.422	3.203	2.821	1.18	0.803	1.211	0.852
52	NORTHRIDGE EARTHQUAKE	SYLMAR - HOSPITAL, 090 (CDMG STATION 24514)	0.325	0.301	0.656	0.541	1.577	1.22	0.533	0.409	0.459	0.339
53	NORTHRIDGE EARTHQUAKE	SYLMAR - HOSPITAL, 360 (CDMG STATION 24514)	0.347	0.332	0.902	0.855	7.561	5.448	0.846	0.716	0.808	0.452
54	NORTHRIDGE EARTHQUAKE	SYLMAR - HOSPITAL, UP (CDMG STATION 24514)	0.37	0.352	0.809	0.769	0.804	0.731	0.706	0.549	0.606	0.456
55	KOCAELI TURKEY	IZMIT, 090 (ERD)	0.098	0.083	0.509	0.336	1.427	0.65	0.331	0.194	0.316	0.126

56	KOCAELI TURKEY	IZMIT, 180 (ERD)	0.076	0.071	0.269	0.225	1.205	0.659	0.2	0.128	0.175	0.096
57	KOCAELI TURKEY	IZMIT, UP (ERD)	0.121	0.117	0.215	0.225	0.363	0.273	0.217	0.179	0.218	0.182
58	KOCAELI TURKEY	YARIMCA, 330 (KOERI)	0.106	0.098	0.366	0.305	1.035	0.571	0.285	0.186	0.233	0.14
59	KOCAELI TURKEY	YARIMCA, 060 (KOERI)	0.102	0.095	0.401	0.313	0.998	0.581	0.284	0.181	0.223	0.134
60	KOCAELI TURKEY	YARMICA, UP (KOERI)	0.152	0.147	0.66	0.5	1.049	0.578	0.492	0.345	0.376	0.225
61	CHI-CHI 09/20/99	TCU065, E	0.311	0.29	0.872	0.649	1.949	1.934	0.7	0.554	0.628	0.383
62	CHI-CHI 09/20/99	TCU065, N	0.222	0.21	0.705	0.579	1.428	0.975	0.545	0.372	0.45	0.288
63	CHI-CHI 09/20/99	TCU065, V	0.11	0.109	0.383	0.313	0.646	0.558	0.32	0.317	0.383	0.22
64	CHI-CHI 09/20/99	TCU067, E	0.201	0.194	0.551	0.441	1.62	0.98	0.432	0.269	0.346	0.209
65	CHI-CHI 09/20/99	TCU067, N	0.138	0.135	0.461	0.403	1.237	0.901	0.381	0.27	0.313	0.191
66	CHI-CHI 09/20/99	TCU067, V	0.125	0.11	0.359	0.313	0.91	0.685	0.298	0.192	0.268	0.196
67	CHI-CHI 09/20/99	TCU084, E	0.415	0.417	4.932	3.042	11.64	11.489	4.194	1.812	2.548	0.785
68	CHI-CHI 09/20/99	TCU084, N	0.199	0.176	0.59	0.438	1.613	0.929	0.416	0.367	0.405	0.309
69	CHI-CHI 09/20/99	TCU084, V	0.156	0.145	0.567	0.554	1.24	0.855	0.556	0.292	0.54	0.215
70	CHI-CHI 09/20/99	TCU102, E	0.093	0.087	0.246	0.21	0.625	0.386	0.2	0.158	0.182	0.119

71	CHI-CHI 09/20/99	TCU102, N	0.061	0.058	0.182	0.156	0.498	0.286	0.142	0.1	0.122	0.075
72	CHI-CHI 09/20/99	TCU102, V	0.065	0.063	0.171	0.155	0.371	0.283	0.149	0.102	0.12	0.073
73	DUZCE 11/12/99	DUZCE, 180 (ERD)	0.148	0.148	0.443	0.406	1.782	0.953	0.399	0.292	0.4	0.197
74	DUZCE 11/12/99	DUZCE, 270 (ERD)	0.234	0.211	0.753	0.489	1.913	2.375	0.452	0.273	0.315	0.252
75	DUZCE 11/12/99	DUZCE, UP (ERD)	0.26	0.261	0.56	0.478	0.631	0.865	0.457	0.407	0.472	0.322
76	DENALI ALASKA 11/03/02	PS10, 047	0.098	0.09	0.388	0.348	1.163	0.732	0.329	0.223	0.253	0.141
77	DENALI ALASKA 11/03/02	PS10, 317	0.105	0.112	0.268	0.231	0.668	0.4	0.233	0.194	0.253	0.179
78	DENALI ALASKA 11/03/02	PS10, UP	0.142	0.157	0.33	0.37	0.682	0.405	0.394	0.3	0.459	0.219

Table 175: Demand of B template buildings (in cm) under near field earthquakes (SDOF system) part one

	Earthquake	**Record and component**	**B1 x**	**B1 y**	**B1 (4fl)x**	**B1 (4fl)y**	**B2 x**	**B2 y**	**B2x (38cm)**	**B2y (38cm)**
1	IMPERIAL VALLEY	CHIHUAHUA, 012 (UNAM/UCSD STATION 6621)	0.24	0.155	0.589	0.285	0.275	0.573	0.282	0.59
2	IMPERIAL VALLEY	CHIHUAHUA, 282 (UNAM/UCSD STATION 6621)	0.244	0.147	0.408	0.269	0.265	0.381	0.268	0.421
3	IMPERIAL VALLEY	CHIHUAHUA, DWN (UNAM/UCSD STATION 6621)	0.25	0.16	0.354	0.287	0.281	0.334	0.285	0.352

4	IMPERIAL VALLEY	EL CENTRO ARRAY #6, 140 (CDMG STATION 942)	0.303	0.333	0.701	0.39	0.371	0.621	0.384	0.707
5	IMPERIAL VALLEY	EL CENTRO ARRAY #6, 230 (CDMG STATION 942)	0.411	0.237	0.682	0.424	0.426	0.66	0.424	0.68
6	IMPERIAL VALLEY	EL CENTRO ARRAY #6, UP (CDMG STATION 942)	2.724	2.478	2.825	2.409	2.308	2.72	2.407	3.018
7	IMPERIAL VALLEY	EL CENTRO ARRAY #7, 140 (USGS STATION 5028)	0.269	0.154	0.561	0.309	0.306	0.529	0.308	0.566
8	IMPERIAL VALLEY	EL CENTRO ARRAY #7, 230 (USGS STATION 5028)	0.393	0.237	0.786	0.42	0.412	0.714	0.417	0.793
9	IMPERIAL VALLEY	EL CENTRO ARRAY #7, UP (USGS STATION 5028)	0.367	0.398	0.343	0.388	0.378	0.33	0.384	0.345
10	IMPERIAL VALLEY	BONDS CORNER, 140 (USGS STATION 5054)	0.071	0.064	0.157	0.102	0.097	0.153	0.1	0.158
11	IMPERIAL VALLEY	BONDS CORNER, 230 (USGS STATION 5054)	0.103	0.058	0.199	0.129	0.126	0.19	0.128	0.2
12	IMPERIAL VALLEY	BONDS CORNER, UP (USGS STATION 5054)	0.074	0.03	0.093	0.072	0.074	0.1	0.071	0.092
13	IRPINIA EQ / ITALY	STURNO, 000	0.348	0.17	0.749	0.407	0.403	0.725	0.406	0.744
14	IRPINIA EQ / ITALY	STURNO, 270	0.52	0.297	1.335	0.75	0.721	1.211	0.742	1.069
15	IRPINIA EQ / ITALY	STURNO, UP	0.171	0.124	0.443	0.219	0.206	0.377	0.215	0.457

16	NAHANNI, CANADA	SITE 1, 010	1.511	0.728	3.164	1.384	1.615	3.044	1.355	3.362
17	NAHANNI, CANADA	SITE 1, 280	1.332	0.588	2.098	1.401	1.471	1.904	1.39	1.944
18	NAHANNI, CANADA	SITE 1, UP	1.138	0.971	2.647	2.435	2.075	2.978	2.403	2.56
19	NAHANNI, CANADA	SITE 2, 240	0.232	0.135	0.425	0.251	0.247	0.411	0.25	0.429
20	NAHANNI, CANADA	SITE 2, 330	0.27	0.231	0.554	0.251	0.255	0.523	0.252	0.557
21	SUPERSTITION HILLS	PTS, 225 (USGS STATION 5051)	0.594	0.243	0.953	0.63	0.629	0.829	0.63	0.965
22	SUPERSTITION HILLS	PTS, 315 (USGS STATION 5051)	0.299	0.204	0.783	0.359	0.351	0.634	0.357	0.795
23	LOMA PRIETA	BRAN, 000	0.673	0.401	0.973	0.716	0.701	0.919	0.712	1
24	LOMA PRIETA	BRAN, 090	1.061	0.537	1.035	0.968	1.011	0.951	0.952	1.085
25	LOMA PRIETA	BRAN, UP	0.579	0.451	0.869	0.502	0.5	0.821	0.502	0.869
26	LOMA PRIETA	CORRALITOS, 000 (CDMG STATION 57007)	0.582	0.29	1.112	0.748	0.725	1.018	0.742	1.207
27	LOMA PRIETA	CORRALITOS, 090 (CDMG STATION 57007)	0.542	0.295	0.92	0.706	0.688	1.032	0.701	0.978
28	LOMA PRIETA	CORRALITOS, UP (CDMG STATION 57007)	0.469	0.335	1.202	0.677	0.654	1.138	0.671	1.245
29	LOMA PRIETA	SARATOGA ALOHA AVE, 000 (CDMG STATION 58065)	0.668	0.346	0.897	0.821	0.813	0.959	0.819	0.897

30	LOMA PRIETA	SARATOGA ALOHA AVE, 090 (CDMG STATION 58065)	0.543	0.259	1.137	0.58	0.571	1.094	0.577	1.324
31	LOMA PRIETA	SARATOGA ALOHA AVE, UP (CDMG STATION 58065)	0.263	0.22	0.464	0.298	0.279	0.44	0.293	0.462
32	ERZICAN TURKEY	ERZICAN EAST-WEST COMP	0.516	0.29	1.481	0.592	0.583	1.371	0.589	1.504
33	ERZICAN TURKEY	ERZICAN - NORTH-SOUTH COMP	0.404	0.261	0.864	0.483	0.473	0.803	0.48	0.872
34	ERZICAN TURKEY	ERZICAN -UP COMP	0.392	0.205	0.435	0.38	0.391	0.435	0.38	0.441
35	CAPE MENDOCINO	CAPE MENDOCINO, 000 (CDMG STATION 89005)	3.156	2.73	5.545	3.544	2.835	4.862	3.527	7.075
36	CAPE MENDOCINO	CAPE MENDOCINO, 090 (CDMG STATION 89005)	1.074	0.748	0.995	1.109	1.149	0.903	1.102	1.015
37	CAPE MENDOCINO	CAPE MENDOCINO, UP (CDMG STATION 89005)	0.823	0.638	1.03	1.047	1.008	1.083	1.045	1.044
38	CAPE MENDOCINO	PETROLIA, 000 (CDMG STATION 89156)	0.458	0.399	0.957	0.544	0.526	1.012	0.539	0.926
39	CAPE MENDOCINO	PETROLIA, 090 (CDMG STATION 89156)	0.667	0.366	0.961	0.759	0.75	0.995	0.757	0.978
40	CAPE MENDOCINO	PETROLIA, UP (CDMG STATION 89156)	0.225	0.167	0.546	0.247	0.245	0.464	0.247	0.552

41	LANDERS 6/28/92	LUCERNE, 260 (SCE STATION 24)	0.768	0.738	1.408	0.657	0.665	1.163	0.658	1.463
42	LANDERS 6/28/92	LUCERNE, 345 (SCE STATION 24)	1.009	0.573	1.133	0.989	1.041	1.02	1.017	1.019
43	LANDERS 6/28/92	LUCERNE, UP (SCE STATION 24)	0.533	0.467	0.577	0.632	0.625	0.517	0.631	0.584
44	NORTHRIDGE EARTHQUAKE	CA:LA;SEPULVEDA VA, BLD 40 GND; 270	0.63	0.393	1.604	1.176	0.944	1.625	1.148	1.415
45	NORTHRIDGE EARTHQUAKE	CA:LA;SEPULVEDA VA, BLD 40 GND; 360	0.973	0.736	3.882	1.726	1.482	2.941	1.709	4.626
46	NORTHRIDGE EARTHQUAKE	CA:LA;SEPULVEDA VA, BLD 40 GND; UP	0.493	0.309	1.037	0.65	0.618	0.962	0.642	0.931
47	NORTHRIDGE EARTHQUAKE	NORTHRIDGE - SATICOY, 090 (USC STATION 90003)	0.552	0.208	1.019	0.704	0.689	1.048	0.7	1.015
48	NORTHRIDGE EARTHQUAKE	NORTHRIDGE - SATICOY, 180 (USC STATION 90003)	0.573	0.326	1.198	0.634	0.628	1.1	0.632	1.3
49	NORTHRIDGE EARTHQUAKE	RINALDI RECEIVING STA, 228	0.732	0.42	2.384	0.944	0.878	2.137	0.933	4.117
50	NORTHRIDGE EARTHQUAKE	RINALDI RECEIVING STA, 318	0.754	0.328	1.338	0.682	0.708	1.295	0.689	2.052
51	NORTHRIDGE EARTHQUAKE	RINALDI RECEIVING STA, UP	1.312	0.897	1.789	1.652	1.715	2.136	1.645	1.677
52	NORTHRIDGE EARTHQUAKE	SYLMAR - HOSPITAL, 090	0.478	0.339	0.923	0.541	0.541	0.91	0.541	0.947

		(CDMG STATION 24514)								
53	NORTHRIDGE EARTHQUAKE	SYLMAR - HOSPITAL, 360 (CDMG STATION 24514)	0.766	0.451	1.621	0.818	0.787	1.343	0.812	2.938
54	NORTHRIDGE EARTHQUAKE	SYLMAR - HOSPITAL, UP (CDMG STATION 24514)	0.706	0.444	0.835	0.814	0.854	0.878	0.822	0.841
55	KOCAELI TURKEY	IZMIT, 090 (ERD)	0.326	0.126	0.584	0.34	0.334	0.622	0.338	0.577
56	KOCAELI TURKEY	IZMIT, 180 (ERD)	0.167	0.096	0.464	0.23	0.221	0.39	0.228	0.473
57	KOCAELI TURKEY	IZMIT, UP (ERD)	0.213	0.182	0.301	0.226	0.224	0.277	0.225	0.302
58	KOCAELI TURKEY	YARIMCA, 330 (KOERI)	0.245	0.14	0.504	0.309	0.301	0.51	0.307	0.499
59	KOCAELI TURKEY	YARIMCA, 060 (KOERI)	0.242	0.134	0.5	0.321	0.308	0.446	0.317	0.506
60	KOCAELI TURKEY	YARMICA, UP (KOERI)	0.415	0.225	0.747	0.493	0.494	0.695	0.494	0.742
61	CHI-CHI 09/20/99	TCU065, E	0.668	0.383	1.266	0.645	0.653	1.02	0.646	1.453
62	CHI-CHI 09/20/99	TCU065, N	0.48	0.288	0.759	0.588	0.574	0.829	0.584	0.756
63	CHI-CHI 09/20/99	TCU065, V	0.388	0.221	0.587	0.313	0.312	0.619	0.313	0.585
64	CHI-CHI 09/20/99	TCU067, E	0.373	0.209	0.853	0.44	0.441	0.842	0.441	0.855
65	CHI-CHI 09/20/99	TCU067, N	0.337	0.191	0.693	0.406	0.4	0.727	0.404	0.719
66	CHI-CHI 09/20/99	TCU067, V	0.293	0.196	0.58	0.317	0.311	0.559	0.315	0.575
67	CHI-CHI 09/20/99	TCU084, E	1.104	0.477	3.457	1.951	1.317	3.128	1.904	7.163

68	CHI-CHI 09/20/99	TCU084, N	0.41	0.309	0.797	0.442	0.435	0.699	0.439	0.816
69	CHI-CHI 09/20/99	TCU084, V	0.575	0.215	0.719	0.558	0.552	0.691	0.556	0.721
70	CHI-CHI 09/20/99	TCU102, E	0.185	0.119	0.329	0.213	0.207	0.293	0.211	0.334
71	CHI-CHI 09/20/99	TCU102, N	0.126	0.075	0.237	0.16	0.154	0.228	0.158	0.239
72	CHI-CHI 09/20/99	TCU102, V	0.129	0.073	0.237	0.155	0.154	0.224	0.155	0.239
73	DUZCE 11/12/99	DUZCE, 180 (ERD)	0.392	0.197	0.632	0.406	0.406	0.564	0.406	0.647
74	DUZCE 11/12/99	DUZCE, 270 (ERD)	0.343	0.252	1.801	0.505	0.482	1.46	0.498	2.318
75	DUZCE 11/12/99	DUZCE, UP (ERD)	0.512	0.322	0.729	0.483	0.474	0.614	0.481	0.746
76	DENALI ALASKA 11/03/02	PS10, 047	0.265	0.141	0.616	0.351	0.345	0.541	0.349	0.622
77	DENALI ALASKA 11/03/02	PS10, 317	0.251	0.179	0.441	0.232	0.231	0.421	0.232	0.441
78	DENALI ALASKA 11/03/02	PS10, UP	0.454	0.219	0.385	0.362	0.376	0.365	0.366	0.38

Table: Demand of B template buildings (in cm) under near field earthquakes (SDOF system) part two

	Earthquake	**Record and component**	**B3x**	**B3y**	**B3x int**	**B3y int**	**B4x**	**B4y**
1	IMPERIAL VALLEY	CHIHUAHUA, 012 (UNAM/UCSD STATION 6621)	1.158	1.386	1.229	1.445	1.187	1.14
2	IMPERIAL VALLEY	CHIHUAHUA, 282 (UNAM/UCSD STATION 6621)	1.184	1.066	1.2	1.005	1.18	1.173
3	IMPERIAL VALLEY	CHIHUAHUA, DWN (UNAM/UCSD STATION 6621)	0.448	0.378	0.551	0.362	0.4	0.5

4	IMPERIAL VALLEY	EL CENTRO ARRAY #6, 140 (CDMG STATION 942)	2.126	1.444	2.087	1.398	2.195	2.071
5	IMPERIAL VALLEY	EL CENTRO ARRAY #6, 230 (CDMG STATION 942)	2.014	1.666	2.335	1.53	2.059	2.177
6	IMPERIAL VALLEY	EL CENTRO ARRAY #6, UP (CDMG STATION 942)	2.885	2.537	3.066	2.501	2.712	2.946
7	IMPERIAL VALLEY	EL CENTRO ARRAY #7, 140 (USGS STATION 5028)	1.897	1.361	1.784	1.348	1.824	1.865
8	IMPERIAL VALLEY	EL CENTRO ARRAY #7, 230 (USGS STATION 5028)	2.013	1.537	2.228	1.456	1.927	2.122
9	IMPERIAL VALLEY	EL CENTRO ARRAY #7, UP (USGS STATION 5028)	1.372	0.932	1.468	0.761	1.301	1.426
10	IMPERIAL VALLEY	BONDS CORNER, 140 (USGS STATION 5054)	0.201	0.18	0.216	0.161	0.208	0.2
11	IMPERIAL VALLEY	BONDS CORNER, 230 (USGS STATION 5054)	0.329	0.257	0.35	0.247	0.309	0.342
12	IMPERIAL VALLEY	BONDS CORNER, UP (USGS STATION 5054)	0.041	0.047	0.039	0.053	0.042	0.04
13	IRPINIA EQ / ITALY	STURNO, 000	2.107	1.233	2.434	1.105	1.866	2.287
14	IRPINIA EQ / ITALY	STURNO, 270	2.568	1.976	2.453	1.698	2.57	2.529
15	IRPINIA EQ / ITALY	STURNO, UP	0.769	0.767	0.636	0.601	0.811	0.708

16	NAHANNI, CANADA	SITE 1, 010	3.304	2.821	3.389	2.284	3.664	3.404
17	NAHANNI, CANADA	SITE 1, 280	3.011	4.255	3.156	3.815	3.192	3.037
18	NAHANNI, CANADA	SITE 1, UP	1.862	1.21	1.876	1.213	1.743	1.897
19	NAHANNI, CANADA	SITE 2, 240	1.57	1.443	1.644	1.37	1.529	1.609
20	NAHANNI, CANADA	SITE 2, 330	1.057	0.832	1.183	0.751	1.019	1.11
21	SUPERSTITION HILLS	PTS, 225 (USGS STATION 5051)	2.274	2.325	2.599	2.081	2.065	2.435
22	SUPERSTITION HILLS	PTS, 315 (USGS STATION 5051)	2.246	1.661	1.998	1.543	2.357	2.108
23	LOMA PRIETA	BRAN, 000	4.842	2.542	5.855	2.24	4.07	4.977
24	LOMA PRIETA	BRAN, 090	3.086	2.762	3.642	2.095	2.596	3.162
25	LOMA PRIETA	BRAN, UP	2.32	1.906	2.699	1.806	2.134	2.758
26	LOMA PRIETA	CORRALITOS, 000 (CDMG STATION 57007)	4.813	3.263	5.357	2.954	4.572	5.08
27	LOMA PRIETA	CORRALITOS, 090 (CDMG STATION 57007)	2.361	1.92	2.342	1.697	2.397	2.3
28	LOMA PRIETA	CORRALITOS, UP (CDMG STATION 57007)	1.193	1.647	1.256	1.813	1.192	1.242
29	LOMA PRIETA	SARATOGA ALOHA AVE, 000 (CDMG STATION 58065)	1.935	1.69	1.86	1.475	1.861	1.93

30	LOMA PRIETA	SARATOGA ALOHA AVE, 090 (CDMG STATION 58065)	2.232	0.904	2.455	0.822	1.922	2.478
31	LOMA PRIETA	SARATOGA ALOHA AVE, UP (CDMG STATION 58065)	0.744	0.553	0.834	0.545	0.672	0.793
32	ERZICAN TURKEY	ERZICAN EAST-WEST COMP	2.81	2.511	3.302	2.604	2.915	3.108
33	ERZICAN TURKEY	ERZICAN - NORTH-SOUTH COMP	2.351	1.872	2.565	1.612	2.254	2.447
34	ERZICAN TURKEY	ERZICAN -UP COMP	1.34	1.202	1.382	0.979	1.225	1.404
35	CAPE MENDOCINO	CAPE MENDOCINO, 000 (CDMG STATION 89005)	8.657	8.369	8.733	8.263	8.339	8.414
36	CAPE MENDOCINO	CAPE MENDOCINO, 090 (CDMG STATION 89005)	2.8	2.154	3.026	2.099	2.727	2.87
37	CAPE MENDOCINO	CAPE MENDOCINO, UP (CDMG STATION 89005)	1.278	1.269	1.595	1.059	1.14	1.467
38	CAPE MENDOCINO	PETROLIA, 000 (CDMG STATION 89156)	2.715	1.788	2.942	1.594	2.558	2.753
39	CAPE MENDOCINO	PETROLIA, 090 (CDMG STATION 89156)	2.38	2.215	2.533	1.873	2.567	2.409
40	CAPE MENDOCINO	PETROLIA, UP (CDMG STATION 89156)	1.109	0.814	1.215	0.788	1.042	1.156

41	LANDERS 6/28/92	LUCERNE, 260 (SCE STATION 24)	1.867	2.261	1.79	2.038	1.82	1.851
42	LANDERS 6/28/92	LUCERNE, 345 (SCE STATION 24)	2.058	1.895	2.071	1.76	2.06	2.04
43	LANDERS 6/28/92	LUCERNE, UP (SCE STATION 24)	1.504	0.804	1.625	0.709	1.372	1.585
44	NORTHRIDGE EARTHQUAKE	CA:LA;SEPULVEDA VA, BLD 40 GND; 270	4.184	2.714	4.933	2.313	3.72	4.247
45	NORTHRIDGE EARTHQUAKE	CA:LA;SEPULVEDA VA, BLD 40 GND; 360	5.641	4.665	5.347	4.429	5.665	4.981
46	NORTHRIDGE EARTHQUAKE	CA:LA;SEPULVEDA VA, BLD 40 GND; UP	2.089	1.185	2.456	1.254	1.82	2.288
47	NORTHRIDGE EARTHQUAKE	NORTHRIDGE - SATICOY, 090 (USC STATION 90003)	2.992	1.858	2.748	1.562	2.924	3.104
48	NORTHRIDGE EARTHQUAKE	NORTHRIDGE - SATICOY, 180 (USC STATION 90003)	3.569	2.236	4.402	1.798	3.078	4.091
49	NORTHRIDGE EARTHQUAKE	RINALDI RECEIVING STA, 228	9.879	7.255	13.158	5.74	8.173	9.689
50	NORTHRIDGE EARTHQUAKE	RINALDI RECEIVING STA, 318	3.107	2.597	3.093	2.46	3.056	3.436
51	NORTHRIDGE EARTHQUAKE	RINALDI RECEIVING STA, UP	2.021	2.787	1.933	2.821	1.994	1.998
52	NORTHRIDGE EARTHQUAKE	SYLMAR - HOSPITAL, 090	2.897	1.83	2.971	1.68	2.819	2.898

		(CDMG STATION 24514)						
53	NORTHRIDGE EARTHQUAKE	SYLMAR - HOSPITAL, 360 (CDMG STATION 24514)	8.976	6.609	10.637	5.89	7.951	9.037
54	NORTHRIDGE EARTHQUAKE	SYLMAR - HOSPITAL, UP (CDMG STATION 24514)	1.065	0.702	1.268	0.71	0.955	1.186
55	KOCAELI TURKEY	IZMIT, 090 (ERD)	1.829	2.047	1.552	1.914	2.018	1.703
56	KOCAELI TURKEY	IZMIT, 180 (ERD)	1.043	1.311	1.088	1.36	1.063	1.034
57	KOCAELI TURKEY	IZMIT, UP (ERD)	0.583	0.428	0.731	0.399	0.556	0.674
58	KOCAELI TURKEY	YARIMCA, 330 (KOERI)	1.542	1.187	1.765	1.129	1.47	1.647
59	KOCAELI TURKEY	YARIMCA, 060 (KOERI)	1.494	1.259	1.664	1.143	1.493	1.559
60	KOCAELI TURKEY	YARMICA, UP (KOERI)	1.302	1.047	1.432	1.043	1.139	1.375
61	CHI-CHI 09/20/99	TCU065, E	2.624	2.474	3.415	2.236	2.171	2.959
62	CHI-CHI 09/20/99	TCU065, N	2.248	1.656	2.281	1.575	2.155	2.264
63	CHI-CHI 09/20/99	TCU065, V	1.24	0.766	1.396	0.703	1.11	1.313
64	CHI-CHI 09/20/99	TCU067, E	3.064	1.753	3.488	1.619	2.443	3.534
65	CHI-CHI 09/20/99	TCU067, N	2.628	1.687	3.241	1.449	2.308	2.799
66	CHI-CHI 09/20/99	TCU067, V	1.034	0.75	0.907	0.776	1.049	0.966
67	CHI-CHI 09/20/99	TCU084, E	7.961	7.721	12.531	6.6	7.529	7.18

68	CHI-CHI 09/20/99	TCU084, N	3.229	2.239	3.527	2.026	2.814	3.196
69	CHI-CHI 09/20/99	TCU084, V	2.593	1.596	2.408	1.38	2.416	2.498
70	CHI-CHI 09/20/99	TCU102, E	1.195	0.756	1.384	0.661	1.149	1.267
71	CHI-CHI 09/20/99	TCU102, N	0.777	0.611	0.857	0.543	0.718	0.834
72	CHI-CHI 09/20/99	TCU102, V	0.572	0.408	0.568	0.359	0.601	0.565
73	DUZCE 11/12/99	DUZCE, 180 (ERD)	2.996	2.262	3.383	2.022	3.397	3.262
74	DUZCE 11/12/99	DUZCE, 270 (ERD)	3.735	2.146	4.15	1.927	3.232	3.94
75	DUZCE 11/12/99	DUZCE, UP (ERD)	1.086	0.785	1.19	0.696	0.979	1.12
76	DENALI ALASKA 11/03/02	PS10, 047	1.758	1.12	1.86	1.207	1.744	1.796
77	DENALI ALASKA 11/03/02	PS10, 317	1.004	0.726	1.118	0.744	0.896	1.066
78	DENALI ALASKA 11/03/02	PS10, UP	0.969	1.099	0.756	0.872	1.112	0.85

Table 177: Demand of C template buildings (in cm) under near field earthquakes (SDOF system) part one

	Earthquake	**Record and component**	**C1Ax**	**C1Ay**	**C1Ax int**	**C1Ay int**	**C1Bx**	**C1By**	**C1Bx (6fl)**	**C1By (6fl)**
1	IMPERIAL VALLEY	CHIHUAHUA, 012 (UNAM/UCSD STATION 6621)	1.159	2.479	1.211	2.452	1.174	2.451	2.275	3.18
2	IMPERIAL VALLEY	CHIHUAHUA, 282 (UNAM/UCSD STATION 6621)	1.185	3.387	0.995	3.005	1.13	2.745	2.096	3.594

3	IMPERIAL VALLEY	CHIHUAHUA, DWN (UNAM/UCSD STATION 6621)	0.447	0.519	0.368	0.536	0.379	0.551	0.591	0.619
4	IMPERIAL VALLEY	EL CENTRO ARRAY #6, 140 (CDMG STATION 942)	2.133	2.902	2.055	2.569	2.202	2.346	2.063	3.429
5	IMPERIAL VALLEY	EL CENTRO ARRAY #6, 230 (CDMG STATION 942)	2.01	3.539	2.038	4.193	2.107	3.971	3.414	4.217
6	IMPERIAL VALLEY	EL CENTRO ARRAY #6, UP (CDMG STATION 942)	3.208	3.654	3.213	3.502	2.957	3.538	3.373	3.204
7	IMPERIAL VALLEY	EL CENTRO ARRAY #7, 140 (USGS STATION 5028)	1.897	2.421	1.443	2.037	1.701	1.986	1.594	3.366
8	IMPERIAL VALLEY	EL CENTRO ARRAY #7, 230 (USGS STATION 5028)	2.01	4.601	1.671	4.873	1.847	4.119	3.388	5.638
9	IMPERIAL VALLEY	EL CENTRO ARRAY #7, UP (USGS STATION 5028)	1.371	1.404	1.18	1.295	1.258	1.345	1.454	2.023
10	IMPERIAL VALLEY	BONDS CORNER, 140 (USGS STATION 5054)	0.201	0.563	0.175	0.485	0.202	0.442	0.366	0.733
11	IMPERIAL VALLEY	BONDS CORNER, 230 (USGS STATION 5054)	0.328	0.486	2.77	0.438	0.297	0.422	0.39	0.865
12	IMPERIAL VALLEY	BONDS CORNER, UP (USGS STATION 5054)	0.041	0.03	0.046	0.031	0.043	0.031	0.033	0.028
13	IRPINIA EQ / ITALY	STURNO, 000	2.106	3.348	1.435	3.347	1.703	3.045	3.011	3.625

14	IRPINIA EQ / ITALY	STURNO, 270	2.322	2.863	2.119	2.746	2.265	2.681	2.526	2.937
15	IRPINIA EQ / ITALY	STURNO, UP	0.77	1.183	0.867	1.18	0.828	1.128	0.922	1.458
16	NAHANNI, CANADA	SITE 1, 010	3.109	3.529	2.972	3.014	3.285	3.094	3.213	4.234
17	NAHANNI, CANADA	SITE 1, 280	3.153	4.027	3.653	4.162	3.175	3.762	3.421	4.694
18	NAHANNI, CANADA	SITE 1, UP	1.86	2.671	1.536	2.66	1.606	2.721	2.474	5.008
19	NAHANNI, CANADA	SITE 2, 240	1.569	2.74	1.484	2.301	1.506	2.196	1.845	4.371
20	NAHANNI, CANADA	SITE 2, 330	1.056	2.717	0.941	2.286	0.994	2.126	1.757	4.627
21	SUPERSTITION HILLS	PTS, 225 (USGS STATION 5051)	2.409	6.068	1.958	6.293	1.971	4.673	3.436	6.179
22	SUPERSTITION HILLS	PTS, 315 (USGS STATION 5051)	2.248	4.5	1.958	3.99	2.244	4.524	3.227	4.249
23	LOMA PRIETA	BRAN, 000	5.856	6.054	3.81	5.228	3.93	6.164	5.626	6.268
24	LOMA PRIETA	BRAN, 090	2.618	7.432	2.737	7.032	2.435	5.879	6.399	8.593
25	LOMA PRIETA	BRAN, UP	2.252	2.525	1.637	2.566	2.02	2.628	2.947	2.466
26	LOMA PRIETA	CORRALITOS, 000 (CDMG STATION 57007)	4.705	5.853	3.995	5.768	4.321	5.588	5.698	6.608
27	LOMA PRIETA	CORRALITOS, 090 (CDMG STATION 57007)	2.273	3.498	2.454	3.869	2.45	3.619	3.191	6.521
28	LOMA PRIETA	CORRALITOS, UP (CDMG STATION 57007)	1.191	1.937	1.484	1.672	1.313	1.545	1.238	2.595

29	LOMA PRIETA	SARATOGA ALOHA AVE, 000 (CDMG STATION 58065)	1.934	2.233	1.694	2.056	1.783	2.114	2.368	3.877
30	LOMA PRIETA	SARATOGA ALOHA AVE, 090 (CDMG STATION 58065)	2.13	3.467	1.295	2.675	1.698	2.503	2.123	3.595
31	LOMA PRIETA	SARATOGA ALOHA AVE, UP (CDMG STATION 58065)	0.742	1.67	0.519	1.651	0.608	1.647	1.581	1.593
32	ERZICAN TURKEY	ERZICAN EAST-WEST COMP	2.968	4.427	2.29	5.028	2.633	3.682	3.092	5.924
33	ERZICAN TURKEY	ERZICAN - NORTH-SOUTH COMP	2.399	3.72	2.229	3.829	2.216	3.492	3.157	4.118
34	ERZICAN TURKEY	ERZICAN -UP COMP	1.337	1.41	1.126	1.391	1.184	1.32	1.186	1.787
35	CAPE MENDOCINO	CAPE MENDOCINO, 000 (CDMG STATION 89005)	8.905	8.497	8.581	8.273	8.804	7.294	7.375	12.301
36	CAPE MENDOCINO	CAPE MENDOCINO, 090 (CDMG STATION 89005)	2.847	3.481	2.483	3.315	2.674	3.465	3.203	3.276
37	CAPE MENDOCINO	CAPE MENDOCINO, UP (CDMG STATION 89005)	1.272	2.275	1.261	2.428	1.222	2.563	2.902	4.138
38	CAPE MENDOCINO	PETROLIA, 000 (CDMG STATION 89156)	2.992	4.628	2.237	4.978	2.421	3.845	3.357	5.728
39	CAPE MENDOCINO	PETROLIA, 090 (CDMG STATION 89156)	2.576	6.212	2.336	6.25	2.722	5.218	4.806	7.532

40	CAPE MENDOCINO	PETROLIA, UP (CDMG STATION 89156)	1.108	2.564	0.837	2.255	0.982	1.973	1.302	2.245
41	LANDERS 6/28/92	LUCERNE, 260 (SCE STATION 24)	1.866	3.751	2.589	3.551	2.025	3.044	2.822	3.774
42	LANDERS 6/28/92	LUCERNE, 345 (SCE STATION 24)	2.059	2.203	2.003	2.15	2.012	2.095	1.91	2.995
43	LANDERS 6/28/92	LUCERNE, UP (SCE STATION 24)	1.501	2.025	1.13	1.987	1.274	1.903	1.564	2.252
44	NORTHRIDGE EARTHQUAKE	CA:LA;SEPULVEDA VA, BLD 40 GND; 270	4.961	9.752	4.199	11.265	3.991	8.983	6.599	12.461
45	NORTHRIDGE EARTHQUAKE	CA:LA;SEPULVEDA VA, BLD 40 GND; 360	6.334	7.049	5.747	7.119	6.324	6.79	7.627	7.443
46	NORTHRIDGE EARTHQUAKE	CA:LA;SEPULVEDA VA, BLD 40 GND; UP	2.085	3.125	1.367	3.2	1.619	3.15	3.062	3.372
47	NORTHRIDGE EARTHQUAKE	NORTHRIDGE - SATICOY, 090 (USC STATION 90003)	2.606	3.631	2.047	3.592	2.579	3.4	3.389	4.097
48	NORTHRIDGE EARTHQUAKE	NORTHRIDGE - SATICOY, 180 (USC STATION 90003)	3.944	5.092	2.769	4.812	2.719	4.303	4.585	5.794
49	NORTHRIDGE EARTHQUAKE	RINALDI RECEIVING STA, 228	13.537	26.437	13.053	30.522	10.587	26.364	22.451	28.22
50	NORTHRIDGE EARTHQUAKE	RINALDI RECEIVING STA, 318	2.798	5.802	2.674	5.739	2.794	4.23	4.475	6.375
51	NORTHRIDGE EARTHQUAKE	RINALDI RECEIVING STA, UP	2.021	3.254	2.161	2.968	1.999	2.725	2.194	4.689

52	NORTHRIDGE EARTHQUAKE	SYLMAR - HOSPITAL, 090 (CDMG STATION 24514)	2.446	7.6	2.541	8.932	2.465	7.419	4.142	12.913
53	NORTHRIDGE EARTHQUAKE	SYLMAR - HOSPITAL, 360 (CDMG STATION 24514)	10.884	16.932	9.988	18.3	9.05	16.369	14.582	16.68
54	NORTHRIDGE EARTHQUAKE	SYLMAR - HOSPITAL, UP (CDMG STATION 24514)	1.061	1.516	0.887	1.578	0.921	1.546	1.408	1.474
55	KOCAELI TURKEY	IZMIT, 090 (ERD)	1.833	1.656	2.046	1.607	2.163	1.672	1.654	2.18
56	KOCAELI TURKEY	IZMIT, 180 (ERD)	1.044	1.872	1.123	1.721	1.075	1.574	1.203	2.79
57	KOCAELI TURKEY	IZMIT, UP (ERD)	0.58	0.79	0.511	0.857	0.56	0.883	0.853	0.883
58	KOCAELI TURKEY	YARIMCA, 330 (KOERI)	1.539	2.718	1.479	2.92	1.542	2.872	2.334	2.864
59	KOCAELI TURKEY	YARIMCA, 060 (KOERI)	1.493	1.276	1.366	2.982	1.52	2.687	2.324	4.699
60	KOCAELI TURKEY	YARMICA, UP (KOERI)	1.299	3.954	1.077	1.336	1.101	1.43	1.574	1.98
61	CHI-CHI 09/20/99	TCU065, E	2.733	4.06	2.298	5.402	2.111	4.543	3.005	4.977
62	CHI-CHI 09/20/99	TCU065, N	2.733	2.146	1.82	3.584	2.036	3.71	3.052	8.446
63	CHI-CHI 09/20/99	TCU065, V	1.237	3.793	0.93	1.933	1.017	1.807	1.645	2.56
64	CHI-CHI 09/20/99	TCU067, E	2.724	2.572	2.066	3.709	2.188	3.367	4.472	5.01

65	CHI-CHI 09/20/99	TCU067, N	2.763	4.754	2.141	5.11	2.082	5.167	4.283	8.398
66	CHI-CHI 09/20/99	TCU067, V	1.035	2.572	0.843	2.432	0.973	2.28	1.842	2.167
67	CHI-CHI 09/20/99	TCU084, E	13.724	30.368	13.362	37.568	9.934	29.829	23.765	29.881
68	CHI-CHI 09/20/99	TCU084, N	3.844	4.124	4.012	4.316	3.468	4.7	3.443	5.366
69	CHI-CHI 09/20/99	TCU084, V	2.468	3.874	1.839	3.368	2.192	3.753	4.209	5.751
70	CHI-CHI 09/20/99	TCU102, E	1.194	2.674	0.883	2.172	1.091	2.042	1.828	4.048
71	CHI-CHI 09/20/99	TCU102, N	0.775	2.074	0.749	1.697	0.73	1.538	1.309	2.508
72	CHI-CHI 09/20/99	TCU102, V	0.572	0.827	0.575	0.786	0.619	0.814	0.78	1.25
73	DUZCE 11/12/99	DUZCE, 180 (ERD)	3.248	5.755	2.714	5.868	3.592	4.876	4.325	6.177
74	DUZCE 11/12/99	DUZCE, 270 (ERD)	3.56	4.204	2.762	3.903	3.11	3.599	3.579	5.106
75	DUZCE 11/12/99	DUZCE, UP (ERD)	1.084	1.189	0.846	1.115	0.896	1.111	1.153	1.047
76	DENALI ALASKA 11/03/02	PS10, 047	1.758	3.14	1.409	3.096	1.691	3.054	2.988	3.695
77	DENALI ALASKA 11/03/02	PS10, 317	1.002	2.772	0.775	2.754	0.805	2.653	2.237	3.028
78	DENALI ALASKA 11/03/02	PS10, UP	0.487	1.248	1.3	1.194	1.212	1.188	1.126	2.119

Table 178: Demand of C template buildings (in cm) under near field earthquakes (SDOF system) part two

	Earthquake	Record and component	C2 x	C2 y	C2Bx (6fl)	C2By (6fl)	C3x	C3y
1	IMPERIAL VALLEY	CHIHUAHUA, 012 (UNAM/UCSD STATION 6621)	1.937	1.202	2.708	1.904	2.399	1.442
2	IMPERIAL VALLEY	CHIHUAHUA, 282 (UNAM/UCSD STATION 6621)	1.645	1.008	3.619	1.624	2.452	0.972
3	IMPERIAL VALLEY	CHIHUAHUA, DWN (UNAM/UCSD STATION 6621)	0.674	0.366	0.609	0.674	0.569	0.355
4	IMPERIAL VALLEY	EL CENTRO ARRAY #6, 140 (CDMG STATION 942)	2.079	2.088	3.114	2.093	2.057	1.358
5	IMPERIAL VALLEY	EL CENTRO ARRAY #6, 230 (CDMG STATION 942)	2.858	2.013	4.024	3.272	3.948	1.563
6	IMPERIAL VALLEY	EL CENTRO ARRAY #6, UP (CDMG STATION 942)	3.365	3.275	3.597	2.598	3.506	2.498
7	IMPERIAL VALLEY	EL CENTRO ARRAY #7, 140 (USGS STATION 5028)	1.469	1.459	3.092	1.473	1.839	1.302
8	IMPERIAL VALLEY	EL CENTRO ARRAY #7, 230 (USGS STATION 5028)	2.839	1.68	4.905	3.225	3.863	1.429

9	IMPERIAL VALLEY	EL CENTRO ARRAY #7, UP (USGS STATION 5028)	1.54	1.188	1.778	1.545	1.402	0.716
10	IMPERIAL VALLEY	BONDS CORNER, 140 (USGS STATION 5054)	0.307	0.177	0.678	0.299	0.392	0.155
11	IMPERIAL VALLEY	BONDS CORNER, 230 (USGS STATION 5054)	0.371	0.278	0.685	0.369	0.405	0.243
12	IMPERIAL VALLEY	BONDS CORNER, UP (USGS STATION 5054)	0.035	0.046	0.028	0.035	0.032	0.054
13	IRPINIA EQ / ITALY	STURNO, 000	3.037	1.455	3.288	3.244	2.967	1.086
14	IRPINIA EQ / ITALY	STURNO, 270	2.26	2.152	2.985	2.236	2.613	1.641
15	IRPINIA EQ / ITALY	STURNO, UP	0.791	0.86	1.319	0.768	0.979	0.567
16	NAHANNI, CANADA	SITE 1, 010	4.245	2.854	4.139	3.127	3.267	2.85
17	NAHANNI, CANADA	SITE 1, 280	3.532	3.558	4.739	3.471	3.407	3.833
18	NAHANNI, CANADA	SITE 1, UP	2.392	1.538	3.893	2.409	2.577	1.289
19	NAHANNI, CANADA	SITE 2, 240	1.757	1.485	3.732	1.751	1.979	1.338
20	NAHANNI, CANADA	SITE 2, 330	1.427	0.945	4.174	1.393	1.948	0.726
21	SUPERSTITION HILLS	PTS, 225 (USGS STATION 5051)	2.953	1.971	5.201	3.309	4.3	1.961

22	SUPERSTITION HILLS	PTS, 315 (USGS STATION 5051)	2.479	1.96	5.295	2.518	4.146	1.516
23	LOMA PRIETA	BRAN, 000	5.605	3.701	6.318	5.884	6.404	2.15
24	LOMA PRIETA	BRAN, 090	4.755	2.75	8.169	6.192	6.411	2.179
25	LOMA PRIETA	BRAN, UP	3.425	1.667	2.366	2.703	2.751	1.834
26	LOMA PRIETA	CORRALITOS, 000 (CDMG STATION 57007)	6.217	4.037	6.982	4.855	5.113	2.887
27	LOMA PRIETA	CORRALITOS, 090 (CDMG STATION 57007)	2.563	2.473	4.881	2.464	3.635	1.671
28	LOMA PRIETA	CORRALITOS, UP (CDMG STATION 57007)	1.266	1.473	2.42	1.278	1.397	1.825
29	LOMA PRIETA	SARATOGA ALOHA AVE, 000 (CDMG STATION 58065)	2.529	1.695	3.401	2.533	2.257	1.388
30	LOMA PRIETA	SARATOGA ALOHA AVE, 090 (CDMG STATION 58065)	2.344	1.321	3.945	2.404	2.283	0.817
31	LOMA PRIETA	SARATOGA ALOHA AVE, UP (CDMG STATION 58065)	1.399	0.527	1.691	1.358	1.625	0.534
32	ERZICAN TURKEY	ERZICAN EAST-WEST COMP	2.881	2.295	4.696	3.875	3.428	2.524
33	ERZICAN TURKEY	ERZICAN - NORTH-SOUTH COMP	2.912	2.246	3.896	3.211	3.368	1.542
34	ERZICAN TURKEY	ERZICAN -UP COMP	1.226	1.123	1.352	1.224	1.181	0.903

35	CAPE MENDOCINO	CAPE MENDOCINO, 000 (CDMG STATION 89005)	6.659	8.606	11.115	8.894	7.342	8.203
36	CAPE MENDOCINO	CAPE MENDOCINO, 090 (CDMG STATION 89005)	3.08	2.514	4.003	2.53	3.52	2.051
37	CAPE MENDOCINO	CAPE MENDOCINO, UP (CDMG STATION 89005)	2.274	1.271	3.091	2.188	2.825	0.994
38	CAPE MENDOCINO	PETROLIA, 000 (CDMG STATION 89156)	3.425	2.256	5.035	4.879	3.639	1.536
39	CAPE MENDOCINO	PETROLIA, 090 (CDMG STATION 89156)	3.671	2.346	8.543	4.196	4.966	1.709
40	CAPE MENDOCINO	PETROLIA, UP (CDMG STATION 89156)	1.179	0.846	2.267	1.216	1.554	0.751
41	LANDERS 6/28/92	LUCERNE, 260 (SCE STATION 24)	2.652	2.587	3.502	2.758	2.868	1.992
42	LANDERS 6/28/92	LUCERNE, 345 (SCE STATION 24)	2.171	1.954	2.504	2.206	1.987	1.669
43	LANDERS 6/28/92	LUCERNE, UP (SCE STATION 24)	1.473	1.14	1.978	1.482	1.744	0.698
44	NORTHRIDGE EARTHQUAKE	CA:LA;SEPULVEDA VA, BLD 40 GND; 270	4.295	4.235	8.956	7.435	8.321	2.346
45	NORTHRIDGE EARTHQUAKE	CA:LA;SEPULVEDA VA, BLD 40 GND; 360	6.406	5.823	9.392	5.956	6.172	4.254

46	NORTHRIDGE EARTHQUAKE	CA:LA;SEPULVEDA VA, BLD 40 GND; UP	2.958	1.381	3.283	2.725	3.14	1.268
47	NORTHRIDGE EARTHQUAKE	NORTHRIDGE - SATICOY, 090 (USC STATION 90003)	2.748	2.064	4.407	2.497	3.25	1.508
48	NORTHRIDGE EARTHQUAKE	NORTHRIDGE - SATICOY, 180 (USC STATION 90003)	5.117	2.842	6.31	4.463	4.629	1.794
49	NORTHRIDGE EARTHQUAKE	RINALDI RECEIVING STA, 228	9.816	13.386	22.103	22.35	25.254	5.576
50	NORTHRIDGE EARTHQUAKE	RINALDI RECEIVING STA, 318	5.628	2.695	6.708	4.125	4.528	2.38
51	NORTHRIDGE EARTHQUAKE	RINALDI RECEIVING STA, UP	1.929	2.126	3.949	1.902	2.452	2.842
52	NORTHRIDGE EARTHQUAKE	SYLMAR - HOSPITAL, 090 (CDMG STATION 24514)	3.85	2.59	8.928	3.001	6.149	1.64
53	NORTHRIDGE EARTHQUAKE	SYLMAR - HOSPITAL, 360 (CDMG STATION 24514)	8.807	10.205	16.162	15.874	15.971	5.854
54	NORTHRIDGE EARTHQUAKE	SYLMAR - HOSPITAL, UP (CDMG STATION 24514)	1.122	0.896	1.268	1.122	1.521	0.742
55	KOCAELI TURKEY	IZMIT, 090 (ERD)	1.567	2.054	2.027	1.546	1.696	1.814

56	KOCAELI TURKEY	IZMIT, 180 (ERD)	1.11	1.117	2.378	1.109	1.382	1.332
57	KOCAELI TURKEY	IZMIT, UP (ERD)	0.816	0.518	0.736	0.81	0.883	0.39
58	KOCAELI TURKEY	YARIMCA, 330 (KOERI)	2.07	1.494	2.83	2.037	2.694	1.109
59	KOCAELI TURKEY	YARIMCA, 060 (KOERI)	1.837	1.391	3.485	1.825	2.553	1.111
60	KOCAELI TURKEY	YARMICA, UP (KOERI)	1.448	1.081	1.907	1.41	1.521	1.048
61	CHI-CHI 09/20/99	TCU065, E	3.262	2.323	4.422	3.403	4.085	2.116
62	CHI-CHI 09/20/99	TCU065, N	2.538	1.805	5.866	2.54	3.267	1.56
63	CHI-CHI 09/20/99	TCU065, V	1.612	0.937	2.206	1.605	1.68	0.69
64	CHI-CHI 09/20/99	TCU067, E	3.643	2.075	4.957	3.74	3.503	1.575
65	CHI-CHI 09/20/99	TCU067, N	4.297	2.171	5.611	5.131	5.005	1.375
66	CHI-CHI 09/20/99	TCU067, V	1.497	0.85	2.26	1.436	2.066	0.806
67	CHI-CHI 09/20/99	TCU084, E	9.068	13.926	21.606	26.653	28.436	6.862
68	CHI-CHI 09/20/99	TCU084, N	3.107	4.131	5.137	3.314	4.396	1.986
69	CHI-CHI 09/20/99	TCU084, V	3.193	1.835	4.95	2.741	4.241	1.324
70	CHI-CHI 09/20/99	TCU102, E	1.495	0.903	3.525	1.477	1.976	0.648

71	CHI-CHI 09/20/99	TCU102, N	1.139	0.751	2.24	1.115	1.424	0.526
72	CHI-CHI 09/20/99	TCU102, V	0.712	0.582	1.09	0.693	0.811	0.361
73	DUZCE 11/12/99	DUZCE, 180 (ERD)	5.904	2.743	6.011	3.719	4.273	1.934
74	DUZCE 11/12/99	DUZCE, 270 (ERD)	4.455	2.823	4.165	4.93	3.572	1.846
75	DUZCE 11/12/99	DUZCE, UP (ERD)	1.358	0.844	1.108	1.382	1.139	0.684
76	DENALI ALASKA 11/03/02	PS10, 047	2.333	1.438	3.35	2.279	3.116	1.206
77	DENALI ALASKA 11/03/02	PS10, 317	1.732	0.78	2.867	1.682	2.499	0.732
78	DENALI ALASKA 11/03/02	PS10, UP	0.955	1.297	1.763	0.923	1.169	0.815

CURRICULUM VITAE

PERSONAL INFORMATION

Surname, Name: Hysenlliu, Marjo

Nationality: Albanian/Shqiptar

Date and Place of Birth: 24.06.1993 Tirane

Marital Status: Single

Phone: 00355696980949

Fax: 0035542266567

E-mail: mariohysenlliu@yahoo.com

EDUCATION

Bachelor in Civil Engineering at Polytechnic University of Tirana 2011-2014

Master in Structural Engineering at Polytechnic University of Tirana 2014-2016

ACADEMIC EXPERIENCE

Pedagogue at Department of Structural Mechanics, Polytechnic University of Tirana 2016-2020

Pedagogue at Faculty of Architecture, Marin Barleti University 2017-2019

FOREIGN LANGUAGES

English C1 Italian B2 Espanol A2

PUBLICATIONS (Journals)

Hysenlliu M.,Bidaj A., Bilgin H., " Influence of material properties on the seismic response of masonry buildings ", Journal of Research on Engineering Structures & Materials, April 2020 DOI: 10.17515/resm2020.177st0120
Available: https://www.researchgate.net/publication/340651860

Hysenlliu M., Bilgin H., " The use of macro element approach for the seismic risk assessment of brick masonry buildings ", Springer Series in Geomechanics and Geoengineering, Romania, November 2019 (Offically accepted for publication) Available: https://www.researchgate.net/publication/341803186

Hysenlliu M., Bilgin H., Bidaj A., "Influence of interventions on the seismic performance of URM buildings designed according to pre-modern codes", Journal of Research on Engineering Structures & Materials, 2020 (Offically accepted for publication) Available: http://dx.doi.org/10.17515/resm2020.177st0120

Hysenlliu M., Bilgin H., Bidaj A., " Analiza e performancës e ndërtesave me murutarë me dhe pa ndërhyrje ", Buletini I Shkencave Teknike, Universiteti Politeknik I Tiranës 2020 (Offically accepted for publication)

Bilgin H., **Hysenlliu M.**, " Comparison of near and far-fault ground motion effects on low and mid-rise masonry buildings ", Jounal of Building Engineering, Romania, 2019, DOI: 10.1016/j.jobe.2020.101248 http://ees.elsevier.com Available: https://www.researchgate.net/publication/339081929

ORAL PRESENTATIONS (Conferences)

Hysenlliu M.,Bidaj A., "Evaluation of capacity and seismic performance of brick masonry buildings with and without structural interventions", International Symposium for Environmental Science and Engineering Research ISESER 2019 Konya, Turkey, 25-27 May 2019

Hysenlliu M., Bilgin H., " The use of macro element approach for the seismic risk assessment of brick masonry buildings ", International Conference Critical Thinking in the Sustainable Rehabilitation and Risk Management of the Built Environment – CRIT-RE-BUILT At: Romania https://www.researchgate.net/publication/341803186

Hysenlliu M., Bilgin H., "Performance of a Typified School Damaged during the 2019 Albanian Earthquake", International Virtual Conference on Emerging Research Trends in Structural Engineering 16 July 2020 organized by School of Civil Engineering VIT Chennai, India (Offically accepted for presenttion)

Hysenlliu M., Gjini A., "Prism testing of most used templates of masonry structures in Albania", International Student Conference of Civil Engineering ISCCE 2018 Polytechnic University of Albania, Faculty of Civil Engineering, Tirane, Albania, 2018

Hysenlliu M., Bidaj A., “Structural system on high rise buildings”, International Conference of Civil Engineering ICCE 2017 , Polytechnic University of Albania, Faculty of Civil Engineering, Tirane, Albania (2017) http://www.icce.al

Bidaj A., Deneko E., **Hysenlliu M.**, “Different reinforcement techniques in damaged buildings”, Published in 3rd International Symposium on Natural Hazards and Disaster Management Van Yuzuncu Yil University TURKEY 25-27 OCT 2019
Available: https://www.researchgate.net/publication/337132297